Final Research Report

Federal Agency and Organization: DOE EERE – Geothermal Technologies Program

Recipient Organization: Impact Technologies LLC
DUNS Number: 141810494

Recipient Address: PO Box 35505, Tulsa, OK 74153

Award Number: DE-EE0002783
Project Title: "Microhole Arrays Drilled with Advanced Abrasive Slurry Jet Technology to Efficiently Exploit Enhanced Geothermal Systems"
Project Period: 1 February 2010 to 31 July 2013
Principal Investigator: Kenneth D. Oglesby
Impact President
kdo2@impact2u.com
918.627.8035

Date of Report Submission: 12 March 2014
Reporting Period: 1 February 2010 to 31 January 2014
Report Frequency: Final

Project Partners: Lawrence Berkeley National Laboratory (Dr. Stefan Finsterle, Dr. Yingqi Zhang, Dr. Lehua Pan, Dr. Patrick Dobson);
University of Tulsa (Dr. Ram Mohan, Dr. Ovadia Shoham);
Dr. Betty Felber and Dr. Dwight Rychel

DOE Project Team: DOE Contracting Officer – Melissa Jacobi (prior-Genevieve Wozniak)
DOE Project Officer – Joshua Mengers (prior-Greg Stillman)
Project Monitor – Elisabet Metcalfe

DISCLAIMER

This report was prepared as an account of work sponsored by an agency of the United States Government. Neither the United States Government nor any agency thereof, nor any of their employees, makes any warranty, express or implied, or assumes any legal liability of responsibility for the accuracy, completeness, or usefulness of any information, apparatus, product, or process disclosed, or represents that the use would not infringe privately owned rights. Reference herein to any specific commercial product, process, or service by trade name, trademark, manufacturer, or otherwise does not necessarily constitute or imply its endorsement, recommendation, or favoring by the United States Government or any agency thereof. The views and opinions of authors expressed herein do not necessarily state or reflect those of the United Sates Government or any agency thereof.

Executive Summary

This project had two major areas of research for Engineered/ Enhanced Geothermal System (EGS) development - study the potential benefits from using microholes (i.e., bores with diameters less than 10.16 centimeters/ 4 inches) and study one method, FLASH ASJ™, to install those microbores. This included the methods and benefits of drilling vertical microholes for exploring the EGS reservoir and for installing multiple (forming an array of) laterals/ directional microholes for creating the in-reservoir heat exchange flow paths.

The stated specific objectives/ goals of the project were to:

1) determine if the FLASH ASJ™ abrasive cutting system was effective in drilling microbores in hard and 260°C/ 500°F temperature rocks. This included evaluating-
   a- various FLASH fluids,
   b- pipes, specifically coiled tubing,
   c- hydraulics of various possible microhole system configurations,
   d- optimal nozzle designs,
   e- directional capabilities, and
   f- safety and environmental;
2) determine the potential benefits for EGS systems by using computer simulations of an EGS reservoir with and without a simplified microbore array; and
3) one unstated, but inferred, side objective of the project was to drill a microhole using the FLASH ASJ™ abrasive drilling system.

The methodologies utilized in the project included:

1) Literature Reviews were made by
   a- Felber/ Lawrence Berkeley National Lab (LBNL)/ Impact identify and characterize all potential fluids that could be used as a FLASH fluid and how they could be obtained in the field,
   b- Rychel/Impact identify and characterize all commercially available pipes (specifically coiled tubing (CT)) useable for the FLASH ASJ™ drilling process,
   c- Rychel/Impact on CT design tools,
   d- LBNL on programing code changes,
   e- TU on erosion, and
   f- TU / Impact on jet pumps;
2) Computer Simulation studies by
   a- LBNL with the TOUGH2 reservoir simulation package (with modifications) to simulate EGS reservoirs with and without microbore arrays in five increasingly sophisticated and complex models, leading up to a Soultz-based 3-D model with 40 microbore,
   b- LBNL with a developed fracture incidence model,
   c- The University of Tulsa (TU) using the Fluent software to aid in the design of a new FLASH ASJ™ nozzle,
   d- Multiphase System Integration (MSI) using SPT Group's WellFlo drilling simulator to hydraulically simulate drilling microholes at 6 depths, 3 supercritical fluids (N_2, CO_2, steam) and various rates and configurations (hole size, pipe size, flow rates of each phase, pressures, nozzle performance, etc…),

e- TU's Dr. Evren Ozbayoglu in modelling the FLASH drilling system for real-time control and operation, and f- by CTES using their proprietary pipe properties program to estimate drill pipe bending for directional control;

3) Bench Tests by
   a- Tulsa University performed studies of supercritical CO_2 jet performance out of a nozzle in a test cell to aid their computer modeling. TU also performed erosion bench tests with simulation studies for a new induction based slurry pump design, and
   b- Impact designed and built over 4 FLASH based nozzles (and other tools) that were then bench tested on granites and sandstones to find the optimal nozzle configuration. Over 250 large scale bench cutting tests were conducted with those nozzles and various combinations of abrasive concentrations, fluids, fluid/gas ratios, flow rates, temperatures and pressures to optimize the FLASH process. Those nozzle and process conditions were used to bench drill granites and sandstones. Bench cutting tests were also conducted on 260°C/500°F granite blocks and then compared again at ambient temperature after cooling. Various tools for abrasive microhole drilling were also developed by Impact. These tool developments and bench tests were successful, although further advancements were identified to increase the FLASH process efficiency. Two marginally successful microhole drilling tests were made at Impact's shop, one using coiled tubing and CT rig and a second test using straight jointed pipe and a hydraulic lift type rig; and
4) Overall review of the processes to determine their feasibility by All.

Outcomes from this project's *simulation efforts* of microbore arrays in EGS reservoirs were:
1) semi-analytical wellbore flow solutions linked to the TOUGH2 reservoir simulator;
2) a very sophisticated and complex Soultz–based 3D TOUGH2 model with and without microbores;
3) microhole arrays increased overall EGS performance due to improved contact of a larger volume of hot rock and higher heat mining performance, thereby doubling the life of an EGS project;
4) microhole arrays were beneficial to EGS projects by lowering development risks via an increased possibility that sufficient microbores would intersect/connect to the targeted fracture conduit and establish the full system flow for a successful project;
5) flow self-regulation between microbores within the array lowered the risk of thermal short circuiting within the imbedded heat exchanger. Regulation occurs due to increased friction as the flow rate increases in any one microbore, resisting flow and balancing upstream pressures;
6) microhole array benefits accrue to the FLASH ASJ™ and all other drilling methods that can install such small lateral bores within EGS reservoirs; and
7) microhole array benefits may apply to slightly larger hole sizes, such as smaller slimholes (less than 4-3/4" bits) which can be drilled with conventional rotary bit drilling methods, but the resulting benefits are estimated to be less and needs to be specifically simulated.

Outcomes from the *FLASH ASJ™ efforts* determined:
8) new FLASH nozzles and tools, based on patented designs, were efficient in cutting rock;
9) overall FLASH system is an efficient rock cutting / reduction method, still estimated at 20 times as efficient as current rock cutting systems of water jetting and bit/ line grinding;

10) the ambient to 500^{o}F to ambient temperature range had no effect on FLASH granite cutting efficiency, thus abrasive systems can be used for drilling or other cutting activities in hot deep EGS rocks;
11) drilling in bench and vertical rock tests were not as successful as desired. Bent pipe or angled jet from the nozzle were suspected. However, both set of tests showed that maintaining a minimum hole size is critical to forward movement even with low viscosity, gaseous FLASH systems. The cause is considered to be- if the bit/nozzle is advanced too fast for FLASH ASJ erosion to create the minimum diameter needed for full return flow, then the bit/ nozzle-

a- cannot physically pass through or, if it can pass through,
b- an annular return flow choke point is created. Multiple less-restrictive reduced diameter/area points can cause the same effect as one fully restrictive point.

As the nozzle/ drill pipe passes through that reduced diameter/ area point(s), both the pressure ahead of the bit/ nozzle increases and frictional drag increases from the higher velocity of the return fluids/solids on the pipe through that choke point. In addition, the increased post-nozzle pressure reduces the FLASH process efficiency (i.e., decreases pressure drop across the nozzle and a higher final pressure for a denser gas in the cutting area). Combined, these actions cause increased reverse forces on the drill pipe and lower cutting efficiency which can overcome the drill assembly weight and stop forward progress. Multiple passes back through that restrictive diameter(s) are not as effective in widening that diameter as the first pass. Reducing the initial forward rate to ensure full bores and the proposed remedial actions take away from the benefits of the faster FLASH rock removal method, slowing the overall drilling process;
12) because of the findings and causes given in 9 above, it is envisioned that FLASH ASJ^{TM} drilling must be combined with a mechanical drilling method (specifically, rotating mechanical bit) that can ensure a minimum hole diameter-without restricting return flow itself. Taken to the extreme end, FLASH ASJ^{TM} can be used to improve or enhance conventional rock bit drilling methods in hard rocks, if the bit is slightly modified for improved return flow. It will take many years of development for this combined drilling system to reach EGS depths;
13) using FLASH ASJ^{TM} to drill deep vertical drilling microholes above the reservoir for exploration were found theoretically hydraulically possible, but deemed not practical due to the high underbalance condition required for optimal FLASH ASJ^{TM} drilling. That required underbalance condition can cause high formation water/ fluid influx, wellbore instability, and well control and safety issues that could not be easily resolved. In addition, in vertical drilling the FLASH process has a very narrow operating range that is significantly impacted by hole size and formation water influx;
14) chemical methods to treat and reduce formation liquid influx were identified and considered, but the time required to stop drilling, chemically treat and cleanup the wellbore and restart drilling was thought to eliminate any benefit from the faster FLASH drilling method;
15) installing the multiple microhole directional laterals within the EGS reservoir had less of those above cited issues in 12 and 13, but the complicated downhole equipment required to maintain the underbalanced condition (estimated at 3 strings all sealed into a packer) was considered too difficult to implement at deep EGS conditions;
16) FLASH ASJ^{TM} and other methods for directional drilling of microholes in EGS reservoirs can use simplified, l950's technology of point (setting initial orientation and angle out of the larger main wellbore) and shoot (direct drilling with computer program forecast of vertical movement based on gravity, created hole diameter at some setoff ahead of the bit/nozzle, pipe diameters and

properties, and bit/nozzle tool diameter) methods to hit a very large target- i.e., the fracture. Since tight tolerances for a given microhole (of many in an array) onto the target position of a very large target are NOT REQUIRED, no extremely complicated and high dollar real-time directional measurement and control systems are needed (or even possible in these very small size pipes and holes) and high temperatures. It is more important to get a large numbers of bores that are spread out instead of precise positioning.

Table of Contents

Tables and Figures

Background of Prior Research

The 2006 MIT report, The Future of Geothermal Energy (21), conducted a detailed investigation of the potential of enhanced geothermal systems (EGS) to contribute up to 10% of U.S. electrical power generation needs in the US by 2050. From regional heat flow maps it was concluded that widespread potential EGS reservoirs at depths of 3 to 10 km would be viable if means were developed to tap this energy source. One key issue identified as critical to exploiting this reserve is the need for better, less costly methods to drill deep wells (21, 27), as drilling costs increase nonlinearly with depth (see Figure 1). A second challenge identified in the MIT report was the need to develop a network of stimulated fractures and wells in the reservoir to create connected flow paths that can achieve optimal heat extraction.

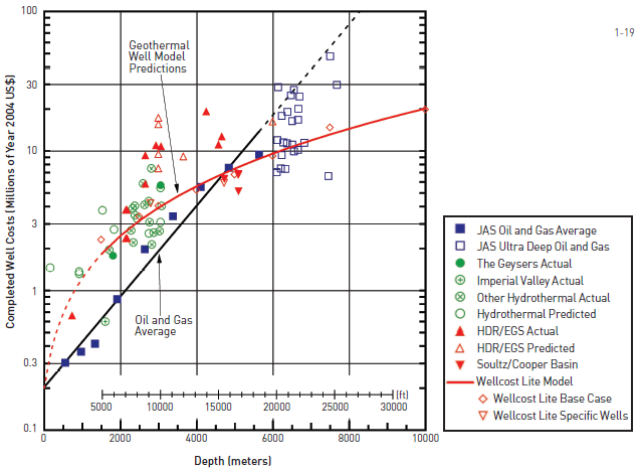

Figure 1. Completed oil, gas, and geothermal well costs as a function of depth in 2004 dollars, including estimated costs (red line) from the Wellcost Lite model (21).

To answer the above needs for geothermal development, this project proposed drilling microholes (defined as boreholes less than 4" diameter) to install microhole arrays (i.e., multiple microholes drilled in parallel) within the reservoir thereby creating a more efficient path to circulate and extract fluids to mine heat from the subsurface. The use of such arrays were simulated to identify the benefits and efficiency. This project also proposed using a special abrasive slurry with a supercritical gas drilling method (called FLASH ASJ™) to efficiently drill those microholes at a high rate of penetration (ROP), although other methods (rotary bit, spallation, abrasive erosion, lasers, millimeter wave directed energy, etc.) may be developed and utilized in the future. Further, it was envisioned in this project that coiled tubing would be utilized to greatly improve drill rate (ROP), maintain the slurry flow and pressure in the tubing and maintain the optimal underbalanced or managed pressure downhole conditions for improved ROP. Each of these technical areas will be further discussed below.

Microhole Drilling

Typical oilfield industry wells use standard 6-1/4" to 24" OD drilling bits, with casing set in sizes from 4-1/2" to 13-3/8". Geothermal wells target bore sizes ending at depth with 8-1/2" at minimum- and up to 36" at the surface. Those sizes require a lot of rock to be removed taking a

lot of energy and very large equipment to do so. The next step down in borehole size is called 'slimhole'. Slimhole drilling (ie. bit sizes from 4" to 6-1/4") has found selected industry applications, primarily in oil and gas directional and horizontal drilling. It is one of the most cost effective methods of oil and gas reserve developments (6). With smaller holes, pipes and casing its advantages include:

1- reduced mud and chemical usage and disposal;
2- smaller (hence less expensive) tubulars and rigs;
3- faster drilling times; and
4- the ability to drill high-angle and horizontal holes from existing wellbores.

The downside is the lower pipe strength and limited space for mechanical equipment and repairs.

Early work in the 1990s applying slimholes to geothermal reservoirs (28) showed considerable potential for smaller geothermal projects (100 to 1,000 kWe) in off-grid remote areas of Latin America, Philippines, Japan (40) and many other Pacific Rim Islands. Conventionally drilled wells were uneconomic, but using slimhole techniques at 1/3 the cost resulted in a generating capacity that was economic. By producing water using binary techniques with a downhole pump, targeting hotter reservoirs and utilizing conventional spontaneous discharge flash steam methods, they concluded that slimholes were technically and economically feasible in cases from a few hundred kilowatts to a megawatt (28).

In about the same time frame, Sandia published a slimhole handbook (6) on the operation of small geothermal power plants (SGPP). Use of diesel generators to provide electricity in remote areas was environmentally harmful and cost 50 cents/kWh. With slimhole drilling a 300 kW geothermal unit extracting 250˚F fluids could produce electricity for 11 cents/kWh. The handbook has a case study on each project and recommendations for slimhole drilling practices (6).
Taking the slimhole concept a step further, the DOE sponsored a Microhole Initiative to promote technology and tools for the drilling of microholes (less than 4" diameter). Sixteen projects (including one with Impact) were funded to develop smaller motors, rigs, steering tools and ancillary drilling equipment. Those tools are now beginning to be applied. From 1996 through 2005, BP and ConocoPhillips drilled over 500 horizontal microholes from larger existing tubing in Prudhoe Bay, as lateral extensions (18). Figure 2 shows a typical conventional, slimhole and microhole configuration in Prudhoe Bay (33). To that end Schlumberger developed "A Built-for-Purpose Coiled Tubing Rig" under a DOE project DE-PS26-03NT15474 that targeted 3.5" bores with conventional rotating bits. There are, however, practical limits for conventional small hole drilling, depending on the knowledge of the crews, fishing tools, sufficient drill rates for weight-on-bit methods, drill string strength and evaluation (logging) tools.

FLASH ASJ™ Drilling

Methods to potentially drill microbores at EGS depths are abrasive water-jetting systems operating at 20,000-40,000 psi (34, 41), the FLASH ASJ™ abrasive cutting system operating at 5,000-10,000 psi (24,25,26), directed energy laser cutting/ drilling system such as the one Foro Energy is developing in a DOE project, and directed energy millimeter wave cutting/ drilling and lining technology being co-developed by MIT and Impact under another DOE project, DE-

EE0005504 entitled “Deep Geothermal Drilling Using Millimeter Wave Technology” (44). The directed energy methods are in early stage development and will not be further discussed herein.

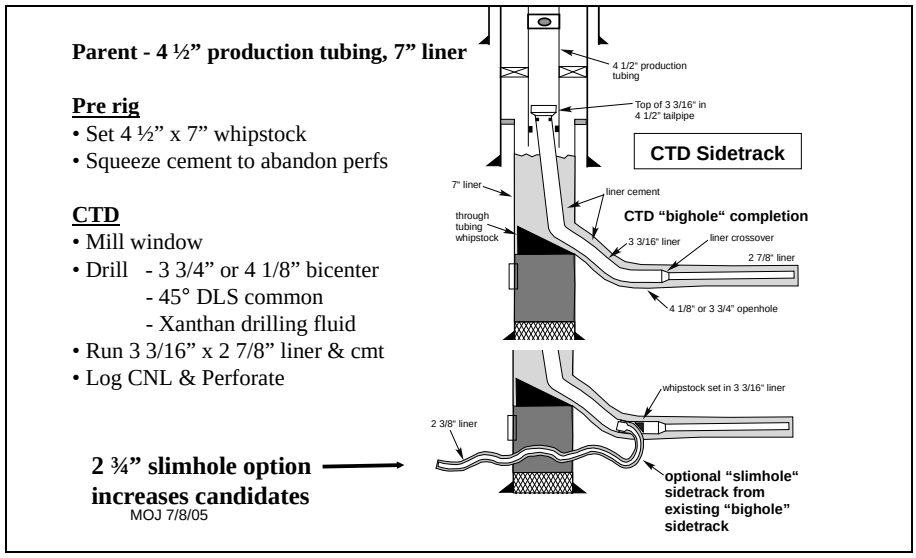

Figure 2. BP Alaska Sidetrack (33)

Abrasive waterjet cutting is used now for cutting materials in machine shops and offshore for platform demolition. It can provide an efficient fast means of cutting (20, 34, 41), either alone or in combination with conventional drilling methods. Gulf Oil Company and others successfully tested ‘lower pressure’ abrasive cutting with rotary drilling in the field to depths of 15,000 ft. High ROP were achieved, but problems with high wear on the pumps, pipes and connections leading to higher costs outweighed the benefits of the higher ROP (34).

Water-jetted abrasive systems were considered potentially not hindered by higher well temperatures AND can be even more effective as the strength and integrity of the rock is reduced with increasing temperature. Temperatures will affect the fluid’s carrying capacity for lifting the injected abrasives and the cut rock debris. That should be compensated by the selection of appropriate fluid types and concentrations (tested as part of this project). Nozzle life (partially tested in this project at surface conditions) may be somewhat reduced by increased temperature, but metal strength and hardness does not significantly degrade below 427^{o}C/ 800^{o}F. Rock and pore pressure at depth (i.e., bottom hole pressure) will impact all abrasive systems as the pressure drop across the nozzle creates the velocity of the abrasive particles and its cutting power. Therefore, higher post-nozzle (bottom hole) wellbore pressure requires a corresponding higher pre-nozzle pressure to keep the same particle velocity and cutting potential. Purely water based abrasive systems have a difficult time in cutting a full bore, mostly requiring rotation of multiple nozzles, but some special nozzles can rotate the abrasive particles for a fuller cut, see Figure 3. FLASH ASJ^{TM} can drill holes without rotation, see Figure 4 cutting sandstone.

Gulf Oil Company and others successfully tested abrasive cutting with rotary drilling in the field to depths of 15,000 ft. High ROP were achieved, but problems with high wear on the pumps, pipes and connections leading to higher costs outweighed the benefits of the higher ROP (34).

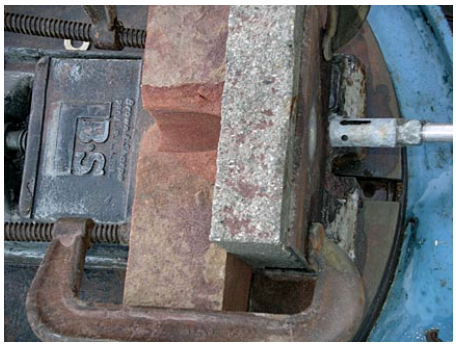

Figure 3. Hole through steel, concrete and rock using only abrasive water-jetting and special nozzles at MS&T (24)

Figure 4. Drilling sandstone using 5,000 psi FLASH ASJ™ at MS&T (24)

Impact and Missouri University of Science and Technology (MS&T) developed the patented FLASH ASJ™ drilling system (developed under DE-FC26-04NT15476, for very fast full-bore drilling without rotation and low (less than 5000 to 10,000 psi) standpipe pressures (24, 42, 47). The FLASH system consists of abrasives, supercritical fluids, chemical additives, a specialized and patented nozzle and modified patented high pressure (some rated at up to 15,000 psi) slurry pumps (HPSP, see Figures 6 & 7, References 24 & 25). The FLASH fluid must be in its liquid or near liquid state inside the drill string and into the nozzle to suspend carry the abrasive particles. It transitions to a low-density gas or fluid across the nozzle. Supercritical fluid and additive selection, tube size (Internal Diameter (ID) and Outer Diameter (OD)), bore or hole diameter, pump / surface/ standpipe pressures, pump rate of each of the various components, nozzle design, hole depth and rock type all impact FLASH ASJ™ drilling rate.

Examples of FLASH fluids include water as steam, carbon dioxide, methane, propane, butane and nitrogen. FLASH ASJ™ is an abrasive cutting system that accelerates the added abrasive particles due to a flow area restriction (i.e., through a nozzle), but it boosts particle velocity an additional 5 to 12 times over the simple nozzle exit velocity by the expansion of the dense (near) liquid supercritical fluid into its low density gaseous phase. Cutting occurs ahead of the nozzle and thus no weight-on-bit (WOB) or reactive force is required. Expansion of the gas phase propels the abrasive into a wider diameter bore. MS&T bench drilled several different rock types, including basalt with FLASH ASJ™ with only 4000 psi - see Figure 5 and Table 1 below. Drill rates of this new system are estimated to be 4 to 20 times faster than conventional drilling systems, but the drill rate of the new system may be more limited by hole cleaning (to be determined in this study) (24).

How 300ºC rocks will erode under FLASH ASJ™ abrasion requires investigation. The downhole temperatures in the drill pipe and in the annulus after the nozzle must also be known to optimize FLASH performance. The temperatures will set the required pressures and required supercritical FLASH fluid type. Thus, heat transfer (from the hot rock to the wellbore fluids and pipe) and hydraulic calculations are essential to the 30,000 foot and 300ºC design. This modeling and/or simulation work has not been attempted to date.

Rock	Jet Pressure (psi)	Nozzle Dia. (in)	ROP Max (ft/min)	ROP Min (ft/min)	Specific Min (j/cc)	Energy Max (j/cc)	Hole Dia. (in)
Roubideaux	3,500	0.044	15.9	3.8	133	560	1.00
Roubideaux	3,000	0.044	11.2	2.1	150	810	0.875
Joachim lls	4,000	0.039	13.8	3.9	410	1,443	0.6
Joachim lls	4,000	0.039	8.9	8.9	360	360	0.80
Joachim lls	4,000	0.039	11.8	2.5	334	1560	0.71
Joachim lls	4,000	0.039	15.7	2.0	560	4,510	0.50
Indiana lls	4,000	0.039	9.8	3.9	207	519	1.00
Missouri do	4,000	0.039	14.8	2.1	216	1,488	0.80
Missouri do	4,000	0.039	14.8	3.2	216	992	0.80
Missouri do	4,000	0.039	8.9	2.0	736	2,210	0.55
Basalt	4,000	0.039	3	-	3,000	-	0.5

Table 1. Performance of a FLASH ASJ™ system in various rocks- tests performed at MS&T during 2004-2008.

Figure 5. Basalt cutting at 4000psi with FLASH ASJ™ at MS&T

Impact Technologies LLC (Impact) previously developed multiple tools for FLASH ASJ™ drilling, including the patented and patented High Pressure Slurry Pumps (HPSP, Figures 6 & 7)

for delivering abrasive particles at high pressure (up to 15,000 psi) without minimal wear, specialized patented cutting nozzles (24,25,42), swivels, inverted motors (26), controls, directional tools (25, 46,45), and surface returns gas-liquid-solids separators (43), see Figures 6- 8.

The fortuitous combination of microholes, ASJ drilling with FLASH fluids, underbalanced/ managed pressure drilling (MPD) and continuous coiled tubing provides an exceptional opportunity to create a new advanced drilling platform. That system would allow very fast drilling with low "weight on bit", reservoir testing while drilling, allowing true vertical and directional capabilities, simplified downhole tools, no downtime for joint connections during tripping or drilling, improved safety due to a smooth OD and continuous operation, so that the drilling process can advance much faster. Many of these benefits are discussed further below.

Figure 6. HPSP#1 in Impact Shop

Figure 7. HPSP#2 in Impact Shop

Figure 8. Gas-Liquid-Solids (GLS) Separator

During FLASH ASJ™ drilling, and due to the expanding gas out of the nozzle, the well annulus is naturally underbalanced when compared to the rock pore pressure at depth. That level of underbalance can be 'managed' with a surface choke utilized to control the return flow rate and increase wellbore pressure. This underbalanced condition allows for testing while FLASH ASJ™

drilling. MPD keeps wellbore pressure at or below reservoir pore pressure. Normally a low density base liquid or a gas is needed to achieve this result. Lower pressure in the wellbore encourages fluid flow during drilling, reducing formation damage, increasing the ROP, prolonging bit life and improving well cleaning. Less drilling fluid is lost during drilling, lowering fluid maintenance costs, lost circulation time and non-productive drilling time. MPD with CT eliminates pressure spikes that can exceed reservoir pressure when adding joints. The main disadvantages are that additional equipment is needed for safe operation and disposal of influx fluids and it requires a fully trained and attentive drilling crew (16, 33). Optimal FLASH ASJ^{TM} drilling requires the lowest density gas possible at the nozzle exist and thus the lowest wellbore pressure possible. Methods to maintain that low pressure during operation were investigated in this project since maintaining that very low underbalance condition for optimal FLASH ASJ^{TM} drilling can be a problem due to fluid influx from the rocks and pores. In addition, such low wellbore pressures can add to well safety and control concerns when drilling /operating at great depths.

It should also be noted that this is an energized pressurized abrasive slurry system both ends- when pumped downhole and in the return flow- and thus safety must always be considered. Design of the surface and downhole systems are important as high velocities of the particles are very erosive. Minimum return velocities in the annulus are also important to ensure that the abrasive particles and the cut rock debris are returned to the surface. Expanding gases also greatly cool the surrounding wellbore at and just above the nozzle due to Joules-Thompson effects. Ice, hydrates and precipitates can form due to the extreme cold.

Directional control with FLASH ASJ^{TM} or abrasive water jetting is fairly simple. The resulting cut holes are naturally straight (in relation to the abrasive jet stream, not the nozzle) and little affected by geological deviations in rock along the well axis. Thus a truly vertical and straight hole can be created and maintained, if desired. However, simple directional drilling and control can be achieved by a change in nozzle alignment, since cutting occurs ahead of the bit. This also makes it important that the pipe is straight and oriented in the proper direction near the nozzle to go in the direction desired.

Drilling with coiled tubing (CT) (collectively CTD) requires special rigs and handling tools (4). Proven advantages to CTD include:

1- can drill on an existing well without killing it,
2- works underbalanced,
3- fast ROP, up to 200 ft/hr, even without FLASH ASJ^{TM} systems,
4- trailer mounted for fast rig up and rig down (mobilization),
5- relatively small footprint compared to rotary rigs,
6- can drill a gauge hole,
7- requires fewer people to operate as there are no pipe joints to add, and
8- are more effective in precise positioning of tools in horizontal and vertical wells.

The biggest disadvantage is in size and weight of the reel of tubing due to road weight and height limits. Other disadvantages are the reduced buckling, burst and collapse strengths of CT limit the sites and depths where they can be used. Coils also only last for 30–50 wells (for 3,000 ft. wells) and are difficult to fish if stuck. Rotation of the bit/ nozzle requires downhole means (motors)

since it is difficult to rotate the full rig. The use of CT for deep hot EGS applications has not been tried and would be challenging. The surface tubing string must be heavy walled, due to weight/tension and temperature.

If the optimal continuous tubing is utilized for FLASH ASJ^{TM} drilling, then methods to deploy such tubing must be investigated. Alternately, and non-optimally, jointed tubulars can be used for the drilling process if used with a downhole check valve to maintain the operating tubing pressure. In all cases the straightness of the pipe, either coiled or jointed, is a concern due to the tight tolerances between the wellbore and pipe sizes. This is more of a problem with coiled tubing if the injector/ straightener is not properly designed or is not performing perfectly.

The Department of Energy, through NETL and Los Alamos National Laboratory, built and tested a Microhole Coiled Tubing Drilling Rig utilizing 1" CT (see Figure 9 below), which Impact obtained during the SBIR Phase II project DE-FG02-07ER-84670 (47).

Figure 9. Los Alamos National Laboratory, Microhole CT Rig Trailers at Impact

Simulation-Optimization Techniques in Geothermal Reservoir Engineering

Numerical models have supported exploration, testing, and management of geothermal reservoirs since the 1980s, and have grown to handle coupled multiphase fluid flow and heat transport in fractured rock.

In this project, the TOUGH suite of simulators (31, 32,14) was used, which originally was developed specifically for geothermal applications, and is routinely used for natural state modeling (2), design and analysis of laboratory experiments and field tests (1, 2, 15, 10) and for the prediction of reservoir behavior under production and injection (for a summary, see reference 23).

The iTOUGH2 code (12) provides inverse modeling and optimization capabilities for the TOUGH suite of non-isothermal multiphase flow simulators. The code was introduced to the geothermal reservoir engineering community in the mid-1990s (7, 8, 9), and has since been applied to various industrial projects and scientific analyses (19, 17, 35), among many other applications in related fields (for an overview, see reference 12). Since iTOUGH2 is capable of minimizing an arbitrary cost function that may depend on operational parameters, it can also be used for the design and optimization of reservoir management strategies (13, 22).

A key feature of geothermal reservoirs and EGS systems is extraction of heat stored in tight rock matrices by circulating fluids through a highly permeable network of natural or induced fractures. Various approaches are available in the TOUGH codes to handle fractured systems, capturing key mechanisms of the fracture-matrix interaction (5, 11). Some methods are based on a statistical description of fracture network characteristics, which have been linked to the probability of intersecting structures such as boreholes, tunnels, or contaminant plumes (36).

In this project, the powerful simulation-optimization capabilities provided by iTOUGH2 was be used as an integration framework for formal sensitivity analyses and design calculations, in which the microhole-array concept is analyzed and optimized for maximum heat recovery, optimum FLASH ASJ^{TM} drilling operation and minimum drilling costs. The goal was to evaluate utilizing one vertical large bore with microhole arrays as both injector and producer OR to improve flow connectivity between multiple vertical large bores.

Prior patented designs by P.H. Moe, et. al. (37) shown in Figure 9 and by Sanyal, et.al. (39) shown in Figure 10, were considered in the simulation designs.

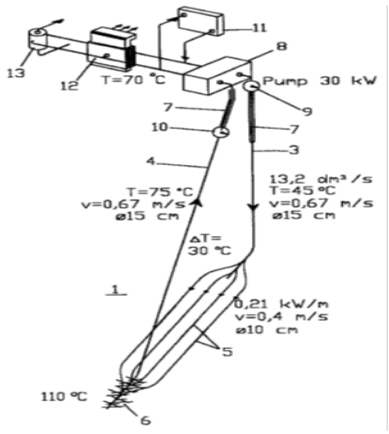

Figure 10. Geothermal System Design, by Per H. Moe (37)

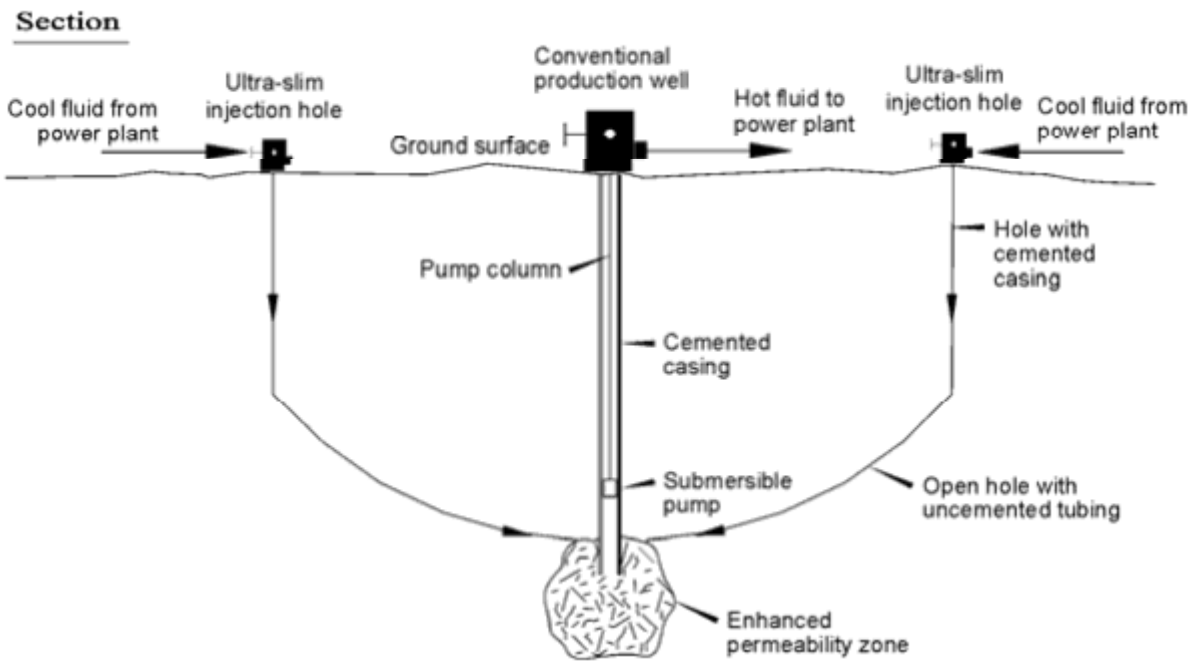

Figure 11. Proposed Energy Extraction System from Sanyal (39)

Discussion of Research

The research performed will be discussed by the original Phase and Tasks/Subtasks outlined for the project.

Phase I Technology and System Feasibility Study

Phase I, Task 1 Evaluation of Microhole ASJ Technology for EGS

Subtask 1.1 Evaluate and Identify FLASH Fluids for EGS Conditions

This effort was led by Dr. Betty Felber with the PI, Ken Oglesby. It researched the potential FLASH fluids and their properties (triple point, critical point, densities, viscosities, heat capacity, etc. -all as a function of pressure and temperature) and then considered their application at high temperature and pressure EGS conditions. There were 3 main components and other additives studied in this subtask-

A) FLASH supercritical fluids;
B) carrier fluid of the solid particles, which can also be the FLASH fluid;
C) additives to the carrier fluid for solids carrying capacity in the system from mixing into and through the nozzle;
D) additives to the carrier fluid for solids (abrasive and formation rock debris) carrying capacity in the system after the nozzle expansion;
E) additives to the carrier fluid to prevent freezing during mixing and through the nozzle (i.e., an antifreeze); and
F) other additives for corrosion protection, friction reduction, surface tension reduction, etc…..

The FLASH fluid components considered included those favorites from prior studies- water/steam/supercritical steam (critical point- 707^{o}F, 3208 psig), nitrogen (N_2), carbon dioxide (CO_2), and methane (CH_4). The properties of alternative gases are given in Table 2. The key properties of nitrogen and carbon dioxide are given in Appendix A. CO_2 cost about $0.97/gallon and it is delivered by truck as a liquid at 10^{o}F and 300psig, requiring pressurized and refrigerated storage, special pumping and handling. CO_2 is more expensive than N_2 to pull out of the air for onsite operations. CO_2 is more expensive than nitrogen for truck delivery due to their cost of separation. However, CO_2 is easier to store, handle and to pump than nitrogen because of each fluid's triple point- N_2 is most always a supercritical gas and not a liquid. N_2 also provides an extra level of health and safety concern due to its required extra cold condition.

In addition, CO_2 has been considered as an alternative to water for the heat transmission fluid for EGS (Brown, 2000; Pruess, 2006, 2008; Pruess and Spycher, 2010; Atrens et al., 2010) and consideration of methane for that function was herein included. See Table 2 below for summaries of some relevant thermo-physical properties of water as well as CO_2 and CH_4 for different pressure and temperature conditions. Initial studies indicated that CO_2 may be superior to water because of the following reasons:

- Larger compressibility and thermal expansivity as compared to water, which increases buoyancy forces and thus reduces power consumption for circulation;
- Lower viscosity, which yields larger flow velocities for a given pressure gradient, compensating for the lower heat capacity of CO2;

- (Dry) CO_2 is much less effective as a solvent for rock minerals, which reduces scaling problems in well and formation;
- Ancillary benefit of geologic carbon sequestration with associated carbon credits.

Density, viscosity, and heat capacity determine the suitability of a fluid regarding (1) wellbore hydraulics (density/viscosity, Figure 4) and (2) as a heat transmission fluid (mass flow rate times heat capacity). Pruess (2006, 2008) concludes that these fluid properties may make CO_2 a suitable working fluid for EGS. Atrens (2010) suggests that CO_2 as a supercritical fluid might experience significant frictional losses in the wellbore, which could be troublesome in trying to produce sufficient volumes of CO_2 needed to extract heat in commercial quantities from the subsurface. As a detriment, CO_2 with any water creates carbonic acid, which at high temperatures and pressures severely corrodes carbon steel and cements.

Methane has not been studied as a working fluid for EGS, but can be used for FLASH ASJ™ drilling. Its (ρ/μ) and Cp values under high T and P conditions appear favorable (much less so, however, for the injection well), moreover, note that the favorable ratio is mainly on account of its low viscosity, an advantage that disappears under turbulent flow conditions in the wellbore). The main (potentially considerable) disadvantage of using CH_4 as a working fluid for EGS is the fact that CH_4 (unlike CO_2) is itself a valuable, expensive energy fluid. Unavoidable fluid losses (which in water-based EGS operations are expected to be on the order of 5%) may render the use of CH_4 unfeasible if the energy generation potential of the lost natural gas outweighs that of the energy gained by the EGS system. Note- The heating value of 1 kg of CH_4 is about 50 MJ (~13 kWh) and if 5 % methane were lost in a EGS system that circulates CH_4 at a rate of 40 kg/s, this methane could produce 100 MWt or 30 MWe, which is significantly more than the 5 MWe that can be produced from the EGS system. Those losses are not expected to be significant in FLASH ASJ™ drilling and thus methane can still be a candidate.

Because of ease of use and potential for use as an EGS working fluid, carbon dioxide (CO_2) will be the primary FLASH fluid used in these tests. However, until CO_2 became available (storage tank and pumping capabilities), water/ steam was used as the initial FLASH fluid.

The carrier fluid mostly discussed was fresh water, although brines and the FLASH fluid itself can provide that service as well. Alcohols, propane and butane were considered as well, but require special handling not desired for these early bench and field tests. Water also has many commercial available additives for improving its performance for FLASH ASJ™ drilling. However, fresh water freezes in cold ambient conditions and when mixed with cold FLASH fluids, has a very low viscosity and low solids holding capacity. Its high heat capacity is not useful for FLASH drilling, but it is for EGS operations. Fresh water is very environmentally friendly. Therefore, fresh water was decided the best carrier fluid choice for FLASH testing at this time.

Antifreeze additives were considered in an internal report “Freezing Point Depression of Xanvis L Solutions”, on 25January2012 by Dr. Felber given in Appendix D. The standards of methanol, ethylene glycol and alcohols were evaluated for environmental, health/ safety

and price. Alcohols were determined the best antifreeze choice, as needed, since they evaporate and pose no other hazards.

	Water	CO_2	CH_4
Molecular weight (g/mol)	18.015	44.01	16.04
Critical temperature (ºC)	373.946	30.95	239.45
Critical pressure (MPa)	22.064	7.38	4.60
Density/viscosity @ 20ºC, 100 bar (kg/(m^3 Pa·s))	1003/1.0e-3 = 1.0e6	856/8.0e-5 = 1.0e7	78/1.4e-5 = 5.7e4
Density/viscosity @ 20ºC, 500 bar (kg/(m^3 Pa·s))	1020/9.9e-4 = 1.0e6	1048/1.4e-4 = 7.4e6	278/3.4e-5 = 8.e6
Density/viscosity @ 200ºC, 100 bar (kg/(m^3 Pa·s))	871/1.4e-4 = 6.4e6	122/2.4e-5 = 5.0e6	41/1.7e-5 = 2.3e6
Density/viscosity @ 200ºC, 500 bar (kg/(m^3 Pa·s))	897/1.5e-4 = 6.2e6	580/5.0e-5 = 1.2e7	171/2.5e-5 = 6.7e6
Heat Capacity (Cp) @ 20ºC, 100 bar (J/g K)	4.15	2.62	3.07
Heat Capacity (Cp) @ 20ºC, 500 bar (J/g K)	4.05	1.75	3.23
Heat Capacity (Cp) @ 200ºC, 100 bar (J/g K)	4.45	1.18	2.98
Heat Capacity (Cp) @ 200ºC, 500 bar (J/g K)	4.28	1.57	3.31

Table 2: Relevant Properties of Alternative EGS Working Fluids, via LBNL, June 2010

Viscosifiers identified for adding solids carrying capacity to the fresh water carrier fluid at both low and high temperatures, prior to (and possibly after) the nozzle, included various polyacrylamides, Xanvis, and SPI gels. Dr. Felber issued the internal report "Xanvis L Viscosity Relationships Vs Temperature for Use in FLASH ASJ™ Drilling Systems" on December 1, 2011 (given in Appendix D) favoring Xanvis L, and it was utilized in this phase of the study. An additional benefit was its use as a friction reducer.

Chemical additives to improve the solids carrying capacity of the carrier and FLASH fluids for the return flow were studied in an internal report- "An Evaluation of Surfactants for Aqueous and Carbon Dioxide Applications" dated 11Jan2010 by Dr. Felber and provided in Appendix D. It identified surfactants additives that were compatible with brines, CO_2 and the pre-nozzle viscosifiers, including Xanvis L and SPI gels. Many also provided friction reduction capabilities. Specifically, Xanthan Gum, Haliburton's Liqui-Dril, Wilcolate's 1247H, and Klean-Foam by Clearwater International for Weatherford International. The report recommended Klean-Foam with isopropanol and glycol ether with our viscosifiers Xanvis L and CO_2. For later foam additives, we reviewed SPE129907 "CO_2 Soluble Surfactants for Improved Mobility Control", by Xing, et al. and SPE129925 "Nanoparticle-Stabilized Supercritical CO_2 Foams for Potential Mobility Control

Applications", by Espinosa, et al. It should be noted that foam additives were not specifically used in the project bench and vertical drill tests conducted in this project.

Subtask 1.2 Evaluate & Identify Pipe Sizing & Configuration

Dr. Dwight Rychel researched coiled tubing and issued a report on October 2010 that is discussed below. Microbores are defined as holes that are less than 10.16 centimeters (cm)/ 4 inches (in) in diameter. Allowing for an equivalent hydraulic return fluid flow area that is 1.5 times the injection flow area (set by internal diameter of the primary drill pipe), this sets the maximum possible pipe sizes (not allowing for collars or external connections) of up to 2" for 4" holes, 1.75" for 3" holes, and 1.25" for 2" holes, if all pipes the same size. Hydraulic studies later will refine the drill pipe size and annular flow area required for a variety of possible drilling scenarios. Table 3 below outlines the typical coiled tubing diameters and strengths.

Nominal OD Inches	Minimum ID Inches	Wall Thickness Inches	Yield 1000#
1.00	0.78	0.11	24
1.25	0.94	0.16	31
1.50	1.15	0.18	40
1.75	1.37	0.19	50

Table 3. Typical Coiled Tubing Properties

There are only three manufacturers of coiled tubing in the world. All have manufacturing facilities in the Houston area. By far the largest (by volume, market share, revenues, product line) is Quality Tubing, a subsidiary of the very large National Oilwell Varco Corporation. They produce 4 types of standard steel coiled tubing, a special chromium line and a line for permanent hang-off installations, plus a number of services including welding, spooling, cleaning and corrosion repair and prevention. Sizes range from ¾ inch to 3 ½ inch OD with varying wall thicknesses.
http://www.nov.com/Tubular_and_Corrosion_Control/Coiled_Tubing_Products_and_Service/Coiled_Tubing_Products.aspx

The second largest and long-time supplier is the former Precision Tubing, now marketed under the Tenaris brand. Tenaris is a Venezuelan owned company with worldwide manufacturing facilities. They manufacture over 6 million tons of steel pipe in 15 countries, with sales of $12 billion. In 2006 they acquired Maverick Tube Company, the then parent of Precision Tubing. Their CT product offering has four lines, including HS-110, a 110,000 psi yield strength coil. They produce products for onshore and offshore, with sizes ranging from 1 inch to 5 inches and were the first to offer integrated coating capabilities. They claimed to have produced the heaviest continuously-milled coiled tubing workstring at 115,000 pounds and the longest at 32,900 feet.
http://www.tenaris.com/en/Products/OCTG/CoiledTubing.aspx

The third, and by far the smallest and newest is Global Tubing. They were organized in 2007, built a state-of-the-art plant in Dayton Texas in 2008 and went into production in early 2009. Their management came from former Quality and Precision executives. They offer three lines of CT products, with three more in the works, including their planned GT-120, a 120,000 psi yield strength coil. They offer sizes ranging from ¾ inches to 5 inch OD and varying wall thicknesses. **http://www.global-tubing.com/products/products.htm.**

All three publish complete technical data on all of their products at the websites given above. Data includes:

- Complete chemical composition
- Minimum Yield Strength, psi
- Minimum Tensile Strength, psi
- Maximum Hardness, Rockwell
- Measurements: ID, OD, thickness
- Plain End Mass, lb/ft
- Pipe Metal Cross Section Area, sq. in.
- Pipe Body Yield Load, lb
- Tensile Load, lb
- Internal Yield Pressure, psi
- Hydro Test Pressure, psi
- Torsional Yield Strength, lb/ft

For a given yield strength and diameter and thickness, the difference in specifications between the three manufacturers are minimal. Decisions as to which manufacturer to select would depend more on product availability, customer service, warrantees and credit worthiness. For that reason, it is recommended staying with Quality Tubing, the predominant supplier. In screening different size and types of tubing for your application, ICOTA has a very quick application online to make CT Performance Calculations- **http://www.icota.com/calcs.asp**

Inputs to that program are: Yield Strength, Outer Diameter, Nominal Wall Thickness, and Length. Calculated Outputs are: Minimal Wall Thickness, Yield Load, Yield Pressure, Yield Torque, Collapse Pressure, Weight of Empty CT, Internal Volume, Volume Displacement, and Elastic Stretch Coefficient.
In addition, CTES LP in Conroe Texas published online their **Coiled Tubing Manual**, Rev 72005-A that has everything from history of coiled tubing development, making of CT, downhole tools, surface tools, inspection tools, etc.

Subtask 1.3 Evaluate Heat Transfer & Hydraulics

Multiphase System Integration (MSI)'s Mehmet Karaaslan and the PI evaluated Halliburton's Wellcat and WellPlan programs and SPT Group's Wellflo program for modelling FLASH ASJ™ drilling at a variety of depths. The Wellflo program was selected since it had a better heat transfer functions to the earth. Over 500 runs were made, but not all were recorded or reported since boundaries of each configuration had to be established. In these studies supercritical steam (where possible, generated at surface or generated by the earth's heat gradient), nitrogen and carbon dioxide were studied. These studies can be utilized both for vertical drilling or for the injection/ return flow in EGS lateral drilling.

Surface to 500 ft, 2000 ft, 5000 ft, 10000ft, 20000 ft, 30000ft drilling cases were run. One deviated well run with water (some nitrogen) in production operation and another with water under injection were run at 20,500 ft. Various CT sizes (0.75, 1, 1.25, 1.5 inch nominal sizes/ ODs) were matched to various hole sizes (up to 10.16 cm/ 4"). Various

water influxes, lowest possible BHP, % hydrates formed were also studied. Operating envelopes developed for each gas at each depth with erosion limit shown were developed. Pressure and temperature plots by depth were also prepared. Selected WellFlo runs are given in Appendix B and the full set of WellFlo study reports are uploaded into the GDR. In all cases the pressure loss across the nozzle was set and the minimum BHP possible was targeted for optimal FLASH ASJ™ performance.

Overall findings were that nitrogen and steam only are possible in deepest cases. Surface generated steam is possible only in the shallowest (limited by heat losses to surrounding rocks) and earth generated heat by surrounding rocks was possible in the deepest runs. CO_2 was found not effective at greater depths than about 10,000 feet.

Solids transport ratios for various cutting particle sizes and casing sizes were studied, but were not relied upon in this study due to various uncertainties.

Hydrate formation or ice was a problem in many shallower cases with minimal water and high Joules-Thompson effect from gas expansion out of the nozzle. Minor amounts of water seemed to mitigate those ice problems.

It is a tough balancing act to keep between the operating envelope of the minimum annular flow rate for proper cuttings transport and the maximum flow rate possible to reduce erosion in these small annular spaces. Erosional concerns due to the return flow velocity are significant. As a note- the erosion limit utilized in this study was at 6-8 gpm for nitrogen in the deeper run and small annular flow cases. This equates to about 1 meter per second velocity of the particles. The effects of larger surface / intermediate casing size and set depth, annular back pressure (i.e. from a surface choke before or after the GLS separator) and water influx were also studied and were significant in reducing annular velocity.

Estimated losses in the 500 feet of coiled tubing on the surface coil unit were 25-50% of the total pressure losses in some cases- this significant loss must be studied more.

Overall, the simulation runs indicate that microhole drilling can occur with the basic FLASH ASJ™ requirements to great depths. However, the mechanics to implement this and the amount of formation liquid influx that would occur due to the high level of underbalance required for optimal FLASH ASJ™ drilling makes this a difficult case. While SPI gels or other PAM system can be pumped to reduce influx once it has occurred and becomes a problem, the time and cost for these remediation efforts reduced the benefits of the faster rock removal FLASH ASJ™ drilling system for vertical EGS.

These WellFlo simulation runs will be used to calibrate the operational program developed for Phase II, Task1, Subtasks 1.1 and 1.4.

Phase I, Task 2 Demonstration of Increased Performance Using Microholes (with simulation)

Subtask 2.1 Define Drilling & Production Scenarios (for Simulation)

To start the simulation effort, we first reviewed the very limited number of installed "conventional" EGS systems (see Table 4) and the P. H. Moe, et. al. (37) and Sanyal, et. al. (39) patented proposed systems, shown previously in the Background Section. Then we developed other possible scenarios for EGS reservoir development and improved heat exchange using microbores, leading to more complex multiple microbores, forming an array, intersecting a large fracture target.

Field	Number of wells	Well depths (km)	Bottom hole distance (m) between wells	Fracture network	References
Habanero	3	4.2-4.4	500-550 m	Subhorizontal fractures, stimulation	Rothert and Baisch, 2010; Chen and Wyborn, 2009
Soultz	5 (3 deep)	5	450-650 m	Multiple stimulations, steeply dipping fractures	Schindler et al., 2010; Genter et al., 2010
Landau	2	3.3	~1200 m	Preexisting fault system, stimulation	Schindler et al., 2010
Groß Schönebeck	2	4.3	475 m	Multiple stimulations, proppant	Moeck et al., 2010; Zimmermann et al., 2010

Table 4. Installed EGS Systems' Information- Well depths, distances between injection and production wells, and stimulated fracture networks for EGS systems

The existing EGS systems' well depth ranges from 3 to 5 km (10,000–15,000 ft); well depths of up to 10 km (30,000 ft) were discussed. There are duplex, triplex and five-spot configurations, see the references listed in Table 3. The distance between injection and production wells ranges from 400 to 1,200 m (1,200–3,600 ft). All installed EGS projects involve stimulation of existing or new fracture systems.

These three final scenarios were modelled:
Scenario 1- Single well heat exchanger with full circulation loop through multiple concentric pipe heat exchangers. **Models 1 and 2** were based on this scenario where a single concentric pipe within a drilled microbore creates a simple heat exchanger in the EGS rock- one of many such exchangers off a single main vertical bore at EGS depths. See Figure 71 in Phase II, Task 2. Each microbore exchange can be kilometers long, in fact, Model 2 length was set at 1500 m. Concentric single pipe extending from within the vertical bore to the end of a microbore. Injected flow goes inside the pipe to the end and return flow occurs in the annular space (between the pipe and drilled rock wall) back to the main vertical well bore to be combined with the other exchanger return flows. Heat would

be mined from the reservoir rock in the return flow of the microbore with some preheating of the injected in-pipe flow via a counter- current heat exchange across the pipe. Problems seen here are the mechanical sealing of multiple microbore pipes within the main vertical wellbore and isolating them from the combined return flow. Also, successfully inserting that many small pipes into the predrilled microholes without bending would be problematic at these great depths. Another possibility is leaving the drill pipe in each drilled hole when depth is reached, but then sealing those multiple pipes then becomes an even bigger problem as is preventing solids fill in other microbores as consecutive microbores are drilled. This option was modelled, but would be very difficult to mechanically implement in the field.

Scenario 2- Models 3 and 4 were based on this scenario, which is based on the concepts shown in Figures 12, 13 and 14 below. In this scenario, 40 microholes emanate from a higher main, large bore production well at spaced depth intervals and at different orientations to prevent interference between microbores. These microbores all extend out to intersect a natural or hydraulically created fracture at different positions and depths. The fracture is hydraulically connected to an injection well which completes the flow circuit to the surface. That scenario can also be reversed from that description.

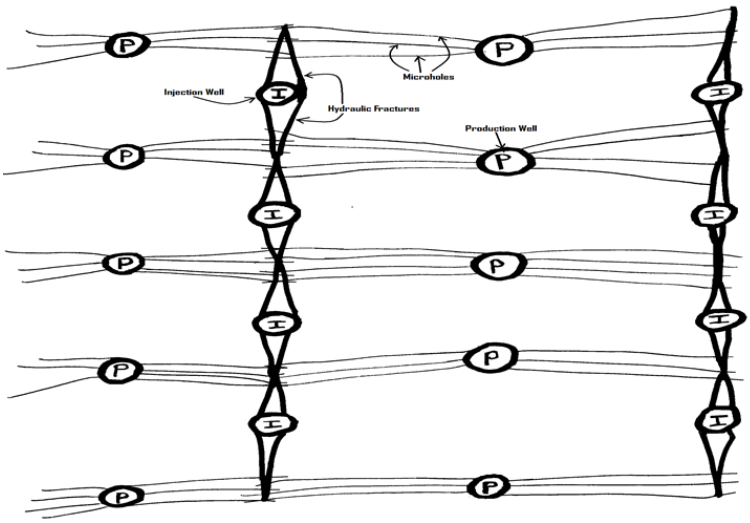

Figure 12. Idealized Microhole Array Plan View. The multiple microbores (lighter lines) emanate from the producers “P” to intersect the large hydraulic fractures (heavier lines) that emanate from the injectors “I”.

Scenario 3- This was based on the Soultz EGS field described earlier from the literature and shown in Figure 15. Model 5 was a complex and sophisticated Soultz-based 3D model using Dual Permeability to model a microbore array of 40 bores.

Subtask 2.2 Develop Geothermal Reservoir Models

This subtask was moved to and combined with Phase II, subtask 2.2 activities because significant changes were needed in the programming to develop the required models.

Subtask 2.3 Compare Fluid Flow & Heat Transfer Scenarios

This subtask was moved to Phase II, Task 2.3. The delay was required to allow all programming to be completed and the models developed.

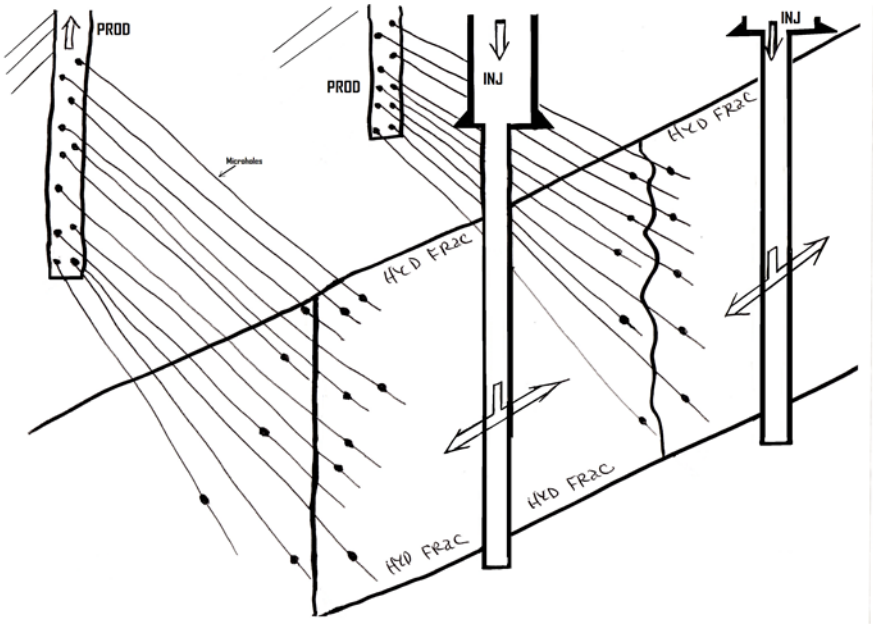

Figure 13. Proposed EGS Microhole Array System

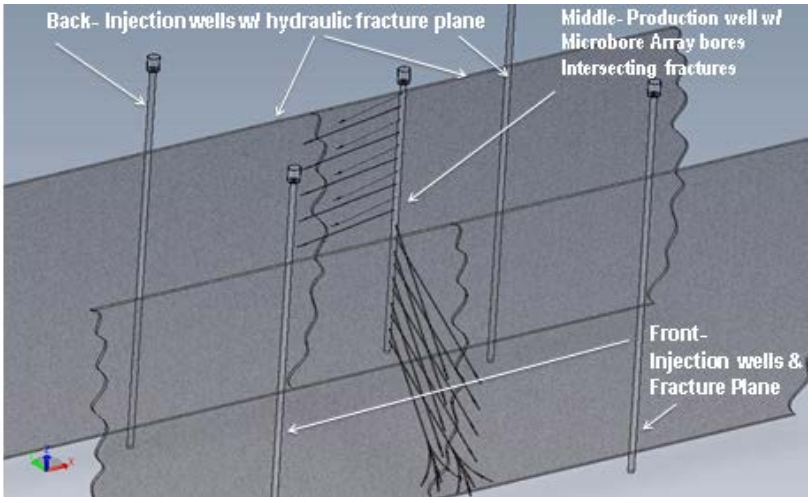

Figure 14. Microbore Array Concept via SolidWorks 3D drawings.

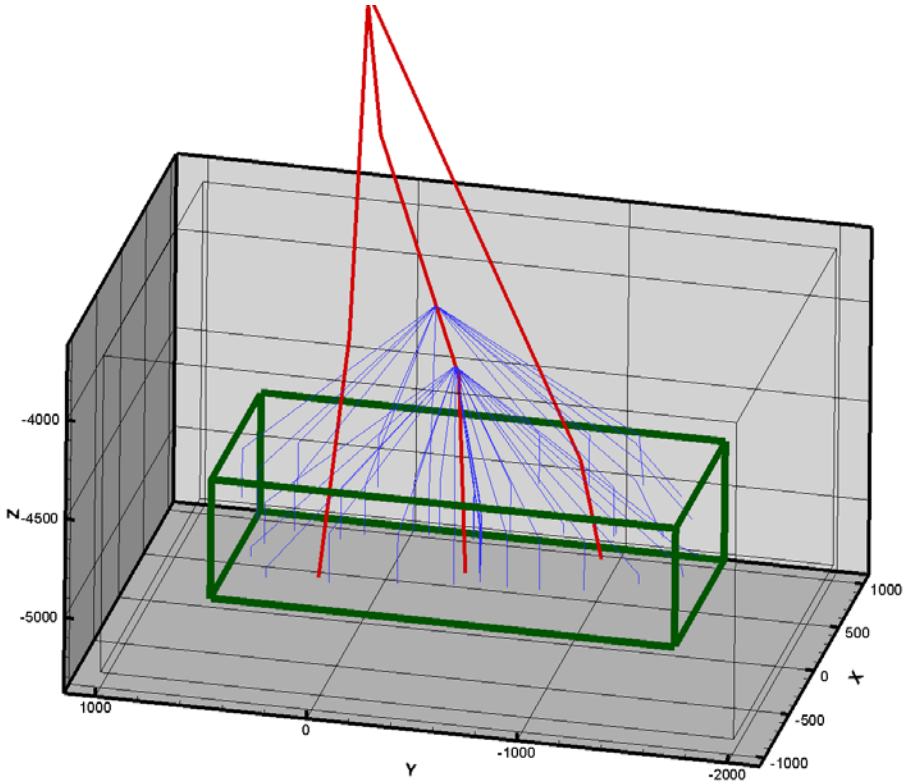

Figure 15. Soultz EGS Field Based Model- Relative locations of conventional wellbores (red lines) and 40 microholes (blue lines) to the fracture zone (outlined by green box).

Phase II Microhole Technology Development for EGS

Phase II, Task 1 Development of Microhole Drilling Technology for EGS

Subtask 1.1 Research & Testing of the Pipe-

The original contractor for this subtask section became busy on other projects and this effort was redirected to computer simulation of bending instead of actual bending tests. Therefore Schlumberger/CTES was hired to perform these simulations and prepare a program to estimate pipe bending for (vertical) directional estimation. This report, manual and program have been uploaded into the GDR.

The basic directional drilling concept for FLASH ASJ™ microhole directional drilling is to use the simple directional drilling concepts developed and utilized in the 1950's into the 1970s. With FLASH drilling no reactive torque on the rock occurs to change the X-Y direction, thus only movement in the vertical Z direction is expected. Thus, in this concept the directional bore is kicked off in a main vertical bore at a known initial depth, orientation (x,y) and angle to vertical. Based on hole diameter, pipe OD, pipe wall thickness and strength, fluid in the pipe, bit and stabilizer ODs and positions on the drill string, the bit direction is estimated as the pipe movement progresses with drilling. If desired, a bent sub can be used to offset the normal expected vertical drop, to increase or decrease vertical section loss. Such a method is not good for hitting a dime sized target miles away, but it is sufficient to hit a large target, such as a large vertical fracture system or wall at anticipated EGS lengths. It is also significantly less expensive than using the advanced real-time monitoring and control directional tools used today, especially for

multiple bores. Those current tools will also not fit into microhole sizes and are not needed for the 500 to 1500 meter (1640 – 4900 feet) microhole laterals for EGS. Note- if vertical laterals are desired, then the length is not important.

The program concept is that the pipe is supported at the intersection of X and Y where it touches the bottom of the previous hole- See Figures 15 and 16. The hole is drilled ahead of, in the direction of the angle of the then current end tip. The cut hole is larger than the pipe at some diameter and at some set distance ahead of the bit/nozzle/pipe. Thus, the pipe and bit/nozzle is free standing until when the weight of the pipe plus internal fluids times the oriented angle provides the true downward force along the pipe's length and a known bending moment. This allows the pipe to remain in the hole not supported by the hole until its combined cantilevered weight overcomes its strength and the pipe again touches and is supported by the drilled hole. This is the new support point for the pipe to again drill ahead.

In Figure 17, a screen shot shows the input values in yellow boxes at the upper left top. The calculated output is shown below the input section and in the plots to the right. For the example shown in Figure 17 the 1.25" drill pipe with known values, de-rated to the 260^{o}C/ 500^{o}F temperature, drops about 0.67 m (2 feet) in 10 m (32 feet) when started at 60^{o} initial angle. At lower initial angles from vertical (i.e. more horizontal), the pipe hits the hole bottom faster and the pipe can drop even faster, unless a bent sub or a larger OD bit/nozzle is utilized to raise the cut hole angle.

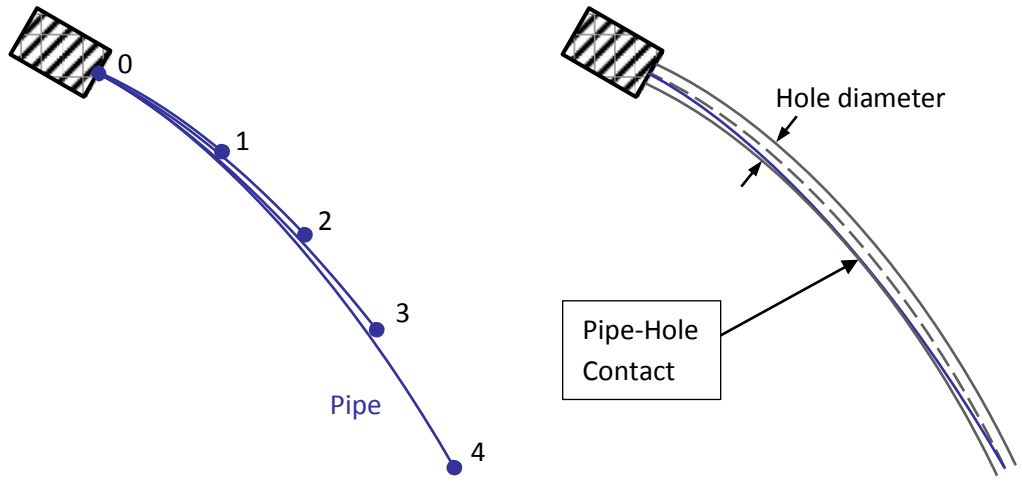

Figure 16. Vertical Drop Estimation for CTES Program

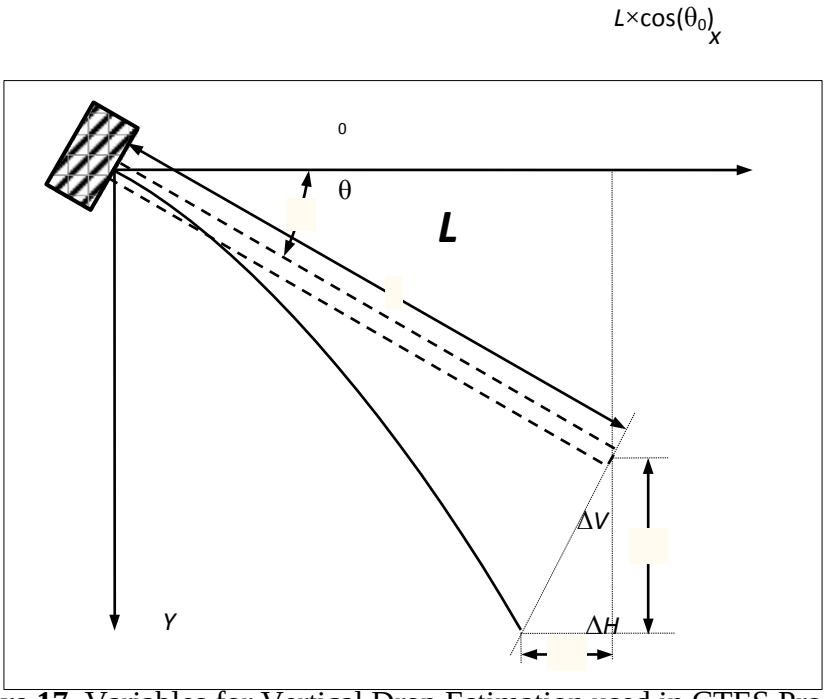

Figure 17. Variables for Vertical Drop Estimation used in CTES Program

Subtask 1.2 Research & Testing of the FLASH Fluids

In this subtask additional research into the various FLASH fluids needed was performed. Specifically, methods to generate onsite desired FLASH supercritical gases were studied. Otherwise purchasing liquid CO_2 or N_2 for delivery were the backup options. It should be noted that pumping CO_2 is much easier than N_2 due to the low temperatures requirements of the pumps and safety concerns. Chemical and membrane methods studied for onsite generation were:

1) a liquid pyrogallol chemical system for oxygen removal that would allow direct use of air (mostly nitrogen);

2) exhaust gas via "An Evaluation Of Exhaust Gas As Possible Carbon Dioxide Replacement For FLASH ASJ™ Systems", report by Dr. Felber, revised 29 March 2012 and given in Appendix C;

3) Onsite chemical CO_2 generation with a Sulfuric Acid and Calcium Carbonate reaction.

4) PCI Technologies' Nitrogen membrane system-Nitrogen Generating Units (NGU) were already commercial and the most cost effective;

5) Portable high pressure N_2 or CO_2 generator proposal from Paul Dunn of Enhanced Energy Group LLC, W. Kingston RI. N_2 is cheaper to generate from air at $500K for 1 ton per day rate at the required pressure;

6) Hughes, W.J. and Dunbar, M. "Nitrogen from Air", USPTO 20050186130 and 20090060801, to US patent 7981379 and #7468173;

7) Prisim Membranes for N_2 onsite generation/ extraction from flue gas, diesel, methane or propane, per report by Dr. Felber.

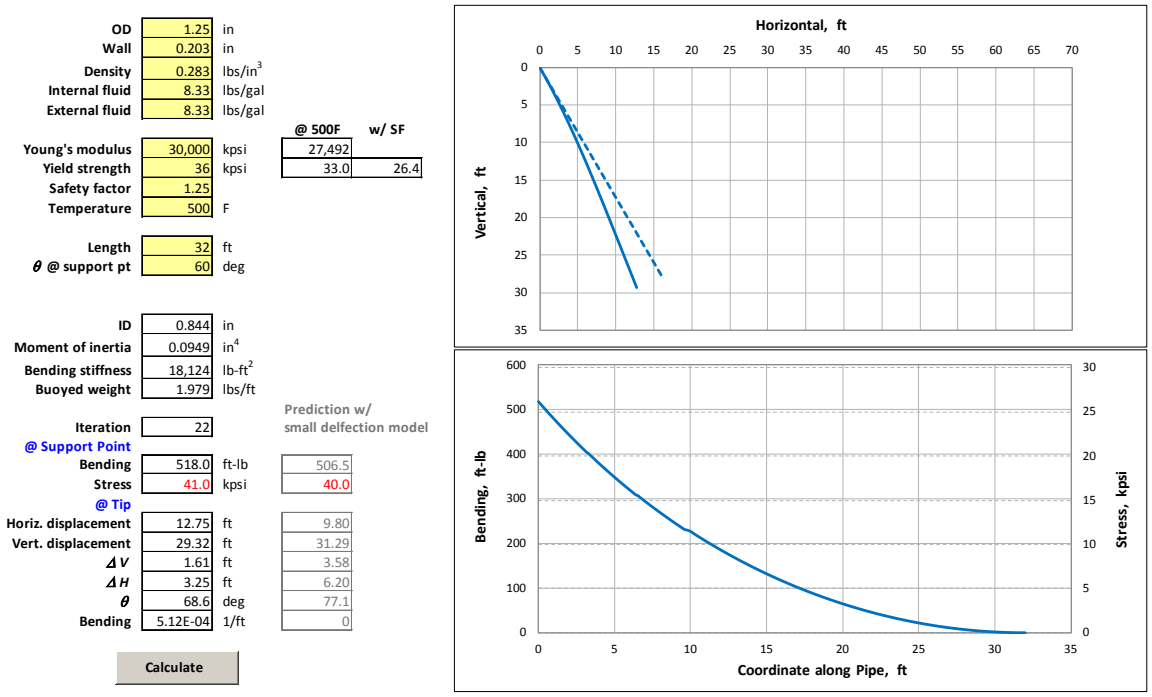

Figure 18. Screen Shot of CTES Directional Program

Overall, the most favorable and cost effective method to obtain the FLASH supercritical gas for onsite field operations is the membrane nitrogen system from the air. More specifically, the PCI nitrogen membrane process appeared the best since it is commercially available now. However, for testing in this study purchased CO_2 will be used due to lower capital investments and easier pumping.

For the other possible chemicals needed in FLASH ASJ™ drilling, we looked at- "pH Sensitive Polymers for Improving Reservoir Sweep and Conformance", 2006, Mukul Sharma, Steve Bryant, Chun Huh, DOE project DE-FC26-04NT15520 and also "High Temperature Chemicals for Drilling Fluids", report by Dr. Felber in February 2012 and given in Appendix C and uploaded into the GDR.

Subtask 1.3 Research the FLASH ASJ Characteristics of 300°C Rocks

This subtask had many various aspects to it and was a central feature of the project. The final proof of the FLASH ASJ™ drilling process was not fully demonstrated in the project, but efforts are continuing to demonstrate and commercialize it in in different formats and in surface and shallower applications.

This subtask effort concentrated on the following efforts:
A) Slurry Pumps- a new Slurry pump was designed, built and demonstrated/ proved for FLASH ASJ™ drilling. Specifics on the slurry pump designs fall under a prior project patent(s) by Impact, with many proprietary aspects, that will not be discussed in this report. A new induction slurry pump was studied via erosion bench tests and simulations at TU;

B) FLASH ASJ™ Nozzles- several new FLASH nozzles were designed off the prior patents, then built and tested. Several nozzle holders and tools were also designed, built and tested with various materials. Nozzle and nozzle holder designs are considered confidential, proprietary and privileged information to Impact, as they fall under a prior project patent. Therefore, their specifics will not be covered in this report;
C) FLASH ASJ™ Pumping Facility- The fluids, materials, procedures/ processes and equipment utilized for the bench cutting / drilling and the rig drilling test were developed in this project and will be discussed;
D) FLASH ASJ™ Bench Tests- cutting efficiency via bench cutting / slicing of various rocks with different nozzles, different FLASH fluids, various pressures, temperatures, gas/slurry ratios and slurry concentrations was demonstrated. Results of those tests are given below in plot format and as an Excel Spreadsheet uploaded into the GDR. Granite blocks at 500°F then cooled to ambient temperature were tested and compared, showing no difference in cutting capabilities; and
D) FLASH ASJ Drilling Tests- FLASH ASJ™ drilling capabilities were demonstrated on the test bench with the target mover, with the coiled tubing rig and with a forklift based jointed tubing rig.

Under effort A, various Impact pumps and their variations were considered. All slurry pumps but HPSP5 requires a pressurized suction to load the slurry. The various pumps are:

HPSP1 is a 1:1 hydraulically driven 15 gpm, 15,000 psi capable pump developed prior to the project that does not have a smooth transition between cylinders. For FLASH ASJ operation, it can be driven with a small 25 hp hydraulic unit. However, it cannot handle CO_2 directly due to its carbon steel materials. It cannot handle gases without modifications, due to its lack of venting capabilities of the cylinders. This could have been easily modified, but since CO_2 was chosen for the testing, it was ruled out. However, it was used in some early steam FLASH ASJ™ testing.
HPSP2 is a hydraulically driven triplex pump with small plungers, see Figure 7. As determined in the prior SBIR Phase II project, it operates at too high a rpm for heavy particles to move into and out of the cylinders. This may be rectified by use of higher viscosity carrier fluids and/or larger plungers that still fit the pump power section and allows it to operate at a slower speed/rpm. Because of the required modifications, it was not used in this project.
HPSP3 is a variable frequency controlled electric motor driven piston pump that is rated at too low a pressure for the FLASH ASJ operation and thus not suited for this application.
HPSP4 is a non-piston pump with clean fluid valves that was built and tested in this project. It is pictured below in Figure 21. Designed December 2010 and built in early 2011, ***this pump did the bulk of the steam and CO_2 slurry testing work starting in early 2011***. If built with other high alloy steel materials, it could utilize CO_2 directly in its operation. It can also be driven with a small 25 Hp, 5 gpm, 5000 psi water pumps, seen in Figure 25.
HPSP5 is potential induction pump under consideration that came from a concept from MS&T. TU performed bench tests and simulations to find the optimal design. API designs were obtained to purchase components that are commercially available from dealers. This pump may utilize CO_2 directly in its operation and can take slurry from ambient to 5000+ per the multi-stage designs. It can also be driven with a small 25 Hp, 5 gpm, 5000 psi water pumps, see Figure 25.

Under effort B) various nozzles, nozzle holders and tools for various uses that are specific to FLASH ASJ operation were designed, made and tested. See Figure 29 top right for a picture of some of the tools developed. They were then used in efforts C and D. Another nozzle design from The University of Tulsa's simulation efforts will be discussed later in this section. Nozzle holders were also designed and built in various configurations for testing. The following nozzles and holders were tested-

1. Three nozzle holders with a 1" outer diameter that holds one newly designed tapered FLASH nozzles. Length with attached tools is 18" to allow a straight section to connect to the pipe, either jointed or coiled or the bench test lance. Heat treated and tungsten carbide outer coated;
2. One 1.5" outer diameter nozzle holder with outer flow channels that holds 3 newly designed tapered FLASH nozzles at specified orientation patterns or nozzle configurations. Heat treated and tungsten carbide coated on the outside;
3. One 3" OD nozzle holder that can hold 4 newly designed tapered FLASH nozzles at specified orientation patterns or nozzle configurations. It was also tungsten carbide coated on the outside. It was designed for creating large holes;
4. Prior-project single nozzle holders of various diameters for bench testing on a lance. Shoulder type nozzles were the proper fit;
5. A slurry swivel for high pressure slurry operation was designed and built, but internal friction prevented free movement, requiring a motor for operation.
6. Four new FLASH tapered nozzles were designed, manufactured (7 of each design) in a Tulsa machine shop made with 4140 carbon steel. They were then coated with Bodycote K-Tech, Inc. ceramic coatings. These coated nozzles did not last over 1 minute of FLASH ASJ^{TM} bench testing in the fall of 2011. In February 2012 ordered new nozzles in one set design made fully with a stronger, proprietary material. With this new material, over 100 hours of nozzle operational life is now expected without significant deterioration of performance. No nozzle of the proprietary materials was significantly worn out in this testing.

Under effort C) the pumping facility to store, mix and pump the FLUIDS and MATERIALS, PROCEDURES and EQUIPMENT were developed and are described below:

FLUIDS

Following the efforts in Phase I, the selected FLASH fluids were obtained and utilized in these tests.

FLASH Fluid- steam and carbon dioxide were used. The steam was generated in diesel heat exchangers and used for early testing. The steam was saturated steam and hot water mixture at upstream nozzle conditions and not supercritical. The CO_2 was purchased as a delivered liquid from AirGas, a national gas company. The delivered CO_2 price was $1807 for 15,000 lbs at about 300psi, 10^oF= $0.1205/lb= $0.964/gallon (at 8ppg density). The tank and other equipment for this storage capability are discussed below. Heating of the very cold (10^oF) CO_2 was important to prevent immediate ice formation when mixed with fresh water and especially after the nozzle. Heating was also needed for improving the cutting efficiency by controlling the density of mixture before, through and after the nozzle.

Carrier Fluid- fresh water. Fresh water has freezing and solids carrying problems.
Carrier Viscosifier- Xanvis L was added to improve solids carrying capacity of the fresh water.
Antifreeze or Freezing Point Depression- none used in these tests.

MATERIALS

Abrasive Material - The abrasive used in all testing was a natural garnet from Barton Mines listed as Super 80HPA and 8HPX. It was an 80 mesh with an average 150 micron size or 0.00591 inches. Average price of the abrasive was $0.28/lb (year 2011). We did recycle some garnet for nozzle design tests, but a minor amount. See Table 5 below for a mesh and micron size converter.

Target Material- Yes, we used a lot of granite grave headstones for the testing, not robbed from grave sites, just obtained from the monument companies where etching errors were made and the stones junked. Names were destroyed so that no family concerns would occur. Granite colors were pink, light and dark grey as well as light and dark brown. No mineralogy tests or strength tests were performed on any rock. The light reddish brown sandstone blocks tested were from the nearby shop area in northeastern Oklahoma.

D100 Separation and API Screen Number

D100 Separation (Microns)	API Screen Number
>780,0 to 925,0	API 20
>655,0 to 780,0	API 25
>550,0 to 655,0	API 30
>462,5 to 550,0	API 35
>390,0 to 462,5	API 40
>327,5 to 390,0	API 45
>275,0 to 327,5	API 50
>231,0 to 275,0	API 60
>196,0 to 231,0	API 70
>165,0 to 196,0	API 80
>137,5 to 165,0	API 100
>116,5 to 137,5	API 120
>98,0 to 116,5	API 140
>82,5 to 98,0	API 170
>69,0 to 82,5	API 200
>58,0 to 69,0	API 230
>49,0 to 58,0	API 270
>41,5 to 49,0	API 325
>35,0 to 41,5	API 400
>28,5 to 35,0	API 450
>22,5 to 28,5	API 500
>18,5 to 22,5	API 635

Table 5. API Screen to Micron Size Conversion

Figure 19. Grey Granite Tombstone slab as a Target

PROCESS AND PROCEDURES

FLASH Slurry Generation - The concentrated slurry was batch mixed into the carrier fluid with viscosifiers to the required specifications, between 17 and 70 wt/wt% of solids. It was mixed in a low pressure vessel and was then transferred into the slurry pump with 15-20 psi pressure on the suction stroke of the HPSP31 or HPSP# 4 slurry pump. This is not a 24/7 type operation and must be automated for higher rates and commercialization.

FLASH Test System Layout – Whether bench or rig based tests, the system schematic is given below in Figure 20. A rural fresh water source was used to mix the slurry at the desired concentrated level. That water was also used as the drive fluid to the slurry drive pump, a Cummins diesel driven, FMC water triplex pump, that then drove the operation of the HPSP4. The concentrated slurry was transferred with 15-20 psi air pressure or a diaphragm pump into the HPSP4 cylinder on its suction stroke. The drive pump displaced the slurry out of the cylinder at pressure and rate desired. Sequenced clean fluid valve processes were used to clean the valves for opening and closing in the HPSP4 operation. The discharged concentrated slurry went from the HPSP4 discharge to the dilution/ mixing point where the FLASH fluid was added.

The FLASH fluid was steam or CO_2. If steam was used, the slurry at the desired concentration was pumped as a single pass process through a two diesel burner heaters with 5000 psi rated pressurized exchanger tubes positioned in series and controlled for final temperature. No other dilution occurred as that heated mixture went directly to the nozzle.

If CO_2 was used, the cold CO_2 was used to cool down the triplex pump fluid end at the 300 psi tank pressure, then pumped back to the tank until the lines were cold. The CO_2 line heater was started to be ready for pumping and heating CO_2 to the mixing/ dilution point. It was required that a water only rate be established at set rates to measure nozzle wear (record pressure and rate, before and after each test), then the water rate was adjusted to near the desired test rate. CO_2 was then started down the line heater. Small step changes in rate were made until the required rates were established. Slurry was started and the test started.

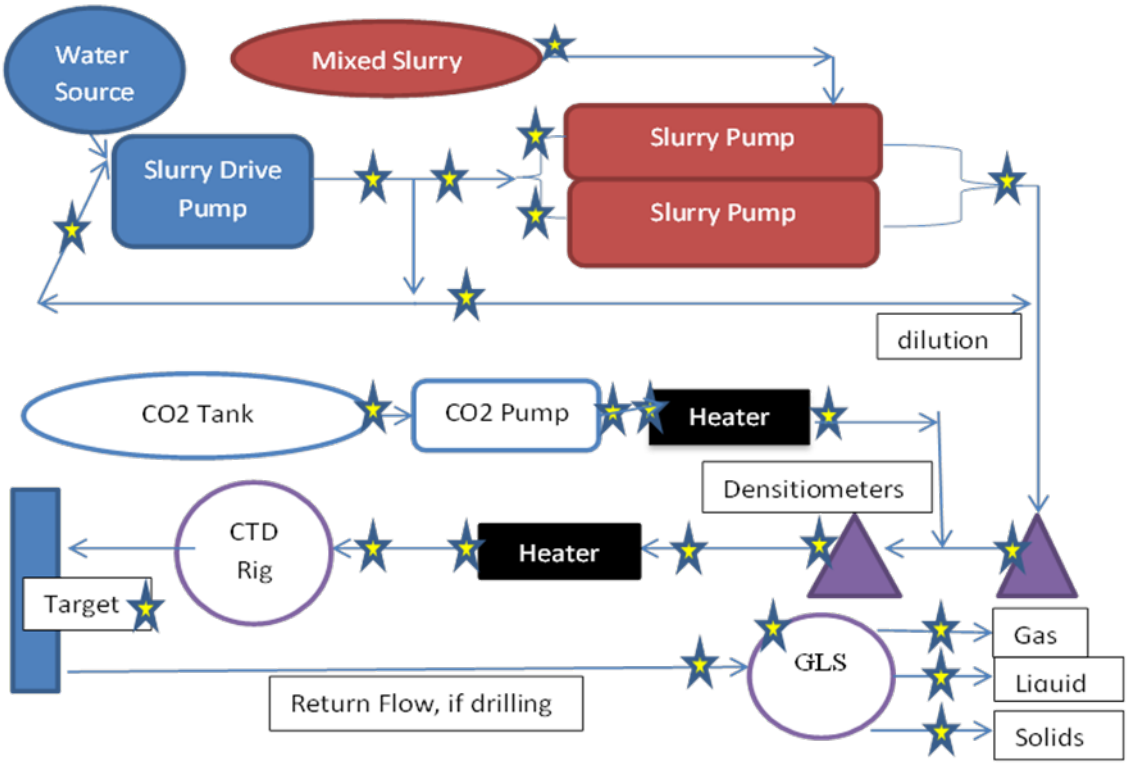

Figure 20. Schematic of FLASH ASJ™ Test Facility at Impact Shop

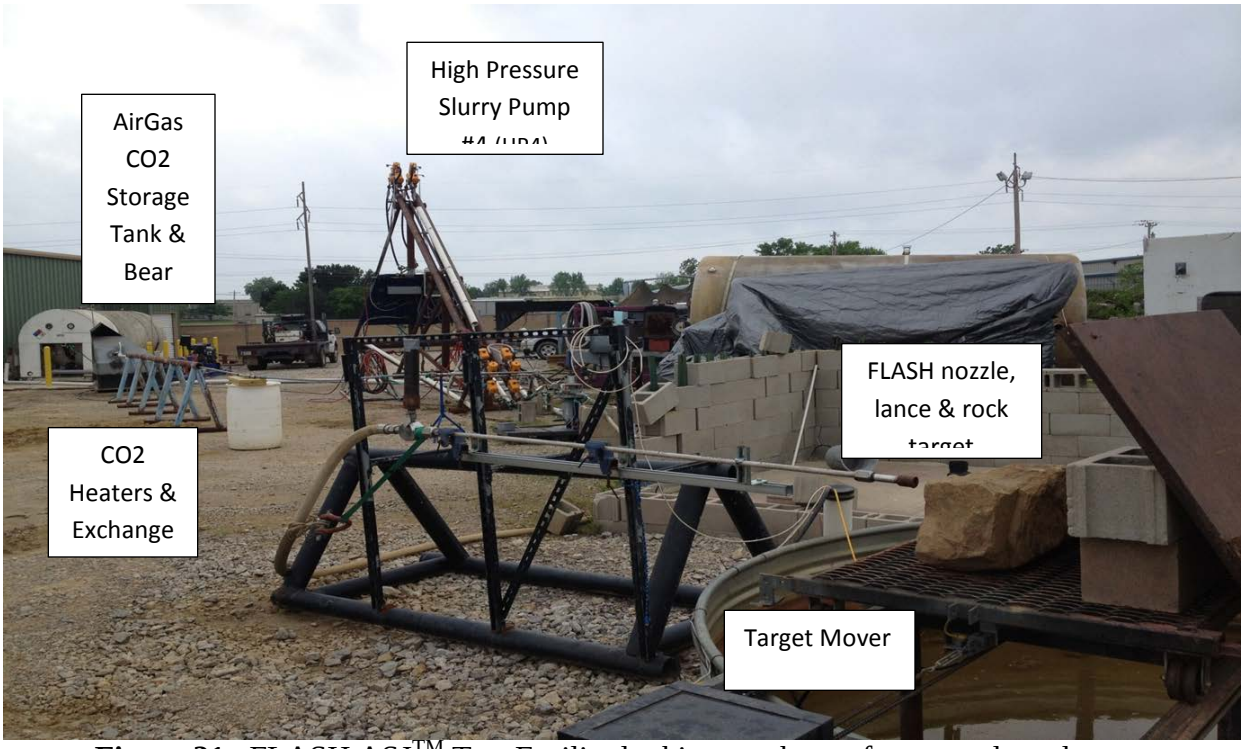

Figure 21. FLASH ASJ™ Test Facility looking south east from nozzle and target.

The final diluted slurry going to the nozzle, was in the range of 10% to 45 % by weight, came from mixing the concentrated slurry from the pump's pressurized discharge with the pumped and heated FLASH fluid (i.e., at the end of the CO_2 heat exchanger). The target mover was started when the densitometers indicated higher concentrations at that mid-point after the final dilution/mixing point. The test was over when the desired volume of slurry was fully utilized and no solids were indicated on the densitometers. *Note- it was not desired to cut through the rock target as this was unsafe and ruined the efficiency calculations as part of the slurry stream was not used to actually cut rock on each subsequent pass.* At that time, CO_2 was stopped and water only was pumped at the desired post rates to measure nozzle wear (record pressure and rate).

Post Test actions- The times and volumes/weights of slurry, supercritical fluids, water, solids, as well as nozzle pressures and temperatures, were calculated for the test. The width and depth of the rock cut was measured to determine volume of rock removed. Efficiency terms were calculated and plotted. Limitations to the mixing and pumping methods selected were reached in this testing.

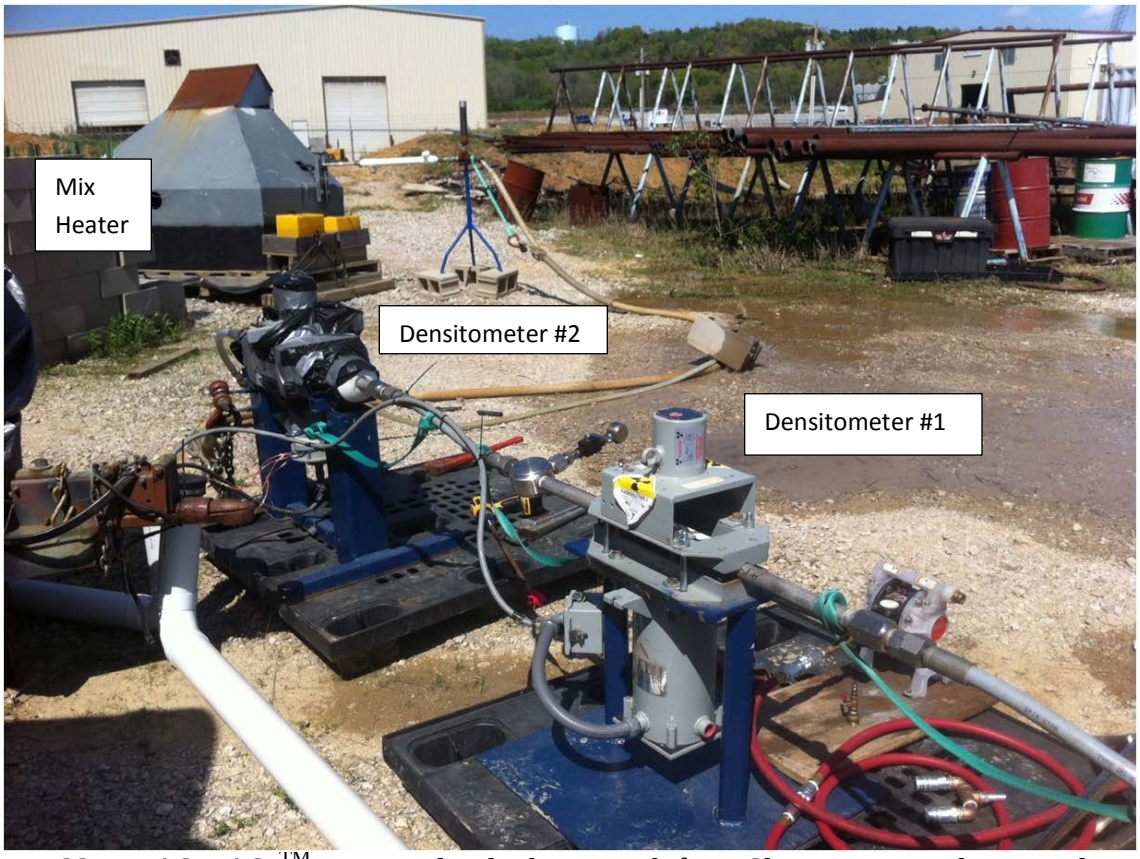

Figure 22. FLASH ASJ™ Test Facility looking North from Slurry Pump outlet toward nozzle

Nozzle Design Testing- various commercially available nozzles were tested in the original round with steam then later with CO_2. The goal was the widest cuts and conditions to obtain the optimal cut width. From those tests, the designed nozzles were built and then tested by water/

CO_2 spray patterns, Figure 24 for the widest cut at 1" standoff from the nozzle tip and the angle of spray growth (ratio of 1" to 6" standoff diameters). Standard rate/ pressure/ gas: slurry ratio tests were run to compare nozzle designs to obtain the optimal design for building with the expensive proprietary material. This nozzle was used as the basis in most other tests.

Optimized FLASH ASJ™ Bench Cutting and Drilling Tests- various CO_2 and slurry flow rates, final diluted abrasive concentrations, pressures and temperatures were tested on a variety of rocks to determine the optimal FLASH ASJ conditions for maximum rock removal and diameter. In most cases a cut process was used as the standard for comparison. This optimum was a product of the equipment, setup and fluids that were selected/ utilized. The pumping procedure for these tests was given above. For bench test drilling the target mover was rotated 90^o so that it went into / away from the nozzle in line with the lance. The target mover was staged on/off to obtain the desired drilling speed.

Hot 260°C/ 500°F Granite Cutting Tests- Red granite blocks were heated in an oven to 260^oC/ 500^oF for several months until the test bench was ready and the granite blocks were quickly moved to the target mover and the cut testing at the standard optimal rate/ ratio/ pressure/ temperature selected was begun. The cutting tests procedures were the same as given above for this type rock at ambient conditions. Once the hot test was completed (about 30 minutes) it was

Figure 23. Bear CO_2 pump and lines cool-down procedure before testing in June 2012

allowed to cool for several days. The same cutting test conditions were replicated to give a direct comparison with no rock variation. *Hint- no statistical difference in cutting was seen with this temperature difference, indicating that 500°F is not high enough to change the abrasive*

erosion potential of granites. However, 500^{o}F is the beginning of the temperature that will significantly degrade metal properties.

Rig Drill Tests- The same FLASH ASJ^{TM} test and pumping system as described earlier was used for the drilling tests. But the high pressure slurry hose from the pumping / mixing dilution point after the densitometers that went to the lance/nozzle was disconnected and instead connected to the inlet of the rigs utilized- either the Los Alamos National Laboratory (LANL) coiled tubing rig or the Impact built forklift based jointed pipe rig, both for shallow hole drilling within the shop yard. The same test procedures were followed for pumping the desired fluids, solids at the pressure and temperature desired. Note that stabilizing the coiled tubing unit took about 40 minutes, indicating that excess tubing was on the coil.

EQUIPMENT

CO_2 Storage Tank- In 2011 (after taking 1 year to obtain and a required 2 year contract) AirGas delivered a 14 ton (3500 gallons at 8ppg density) insulated steel CO_2 horizontal storage tank. It required an electric heater and refrigerator unit to maintain the 300psi operating pressure. Relief pressure was set at 350 psig, which did vent during summer months. The cold (estimated 10^{o}F) CO_2 was a liquid as needed to pump, but it needed heating before contact with water to prevent ice or hydrate formation. Truck deliveries kept the tank full. To imitate what we would need in the field, we tried to utilize the delivery trucks instead of a set tank, but AirGas would not allow their truck to be tied up for any period of time. Those would need to be purchased.

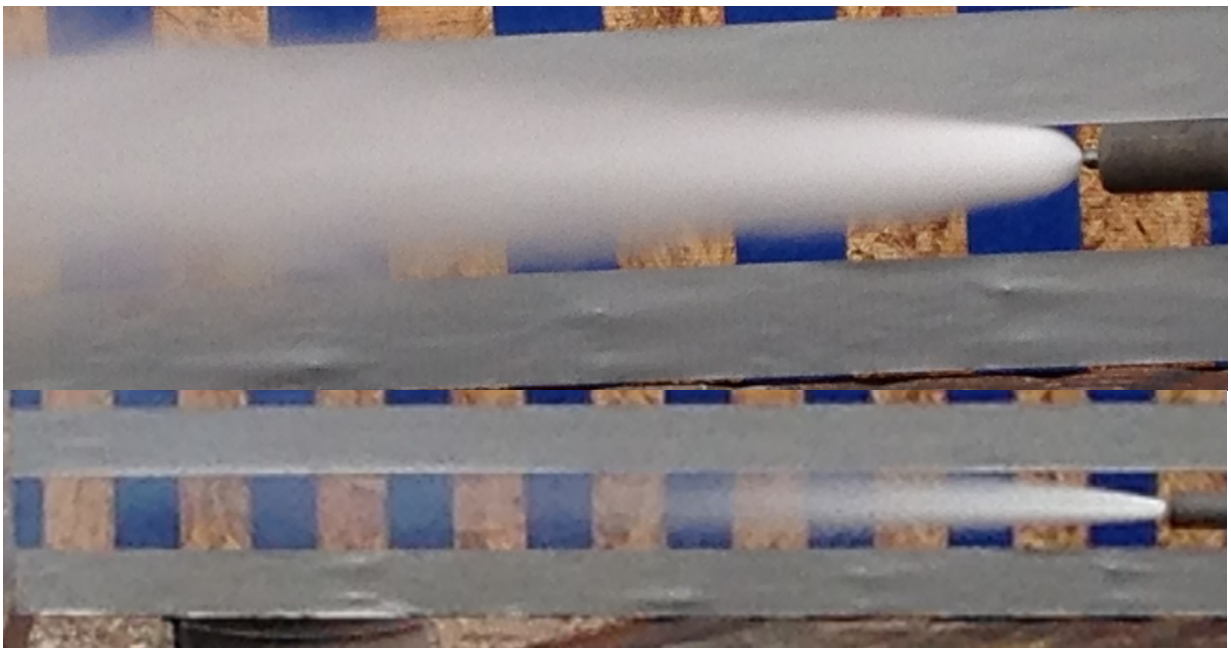

Figure 24. Spray Pattern Testing March 2013 - 2” patterns behind spray. Top-Good Wide Cut. Bottom,Test 248b-Poor Narrow Cut.

Figure 25. AirGas CO_2 storage tank, Bear triplex pump skid, charge pump and header

CO_2 Charge Pump- Even though AirGas and other experts said that a charge pump was not needed, we found that it was needed to ensure full pump cylinder loading during summer months. Gas lock was occurring. Without full cylinder loading the full pressure required could not be maintained. The vane charge pump was installed in April 2013 and used for recirculation back to the tank to cool the triplex pump fluid end and the lines before testing begins. Also it was used to keep the pressure above saturation so that no gas would form during testing. The difference between actual and the experts was due to the low rates being pumped allowing some slight temperature increase of the saturated CO_2 liquid (and therefore gas formation) at and in the pump fluid end during the pump's suction stroke. Most experts were apparently only familiar with higher rates. Shown in Figure 26.

Figure 26. CO_2 Charge Pump installed April 2013

CO_2 Triplex Pump- In August 2011 the National Oilwell Varco (NOV) Bear^{TM} BD-60H triplex plunger pump package for CO_2 service was delivered, however, it took many shop repairs (primarily for bearings to get it working right- estimated 3 months delay. The pump had all metal valves in the fluid end. The pump is driven by a 60 hp Duetz diesel engine (oil bath air breather) and a Siemens gear box reducing the rpm by 4:41:1. Shown in Figure 25.

Densitometers- Two ThermoFisher Density Pro Plus (20 & 50 mCi) Cesium CS-137 gama-ray densitometers with scintillation detectors in a Nema 4 housing and 2" pipe saddles, reduced by Impact to 1" horizontal pipes, were used to detect final mixture density that was going to the nozzle, not to measure exact densities. Shown in Figure 22. The relative readings were used to determine the timing of switching HP4 pump cylinders and for monitoring maximum density timing. A 1" pipe was used to maintain sufficient velocities to fully mix the slurry, but it provided too small a volume of slurry in the cross section for exact measurements. A new design to shoot down a 3" to 6" section of 1" pipe length was considered but not purchased or built, due to cost and timing.

Flow Meters- for the water/slurry and CO_2 were Hoffer CO_2 Flow Meter Model HO1X5/8A-1.75-16-BP-1MX-NPT-SP for liquid carbon dioxide service. Flow rate range- 1.75 to 16 GPM (6.62 TO 60.57 LPM). Construction - 316/316L stainless steel with ceramic, self-lubricating hybrid ball bearings. Maximum pressure of 7000 psig. The Hoffer Water Flow Meter (on FMC pump) Model HO½X¼A-0.25-4.5-BP-1(RP51S)X8S-NPT-X. Flow rate range - 0.25 to 4.5 GPM. Maximum pressure of 7000 psig.

Inline Heaters- Dual, diesel fired, NorthStar Pressure Washer Heater/Steamers were used to heat the CO_2 via through a custom coiled pressurized (5000 psi rated) 1" tube heat exchanger, used for steam generation. Seen in Figures 22 and 28, lower left.

Slurry Drive Pump- Impact already owned a Freemeyer Industrial fabricated, triplex pump package with a 180hp Cummings diesel engine, a FMC triplex pump geared down from the diesel rpm at about a 4:1 ratio, and a specialty custom designed stainless steel fluid end for clean water service. That pump can be seen in Figure 28 top left. The pump fluid end and available power was rated for 20,000 psi and 20 gpm. It should be noted that a 25 hp water pump, rated for the 5 gpm rate and 5000 psi, as the gasoline driven pump in Figure 27 below, can be used as the slurry drive pump for lower slurry rates.

Temperature Readings- The thermocouple at the end of CO_2 heat exchange unit was an external (taped to the CO_2 delivery pipe and insulated) RTD type from Red Lion.

Hoses- All slurry hoses were from SpirStar and were secured at both ends and in the middle in case of breakage/failure under pressurized slurry operation. The hoses were rated for 20,000 psi and higher with an outer wear guard.

Figure 27. Small 5gpm and 5000psi 25hp water jet sprayer used for some steam tests.

Figure 28. Clockwise-Freemyer slurry drive water pump, HPSP#4 control valves, AirGas CO_2 Tank, Bear CO_2 pump, dual NorthStar heaters, ThermoFisher densitometer, polymer mixing tank

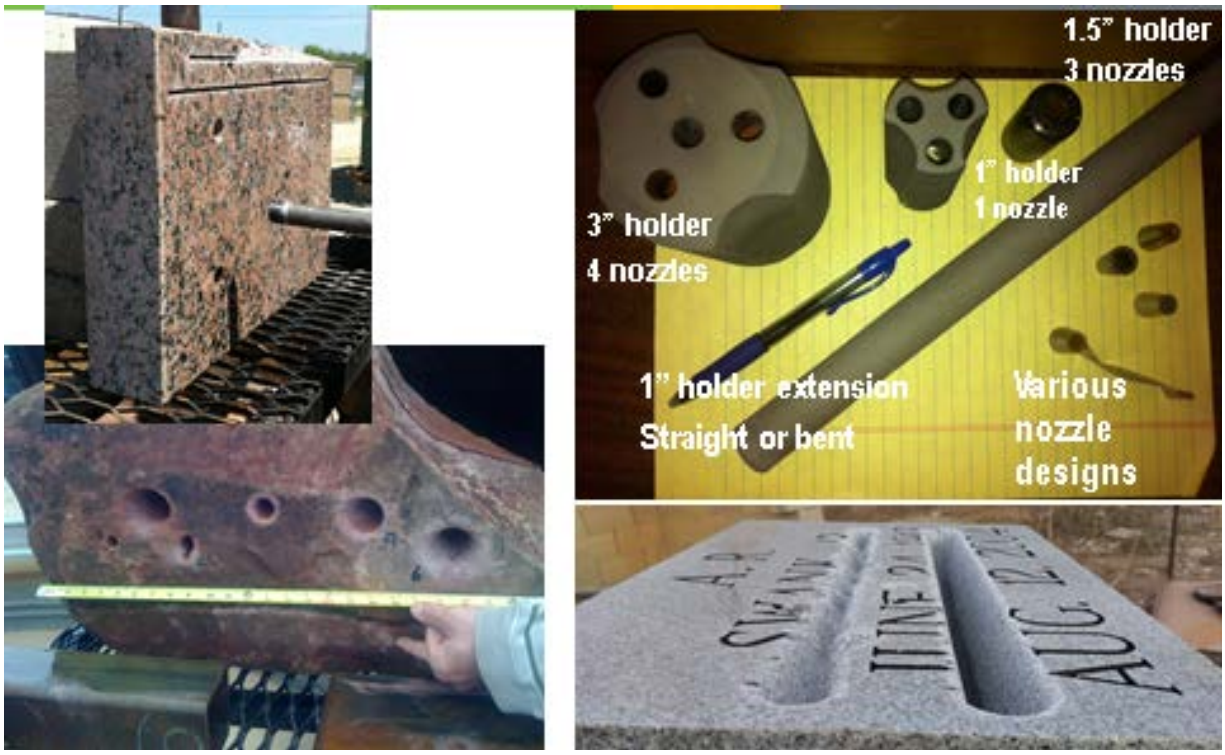

Figure 29. Left- Rose granite and red sandstone blocks under steam FLASH ASJ cutting and boring; Right- tools and cut grey granite with CO_2 FLASH ASJ™ cutting.

Figure 30. FLASH ASJ Drilling Hole in Granite Block on bench target mover - Spring 2013

Figure 30 shows one granite bench test in the spring of 2013 that had multiple cuts on both sides to optimize the nozzle or FLASH fluids ending in drilling several bores through it. Figures 31and 32 show a red sandstone under FLASH bench cutting with the 3 nozzle holder in the summer of 2013. One nozzle became plugged during testing which increased flow to the

remaining 2 nozzles and an uneven cut. Note, it was not desired to cut all the way through the rock block.

Figure 31. Three Nozzle CO_2 Bit FLASH Cut through Rock. Measuring back side hole.

Figure 32. Use of a 3 Nozzle Bit with CO_2 FLASH. Measuring cut depth.

In 2012 it was determined that the CT on the LANL rig was damaged and could not be repaired. It was taken off the reel and junked. Over 500 feet of new 1.0" high alloy steel coiled tubing (CT) were purchased and spooled onto the LANL CT rig reel. It was later apparent that we received at least 800 feet probably from the end of their roll. The LANL CT rig, shown in Figure 33, was modified for easier remote control so that the operator would not be near the pressurized inlet abrasive hose or near the wellbore. It was used for vertical bore drilling in the earth, discussed later.

Figure 33. LANL Coiled Tubing Rig with new 1.0" high alloy steel CT

In the summer of 2013, Impact developed a forklift-based drill rig, seen in Figures 34, 35a and 35b, that utilized straight thick wall carbon steel pipe in 3/4" and 1/2" ODs and 20 feet lengths. The pipe was made up in alternating sizes (i.e., smaller pipe threaded into the larger pipe on both ends) so that the outer diameter was nearly smooth when made up- no exterior joints. Internal and external edges were beveled to prevent flow disruption or sticking in the hole. Different lift and handling tools were needed for each size. A high pressure swivel was used to make up the pipe while lifted by the rig.

Figure 34. Wellhead & Return Tank for Vertical Drilling

PROBLEMS during testing-
A) Safety danger of cutting through the rock and back steel during testing. Figure 36 showed a jet that cut through a thick rock slab and a ¼" steel plate very fast during early steam testing. Narrow focused jets were avoided because of that and because we wanted wider cuts anyway. Note- in all tests we did not want to cut all the way through the rock because that is dangerous and it prevents accurate measurement of cutting efficiencies (because some of the slurry misses and removes no rock).
B) Cavitation of the thick slurry in the pumps destroying valves, see Figure 37. HPSP1 and HPSP2 (July-August 2010) endured valve damage due to cavitation from incomplete cylinder filling during the suction stroke. This was solved by going to a long slower stroke pump.
C) Icing of target, seen in Figure 38, occurred at times reducing the effectiveness of slurry cutting since no antifreeze was added. Heating of the CO_2 and/or mixture solved this problem which mainly occurred at high gas/slurry ratios.
D) Goal was thick wide cuts which would lead to drilling/ boring holes. However, many different nozzle and fluid combinations were tried to finally obtain the desired wide cuts. Thin width cuts and cone shaped holes often occurred in certain nozzle/ fluid configurations during boring and drilling. Ultimately, we achieved the goal for drilling and slotting by obtaining wide flat bottom cuts/ bores with straight even sides.

Figure 35a. Forklift-Based Jointed Pipe Rig

Figure 35b. Jointed Pipe Rig w/ Wellhead

Figure 36. Danger if nozzle focused. Here with Steam as the FLASH fluid.

Figure 37. HPSP1 Valve Damage due to Cavitation.

Figure 38. Icing at High Gas: Slurry Ratio Tests, if not heated-May2013 tests

Steam cutting tests results-

These tests were used to evaluate steam as a FLASH ASJ fluid and to evaluate various nozzle designs. This was low quality (maybe 70% steam, 30% water) steam at best. Need higher temperatures instead of the maximum 400^{o}F temperatures available on the heater coils in series utilized as a single pass. Temperature control was set on the second burner. Pictures below in Figures 39- 44 are from the May 2010 steam cutting/ boring testing on a red Oklahoma sandstone.

Figure 39. Early FLASH ASJ^{TM} Steam Cutting and Boring Tests on sandstone, May 2010

Figure 40. Steam FLASH ASJ Cutting and Boring, May 2010. Cutting through the back steel.

Figure 41. Results of the May 2010 Steam FLASH ASJ™ testing on Sandstone

Figures 42, 43 and 44, clockwise. Steam FLASH ASJ cutting on sandstone May 2010. Showing deep tapered cuts with standard nozzles; variable stray cuts due to partial nozzle plugging; standoff effect with higher standoff (distance from nozzle to target in a gas) showing a wider cut.

Figure 45. CO_2 FLASH ASJ™ Cutting on Sandstone in June 2012

TABULIZED RESULTS:

a) ***Nozzle Spray Tests-*** These tests identified several nozzle and FLASH fluid combinations that were useful for obtaining wide cuts. See Figures 46 and 47 below. They were run with only gas and water, no solids. Thus these patterns may not fully match a full FLASH ASJ™ cutting / drilling system. The jet width at 1" cutoff was 1.2 inches. Above that size it was felt that the cut bore would be sufficient to allow return flow. The ratio of the jet diameter at 6" and 1" identified those jets that were growing and could create a proper cutting pattern.

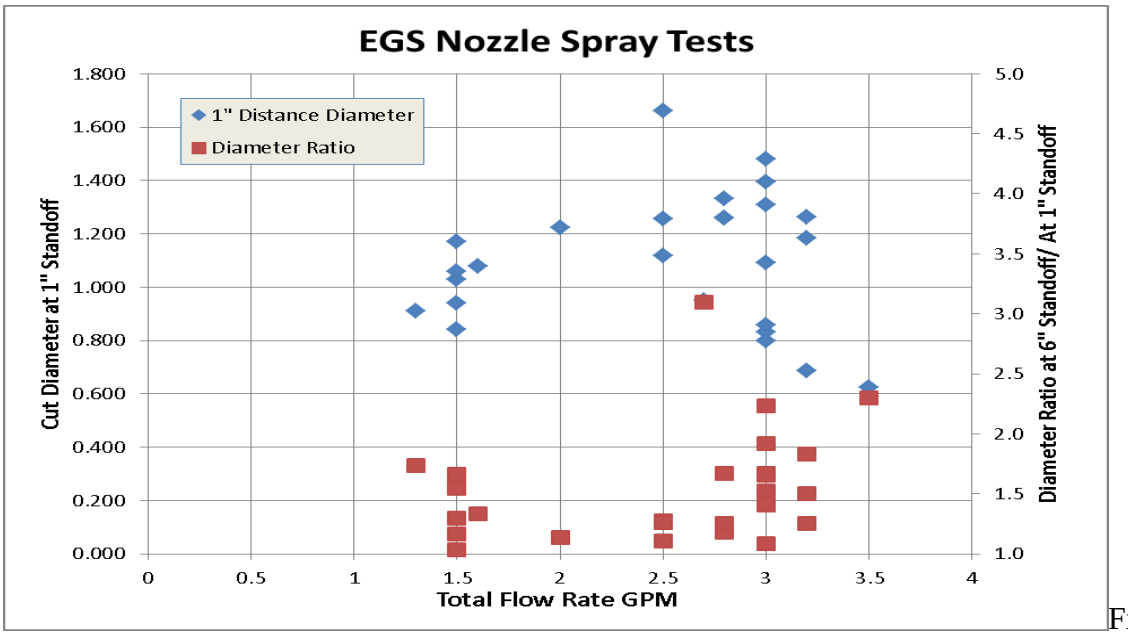

Figure 46

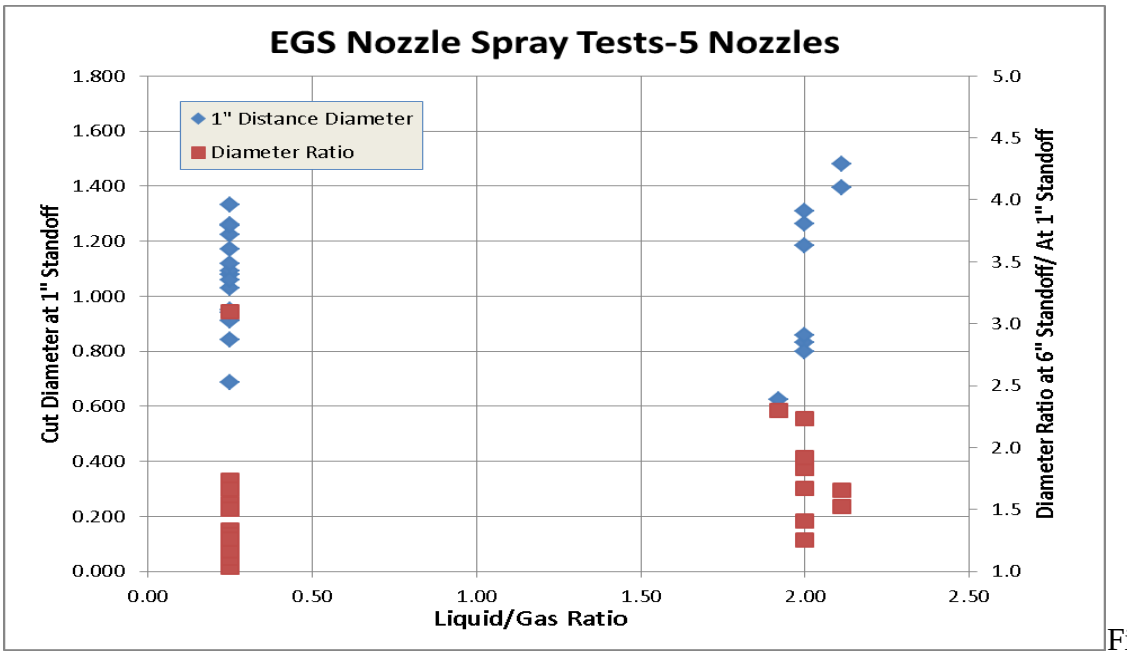

Figure 47

b) ***Hot Granite Rock Cutting tests*** – Tests 46, 47, 48 and 49 were conducted during April to June of 2013 on 500^{o}F granite that had been heating for several months. The same optimal FLASH setting/ conditions were used to cut these hot rocks, then allow to cool for a few days and recuts on the other face. Pictures of those cut rocks are given in Figures 48 and 49 below. The plot of that data as a modified specific energy number is given in Figure 50 below the pictures.

Figure 48. Hot Rocks- Part 1

Figure 49. Hot Rock Tests- Part 2

In terms of the various efficiency terms utilized to compare each test, the specific energy term utilized (calculation shown on Figure 50) was the most beneficial in making this comparison between tests. Test R1.0-Q2.65-P330 cut off the rock and thus considered not valid for direct comparison.

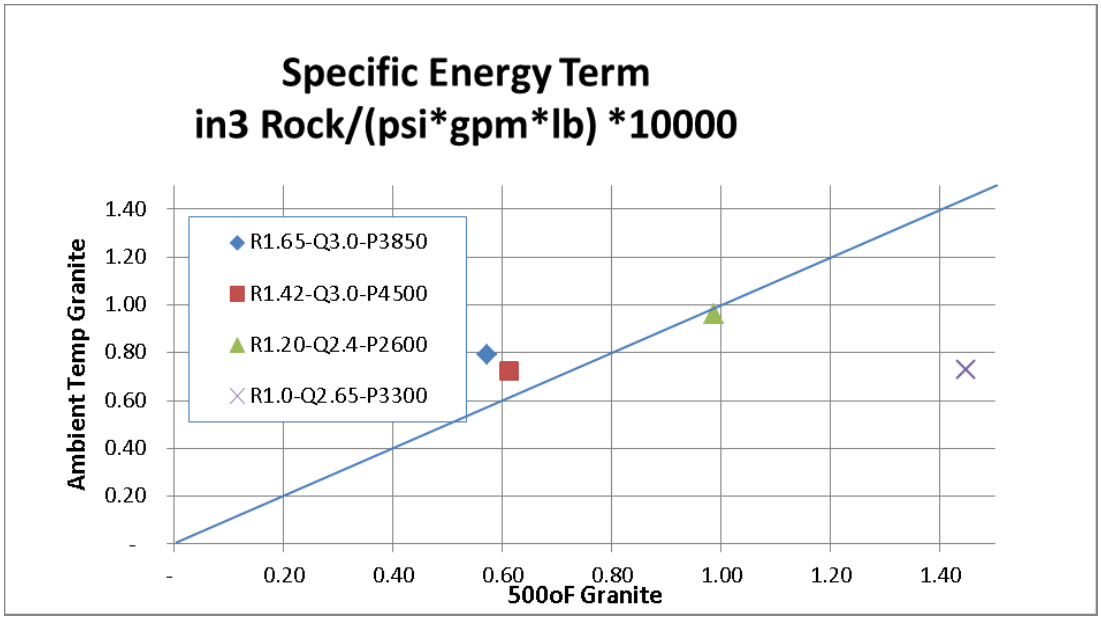

Figure 50. Specific Energy Term in comparing 500°F Rock to room temp rock cutting

RESULTS of NOZZLE DESIGN AND FLASH ASJ™ BENCH CUT TESTING

The calculation methods for each efficiency term (note-no conversion constants utilized herein since most of the effort dealt with comparison of one test over another) used in the spreadsheets and plots were as follows-

- Slurry based Abrasive Cutting Efficiency Factor= volume (cubic inch) of rock removed per pound (lb) of abrasive used;
- Rate Based Time Cutting Efficiency Factor= volume (cubic inch) of rock removed per test minute. Rate based test minute= total concentrated slurry volume (gallons) through pump utilized / average concentrated slurry rate (gpm) during the test;
- Specific Energy Term= volume (cubic inch) of rock removed / (total flow rate of FLASH and concentrated slurry (gpm) * average pressure (PSIG) * lbs of slurry used) during the test with no conversion factors;
- KDO Factor for correlation purposes only.

It was important that the CO_2 density be corrected for the upstream temperature and pressure at the nozzle. The only temperature sensor available for CO_2 was after its heat exchanger and before the phases were mixed together. The concentrated slurry temperature was estimated based on seasonal weather, since it was not recorded during the tests. The upstream nozzle mixture temperature was then estimated based on mass contribution of each phase to the total mix. The

pressure was taken off the water drive pump in most cases. Where there was a concern as to accuracy, the average of the CO_2 and water drive pressures were used.

Plots from the summary report, dated May 2013, are given below. The table of data will be uploaded to and made available from the GDR. In these plots the various efficiency factors were plotted versus the variables considered important to FLASH ASJ cutting and drilling. These factors are:

- Volume ratio of slurry/ gas, corrected to the upstream nozzle conditions;
- Total flow rate to the nozzle in gpm, corrected to the upstream nozzle conditions;
- Pressure of the mixture upstream of the nozzle, as measured from the pumps;
- Temperature of the diluted mixture upstream of the nozzle, estimated as discussed above.

The resultant cutting efficiency terms for each test were plotted against each of these controllable factors below:

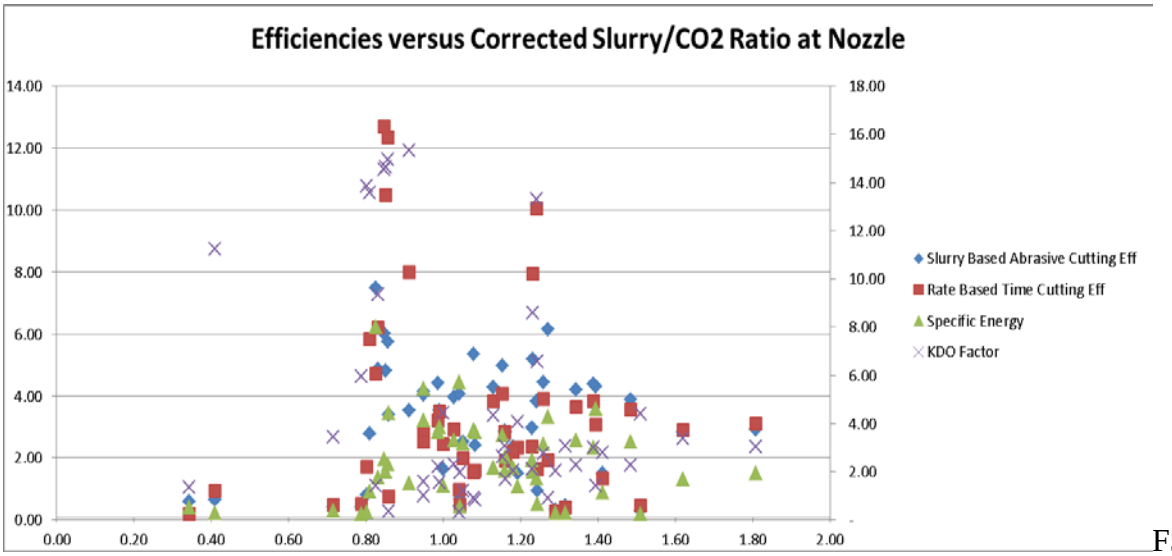

F51

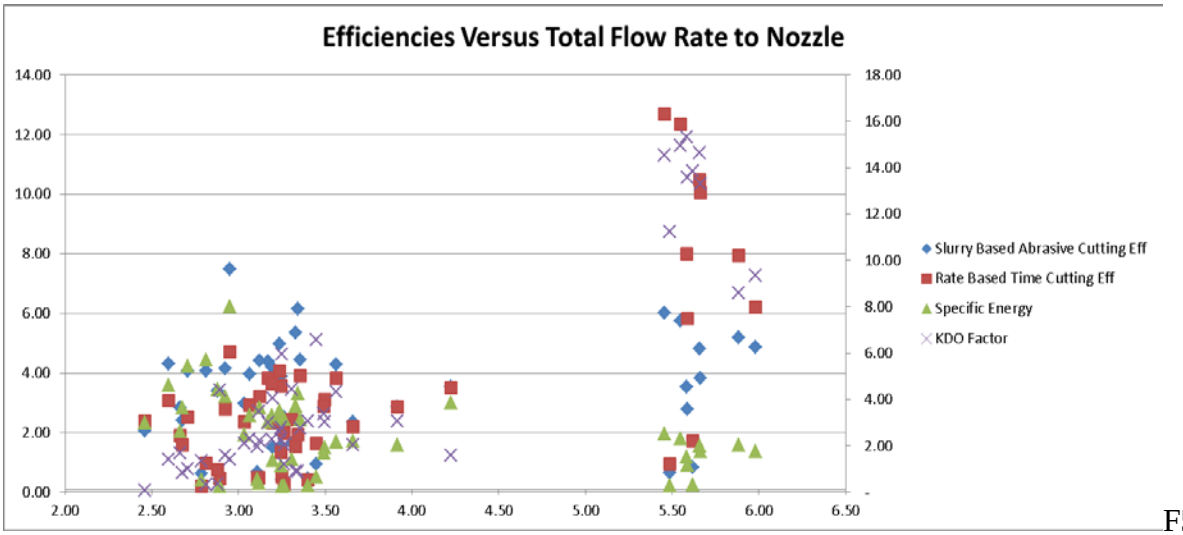

F52

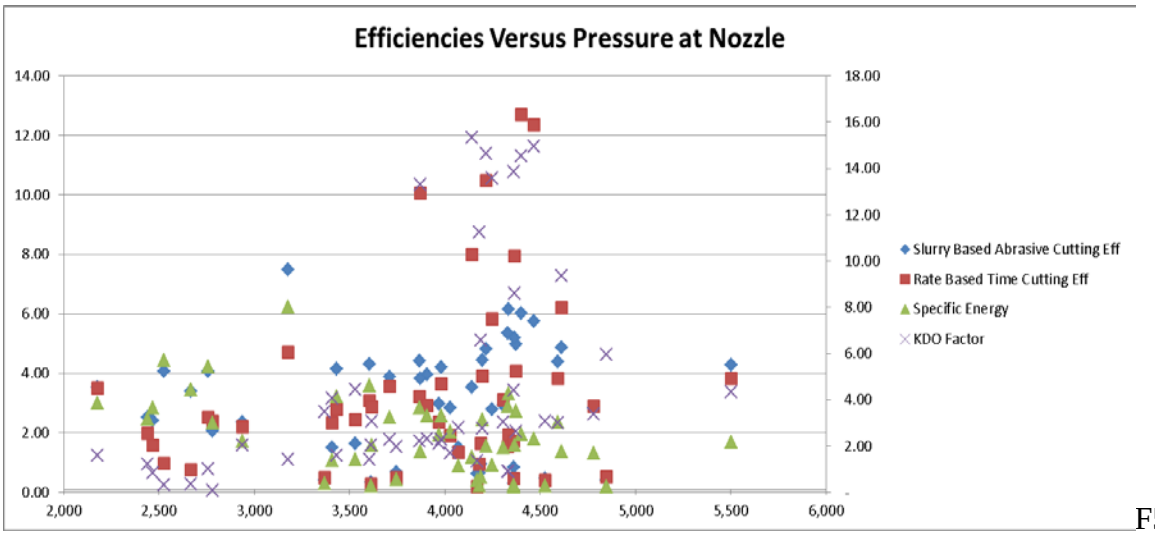
Efficiencies Versus Pressure at Nozzle
14.00
12.00
10.00
8.00
6.00
4.00
2.00
0.00
18.00
16.00
14.00
12.00
10.00
8.00
6.00
4.00
2.00
-
2,000
2,500
3,000
3,500
4,000
4,500
5,000
5,500
6,000
Slurry Based Abrasive Cutting Eff
Rate Based Time Cutting Eff
Specific Energy
KDO Factor

F53

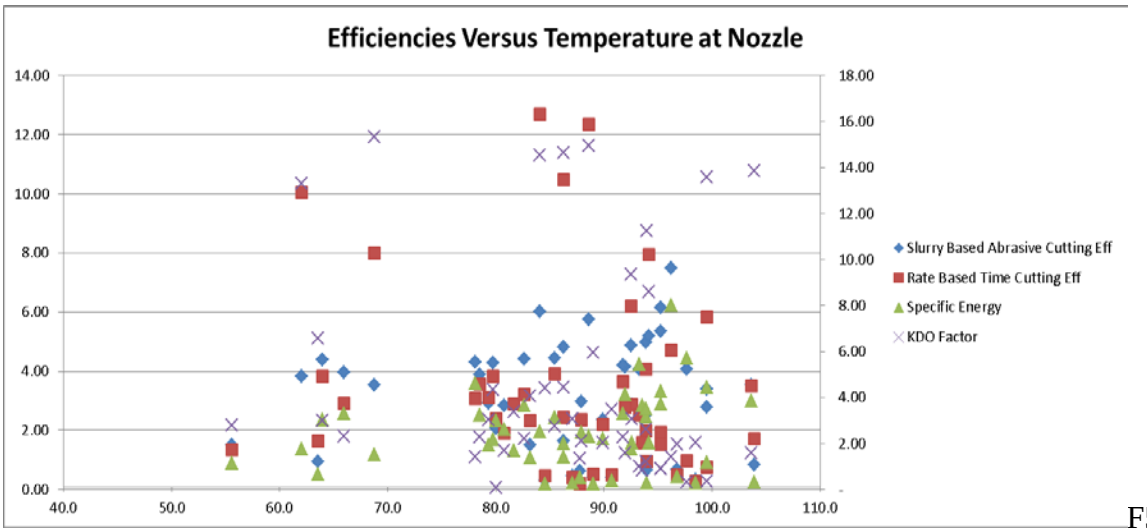
Efficiencies Versus Temperature at Nozzle
14.00
12.00
10.00
8.00
6.00
4.00
2.00
0.00
18.00
16.00
14.00
12.00
10.00
8.00
6.00
4.00
2.00
-
40.0
50.0
60.0
70.0
80.0
90.0
100.0
110.0
Slurry Based Abrasive Cutting Eff
Rate Based Time Cutting Eff
Specific Energy
KDO Factor

F54

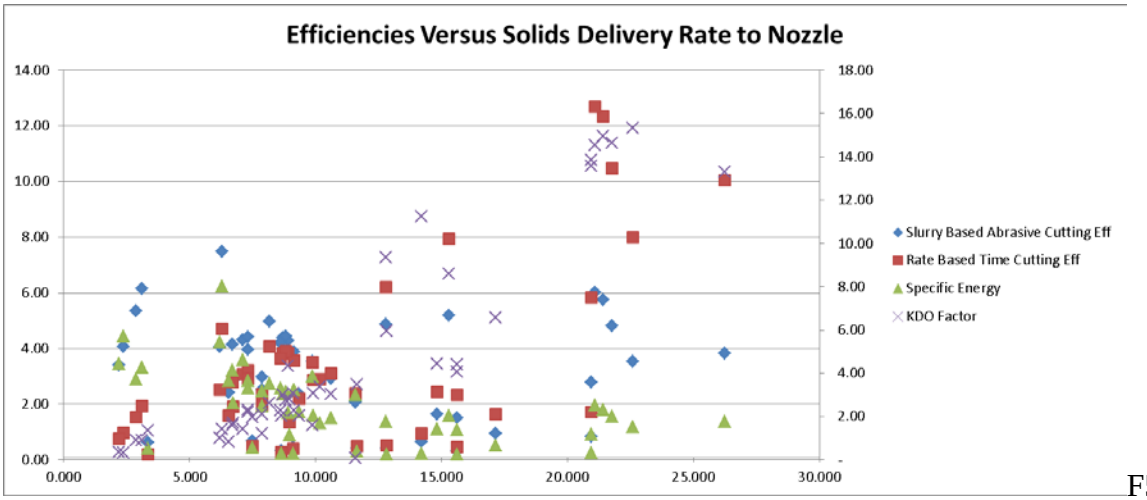
Efficiencies Versus Solids Delivery Rate to Nozzle
14.00
12.00
10.00
8.00
6.00
4.00
2.00
0.00
18.00
16.00
14.00
12.00
10.00
8.00
6.00
4.00
2.00
-
0.000
5.000
10.000
15.000
20.000
25.000
30.000
Slurry Based Abrasive Cutting Eff
Rate Based Time Cutting Eff
Specific Energy
KDO Factor

F55

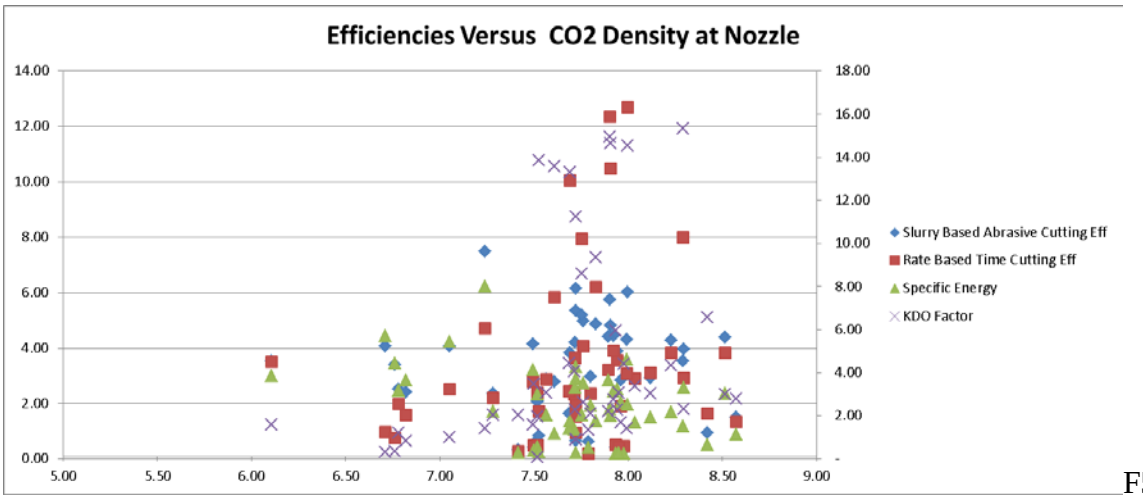
Efficiencies Versus CO2 Density at Nozzle
Slurry Based Abrasive Cutting Eff
Rate Based Time Cutting Eff
Specific Energy
KDO Factor

F56

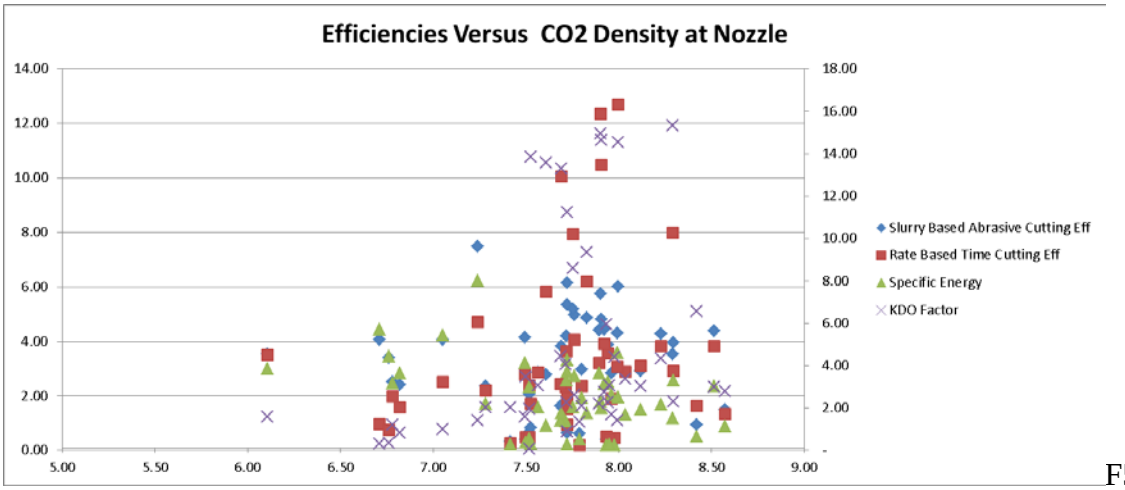
Efficiencies Versus CO2 Density at Nozzle
Slurry Based Abrasive Cutting Eff
Rate Based Time Cutting Eff
Specific Energy
KDO Factor

F57

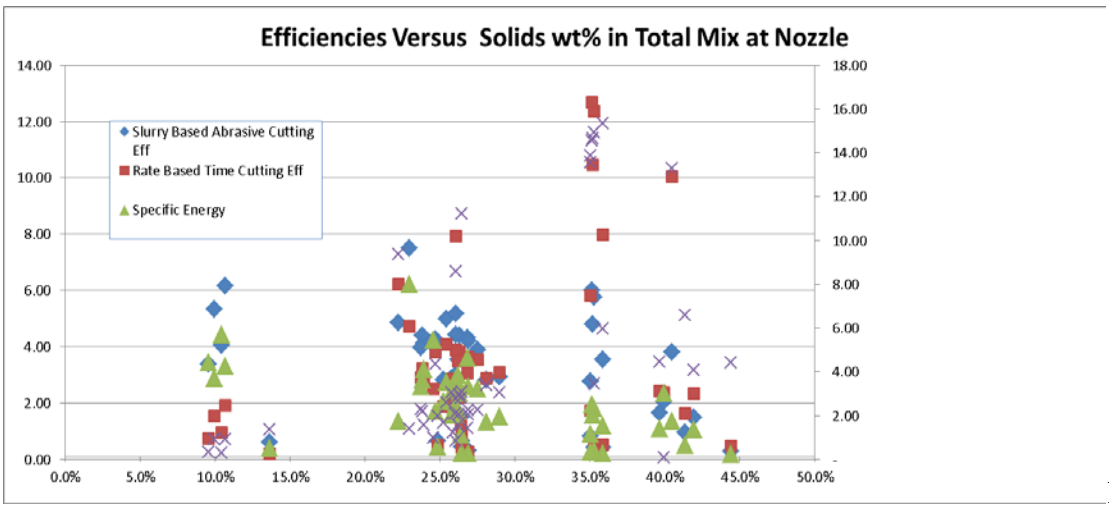
Efficiencies Versus Solids wt% in Total Mix at Nozzle
Slurry Based Abrasive Cutting Eff
Rate Based Time Cutting Eff
Specific Energy

F58

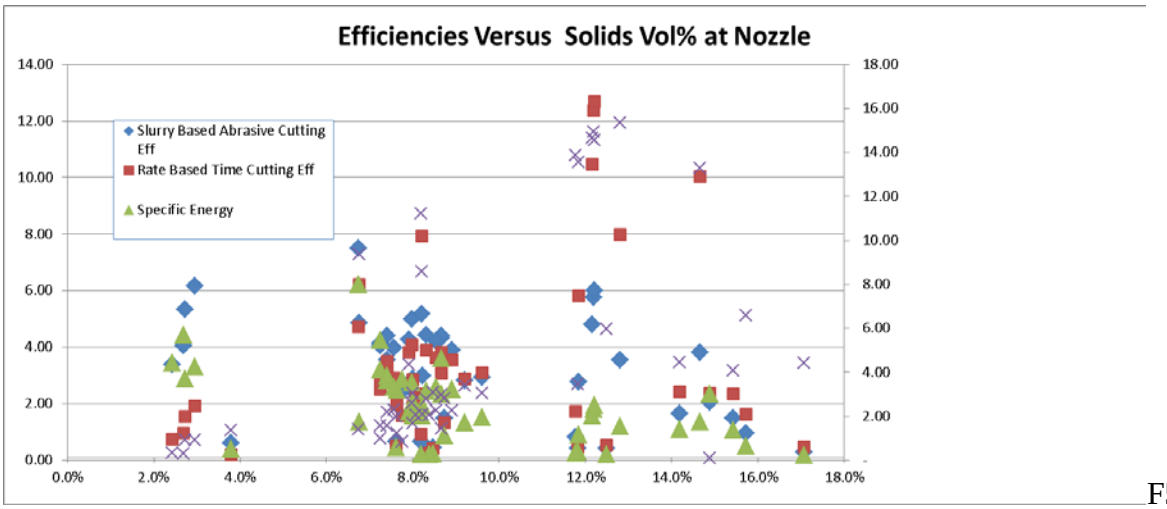

F59

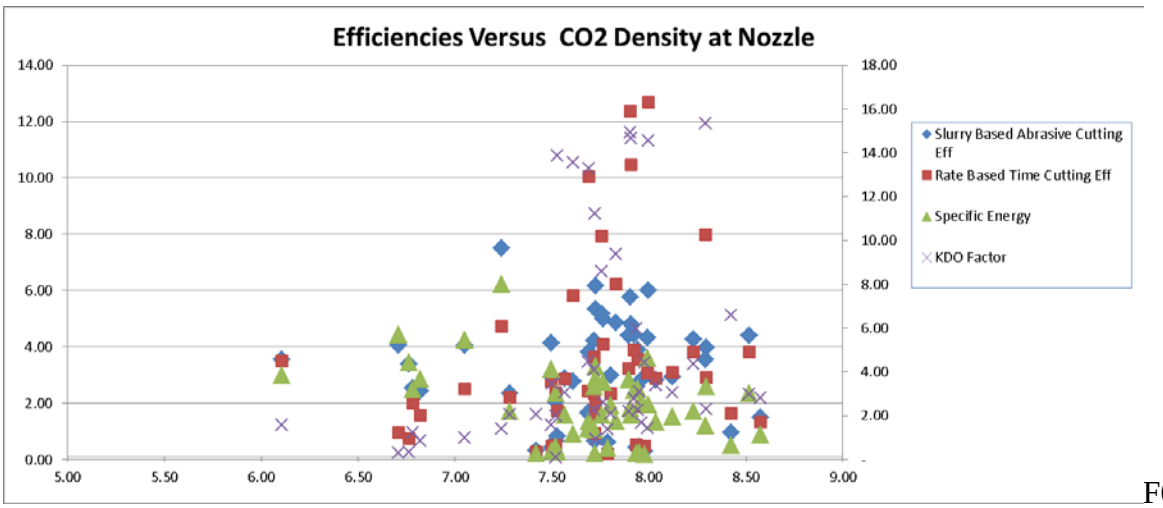

F60

DRILLING AND BORING BENCH TESTS

Once the nozzles were designed and the optimal FLASH conditions determined, bench drilling began on sandstone and granites in the summers of 2012 and 2013. It was found that if the bit/nozzle was advanced too fast then too small a hole is formed, which allows for pipe advancement just into the restriction, but no further advancement is possible due to pressure buildup ahead of the nozzle. The hole beyond the restriction continues to be eroded ahead and outward creating a larger diameter section. Very slow drilling can prevent such restrictions, but lowers the overall drill rate and process efficiency- driving up cost/foot of hole drilled. Rotation of the nozzle(s) with a motor and proper flow channels appears to be a solution. If a motor is added then the possibility of a mechanical bit to keep the hole to a minimum size exists. To that end a 3” OD swivel was built and tested on the bench, but no further work with it was accomplished during the project.

Drilling sandstone tests on the bench target mover in June and July 2012 are shown below.


Figure 61


Figure 62. Bench Boring a long Sandstone


Figure 63. Exiting through the sandstone


Figure 64. Exit wound due to flow choking

CT Rig Drilling- After all nozzle design and FLASH optimization tests were completed and several bench drill/ boring tests were conducted on granite and sandstone, it was decided to drill into the earth. Those bench/boring tests were only successful if the bit/nozzle was not advanced too fast. Bench cutting tests also showed that all rocks could be cut and therefore drilled under the right conditions. In 2012 a site in Impact's yard was selected and a 4" nipple driven a few inches through the yard's gravel bedding. The 1" nozzle holder and a FLASH ASJ^{TM} nozzle to cut a 3" hole were inserted. The 18" length of the 1.0" pipe was added then attached to the 1.0" coil. With this setup the FLASH facility process was started and water was pumped at selected rates through the HPSP4 pump, densitometers, CT coil and nozzle above the surface. Optimal FLASH fluids rates were begun when the pumps were ready and all was pumped to the nozzle. It took almost 40 minutes from the pump for a change to be seen at the nozzle- indicating excess pipe was on the reel. Pressure loss through the reeled CT exceeded 800 psi over what the bench test setup operated at for the same rate/ nozzles. Abrasive was started and, when seen coming out of the nozzle, the drill assembly was slowly lowered. The CT rig had a reel reversing system that was hard to overcome to go forward. However, sufficient forward force was applied to lower the bit into the pipe. Care was taken to advance slowly and stroke the drilled hole repeatedly. However at about 6 feet of new hole the pipe would not advance further, even with repeated jarring down with the hydraulic unit. The pipe and drill assembly was pulled out and inspected with no marks noted on the nozzle holder or pipe. It was thought that the coil straightener on the injector head (a series of rollers) did not work as desired and the resultant bent pipe caused sufficient friction onto the drilled hole to stop drilling. This could not be confirmed on the surface.

Jointed Pipe Rig Drilling- In 2013 a new site in Impact's yard was selected and a pipe driven down to rock through a gravel layer. The rig was aligned over the installed wellhead and the pipe and same drilling assembly as used with the CT rig was inserted into the wellhead. The FLASH Facility was started and water was pumped to establish a base rate/pressure. FLASH fluids were started and the rate maintained until stabilized, then abrasive was begun. Once abrasive and FLASH fluids were seen at the nozzle, the drill assembly was slowly lowered and drilling began. The hole was easily drilled in a few minutes to 15 feet, with repeated strokes to ensure an open hole, but it stopped drilling once again and could not be advanced further. Examining the hole was not accomplished since it collapsed before it could be fully inspected.

With only a minimal depth obtained even with the jointed pipe, bent pipe causes were ruled out for the current problem, but it still should be investigated more thoroughly. Later testing with that same nozzle did not demonstrate any off angle cutting, although minor angles can accumulate to become significant, so this may still be a problem but it would be hard to identify and solve. Therefore, the limited penetration seen in the FLASH ASJ^{TM} drilling tests were possibly caused by one or more of the following causes:

1) slight bend in the pipe causing increased friction with the drilled wall;
2) uneven abrasive spray pattern causing a directional bore; and/ or
3) too fast advancement relative to the rock erosion leaving a return flow restriction(s).

It is now determined that, for deeper holes to be FLASH ASJ™ drilled, a rotation device (ie., a motor) will be needed. Minimum rotational speed and orientation of the nozzles will have to be determined later.

THE UNIVERSITY OF TULSA

The University of Tulsa's efforts in Phase II, Task 1, subTask 1.3 were focused on a) improving the design of the patented FLASH nozzle through numerical simulation, b) laboratory test cell bench tests of supercritical carbon dioxide exiting out of a nozzle, c) bench tests of the erosional characteristics of a new induction slurry pump, and d) simulation of that erosion potential in the pump. These efforts supported one professor, one Ph.D graduate student and one M.S. graduate student.

FLASH ASJ Nozzle Design-

Models were developed using the FLUENT program and the post-nozzle behavior of supercritical CO_2 was examined in laboratory bench tests, seen in Figure 62 below.

Figure 62. TU Experimental Laboratory Equipment

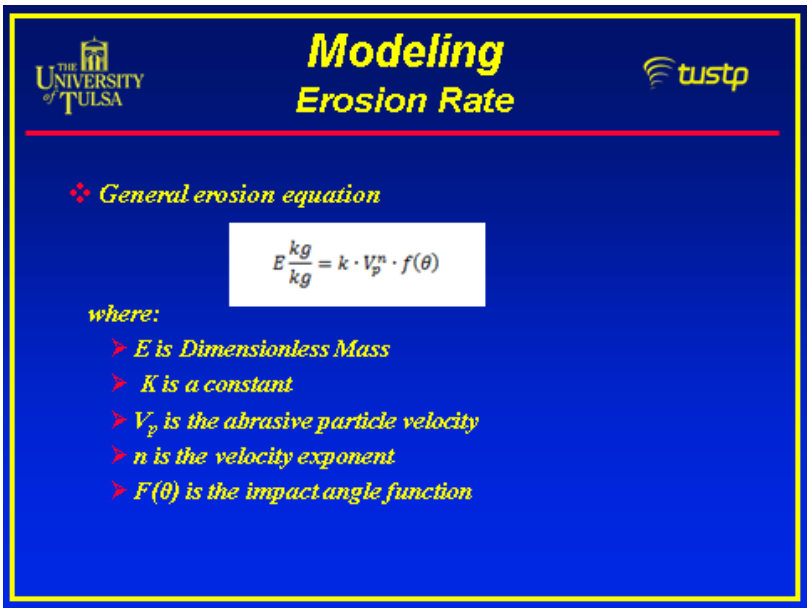

Figure 63. General Erosion Equation.

General Erosion Equation given in Figure 63 shows the significance of particle velocity, impact angle and the (abrasive) particles mass on erosion (i.e., rock mass removed). Particle velocity is raised to a power; therefore, for optimal erosion/ cutting the particle must exit the nozzle at the highest rate possible. In reality, the velocity term is more exactly correct right when the particle hits the target.

Particle velocity is first created by the nozzle flow restriction that changes the flow area of the slurry mixture from the large diameter at entrance to the very narrow nozzle diameter, which increases the velocity of the mixture within the nozzle. The particle velocity is imparted by the drag of the slurry carrier fluid on the particles as they accelerate in this change. If acceleration is too high (i.e., nozzle entrance too steep or abrupt), then a concentration of particles will occur at the nozzle inlet/ entrance as the carrier fluid leaves the particles behind. This solids build-up can interfere with slurry flow coming into the nozzle. If the carrier fluid density and viscosity is high, then it will accelerate the particles better.

In the patented FLASH ASJ systems a second acceleration of the slurry mix occurs after (and sometimes within) the nozzle. This is the expansion of the supercritical fluids from a liquid to a gas, a significant volume change of 8 to 20 times. This expansion increases the velocity of the slurry mixture and the entrained particles on top of the previous described flow restriction caused velocity increase.

Furthermore, that velocity term is when the particle hits the target, not just exiting the nozzle. The rapid velocity reduction profile that occurs in water after a nozzle can be seen in Figure 64. Note that 50% of the velocity is lost at 1” from the nozzle when jetting through a water phase. Thus the standoff (distance between the nozzle exit and the target) must be as small as possible, and the fluid density and viscosity within that standoff region should be as low as possible (gas preferred). It is therefore good that the FLASH ASJ fluid expansion creates a lower density, lower

viscosity gas phase after the nozzle in the standoff region that less restricts the jetted particles on their path to the target.

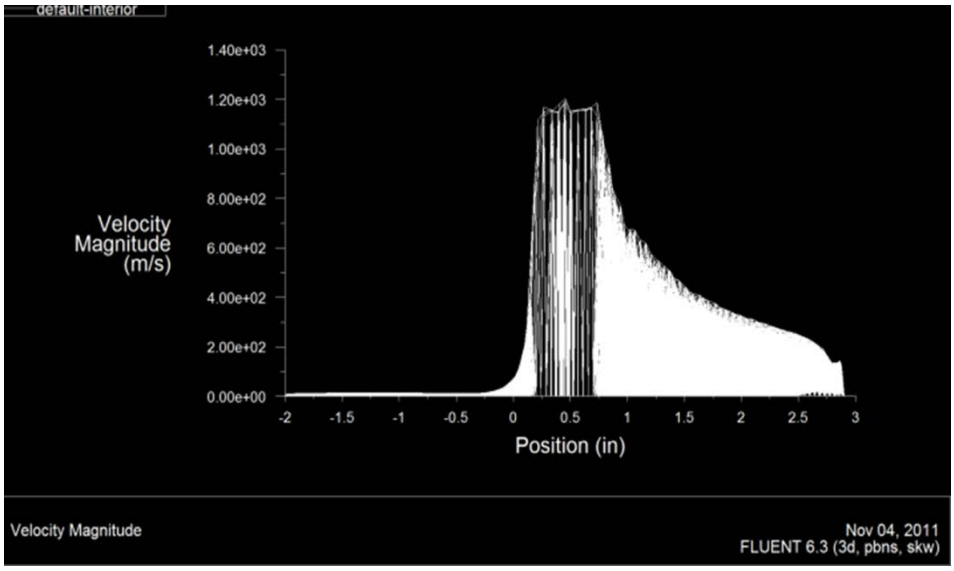

Figure 64. Velocity of fluid before, through and existing a standard nozzle.

Also important in the General Erosion Equation is the angle of impact of the particle to the target, with a more perpendicular (direct, high angle) strike more effective at erosion than a low angle glancing blow. This is important in creating a full open bore in drilling because the original cut (first pass) has a perpendicular rock face to the nozzle exiting jet for optimal erosion/cutting. If the full desired bore diameter is not cut in that first pass, then subsequent passes back through that bore section will only have low angle glancing opportunities and; therefore, less effective. Further, return flow is at a very low angle and is also less effective in eroding the rock bore wall. It appears that the best way to enlarge a given hole diameter size, after the first pass is with a different nozzle with a radial flow design.

The next variable of importance in erosion is the mass of the particles, where a denser particle material is desired, as well as a higher particle concentration.

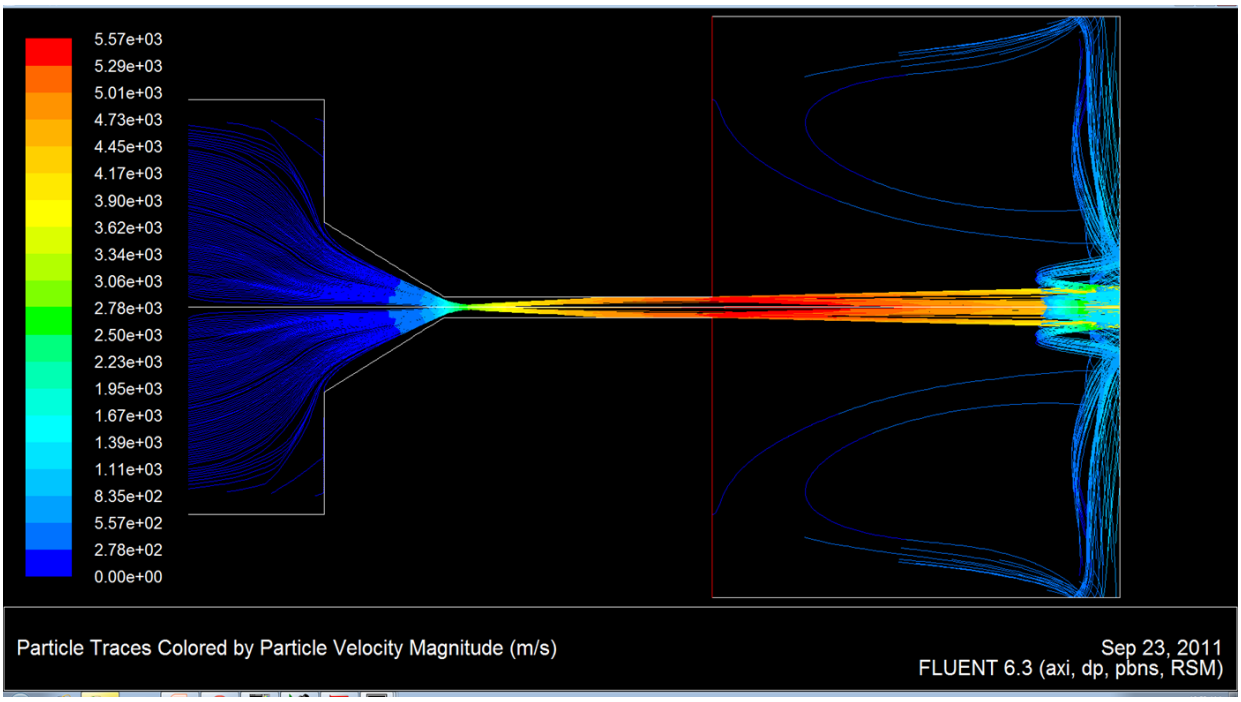

Figure 65. Fluent Particle Trace from a Fluent Simulation for a Standard Nozzle

This work is not completed. The nozzle design effort will continue at TU even after the project period ends and this report is issued.

Induction Slurry Pump Studies-

Figure 67 shows a generalized concept of the proposed induction slurry pump. Impact licensed the concept from MS&T for development in this project. Certain components are commercially available from various vendors. In fact, there is an American Petroleum Institute bulletin for standard designs of these components that was obtained for this project. However, the erosion potential of such a system is a concern and was studied in this project. To that end, components were designed and built and bench erosion tests were conducted and later modelled. Figure 68 shows the basic model that was built and simulated in this study. This effort continues after this project and after this report is issued.

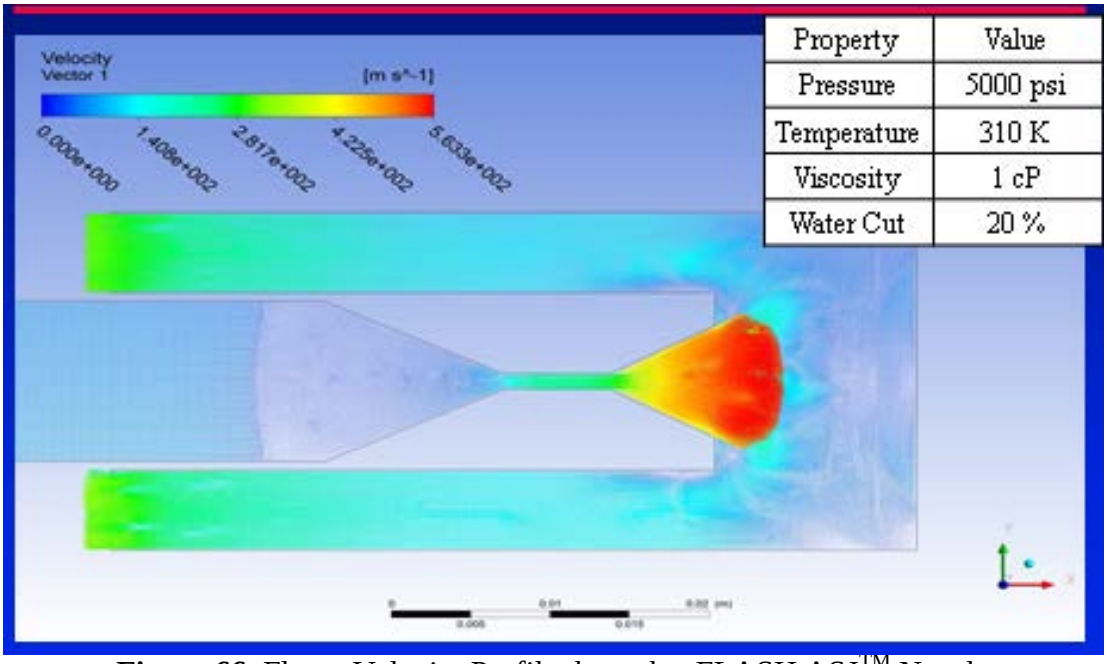

Figure 66. Fluent Velocity Profile through a FLASH ASJ™ Nozzle

.

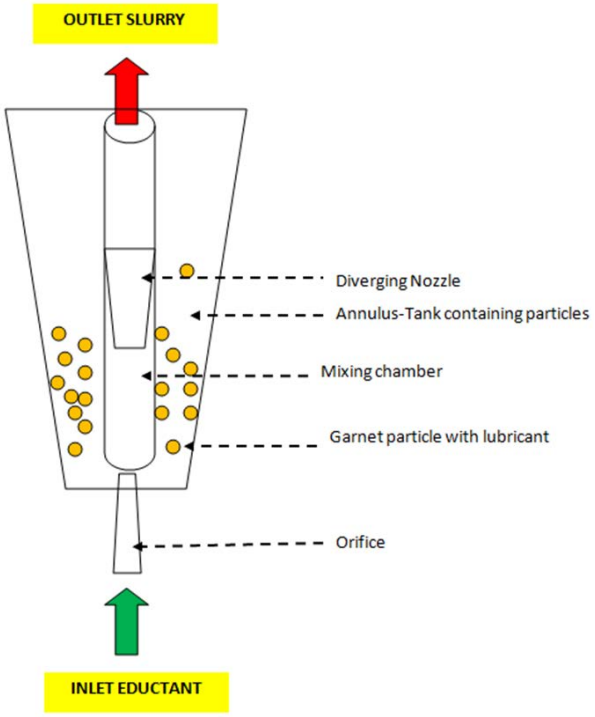

Figure 67. Induction Slurry Pump Concept

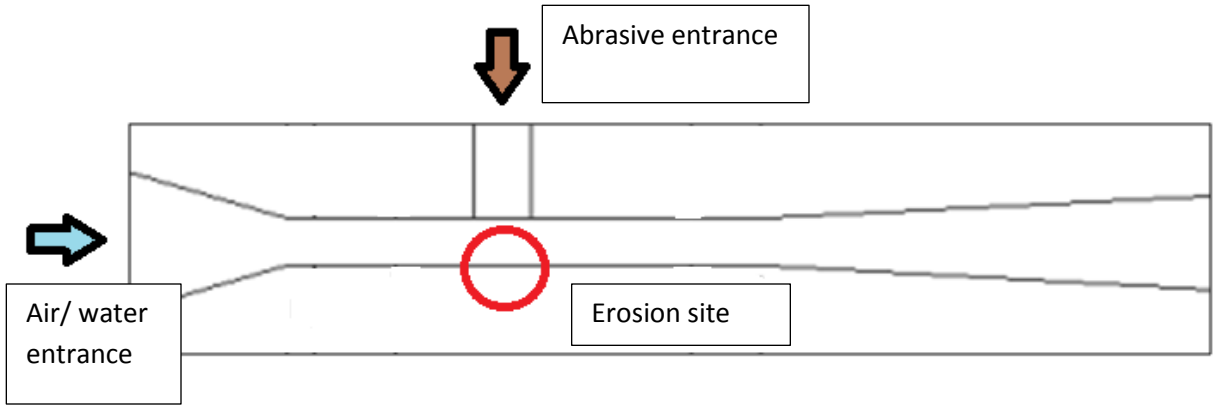

Figure 68. Basic Erosion Test model for components and simulation.

Subtask 1.4 Expand the Directional Capabilities of Microholes

It is proposed that a large main vertical bore be drilled from the surface down to above the EGS depth, then multiple microhole sized bores be directional drilled from that well some distance out to intersect a fracture that is hydraulically connected to another main vertical well to the surface. This establishes a flow loop for the working heat transfer fluid. The level and control of those installed microbore sized directional laterals were discussed in the prior subTask 1.1 of this Phase and Task.

As discussed previously, the depth of the kick-off point for the laterals in the main vertical large bore would be well known with current technology and tools. Likewise, the orientation of a standard whip-stock tool that is set in that main bore is also well known, as is the angle off-vertical of that whip-stock curve, especially in hard rocks. Thus the direction and orientation of the nozzle when immediately exiting the main vertical bore would be well known. It is, therefore, of most interest how to measure, monitor and control the lateral direction between the two vertical bores/ fracture. The CTES program developed in subTask 1.1 was meant to allow estimation of the vertical movement of the microbore in that interval. Standard directional tools of whip-stocks and bent subs were developed prior to this project.

It is envisioned that the microhole size will be between 5.08 to 10.2 cm (2” and 4”) in diameter. That requires pipe in the outer diameter range of 2.54 to 5.08 cm (1” to 2”) with reduced internal diameters. This makes the effective size of tools that can pass through the pipe down to 1.25 to 3.2 cm (0.5” to 1.25”). It is also important to note that EGS conditions of temperature and pressure will apply. There are no current directional tools that will allow real-time measurement, monitoring of and for control of bit/nozzle inclination and azimuth. There are not even single-shot tools of that size and rating that can be dropped and retrieved at given intervals to mark the path of the bore that was drilled. Furthermore, there are no such tools available for post measurement of the larger holes that size at the temperatures and pressures described. Directional tools in the pipe can be pumped down and retrieved with wireline, but such tools in the open-hole lateral would require attachment to the end of a pipe to push it to the end of the hole. Alternatively and more expensive, a tractor device can be used in the open hole.

No such survey tools now exist, however, the most likely directional monitoring tool to be first developed would be a single shot digital tool that would be timed to take multiple shots at set timed intervals. Because of other problems in subtask 1.3, no further work was done for this subtask.

Subtask 1.5 Safety and Control Issues

FLASH ASJ^{TM} drilling uses CO_2, N_2 or other gases in an energized abrasive system that create a safety and control issue on the injection side (from the pumps to and down the drill string to the nozzle) and on the return side (from the nozzle, up the annular space between the drill string and the casing/ hole wall through a surface choke and to a separator). Both high velocities (erosion) and low velocities (allowing settling of the solids) are of concern- seen in the Phase I, Task 1.3 WellFlo simulation runs. Velocities greater than 1 meter/ second are considered erosional. Minimal velocities to prevent settling are based on flow rate, fluid density, fluid viscosity, particle density and particle diameter. In addition to these concerns, we must add an underbalanced condition in the wellbore, where the wellbore pressure is lower than the pore fluid pressure in the rocks and encourages formation fluid (brine, crude oil, natural gas) influx.

The surface injection side can be safely operated with proper designed equipment and keeping the velocity of the slurry within safe levels and with minimal sharp bends. Noting hours of operation of all surface injection equipment is needed at this beginning effort to set a base line of operational life. Regular inspections are needed as well. No (excepting pumps and, nozzle) operational wear problems were identified during the several hundred hours of slurry operations during all project (and prior period) testing.

On the return side, high velocity solids, liquids and gases are returned to the surface. During bench and surface testing this return was focused back toward the nozzle and lance. Because of the low return flow rates, the Gas-Liquid-Solid (GLS) Separator (Figure 8, in the Background Section) was not used during this surface testing. However, in anticipation of drilling during the project, improvements in that system were begun early in the project to install a ceramic sleeve inside the GLS separator where the very high velocities are encouraged to force centrifugal separation. The ceramic lining was purchased from CLS Ceramics (Missouri) a C.L. Smith Industrial Company, although ceramic tiles were also found at Superior Ceramics Technical Corporation. Those tiles were not installed as of the time of this report.

Also, in anticipation of drilling within the project timing, a drilling control program was developed by Dr. Evren Ozbayoglu, a professor at The University of Tulsa, to guide the real-time drilling operation of a FLASH ASJ^{TM} drill rig. This C++ program took all available real-time inputs of pressure (injected and return/separator), rates (gas, liquid, solids), temperatures and depths, processed them to estimate and report the real-time downhole conditions, allowing an operator to maintain safe, secure and effective operations under full control. In addition to that hydraulic model a heat transfer component was included that tied to the CO_2 and Nitrogen physical properties. Figure 69 below is a flow diagram of the decision tree in the program. This C++ program was completed and its code, operating manual and PDF report will be uploaded to the GDR.

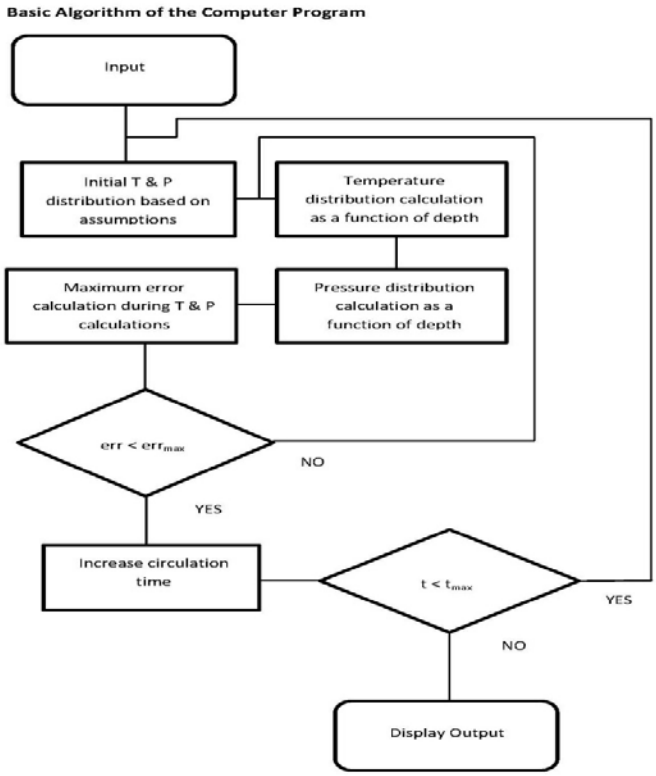

Figure 69. Decision Tree for Developed Operation Control Program

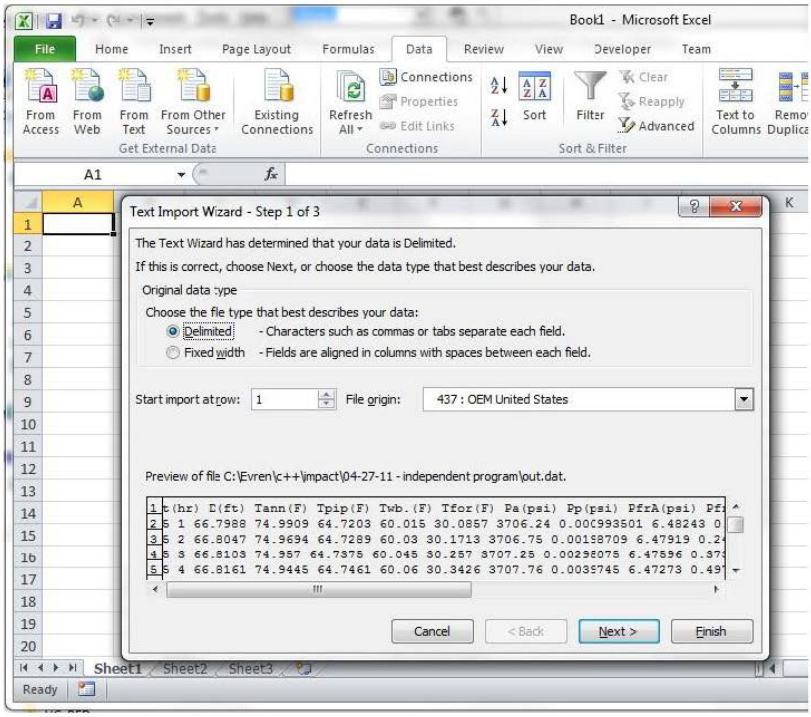

Figure 70. Screen Shot of Operation Control Program Inputs

Phase II, Task 2 Development of Simulation Capabilities for Microhole Technology

Subtask 2.1 Development of a Non-Isothermal Wellbore Simulator
Subtask 2.2 Coupling of Wellbore Simulator to Reservoir Simulator

In Phase I, Task 2 the scenarios for microhole arrays were developed, however the required programming code was not available to properly model those scenarios. Thus, further simulation work was moved to this Task. All project program coding changes and modelling efforts were reported in References [40-51] and published in [52]. Lawrence Berkeley National Lab (LBNL) did the work in this section.

As background, TOUGH2/EOS1 is a module of the TOUGH2 reservoir simulator that describes pure water in its liquid, vapor and two-phase state. It is also capable of solving the energy equation, therefore handling non-isothermal conditions. This module has been selected to simulate conditions typical of geothermal reservoirs. iTOUGH2 provides inverse modeling capabilities for the non-isothermal multiphase flow simulator TOUGH2 [*Pruess*, 1989, 1991]. A module described in "EOS16:An iTOUGH2 Module for Two-Phase Flow of Water, Air, and Methane Under Choked Gas Flow Conditions- Users Manual" was added for multiphase flow.

Further prior-project changes to TOUGH2 included inclusion of non-darcy flow. The Darcy-Buckingham law is commonly used to describe fluid flow through porous and fractured geologic media. However, deviations from the classical Darcy law have been observed under high-velocity flow conditions, which may occur in the region near an injection or extraction well. In particular, it may well occur within the microbores cited in this project. This non-Darcy flow can be described using the Forchheimer equation, which predicts the additional pressure loss on account of high-velocity flow to be a quadratic function of average flow velocity. A non-Darcy flow coefficient is thus introduced, which in its most general form is a function of effective permeability, water content and tortuosity. The Forchheimer equation was, therefore, previously incorporated into the iTOUGH2 simulator [*Finsterle*, 1999abc] and was used herein.

By April 2011 LBNL had incorporated a Time-Convolution Approach to account for Heat Exchange between the wellbore and the formation. The method remembers the temperature history of the rock in this approach. This is an overall semi-analytical solution to the problem since it incorporates an analytical solution for radial heat flow with constant temperature at wellbore, with a Supersition /Time convolution, link to the wellbore simulator, which is also linked to the reservoir simulator (TOUGH2). This report is included in Appendix E and uploaded to GDR. A movie of one run will be also uploaded to GDR.

By October 2011 LBNL coupled a wellbore simulator to the TOUGH2 EOS1 module. The momentum equation can be reduced to Darcy's law when the friction term dominates, i.e., the inertial term can be ignored. For the wellbore simulator, the Darcy flow equation was replaced by

the multiphase momentum conservation equation. The wellbore simulator does not need to make the assumption that the inertial term in the momentum equation can be ignored, which is the condition to use a Darcy flow simulation.

The wellbore simulator was built to be capable of simulating time-varying temperature boundary conditions at the wall of a flowing well and the corresponding heat transfer with the formation. Considering time-dependent boundary conditions for the calculation of transient heat exchange provides the flexibility needed to efficiently evaluate heat extraction from geothermal reservoirs using many microholes. The significance of this accurate semi-analytical solution to calculate the heat exchange between the wellbore and its surrounding formation work is that the computational cost can be significantly reduced, which makes large-scale accurate reservoir simulations with multiple wells and microholes feasible. The model was tested to ensure that the developed code is capable of simulating heat exchange with a flowing well with non-monotonic time-varying fluid temperature.

The wellbore flow was calculated based on the drift-flux model (DFM) for transient two-phase non-isothermal flow of fluid. Conservation equations for mass, momentum and energy under different flow regimes in the wellbore were solved numerically while wellbore formation heat exchange was calculated either numerically (if formation is represented in the numerical grid) or semi-analytically (if formation is omitted). The basic idea of the DFM was to consider the two-phase liquid-gas mixture as a single effective fluid phase with slip between gas and liquid arising from their different fluid properties, accounted for by empirically relating phase fractions and velocities to the mixture velocity. Following the scheme proposed by Shi et al. (2005), that drift velocity can be determined as a function of gas saturation and other properties of the fluids.

LBNL also included the effects of the inflow/outflow on the velocity along the z-direction of the wellbore in the feeding/leakage zone (i.e., the perforated section). By approximating that the density, the phase saturation, and the velocities along the z-direction are considered all independent of the radius (they are averaged values already), we can get the area-averaged net momentum flux in z-direction due to radial inflow or outflow. This code was tested using a basic heat exchange model between a microhole and the formation.

Subtask 2.3 (moved from Phase I) Compare Fluid Flow & Heat Transfer Scenarios

Based on the conceptual model shown in Figure 71, the simplest microbore scenario that was first reported in an internal report in October 2010, **Model 1** was built to provide a first approximation of how much heat can be extracted from formation. In that simulation, the geothermal reservoir (and thus the microhole) is assumed to be 3000 km below the ground surface. All the models are 2-D radial (i.e., cylindrical), with a radial extent of 1000 m. The geothermal gradient is usually between 15~50ºC/km and this simulation used 40ºC/km. Based on this evaluation, the temperature penetration distance after 20 years of operation is less than 50 m, which is a conservative estimate. Therefore, the mesh in radial direction beyond 50 m will be very coarse in all subsequent radial models.

A more detailed version of **Model 1,** reported in the Jan 2012 Stanford Workshop [49] and subsequent paper [50-52], was discretized into 2 elements (each element was 1000 m thick) in the vertical direction, and 70 elements in radial (horizontal) direction. In the radial direction, the first 3 elements coincide with the inner and outer steel tube geometry. The the radial discretization started using very small element sizes, then gradually increased using a logarithm scheme. Initially, formation temperature was at 140 ºC (upper layer), and 180 ºC (lower layer). The injected fluid was assumed to be 50 ºC. Results (no plot provided herein, see the referenced paper)- Temperatures in the inner tube and outer tube were very similar due to the large heat conductivity of steel. The outflow temperature gradually goes from 93 ºC initially to 81 ºC after 30 years. The temperature change in the formation extends to about 100 m radially.

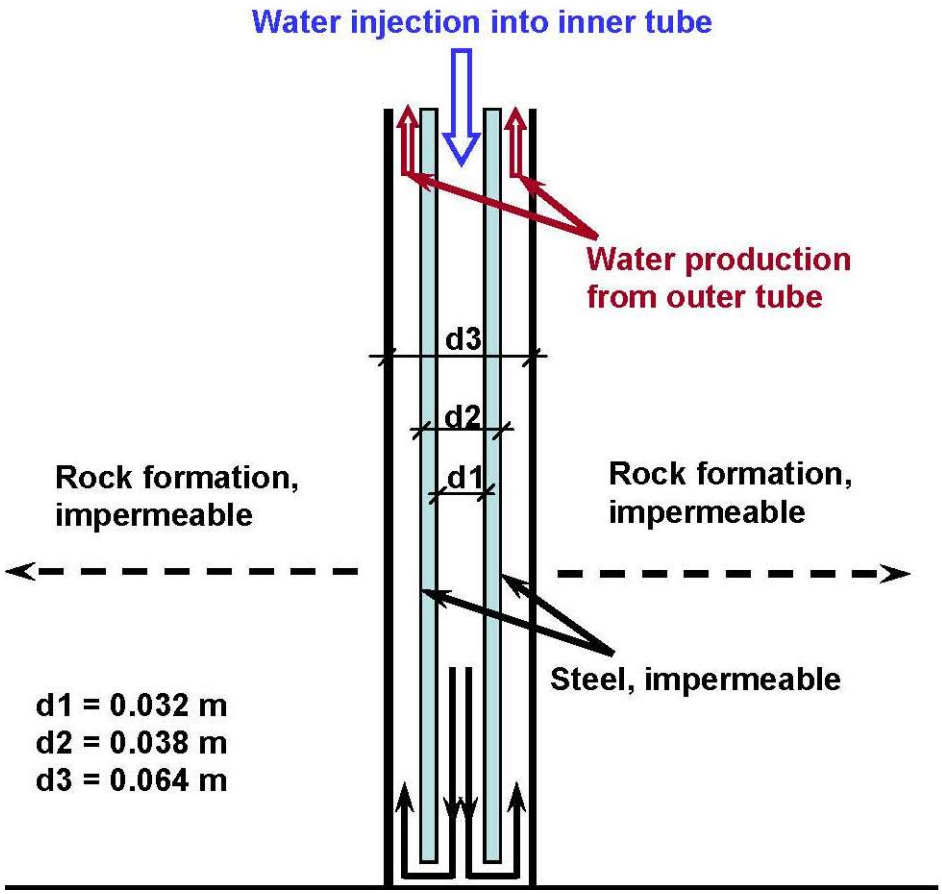

Figure 71- Model 1&2 -concentric pipe microhole configuration with preheating counter-flow heat exchange with the internal pipe flow.

Also based on Figure 71, Model 2 considered the microhole to be 1500 m/ 4920 ft long, and the temperature of the corresponding reservoir ranges from 140 to 200 ºC. The model was discretized vertically into 10 m long elements vertically, with the exception of the bottom 10 m, where finer discretization was used. Again, radial discretization was increased logarithmically, injected water was assumed to be at 50 ºC. The boundary condition at the top of the reservoir was kept at a constant pressure and temperature, and at the bottom boundary there was no fluid flow and it had

a constant temperature. Fluid injection rate into the inner tube is 2 Kg/s, the pressure at the outlet was kept constant. Simulation results used wellbore simulator.

Figures 72 and 73 show a comparison between the wellbore simulator (T2Well/EOS1) and TOUGH2/EOS1 using Darcy flow for wellbore behavior for this Model 2. The difference between the two simulations was not significant for three reasons:

1. the entire borehole was under single-phase liquid flow conditions;
2. larger differences were expected if two phases flow occurred in the microhole; and
3. there was no fluid exchange between the wellbore and the formation, ie., the mass in the system did not change.

Overall, both simulators predict that the energy flow rate will decrease with time before reaching some kind of steady state heat flow condition. However, two-phase flow conditions and high flow rates in small tubes (creating a self-regulation or choking effect) were expected for microhole EGS, in fact that was incorporated into the design. Therefore, simulation results using the modified wellbore simulator were expected to have significant differences compared to a Darcy flow simulation. The LBNL internal reports for the Models 1 and 2 simulations are provided in Appendix F, are reported in referenced [49-52] and uploaded into the GDR.

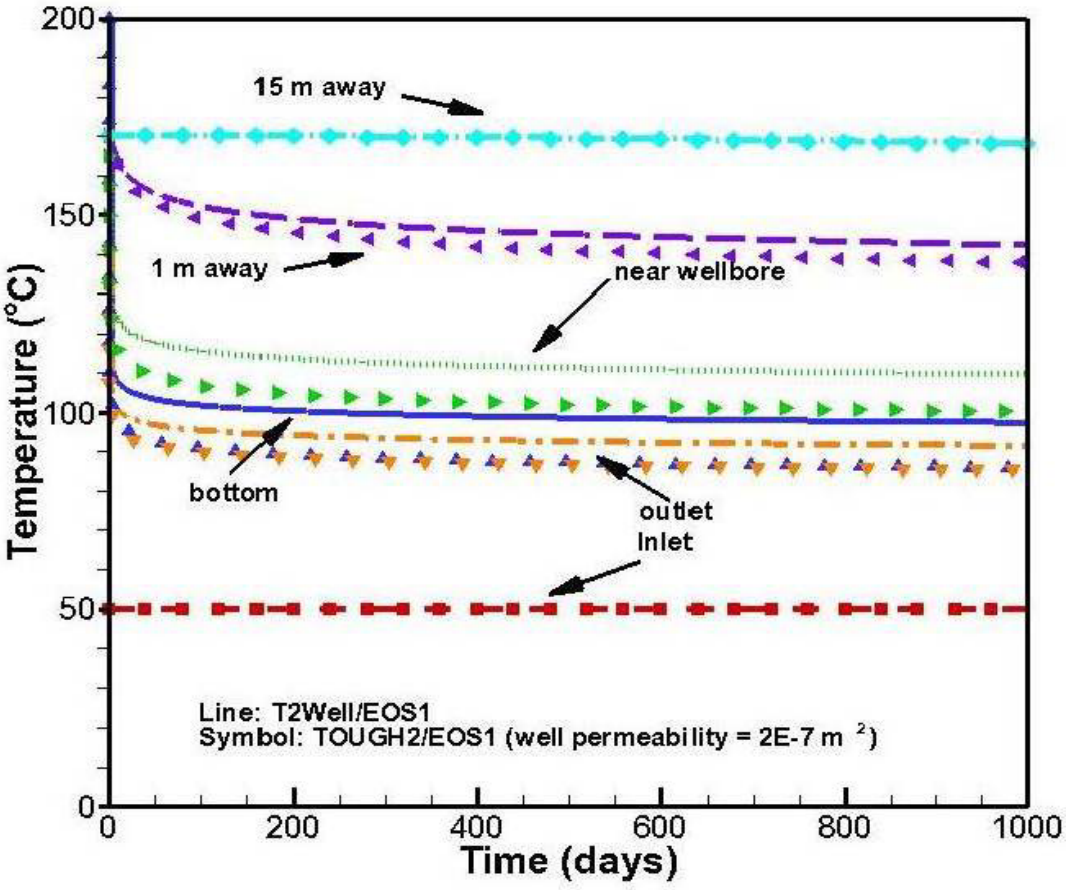

Figure 72. Model2 Results showing Formation Temperature Distribution after the 1st 1000 days of water injection. Both the full wellbore simulator (T2Well/EOS1, as lines) and the regular TOUGH/EOS1 (as points/ symbols) with the Darcy flow equation are given.

In February 2011 a more complex microbore array model (**Model 3**) was developed, see Figure 74, and simulated in March-July 2011. Geothermal reservoir parameters used for this model are listed in Table 5. Model 3 was a synthetic system that contains a doublet – an injection well and a production well, as shown in Figure 74. The two wells are 500 m apart, with a fracture zone between. The fracture zone under consideration is assumed to be 100 meters thick and 50 m wide. For the microhole design, the second wellbore, which is connected to 40 microholes, is drilled outside the fracture zone, then the 40 microholes are drilled into the fracture zone, as shown in Figure 74.

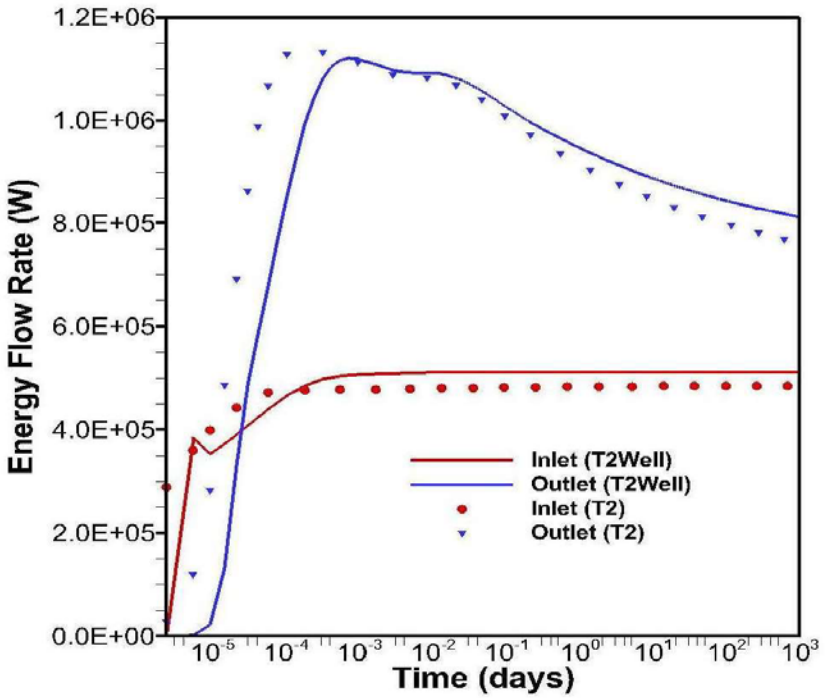

Figure 73. Model 2 Results showing Energy Flow Rate at Outlet.
Wellbore Simulator (T2Well/EOS1, as lines) and the regular TOUGH2/EOS1with Darcy flow

For Model 3, we assume that four microholes (10% of the total) missed the fracture zone and were drilled into the impermeable rock matrix. The remaining 36 microholes were able to hit the fracture zone, which was created by fracturing the first main borehole. Fluid flow in the fracture zone could reach equilibrium instantly. As a result, a single-continuum approach can be applied for this scenario. In other words, fracture properties are applied to the fracture zone, and for the rest of the model, matrix properties listed in Table 6 are used.

Figures 74 and 75 show the temperature profiles within the plane of the fracture zone at the end of 10 years for the conventional EGS design and EGS design with microholes, respectively. Figure 77 is a comparison of the temperatures of the produced fluid over time for the two designs. An additional simulation considering impermeable matrix was performed to investigate the influence of matrix permeability. Figure 78 is the comparison of the corresponding heat flux at the outlet of the production well.

Fracture permeability	1 D
Fracture porosity	0.07
Fracture depth	-4060 ~ -3960 m
Matrix permeability	0.1 mD
Matrix porosity	0.05
Injection fluid temperature	50 ºC
Geothermal gradient	40 ºC/km

Table 6: Reservoir parameters for Model 3.

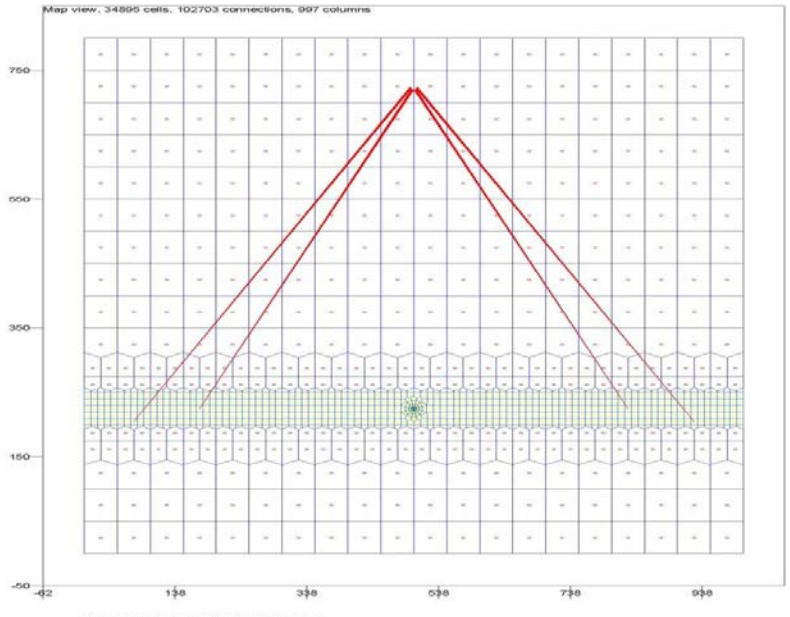

Figure 74. Model 3- Plan View with the Microhole Array (red lines). Notice- the 40 microholes are collapsed into 4 lines in this view.

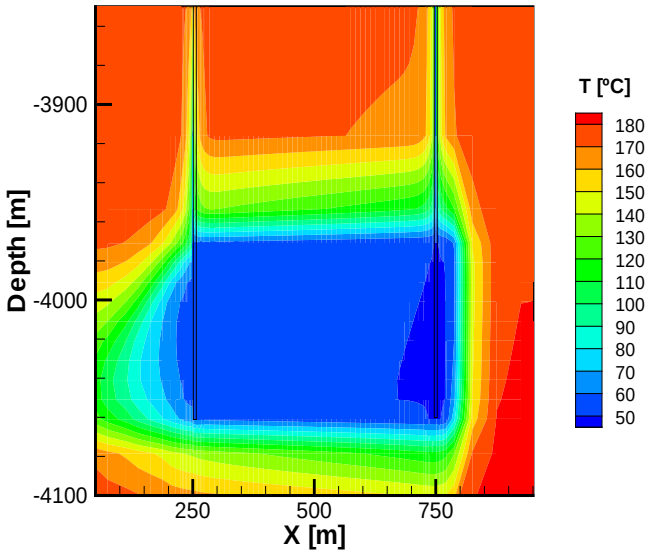

Figure 75. Model 3- Temperature Distribution for Conventional EGS Design after 10 years. The injection well is on the right.

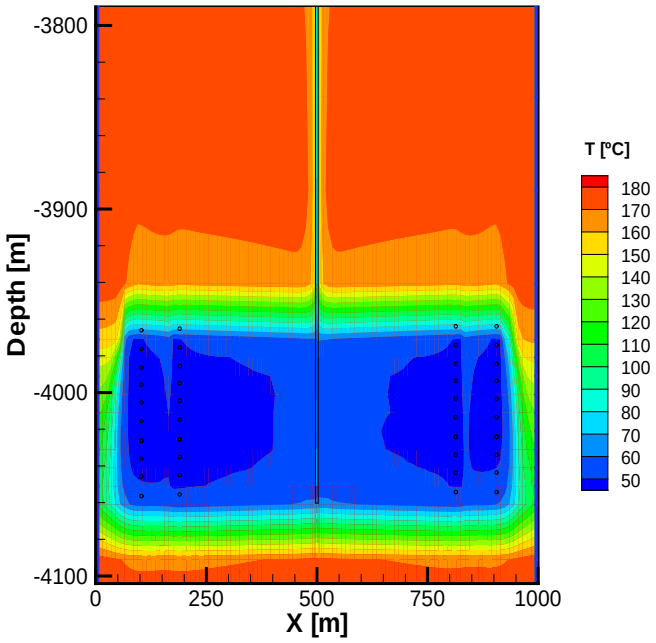

Figure 76. Model 3- Temperature Distribution for the Microhole EGS Design after10 years. Injection takes place through the microhole array.

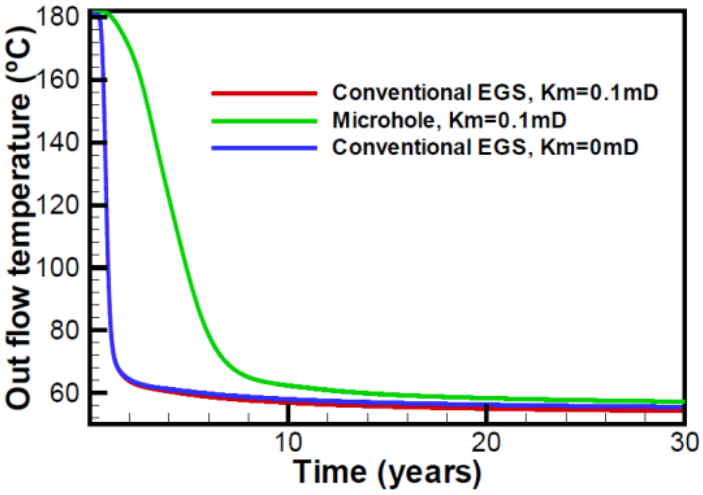

Figure 77. Model 3- Comparison of the Outflow Temperature Change over Time.

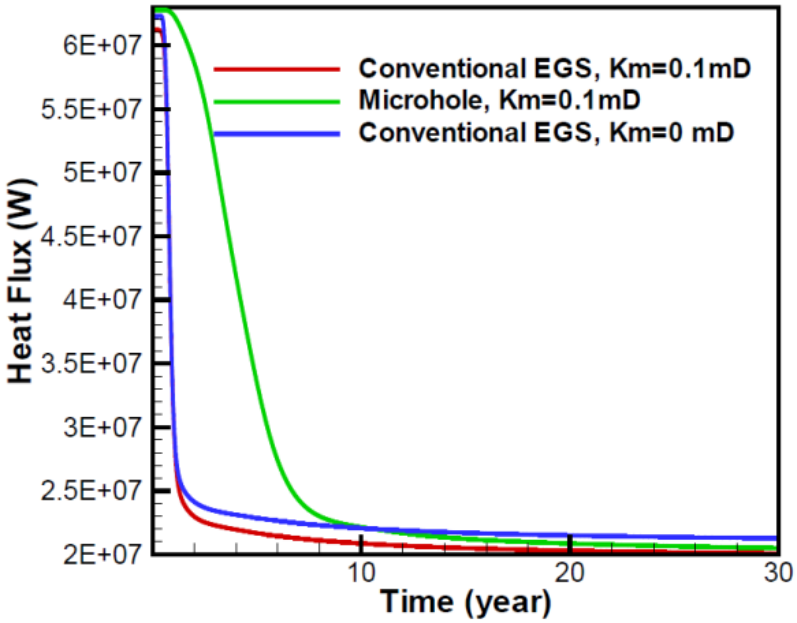

Figure 78. Model 3- Comparison of the Heat Flux at the Production Well.

Model 3 preliminary results, from Figure 77 & 78, show:

- Significant improvement in energy production can be achieved by injecting working fluids from a microhole array into the fracture network;
- When a single continuum approach is used to model the system, the energy production is not very sensitive to matrix permeability;
- For the microhole design, if some of the microholes have missed the fracture zone, the design is able to self-regulate and assign more flow to other microholes. As a result, microhole design is robust to drilling uncertainties.
- Break-through time for the microhole design is five longer than the conventional EGS configuration, based on a 120^{o}C temperature.

Model 4, based on Scenario 2 and a variant of Model 3 as seen in Figure 74, assumed that there is a fast flow path in the middle of the fracture zone. This was a very high permeability path that would show the flow self-regulation capabilities of microhole arrays. Preliminary results from Model 4, plotted in Figure 79, shows that both reservoir designs have poorer performance relative to Model 3. This is due to the high flow path leading to early thermal breakthrough. However, the microhole configuration again shows a strong improvement over the conventional EGS design, indicating robustness in EGS design.

In August 2011, LBNL started collecting geological and well data from the Soultz EGS project and developing a 3D dual permeability (K) model based on that EGS project (**Model 5**). It used all prior code developments already incorporated, including the option of with microhole arrays and without (conventional) such an array. As shown in Figures 80 and 81, there are two production wells and one injection well (in the middle) for the conventional design (Model 5a). For the microhole configuration (Model 5b), the injection wellbore is connected to 40 microholes.

By December 2011, the dual permeability model was built based on a 30 m thick fracture zone, where most flow occurs, that is approximately delineated by micro seismicity data collected at Soultz [Sausse et al., 2010]. The model domain is between -3800 m ~ -5300 m. The fracture zone is assumed to be between -4400 m ~ -4800 m. Well sections above the numerical mesh uses a semi-analytical radial heat-exchange model.

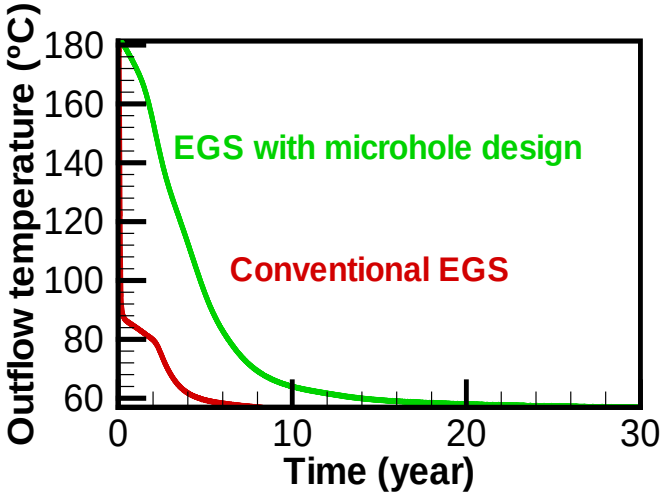

Figure 79. Model 4- Outflow Temperature.
A very high fast-flow path exists within the fracture.

For the microhole case (Model 5b), the lower part of the injection well was replaced by 40 microholes. The dual permeability zone is about 400 meters thick. The geothermal gradient is given by temperatures of T=160ºC at a depth h=-3800 m, and T=200ºC at h= -5000 m. A base case scenario is defined in which the major fault zone permeability is two orders of magnitude higher than the fracture permeability in the highly fractured system.

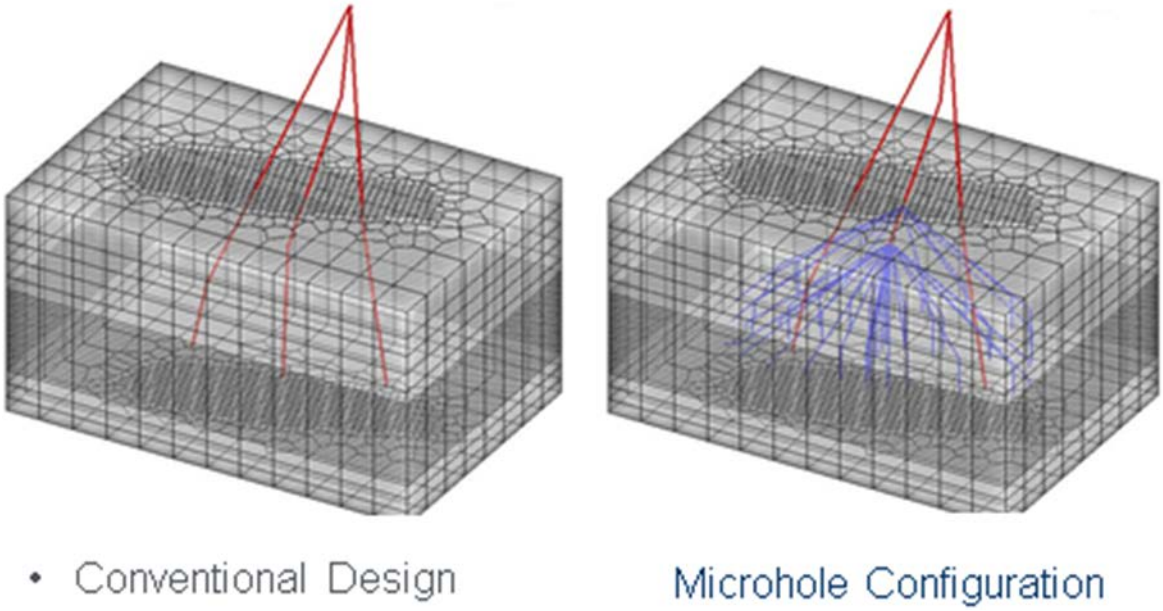

Figure 80. Model 5a & 5b are Soultz-based models

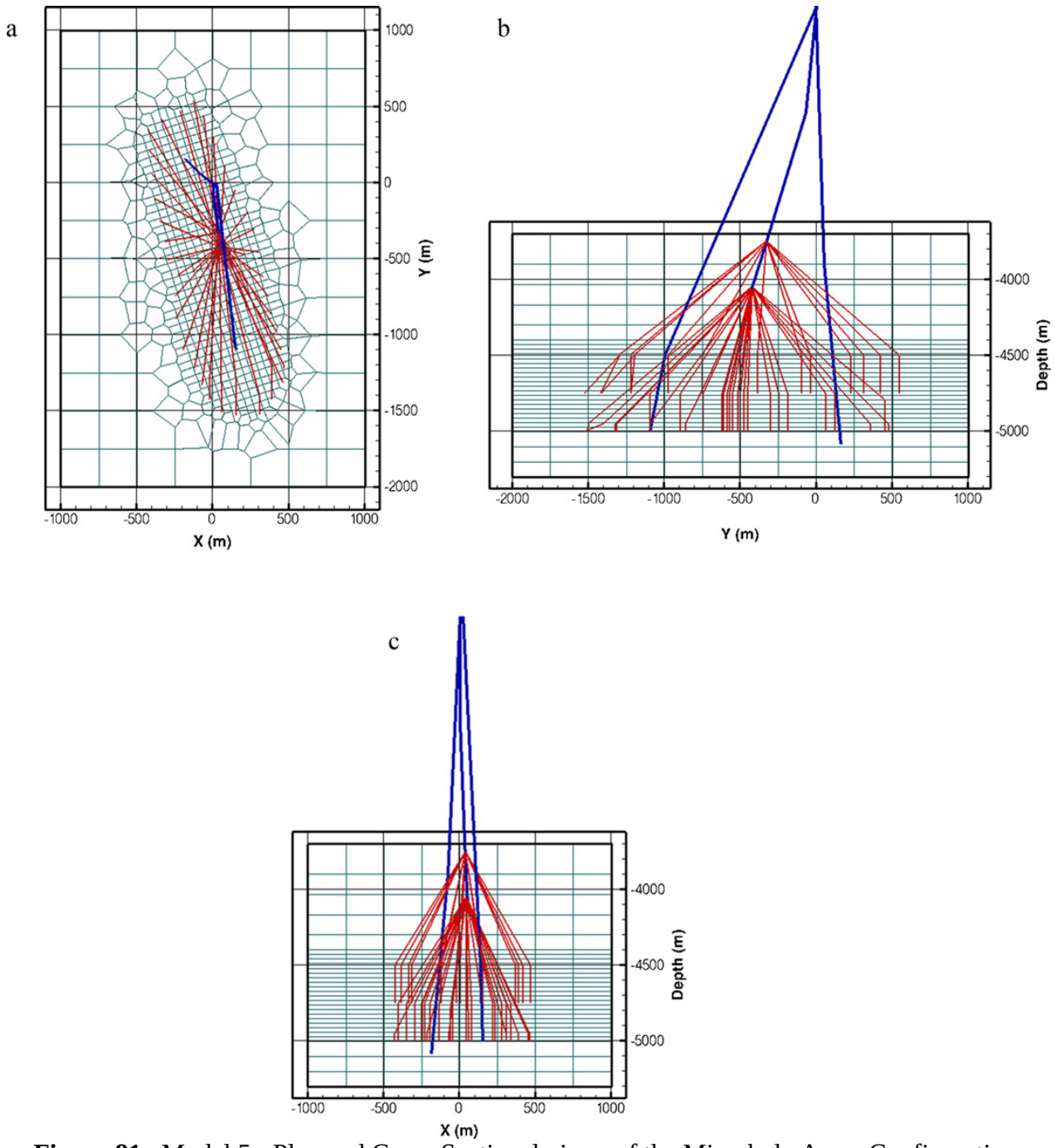

Figure 81. Model 5 - Plan and Cross-Sectional views of the Microhole Array Configuration. Conventional Wells shown in blue and Microholes shown in red. The numerical mesh is shown in green.

The temperature distributions of the model domain after 10 years for both designs is plotted in Figures 82 and 83, and for 30 years in Figure 84. Temperatures at the two production wells for

both designs are plotted in Figure 85 for 30 years only. Comparing the two designs, the production temperature using conventional EGS is higher for the first few years and lower later on as shown in Figure 85. Figure 86 shows the reason that, in the conventional EGS design, the heat mainly comes from the major fault zone, which is at the lower part of the geothermal reservoir, and thus has a higher temperature than the upper part of the reservoir. Once the heat from the fault zone is exhausted, the temperature decreases. Compared to the conventional EGS, more flow in the microhole design goes through the somewhat cooler fracture zone, which explains the lower temperature at earlier time, but provides access to a larger rock volume and allows more heat mining from the matrix of the dual permeability zone. Therefore, the temperature at the end of the ten and 30 years is higher for the microhole array system allowing for a more sustainable operation of the EGS system.

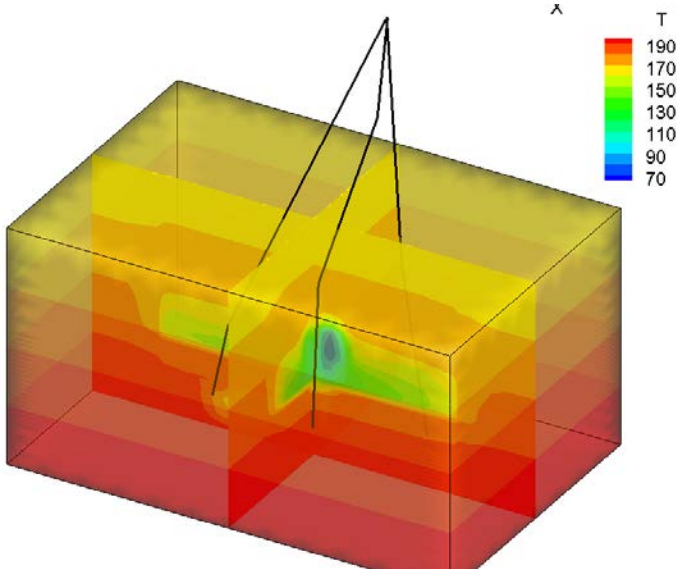

Figure 82. Model 5a- Temperature Distribution for Conventional EGS after 10 years. The injection well is in the middle of the system.

Two facets of microholes were also studied- preheating of the injected fluid and flow self-regulating between microbores in an array. In a sub-model that was developed to consider fluid flow through a 4 km long conventional well of radius 0.1 m, which is connected to forty 1.3 km long microholes of radius 0.032 m. The microholes fan out symmetrically from the central well at a 45^{o} angle for 1 km, and then become vertical for the remaining 300 m. This sub-model was very similar to the actual configuration studied in the 3D model. Water of 50^{o}C was injected at a rate of 80 kg/s; each microhole takes 2 kg/s, assuming symmetry. Fluid exited the well system at the bottom of the microholes, which is different from the scenario studied in the full model, where water may exit the microhole at any location according to the local injectivity. The formation temperature follows a geothermal gradient of 30^{o}C/km. Assuming that preheating of the working fluid in the injection well system occurs by radial heat conduction only, and that there is no interference among the microholes, we can employ a semi-analytical solution for calculating transient, radial heat exchange between a flowing wellbore and a conductive formation.

This sub-model demonstrated that preheating of the large diameter conventional well is relatively small (approximately 6°C over a flow distance of 4 km). Once the fluid enters one of the microholes, the temperature increases from 55 to above 100°C at early times, i.e., significantly more than in the upper part of the well system despite the shorter flow distance. This is due to several factors, notably the smaller flow velocity in the microholes (0.55 m/s) compared to that in the large-diameter section of the injection system (2.2 m/s), which substantially increases the heat uptake. Moreover, the microholes are located in the deeper parts of the reservoir and thus encounter higher rock temperatures. The inclination of the microholes also contributes to the

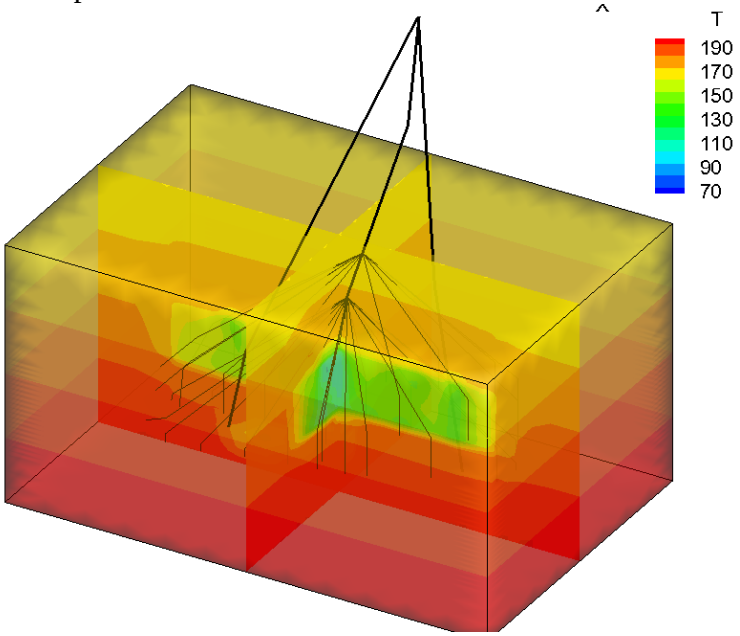

Figure 83. Model 5b- Temperature Distribution for microhole array EGS after 10 years. Injection takes place through the microhole array.

Pre-heating effect, as it prolongs the length of the flow path to reach the target depth. However, as time goes on, cooling of the rock around the microholes gradually reduces the reheating effect, with temperatures dipping below 100°C after about 4 years. After 30 years, the temperature reaches about 90°C, and the radial extent of the cooling zone around a microhole, defined as the radius with a temperature change of 50% and 10% of the total cooling amount after 30 years, is about 1 m and 15 m, respectively. This means that the rock volume from which thermal energy is extracted by conductive preheating is on the order of 105 m3 for the entire microhole array, a volume very small compared to the stimulated reservoir volume, which is on the order of 109 m3. This larger volume of hot rock could potentially be accessed by injecting the working fluid through a microhole array, thus inducing a widely distributed flow pattern in the fracture network.

The last aspect of microhole arrays is the prospect of self-regulation of flow between microholes. The fact that the total amount of injected working fluid is distributed over many microholes provides an opportunity for self-regulation. Unlike in a conventional configuration, where most of the fluid is taken up by one or a few high-injectivity features encountered by the well, microhole arrays are likely to intersect many geological features of varying injectivity. Fractures with high

permeability tend to induce high flow velocities in the vicinity of the microhole and in the microhole itself. However, high velocities in the microholes lead to turbulent flow and thus higher flow resistance that is transmitted back to the entrance of that specific microbore. As a consequence, as the pressure in one microhole increases, the injected fluid is redistributed to

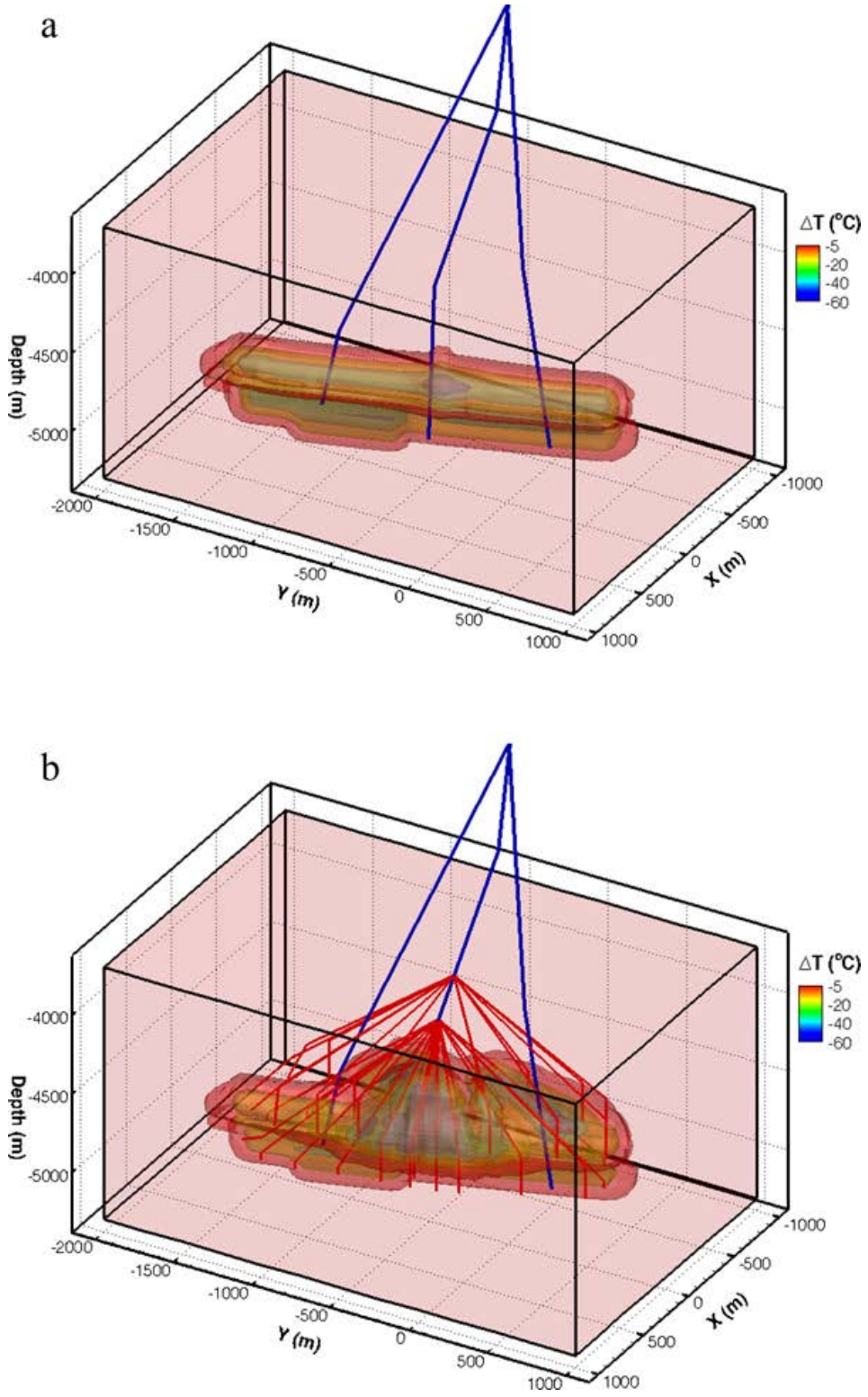

Figure 84a and b. Model 5- Simulated Temperature-Change Distribution after 30 years of exploitation for both (a) conventional and (b) microhole EGS configurations.

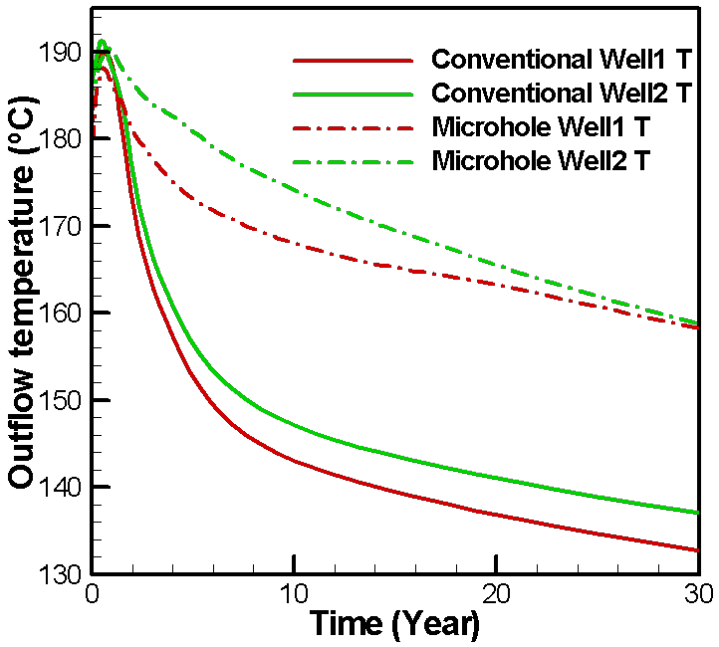

Figure 85. Model 5- Production Well Outflow Temperatures over 30 years.
For both Production Wells and both Conventional and Microhole Array EGS Designs.

other microholes, resulting in a more even and widespread distribution of injection rates. To test this hypothesis, we compare the injection-rate distribution using a standard model based on Darcy's law, where potential impacts of inertia and turbulence are neglected, and one based on the Forchheimer (1901) equation, where velocity-dependent flow resistance is accounted for. The non-Darcy flow coefficient is calculated using the model of Geertsma (1974). Accounting for velocity-dependent flow resistance in the microholes, the standard deviation of the flow rates at the head of the 40 microholes is reduced from 2.9 to 1.6 kg/s, indicating a more uniform injection distribution. We conclude that self-regulation of a microhole array reduces the sensitivity of the EGS operation to generally uncertain or unknown heterogeneity in the system, making it more robust.

Lastly in this section and based on Model 5, Figure 87 shows the outflow temperature result of a statistical analysis of the connecting flow area of the fracture-matrix that results from the intersection of various microhole angles. In all cases the microhole EGS configuration out performs the conventional EGS case, again showing robustness of the design.

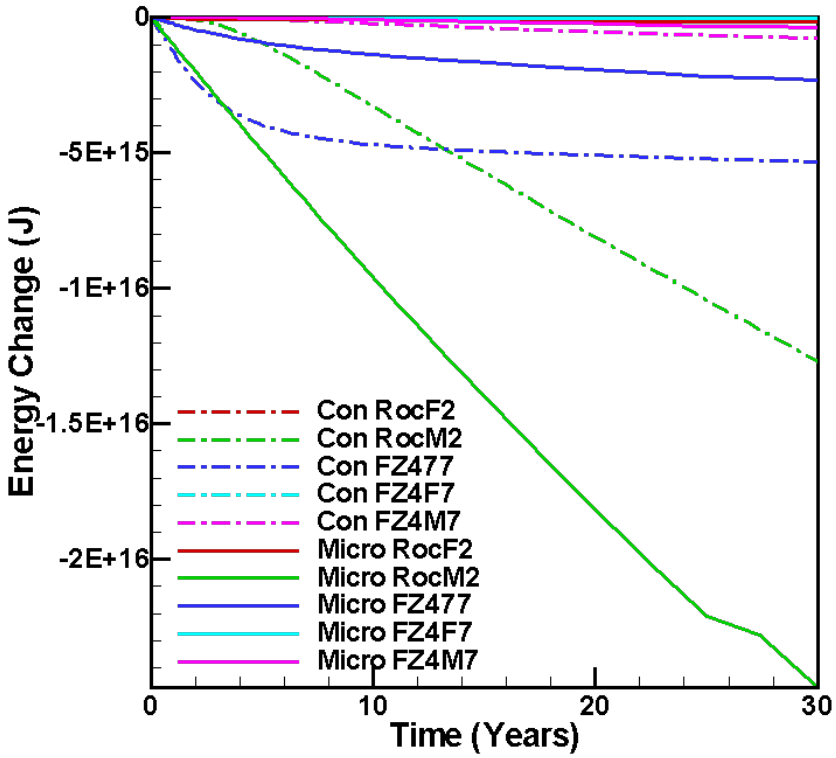

Figure 86. Model 5- Energy Change in Each Component of the EGS System- Matrix Rock, Fracture System, Microholes

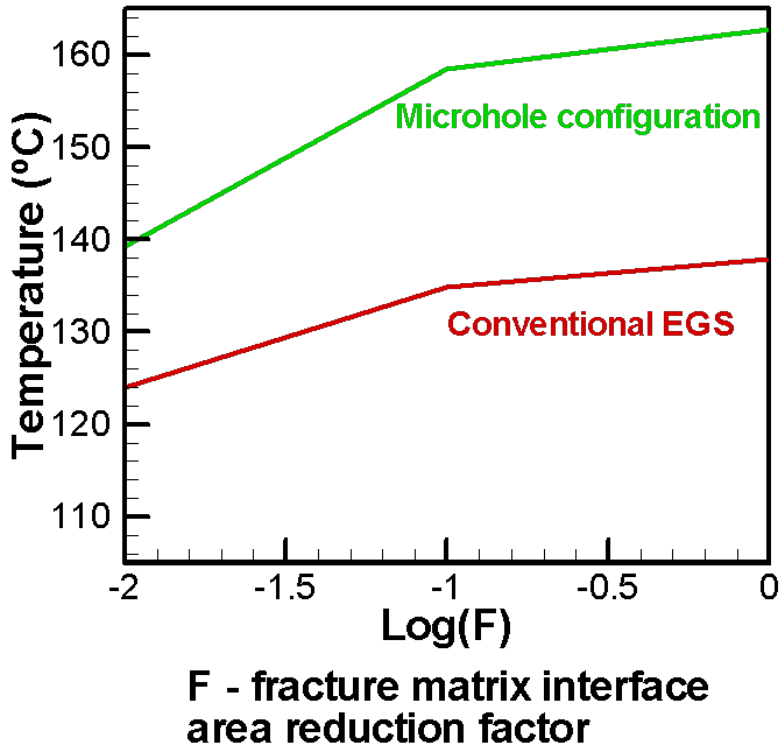

Figure 87. Model 5- Area Reduction Factor for the Fracture Interface.

Conclusions from the Simulation Efforts in Phase II-

1. Models 1 and 2 represented the self-contained heat exchanger that was found not an effective way to mine heat, even if microholes are used.

2. A microhole design like Models 3-5 has the potential to improve the heat mining efficiency compared to the conventional EGS design.

3. For a Model 3 doublet design of a conventional EGS, it is challenging to guarantee the second wellbore will hit the fracture zone. The probability that the two wells get connected may not be very high. In contrast, if some of the microholes in Model 4 missed the fracture zone, the circulating fluid can self-regulate and flow through the remaining microholes that intersect the fracture zone. Therefore, using a microhole design reduces the possibility of a failed EGS design.

4. The basic idea of improving the robustness and sustainability of an EGS using microhole arrays is conceptually demonstrated. Conditions leading to thermal breakthrough are reduced, and a larger area between the flowing working fluid and the hot rock is created by distributing injection points over a much larger volume of the reservoir.

5. The performance of the microhole-based EGS could be higher than demonstrated here for different locations of preferential flow zone and can potentially be further increased by optimizing the configuration of the microhole array. Specifically, more than only 40 microbores can be used in any given array. A given wellbore has sufficient height to allow room for over a hundred such lateral kickoffs. Also, additional arrays emanating out of the same wellbore, but going opposite directions to another pattern, are possible.

6. Flow self-regulation between microholes in a given array prevents early thermal breakthrough and provides a longer heat mining life of an EGS project.

7. Preheating of the fluids in the large diameter conventional well is relatively small (approximately $6^{o}C$ over a flow distance of 4 km).

Phase III Design & Optimize Microhole Array Deployment for EGS
Phase III, Task 1 Operation Plan for Drilling & Completion of EGS Microhole Arrays

From this work it became apparent that a low bottom-hole pressure (BHP) was essential to maintain optimal FLASH ASJ^{TM} drilling conditions. As discussed earlier in the Background Section, this is to ensure that a low density gas exists between the nozzle exit and the rock target. That strong underbalanced condition also aids in formation rock failure at the bit/ nozzle and in hole cleaning. That needed optimal BHP ranged from 100-300 psi for CO_2 and from 100 to 1000

psi for N_2. Nitrogen's larger BHP range is due to its higher injection pressure during drilling operations (needed to get density high enough to easily pump).

It is not desired to keep the full wellbore annulus at that low pressure due to possible casing failure and well control concerns. Therefore, a downhole seal or packer assembly would be needed with water, heavy brine or drilling mud in the annular space (space between the casing and tubing) and restrict the required low drilling return pressure within the tubing to the surface. It is envisioned further that the drill string pipe is inside one tubing string with a second blow-out preventer (BOP, 1st one on the casing) in-place around the drill pipe at the surface. Furthermore, is it not desired to have the return flow from the bottom depths below the packer/ seal assembly to the surface of all fluids (gases and liquids, drilling or formation) and solids (drilling or formation) occur in the tubing/drill string pipe annulus. This is because of the high velocities possible in the return flow with abrasives and gases and the possible erosive wear on the drill string. Another reason is the possibility of solids settling in that annular space and around the drill pipe if pumping were to slow stop at any time, which would stick the drill pipe in the tubing. A better solution is to have a separate tubing string designed specifically for that return flow, with a smaller diameter at bottom and a larger diameter tubing nearer the surface (see WellFlo simulation section (Phase I). This means that a 2nd tubing string must be run from the surface to the downhole packer/ seal assembly to take this return flow- to be connected to a surface adjustable choke and separation facilities (GLS, tanks, etc..). The FLASH ASJ^{TM} system is naturally underbalanced as it introduces gas into the flow stream which lightens the hydrostatic head and allows upward flow; however this drill gas flow rate may not be sufficient to lift all drill water, abrasive solids, formation liquid influx and formation rock debris as it is drilled. Additional lift may be needed and two options were identified:

1) *Gas Lift*- an additional string was envisioned that would extend from the surface to the downhole packer/ seal to allow injection of additional CO_2 or N_2 to help the return flow to the surface. CO_2 has a higher density under pressure and would inject at a lower pressure, while N_2 would provide a better return lift due to its much lower critical point. Mixing of the separately injected gas with the drilling and formation fluids and solids would occur below the packer/ seal assembly. The flow rates, pressure and velocities for different equivalent diameters can be seen in the WellFlo simulation runs in Phase I. The open dual tubing strings allow close surface monitoring of the operation. There is a limit as to how low the BHP can be maintained with gas only lifting when increasing fluid influx from the formation occurs. There is also a concern as to the feasibility of running 2 parallel tubing strings to EGS depths and sealing both within a packer/seal assembly. Concurrent running of two coiled tubing strings with the packer already assembled should be seriously considered for this application. This means that, at completion and with drilling ongoing, now 3 coiled tubing strings would be in the wellbore (the CT drill string internal to another CT).

2) *Jet Pump*- With higher influx rates additional lift methods are needed that are not dependent on gas only lift. One preferred method is based on the Hughes, W.J., and Renfro, J.J., US Patent Application #2003004048, "Down hole drilling assembly with independent jet pump", March 2003 and USPTO#6877571. In this method a jet pump would provide the means to allow a higher lift pressure above the jet pump and a lower desired pressure below the jet pump, even with solids

and gases. Since Flash ASJ™ provides a very fine (20 micron or smaller) drilled rock debris, it would pass through a properly designed jet pump orifice, although with erosional wear expected. A more incompressible fluid is needed to efficiently operate the jet pump, requiring the use of denser CO_2, water/brine or oil and not N_2. As the power fluid CO_2 turns into a gas higher in the return tubing, it will help lift the mixture to the surface. Since abrasive solids are still not desired in the same tubing string as the drill string, the jet pump assembly would be placed at the packer/ seal assembly on the return flow tubing end. The problem comes in delivering the higher pressured fluid to the jet pump. First, the transfer of the high pressure pump operating fluid from one injection tubing string to the return flow string containing the jet pump must occur through a flow path assembly within or attached to the downhole packer/ seal assembly. To pump this pressurized operating fluid down the tubing containing the drill string would require seals (outer tubing to the inner sliding drill string) both at the surface and at the downhole packer/ seal assembly. This would be possible, but difficult and would block one method of monitoring downhole operations. Alternatively, a separate operating fluid injection tubing string could be used, requiring an additional 3rd tubing string from the surface to the downhole packer/ seal assembly at depth (4 tubing strings after completion and during drilling). This could only be done with coiled tubing for all strings. The space within the normally EGS type 7" or larger internal diameter casing is not the problem, if the tubing strings are 3" or less with no external connectors.

In conclusion, methods are available to implement FLASH ASJ™ at EGS depths, but that drilling process must be proven first at the surface and then at ever increasing depths before reaching EGS depths. No operator would jump from the surface to EGS depths in just one step. Therefore, no further design or planning work was performed in this Phase and Task as all efforts were devoted toward proving the FLASH ASJ™ drilling at the surface and in shallow applications.

Phase III, Task 2 Optimized EGS Performance Using Microhole Technology

Subtask 2.1 Evaluate Intersection Probability of Microholes with Fracture Network Microbores in EGS reservoirs.

With the model development and simulations completed, in October 2012, LBNL developed a discrete fracture network using Fracman and developed an algorithm to calculate the number of intersections between the wellbore and fractures. This was used to calculate the wellbore and fracture intersection for multiple fracture network realizations. The results were used to evaluate intersection probability of microholes with fractures in a fracture network for comparison with conventional EGS injection and production wells. Model 5 was used as the basis, where half of the injection wellbore GPK3 was replaced by 40 microholes and a discrete fracture network using FracMan was generated within a square zone (1000 x 2200 x 600 m^3) that represents the stimulated fracture zone (see Figure 1). Each fracture was defined as a planar polygon in a 3-D space. The fracture distribution was simulated by a random walk process called Levy Flight (Mandelbrot, 1985), for which the length L of each step was given by a probability function. The fracture orientation was assumed to be randomly distributed along the mean trend and plunge following the univariate Fisher distribution. The fracture size was assumed to follow a uniform distribution with a mean of 100 m and a standard deviation of 50 m. All fractures were of square shape (4 sides) except for those intersected with the boundary of the fracture zone where it will be

truncated accordingly. Finally, an algorithm was developed to calculate the intersection of the wellbores with such a fracture network. Results are shown in Table 7 below.

In Table 8, intersections of the wellbores with fractures are at different dipping angles. Hitting rate is the number of intersected fractures divided by the total number of fractures. Intersection frequency is defined as the number of the intersected fractures scaled by the total length of the given wellbore(s) within the box.

The intersection probability between microholes and fractures depends on the numbers and spatial distributions of the microholes. Here, we compare one vertical conventional well (1000 m) with 11 microholes (with the same length) distributed like a fan that is perpendicular to the mean trend of the fractures.

Average dip (degree)	Total Number of fractures	Fractures intersected		Hitting rate (%)		Intersection frequency	
		GPK3	Microholes	GPK3	Microholes	GPK3	Microholes
0 (horizontal)	14414	293	7235	2.033	50.194	0.4954	0.3795
15	15085	361	6121	2.393	40.577	0.6103	0.3210
30	14707	361	6419	2.455	43.646	0.6103	0.3367
45	15256	78	4366	0.511	28.618	0.1319	0.2290
60	14891	152	3212	1.021	21.570	0.2570	0.1685
75	15450	57	2438	0.369	15.780	0.0964	0.1279
90 (vertical)	15197	51	1834	0.336	12.068	0.0862	0.0962
Average	15000.00	193.29	4517.86	0.33	30.35	0.33	0.24
STD	354.78	141.43	2114.41	0.24	14.73	0.24	0.11
STD/Average	0.02	0.73	0.47	0.73	0.49	0.73	0.47

Table 7. Wellbore/ Microhole Intersection Frequency

The fracture centers are randomly but uniformly distributed in space. Other parameters related to fracture distributions are described in Tables 8 & 9 below. For each combination of parameters, 100 realizations are generated.

	Center (m)	Size (m)
X	0.0	3000.0
Y	0.0	3000.0
Z	0.0	3000.0

Table 8. Geometry of the Fracture Zone

Figure 88 shows the relative number of intersected fractures as a function of mean dipping angles of the fractures. In the conventional vertical well case, this relative number goes down as the dipping angle of fracture goes to 90º, following the cosine curve. Dipping angle of 90º gives vertical fractures, which are parallel to vertical wellbore and are the worst case, resulting in very low intersection probability. However, in the microhole case, microholes are of multiple orientations in general and therefore are of less chance to get into the worst situation (i.e., all

wells are parallel to the mean orientation of the fractures). The intersection probability between microholes and fractures never goes as low as the one in the conventional case. This makes the microhole designs more robust than the conventional vertical wellbore design.

Parameter	Value	Note
P_{32} (m^2/m^3)	0.4	Equation (3)
Mean trend (degree)	0	Bivariate Normal Distribution STD = 10 in both trend and dipping 0 dipping angle indicating horizontal fracture
Mean dipping (degree)	0, 15, 30, 45, 60, 75, or 90	
Mean size (m)	100	Normal distribution
Deviation of size (m)	±20	
Number of sides	5	except for those intersected with the boundary of the fracture zone where it will be truncated accordingly

Table 9. Parameters used for Generating Fracture Networks.

Subtask 2.2 Develop Integrated EGS Approach Using Microhole Technology

Used modified TOUGH2 simulator with a Wellbore Simulator for non-Darcy flow in the microbores to ultimately develop a sophisticated and complex Soultz-based model to evaluate the benefits of installed microhole arrays in EGS reservoirs compared to conventional EGS systems. The robustness and heat mining benefits of using microhole arrays in EGS reservoirs was demonstrated fully in the above efforts.

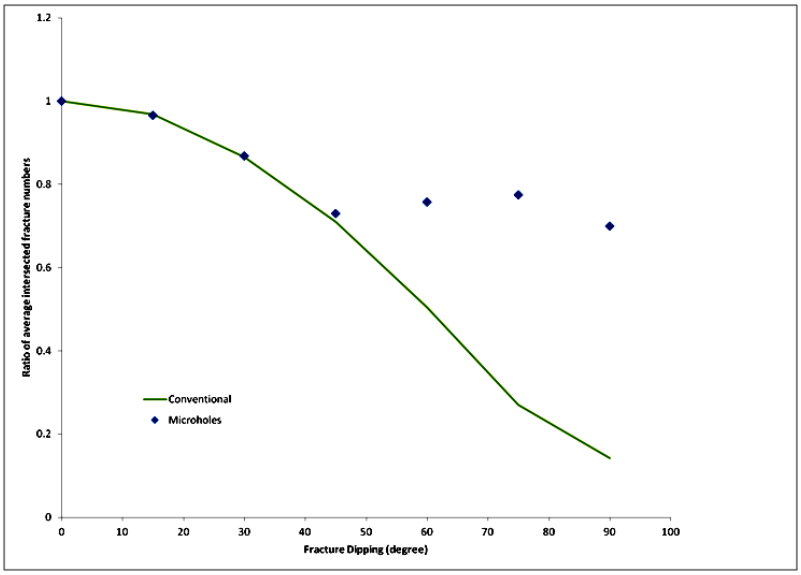

Figure 88. Fracture Incidence versus Dipping Angles of the Fractures

Phase IV Final Reporting & Technology Transfer
Phase IV, Task 1 Project Management & Reporting

Most all Quarterly financial and technical reports were filed on time. Presentations at the annual Peer Review Meetings in 2010, 2011, 2012 and 2013 were made and feedback considered. This Final Report is late to allow additional testing and drilling with the FLASH ASJ™ system. In addition the following additional deliverables were made:

Training and Professional Development-
One graduate student at the University of Tulsa earned a Master of Science degree in Mechanical Engineering from this project. One PhD candidate performed much of his graduate studies on this project.

Publications, Conference Papers, and Presentations-
"Use of Microholes in the Development of Improved Fluid Flow and Heat Transfer in EGS Reservoirs: Initial Modeling Results" by Stefan Finsterle, Yingqi Zhang, Lehua Pan, Patrick Dobson (Lawrence Berkeley National Laboratory) and Ken Oglesby (Impact Technologies LLC) at the AAPG/SPE/SEG Hedberg Conference on Enhanced Geothermal Systems, on March 14-18, 2011 in Napa, California.

"Microholes for Improved Heat Extraction from EGS Reservoirs: Numerical Evaluation", by Yingqi Zhang, Lehua Pan, Patrick Dobson (Lawrence Berkeley National Laboratory), Ken Oglesby (Impact Technologies LLC), and Stefan Finsterle (LBNL), SGP-TR-194 Proceedings of the Thirty-Seventh Workshop on Geothermal Reservoir Engineering at Stanford University, Stanford, California, on January 30 - February 1, 2012.

"Simulating Microhole-Based Heat Mining from Enhanced Geothermal Systems", by Yingqi Zhang, Lehua Pan, Patrick Dobson (Lawrence Berkeley National laboratory), Ken Oglesby (Impact Technologies LLC), and Stefan Finsterle (LBNL), TOUGH2 Symposium 2012, Berkeley, California
http://esd.lbl.gov/files/research/projects/tough/events/symposia/toughsymposium12/Zhang_Yingqi-Microholes.pdf.

"Microhole Arrays for Improved Heat Mining from Enhanced Geothermal Systems" by Stefan Finsterle, Yingqi Zhang, Lehua Pan, Patrick Dobson (all at LBNL) and Ken Oglesby (at Impact) published in *Geothermics, 47 (2013) 104-115.*

DOE Peer Review Presentations –
May 2010 in Crystal City VA, June 2011 in Bethesda MD, May 2012 in Westminster CO, April 2013 in Denver CO

Tulsa University Separation Technology Projects (TUSTP) board presentations –
"High Pressure Multiphase Slurry Flow in Micro-channels" by Ashwin Padsalgikar on May 16, 2012 at the TUSTP meeting in Tulsa OK

"Multiphase Slurry Jet Technology for Enhanced Geothermal Systems" by Thierry Groga-Bada on May 16, 2012 at the TUSTP meeting in Tulsa OK

ASME student presentations-
"High Pressure Multiphase Slurry Flow in Microchannels", by Ashwin Padsalgikar, ASME Oklahoma Symposium, March 10, 2012 in Tulsa OK
"Nozzle Geometry Optimization for High Pressure Multiphase Slurry Flows" by A. Padsalgikar, R. S. Mohan, Ph.D. and O. Shoham, Ph.D.(The University of Tulsa) and Ken Oglesby (Impact Technologies LLC) on March 2013 at the ASME Oklahoma Symposium, Tulsa Oklahoma

website www.impact2u.com

Conclusions

The original concept of the project was that multiple (100's to create an array) directionally drilled microholes (e.g., bores< 5.08cm/ 4") emanating from a 1st EGS primary large bore vertical wellbore to intersect fracture networks (natural or induced) that are hydraulically connected to a 2nd EGS large bore vertical wellbore to form a flow circuit to the surface. That full circuit creates a heat exchanger that contacts a larger volume of hot EGS rock. Several different EGS patterns or circuits can be serviced from one EGS well with multiple microhole arrays.

That concept was focused to address the DOE GTP goals of improved reservoir rock contact for higher heat transfer / mining creating more efficient EGS projects with fewer vertical large bores and longer lives and thus lower LCOE. This is because the success and sustainability of energy production from EGS largely depends on the ability of the working fluid to get in contact with a substantial volume of hot reservoir rock.

The original project objectives were:
Demonstrate EGS heat mining potential benefits in performance with microhole arrays with TOUGH2 computer simulations.
Demonstrate technologies to install such microholes in EGS systems. No known method now, but potential methods are high frequency millimeter wave directed energy, laser systems and FLASH ASJ^{TM}. This project focused on demonstrating microholes drilled with FLASH abrasive slurry jetting method.

Microhole Array Performance Simulation Efforts -
Modules linked to the TOUGH2 reservoir simulation program were coded/ modified for-

1) pre-heating above the EGS reservoir with semi-analytical methods,
2) non-darcy flow in the microholes with a modified Wellbore Simulator,
3) time/temperature memory of the reservoir rock by depth, and
4) fracture incidence.

Five microhole array EGS models were built to evaluate microhole systems-

1&2) single bore, concentric pipe/ counter flow heat exchange model (simplified and complex radial),
3&4) doublet model with and without a 40 bore microhole array, and
5) sophisticated dual permeability (Dual-K) model adapted from the Soultz EGS field geological data, with and without a 40 bore microhole array.
Extra) Soultz-based fracture network model was built for statistically estimating microbore fracture intersection probabilities.

Most all the simulation findings were earlier reported in the published 2013 *Geothermics* paper, "Microhole arrays for improved heat mining from enhanced geothermal systems" (52), but are listed herein for completeness-

- Models 1 and 2 represented the self-contained concentric heat exchanger. It was found to be not an effective way to mine EGS heat, even if microholes are used.
- The improved robustness and sustainability of an EGS using microhole arrays was conceptually demonstrated. Models 3-5 results showed that microhole arrays can make a

significant impact on long term heat transfer efficiency of EGS. Outflow temperatures of production wells, with and without a 40 microhole array, showed a 2-7 times longer life expectancy, with corresponding levels of mined heat/ energy.

- Microhole arrays offer flexibility to an EGS system by allowing for distributed flow through a larger volume of EGS reservoir rock and across a larger surface area of the fracture for improved heat exchange between the hot matrix rock and the working fluid.
- Flow self-regulation between microholes in a given array prevents early thermal breakthrough and therefore provides for a longer heat mining life of an EGS project.
- The basic idea of improving the robustness and sustainability of an EGS using microhole arrays was conceptually demonstrated.
- Microhole design is more robust to uncertainty in matrix-fracture interface area reduction factor
- Fracture Network model showed that microhole arrays can provide robustness (lower risk) in fractured EGS system development. This is because microhole arrays lower the risk that the directionally drilled bores will completely miss (i.e., NOT intersect) the fracture network that is hydraulically connected to the second well. Not connecting to the fracture network with only one bore would constitute a failed EGS design. In contrast, if some of the microholes missed the fracture zone, the circulating fluid can self-regulate and flow through the remaining microholes that intersect the fracture zone.
- For the Model 3 doublet design of a conventional EGS, it was and still is challenging to guarantee that the second wellbore will hit the fracture zone and form the flow circuit. The probability that the two wells get connected may below and the EGS system design will therefore fail. In contrast, if some of the microholes in Model 4 missed the fracture zone, the circulating fluid can self-regulate and flow through the remaining microholes that intersect the fracture zone. Therefore, using a microhole array design reduces the possibility of a failed EGS design.
- Other microhole array designs could be more beneficial than those modelled. Optimizing microhole configuration including better matching bore size and flow rates may further improve performance. Optimizing microbore count and placement on the vertical bore, within the reservoir, and connecting to the fracture system may further improve performance.
- Overall array designs could include hundreds of microholes and connect to multiple patterns out of just one main vertical, large bore wellbore. A given wellbore has sufficient height to allow room for over a hundred such lateral kickoffs, instead of just 40.
- Preheating of the fluids in the large diameter conventional well is relatively small (approximately 6^{o}C over a flow distance of 4 km).

FLASH ASJ^{TM} Drilling-

From hundreds of tests on nozzle designs, FLASH ASJ^{TM} optimal conditions, bench drilling and vertical drilling, with a variety of nozzles and rocks, the following conclusions are drawn:

- FLASH ASJ^{TM} systems (combination of FLASH supercritical fluids, abrasive materials, carrier fluids, slurry nozzles and slurry pumps) are very efficient in cutting very hard rocks. It was previously estimated to be 20 times faster than conventional cutting and drilling systems, and that estimate still holds.
- FLASH ASJ^{TM} system can cut very hard rocks with very low 5000 psi pressures. This is in contrast to water jet systems that operate at 20-40,000 psi pressures. Newer shallower rigs

operate at 5000 psi with newer deep rigs operating at up to 7500 psi mud pump pressures. This puts FLASH ASJ™ within reach of normal rig operating pressures.

- Rotation methods are apparently needed for drilling bores to any great depth. This ensures a wider cut and allows for return flow to bypass the nozzle. However, to ensure a full bore cut, FLASH ASJ™ must be combined with a motor driven bit that is specially designed for FLASH operations. This directs the long term effort toward combining FLASH ASJ™ with the patented Inverted Motors for high pressure slurry operations and/ or with conventional drilling / cutting systems, especially targeting nitrogen underbalanced drilling methods.
- Multiple FLASH fluids were identified and evaluated including air (de-oxygenated), water/ steam, CO_2, N_2 and flue gas (de-oxygenated, de-watered, and mostly N_2 and CO_2). Only CO_2 and steam has been bench tested.
    - Steam or supercritical steam is useful only at the surface, very shallow (6-10 feet) or very deep, at EGS depths. This is because it loses heat too fast in the cooler shallower depths. Conversely, it is useful at great hot depths because it can self-generate with heat from the earth, if pumped slow enough. Steam systems are the simplest to create/ equip (slurry pump and heaters only), easiest to generate (burn diesel in the heater), and may be the cheapest to utilize in the field. They have a higher safety concern due to the pressure, energized abrasive fluid with a high heat content. It must be generated and used at very high quality to be useful for FLASH drilling and cutting. Even then it has a very low multiple volume expansion, at about 5-8.
    - CO_2 is useful from the surface down to about 10,000 feet, based on the SPT WellFlo program simulation runs. Deeper than 10,000 feet CO_2's higher liquid density creates too much back-pressure on the downstream side of the FLASH nozzle for optimal FLASH ASJ cutting. CO_2 has an expansion ratio from liquid to gas that can be up to 20, making it better than N_2 or supercritical steam. CO_2 must be pumped cold then slightly heated for FLASH use. CO_2 has been used in the oilfield for hydraulic fracturing in the 1970-1980s. There are some minor freezing safety concerns.
    - N_2 is the cheapest to purchase or obtain in the field (membrane systems). N_2 is routinely used in the oilfield for drilling. It has a wide range of operational depths. It has a volume expansion factor (gas to gas) of only about 8. N_2 requires very cold pumping requirements then high heating loads to allow for FLASH use. Therefore, it has a high freezing safety concern.
- Multiple FLASH carrier fluids were evaluated, including fresh water, brine water, mineral oils, alcohols, the supercritical FLASH fluids, but fresh water was selected due to its low cost, environmentally friendly nature, variety of additive chemicals and ease of handling.
- The designed nozzles performed very good, but additional optimization of their dimensions can still occur. In particular, nozzle length, its throat diameter, entrance and exit shape can be better matched to the desired slurry flow rate. This can be based on the TU simulations now being performed and/or in further bench testing. Full cut widths of over 2" with only 1 nozzle were obtained with the right combination of nozzle and FLASH conditions (rates, gas/slurry ratios, temperature and pressure) which allow entry of a 1" or smaller nozzle and pipe. The proprietary material that one nozzle was made from and tested in this project showed little to no wear during testing. This would indicate that such nozzles would have 200 or more hours of operational life.

- The HPSP4 slurry pump with clean fluid valving performed very good for these bench and drilling FLASH ASJ™ operations. The pump can be shortened to allow for mobilization and can be made of higher alloy steels for direct CO_2 utilization. However, the pump allows for temporary drops in slurry concentration going to the nozzle during cylinder changes that needs to be reduced or eliminated.
- The induction slurry pump (denoted as HPSP5) has great potential for reducing the footprint and operational steps needed for continuous and steady FLASH ASJ™ operations. Its key components need to be purchased off the API design and / or made so that testing can begin.
- A coiled tubing (CT) rig would still be desired for deep operations because it allows continuous FLASH operations, without blow-down on joint makeups and faster tripping. In those deeper operations pipe weight would keep the pipe straight.
- In very shallow (500 ft or less) drilling operations a jointed pipe rig (very common) may be preferred. However, a CT rig with very small (1/2" - 3/4") stainless steel CT or a 2" hose CT would be desired due to the concern about CT pipe bending. Improved CT straighteners on the injection head may correct this problem, but steel has a memory.
- Coiled tubing in the 1" and 1.25" sizes are the most versatile and cheapest. With the low pressure required for CO_2 FLASH ASJ™ operations, even thinner wall CT can be used- not the case for use with N_2. Removing or "de-flashing" the internal metal weld seal in CT pipe is required for FLASH ASJ™ operation as the metal seam will be eroded and can plug the nozzle, however, deflashed CT is more expensive. As discussed above, shielded and re-enforced hoses or smaller diameter CT can be used for shallow (non-EGS) applications.
- The hydraulics to FLASH ASJ™ drill microholes vertically to great depth is theoretically possible, per the WellFlo program. However, the very narrow clearances in such a hole, and the small annular volume for controlled response, and the highly pressure underbalanced wellbore condition for FLASH ASJ™ drilling and subsequent liquid influx makes this unlikely to be accomplished. However, the hydraulics determined in the program point to the use of FLASH ASJ™ as a strong completion method, if properly designed. Other concerns-
    - Handling of formation influx so as not to lower or stop the drilling efficiency.
    - CO_2 and N_2 can form ice or hydrates downhole at the nozzle bit, based on Joules-Thompson effects with low water content. Adding more water or liquid with the slurry, adding an anti-freeze chemical, allowing higher formation fluid influx or choking the annular return flow can mitigate this problem.
    - High return velocities (estimated at greater than 1 meter per second, 180 feet/ minute) in the annulus can cause erosion of the well and pipes. This can be mitigated by proper design of the downhole return flow area (tubing/casing size) by depth, choking of the annular return flow (increased back-pressure down to the nozzle) and increased water in the slurry.
- The Operations Control C++ program is a good start in controlling FLASH ASJ™ drilling rig operations.
- Simplified directional methods and tools can be used with microhole directional drilling, especially for hitting large, close targets. In fact, such tools must be used since no other real-time tools are available in such small size holes/ pipes and at those temperatures and pressures. The Schlumberger/ CTES directional program for vertical movement would be useful in such applications.
- Impact will continue developing the FLASH ASJ™ technology for cutting and drilling, but starting in surface and shallow operations.

Acknowledgements

Department of Energy (DOE), Geothermal Technology Program (GTP), without whom many new ideas would not be tested.

Lawrence Berkeley National Laboratory (LBNL)- Dr. Stefan Finsterle, Dr. Yingqi Zhang, Dr. Lehua Pan and Dr. Patrick Dobson who did a brilliant job in developing the programming code changes, modelling three versions of microhole array systems in EGS reservoirs and developing a statistical analysis of microbores intersections with the EGS fracture.

The University of Tulsa (TU)- Dr. Dean Bellovich (in memory), Dr. Ram Mohan, Dr. Ovadia Shoham, Ashwin Padsalgikar (PhD candidate), Thierry Groga-Bada (Masters graduate student) and the Tulsa University Separation Technology Projects (TUSTP) corporate membership for their development of erosion theory and modelling of the nozzles and slurry pump.

Dr. Betty Felber, for her extensive knowledge of chemicals for the oilfield.

Dr. Dwight Rychel, for his expertise and contacts within the coiled tubing industry.

Dr. Summers at Missouri University of Science and Technology (MS&T, retired), for his extensive knowledge of and for his introduction of the PI to the depths of abrasive cutting and drilling history.

Impact Technologies- Pat Oglesby, Nick Novak, Tim Loscuito, Greg Morgan, Bryan Oglesby and Bryan McCollam for all their efforts in the development and testing of the various technologies utilized in this project.

Some are pictured below:


Folgers


BABCO

References

1. Bodvarsson, G.S., S.M. Benson, O. Sigurosson, V. Stefansson, and E.T. Elliasson, "The Krafla Geothermal Field, Iceland. I. Analysis of well tests data", *Water Resources Res.*, 20:1515–1530, 1984a.
2. Bodvarsson, G.S., K. Pruess, V. Stefansson, and E.T. Eliasson. 1984b. "The Krafla Geothermal Field, Iceland. 2. The natural state of the system", *Water Resources Res*., 20:1531–1544, 1984b.
3. DOE, Geothermal Technologies Program, Multi-Year Research, Development and Demonstration Plan, 2009–2015 with Program Activities to 2025, 2008.
4. DOE NETL, Coiled Tubing: State of the Industry and Role for NETL, Topical Report, NETL, 2005.
5. Doughty, C., "Investigation of conceptual and numerical approaches for evaluating moisture, gas, chemical, and heat transport in fractured unsaturated rock", *Journal of Contaminant Hydrology*, 38:69–106, 1999.
6. Finger, J., R. Jacobson, C. Hickox, J. Combs, G. Polk, and C. Goranson, Slimhole Handbook: Procedures and Recommendations for Slimhole Drilling and Testing in Geothermal Exploration, Report SAND99-1976, Sandia National Laboratories, Albuquerque, New Mexico, October 1999,. USA, 164 pp.
7. Finsterle, S., and K. Pruess, "Automatic history matching of geothermal field performance", *Proceedings*, 17th New Zealand Geothermal Workshop, November 8–10, pp. 193–198, Auckland, New Zealand, 1995.
8. Finsterle, S., K. Pruess, D. P. Bullivant, and M. J. O'Sullivan, "Application of inverse modeling to geothermal reservoir simulation", *Proceedings*, Twenty-Second Workshop on Geothermal Reservoir Engineering, Stanford University, Stanford, California, January 27–29, pp. 309–316, 1997.
9. Finsterle, S., and K. Pruess, "Development of inverse modeling techniques for geothermal applications", *Proceedings*, Geothermal Program Review XV, pp. 2-47–2-54, San Francisco, Calif., March 24–26, 1997.
10. Finsterle, S., K. Pruess, G. Björnsson, and A. Battistelli, "Evaluation of geothermal well behavior using inverse modeling", Faybishenko (ed.) *Dynamics of Fluids in Fractured Rocks*, Geophysical Monograph 122, pp. 377–387, American Geophysical Union, Washington DC, 2000.
11. Finsterle, S.,"Using the continuum approach to model unsaturated flow in fractured rock", *Water Resources Res.*, 36(8), 2055–2066, 2000.
12. Finsterle, S., "Multiphase inverse modeling: Review and iTOUGH2 applications", *Vadose Zone J*., 3: 747–762, 2004.
13. Finsterle, S., "Demonstration of optimization techniques for groundwater plume remediation using iTOUGH2", Environmental Modeling and Software, (21)5, 665–680, doi:10.1016/j.envsoft.2004.11.012, 2005.
14. Finsterle, S., C. Doughty, M.B. Kowalsky, G.J. Moridis, L. Pan, T. Xu, Y. Zhang, and K. Pruess, "Advanced vadose zone simulations using TOUGH", *Vadose Zone J.*, 7:601–609, doi:10.2136/vzj2007.0059, 2008.

15. Guerrero, M. T., C. Satik, S. Finsterle, and R. Horne, "Inferring relative permeability from dynamic boiling experiments", *Proceedings*, Twenty-Third Workshop on Geothermal Reservoir Engineering, Stanford University, Stanford, California, 389–396, January 26–28, 1998.
16. Hannegan, D.M., "Managed Pressure Drilling", SPE Distinguished Lecturer Presentation, 2006- 2007.
17. Kiryukhin, A.V., N.P. Asaulova, and S. Finsterle, "Inverse modeling and forecasting for the exploitation of the Pauzhetsky geothermal field, Kamchatka, Russia", *Geothermics*, 37, 540–562, doi:10.1016/j.geothermics.2008.04.003, 2008.
18. Johnson, M.O., et al., "Unique 'Through Tubing' Completions Maximize Production and Flexibility", SPE Paper 92392, Presented at the SPE/IDC Drilling Conference, Amsterdam, The Netherlands, 23–25 February, 2005.
19. Mannington, W., M. O'Sullivan, and D. Bullivant, "Computer modeling of the Wairakei-Tauhara geothermal system", New Zealand, *Geothermics*, 33(4), 401-419, 2004.
20. Maurer, W.C., Advanced Drilling Techniques, Petroleum Publishing Company, Tulsa, OK, ISBN 0-87814-117-0, 1980.
21. Tester, J.W., Anderson, B.J., Batchelor, A.S., Blackwell, D.D., DiPippo, R., Drake, E.M., Garnish, J., Livesay, B., Moore, M.C., Nichols, K., Petty, S., Toksöz, M.N. and Veatch, R.W., Jr., The Future of Geothermal Energy – Impact of Enhanced Geothermal Systems (EGS) on the United States in the 21st Century, Massachusetts Institute of Technology Press, Boston, USA, 372 pp., 2006.
22. Moridis, G. J., S. Finsterle, and J. Heiser, "Evaluation of alternative designs for an injectable barrier at the Brookhaven National Laboratory Site, Long Island, New York", *Water Resour. Res*., 35(10), 2937–2953, 1999.
23. O'Sullivan, M.J., K. Pruess, and M.J. Lippmann. 2001. "State of the art of geothermal reservoir simulation", *Geothermics*, 30:395–429, 2001.
24. Oglesby, K., Impact Technologies, "Advanced Mud System for Microhole Coiled Tubing Drilling", Final Report DE-FC26-04NT15476, March 2009.
25. Oglesby, K., US Patent Office Patent No. 7,118,349B2 and 7,794,215, "High Pressure Slurry Pumps".
26. Oglesby, K., US Patent Office Patent No. 6,920,946 and 7,055,629, "An Inverted Motor for Drilling Rocks and Man- Made Materials and for Re-entry and Cleanout of Existing Wells and Pipes".
27. Polsky, Y., Capuano Jr., L., Finger, J., Huh, M., Knudsen, S. Mansure, A.J.C., Raymond, D., and Swanson, R., Enhanced Geothermal Systems (EGS) Well Construction Technology Evaluation Report, Report SAND2008-7866, Sandia National Laboratories, December 2008.
28. Prichett, P.W., Electrical Generating Capacities of Geothermal Slim Holes, Report MTSD-DFR-98-16223, DOE/ID/13455, Maxwell Technologies Systems Division, Inc., San Diego, Calif., October 1998.
29. Pruess, K., and G.S. Bodvarsson. "Thermal effects of reinjection in geothermal reservoirs with major vertical fractures", J. Pet. Technol., 36:1567–1578, 1984.

30. Pruess, K., C. M. Oldenburg, G. J. Moridis, and S. Finsterle, S.," Water injection into vapor- and liquid-dominated reservoirs: Modeling of heat transfer and mass transport", *Proceedings*, DOE Geothermal Program Review XV, San Francisco, Calif., March 25–26, 1997.

31. Pruess, K., C. Oldenburg, G. Moridis, TOUGH2 User's Guide, Version 2.0, Report LBNL-43134, Lawrence Berkeley National Laboratory, Berkeley, Calif., 1999.

32. Pruess, K., "The TOUGH codes—a family of simulation tools for multiphase flow and transport processes in permeable media", Vadose Zone J., 3:738–746, 2004.

33. Rehn, B., et al., Managed Pressure Drilling, Gulf Publishing, 2009.

34. Summers, D.A., Waterjetting Technology, E&FN Spon, Chapman & Hall, London, 1995.

35. Zarrouk, S., M. O'Sullivan, A. Croucher, and W. Mannington, "Numerical modeling of production from the Poihipi dry steam zone: Wairakei geothermal system, New Zealand", *Geothermics*, 36. 289-303, 2007.

36. Zhang, Y. C.M. Oldenburg, and S. Finsterle, "Percolation-theory and fuzzy rule-based probability estimation of fault leakage at geologic carbon sequestration site", *Env. Earth Sci*., doi: 10.1007/s12665-009-0131-4, 2009.

37. Moe, P.H., and Rabben, K.M., US Patent Office 6,247,313 B1, "Plant for Exploiting Geothermal Energy", June 2001

38. Al Adwani, Faisal Abdullah, Ph.D. dissertation, "Mechanistic Modeling of an Underbalanced Drilling Operation Utilizing Supercritical Carbon Dioxide", Louisiana State University, August 2007.

39. Sanyal, S.K., Eduardo E. Granados, Steven J. Butler and Roland N. Horne, "An Alternative and Modular Approach to Enhanced Geothermal Systems", *Proceedings* World Geothermal Congress 2005, Antalya, Turkey, 24-29 April 2005.

40. Garg, S.K. and Jim Combs, "A study of Production/ Injection Data from Slim Holes and Large-Diameter Wells at the Okuaizu Geothermal Field, Tohoku, Japan", June 2002, INEEL/EXT-02-01429, Idaho National Engineering and Environmental Laboratory, Idaho, USA, 257 pp.

41. Gupta, Anuj, "Performance Optimization of Abrasive Fluid Jet for Completion and Stimulation of Oil and Gas Wells", *ASME Journal of Energy Resources Technology*, June 2012, Vol134/021001-1, DOI: 10.1115/1.4005775.

42. Oglesby, K.D., US patent 8,257,147, "Method and Apparatus for Jet-Assisted Drilling or Cutting".

43. Oglesby, K.D., US patent 7,569,098, "Gas-Liquid-Solids Compact Separator".

44. Woskov, P.W., and Cohn, D., US patent 8,393,419B2, "Millimeter-Wave Drilling System", March 2013.

45. Oglesby, K.D., US patent 7,934,563, "Inverted Drainholes".

46. Oglesby, K.D., US patent 8,474,529, "Concentric Tubing Directional Control".

47. Oglesby, K.D., Final Report for SBIR Phase II project DE-FG02-07ER-84670.

48. Sausse, J., C. Dezayes, L. Dorbath, A. Genter, and J. Place," 3D model of fracture zones at Soultz-sous-Foreˆts based on geological data, image logs, induced microseismicity and vertical seismic profiles". *C. R. Geoscience* 342 (2010) 531–545.

49. Finsterle, S., Zhang, Y., Pan, L., Dobson, P., and Oglesby, K., "Use of Microholes in the Development of Improved Fluid Flow and Heat Transfer in EGS Reservoirs: Initial Modeling Results", AAPG/SPE/SEG Hedberg Conference on Enhanced Geothermal Systems, March 14-18, 2011, Napa, California.

50. Zhang, Y., Pan, L., Dobson, P., Oglesby, K., and Finsterle, S., "Microholes for Improved Heat Extraction from EGS Reservoirs: Numerical Evaluation", SGP-TR-194 Proceedings of the Thirty-Seventh Workshop on Geothermal Reservoir Engineering at Stanford University, Stanford, California, on January 30 - February 1, 2012.

51. Zhang, Y., Pan, L., Dobson, P., Oglesby, K., and Finsterle, S., "Simulating Microhole-Based Heat Mining from Enhanced Geothermal Systems", TOUGH2 Symposium 2012, Berkeley CA, online at-http://esd.lbl.gov/files/research/projects/tough/events/symposia/toughsymposium12/Zhang_Yingqi-Microholes.pdf.

52. Finsterle, S., Zhang, Y., Pan, L., Dobson, P., and Oglesby, K., "Microhole Arrays for Improved Heat Mining from Enhanced Geothermal Systems", *Geothermics, 47 104-115, 2013.*

Additional Reference Documents-

Albright, J.N., Dreesen, D.S., "Microhole technology lowers reservoir exploration, characterization costs", Oil and Gas Journal 98(2), 39–41, January 10, 2000.

Bracke, R. and Wittig, V. "Design of a multi-sidetrack geothermal system based on coiled-tubing drilling technology," AAPG/SPE/SEG Hedberg Conference "Enhanced Geothermal Systems" March 14-18, 2011 – Napa, California(2011)

Coiled Tubing Manual by CTES, LP, Conroe Texas, Rev 72005

Combs, Jim, Clutter, Ted, "Slimhole Primer- Sandia National Laboratories Proves Cost-Savings and Other Attributes of Slimhole Drilling for Geothermal Exploration and Development Projects", GRC Bulletin, 2003.

Combs Jim Garg Sabodh K. ,"Discharge Capability And Geothermal Reservoir Assessment Using Data From Slim Holes", World Geothermal Congress Proceedings, Kyushu-Tohoku, Japan, 2000.

Combs, J. and Dunn, J.C., "Geothermal Exploration and Reservoir Assessment: The Need for a U.S. Department of Energy Slim-Hole Drilling R&D Program in the 1990's", Geothermal Resources Council Bulletin, Vol. 21(10), pp. 329- 337, 1992.

Combs, J. and Goranson, C., "Reservoir Evaluation Using Discharge and Injection Data from Slim Holes and Large-Diameter Production Wells at the Steamboat Hills Geothermal Field, Nevada, USA.", Proceedings World Geothermal Congress, Florence, Italy, 18-31 May, Vol. 3, pp. 1517-1524, 1995.

Cuenot, N., Dorbath, C., Dorbath, L., “Analysis of the microseismicity induced by fluid injections at the EGS Site of Soultz-sous-Forêts (Alsace, France): Implications for the characterization of the geothermal reservoir properties”, Pure and Applied Geophysics 165, 797–828, 2008.

Doughty, C.,” Investigation of conceptual and numerical approaches for evaluating moisture, gas, chemical, and heat transport in fractured unsaturated rock”, Journal of Contaminant Hydrology 38(1–3), 69–106, 1999.

Dukler, A.E., Wicks III, M. and Cleveland, R.G., “ Frictional Pressure Drop in Two-Phase Flow —B. An Approach Through Similarity Analysis”, American Institute Chemical Engineering Journal, Vol. 10, pp. 44-51, (1964).

Finger, J.T., Hickox, C.E., Eaton, R.R. and Jacobson, R.D., “Slim-hole Exploration at Steamboat Hills Geothermal Field”, Geothermal Resources Council Bulletin, Vol. 23(3), pp. 97-104, 1994.

Finger, J.T., Jacobson, R.D., Hickox, C.E., and Eaton, R.R., “Slimhole Drilling for Geothermal Exploration”, Proceedings World Geothermal Congress, Florence, Italy, 18-31 May 1995, Vol. 2, pp. 1473-1477.

Finger, J.T., Jacobson, R.D., and Hickox, C.E., “Vale Exploratory Slimhole: Drilling and Testing”, Report SAND96- 1396, June, Sandia National Laboratories, Albuquerque, NM, 1996.

Finger, J.T., Jacobson, R.D., and Spielman, P.B., “Newberry Exploratory Slimhole”, Geothermal Resources Council Transactions, Vol. 21, pp. 97-102, 1997.

Finsterle, S., “Parallelization of iTOUGH2 Using PVM”, Report LBNL-42261, Lawrence Berkeley National Laboratory, Berkeley, California, USA, 37 pp, 1998.

Finsterle, S., “Multiphase inversion modeling: Review and iTOUGH2 applications”, *Vadose Zone Journal* 3, 747–762, 2004.

Finsterle S., Witherspoon, P.A., “Implementation of the Forchheimer Equation in iTOUGH2”, Project Report, Witherspoon Inc., Berkeley, California, USA, 43 pp, 2001.

Finsterle, S., Zhang, Y., “Solving iTOUGH2 simulation and optimization problems using the PEST protocol”, Environmental Modelling and Software 26, 959–968, 2011. doi:10.1016/j.envsoft.2011.02.008.

Garg, S.K. and Combs, J., “Production/Injection Characteristics of Slim Holes and Large-Diameter Wells at the Sumikawa Geothermal Field, Japan”, Proceedings Twentieth Workshop on Geothermal Reservoir Engineering, 24-26 January, Stanford University, Stanford, California, pp31-39, 1995.

Garg, S.K. and Combs, J., "Use of Slim Holes with Liquid Feedzones for Geothermal Reservoir Assessment", *Geothermics*, Vol. 26(2), pp. 153-178, 1997.

Garg, S.K., Combs, J. and Abe, M., " Study of Production/Injection Data From Slim Holes and Large- Diameter Production Wells at the Oguni Geothermal Field, Japan", Proceedings World Geothermal Congress, Florence, Italy, 18-31 May, Vol. 3, pp. 1861-1868, 1995a.

Garg, S.K., Combs, J. and Goranson, C. "Use of Slim Holes for Geothermal Reservoir Assessment: An Update", Proceedings Seventeenth New Zealand Geothermal Workshop, The University of Auckland, Auckland, 8-10 November, pp. 151-156, 1995b.

Garg, S.K., Combs, J., Ozawa, F. and Gotoh, H., "A Study of Production/Injection Data from Slim Holes and Large-Diameter Wells at the Takigami Geothermal Field, Kyushu, Japan", Geothermal Resources Council Transactions, Vol. 20, pp. 491-502, 1996.

Garg, S. K., Combs, J., Kodama, M., and Gokou, K., "Analysis of Production/Injection Data from Slim Holes and Large-Diameter Wells at the Kirishima Geothermal Field, Japan", Proceedings Twenty-Third Workshop on Geothermal Reservoir Engineering, 26-28 January. Stanford University, Stanford, California, pp. 64-76, 1998.

Garg, S.K., Combs, J., "Appropriate use of USGS volumetric 'heat in place' method and Monte Carlo calculations". In: Proceedings of the 34th Workshop on Geothermal Reservoir Engineering, Stanford University, Stanford, California, USA, pp. 80–86, 2010.

Gérard, A., Kappelmeyer, O., "The Soultz-sous-Forêts project", Geothermics 16 (4), 393–399, 1987.

Geertsma, J., "Estimating the coefficient of inertial resistance in fluid flow through porous media", Soc. Pet. Eng. J., 445–450, 1974.

Grant, M.A., Garg, S.K.,"Recovery factor for EGS", Proceedings of the 37th Workshop on Geothermal Reservoir Engineering, Stanford University, Stanford, California, USA, pp. 738–740,2012.

Hadgu, T., Zimmermann, R.W. and Bodvarsson, G.S. (1994), "Theoretical Studies of Flowrates from Slimholes and Production-Size Geothermal Wells", *Proceedings* Nineteenth Workshop on Geothermal Reservoir Engineering, 18-20 January. Stanford University, Stanford, California, pp. 253-260.

Heuze, F., 1995. "Slimhole Drilling and Directional Drilling for On-Site Inspections Under a Comprehensive Test Ban – An Initial Assessment". Report UCRL-ID-121295, Lawrence Livermore National Laboratory, Livermore, California, USA, 16 pp

Hughes, W.J., and Renfro, J.J., US Patent Application #2003004048 and #6877571, "Down hole drilling assembly with independent jet pump", March 2003.

Hughmark, G.A. (1962). “Holdup in Gas-Liquid Flow”, Chemical Engineering Progress, Vol. 53, pp. 62-65

International Formulation Committee, “A Formulation of the Thermodynamic Properties of Ordinary Water Substance”, IFC Secretariat, Düsseldorf, Germany, 34 pp, 1967.

Johnson, M.O., Hyatt, P.G., 2005, “ Unique ‘through tubing’ completions maximize production and flexibility”, SPE Paper 92392, presented at the SPE/IDC Drilling Conference, Amsterdam, The Netherlands, 23–25 February, 2005.

Liu, H.H., Doughty, C., Bodvarsson, G.S., 1998, “An active fracture model for unsaturated flow and transport in fractured rocks”, Water Resour. Res. 34(10), 2633–2646.

Maurer, W.C., 1980. Advanced Drilling Techniques. Petroleum Publishing Company, Tulsa, OK, ISBN 0-87814-117-0, 698 pp.

McSpadden, A, Newman K, “Development of a Stiff-String Forces Model for Coiled Tubing”, SPE74831, SPE/ ICoTA Coiled Tubing Conference and Exhibition, Houston TX April 2002

McDermott, C.I., Randriamanjatosoa, A.R.L., Tenzer, H., Kolditz, O., 2006, “ Simulation of heat extraction from crystalline rocks: The influence of coupled processes on differential reservoir cooling”, *Geothermics* 35(3), 321–344.

Michelet, S., Toksöz, M.N., 2007, “Fracture mapping in the Soultz-sous-Forêts geothermal field using microearthquake locations”, Journal of Geophysical Research 112, B07315, pp. 14, doi:10.1029/2006JB004442.

Morris, M.D., 1991, “ Factorial sampling plans for preliminary computational experiments”, *Technometrics* 33(2), 161–174.

Nalla, G. and Shook, G.M. (2004). “Engineered geothermal systems using advanced well technology,” *Geothermal Resources Council Transactions*, 28, 117-124.

Narasimhan, T.N., Witherspoon, P.A., 1976, “An integrated finite difference method for analyzing fluid flow in porous media”, Water Resources Research 12, 57–64.

Newman, K., “Coiled-Tubing Stretch and Stuck-Point Calculations”, SPE 54458, SPE/ICoTA Coiled Tubing Roundtable, Houston, Texas, May 1999.

Newman, K, Sathuvali, UB, Wolhart, S, “Elongation of Coiled Tubing during its Life”, SPE3808, 2nd North American Coiled Tubing Roundtable, Montogomery TX, April 1997

Newman, K, Aasen, Jan, “Catastrophic buckling of Coiled Tubing in the Injector”, SPE46007, 1998 SPE/ ICoTA Coiled Tubing Roundtable, Houston TX, April, 1998

Oglesby, K., 2009, " Advanced Mud System for Microhole Coiled Tubing Drilling", Final Technical Report, DE-FC26-04NT15476, 97 pp.

Pan, L., Oldenburg, C.M., Pruess, K., Wu, Y.S., 2011, " Transient CO_2 leakage and injection in wellbore-reservoir systems for geologic carbon sequestration", Greenhouse Gases: Science and Technology 1(4), 335–350.

Pritchett, J.W. " WELBOR: A Computer Program for Calculating Flow in a Producing Geothermal Well", Report No. SSS-R-85-7283, S-Cubed, La Jolla, California, 1985.

Pritchett, J.W., "Preliminary Study of Discharge Characteristics of Slim Holes Compared to Production Wells in Liquid-Dominated Geothermal Reservoirs", *Proceedings* Eighteenth Workshop on Geothermal Reservoir Engineering, 26-28 January. Stanford University, Stanford, California, pp.181-187, 1 993

Pritchett John W. "Preliminary Estimates of Electrical Generating Capacity of Slim Holes a Theoretical Approach", *Proceedings*, Twentieth Workshop on Geothermal Reservoir Engineering, Stanford University, Stanford, California, January 1995, SGP-TR-150

Pritchett, J.W., 1998, " Electrical Generating Capacities of Geothermal Slim Holes", Report MTSD-DFR-98-16223, Maxwell Technologies Systems Division, Inc., San Diego, California, USA, 7 pp.

Pritchett, J.W. (1995). "Preliminary estimates of electrical generating capacity of slim holes – a theoretical approach," *Proceedings*, Twentieth Workshop on Geothermal Reservoir Engineering, 41-46.

Pritchett, John W., "Electrical Generating Capacities of Geothermal Slim Holes", DE-FG-961DI 3455 Final Report, Maxwell Technologies Systems Division Inc., MTSD-DFR-98-I 6223 WIO 11438, October 1998

Pruess, K., Narasimhan, N.T., 1982, "On fluid reserves and the production of superheated steam from fractured, vapor-dominated geothermal reservoirs", J. Geophys. Res. 87(B11), 9329–9339.

Pruess, K., Narasimhan, N.T., 1985, "A practical method for modeling fluid and heat flow in fractured porous media", Soc. Pet. Eng. J. 25(1), 1567–1578.

Pruess, K., Oldenburg, C., Moridis, G., 1999. TOUGH2 User's Guide, Version 2.0. Report LBNL-43134, Lawrence Berkeley National Laboratory, Berkeley, California, USA, 210 pp

Quigley, MS, Stone, LR, "The Benefits of Real-Time Coiled Tubing Diameter Measurements", SPE46040, 1998 SPE/ICoTA Coiled Tubing Roundtable, Houston TX, April 1998.

Saltelli, A., Ratto, M., Andres, T., Campolongo, F., Cariboni, J., Gatelli, D., Saisana, M., Tarantola, S., 2008, "Global Sensitivity Analysis, the Primer", John Wiley & Sons Ltd., West Sussex, England, 292 pp.doi:10.2118/92392--MS.

Sanyal, S.K., Butler, S.J., 2005, " An analysis of power generation prospects from enhanced geothermal systems", Transactions Geothermal Resources Council 29, 131–138.

Sanyal, S.K., Granados, E.E., Butler, S.J., Horne, R.N., 2005, "An alternative and modular approach to enhanced geothermal systems",Transactions Geothermal Resources Council 29, 139–144.

Sausse, J., Dezayes, C., Dorbath, L., Genter, A., Place, J. "3D model of fracture zones at Soultz-sous-Forêts based on geological data, image logs, induced microseismicity and vertical seismic profiles", C. R. Geoscience 342, 531–545, 2010.

Schulte, T., Zimmermann, G., Vuataz, F., Portier, S., Tischner, T., Junker, R., Jatho, R. and Huenges, E. (2010), "Enhancing Geothermal Reservoirs," Geothermal Energy Systems, Wiley-VCH, pp. 173-244.

Stauffer, P.H., Stein, J.S., Travis, B.J., 2003,"The Correct Form of the Energy Balance for Fully Coupled Thermodynamics in Liquid Water", Report LA-UR-03-1555, Los Alamos National Laboratory, Los Alamos, New Mexico, USA, 9 pp.

Summers, D., Oglesby, K., Galecki,G.,Woelk,K.,2007, "Method and Apparatus for Jet-Assisted Drilling and Cutting", US patent application 12/400,507; issued.

Tipton, S., "The Varying Modulus of Elasticity for Coiled Tubing Material", SPE54461, 1999 SPE/ ICoTA Coiled Tubing Roundtable, Houston, May 1999.

Vogt, C., Kosack, C., Marquart, G., 2012, "Stochastic inversion of the tracer experiment of the enhanced geothermal system demonstration reservoir in Soultz-sous-Forêts—Revealing pathways and estimating permeability distribution", *Geothermics* 42, 1–12.

Warren, J.E., Root, P.J., 1963. "The behavior of naturally fractured reservoirs", Society of Petroleum Engineering Journal Transactions, AIME 228, 245–255.

Zhang, Y., Pan, L., Pruess, K., Finsterle, S., 2011, "A time-convolution approach for modeling heat exchange between a wellbore and surrounding formation", *Geothermics* 40(4), 261?/251–266, doi:10.1016/j.geothermics.2011.08.003.

Zhou, Zhengcai Anhui "Blasting Device for Premixed Abrasive Slurry Jet", USPTO 2008/0299876 A1, pending, Dec 2008

Appendices
Appendix A
Properties of Nitrogen and Carbon Dioxide for FLASH ASJ™

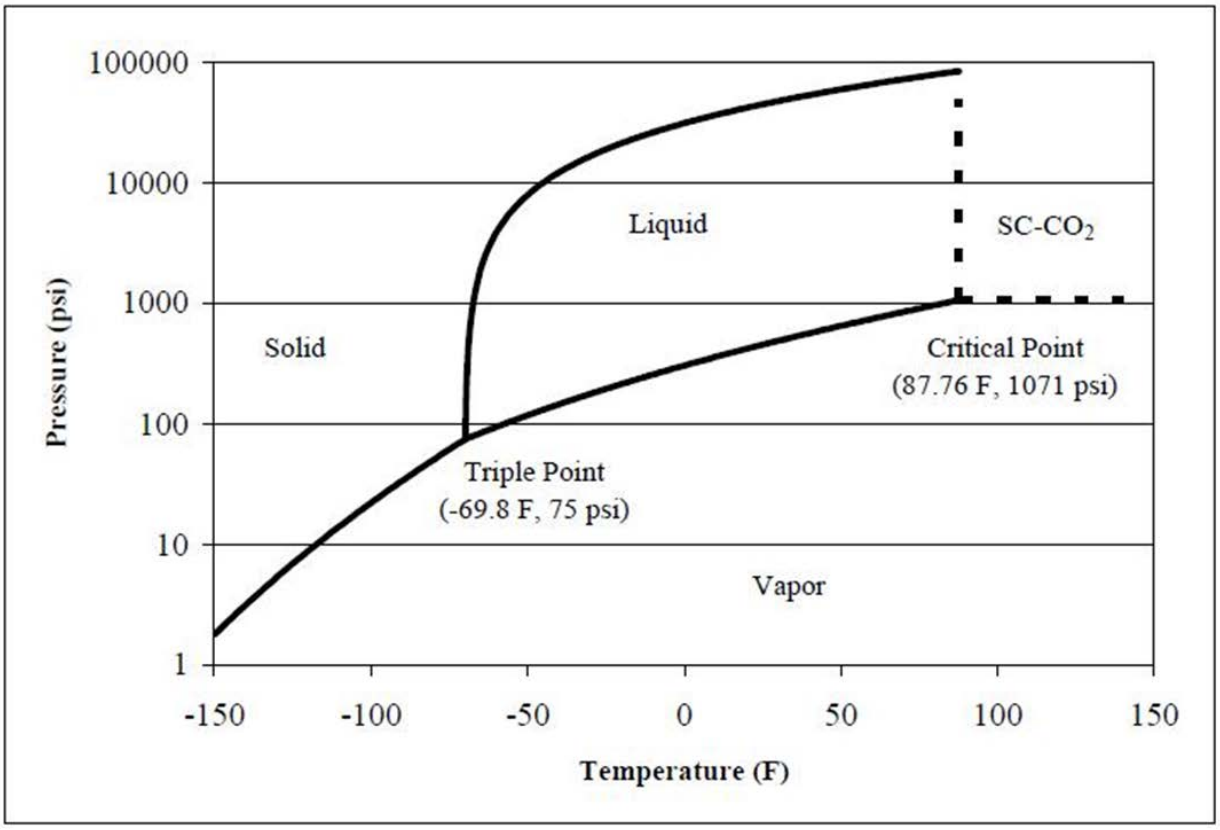

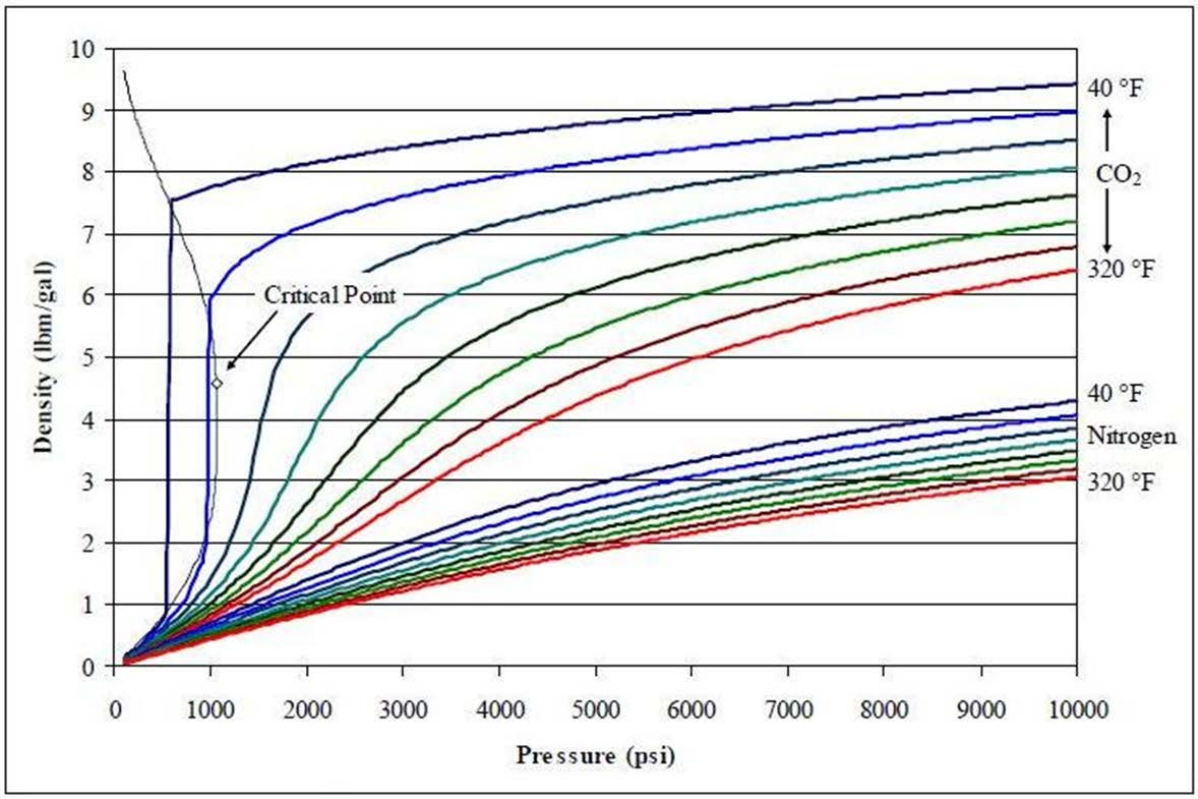
Density (lbm/gal)
Pressure (psi)
Critical Point
40 °F
CO2
320 °F
40 °F
Nitrogen
320 °F

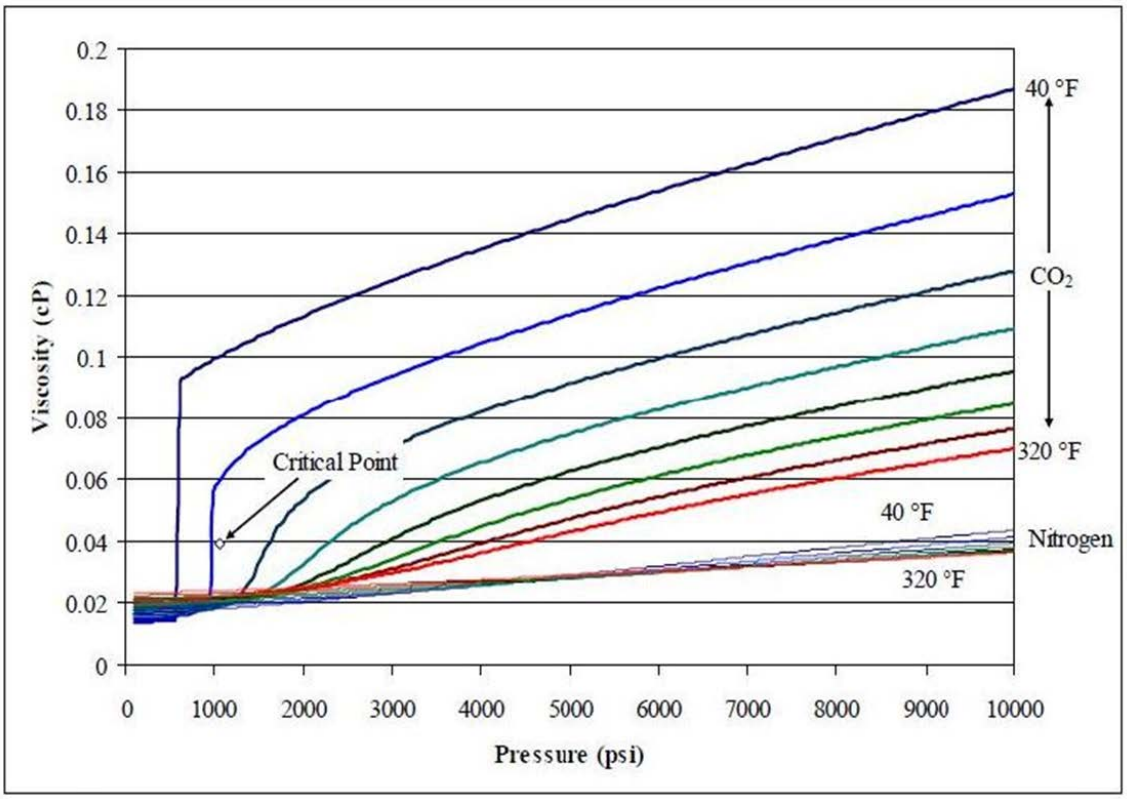
Viscosity (cP)
Pressure (psi)
Critical Point
40 °F
CO2
320 °F
40 °F
Nitrogen
320 °F

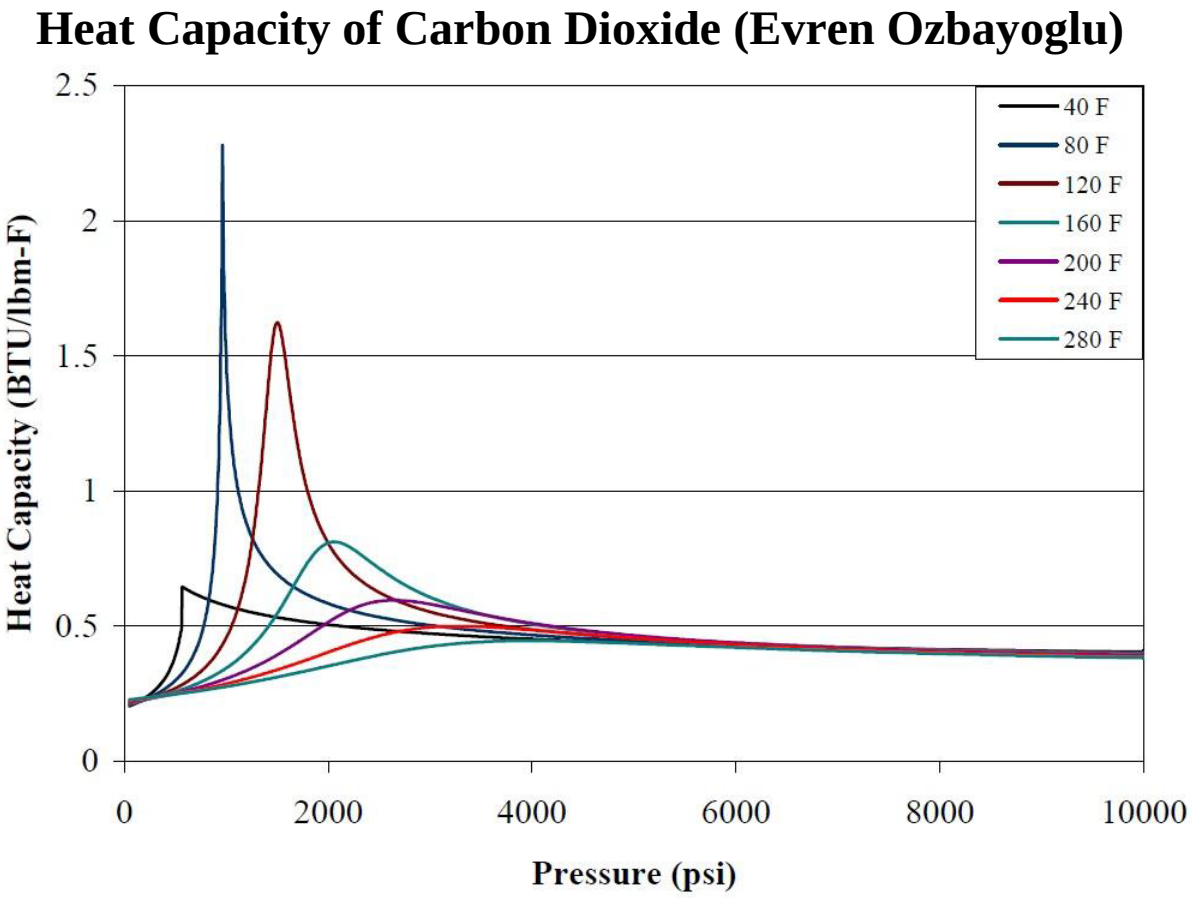
Heat Capacity of Carbon Dioxide (Evren Ozbayoglu)
Heat Capacity (BTU/lbm-F)
2.5
2
1.5
1
0.5
0
0
2000
4000
6000
8000
10000
Pressure (psi)
40 F
80 F
120 F
160 F
200 F
240 F
280 F

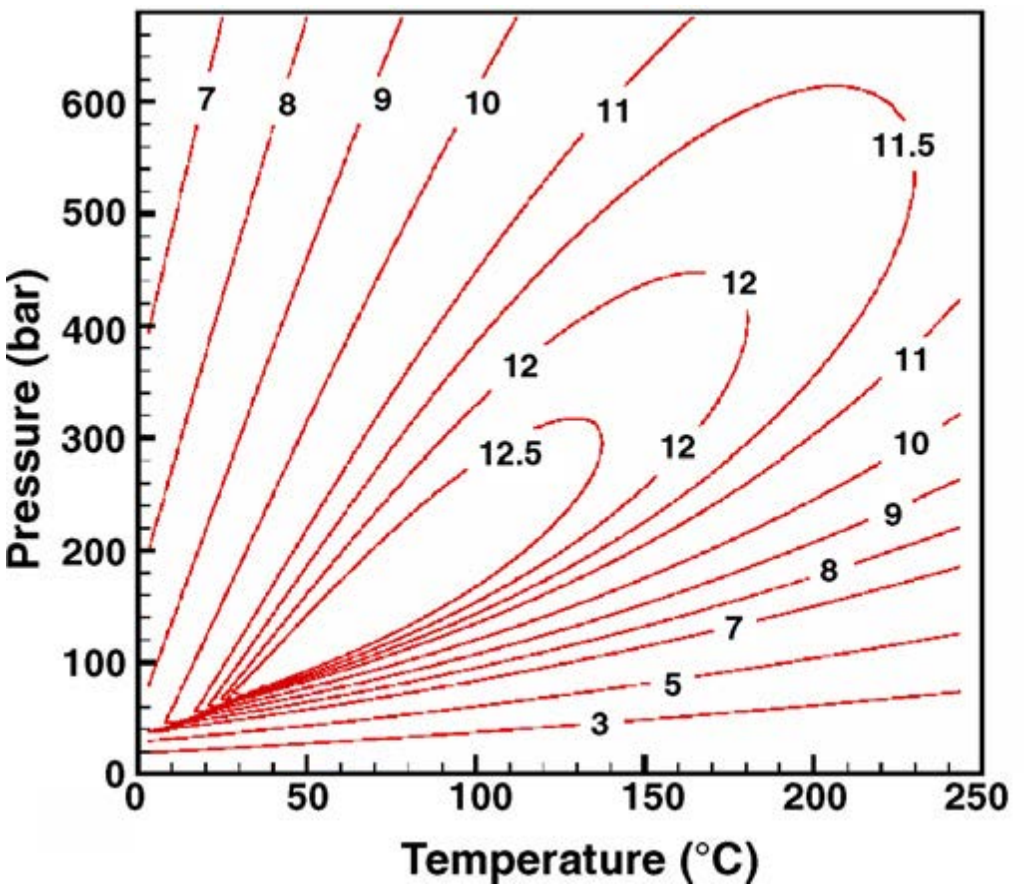

Ratio of CO_2 fluid density to viscosity (ie., inverse kinematic viscosity) in units of 10^6 s m^{-2} (Pruess, 2008) as possible EGS working fluid as well.

Appendix B

Two WellFlo Drilling Simulation Cases at 20,000 feet
Full MSI Report runs are uploaded into GDR

Nitrogen WellFlo Simulation Run-

Total Depth: 20,000 ft
QN2= 8 gpm AND Qslurry= 1 gpm
Coiled Tubing: 1.25”OD
Surface Pipe: 0-5000 ft, Casing ID:5’’
Hole Size: 2.5’’ from 5000 ft to TD
ΔPnozzle= 6000 psi fixed by design
Water Influx=0 gpm

Other Input Parameters

	CASE-1		CASE-2
	N2 Only	N2&Water	All Runs
Formation	Sandstone	Sandstone	Sandstone
Geothermal Gradient (°F/ft)	0.015	0.015	0.015
Surface Temperature (°F)	60	60	60
Injected Fluid Temperature (°F)	75	75	75
Return Choke Pressure (psia)	50	50	50
Nozzle Pressure Drop (psi)	7500	5000	8000
Cutting Size (micron)	25-100	25-100	25-100
ROP (ft/hour)	400	400	400

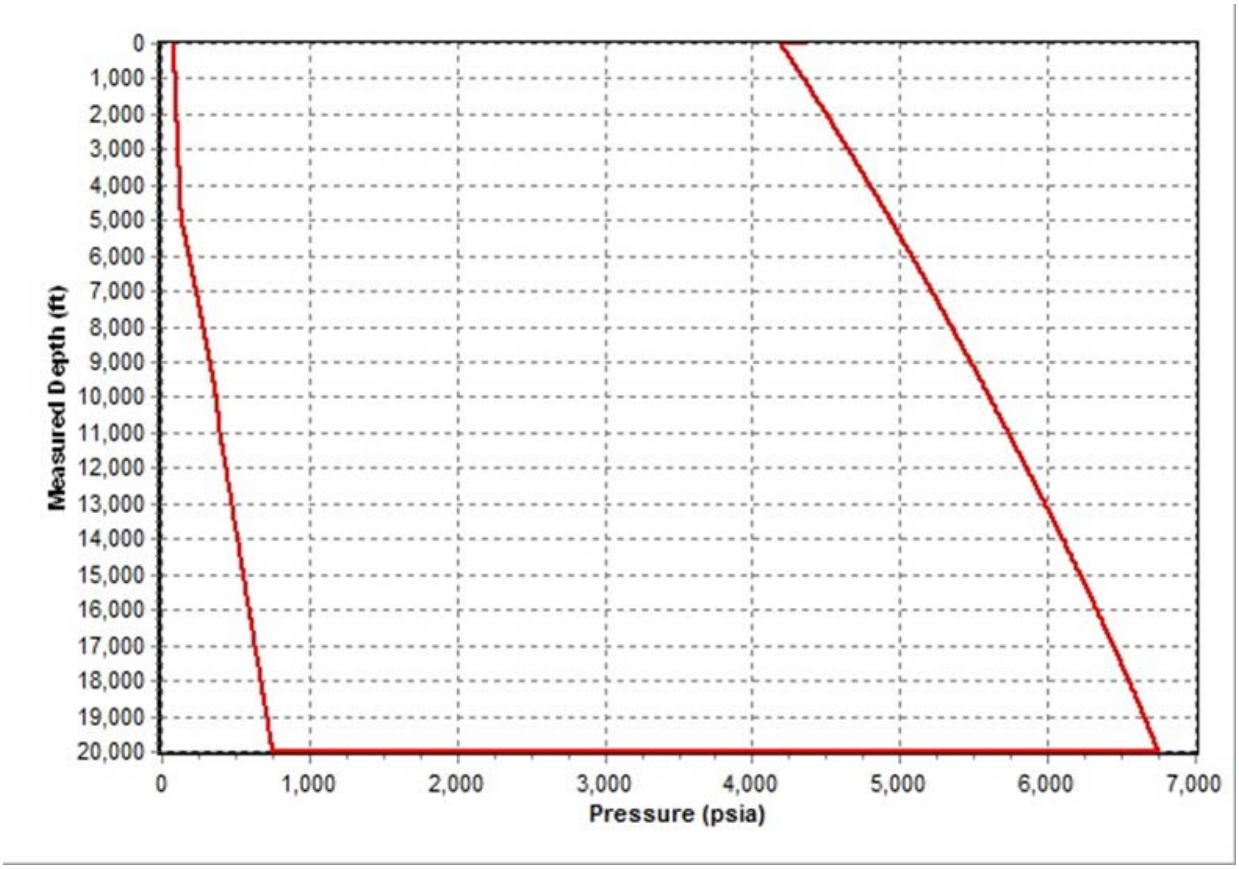
Measured Depth (ft)
0
1,000
2,000
3,000
4,000
5,000
6,000
7,000
8,000
9,000
10,000
11,000
12,000
13,000
14,000
15,000
16,000
17,000
18,000
19,000
20,000
0
1,000
2,000
3,000
4,000
5,000
6,000
7,000
Pressure (psia)

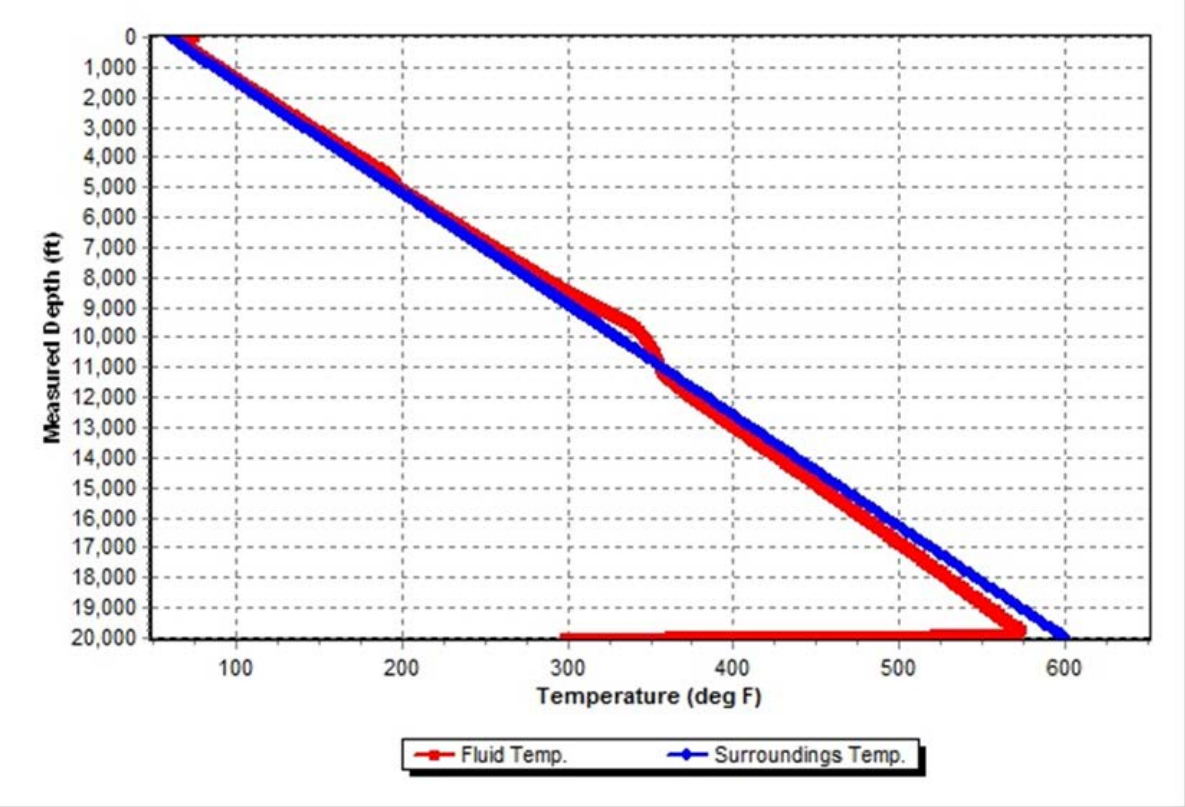
Measured Depth (ft)
0
1,000
2,000
3,000
4,000
5,000
6,000
7,000
8,000
9,000
10,000
11,000
12,000
13,000
14,000
15,000
16,000
17,000
18,000
19,000
20,000
100
200
300
400
500
600
Temperature (deg F)
Fluid Temp.
Surroundings Temp.

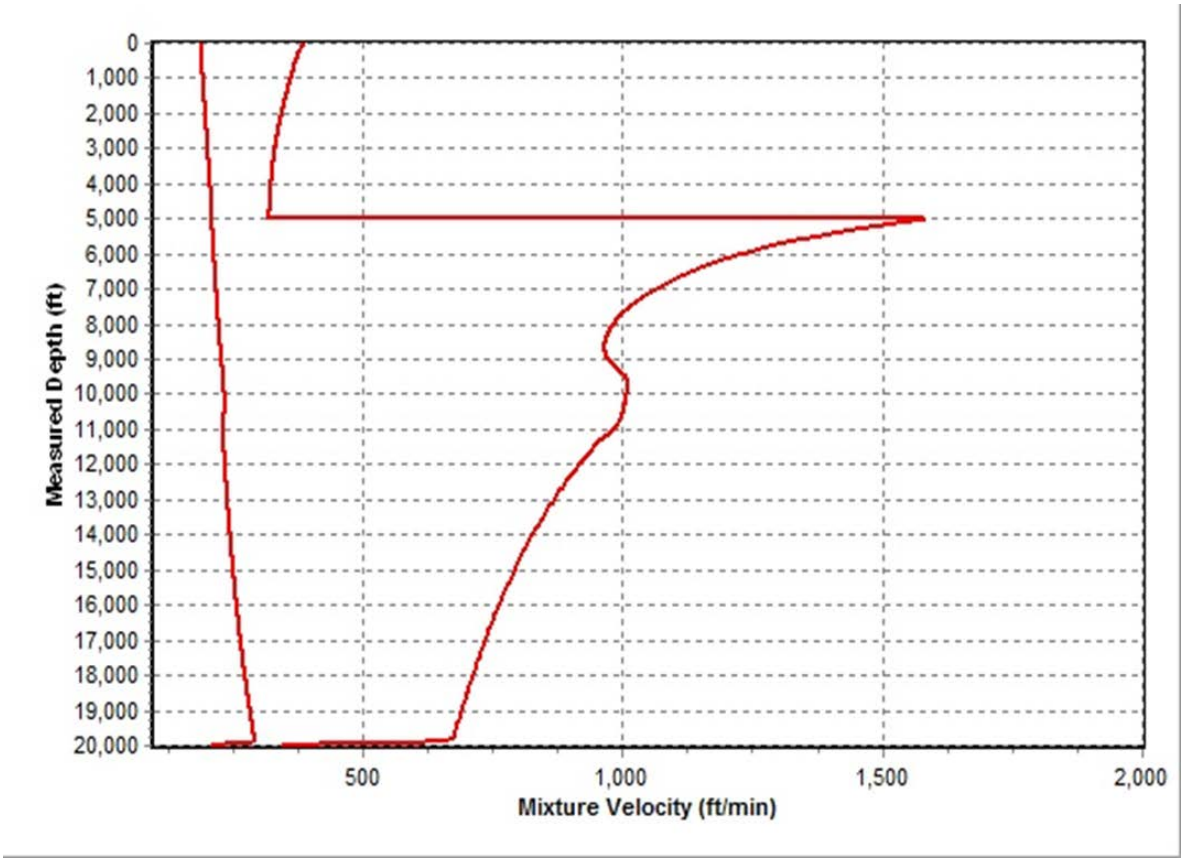
Measured Depth (ft)
0
1,000
2,000
3,000
4,000
5,000
6,000
7,000
8,000
9,000
10,000
11,000
12,000
13,000
14,000
15,000
16,000
17,000
18,000
19,000
20,000
500
1,000
1,500
2,000
Mixture Velocity (ft/min)

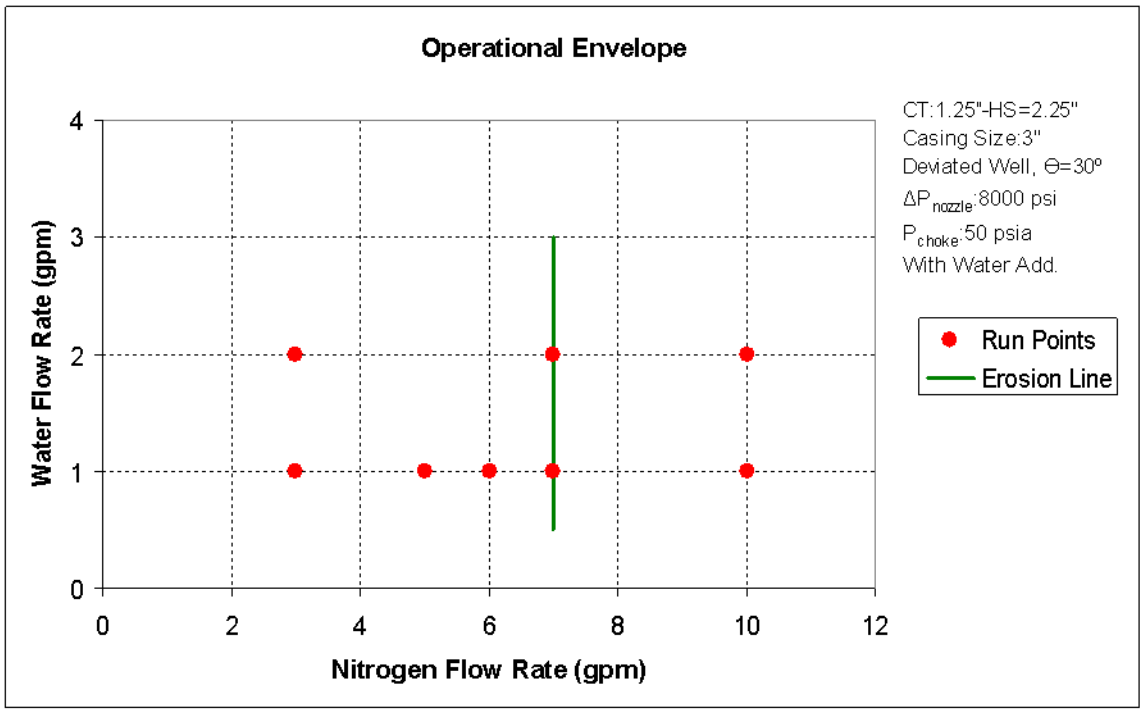
Operational Envelope
Water Flow Rate (gpm)
Nitrogen Flow Rate (gpm)
0
1
2
3
4
0
2
4
6
8
10
12
CT:1.25"-HS=2.25"
Casing Size:3"
Deviated Well, Θ=30°
ΔP nozzle:8000 psi
P choke:50 psia
With Water Add.
Run Points
Erosion Line

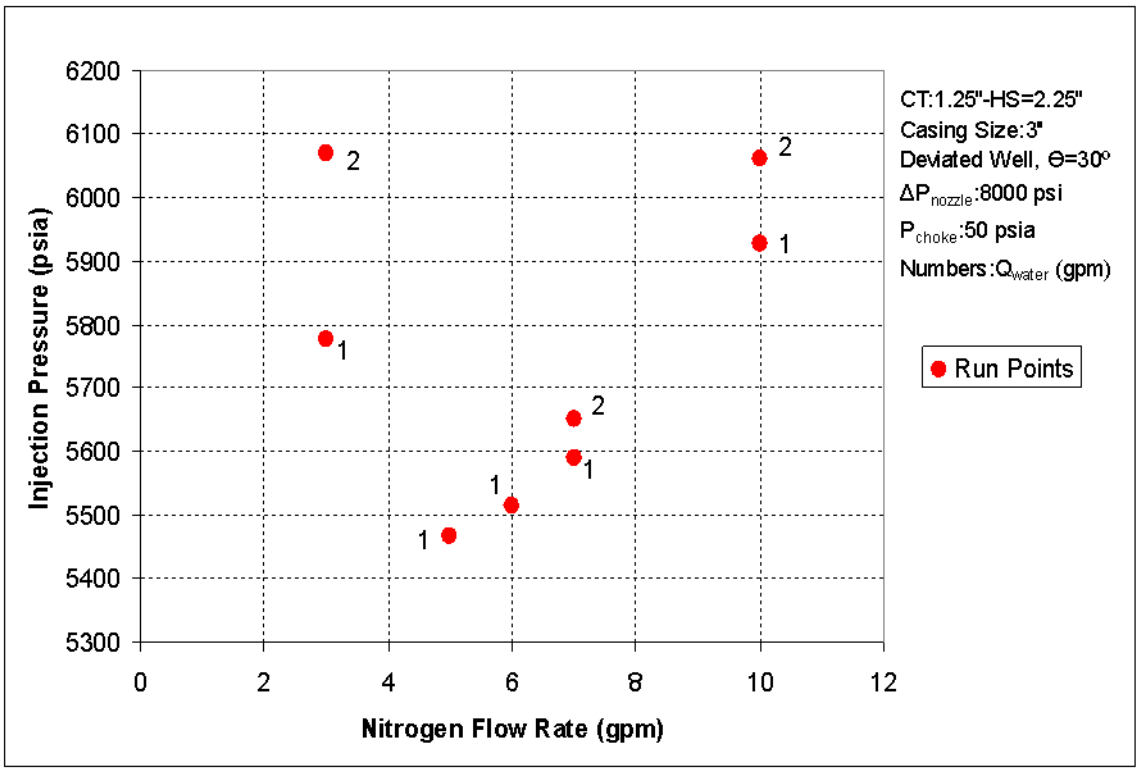
Injection Pressure (psia)
Nitrogen Flow Rate (gpm)
5300
5400
5500
5600
5700
5800
5900
6000
6100
6200
0
2
4
6
8
10
12
CT:1.25"-HS=2.25"
Casing Size:3"
Deviated Well, Θ=30°
ΔP nozzle:8000 psi
P choke:50 psia
Numbers:Q water (gpm)
Run Points

Carbon Dioxide WellFlo Run

Total Depth: 20,000 ft
QCO2= 8 gpm AND Qslurry= 3 gpm
Coiled Tubing: 1.25”OD
Surface Pipe: 0-5000 ft, Casing ID: 5.5’’
Hole Size: 2.5’’ from 5000 to Total Depth
ΔPnozzle= 4750 psi fixed
No water Influx

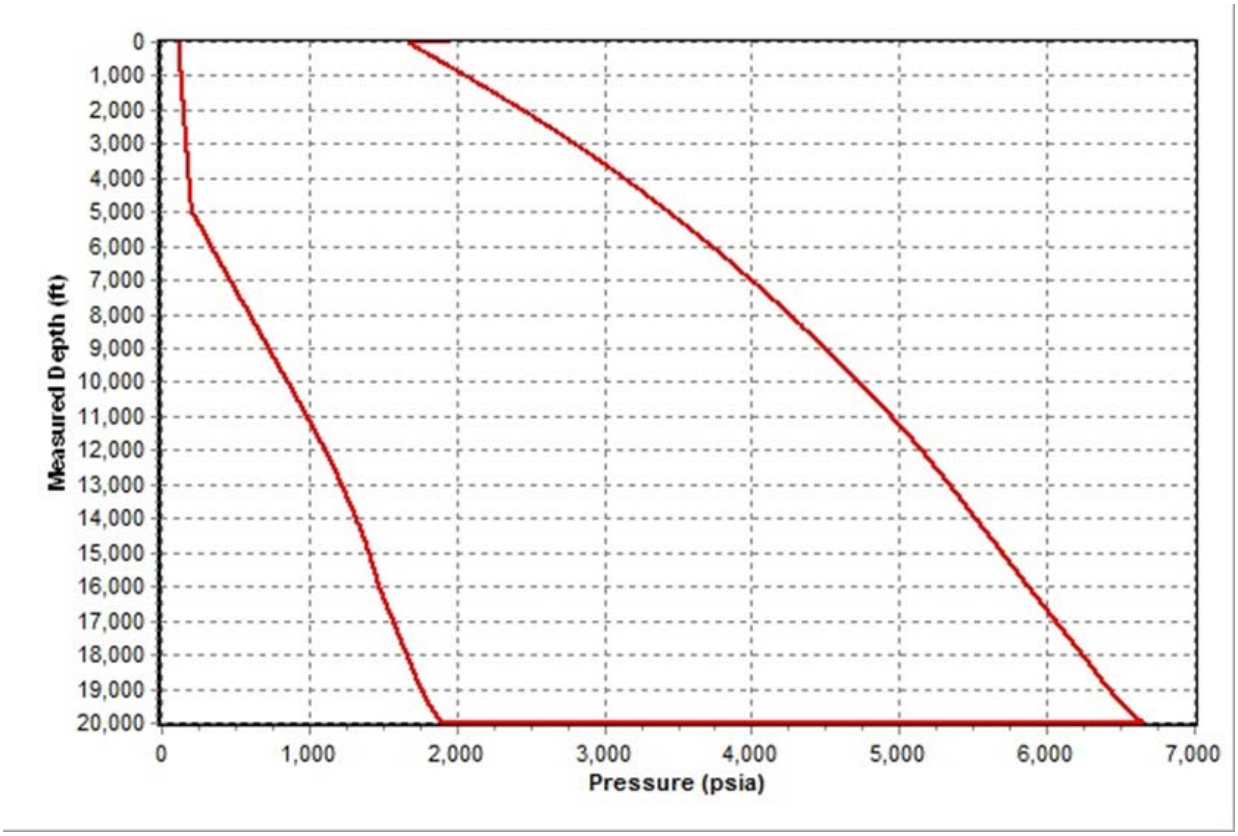

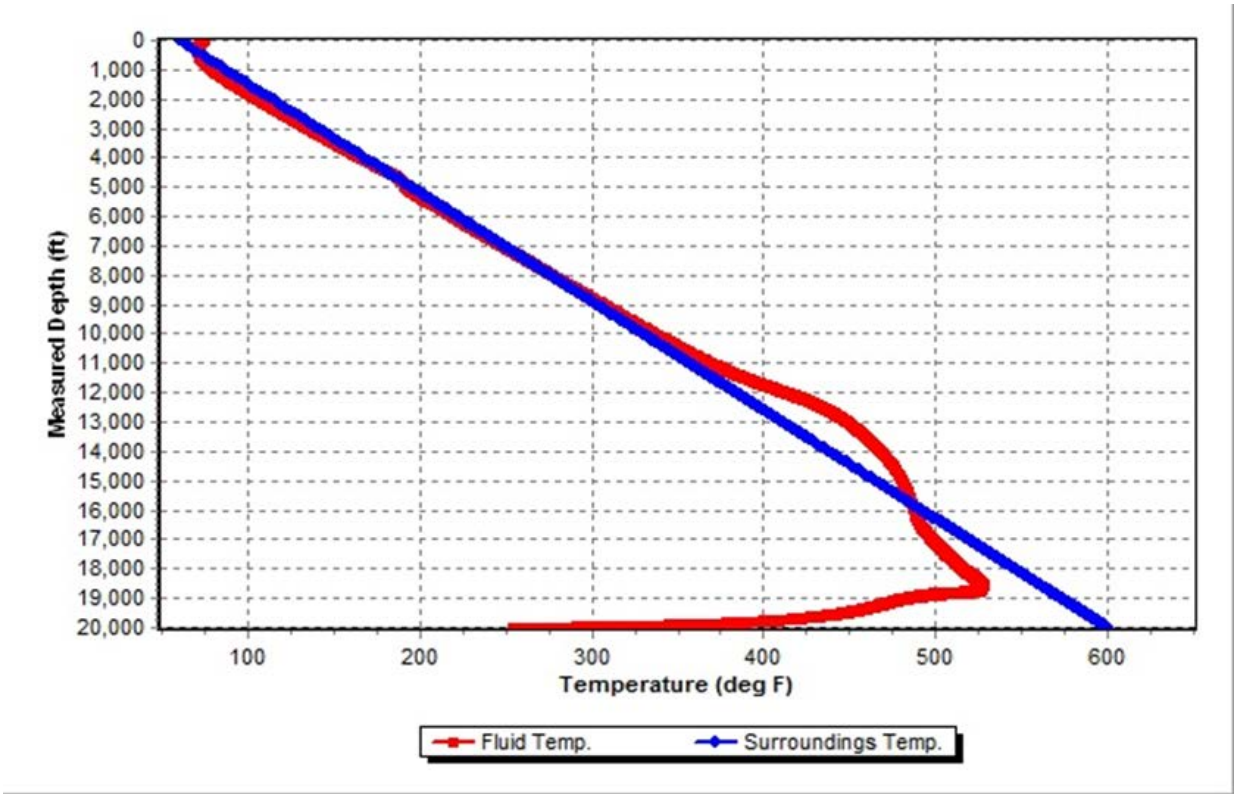
Measured Depth (ft)
0
1,000
2,000
3,000
4,000
5,000
6,000
7,000
8,000
9,000
10,000
11,000
12,000
13,000
14,000
15,000
16,000
17,000
18,000
19,000
20,000
100
200
300
400
500
600
Temperature (deg F)
Fluid Temp.
Surroundings Temp.

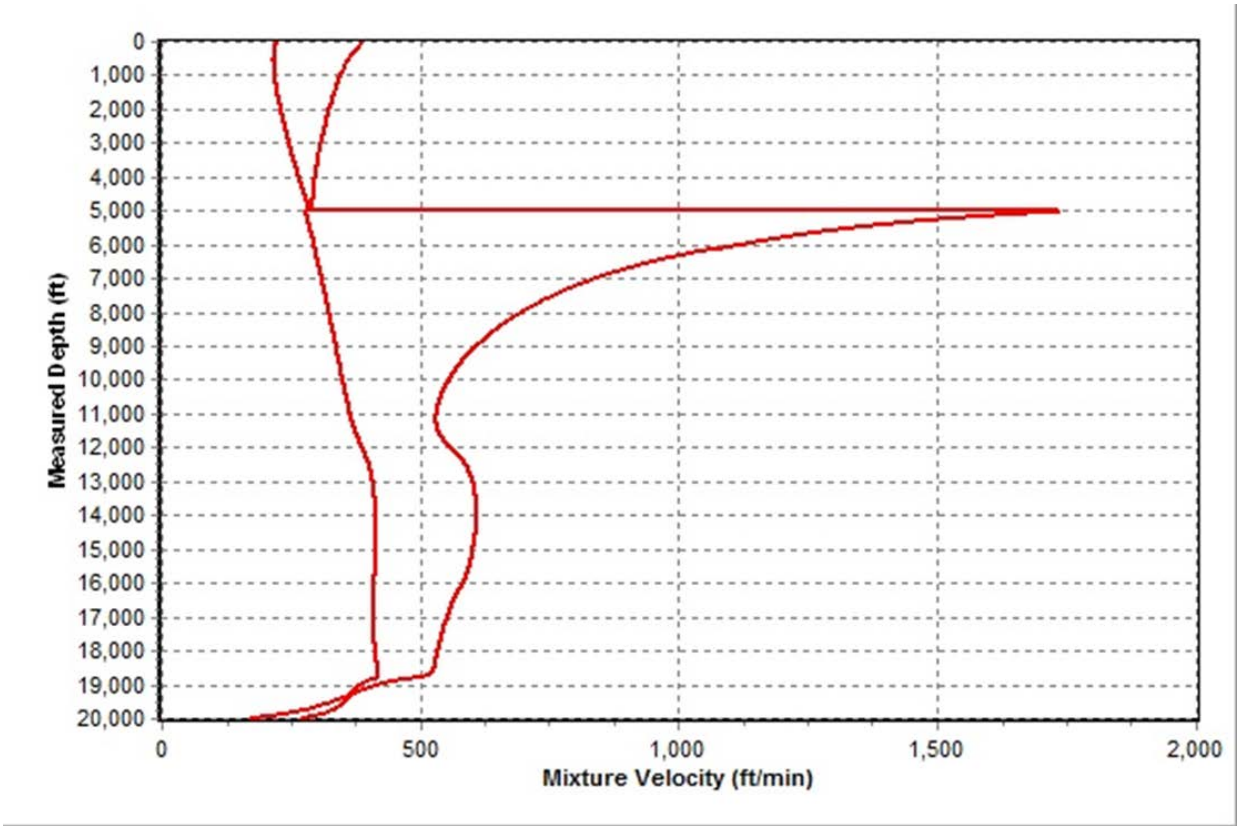
Measured Depth (ft)
0
1,000
2,000
3,000
4,000
5,000
6,000
7,000
8,000
9,000
10,000
11,000
12,000
13,000
14,000
15,000
16,000
17,000
18,000
19,000
20,000
0
500
1,000
1,500
2,000
Mixture Velocity (ft/min)

Appendix C
FLASH Fluid Internal Reports by Dr. Felber

Executive Summary

This data reflects some of the viscosities recently measured for 0.875 wt % Xanvis L solutions. Comparison data from Kelco at lower polymer concentrations and lower temperatures are also included.

Explanation Of Figure

This Figure shows some of the viscosity data that is available for Xanvis L. The 0.88 Wt % data was measured at the Bartlesville laboratory of Clean Environmental Solutions during June 2011. This data was taken using a Brookfield LV Series Viscometer with the LV-3 spindle. The concentrated polymer solutions were diluted using fresh water—Sapulpa drinking water. The Figure depicts some of the 72 and 140 °F data generated with the 0.875 Wt % polymer solutions.

The data are consistent with normal viscosity measurements. The lower the temperature is the higher the measured viscosities. This inverse relationship is directly opposite of the Xanvis L concentration which also influences the viscosities. There is a direct correlation with concentration. The lower the concentration the lower the viscosities are.

Two temperatures for the 0.875 wt % Xanvis L are shown. The red solid line represents some of the data taken at 72°F. The highest viscosity recorded was 60,400 cP. The direct comparison of the 72°F at 6 RPM shows that it is 4,500 cP while the data at 140°F is 3,240 cP. The light green, dashed line is an estimation of what the viscosities might be at lower shear rates for the 140°F solutions.

For comparison data created by Kelco scientists is included. This work was reported in SPE papers. The data chosen was the highest weight percent that they have reported—0.71 Wt %. The comparison data was generated at 75 °F using ASTM Seawater. (SPE 64982) This work is depicted by the dashed brown line.

The other comparison data chosen was because the temperature (120°F) is close to that in this work—140°F. Their work utilized 0.57 Wt % Xanvis L in 3% KCl. This is the highest polymer concentration that they reported at this temperature. (SPE 62790) It is shown by the dashed blue line. The effect of lower polymer concentration contributes to the lower viscosities as well as the 120°F.

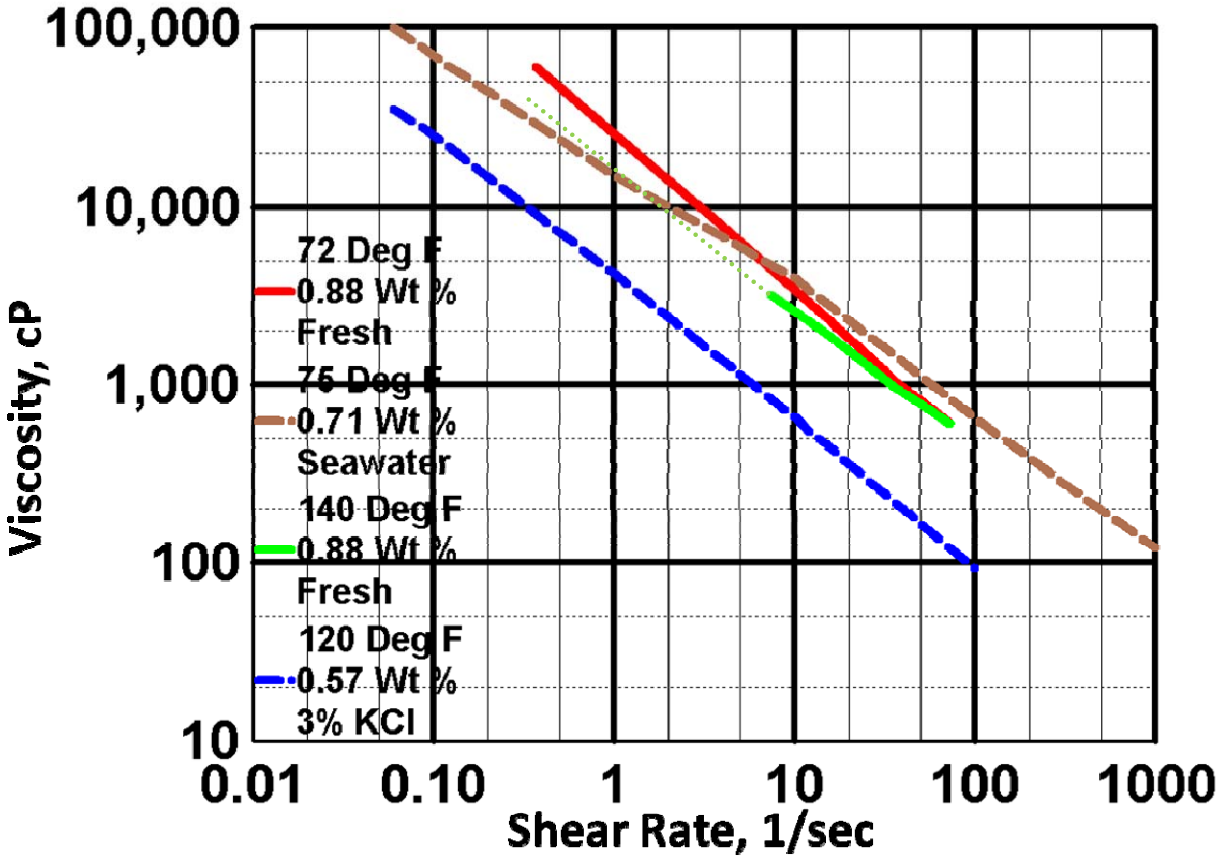

References

Navarrete, R. C., Seheult, J. M., and Coffey, M. D., "New Bio-Polymers for Drilling, Drill-In, Completions, Spacer Fluids and Coiled Tubing Applications", IADC/SPE 62790, presented at 2000 IADC/SPE Asia Pacific Drilling Technology, Kuala Lumpur, Malaysia, September 2000.

Navarrete, R. C., Seheult, J. M., and Coffey, M. D., "New Biopolymers for Drilling, Drill-In, Completions, Spacer, and Coil-Tubing Fluids, Part II", SPE 64982, presented at 2001 SPE International Symposium on Oilfield Chemistry, Houston, Texas, February 2001.

An Evaluation Of Exhaust Gas As Possible Carbon Dioxide Replacement For FLASH ASJ™ Systems

Study Conducted For

Impact Technologies LLC

June 10, 2011

Work Performed by

Betty Felber, Ph D.

Consultant

Table Of Contents

List Of Figures

List Of Tables

Introduction

This work was undertaken to determine if exhaust gases from generators and other field equipment could be used as sources for the gas necessary for FLASH ASJ™ drilling.

Literature reviews of various generators, ancillary equipment and technical papers were conducted. This review did indeed determine that one can use exhaust gases for underbalanced drilling techniques utilized by **Impact Technologies, LLC.**

Executive Summary

A source of gas is required to drill a 2", 5000 ft well requires a minimum volume of 109 ft^3 (815.38 gallons). This volume is that required to have gases present in the entire drilling column. Another requirement is that the gas volume must be able to be produced at rates of 5 gallons/minute. It is possible to have enough volume to achieve this goal based on the exhaust gas rates from several generator manufacturers. The goal is to develop the necessary expertise to implement the FLASH ASJ system when there is not sufficient supercritical CO_2 or nitrogen on location. Ultimately solving this challenge could lead to even broader FLASH ASJ applications.

Several generator specifications were reviewed to determine suitability. There were some which are capable of generating large enough volumes of exhaust gas to be utilized. There is no general "rule of thumb" for using exhaust gas to drill wells. Each well must have separate laboratory tests conducted at near reservoir conditions to determine if exhaust gases are safe to use. By safe, it means that no explosions or fires will occur either downhole or in surface equipment.

Using exhaust gas for drilling has been conducted in Canada over the last 20 years. The physical properties and phase diagrams for a typical exhaust system were also developed.

Using flue gas as a FLASH ASJ source was also reviewed. It is possible to use this gas as a source for the underbalanced drilling system.

The type and sources for ancillary equipment were also defined. Neither the ancillary equipment costs nor the delivery time for each unit was determined.

Current Exhaust Gas Underbalanced Drilling Technology Review

A current technology review was conducted. It is important to note that published current underbalanced drilling technology involves using gases as an adjunct to liquid muds. This is in contrast to the technology for FLASH ASJ in which gas is an integral part of the drilling fluid mixture not just an adjunct used to lighten conventional muds. Some comparisons and contrasts are noted in the following sections.

The growing demand for maximizing production in a cost-effective manner has led to development of novel technologies. Underbalanced drilling (UBD) has proven to be a viable technique to reduce drilling damage caused by drilling fluid invasion. Underbalanced drilling also has many other potential advantages, such as

- increased rate of penetration,
- productivity testing while drilling,
- drilling fluid options,
- eliminating differential sticking, and
- reducing completion costs.

Gas is injected and/or circulated with the drilling mud to reduce potential for formation damage from whole mud, fluid filtrate or solids invasion into the hydrocarbon-bearing formation. This procedure involves gas injection *via* a separate string to that through which the drilling mud is injected. The gas employed is usually nitrogen, in order to prevent fire and explosion hazards. However, nitrogen injection adds a significant cost. Another major challenge for remote or long duration UBD operations is the liquid nitrogen supply. This has increased interest in the use of air or deoxygenated air (membrane) technology to reduce costs and logistical challenges associated with liquid nitrogen.

If nitrogen injection were replaced with that of air, the cost could be reduced considerably. Nitrogen, natural gas, normal air or an oxygen-containing gas (usually vitiated air, which is air mixed with nitrogen, or de-oxygenated air, which is air with some of the oxygen removed) are used. Of these choices, the oxygen containing gases are the least expensive; however, there is a potential for flammable, explosive mixtures to be present in the wellbore and surface piping.

Horizontal well underbalanced drilling is also practiced. Injection either with the drilling mud or via a separate string is common. Just as for vertical wells, safe operational ranges of oxygen-containing gas/live oil/drilling mud mixtures can be determined if the flammability has been measured. (Metha 1995)

Flammability limits are affected by a number of different factors. The most important are temperature and pressure. For some fuels, small amounts of moisture can widen flammability limits, as can presence of hydrocarbon containing liquids. Significant widening of the flammability limits of complex fuel mixtures can also be caused by presence of low levels of hydrogen sulfide, carbon monoxide and hydrogen.

Many complex mixtures could be encountered with injection of an oxygen-containing gas. Drilling mud may ignite at concentrations of oxygen significantly lower than 21 percent. It is possible that explosions may occur at concentrations as low as five percent oxygen. It has been found that high pressure flammability limit behavior is neither simple nor uniform, but is specific to the mixture examined. It must therefore be stressed that flammability characteristics for a given reservoir and operating conditions are case specific. (Metha, 1995)

Laboratory studies to test for ignition characteristics and flammability of gas, oil, and drilling mud mixtures must be conducted for each specific reservoir. To conduct these tests, the reaction vessel contains mixtures of air, the drilling polymer such as Xanvis, and live oil. The pressure

ranges are based on the reservoir. The temperature range is also determined by that expected to be encountered in the reservoir. Flammability limits are determined. Results are then used to design safety features for a field application horizontal drilling program using underbalanced methods at depth. This technique has proven successful, and a significant cost saving was realized by utilizing a 40 percent nitrogen, 60 percent air mixture instead of pure nitrogen. (Metha, 1995)

The mixtures were classified as "flammable", since using de-oxygenated air there is a continuous supply 5 % O_2. Ignition was classified in two categories: 'Strong Reactions', when the temperature rise was instantaneous after the introduction of a spark with a total temperature rise in excess of 50 °F; and 'Weak Reactions', when the rate of temperature rise was relatively slow after the introduction of a spark with a total temperature rise of more than 41 °F but less than 50°F.

Where a limited amount of reaction was observed with very low rate of temperature rise after the introduction of a spark with a total temperature rise of less than 41 °F, it was designated as 'Limited Reactions' and classified as no ignition. The hydrocarbon mixture flammability was significantly affected (widened) by the presence of hydrogen sulfide. In addition, operating pressure and temperature had a strong influence on mixture ignition characteristics.

Other studies were performed to determine safe conditions for underbalanced drilling using compressed air and liquid nitrogen. The main objectives were:

- to establish flammability of mixtures of air, live heavy oil and drilling mud as a function of pressure, and

- to determine optimum composition of vitiated air (nitrogen-air mixture), based on flammability data, in order to minimize ignition or explosion potential during underbalanced drilling operations.

Currently, there are no general "rules-of-thumb" which can be used to predict if an underbalanced drilling operation will be conducted in a safe, effective manner. (Metha, 1996) Using exhaust gas for underbalanced drilling has killed the market for nitrogen membrane units. (jonralph)

Hydrogen Sulfide Effects

Studies have also been conducted to determine flammability of complex mixtures of fuel gases containing H_2S, hydrocarbon condensate and drilling mud in de-oxygenated air (consisting of 5 % O_2 with the balance being N_2). Flammability tests at realistic reservoir pressures and temperatures and at the types of operating conditions which might be encountered during sour underbalanced drilling operations should be conducted for each project. The goal is to establish hydrogen sulfide concentration effects on flammability. Establishing safe design and operation of underbalanced drilling projects in sour hydrocarbon fields using de-oxygenated air containing 5% oxygen with the balance being nitrogen is important.

It was determined that de-oxygenated air containing 5 % oxygen was the benchmark for a safe underbalanced drilling operation in reservoirs containing very small amounts of hydrogen sulfide

(up to 3000 ppm). This particular composition of deoxygenated air is economically achievable. Work was conducted at near-atmospheric conditions and is not valid at elevated pressures and temperatures. The pressure range chosen was from 0.0 to 3000 psig.

It is well known that increases in pressure and temperature have a widening effect on flammability range. Therefore, it was concluded that optimizing compositions at atmospheric conditions using correlations and extending the values to higher pressures and temperatures would lead to the "worst-case" flammability scenario.

Again, it must be stressed that results are highly case-specific. They are valid only for specific fuel gas, hydrocarbon and drilling mud mixtures and the run conditions investigated. The test parameters were designed for a specific set of reservoir conditions; thus, the ignition characteristics described herein should **NOT** be applied to other reservoirs.

It should **NOT** be assumed that de-oxygenated air containing five percent oxygen by volume with the balance being nitrogen can be safely used during an underbalanced drilling operation for a hydrocarbon system containing other gases. The flammability limits for each system must be tested. (Metha, 1996)

Also note that the underbalanced drilling discussed here does not relate specifically to mixing the gas at the surface to create underbalanced fluids. Rather the gas is added subsurface to create an underbalanced fluid. This is in contrast to **Impact Technologies** methods but still gives one insight into how the fluids could behave downhole. The exhaust gas system could be used for FLASH ASJ drilling.

Field Applications

Over the past two decades, the underbalanced drilling technology has evolved significantly. It can yield benefits such as

- increasing ROP (reduced well cost)
- reducing formation damage (increased productivity)
- limiting lost circulation problems
- reducing differential sticking
- providing formation testing/evaluating while drilling and
- picking TD from production rate or first water influx.

Underbalanced drilling has several advantages over conventional drilling, but it also has several disadvantages as well. ***The principle advantage is that the penetration rates are usually 3-6 times greater that mud drilling. The disadvantage is that the penetration rates are higher.*** Although penetration rates are higher, you're basically limited by the rig crew's capability to be

able to "keep-up" and also recognize when the well "tells" them that something is happening downhole that isn't "right". There problems can lead one to a "fishing" job.

In well pre-planning, determine what a "safe" penetration rate would be, even though the capability exists to drill faster and, adhere to it during implementation. Plan to schedule enough time for "circulating" before making connections to make sure you have a reasonable clean annulus prior to shutting down the injection gas. If one is using coiled tubing, the requirements are different.

The people responsible have to be educated, that once the air is cut-off "mother nature" takes over (gravity), and the cuttings in the annulus will fall, as "air" has very little carrying capacity. "Velocity", is the primary carrying agent for straight "air" drilling (commonly called "Dusting"). (Redman69)

That said, by 2003, out of over 15,000 wells drilled under “so called” UBD conditions in North America, approximately 9,000 wells were drilled with truly underbalanced conditions over the entire planned depth/length and completion. Worldwide, the percentage drilled through the pay zone and completed underbalanced is considerably less. A variety of techniques have been employed relevant to different applications, such as:

- air drilling and use of air hammers
- flow drilling
- gas injection (via drill string; parasite string; inner string)
- mist and
- foam drilling.

Depending on the application and availability, gases such as air, deoxygenated air created through membrane separation or exhaust gas recompression, vitrified air, cryogenic nitrogen and natural gas have been injected in order to achieve these conditions. (Pratt) Another method is being tried in Australia using natural gas and nitrogen. Weatherford is championing this system. (Santarelli)

Using Exhaust Gas For Drilling

A schematic of an exhaust gas system is shown in Figure 1 below. (Pratt) The two engines supply the input to the catalytic converter which eliminates oxygen from the stream. Through a series of heat exchangers and scrubbers the gas is made ready for using in the underbalanced drilling operation. Note that the final injection stream has no oxygen.

This technique has been used successfully on remote Canadian locations for many years. It should be noted that drilling with exhaust gas units can cause very serious problems. (CamT) This occurs when the gas generated was not treated properly or when surface equipment fails.

Exhaust gas systems are not as simple as one would believe. One can’t just hook up a compressor to some diesel engine exhaust and go with it. If this is done, you'll also have no

drillpipe, no casing, and no surface injection piping. The compressors can also be damaged. If one is under the impression that membranes give bad corrosion with oxygen, saltier water and temperature, then one should see what a poorly controlled exhaust gas corrosion management system can do. Fortunately this is extremely rare, however it does occur 2 or 3 times every 4 to 6 months. (Kevin S) A well controlled exhaust gas system produces approximately 87% N_2 and 13% CO_2 as the injection gas as shown in Figure 1.

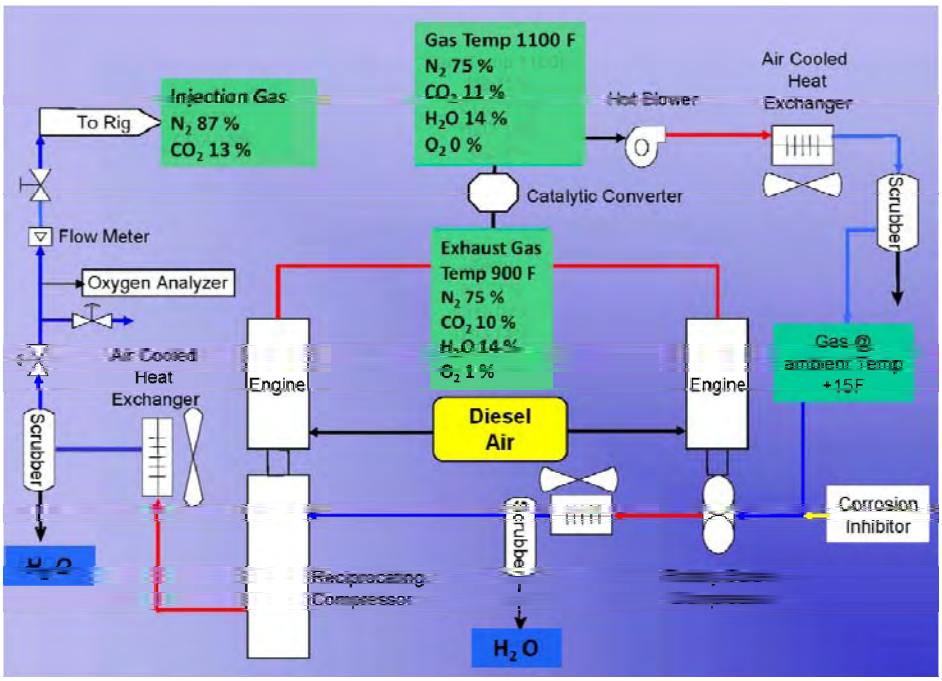

Figure 1: Exhaust Gas Schematic

Figure 2 is an example of how a field application layout using exhaust gas for underbalanced drilling looks. (Pratt)

Figure 2: Exhaust Gas Field Equipment Layout

Nitrogen Drilling

In contrast to the exhaust gas system, one of the fluids used in underbalanced drilling operations is cryogenic nitrogen, the liquid form of nitrogen, which is at a temperature of -321°F. Some of the characteristics of it are it is transported in tractor/trailer bulkers and stored at the drilling location in "Queen storage tanks" (typically 503 barrels).

The cryogenic N_2 is pressure transferred to a Cryogenic N_2 pumping unit which is capable of pumping 1 to 80 scfm at 1 to 50,000 psi or greater. The pumps are generally from the fracing industry. The N_2 pumper has a liquid N_2 storage tank, (about 63 barrels) and that is held at a fixed pressure, pressure feeding a downstream pump. This pump then pre-charges the liquid nitrogen to a couple hundred psi and forces it to the cryogenic pumps, which is usually a triplex. The triplex pressurizes the cryogenic nitrogen to its operating pressure and forces it to the heat convertor, which converts the cryogenic nitrogen to gaseous nitrogen at 77°F.

For the average two-phase system drilling a 6 1/4" hole with saltwater and nitrogen, it takes about 200 gpm water and about 1500 scfm nitrogen (11,221 gpm) at a drilling pressure of 1100 psi. (KevinS) These numbers are important to remember since the FLASH ASJ system requires a higher pressure and 5 gpm availability for the drilling fluid.

Cryogenic nitrogen is not inexpensive when compared to other gas methods. The cryogenic pumping equipment and cryogenic storage equipment can run about $15-$20K per day; then there is the cost of the nitrogen—30 scm * $0.75/scm * 24 (pumping about 75—85 % of the time on underbalanced drilling jobs, but there are also cryogenic losses so one can almost say pumping is 100%).

Cryogenic nitrogen costs vary on location and weather conditions. For example, if one is in Alberta, Canada, where there is one of the world's largest N_2 factories, costs are significantly lower than if one is in South Dakota where one may only get 1 bulker of nitrogen every 24 hours delivered. The cost delivered to site in Canada, including trucking and standard losses run about $0.75/scm.

A deoxygenated air system for 1500 scfm at 2200 psi costs around CAN $2.8 Mil and takes 6 months to build. The system is extremely portable. However, one of the disadvantages is the remaining 5% oxygen which given the right downhole chemistry causes massive corrosion. Some mud companies are close to conquering this 10 year old problem, however only close. On a high rate, remote location, this is the only economical way to go, unless you have exhaust gas or a gas line you can tie into. There is also air, but this is not very common in places outside of the U. S.; most likely due to lack of experience elsewhere. (KevinS)

So using nitrogen or exhaust gas for underbalanced drilling is not unheard of. The EPA requirements have complicated this use by limiting nitrogen in the exhaust from off road equipment.

EPA Off Road Standards

There is a requirement that off road diesel equipment must meet exhaust emission standards. Some of the requirements are summarized below.

Tier 1-3 Standards

The first Federal standards (Tier 1) for new nonroad (or off-road) diesel engines were adopted in 1994 for engines over 50 hp. The requirements were to be phased-in from 1996 to 2000. In 1996, a Statement of Principles (SOP) pertaining to nonroad diesel engines was signed between EPA, California Air Resources Board and engine makers (including Caterpillar, Cummins, Deere, Detroit Diesel, Deutz, Isuzu, Komatsu, Kubota, Mitsubishi, Navistar, New Holland, Wis-Con, and Yanmar). On August 27, 1998, EPA signed the final rule reflecting the SOP provisions. The 1998 regulation introduced Tier 1 standards for equipment under 50 hp and increasingly more stringent Tier 2 and Tier 3 standards for all equipment with phase-in schedules from 2000 to 2008. Tier 1-3 standards were met through advanced engine design, with no or only limited use of exhaust gas after treatment such as oxidation catalysts. Tier 3 standards for NO_x+ HC are similar in stringency to the 2004 standards for highway engines; however Tier 3 standards for PM (Particle Matter) were never adopted.

Tier 4 Standards

On May 11, 2004, the EPA signed the "final" rule introducing Tier 4 emission standards, which are to be phased-in over the period of 2008-2015. Tier 4 standards require PM and NO_x emissions be further reduced by about 90%. Such emission reductions can be achieved through the use of control technologies—including advanced exhaust gas after treatment—similar to those required by the 2007-2010 standards for highway engines.

Nonroad Diesel Fuel

The other element for nonroad equipment is diesel. At the Tier 1-3 stage, sulfur content in nonroad diesel fuels was not limited. The oil industry specification was 0.5% (wt., max), with the average in-use sulfur level of about 0.3% = 3,000 ppm. To enable sulfur-sensitive control technologies in Tier 4 engines—such as catalytic particulate filters and NO_x absorbers—EPA mandated reductions in sulfur content in nonroad diesel fuels, as follows:

- 500 ppm effective June 2007 for nonroad, locomotive and marine (NRLM) diesel fuels
- 15 ppm (ultra-low sulfur diesel) effective June 2010 for nonroad fuel, and June 2012 for locomotive and marine fuels

The Figure below shows the EPA timeline for reduced particle matter and NO_x implementation. Included are the years when new emissions are active as well as the NO_x, hydrocarbon, carbon monoxide, and particle matter limits. (Caterpillar)

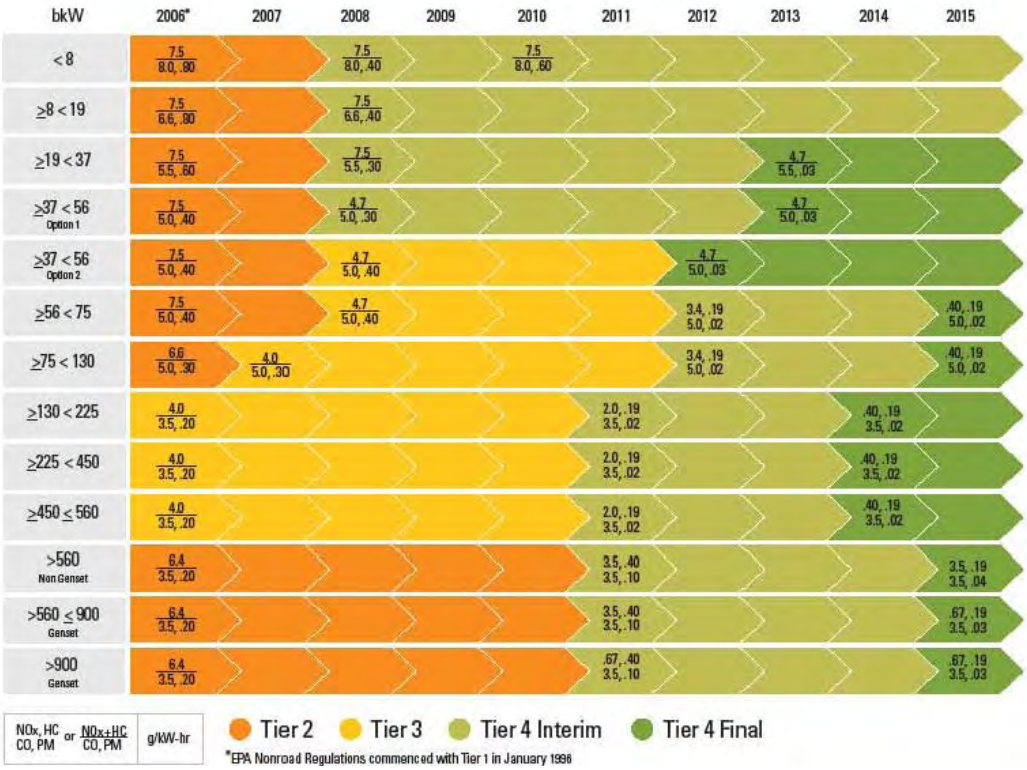

Figure 3: EPA Emission Requirements--Nonroad

Industries Where Applicable

The nonroad standards cover mobile *nonroad diesel engines* of all sizes used in a wide range of construction, agricultural and industrial equipment. Examples of regulated applications include farm tractors, excavators, bulldozers, wheel loaders, backhoe loaders, road graders, diesel lawn tractors, logging equipment, portable generators, skid steer loaders, or forklifts.

EPA defined *nonroad engines* as based on the principle of mobility/portability, and includes engines installed

(1) on self-propelled equipment,

(2) on equipment that is propelled while performing its function, or

(3) on equipment that is portable or transportable, as indicated by the presence of wheels.

In other words, nonroad engines are all internal combustion engines except motor vehicle (highway) engines, stationary engines (or engines that remain at one location more than 12 months), engines used solely for competition, or aircraft engines.

Effective May 14, 2003, the definition of nonroad engines was changed to also include all diesel powered engines—including stationary ones—used in California agricultural operations. This change applies only to engines sold in California. Stationary engines sold in other states are not classified as nonroad engines.

The nonroad diesel emission regulations are not applicable to all nonroad diesel engines. Exempted are the following nonroad engine categories:

- Engines used in railway locomotives; those are subject to separate EPA regulations.

- Engines used in marine vessels, also covered by separate EPA regulations. Marine engines below 37 kW (50 hp) are subject to Tier 1-2—but not Tier 4—nonroad standards. Certain marine engines that are exempted from marine standards may be subject to nonroad regulations.

- Engines used in underground mining equipment. Diesel emissions and air quality in mines are regulated by the Mine Safety and Health Administration (MSHA).

- Hobby engines (below 50 cm^3 per cylinder)

A new definition of a compression-ignition (diesel) engine is used in the regulatory language since the 1998 rule. The definition focuses on engine cycle, rather than ignition mechanism, with the presence of a throttle as an indicator to distinguish between diesel-cycle and otto-cycle operation. Regulating power by controlling the fuel supply in lieu of a throttle corresponds with lean combustion and diesel-cycle operation. This language allows the possibility that a natural gas-fueled engine equipped with a sparkplug is considered a compression-ignition engine. (DieselNet)

So what do these requirements mean for oil field equipment? The next section details some examples.

Compressor Review

EPA has entered into an agreement with several companies who have agreed to limit exhaust of NO_x and particular matter. These companies were listed previously.

Two compressor manufacturers were reviewed—Cummins and Caterpillar. In both cases the company was proud that they were in compliance with EPA nonroad diesel requirements. Even with the engines meeting EPA standards, there is enough nitrogen + carbon dioxide exhaust volume being emitted that the exhaust can be the gas source for the **Impact Technology** FLASH ASJ system.

One would still need to choose a generator that could support the rates needed for this application. In order for a generator to meet the rate requirements for the FLASH ASJ system, it must be capable of producing exhaust gas at a rate of 8,898 ft^3/min. Examples of the Cummins engines are the Genset PC880 series (Appendix A, page A-1). Caterpillar diesel examples are in the PRIME 1360 ekW, 1700 kVA engine series Appendix A, page A-9.

One could also use 2 much smaller generators—4000 ft^3/min each. This arrangement may allow for more rate variations. It could also lower the acquisition costs. Appendix A, page A-5 is an example of the ± 4000 rated generator from Cummins. A Cat PRIME 580 eKW example is included on page A-15.

More information from each company is included in Appendix A. Each generator highlighted will produced enough exhaust gas to meet FLASH ASJ requirements for a 2" 5000' wellbore.

Ancillary Equipment Sources

In order to successfully apply the exhaust gas system several pieces of ancillary equipment must be used. This section is targeted toward locating this equipment. See Appendix B for more information on the ancillary equipment types and sources.

Using Figure 1 as an example, the ancillary equipment is listed as it appears on this figure. The first item is the catalytic converter. PTX purifiers are used to control commercial equipment exhaust powered with engines using unleaded gasoline, diesel fuel, or LPG, allowing the safe use of such equipment in enclosed spaces. PTX purifiers are used on fork lifts, trucks, floor sweepers, underground locomotives, stationary or portable engines. (Cohn) These catalytic converters may be purchased from Optimized Process Design. They do not have literature available on the Internet. The contact information is OPD, 25610 Clay Road, Katy, TX 77493. The phone number is (281) 371-7500.

There are also several other prominent catalytic converter sources. One of them is BASF. The contact information is BASF Catalysts LLC, 101 Wood Avenue, Iselin, NJ 08830-0770. The phone number is (732) 205-5000. The web site is www.basf-catalysts.com. A description of one of their products begins on page B-1of Appendix B.

A hot blower that can handle 1100 °F can be supplied through The New York Blower Company. The contact information is 7660 Quincy Street, Willowbrook, IL 60527-5530. The phone number is 800-208-7918 and the web site is www.nyb.com. Product descriptions are listed in Appendix B beginning on page B-3.

For the miniature air cooled heat exchangers, www.wholesalehydraulics.com is a good source. They market several brands—American Heat Transfer, American Standard Thermal Transfer, and Young Radiator for example. These are all manufacturers on miniature air cooled heat exchangers. Depending on the model, cooling rates range from 1 to 1000 gpm. They do not have brochures that one can download but they do have brief descriptions of several of their heat exchangers.

The toll free number is 1-800-329-6888**.** E-mail is info@wholesalehydraulics.com. The parent company is Advanced Fluid Power, Inc. It is located in Mobile, Alabama. Advanced Fluid Power, Inc. has over 75 years of combined experience. The address is I-10 Industrial Parkway, Theodore, Alabama 36582. Examples of their product lines are in Appendix B on page B-6.

For the scrubbers in Figure 1, it is suggested that **Impact** use the **Tulsa University** designed separators. It should be fairly inexpensive to design and fabricate them for the throughput necessary for rate, temperature and pressure ranges expected. **Impact** or MSI should be able to manufacture the two phase separator equipment required. Appendix B, page B-8 contains some of MSI's information.

The rotary screw compressor is marketed by Kaeser. More information can be obtained at http://us.kaeser.com/Products. The closest distributor is MIS Group, Inc. The phone number is (713) 671-9565. The address is 9402 North Loop E, Houston, TX 77029-1228. Or the Kaeser

number is (800) 777-7873. Some more compressor information is contained in Appendix B on page B-9.

The reciprocating compressor can be provided by Dresser Rand or GE. The Dresser contact information is Dresser-Rand, West8 Tower Suite 1000, 10205 Westheimer Road, Houston, TX 77042. The phone number is (713) 354-6100. An example of their reciprocating compressor is shown in Appendix B on page B-10.

The oxygen analyzer can be purchased from Alpha Omega Instruments Corporation. It is located at 30 Martin Street, Cumberland, RI 02864. The phone number is (800) 262-5977. The web site is http://www.aoi-corp.com. The analyzers which could be used are Series 2520 & 3520 Portable Oxygen Analyzers. The product information sheet is in Appendix B on page B-12.

Now that the compressors and ancillary equipment have been reviewed, what are the exhaust gas fluid properties which might be utilized in the underbalanced drilling operations?

Fluid Properties

Exhaust Gas

A physical properties study of the typical cleaned up exhaust gas is made up of 87 % Nitrogen and 13 % Carbon Dioxide was conducted. See Figure 1 above. Some of the exhaust gas mixture physical properties were determined and are included in Table 1 below.

Table 1: 87 % Nitrogen + 13 % Carbon Dioxide Mixture Physical Properties

English Units		Normal Freezing Point (1 atm)		Gas Phase Properties @ 68°F & @1 atm		Liquid Phase Properties @ B P& @ 1 atm		Triple Point		Critical Point		
		Temp.	Latent Heat of Vaporization	Specific Gravity	Specific Heat (Cp)	Specific Gravity	Specific Heat (Cp)	Temp.	Pressure	Temp.	Pressure	Density
Substance	Mol. Weight	° F	BTU/lb	Air = 1	BTU/lb °F	Water = 1	BTU/lb °F	°F	psia	°F	psig	lb/cu ft
N_2 + CO_2 Mixture	29.40	-273.3	---	---	7.21	---	12.95	-373.0	1.00	-178.9	1073.4	25.99

The phase diagram for exhaust gas is shown in Figure 4. The nitrogen—carbon dioxide mixture is shown in black. The important features are that it goes supercritical at -180°F. Low temperatures are required to drive it to the supercritical region. The carrying capacity of this fluid might be lower compared to carbon dioxide since the molecular weight is 29 while it is 44 for CO_2.

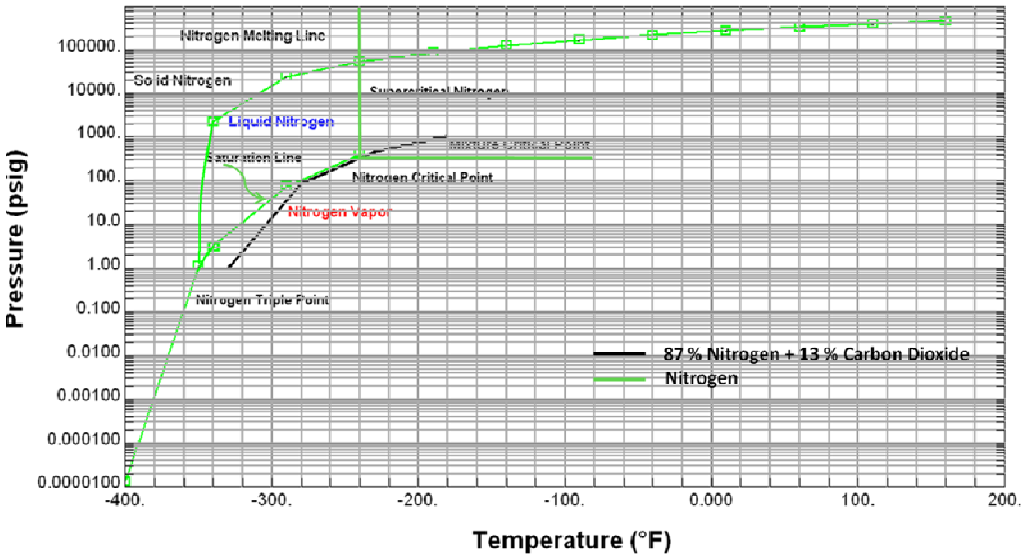

Figure 4: 87 % Nitrogen + 13 % Carbon Dioxide Mixture Phase Diagram

On Figure 4 the nitrogen phase diagram is included for reference. It is depicted in green. The conversion of 1 ft^3 of this mixture would be between that of carbon dioxde—533 ft^3 and that of nitrogen which is 694 ft^3 at 60 and 14.696 psi. If one assumes each element contributes its respective amount of volume to the expansion, then the number would be 673 ft^3 (0.87 *694 ft^3 + 0.13 * 533 ft^3), however it is unclear if one can really assume that the mixture would vaporize in this manner.

Sample Of Expanded Physical Properties—Nitrogen + Carbon Dioxide Mixture

The table shows some more physical properties of the 87 % nitrogen + 13 % carbon dioxide mixture. The differences at these two temperatures—60 and 70 —are slight. These two temperatures were chosen because they are the ambient temperature range which might be most frequently encountered.

Table 2: Expanded 87 % Nitrogen + 13 % Carbon Dioxide Mixture Physical Properties List

Temp.,	Press., psig	Density, lbm/ft^3	Enthalpy, (Btu/lbm)	Entropy, (Btu/lbm-°R)	Heat Capacity, C_v (Btu/lbm-°R)	Heat Capacity, C_p (Btu/lbm-°R)
60	0	0.08	139.93	1.5185	0.17457	0.24257
	100	0.61	139.07	1.3782	0.17516	0.24601
	1000	5.50	131.67	1.2187	0.17997	0.27792
	2000	10.88	124.81	1.1604	0.18419	0.30948
	3000	15.73	119.84	1.1239	0.18724	0.32979
	4000	19.83	116.71	1.0978	0.18950	0.33932
	5000	23.21	115.01	1.0780	0.19132	0.34239
	6000	26.00	114.36	1.0623	0.19293	0.34232
	8000	30.35	115.06	1.0384	0.19589	0.33924
	10000	33.62	117.34	1.0205	0.19865	0.33582
70	0	0.08	142.36	1.5231	0.17477	0.24275
	100	0.60	141.53	1.3829	0.17532	0.24602
	1000	5.37	134.45	1.2239	0.17987	0.27614
	2000	10.61	127.88	1.1663	0.18388	0.30585

	3000	**15.34**	**123.11**	**1.1301**	**0.18685**	**0.32545**
	4000	**19.37**	**120.08**	**1.1042**	**0.18908**	**0.33521**
	5000	**22.71**	**118.42**	**1.0845**	**0.19090**	**0.33883**
	6000	**25.49**	**117.77**	**1.0687**	**0.19251**	**0.33930**
	8000	**29.85**	**118.44**	**1.0448**	**0.19545**	**0.33697**
	10000	**33.14**	**120.69**	**1.0269**	**0.19819**	**0.33398**

The enthalpy curves are depicted in the Figure below. Note the similarity at the two temperatures reported. There is, however, some separation.

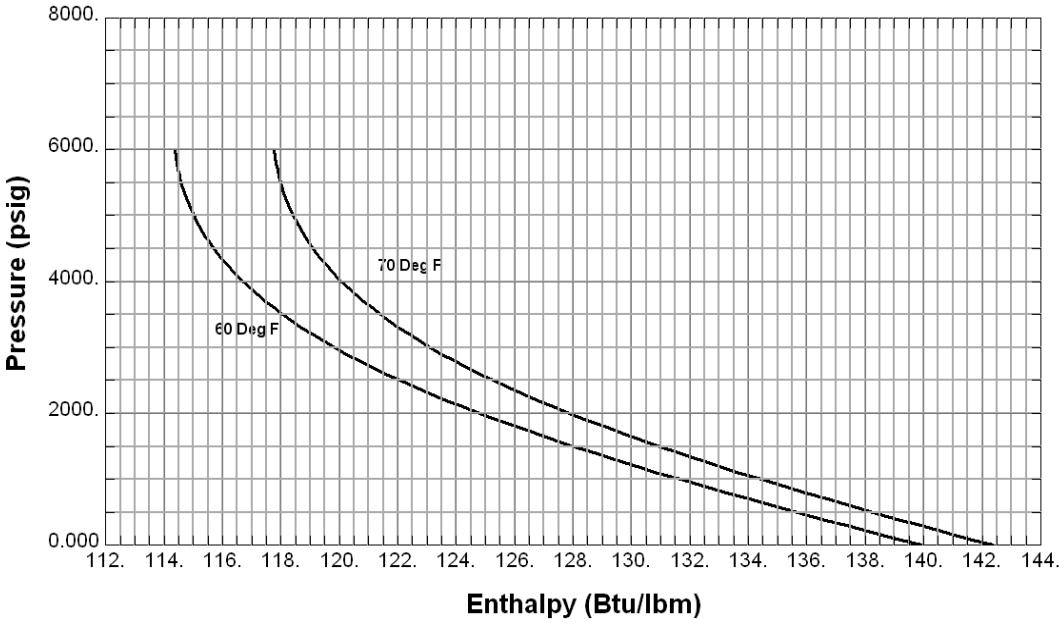

Figure 5: 87 % Nitrogen + 13 % Carbon Dioxide Enthalpy Curves

The entropy curves for the nitrogen—carbon dioxide mixture are shown in the Figure below. Unlike the enthalpy curves the entropy curves are essentially on top of each other. See Figure 6.

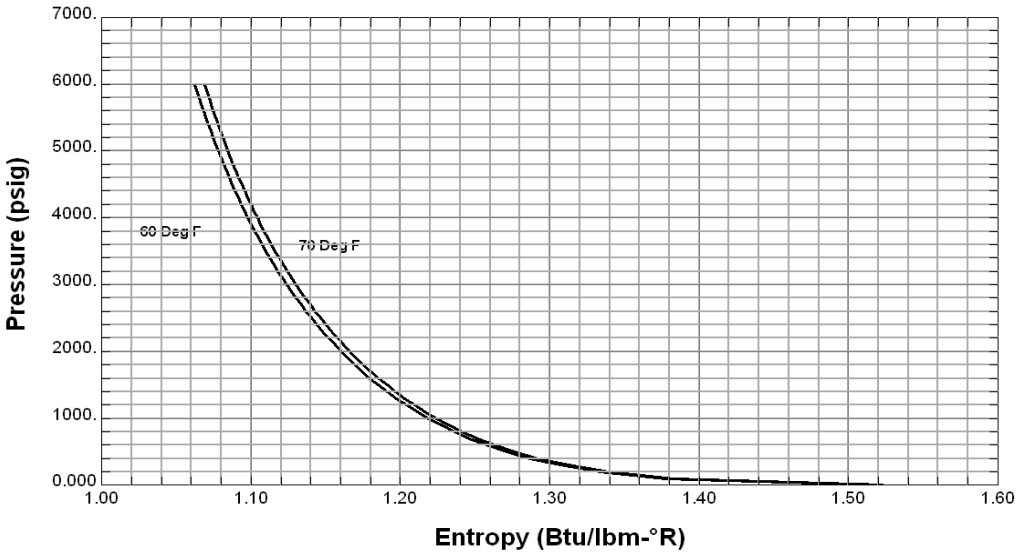

Figure 6: 87 % Nitrogen + 13 % Carbon Dioxide Mixture Entropy Curves

The density-pressure plots are included for the nitrogen—carbon dioxide mixture. Because they

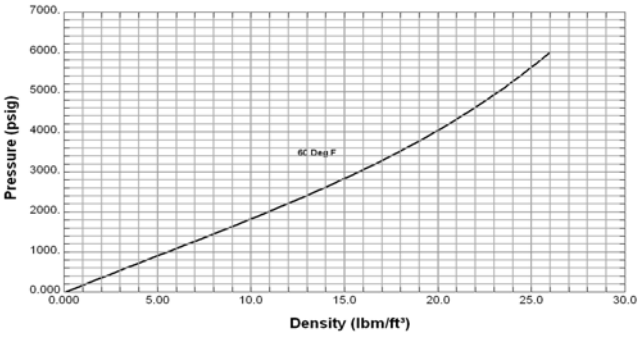

Figure 8: 87 % Nitrogen + 13 % Carbon Dioxide Density Curve @ 60 Degrees F

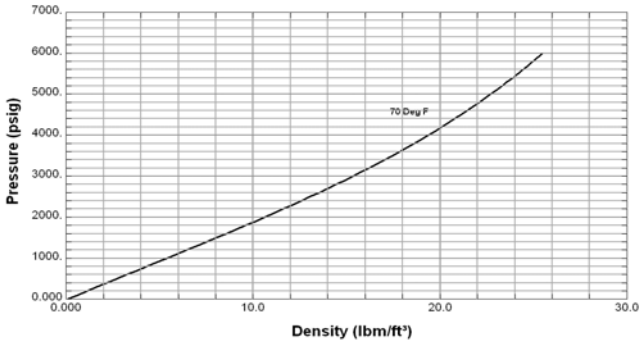

Figure 7: 87 % Nitrogen + 13 % Carbon Dioxide Density Curve @ 70 Degrees F

are so close, the plots are shown separately.

The constant volume heat capacities are also shown separately because they too are also very close. The variances are slight throughout the pressure range investigated.

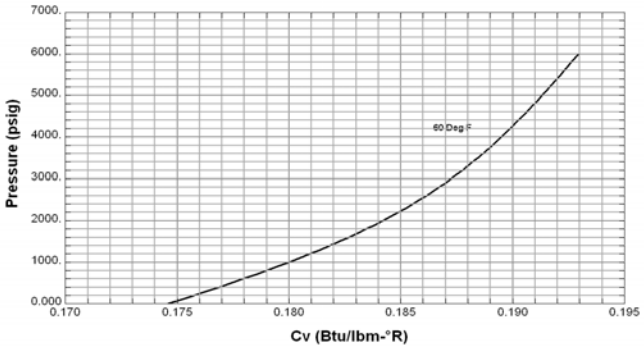

Figure 10: 87 % Nitrogen + 13 % Carbon Dioxide Constant Volume @ 60 Degrees F

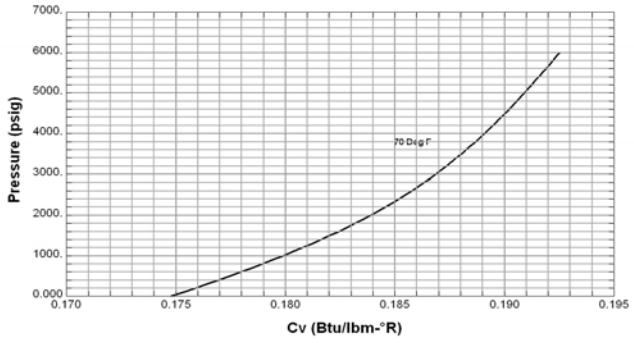

Figure 9: 87 % Nitrogen + 13 % Carbon Dioxide Constant Volume @ 70 Degrees

The heat capacities at constant pressure are shown in the Figure below. Note that in the pressure range (Highlighted by red line) important for this work the differences are almost indistinguishable.

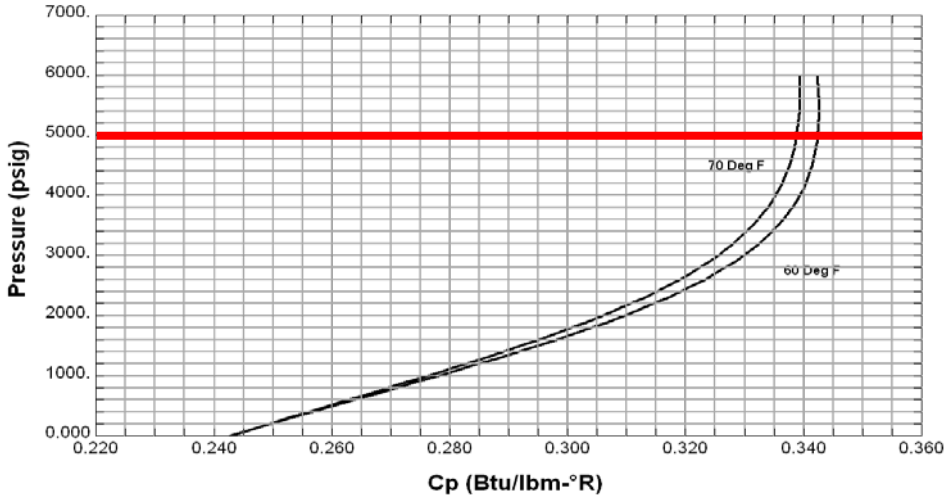

Figure 11: 87 % Nitrogen + 13 % Carbon Dioxide Constant Pressure Heat Capacities

Flue Gas

Flue gas was also reviewed. It is defined as the gas that exits to the atmosphere via a flue, which is a pipe for conveying exhaust gases from a fireplace, oven, furnace, boiler or steam generator. Quite often, it refers to the combustion exhaust gas produced at power plants. The emissions are different for each source.

Flue gas emissions from fossil fuel combustion refer to the combustion product gas resulting from 10 to 25 volume percent or more of flue gas. Its composition depends on what is being burned, but it will usually consist of mostly nitrogen (typically more than two-thirds) derived from the combustion air, carbon dioxide (CO_2) and water vapor as well as excess oxygen (also

derived from the combustion air). This is closely followed in volume by water vapor created by combustion of the hydrogen in the fuel with atmospheric oxygen. Much of the 'smoke' seen pouring from flue gas stacks may in fact be water vapor forming a cloud as it contacts cool air. It further contains a small percentage of pollutants such as particulate matter, carbon monoxide, nitrogen oxides and sulfur oxides.

A typical flue gas from the combustion of fossil fuels will also contain nitrogen oxides (NO_x), sulfur dioxide (SO_2) and particulate matter. The nitrogen oxides are derived from the nitrogen in the air as well as from any nitrogen containing compounds in the fossil fuel. Sulfur dioxide is derived from any sulfur-containing compounds in the fuels. The particulate matter is composed of very small particles of solid materials and very small liquid droplets which give flue gases their smoky appearance.

At power plants, flue gas is often treated with a series of chemical processes and scrubbers, which remove pollutants. Electrostatic precipitators remove particulate matter and flue gas desulfurization captures the sulfur dioxide produced by burning fossil fuels, particularly coal. Nitrogen oxides are treated either by modifications to the combustion process to prevent their formation, or by high temperature or catalytic reaction with ammonia or urea. In either case, the aim is to produce nitrogen gas, rather than nitrogen oxides.

The steam generators in large power plants and the process furnaces in large refineries, petrochemical and chemical plants, and incinerators burn large amounts of fossil fuels and therefore emit large amounts of flue gas. The table below presents the total amounts of flue gas typically generated by the burning of fossil fuels such as natural gas, fuel oil and coal. Data in the table were obtained by stoichiometric calculations. (Gas Emissions)

Table 3: Flue Gas Generated By Fossil Fuel Combustion

Combustion Data	Fuel Gas	Fuel Oil	Coal
Fuel Properties:			
Gross heating value, Btu/scf	1,093		
Gross heating value, Btu/gal		150,000	
Gross heating value, Btu/lb			11,150
Molecular weight	18		
Specific gravity		0.9626	
Gravity, °API		15.5	
Carbon/hydrogen ratio by weight		8.1	
weight % carbon			61.2
weight % hydrogen			4.3
weight % oxygen			7.4
weight % sulfur			3.9
weight % nitrogen			1.2
weight % ash			12.0
weight % moisture			10.0
Combustion Air:			
Excess combustion air, %	12	15	20

Wet Exhaust Flue Gas:			
Amount of wet exhaust gas, scf/10^6 Btu of fuel	11,600	11,930	12,714
CO_2 in wet exhaust gas, volume %	8.8	12.4	13.7
O_2 in wet exhaust gas, volume %	2.0	2.6	3.4
Molecular weight of wet exhaust gas	27.7	29.0	29.5
Dry Exhaust Flue Gas:			
Amount of dry exhaust gas, scf/10^6 Btu of fuel	9,510	10,600	11,554
CO_2 in dry exhaust gas, volume %	10.8	14.0	15.0
O_2 in dry exhaust gas, volume %	2.5	2.9	3.7
Molecular weight of dry exhaust gas	29.9	30.4	30.7

Note: scf is standard cubic feet at 60 °F and 14.696 psia.

It is of interest to note that the total amount of flue gas generated by coal is only 10 percent higher than the flue gas generated by natural gas. ***This means that changing to gas fired electrical plants will have virtually no impact on air emissions released.***

Also in the US there are a range of emerging technologies for removing pollutants emitted from power plants. One of these is the deployment of technologies to remove mercury from flue gas—typically by adsorption on sorbents or by capture in inert solids as part of the flue gas desulfurization product. There is very little performance data from large-scale industrial applications of such technologies. None has achieved significant worldwide market penetration so valid conclusions based on this implementation are premature.

Conclusions and Recommendations

History has shown that successful underbalanced drilling applications using exhaust gas have been applied for over two decades. A brief review of available diesel powered generators indicates that the exhaust gas rate is sufficient to be applied with **Impact Technologies'** FLASH ASJ system. The ancillary equipment required for safe operation of an exhaust gas drilling system is also available. If one wanted to pursue the flue gas system for underbalanced drilling, it is expected that similar equipment would be required to use flue gas as that for exhaust gas drilling.

It is recommended that serious consideration of the exhaust gas system be undertaken.

References

CamT, Posted on Underbalanced Drilling Thread, December 31, 2003.
http://drillingclub.proboards.com/index.cgi?board=ubd&action=display&thread

Caterpillar, "Guide to EPA Tier 4 Emissions for Diesel Generator Sets", 2011.

Cohn, J. G., "Catalytic Converters for Exhaust Emission Control of Commercial Equipment Powered by Internal Combustion Engines", Environmental Health Perspectives, Vol. 10, pp. 159-164, April 1975.

DieselNet, "Emission Standards, Nonroad Diesel Engines", Dieselnet.org, Downloaded March, 2011.

EPA Program Update, "Reducing Air Pollution From Nonroad Engines," United States Environmental Protection Agency, EPA420-F-03-011, April 2003.

Gas Emissions From Fossil Fuel Combustion, Wikipedia, http://en.wikipedia.org/wiki/flue_gas_emissions_from_fossil_fuel_combustion, Downloaded April 2011.

Jonralph, Posted on Chemical Engineering Other Topics, June 13, 2001. http://www.eng-tips.com/viewthread.cfm?qid=7819&page=48

KevinS, Posted on Underbalanced Drilling Thread, March 11, 2004 . *http://drillingclub.proboards.com/index.cgi?board=ubd&action=display&thread*

Mehta, S.A., Moore, R.G., Samuel, P., Laureshen, C.J., Bennion, D.B., and Teichrob, R., "High Pressure Flammability Limits Of Drilling Mud/Live Heavy Oil Mixtures In Pure Air And Nitrogen/Air Mixtures", Proceedings of Sixth UNITAR International Conference on Heavy Oil and Tar Sands, Houston, TX, February 1995.

Mehta, S. A., Moore, R.G., Laureshen, C. J., Samuel, P., Teichrob, A. R., Bennion, O. B., "Safety Considerations For Underbalanced Drilling Of Horizontal Wells Using Air Or Oxygen-Containing Gas", CIM Paper 95-135, Presented At The Sixth Petroleum Conference Of The South Saskatchewan Section, The Petroleum Society Of CIM, Regina, Saskatchewan, CA, October 1995.

Mehta, S. A., Moore, R. G., Pratt, C. A., (Kip), Gair, S. D., Hoyer, C.W.J. "High-Pressure Flammability of Drilling Mud/Condensate/Sour Gas Mixtures in De-Oxygenated Air for Use in Underbalanced Drilling Operations", SPE 37067, Presented at 1996 Conference on Horizontal Well Technology, Calgary, Alberta, CA, November 1996.

Pratt, C. A. (Kip), "Underbalanced Drilling: The Past, The Present and The Future" SPE Distinguished Lecturer Presentation, 2003.

Redman69, Posted on Underbalanced Drilling Thread, April 8, 2003 *http://drillingclub.proboards.com/index.cgi?board=ubd&action=display&thread*

Santelli, N., Posted on Underbalanced Drilling Thread, Mar 31, 2003. *http://drillingclub.proboards.com/index.cgi?board=ubd&action=display&thread*

The New York Blower Company, Brochure, Downloaded June 2011.

Appendix A—Example Generator Brochures

Cummins

and Caterpillar

CATERPILLAR®

ISO 9001:2000

PowerWorld®
Diesel Generator

GensetModel:PC880

POWERBYCUMMINS

110V-440V 3P4W

Standard Features and Characteristics

● QUALITY STANDARDS

- ○ The POWERWORLD generator set compliance with all main standards, such as ISO8528 GB/T2820-97), GB755 BS5000, VDE0530, ISO3046, IEC34-1, CSA22-2, AS1359, ISO14001.
- ○ Diesel engine and alternator from the exclusive manufacturer in china and their quality assurance.
- ○ Other standards and certifications can be considered on request.

● ASSEMBLY

- ○ The engine and alternator are close coupled by means of an SAE flange . A full torsional analysis has been carried out to guarantee no harmful vibration will occur b
- ○ Anti-vibration pads are affixed between engine alternator feet and the base frame. Thus ensuring complete vibration isolation of the rotating assemblies and enabling the machine to be placed on an uneven surface without any detrimental effects.
- ○ For durability and corrosion resistance, all iron and steel surfaces of canopy fabrications have been treated for coating by grit blast cleaning. Then covered by special three layers painting which provides an excellent corrosion resistant surface.

● CONTROL SYSTEM AND PROTECTION

- ○ Controllers are available for all applications. The controller system is used to start and stop the engine , indicate electric date and protect the generator set. See controller features inside.
- ○ The revolving parts are covered by safety net , and the place which easy to scald and got an electric shock all to have been put on obvious warning slogan

● WARRANTY

- ○ Each POWERWORLD generating set has been got through 2 hours load test for running 0%, 25%, 50%, 75%, 100% and 110% load, all protective devices and control function are simulated and checked before despatch.
- ○ POWERWORLD Company provides one-source responsibility for the generator set and accessories.
- ○ Engine and Alternator are guaranteed for a period of 12 months from the date of commissioning or 18 months from shipping, whichever occurs first.
- ○ Convenience for operation and maintenance, backed by CUMMINS and STAMFORD global service

RATINGS: All three-phase units are rated at 0.8 power factor. Standby ratings : Standby ratings apply to installations served by a reliable utility source. The standby rating is for this rating. Ratings are in according with ISO-3046/1, BS 5514 ,AS 2789 , and DIN 6271. Prime Power Ratings: Prime power ratings apply to installations where utility power is unavailable or unreliable. At varying load, the number of generator set operating hours is unlimited. A 10% overload capacity is available for one hour in twelve. Ratings are in accordance with ISO-8528/1, overload capacity in accordance with ISO-3046/1, BS 5514, AS 2789, and DIN 6271. For limited running time and base load ratings, consult the factory. The generator set manufacturer reserves the right to change the design or specifications without notice and without any obligation or liability whatsoever. GENERAL GUIDELINES FOR DERATION: Altitude: Derate 2.0% per 300m (984 ft) elevation above 1000m (3279 ft) up to a maximum elevation of 2450m (8000 ft). More than 2450m (8000ft), please contacts with us or our dealer seek the help. Temperature: Derate 6.0% per 11 (20) temperature above 40 (104).

Rating Range

		RPM1500 50Hz
Standby:	kW	880
	kVA	1100
Prime:	kW	800
	kVA	1000

GENERATOR SET RATINGS

Alternator Model	STAMFORD				MARATHON		
Frequency and Speed	50Hz 1500rpm				50Hz 1500rpm		

Prime Power Data

Class-TEMP Rise( )	Cont.H-125K/40				Cont.H-125K/40		
Voltage series star	380	400	415	440	380	400	415
Voltage parallel star	190	200	208	220	190	200	208
Voltage series delta	220	230	240	254	220	230	240
Rating capacity(kVA)	1000	1030	1000	1000	1025	1025	1025
Rating power(kW)	800	824	800	800	820	820	820
Power efficiency(%)	95.0	95.1	95.3	95.4	95.1	95.1	95.1
Input power(kW)	842	866	839	839	863	863	863

Standby Power Data

Class-TEMP Rise( )	Standby.H-125K/40				Standby.H-150K/40		
Voltage series star	380	400	415	440	380	400	415
Voltage parallel star	190	200	208	220	190	200	208
Voltage series delta	220	230	240	254	220	230	240
Rating capacity(kVA)	1060	1070	1060	1060	1075	1075	1075
Rating power(kW)	848	856	848	848	860	860	860
Power efficiency(%)	94.7	94.9	95.1	95.3	94.9	94.9	94.9
Input power(kW)	895	902	892	890	906	906	906

ALTERNATOR

Specification	1500RPM 50HZ
Type	4-Pole, Rotating Field
Exciter type	Brushless, Self excited
Voltage regulator	Solid State, Volts/Hz
Voltage regulation	1.0%
Insulation	Class H
Protection	IP23
Rated power factor	0.8
Stator winding	Double layer concentric
Winding pitch	Two thirds
Winding leads	12
Maximum overspeed	2250 Rev/min
Sustained short circuit	Self excited machines do not sustain a short circuit current
Waveform distortion	No load < 1.5% Non-distorting balanced linear load < 5.0%
Altitude	1000 m

- Alternators meet the requirement of BS EN 60034 and the relevant section of other international standards such as BS5000, VDE 0530, NEMA MG1-32, IEC34, CSAC22.2-100, As1359, and other standards and certifications can be considered on request.
- The 2/3 pitch design avoids excessive neutral currents. With the 2/3 pitch and carefully selected pole and tooth designs, ensures very low waveform distortion.
- Brushless alternator with brushless pilot exciter for excellent load response.
- The insulation system is class H, easy parallelling with mains or other generators, standard 2/3 pitch stator windings avoid excessive neutral currents.
- Backed by worldwide service network

DIESEL ENGINE

- KTA38-G5 diesel engines are manufactured by CHONGQING CUMMINS Engines Company Limited.

Application Data

EngineSpecifications	1500RPM 50HZ
Manufacturer	CUMMINS
Number of cylinders	12
Cylinder arrangement	60° V
Cycle	Four stroke
Aspiration	Turbocharged Aftercooler
Compression ratio	13.9:1
Bore Stroke	159 mm 159mm
Displacement	37.8litres
Direction of rotation	Clockwise viewed from front
Max.Power at rated rpm	970kW
Estimated total weight(dry)	4231kg
Frequency regulation steady state	0.25%
Mean piston speed	7.9m/s

Exhaust

Exhaust System	1500RPM 50HZ
Maximum back pressure	10.05 kPa (3 in Hg)
Exhaust gas flow (max)	3306 litre/s
Exhaust gas temperature (max)	513 (955℉)

Lubrication

Lubrication system	1500RPM 50HZ
Oil Pressure At idle speed At governed speed	 138kPa 310-448kPa
Maximum Oil Temperature	121 ℃(250℉)
Total System Capacity (with Combo Filter)	135 litre(35.7 US gal)

Engine Electrical

Engine Electrical System	1500RPM 50HZ
Battery charging alternator:	
Ground(negative/positive)	Negative
Volts(DC)	24V
Starter motor rated voltage(DC)	24V
Battery voltage	12V
Battery charging ampere	35A
Maximum allowable resistance of cranking circuit	0.002 ohm
Minimum Recommended Battery Capacity:	
Cold Soak @ 10 ℉ and Above	1200 CCA
Cold Soak @ 0 to 10 ℉ ℉	1280 CCA
Cold Soak @ -18 to 0℉ ℉	1800 CCA

Fuel

Fuel System	1500RPM 50HZ
Type of injection	Direct Injection Cummins PT
Maximum restriction at PT fuel injection pump with clean fuel filter with dirty fuel filter	 13.4kPa 26.8kPa
Maximum allowable head on injector return line	6.5 in Hg
Maximum fuel flow to injection pump	TBA litre/hour

Fuel consumption	1500RPM 50HZ
Standby power	228 litre/hr
100% prime power	209 litre/hr
75% prime power	161 litre/hr
50% prime power	113 litre/hr
25% prime power	65 litre/hr
Continuous power	N.A litre/hr

Specifications may change without notice

Http://www.dieselgeneratorcn.com

Application Data

Cooling System

Cooling System	1500RPM 50HZ
Total system capacity	
Engine Only	30 litres
Radiator	71 litres
Fan gas flow	29950m³/hr
Thermostat operation range	82 - 95 ¥
Maximum water temperature	100 (212¥) &»
Minimum Pressure of radiator cap	69kPa
Max. coolant temp. permitted	
for Standby Power	104 (220¥) &»
for Prime Power	100 (212¥) &»

NOTE:

All data is based on:

1. Engine operating with fuel system, water pump, lubricating oil pump, air cleaner and exhaust silencer; not included are battery charging alternator, fan, and optional driven components.
2. Engine operating with fuel corresponding to grade No. 2-D per ASTM D975.
3. ISO 3046, Part 1, Standard Reference Conditions of:
   Barometric Pressure : 100 kPa (29.53 in Hg)
   Air Temperature : 25 (77¥) &»
   Altitude : 110 m (361 ft)
   Relative Humidity : 30%
   Air Intake Restriction : 254 mm H2O (10 in H2O)
   Exhaust Restriction : 51 mm Hg (2 in Hg)

TBA: To Be Determined

CONTROLLERS

GTR-168 MANUAL CONTROLLER

The Model GTR-168is a Manual Engine Control Module designed to control the engine via a key switch and pushbuttons on the front panel. The module is used to start and stop the engine and indicate fault conditions, automatically shutting down the engine and indicating the engine failure by LED, giving true, first up fault annunciation.

Panel introduction:

- Indicator type frequency, voltmeter and ampere meter demonstration unit's electrical parameter.
- The voltage change-over switch and the rheotrope uses for to choose the different phase voltage and current to display.
- The big red button uses for the operator to stop the genset peremptorily
- The oil pressure gauge, coolant temperature gauge and the battery voltage gauge.
- The controller. And an integral anti-tamper LCD hours run counter is also provided.
- If the customer needs to use the preheating function, we will be able to increase the preheating button.

Protection:

Low Oil Pressure
High Engine Temperature
Auxiliary Shutdown
Over speed

DC Supply: 8 to 35 V Continuous.

PLC5110 CONTROLLER

Panel introduction:

- Indicator type frequency, voltmeter and ampere meter demonstration unit's electrical parameter.
- The voltage change-over switch and the rheotrope uses for to choose the different phase voltage and current to display.
- The oil pressure gauge, coolant temperature gauge and the battery voltage gauge.
- The controller.
- Preheating button.

Protection:

Over Speed Shutdown.
Low Oil Pressure Shutdown.
High Engine Temp Shutdown.
Charger failure alarm.
Mains failure alarm.
Optional Under speed Protection.

DC Supply: 8 to 35 V Continuous.

PLC5220 INTELIGENT CONTROL SYSTEM

The AMF25 is an Automatic Mains Failure module with generator monitoring, protection and start facilities. The controller has a large LCD screen, display the generator's each parameter, running and alarm information. The off/replacement button, mode switch button, start/stop button and the LED indicator light, makes the user easy to operate and maintain the generator.

Panel introduction:

- Indicator or digital type frequency, voltmeter and ampere meter demonstration unit's electrical parameter.
- The big red button uses for the operator to stop the genset peremptorily
- The controller.

Function:

- Communication: RS232 connection, uses the industry rank MODBUS protocol can easily communicate with others intelligence control system.
- Display function: LCD screen can display the generator's parameter and the control system's running information.
- Set up parameter: Engineer can set up the controller parameter from the control panel or through the PC, 6 programmable fan-out may satisfy the user each kind of demand.
- Protection: The control system can protect the generator set, manage each kind of electrical failure.
- Control Function of ATS.

DC Supply: 8 to 35 V Continuous.

Standard Features and Accessories

Paralleling System

- ❑ Reactive Droop Compensator
- ❑ Voltage Adjust Control
- ❑ Voltage Regulator Relocation Kit

Controller System

- ❑ Common Failure Relay Kit
- ❑ Customer Connection Kit(Except Open Style)
- ❑ Communications Products and PC Software
- ❑ Engine Pre-alarm Sender Kit
- ❑ Remote Annunciator Panel
- ❑ Remote Audiovisual Alarm Panel
- ❑ Remote Emergency Stop Kit
- ❑ PCRC series control system, with RS232 or RS485 communication connection and communication agreement.

Miscellaneous Accessories

- ❑ _____
- ❑ _____
- ❑ _____
- ❑ _____
- ❑ _____

Dimensions and Weights

Open Style

Overall Size, L*W*H(mm)	4850*1830*2400
Weight(radiator model),net,Kg	8900Kg

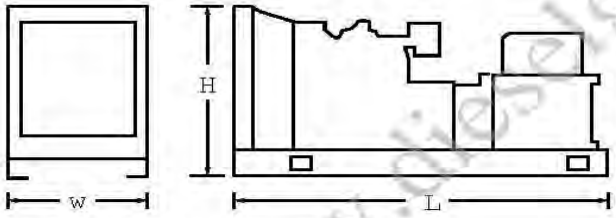

Soundproof Style

Overall Size, L*W*H(mm)	N/A
Weight(radiator model),net,Kg	N/A

NOTE: This drawing is provided for reference only and should not be used for planning installation. Contact your local distributor for more detailed information.

DISTRIBUTED BY:

Standard Features

- Battery, Battery Rack and Battery Cables
- Integral Vibration Isolation
- Oil Drain Extension
- Air cleaner ,Heavy Duty
- 3 Pole Circuit Breaker
- Heavy duty industrial type exhaust silencer with flexible pipe(supplied loose).

Maintenance and Literature

- General Maintenance Literature Kit
- Test Certificate and design paper
- Quality certificate and Maintenance card

Accessories

Enclosed Unit

- ❑ Sound Enclosure
- ❑ Weather Enclosure (with enclosed critical silencer)
- ❑ Weather Housing (with roof-mounted critical silencer)
- ❑ Trailer(Causes the genset easily to move)

Open Unit

- ❑ Exhaust Silencer, Critical kit
- ❑ Flexible Exhaust Connector, Stainless Steel

Cooling System

- ❑ Block Heater (recommended for ambient temperatures below 0 ¥)
- ❑ Radiator Duct Flange
- ❑ Remote Radiator Cooling

Fuel System

- ❑ Auxiliary Fuel Pump
- ❑ Flexible Fuel Lines
- ❑ Mechanical dipstick or fuel level sensor
- ❑ Subbase Fuel Tank with Day Tank
- ❑ Fuel fill cap with breather
- ❑ 10 hours running tank
- ❑ Automatic fuel--providing device
- ❑ Hand primer pump

Electrical System

- ❑ Battery Charger, Equalize/Float Type

Engine and Alternator

- ❑ 3 or 4 Pole Circuit Breaker with Shunt Trip
- ❑ Fuel/Water Separator
- ❑ Oil Preheater
- ❑ Air Preheater
- ❑ Alternator Strip Heater

Maintenance and Literature

- ❑ Maintenance Kit (includes air, oil, and fuel filters)
- ❑ Overhaul Literature Kit

Specifications may change without notice

Http://www.dieselgeneratorcn.com

Model: DFHA
KW rating: 620 standby
560 prime
Frequency: 50
Fuel type: Diesel

Generator set data sheet

Our energy working for you.™

Cummins Power Generation

Exhaust emission data sheet:	**EDS-251**
Exhaust emission compliance sheet:	
Sound performance data sheet:	**MSP-249**
Cooling performance data sheet:	
Prototype test summary data sheet:	**PTS-226**
Standard set-mounted radiator cooling outline:	**0500-3134**
Optional set-mounted radiator cooling outline:	
Optional heat exchanger cooling outline:	
Optional remote radiator cooling outline:	

Fuel consumption

	Standby				Prime				Continuous
	kW (kVA)				kW (kVA)				kW (kVA)
Ratings	620 (775)				560 (700)				
Load	1/4	1/2	3/4	Full	1/4	1/2	3/4	Full	Full
US gph	12.6	23.2	33.0	44.7	11.7	20.7	30.7	40.3	
L/hr	48	88	125	169	44	78	116	153	

Engine

	Standby rating	Prime rating	Continuous rating
Engine manufacturer	Cummins Inc.		
Engine model	QST30-G1		
Configuration	Cast iron, 50°V 12 cylinder		
Aspiration	Turbocharged and aftercooled		
Gross engine power output, kWm (bhp)	701.2 (940.0)	634.1 (850.0)	
BMEP at rated load, kPa (psi)	1840.9 (267.0)	1661.6 (241.0)	
Bore, mm (in)	140.0 (5.51)		
Stroke, mm (in)	165.1 (6.50)		
Rated speed, rpm	1500		
Piston speed, m/s (ft/min)	8.3 (1634.0)		
Compression ratio	14.0:1		
Lube oil capacity, L (qt)	132.5 (140.0)		
Overspeed limit, rpm	2100 ± 50		
Regenerative power, kW	78.00		

Fuel flow

Fuel flow at rated load, L/hr (US gph)	355.8 (94.0)	
Maximum inlet restriction, mm Hg (in Hg)	101.6 (4.0)	
Maximum return restriction, mm Hg (in Hg)	254.0 (10.0)	

Air	Standby rating	Prime rating	Continuous rating
Combustion air, m^3/min (scfm)	45.6 (1610.0)	42.4 (1500.0)	
Maximum air cleaner restriction, kPa (in H_2O)	6.2 (25.0)		
Alternator cooling air, m^3/min (scfm)	96.8 (3420.0)		

Exhaust			
Exhaust flow at rated load, m^3/min (cfm)	130.1 (4596.0)	119.6 (4225.0)	
Exhaust temperature, °C (°F)	537.8 (1000.0)	526.7 (980.0)	
Maximum back pressure, kPa (in H_2O)	10.2 (41.0)		

Standard set-mounted radiator cooling			
Ambient design, °C (°F)	40 (104)		
Fan load, kW (HP)	18.4 (24.7)		
Coolant capacity (with radiator), L (US gal)	200.6 (53.0)		
Coolant system air flow, m^3/min (scfm)	707.5 (25000		
Total heat rejection, MJ/min (Btu/min)	30.9 (29140)	27.1 (25560)	
Maximum cooling air flow static restriction, kPa (in H_2O)	0.12 (0.5)		

Optional set-mounted radiator cooling			
Ambient design, °C (°F)			
Fan load, kW_m (HP)			
Coolant capacity (with radiator), L (US gal)			
Cooling system air flow, m^3/min (scfm)			
Total heat rejection, MJ/min (Btu/min)			
Maximum cooling air flow static restriction, kPa (in H_2O)			

Optional heat exchanger cooling			
Set coolant capacity, L (US gal)			
Heat rejected, jacket water circuit, MJ/min (Btu/min)			
Heat rejected, after-cooler circuit, MJ/min (Btu/min)			
Heat rejected, fuel circuit, MJ/min (Btu/min)			
Total heat radiated to room, MJ/min (Btu/min)			
Maximum raw water pressure, jacket water circuit, kPa (psi)			
Maximum raw water pressure, aftercooler circuit, kPa (psi)			
Maximum raw water pressure, fuel circuit, kPa (psi)			
Maximum raw water flow, jacket water circuit, L/min (US gal/min)			
Maximum raw water flow, aftercooler circuit, L/min (US gal/min)			
Maximum raw water flow, fuel circuit, L/min (US gal/min)			
Minimum raw water flow @ 27 °C (80 °F) Inlet temp, jacket water circuit, L/min (US gal/min)			
Minimum raw water flow @ 27 °C (80 °F) Inlet remp, after-cooler circuit, L/min (US gal/min)			
Minimum raw water flow @ 27 °C (80 °F) Inlet temp, fuel circuit, L/min (US gal/min)			
Raw water delta P @ min flow, jacket water circuit, kPa (psi)			
Raw water delta P @ min flow, after-cooler circuit, kPa (psi)			
Raw water delta P @ min flow, fuel circuit, kPa (psi)			
Maximum jacket water outlet temp, °C (°F)			
Maximum after-cooler inlet temp, °C (°F)			
Maximum after-cooler inlet temp @ 25 °C (77 °F) ambient, °C (°F)			

Optional remote radiator cooling[1]	
Set coolant capacity, L (US gal)	

Our energy working for you.™

www.cumminspower.com

D-3412 (7/08)

Cummins Power Generation

Max flow rate @ max friction head, jacket water circuit, L/min (US gal/min)			
Heat rejected, jacket water circuit, MJ/min (Btu/min)			
Total heat radiated to room, MJ/min (Btu/min)			
Maximum friction head, jacket water circuit, kPa (psi)			
Maximum static head, jacket water circuit, m (ft)			
Maximum jacket water outlet temp, °C (°F)			

Weights[2]

Unit dry weight kgs (lbs)	7676 (16922)
Unit wet weight kgs (lbs)	7973 (17578)

Notes:

[1] For non-standard remote installations contact your local Cummins Power Generation representative.

[2] Weights represent a set with standard features. See outline drawing for weights of other configurations.

Derating factors

Standby	Rated power available up to 1524 m (5000 ft) at ambient temperatures up to 35 °C (95 °F). Above 1524 m (5000 ft), derate at 4% per 305 m (1000 ft), and 2% per 11 °C (1% per 10 °F) above 35 °C (95 °F).
Prime	
Continuous	

Ratings definitions

Emergency standby power (ESP):	**Limited-time running power (LTP)**:	**Prime power (PRP)**:	**Base load (continuous) power (COP)**:
Applicable for supplying power to varying electrical load for the duration of power interruption of a reliable utility source. Emergency Standby Power (ESP) is in accordance with ISO 8528. Fuel Stop power in accordance with ISO 3046, AS 2789, DIN 6271 and BS 5514.	Applicable for supplying power to a constant electrical load for limited hours. Limited Time Running Power (LTP) is in accordance with ISO 8528.	Applicable for supplying power to varying electrical load for unlimited hours. Prime Power (PRP) is in accordance with ISO 8528. Ten percent overload capability is available in accordance with ISO 3046, AS 2789, DIN 6271 and BS 5514.	Applicable for supplying power continuously to a constant electrical load for unlimited hours. Continuous Power (COP) is in accordance with ISO 8528, ISO 3046, AS 2789, DIN 6271 and BS 5514.

Our energy working for you.™

www.cumminspower.com

D-3412 (7/08)

Power Generation

Alternator data

Three phase table[1]		105 °C	125 °C	125 °C								
Feature code		B325	B324	B360								
Alternator data sheet number		310	309	309								
Voltage ranges		110/190 thru 127/220 220/380 thru 254/440	110/190 thru 127/220 220/380 thru 254/440	220/380 thru 254/440								
Surge kW		650	644	644								
Motor starting kVA (at 90% sustained voltage)	Shunt											
	PMG	2250	2000	2000								

Full load current amps at standby rating	120/208	220/380	230/240	240/416
	2151	1177	1118	1076

[1] Single phase power can be taken from a three phase generator set at up to 40% of the generator set nameplate kW rating at unity power factor.

Formulas for calculating full load currents:

Three phase output

$$\frac{\text{kW} \times 1000}{\text{Voltage} \times 1.73 \times 0.8}$$

Single phase output

$$\frac{\text{kW} \times \text{SinglePhaseFactor} \times 1000}{\text{Voltage}}$$

Cummins Power Generation
1400 73rd Avenue N.E.
Minneapolis, MN 55432 USA
Phone: 763 574 5000
Fax: 763 574 5298

Warning: Back feed to a utility system can cause electrocution and/or property damage. Do not connect to any building's electrical system except through an approved device or after building main switch is open.

Our energy working for you.™

www.cumminspower.com

D-3412 (7/08)

Power Generation

DIESEL GENERATOR SET

CATERPILLAR®

Image shown may not reflect actual package.

PRIME
1360 ekW 1700 kVA 60 Hz 1800 rpm 12 470 Volts

Caterpillar is leading the power generation marketplace with Power Solutions engineered to deliver unmatched flexibility, expandability, reliability, and cost-effectiveness.

FEATURES

FUEL/EMISSIONS STRATEGY
- EPA Certified for Stationary Emergency Application (EPA Tier 2 emissions levels)

DESIGN CRITERIA
- The generator set accepts 100% rated load in one step per NFPA 110 and meets ISO 8528-5 transient response.

FULL RANGE OF ATTACHMENTS
- Wide range of bolt-on system expansion attachments, factory designed and tested
- Flexible packaging options for easy and cost effective installation

SINGLE-SOURCE SUPPLIER
- Fully prototype tested with certified torsional vibration analysis available

WORLDWIDE PRODUCT SUPPORT
- Cat dealers provide extensive post sale support including maintenance and repair agreements
- Cat dealers have over 1,800 dealer branch stores operating in 200 countries
- The Cat® S•O•S℠ program cost effectively detects internal engine component condition, even the presence of unwanted fluids and combustion by-products

CAT 3512C DIESEL ENGINE
- Reliable, rugged, durable design
- Four-stroke-cycle diesel engine combines consistent performance and excellent fuel economy with minimum weight

CAT EMCP 3 SERIES CONTROL PANELS
- Simple user friendly interface and navigation
- Scalable system to meet a wide range of customer needs
- Integrated Control System and Communications Gateway

SEISMIC CERTIFICATION
- Seismic Certification available
- Anchoring details are site specific, and are dependent on many factors such as generator set size, weight, and concrete strength. IBC Certification requires that the anchoring system used is reviewed and approved by a Professional Engineer
- Seismic Certification per Applicable Building Codes: IBC 2000, IBC 2003, IBC 2006, IBC 2009, CBC 2007
- Pre-approved by OSHP and carries an OPA#(OSP-0084-01) for use in healthcare projects in California

PRIME 1360 ekW 1700 kVA

60 Hz 1800 rpm 12 470 Volts

CATERPILLAR®

FACTORY INSTALLED STANDARD & OPTIONAL EQUIPMENT

System	Standard	Optional
Air Inlet	• Single element canister type air cleaner with service indicator	[ ] Dual element & heavy duty air cleaners (with pre-cleaners) [ ] Air inlet adapters & shutoff
Cooling	• Radiator fan and fan drive • Fan and belt guards • Coolant level sensors* • Cat Extended Life Coolant*	[ ] Coolant level switch gauge [ ] Heat exchanger and expansion tank
Exhaust	• Exhaust manifold - dry - dual - 8 in • 203 mm (8 in) ID round flanged outlet	[ ] Mufflers [ ] Stainless steel exhaust flex fittings [ ] Elbows, flanges, expanders & Y adapters
Fuel	• Secondary fuel filters • Fuel cooler* • Fuel priming pump • Flexible fuel lines-shipped loose	[ ] Duplex secondary fuel filter [ ] Primary fuel filter with fuel water separator
Generator	• Class F insulation • Cat digital voltage regulator (CDVR) with kVAR/PF control, 3-phase sensing • Winding temperature detectors • Anti-condensation space heaters	[ ] Oversized generators [ ] Bearing temperature detector [ ] Cross current compensation transformer
Power Termination	• Bus bar (NEMA mechanical lug holes) • Right hand cable entry • Top or bottom cable entry	[ ] Left hand cable entry
Governor	• ADEM™ 3	[ ] Load share module
Control Panel	• EMCP 3.1 • User Interface panel (UIP) - rear mount • AC & DC customer wiring area (right side) • Emergency stop pushbutton	[ ] EMCP 3.2 ... [ ] EMCP 3.3 [ ] Option for right or left mount UIP [ ] Local & remote annunciator modules [ ] Digital I/O Module [ ] Generator temperature monitoring & protection [ ] Remote monitoring software
Lube	• Lubricating oil and filter • Oil drain line with valves • Fumes disposal • Gear type lube oil pump	[ ] Oil level regulator [ ] Deep sump oil pan [ ] Electric & air prelube pumps [ ] Manual prelube with sump pump [ ] Duplex oil filter
Mounting	• Rails - engine / generator / radiator mounting • Anti-vibration mounts (shipped loose)	[ ] Spring-type vibration isolator [ ] IBC Isolators
Starting/Charging	• 24 volt starting motor(s) • Batteries with rack and cables • Battery disconnect switch	[ ] Battery chargers (10 & 20 Amp) [ ] 45 amp charging alternator [ ] Oversize batteries [ ] Ether starting aids [ ] Heavy duty starting motors [ ] Barring device (manual) [ ] Air starting motor with control & silencer
General	• Right hand service • Paint - Caterpillar Yellow (with high gloss black rails & radiator) • SAE standard rotation • Flywheel and flywheel housing - SAE No. 00	[ ] CSA certification [ ] CE Certificate of Conformance [ ] Seismic Certification per Applicable Building Codes: IBC 2000, IBC 2003, IBC 2006, IBC 2009, CBC 2007 * Not included with packages without radiators

PRIME 1360 ekW 1700 kVA

60 Hz 1800 rpm 12 470 Volts

CATERPILLAR®

SPECIFICATIONS

CAT GENERATOR

SR4B Generator

Frame Size	2730
Excitation	Permanent Magnet
Pitch	0.6670
Number of poles	4
Number of bearings	2
Number of Leads	006
Insulation	Class F
IP Rating	Drip Proof IP22
Alignment	Closed Coupled
Overspeed capability- % of rated	125
Wave form	002.00
Paralleling kit/Droop transformer	Standard
Voltage Regulator	3 Phase sensing with volts/Hz
Telephone influence factor	Less than 50

CAT DIESEL ENGINE

3512C ATAAC, V-12, 4 stroke, water-cooled diesel

Bore	170.00 mm (6.69 in)
Stroke	190.00 mm (7.48 in)
Displacement	51.80 L (3161.03 in^3)
Compression Ratio	14.7:1
Aspiration	TA
Fuel System	Electronic unit injection
Governor Type	ADEM3

CAT EMCP SERIES CONTROLS

- EMCP 3.1 (Standard)
- EMCP 3.2 / EMCP 3.3 (Option)
- Single location customer connector point
- True RMS AC metering, 3-phase
- Controls
  - Run / Auto / Stop control
  - Speed Adjust
  - Voltage Adjust
  - Emergency Stop Pushbutton
  - Engine cycle crank
- Digital Indication for:
  - RPM
  - Operating hours
  - Oil pressure
  - Coolant temperature
  - System DC volts
  - L-L volts, L-N volts, phase amps, Hz
  - ekW, kVA, kVAR, kW-hr, %kW, PF (EMCP 3.2 / 3.3)
- Shutdowns with common indicating light for:
  - Low oil pressure
  - High coolant temperature
  - Low coolant level
  - Overspeed
  - Emergency stop
  - Failure to start (overcrank)
- Programmable protective relaying functions: (EMCP 3.2 & 3.3)
  - Under and over voltage
  - Under and over frequency
  - Overcurrent (time and inverse time)
  - Reverse power (EMCP 3.3)
- MODBUS isolated data link, RS-485 half-duplex (EMCP 3.2 & 3.3)
- Options
  - Vandal door
  - Local annunciator module
  - Remote annunciator module
  - Input / Output module
  - RTD / Thermocouple modules
  - Monitoring software

PRIME 1360 ekW 1700 kVA

60 Hz 1800 rpm 12 470 Volts

CATERPILLAR®

TECHNICAL DATA

Open Generator Set - - 1800 rpm/60 Hz/12 470 Volts	DM8261	
EPA Certified for Stationary Emergency Application (EPA Tier 2 emissions levels)		
Generator Set Package Performance		
Genset Power rating @ 0.8 pf	1700 kVA	
Genset Power rating with fan	1360 ekW	
Coolant to aftercooler		
Coolant to aftercooler temp max	47 ° C	117 ° F
Fuel Consumption		
100% load with fan	364.5 L/hr	96.3 Gal/hr
75% load with fan	286.2 L/hr	75.6 Gal/hr
50% load with fan	201.8 L/hr	53.3 Gal/hr
Cooling System[1]		
Air flow restriction (system)	0.12 kPa	0.48 in. water
Air flow (max @ rated speed for radiator arrangement)	2075 m³/min	73278 cfm
Engine Coolant capacity with radiator/exp. tank	390.8 L	103.2 gal
Engine coolant capacity	156.8 L	41.4 gal
Radiator coolant capacity	234.0 L	61.8 gal
Inlet Air		
Combustion air inlet flow rate	124.7 m³/min	4403.7 cfm
Exhaust System		
Exhaust stack gas temperature	388.4 ° C	731.1 ° F
Exhaust gas flow rate	293.5 m³/min	10364.9 cfm
Exhaust flange size (internal diameter)	203.2 mm	8.0 in
Exhaust system backpressure (maximum allowable)	6.7 kPa	26.9 in. water
Heat Rejection		
Heat rejection to coolant (total)	580 kW	32985 Btu/min
Heat rejection to exhaust (total)	1213 kW	68983 Btu/min
Heat rejection to aftercooler	443 kW	25193 Btu/min
Heat rejection to atmosphere from engine	118 kW	6711 Btu/min
Heat rejection to atmosphere from generator	71.6 kW	4071.9 Btu/min
Alternator[2]		
Motor starting capability @ 30% voltage dip	2788 skVA	
Frame	2730	
Temperature Rise	105 ° C	189 ° F
Lube System		
Sump refill with filter	310.4 L	82.0 gal
Emissions (Nominal)[3]		
NOx g/hp-hr	4.33 g/hp-hr	
CO g/hp-hr	.41 g/hp-hr	
HC g/hp-hr	.13 g/hp-hr	
PM g/hp-hr	.032 g/hp-hr	

[1] For ambient and altitude capabilities consult your Cat dealer. Air flow restriction (system) is added to existing restriction from factory.
[2] UL 2200 Listed packages may have oversized generators with a different temperature rise and motor starting characteristics. Generator temperature rise is based on a 40 degree C ambient per NEMA MG1-32.
[3] Emissions data measurement procedures are consistent with those described in EPA CFR 40 Part 89, Subpart D & E and ISO8178-1 for measuring HC, CO, PM, NOx. Data shown is based on steady state operating conditions of 77°F, 28.42 in HG and number 2 diesel fuel with 35° API and LHV of 18,390 btu/lb. The nominal emissions data shown is subject to instrumentation, measurement, facility and engine to engine variations. Emissions data is based on 100% load and thus cannot be used to compare to EPA regulations which use values based on a weighted cycle.

PRIME 1360 ekW 1700 kVA

60 Hz 1800 rpm 12 470 Volts

CATERPILLAR®

RATING DEFINITIONS AND CONDITIONS

Meets or Exceeds International Specifications: AS1359, CSA, IEC60034-1, ISO3046, ISO8528, NEMA MG 1-22, NEMA MG 1-33, UL508A, 72/23/EEC, 98/37/EC, 2004/108/EC

Prime - Output available with varying load for an unlimited time. Average power output is 70% of the prime power rating. Typical peak demand is 100% of prime rated ekW with 10% overload capability for emergency use for a maximum of 1 hour in 12. Overload operation cannot exceed 25 hours per year. Prime power in accordance with ISO3046. Prime ambients shown indicate ambient temperature at 100% load which results in a coolant top tank temperature just below the alarm temperature.

Ratings are based on SAE J1349 standard conditions. These ratings also apply at ISO3046 standard conditions.

Fuel rates are based on fuel oil of 35° API [16° C (60° F)] gravity having an LHV of 42 780 kJ/kg (18,390 Btu/lb) when used at 29° C (85° F) and weighing 838.9 g/liter (7.001 lbs/U.S. gal.). Additional ratings may be available for specific customer requirements, contact your Cat representative for details. For information regarding Low Sulfur fuel and Biodiesel capability, please consult your Cat dealer.

PRIME 1360 ekW 1700 kVA

60 Hz 1800 rpm 12 470 Volts

CATERPILLAR®

DIMENSIONS

Package Dimensions		
Length	6452.6 mm	254.04 in
Width	2324.5 mm	91.52 in
Height	2711.4 mm	106.75 in
Weight	15 926 kg	35,111 lb

NOTE: For reference only - do not use for installation design. Please contact your local dealer for exact weight and dimensions. (General Dimension Drawing #2846050).

Performance No.: DM8261

Feature Code: 512DE6D

Gen. Arr. Number: 2524216

Source: U.S. Sourced

October 27 2010

16297658

www.CAT-ElectricPower.com

DIESEL GENERATOR SET

CATERPILLAR®

Image shown may not reflect actual package.

PRIME
580 ekW 725 kVA
50 Hz 1500 rpm 400 Volts

Caterpillar is leading the power generation marketplace with Power Solutions engineered to deliver unmatched flexibility, expandability, reliability, and cost-effectiveness.

FEATURES

FUEL/EMISSIONS STRATEGY
- Low Fuel consumption

FULL RANGE OF ATTACHMENTS
- Wide range of bolt-on system expansion attachments, factory designed and tested
- Flexible packaging options for easy and cost effective installation

SINGLE-SOURCE SUPPLIER
- Fully prototype tested with certified torsional vibration analysis available

WORLDWIDE PRODUCT SUPPORT
- Cat dealers provide extensive post sale support including maintenance and repair agreements
- Cat dealers have over 1,800 dealer branch stores operating in 200 countries
- The Cat® S•O•S℠ program cost effectively detects internal engine component condition, even the presence of unwanted fluids and combustion by-products

CAT® 3412C TA DIESEL ENGINE
- Reliable, rugged, durable design
- Field-proven in thousands of applications worldwide
- Four-stroke-cycle diesel engine combines consistent performance and excellent fuel economy with minimum weight

CAT GENERATOR
- Designed to match the performance and output characteristics of Cat diesel engines
- Single point access to accessory connections
- UL 1446 recognized Class H insulation

CAT EMCP 3 SERIES CONTROL PANELS
- Simple user friendly interface and navigation
- Scalable system to meet a wide range of customer needs
- Integrated Control System and Communications Gateway

PRIME 580 ekW 725 kVA

50 Hz 1500 rpm 400 Volts

CATERPILLAR®

FACTORY INSTALLED STANDARD & OPTIONAL EQUIPMENT

System	Standard	Optional
Air Inlet	• Single element canister type air cleaner • Service indicator	[ ] Dual element air cleaner [ ] Heavy-duty air cleaner
Cooling	• Radiator with guard • Coolant drain line with valve • Fan and belt guards • Cat® Extended Life Coolant • Low coolant level alarm or shutdown	[ ] Radiator duct flange [ ] Jacket water heater with shutoff valve [ ] Heat exchanger and expansion tank
Exhaust	• Stainless steel exhaust flex and ANSI style outlet flange, gasket, bolts and mating weld flange, shipped loose	[ ] Mufflers (10 or 35 dBA) [ ] Elbow kit and through-wall installation kit [ ] Manifold and turbocharger guards
Fuel	• Primary and secondary fuel filters • Water separator • Fuel priming pump • Flexible fuel lines	[ ] Manual transfer pump [ ] Choice of three Automatic Transfer Systems
Generator	• Class H insulation • Class F temperature rise • VR6 Voltage Regulator, 3-phase sensing, 2:1 Volts/Hz • Reactive droop • Extension box • Bus bar connection • Segregated low voltage (AC/DC) wiring panel	[ ] Digital Voltage Regulator with kVAR/PF control [ ] Anti-condensation space heater [ ] Oversize and premium generators [ ] Circuit breakers, IEC Compliant, 3-pole or 4-pole with shunt trip
Governor	• PEEC - Cat Electronic	[ ] Electronic load sharing
Control Panels	• EMCP 3.1 (mounted inside power center) • Rear facing • Speed adjust • Emergency stop pushbutton • Voltage adjustment	[ ] EMCP 3.2 ... [ ] EMCP 3.3 [ ] Right-hand mounting of control panel [ ] Local annuniciator modules (NFPA 99/110) [ ] Remote annunicator modules (NFPA 99/110) [ ] Discrete I/O module
Lube	• Lubricating oil and filter • Oil drain line with valves • Fumes disposal	[ ] Manual sump pump
Mounting	• Formed steel base • Linear vibration isolators between base and engine-generator	[ ] Integral fuel tank base [ ] Sub base fuel tank [ ] Wide base [ ] Skid base
Starting/Charging	• 45 amp charging alternator • Fuel shutoff solenoid • 24 volt starting motor • Battery with rack and cables	[ ] Heavy-duty starting system [ ] 5 or 10 amp battery charger [ ] Oversize batteries [ ] Ether starting aid [ ] Battery disconnect switch
General		[ ] Enclosures - sound attenuated, weather protective [ ] Automatic transfer switches (ATS) [ ] Floor standing circuit breakers [ ] EU Certificate of Conformance (CE)

PRIME 580 ekW 725 kVA

50 Hz 1500 rpm 400 Volts

CATERPILLAR®

SPECIFICATIONS

CAT SR4B GENERATOR

Frame Size.....597
Excitation.....Self Excited
Pitch..... 0.8000
Number of poles.....4
Number of bearings..... Single Bearing
Insulation..... UL 1446 Recognized Class H with tropicalization and antiabrasion
IP Rating.....Drip Proof IP22
Alignment..... Pilot Shaft
Overspeed capability - % of rated..... 180
Wave form..... Less than 5% deviation
Paralleling kit/Droop transformer..... Standard
Voltage regulator.3 Phase sensing with selectible volts/Hz
Voltage regulation.....Less than +/- 1/2% (steady state) Less than +/- 1% (no load to full load)
Telephone Influence Factor..... Less than 50
Harmonic distortion..... Less than 5%

CAT DIESEL ENGINE

3412C TA V-12, 4-stroke-cycle watercooled diesel
Bore - mm..... 137.20 mm (5.4 in)
Stroke - mm..... 152.40 mm (6.0 in)
Displacement - L..... 27.02 L (1648.86 in^3)
Compression Ratio..... 13.0:1
Aspiration..... TA
Fuel system.....Pump and Lines
Governor type..... PEEC - Cat Electronic

CAT CONTROL PANELS

- EMCP 3.1 (Standard)
- EMCP 3.2 / EMCP 3.3 (Option)
- Single location customer connector point
- True RMS metering, 3-phase
- Controls
  - Run / Auto / Stop control
  - Speed Adjust
  - Voltage Adjust
  - Emergency Stop Pushbutton
  - Engine cycle crank
- Digital Indication for:
  - RPM
  - Operating hours
  - Oil pressure
  - Coolant temperature
  - System DC volts
  - L-L volts, L-N volts, phase amps, Hz
  - ekW, kVa, kVAR, kW-hr, % kW, PF (EMCP 3.2 / 3.3)
- Shutdowns with indicating lights for:
  - Low oil pressure
  - High coolant temperature
  - Low coolant level
  - Overspeed
  - Emergency Stop
  - Failure to start (overcrank)
- Programmable protective relay functions: (EMCP 3.2 & 3.3)
  - Under and over voltage
  - Under and over frequency
  - Overcurrent (time and inverse time)
  - Reverse power (EMCP 3.2 & 3.3)
- MODBUS isolated data link RS–485 half-duplex (EMCP 3.2 & 3.3)
- Options
  - Vandal door
  - Local annunciator module
  - Remote annunciator module
  - Input / Output module
  - RTD / Thermocouple Modules
  - Monitoring software

PRIME 580 ekW 725 kVA

50 Hz 1500 rpm 400 Volts

CATERPILLAR®

TECHNICAL DATA

Open Generator Set - - 1500 rpm/50 Hz/400 Volts	DM0627	
Package Performance		
Genset Power rating @ 0.8 pf	725 kVA	
Genset Power rating with fan	580 ekW	
Fuel Consumption		
100% load with fan	153.7 L/hr	40.6 Gal/hr
75% load with fan	117.5 L/hr	31.0 Gal/hr
50% load with fan	82.5 L/hr	21.8 Gal/hr
Cooling System[1]		
Air flow restriction (system)	0.12 kPa	0.48 in. water
Air flow (max @ rated speed for radiator arrangement)	1236 m³/min	43649 cfm
Engine coolant capacity	59.0 L	15.6 gal
Radiator coolant capacity	84.0 L	22.2 gal
Engine Coolant capacity with radiator/exp. tank	143.0 L	37.8 gal
Exhaust System		
Combustion air inlet flow rate	44.2 m³/min	1560.9 cfm
Exhaust stack gas temperature	534.0 °C	993.2 °F
Exhaust gas flow rate	125.4 m³/min	4428.5 cfm
Exhaust flange size (internal diameter)	203.2 mm	8.0 in
Exhaust system backpressure (maximum allowable)	6.7 kPa	26.9 in. water
Heat rejection		
Heat rejection to coolant (total)	347 kW	19734 Btu/min
Heat rejection to exhaust (total)	571 kW	32473 Btu/min
Heat rejection to atmosphere from engine	95 kW	5403 Btu/min
Heat rejection to atmosphere from generator	27.3 kW	1552.5 Btu/min
Alternator[2]		
Motor starting capability @ 30% voltage dip	1815 skVA	
Frame	597	
Temperature Rise	105 °C	189 °F
Lube System		
Sump refill with filter	139.0 L	36.7 gal
Emissions[3]		
NOx mg/nm3	2932.1 mg/nm³	
CO mg/nm3	171.7 mg/nm³	
HC mg/nm3	102.6 mg/nm³	
PM mg/nm3	45 mg/nm³	

[1] For ambient and altitude capabilities consult your Cat dealer. Air flow restriction (system) is added to existing restriction from factory.
[2] UL 2200 Listed packages may have oversized generators with a different temperature rise and motor starting characteristics. Generator temperature rise is based on a 40°C ambient per NEMA MG1-32.
[3] Emissions data measurement procedures are consistent with those described in EPA CFR 40 Part 89, Subpart D & E and ISO8178-1 for measuring HC, CO, PM, NOx. Data shown is based on steady state operating conditions of 77°F, 28.42 in HG and number 2 diesel fuel with 35° API and LHV of 18,390 btu/lb. The nominal emissions data shown is subject to instrumentation, measurement, facility and engine to engine variations. Emissions data is based on 100% load and thus cannot be used to compare to EPA regulations which use values based on a weighted cycle.

PRIME 580 ekW 725 kVA

50 Hz 1500 rpm 400 Volts

CATERPILLAR®

RATING DEFINITIONS AND CONDITIONS

Meets or Exceeds International Specifications: AS1359, CSA, IEC60034-1, ISO3046, ISO8528, NEMA MG 1-22, NEMA MG 1-33, UL508A, 72/23/EEC, 98/37/EC, 2004/108/EC

Prime - Output available with varying load for an unlimited time. Average power output is 70% of the prime power rating. Typical peak demand is 100% of prime rated ekW with 10% overload capability for emergency use for a maximum of 1 hour in 12. Overload operation cannot exceed 25 hours per year. Prime power in accordance with ISO3046. Prime ambients shown indicate ambient temperature at 100% load which results in a coolant top tank temperature just below the alarm temperature.

Ratings are based on SAE J1349 standard conditions. These ratings also apply at ISO3046 standard conditions.

Fuel rates are based on fuel oil of 35° API [16° C (60° F)] gravity having an LHV of 42 780 kJ/kg (18,390 Btu/lb) when used at 29° C (85° F) and weighing 838.9 g/liter (7.001 lbs/U.S. gal.). Additional ratings may be available for specific customer requirements, contact your Cat representative for details. For information regarding Low Sulfur fuel and Biodiesel capability, please consult your Cat dealer.

PRIME 580 ekW 725 kVA

50 Hz 1500 rpm 400 Volts

CATERPILLAR®

DIMENSIONS

Package Dimensions		
Length	**4485.0 mm**	**176.57 in**
Width	**1798.1 mm**	**70.79 in**
Height	**1986.7 mm**	**78.22 in**
Weight	**5693 kg**	**12,551 lb**

NOTE: For reference only - do not use for installation design. Please contact your local dealer for exact weight and dimensions. (General Dimension Drawing #2923106).

Performance No.: DM0627

Feature Code: 412DEQ9

Gen. Arr. Number: 1492443

Source: European Sourced

October 27 2010

16282242

www.CAT-ElectricPower.com

Appendix B—Example Ancillary Equipment Brochures

BASF
The Chemical Company

PTX™ and DPX™

For mining applications

Product data

Watery eyes. Itchy throats. Headaches and nausea. They are the "occupational hazards" of almost everyone who works with diesel equipment. Worse yet, the fumes and noxious chemicals emitted from this machinery can lead to long-term health problems, causing increased sick time and employee turnover.

Yet with BASF ingenuity, your company can do more than improve the work environment of its employees. You can actually enhance productivity; protect workers and materials on the job site, while complying with today's increasingly stringent anti-pollution legislation.

As a world leader in emissions control technologies, BASF has extensive experience in reducing carbon monoxide (CO), hydrocarbons (HC) and particulate matter (PM) produced in diesel engine environments, including mining.

PTX Diesel Oxidation Catalyst
BASF innovative PTX catalyst was specifically designed to control carbon monoxide and hydrocarbon emissions from diesel engines.

- Reduces CO up to 95%
- Reduces HC up to 95%
- Extremely durable
- Withstands up to 590°C (1100°F)
- Simple to install
- Easy to clean and maintain

DPX™ Diesel Particulate Filter
BASF DPX soot filter is remarkably effective for eliminating soot and other pollutants.

- Proven on tens of thousands vehicles retrofitted worldwide
- Verified by the US EPA
- Can reduce PM,CO, HC by 90+%
- Can regenerate at normal diesel operating temperatures

About BASF
As the world's leading chemical company, BASF's portfolio ranges from chemicals, plastics, performance products, agricultural products and fine chemicals to crude oil and natural gas. BASF's intelligent system solutions and high-value products help its customers to be more successful. BASF develops new technologies and uses them to open up additional market opportunities. It combines economic success with environmental protection and social responsibility, thus contributing to a better future.

BASF Emission Control Technologies for Retrofit Mining Applications			
Technology	**Carbon Monoxide**	**Hydrocarbons**	**Particulate Matter**
PTX	✓	✓	
DPX	✓	✓	✓

BASF

The Chemical Company

BASF DPX™ Diesel Particulate Filter

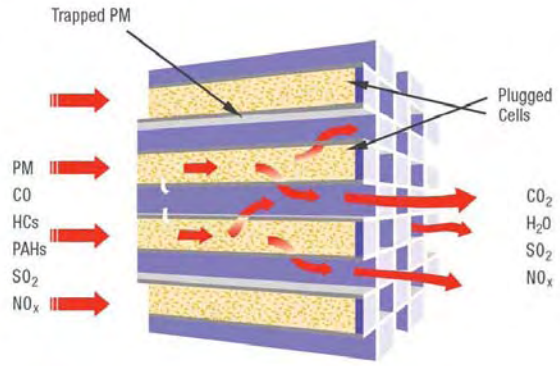

BASF PTX™ Diesel Oxidation Catalyst

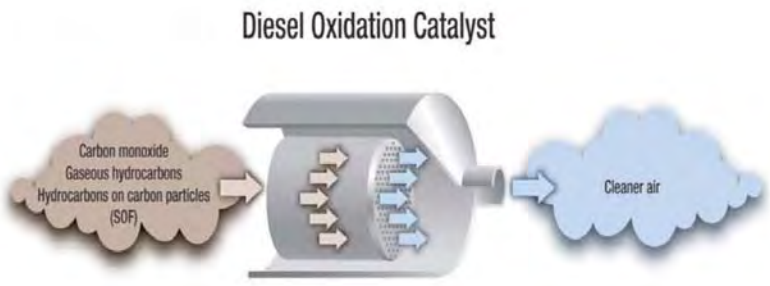

BASF Catalysts LLC
101 Wood Avenue
Iselin, NJ 08830-0770
Telephone: 732 205-5000
Fax: 732 205-5915
Web site: www.basf-catalysts.com

BF-8503 Rev. 11/2006

MATERIAL SPECIFICATIONS [INCHES, POUNDS, WR² IN LB.-FT.²]

CLASS II PLUG FANS

Size	PLR bare fan weights				AcoustaFoil bare fan weights				B†	Wheel WR²				Shaft diameter				
	450°F.	800°F. Uninsulated	800°F. Insulated	1000°F. Insulated	450°F.	800°F. Uninsulated	800°F. Insulated	1000°F. Insulated		AcF	PLR	SST AcF	SST PLR	450°F.		800°F.	1000°F.	800°F./ 1000°F.
														at wheel	at bearings	at wheel	at wheel	at bearings
12	137	158	181	—	—	—	—	—	A	—	2	—	—	1 7/16	1 7/16	1 7/16*	—	1 15/16
15	148	165	188	—	—	—	—	—	A	—	5	—	—	1 7/16*	1 11/16	1 7/16*	—	1 15/16
18	132	253	290	307	233	254	291	308	A	11	10	13	12	1 11/16*	1 15/16	1 11/16*	1 15/16*	2 3/16
20	255	290	327	335	253	288	325	333	A	17	19	21	19	1 15/16	1 15/16	1 15/16	1 15/16	2 7/16
22	263	298	335	343	259	294	331	339	A	24	27	29	27	1 15/16	1 15/16	1 15/16	1 15/16	2 7/16
24	389	416	466	489	385	413	462	485	C	38	42	55	47	1 15/16	2 3/16	1 15/16	2 3/16	2 7/16
27	400	428	477	500	395	423	472	495	C	55	60	79	65	1 15/16	2 3/16	1 15/16	2 3/16	2 7/16
30	488	524	591	622	475	511	578	609	D	87	103	121	103	1 15/16	2 3/16	1 15/16	2 7/16	2 7/16
33	525	561	628	658	507	543	610	640	D	103	158	174	157	2 3/16	2 3/16	2 3/16	2 7/16	2 7/16
36	623	680	771	1022	607	664	755	1006	D	219	249	304	276	2 3/16	2 3/16	2 3/16	2 7/16	2 11/16
40	696	723	814	1077	669	707	798	1061	D	321	382	446	428	2 7/16	2 7/16	2 7/16	2 7/16	2 11/16
44	1230	1340	1315	1395	1190	1230	1270	1350	F	523	645	755	658	2 11/16	3 7/16	2 11/16	2 15/16	3 7/16
49	1325	1470	1410	1560	1300	1340	1380	1530	F	891	964	1251	1054	2 15/16	3 7/16	2 15/16	2 15/16	3 7/16

†Bearing types: A–Link-Belt P3-U200. C–Sealmaster SPM. D–Sealmaster MPD. F–Link-Belt P-B22400.
*Shaft diameter at drive end and wheel. For all others, shaft diameter at bearings same as at drive.
nyb reserves the right to substitute bearings of equal ratings.

CLASS III PLUG FANS

Size	PLR bare fan weights				AcoustaFoil bare fan weights				B†‡	Wheel WR²				Shaft diameter					
	450°F.	800°F. Uninsulated	800°F. Insulated	1000°F./1300°F. Insulated	450°F.	800°F. Uninsulated	800°F. Insulated	1000°F. Insulated		AcF	PLR	SST AcF	SST PLR	450°F.		800°F.	1000°F./ 1300°F.	800°F./1000°F./ 1300°F.	1000°F./ 1300°F.
														at wheel	at bearings	at wheel	at wheel	at bearings	at drive
18	305	329	366	399	304	328	365	398	A★	12	12	14	12	1 11/16*	2 3/16	1 11/16*	2 7/16	2 7/16	1 15/16
22	331	392	429	491	327	388	425	487	D♦	28	30	36	27	1 15/16	2 7/16	1 15/16	2 11/16	2 11/16	2 7/16
24	507	541	590	624	507	541	590	624	D	42	49	55	47	1 15/16	2 7/16	1 15/16	2 11/16	2 11/16	2 7/16
27	523	557	606	640	522	556	605	639	D	63	71	79	65	1 15/16	2 7/16	1 15/16	2 11/16	2 11/16	2 7/16
30	702	735	802	902	713	746	813	913	E	96	113	121	111	2 3/16	2 11/16●	2 3/16	2 15/16	2 15/16	2 15/16
33	736	769	836	936	736	768	865	965	E	169	166	187	157	2 3/16	2 11/16♦	2 3/16	2 15/16	2 15/16	2 15/16
36	898	928	1019	1085	901	931	1022	904	E	240	279	319	309	2 7/16	2 11/16	2 7/16	2 15/16	2 15/16	2 15/16
40	943	973	1064	1130	943	973	1064	1130	E	374	454	508	477	2 7/16	2 11/16	2 7/16	2 15/16	2 15/16	2 15/16
44	1300	1345	1385	1460	1240	1280	1320	1395	F	628	701	823	841	2 15/16	3 7/16	2 11/16	2 15/16	3 7/16	3 7/16
49	1510	1550	1595	1640	1305	1345	1390	1435	F	913	1043	1321	1316	2 15/16	3 7/16	2 15/16	2 15/16	3 7/16	3 7/16

†Bearing types: A–Link-Belt P3-U200. D–Sealmaster MPD. E–Link-Belt P-U300. F–Link-Belt P-B22400. ♦Link-Belt P3-U200 used on 450°F. units.
‡The inboard bearing on all 1300°F. Plug Fans is an expansion-type bearing.
★Size 18 1300°F. Plug Fan utilizes Sealmaster MPD bearings in lieu of the 200 Series bearings shown.
*Shaft diameter at drive end and wheel. ●Shaft diameter at drive end is 2 7/16". For all others, shaft diameter at bearings same as at drive.
nyb reserves the right to substitute bearings of equal ratings.

EXHAUST FAN CHOICES

New York Blower Duct Fans, with heat-fan construction, are ideal for industrial oven and dryer exhaust systems where pressure requirements are minimal and compact, light-weight designs are advantageous. With heat-fan construction, Duct Fans are capable of handling airstream temperatures to 350°F. in ambient environments up to 120°F. The Duct Fan, with heat-fan construction, includes a flow of cooler, ambient air through the belt well and inner tube, cooling the fan's internal components. Depending on temperature requirements, modifications include high-temperature fan wheel, special drive components, and modifications to provide internal ambient-air cooling.

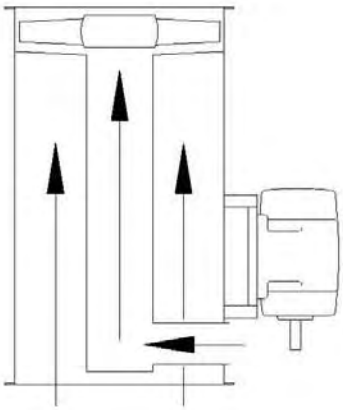

DRAWINGS/DIMENSIONS [INCHES] Not to be used for construction unless certified.

DIMENSIONS [INCHES]–for drawings on page 19

Size	Wheel dia.*	A	E	F●	G max. Class II	G max. Class III	H 450°F.	H 800°F.	H 1000°F./1300°F. 6" panel	H 1000°F./1300°F. 8" panel	K	M 450°F.	M 800°F.	M 1000°F./1300°F. 6" panel	M 1000°F./1300°F. 8" panel	N	P†	R	S	T	Wheel cone clear.	Class II C-NW■ max.	Class II Max. motor frame■	Class III C-NW■ max.	Class III Max. motor frame■
12	12 1/4	21	19	4	18	–	34 1/4	38 1/4	–	–	3	10	14	–	–	21 1/4	17	15 3/8	14 5/8	8-11/16	4 1/2	17	215T	–	–
15	15	21	19	4	18	–	35 3/8	39 3/8	–	–	3	11 1/8	15 1/8	–	–	21 1/4	17	18 5/8	17 7/8	8-11/16	5 1/2	17	215T	–	–
18	18 1/4	28	26	6	26 3/4	25 1/4	42 1/8	46 1/8	48 1/8	50 1/8	4	14	18	20	22	24 1/8	24	22 3/4	21 3/4	16-7/8	7	22 3/4	284T	22 3/4	284T
20	20 1/8	28	26	6	26 3/4	26	43 1/4	47 1/4	49 1/4	51 1/4	4	15 1/8	19 1/8	21 1/8	23 1/8	24 1/8	24	24 1/2	23 1/2	16-7/8	7 1/2	22 3/4	284T	22 3/4	284T
22	22 1/4	28	26	6	26 3/4	26	44 3/4	48 3/4	50 3/4	52 3/4	4	16 5/8	20 5/8	22 5/8	24 5/8	24 1/8	24	27 1/8	26 1/8	16-7/8	8 1/4	22 3/4	284T	22 3/4	284T
24	24 1/2	33	31	6	29 1/4	27 1/2	50	54	56	58	5	18 1/4	22 1/4	24 1/4	26 1/4	26 3/4	29	30 1/2	29 1/8	16-1	9 1/4	25 1/4	324T	25 1/4	324T
27	27	33	31	6	29 1/4	28 1/4	51 1/2	55 1/2	57 1/2	59 1/2	5	19 3/4	23 3/4	25 3/4	27 3/4	26 3/4	29	33 1/8	31 3/4	16-1	10 1/8	25 1/4	324T	25 1/4	324T
30	30	39	37	5 1/2	30 1/8	30 1/4	57 1/8	61 1/8	63 1/8	65 1/8	6	21 7/8	25 7/8	27 7/8	29 7/8	29 1/4	34	36 1/2	35 1/8	16-1	11 1/4	27 3/4	364T	27 3/4	364T
33	33	39	37	5 1/2	20 1/3	30 1/4	59 1/8	63 1/8	65 1/8	67 1/8	6	23 7/8	27 7/8	29 7/8	31 7/8	29 1/4	34	39 3/4	38 3/8	16-1	12 1/4	27 3/4	364T	27 3/4	364T
36	36 1/2	46	44	6	31 3/8	31 3/4	63 7/8	67 7/8	69 7/8	71 7/8	7	26 3/8	30 3/8	32 3/8	34 3/8	30 1/2	41	44 1/8	42 3/8	16-1	13 3/8	29	365T	29	365T
40	40 1/4	46	44	6	31 3/8	31 3/4	66 3/8	70 3/8	72 3/8	74 3/8	7	28 7/8	32 7/8	34 7/8	36 7/8	30 1/2	41	47 1/2	46 1/8	24-1	14 3/4	29	365T	29	365T
44	44 1/2	56	54	6	52	52	71 1/8	75 1/8	77 1/8	79 1/8	8	31 3/4	35 3/4	37 3/4	39 3/4	31 3/8	51	52 1/2	51 1/8	24-1	16 1/4	28 5/8	365T	28 5/8	365T
49	49	56	54	6	52	52	74 1/4	78 1/4	80 1/4	82 1/4	8	34 7/8	38 7/8	40 7/8	42 7/8	31 3/8	51	57 1/2	56 1/8	24-1	17 1/8	28 5/8	365T	28 5/8	365T

*O.D. of blades. †P is square dimension of panel. ●Plus corner holes. Tolerance: ±1/8"

Mounting panel thickness: Sizes 12-22, 10 gauge; Sizes 24-40, 7 gauge; Sizes 44-49, 1/4".

■In some cases, larger frame motors may fit. In all cases, maximum motor frame size is limited to C-NW maximum dimension.

PLUG FANS WITH INTEGRAL INLET-CONE ASSEMBLIES

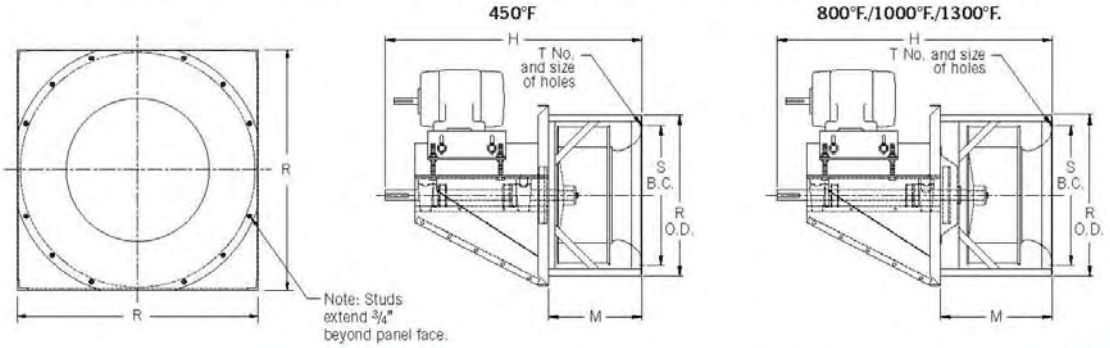

L = all holes 9/16" diameter and on centerline. Sizes 12–27, 24 holes; Sizes 30–40, 32 holes.

DERATES

The integral inlet-cone assembly incorporates reduced-depth inlet cones in Sizes 18 through 49 [not available Size 20] for substantial reduction in fan depths ranging from 2" on the Size 18 to 6" on the Size 49. Due to the shorter-length cone, air performance derates are required as follows: Size 18–8%, Size 22–4 1/2%, and Size 24–3%. Size 20 and Sizes 27 and larger do not require a derate.

DIMENSIONS [INCHES]

Size	H Class II 450°F.	H Class II 800°F.	H Class II 1000°F. 6" panel	H Class II 1000°F. 8" panel	H Class III 450°F.	H Class III 800°F.	H Class III 1000°F./1300°F. 6" panel	H Class III 1000°F./1300°F. 8" panel	M 450°F.	M 800°F.	M 1000°F./1300°F. 6" panel	M 1000°F./1300°F. 8" panel	R	S	T
12	34 1/4	38 1/4	NA	NA	34 1/4	38 1/4	NA	NA	10	14	NA	NA	17	14 5/8	8-11/16
15	35 3/8	39 3/8	NA	NA	35 3/8	39 3/8	NA	NA	11 1/8	15 1/8	NA	NA	17	17 7/8	8-11/16
18	40 1/8	44 1/8	46 1/8	48 1/8	40 1/8	44 1/8	46 1/8	48 1/8	12	16	18	20	24	19 3/4	16-7/8
20	43 1/4	47 1/4	49 1/4	51 1/4	NA	NA	NA	NA	15 1/8	19 1/8	21 1/8	23 1/8	24	23 1/2	16-7/8
22	42 1/8	46 1/8	48 1/8	50 1/8	42 1/8	46 1/8	48 1/8	50 1/8	14	18	20	22	24	24	16-7/8
24	47 1/4	51 1/4	53 1/4	55 1/4	47 1/4	51 1/4	53 1/4	55 1/4	15 1/2	19 1/2	21 1/2	23 1/2	29	26 1/8	16-1
27	48 1/2	52 1/2	54 1/2	56 1/2	48 1/2	52 1/2	54 1/2	56 1/2	16 3/4	20 3/4	22 3/4	24 3/4	29	29 1/8	16-1
30	53 3/4	57 3/4	59 3/4	61 3/4	53 3/4	57 3/4	59 3/4	61 3/4	18 1/2	22 1/2	24 1/2	26 1/2	34	31 3/4	16-1
33	55 3/8	59 3/8	61 3/8	63 3/8	55 3/8	59 3/8	61 3/8	63 3/8	20 1/8	24 1/8	26 1/8	28 1/8	35	35 1/8	16-1
36	59 3/8	63 3/8	65 3/8	67 3/8	59 3/8	63 3/8	65 3/8	67 3/8	21 7/8	25 7/8	27 7/8	29 7/8	41	38 3/8	16-1
40	61 1/2	65 1/2	67 1/2	69 1/2	61 1/2	65 1/2	67 1/2	69 1/2	24	28	30	32	42	42 3/8	24-1
44	65 5/8	69 5/8	71 5/8	73 5/8	65 5/8	69 5/8	71 5/8	73 5/8	26 1/4	30 1/4	32 1/4	34 1/4	51	46 5/8	24-1
49	68 1/4	72 1/4	74 1/4	76 1/4	68 1/4	72 1/4	74 1/4	76 1/4	28 7/8	32 7/8	34 7/8	36 7/8	51	51 1/8	24-1

NA=Not available Tolerance: ±1/8"

DRAWINGS

■ Plug Fan motors are mounted as space permits as measured by dimension C-NW. To determine fit, compare the desired motor's frame size with the frame size listed below. If the frame size and C-NW dimension are no larger than that shown, the combination is satisfactory. If the C-NW dimension is larger than that shown, a different motor or fan must be selected.

CLASS II SIZES 12-40

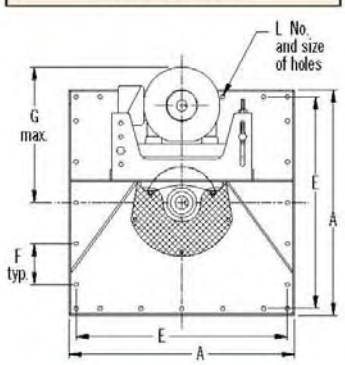

450°F.

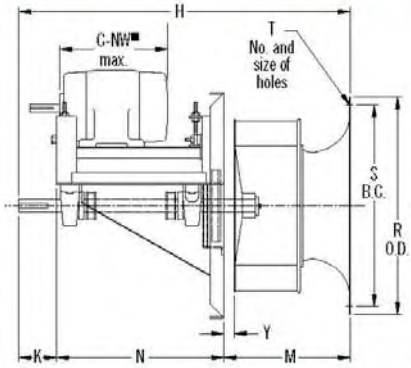

800°F.–1000°F.

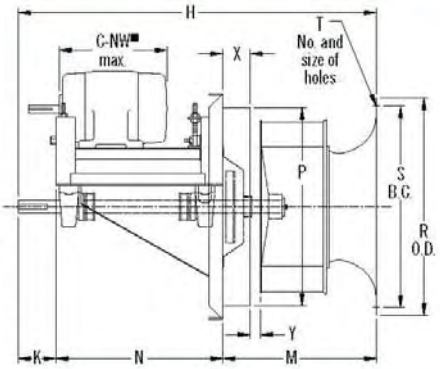

CLASS III SIZES 18-40

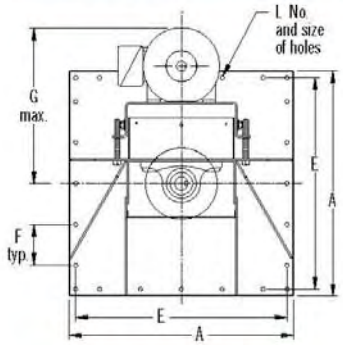

450°F.

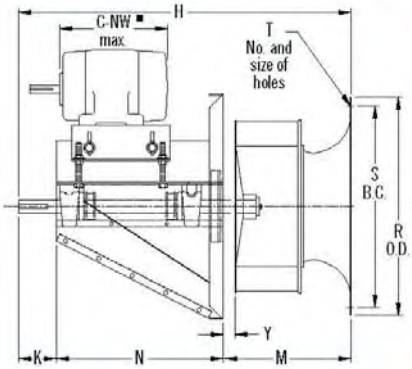

800°F.–1000°F.–1300°F.

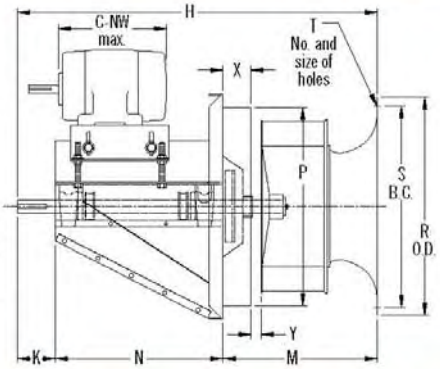

CLASS II*/III SIZES 44-49

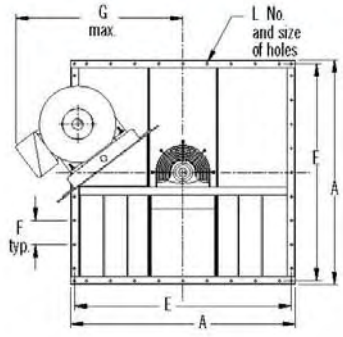

450°F.

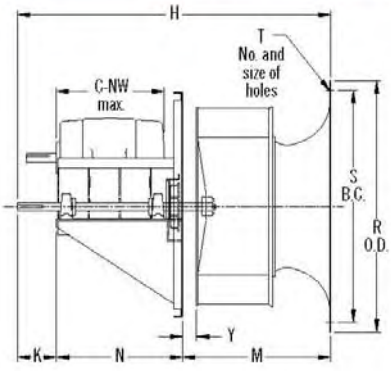

800°F.–1000°F.–1300°F.

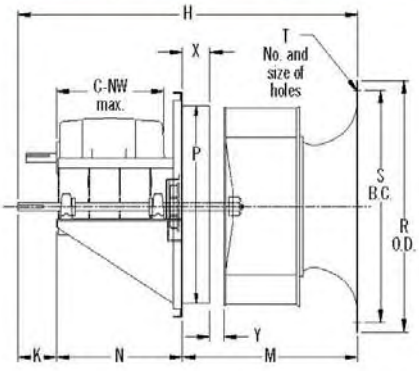

*Class II Sizes 44 and 49 Plug Fans are only available to 1000°F.
Y = 1½" on all models. X = 4" on 800°F. fans, 6" on 1000°F./1300°F. fans. Dimensions not to be used for construction unless certified.
L = All holes 9/16" diameter and on centerline. Sizes 12-27, 24 holes; Sizes 30-40, 32 holes; Sizes 44-49, 40 holes.

The New York Blower Company has a policy of continual product improvement and reserves the right to change designs and specifications without notice.

PRODUCT CATALOG

- OIL FILTER CRUSHER
- DRUM CRUSHER
- HYDRAULIC POWER UNIT
- ACCUMULATOR
- HYDRAULIC PUMP
  - GEAR PUMP
  - VANE PUMP
  - VARIABLE PISTON PUMP
  - VARIABLE VANE PUMP
- HEAT EXCHANGER
  - SHELL & TUBE
  - AIR COOLED
  - PLATE TYPE
- HYDRAULIC CYLINDER
- HYDRAULIC DIRECTIONAL CONTROL VALVE
- HYDRAULIC PRESSURE CONTROL VALVE
- HYDRAULIC FLOW CONTROL VALVE
- PNEUMATIC CYLINDER
- PNEUMATIC CONTROL VALVE
- PNEUMATIC FRL UNIT AND AIR PREPARATION
- SHOCK ABSORBER
- PRESSURE GAUGE

Air Cooled - HEAT EXCHANGER

MOBILE AIR COOLED HEAT EXCHANGERS		
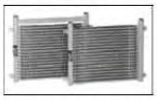 MODEL SEARCH	mount on Mobile Equipment mounts in front of Engine Radiator pressure to 300 PSI flow rate 1GPM to 100 GPM CALL 800-329-6888	AMERICAN HEAT TRANSFER AMERICAN STANDARD THERMAL TRANSFER YOUNG RADIATOR

SMALL AIR COOLED HEAT EXCHANGERS		
 MODEL SEARCH	different flow rates up to 25 GPM AC, or DC Motor Drive with or without Motor can mount behind Electric Motor CALL 800-329-6888	AMERICAN HEAT TRANSFER AMERICAN STANDARD THERMAL TRANSFER YOUNG RADIATOR

AC or DC Fan Drive		
 MODEL SEARCH	explosion proof option flow rates of 1 to 30 GPM 1, 2, 4 Fan Drives CALL 800-329-6888	AMERICAN HEAT TRANSFER AMERICAN STANDARD THERMAL TRANSFER YOUNG RADIATOR

HEAVY DUTY AIR COOLED HEAT EXCHANGER		
 MODEL SEARCH	different flow rates of 1 to 600 GPM pressure to 300 PSI AC, DC or Hydraulic Motor Drive NPT, SAE, or Flanged connections CALL 800-329-6888	AMERICAN HEAT TRANSFER AMERICAN STANDARD THERMAL TRANSFER YOUNG RADIATOR

HEAY DUTY INDUSTRIAL HEAT EXCHANGERS		
 MODEL SEARCH	different flow rates 20 to 1000 GPM Steel or Stainless Steel AC, DC, or Hydraulic Motor Driven Severe Duty Construction CALL 800-329-6888	AMERICAN HEAT TRANSFER AMERICAN STANDARD THERMAL TRANSFER YOUNG RADIATOR

MOBILE AIR COOLED HEAT EXCHAGERS		
	with or without Fans Single, Double, or Quad fans AC, or DC voltages for fans flow rates up to 150 GPM CALL 800-329-6888	AMERICAN HEAT TRANSFER AMERICAN STANDARD THERMAL TRANSFER YOUNG RADIATOR

TEMPERATURE SWITCH		
 MODEL SEARCH	with in-tank Thermal Wet Bulb sensor adjustable temperture settings Start and Stop Fan CALL 800-329-6888	AMERICAN HEAT TRANSFER AMERICAN STANDARD THERMAL TRANSFER YOUNG RADIATOR

COMPACT AIR COOLED HEAT EXCHANGER		
 MODEL SEARCH	MOUNT IN REAR OF ELECTRIC MOTOR uses Electric Motor Fan to Cool CALL 800-329-6888	AMERICAN HEAT TRANSFER AMERICAN STANDARD THERMAL TRANSFER YOUNG RADIATOR

COMPACT AIR COOLED HEAT EXCHANGER		
 MODEL SEARCH	For Industrial or Mobile applications AC, DC, or Hydraulic Motor driven fan flow rates of 1 GPM to 150 GPM Single or Double Fans CALL 800-329-6888	AMERICAN HEAT TRANSFER AMERICAN STANDARD THERMAL TRANSFER YOUNG RADIATOR

LARGE AIR COOLED HEAT EXCHANGERS		
 MODEL SEARCH	flow rates up to 1000 GPM EXPLOSION PROOF OPTION CALL 800-329-6888	AMERICAN HEAT TRANSFER AMERICAN STANDARD THERMAL TRANSFER YOUNG RADIATOR

COMPACT AIR COOLED HEAT EXCHANGER		
 MODEL SEARCH	1, 2, 4 FAN COOLED Heat Exchanger AC or DC drives flow rates 1 to 30 GPM CALL 800-329-6888	AMERICAN HEAT TRANSFER AMERICAN STANDARD THERMAL TRANSFER YOUNG RADIATOR

LARGE AIR COOLED HEAT EXCHANGERS		
	different flow rates of 10 to 1000 GPM THERMAL CAPACITY TO 750 hp (560 Kw) AC, DC or Hydraulic Motor Driven in Steel or Stainless Steel CALL 800-329-6888	AMERICAN HEAT TRANSFER AMERICAN STANDARD THERMAL TRANSFER YOUNG RADIATOR

Products & Services

msi multiphase systems integration

Multiphase Technology Design & Manufacturing

MSI has earned an excellent worldwide reputation through Research, Development & Modeling of Multiphase Separation Technologies, achieving world leading expertise in the design of compact gas, oil, water, and solids separation systems and technologies. We offer design, fabrication, installation, and troubleshooting of the following technologies:

GLCC – Gas-Liquid Cylindrical Cyclone compact separators
LLCC – Liquid-Liquid Cylindrical Cyclone compact separators
LLHC – Liquid-Liquid Hydrocyclone (Deoling and FWKO)
SLHC – Solid-Liquid Hydrocylone for solids removal
SD – Slug Damper

Consulting & Engineering Solutions
Multiphase Technology Design & Manufacturing
Oilfield Services
Research & Development
Technical Training

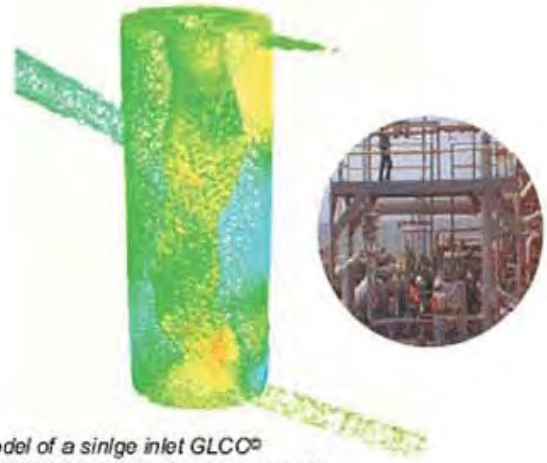

CFD model of a sinlge inlet GLCC®
(Gas-Liquid Cylindrical Cyclone) compact separator

KAESER COMPRESSORS

More Compressed Air for Less Energy

Lower Long Term Costs

Energy costs are a significant portion of any compressed air system's total lifetime cost. In fact, the amount of energy required to run a compressor for just one year can exceed the compressor purchase price. Over a period of 10 years, energy normally totals 70% of the overall costs.

Since Kaeser's energy-saving screw compressors deliver up to 20% more air per kilowatt, the cost-efficient choice is clear.

The Revolutionary Sigma Control

Sigma Control automatically regulates and monitors the compressor. It is an industrial-based PC with a real-time operating system. Easy-to-understand, color-coded LEDs indicate operating status. The four-line, plain-text display with touch keys and menu-guided screens offer clear function choices.

The Energy-saving Sigma Profile Airend

Larger, slower-running airends are more efficient and deliver more compressed air for the same input power. Kaeser's Sigma Profile airends are optimized and designed to operate at the lowest possible speeds. Every Kaeser rotary screw compressor is equipped with a highly efficient airend and will quickly pay for itself through power cost savings.

The Proprietary Sigma Profile

Kaeser's proprietary Sigma Profile airend was introduced in 1975. It is up to 20% more efficient than conventional rotary screw designs, offering more compressed air per kilowatt.

Efficiency and reliability are designed into the Sigma Profile airend with excellent airend inlet flow characteristics and a five-to-six lobe, assymmetrical design. Kaeser also uses precision-aligned, high-quality roller bearings designed to withstand the most demanding conditions and extend service life.

Kaeser continues to refine and improve the airend design, and as a result, the optimized Sigma Profile airends offer unparalleled performance.

DRESSER-RAND.

Bringing energy and the environment into harmony.®

ESH Horizontal, Single-Throw Process Compressors

Application versatility and unmatched dependability.

The ESH horizontal single-throw reciprocating compressor is one of the simplest and most basic of all compressor designs. ESH compressors have unmatched versatility and dependability. Basic components are pre-engineered, pre-assembled and pre-tested. The final selection is verified by special computer programs that will calculate the performance, select cylinders, frames and distance pieces, compute the gas and inertia loads and torsional stresses which will be encountered in your service.

Features

- All running gear components are pressure-lubricated with filtered oil, distributed through internal rifle-drilled passages (see Figure 1 below). The complete system is protected by an oil pressure shutdown switch. Units have a pressure gauge and a crankcase window-type oil level indicator. Oil filter is automotive cartridge-type for easy replacement.
- Cylinders for any gas or pressure are available for either lubricated or non-lubricated service. Cylinder materials include cast iron, nodular iron and steel.
- Main, crankpin and crosshead pin bearings are full-floating - free to rotate on the bearing journal and within the bearing housing. Due to the unique design having pressurized oil on both sides of the floating bearings, friction is reduced and wear is distributed evenly on both sides of the bearing.
- ESH compressors can be packaged for ease of installation and reduced installation costs (see Figure 2 below).
- Piston rods are induction hardened for reduced wear and longer life in continuous heavy-duty operation. Standard material is AISI 4142 carbon steel; other materials available as required including our tungsten-carbide coating.
- Full-floating rod packing with latest technology, non-metallic packing ring materials are vented and water-cooled which contribute to long, trouble-free operation with minimum leakage.
- Pistons are provided with latest technology, non-metallic piston ring and rider band materials to ensure maximum reliability.

ESH Model Data

Stroke, in. (mm)	7 (178)	11 (279)
Max BHP (kW)	70 (52)	180 (134)
Max RPM	600	450
(A) Length, in. (mm)	125 (3175)	125 (3175)
(B) Piston Removal, in. (mm)	43 (1092)	66 (1676)

(C) Width, in. (mm)	40 (216)	40 (216)
(D) Height, in. (mm)	30 (762)	30 (762)
Weight, lbs. (kg)	2550 (1157)	6030 (2735)

Weight does not include driver or sheave.

- Length = average distance along axis running perpendicular to crankshaft from outer head to outer head with standard cylinders and API Type B distance piece.
- Piston Removal = average distance required to remove piston and rod with standard cylinders and API Type B distance piece.
- Width = average distance along axis running from drive-end of crankshaft to oil pump.
- Height = average distance from top of foundation/skid to top of frame.

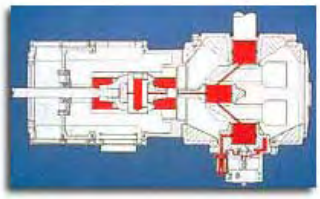

Figure 1. Pressurized Oil to All Bearing Surfaces

Figure 2. Two-Stage Tandem ESH Package with Overhead Motor Mount

Dresser-Rand
Reciprocating Operations
100 Chemung Street
Painted Post, NY 14870 USA
Tel: (Int'l +1) 607-937-2011
Fax: (Int'l +1) 607-937-2905

SERIES 2520 & 3520
Portable Oxygen Analyzers

ALPHA OMEGA
INSTRUMENTS

FEATURES	***BENEFITS***
√ State-of-the-Art Sensor Technology	High Precision Measurements.
√ Light Weight/Compact Design	Easy to Carry and Transport.
√ Rapid Speed of Response	Senses Changes in Gas Composition in Seconds.
√ Built-in NICAD Batteries	Provides >12 Hours of Continuous Operation with the Optional DC Sample Pump in Use.
√ Uses Standard NICAD's	Replacement Batteries Can be Purchased Worldwide.
√ Built-in Battery Charger	Can be Powered From AC Adapter.
√ Minimum Maintenance	Low Cost of Ownership.

System Description

Series 2520 Portable *Percent* Oxygen Analyzer

The Series 2520 Portable Percent Oxygen Analyzer is a light-weight, easy-to-use analyzer that provides accurate and repeatable percent oxygen measurements in a variety of gases. The rugged and compact design of the Series 2520 makes it ideal for industrial applications where spot oxygen measurements need to be made. The Series 2520 can be configured with one of several measuring ranges from 0-1% to 0-100% oxygen. The standard Series 2520 Portable Percent Oxygen Analyzer is equipped with a 3-1/2 digit liquid crystal display, in-line filter, built-in NICAD batteries, and an AC adapter that provides the ability to recharge the NICAD batteries even while powering the analyzer from the adapter.

The Series 2520 Portable Percent Oxygen Analyzer features a patented, extended life oxygen sensor with EES (Enhanced Electrolyte System) that provides exceptional measurement accuracy and stability. For applications where carbon dioxide is present in the sample gas, the EES retards passivation of the sensor anode by allowing the products of oxidation to dissolve in the electrolyte. In effect, the sensor is renewed continuously, resulting in an increase in sensor life. The output from the sensor is temperature compensated.

Series 3520 Portable *Trace* Oxygen Analyzer

The Series 3520 Portable Trace Oxygen Analyzer is a high precision instrument designed to provide accurate trace oxygen measurements in a variety of laboratory and process gases. The Series 3520 can be configured with one of several measuring ranges from 0-50 parts per million (ppm) to 0-10,000 ppm. The Series 3520 is equipped with either a 3-1/2 or 4-1/2 digit liquid crystal display (depending on the range selected), built-in NICAD batteries, and an AC adapter that provides the ability to recharge the NICAD batteries even while powering the analyzer from the adapter.

The 3520 features an advanced electrochemical oxygen sensor. The improved mechanical design of the sensor ensures longer life and virtually eliminates leakage of caustic electrolyte, a nagging problem associated with sensors that require periodic electrolyte maintenance. The output from the sensor is temperature compensated. In addition, the sensor is equipped with manual isolation valves so that during times of inactivity, the sensor can be kept inerted and ready for use. A major advantage of the Series 3520 is that it does not require users to apply a correction factor to the readings when exposed to different gas compositions. With other analyzer types, if correction factors are not applied, readings can be off by a factor of three!

Specifications	Series 2520	Series 3520
Measurement Ranges:	0-1, 0-5, 0-10, 0-25, 0-50, and 0-100%.	0-50, 0-100, 0-500, 0-1,000, 0-5,000, and 0-10,000 ppm.
Accuracy:	± 1% of full scale.	± 1% of full scale.
Linearity:	± 1% of full scale.	± 1% of full scale.
Response Time:	90% of full scale in <15 seconds.	90% of full scale in <20 seconds typical.
Sensor Type:	Electrochemical.	Electrochemical.
Temperature Compensation:	Standard.	Standard.
Operation Temperature Range:	40° to 100°F (5° to 38° C).	40° to 100°F (5° to 38° C).
Sample Gas Pressure Limits:	0.1 to 1.0 psig.	0.1 to 1.0 psig.
Sample Flow Rate:	1.0 to 2.0 SCFH (0.5 to 1.0 liters/minute).	1.0 to 2.0 SCFH (0.5 to 1.0 liters/minute).
Power Source:	Rechargeable NICAD batteries or 115 VAC/60 Hz using the AC adapter.	Rechargeable NICAD batteries or 115 VAC/60 Hz using the AC adapter.
Analog Output:	Not available.	Not available.
Warranty:	Two years electronics/1 year sensor.	Two years electronics/1 year sensor.
Enclosure:	Polycarbonate-rated NEMA 1.	Polycarbonate-rated NEMA 1.
Display:	3-1/2 digit liquid crystal display.	3-1/2 or 4-1/2 digit liquid crystal display.
Gas Connections:	Quick connect.	1/4"compression fittings.
Dimensions:	5.8" H x 6.7" W x 3.4" D.	5.8" H x 8.8" W x 3.4" D.
Weight:	<2 pounds.	<4 pounds.

Optional Equipment

DC Sample Pump
High Capacity Filter
Pressure Regulator
Flow Meter

Call Us Toll Free
800-262-5977

ALPHA OMEGA INSTRUMENTS

Alpha Omega Instruments Corp., 30 Martin Street, Cumberland, RI 02864
Telephone: 800.262.5977 or 401.333.8580, Fax: 401.333.5550
Email: aomega@aoi-corp.com, Web Site: http://www.aoi-corp.com

Table of Contents

An Exhaust Gas Evaluation As Possible Carbon Dioxide Replacement For FLASH ASJ™ Systems

Study Conducted For

Impact Technologies LLC

In Support Of

DE-EE0002783

Revised Report Issued

March 29, 2012

Work Performed by

Betty Felber, Ph D.

Consultant

Table Of Contents

List Of Figures

List Of Tables

Introduction

Previous work (Felber, 2008 – 2011) evaluated polymers, surfactants and various aspects of carbon dioxide for underbalanced drill applications. This work was undertaken to determine if exhaust gases from generators and other field equipment could be used as sources for the gas necessary for FLASH ASJ™ drilling. This report contains several new figures and a revised Appendix B.

Literature reviews of various generators, ancillary equipment and technical papers were conducted. This review did indeed determine that one can use exhaust gases for underbalanced drilling techniques utilized by **Impact Technologies, LLC.**

Executive Summary

A source of gas is required to drill a 2", 5000 ft well requires a minimum volume of 109 ft^3 (815.38 gallons). This volume is that required to have gases present in the entire drilling column. Another requirement is that the gas volume must be able to be produced at rates of 5 gallons/minute. It is possible to have enough volume to achieve this goal based on the exhaust gas rates from several generator manufacturers. The goal is to develop the necessary expertise to implement the FLASH ASJ system when there is not sufficient supercritical CO_2 or nitrogen on location. Ultimately solving this challenge could lead to even broader FLASH ASJ applications.

Several generator specifications were reviewed to determine suitability. There were some which are capable of generating large enough volumes of exhaust gas to be utilized. There is no general "rule of thumb" for using exhaust gas to drill wells. Each well must have separate laboratory tests conducted at near reservoir conditions to determine if exhaust gases are safe to use. By safe, it means that no explosions or fires will occur either downhole or in surface equipment.

Using exhaust gas for drilling has been conducted in Canada over the last 20 years. The physical properties and phase diagrams for a typical exhaust system were also developed.

Using flue gas as a FLASH ASJ source was also reviewed. It is possible to use this gas as a source for the underbalanced drilling system.

The type and sources for ancillary equipment were also defined. Neither the ancillary equipment costs nor the delivery time for each unit was determined.

Current Exhaust Gas Underbalanced Drilling Technology Review

A current technology review was conducted. It is important to note that published current underbalanced drilling technology involves using gases as an adjunct to liquid muds. This is in contrast to the technology for FLASH ASJ in which gas is an integral part of the drilling fluid mixture not just an adjunct used to lighten conventional muds. Some comparisons and contrasts are noted in the following sections.

The growing demand for maximizing production in a cost-effective manner has led to development of novel technologies. Underbalanced drilling (UBD) has proven to be a viable

technique to reduce drilling damage caused by drilling fluid invasion. Underbalanced drilling also has many other potential advantages, such as

- increasing rate of penetration,
- testing while drilling,
- drilling fluid options,
- eliminating differential sticking, and
- reducing completion costs.

Gas is injected and/or circulated with the drilling mud to reduce potential for formation damage from whole mud, fluid filtrate or solids invasion into the hydrocarbon-bearing formation. This procedure involves gas injection *via* a separate string to that through which the drilling mud is injected. The gas employed is usually nitrogen, in order to prevent fire and explosion hazards. However, nitrogen injection adds a significant cost. Another major challenge for remote or long duration UBD operations is the liquid nitrogen supply. This has increased interest in the use of air or deoxygenated air (membrane) technology to reduce costs and logistical challenges associated with liquid nitrogen.

If nitrogen injection were replaced with that of air, the cost could be reduced considerably. Nitrogen, natural gas, normal air or an oxygen-containing gas (usually vitiated air, which is air mixed with nitrogen, or de-oxygenated air, which is air with some of the oxygen removed) are used. Of these choices, the oxygen containing gases are the least expensive; however, there is a potential for flammable, explosive mixtures to be present in the wellbore and surface piping.

Horizontal well underbalanced drilling is also practiced. Injection either with the drilling mud or via a separate string is common. Just as for vertical wells, safe operational ranges of oxygen-containing gas/live oil/drilling mud mixtures can be determined if the flammability has been measured. (Metha 1995)

Flammability limits are affected by a number of different factors. The most important are temperature and pressure. For some fuels, small amounts of moisture can widen flammability limits, as can presence of hydrocarbon containing liquids. Significant widening of the flammability limits of complex fuel mixtures can also be caused by presence of low levels of hydrogen sulfide, carbon monoxide and hydrogen.

Many complex mixtures could be encountered with injection of an oxygen-containing gas. Drilling mud may ignite at concentrations of oxygen significantly lower than 21 percent. It is possible that explosions may occur at concentrations as low as five percent oxygen. It has been found that high pressure flammability limit behavior is neither simple nor uniform, but is specific to the mixture examined. It must therefore be stressed that flammability characteristics for a given reservoir and operating conditions are case specific. (Metha, 1995)

Laboratory studies to test for ignition characteristics and flammability of gas, oil, and drilling mud mixtures must be conducted for each specific reservoir. To conduct these tests, the reaction vessel contains mixtures of air, the drilling polymer such as Xanvis, and live oil. The pressure ranges are based on the reservoir. The temperature range is also determined by that expected to be encountered in the reservoir. Flammability limits are determined. Results are then used to design safety features for a field application horizontal drilling program using underbalanced methods at depth. This technique has proven successful, and a significant cost saving was realized by utilizing a 40 percent nitrogen, 60 percent air mixture instead of pure nitrogen. (Metha, 1995)

The mixtures were classified as "flammable", since using de-oxygenated air there is a continuous supply 5 % O_2. Ignition was classified in two categories: 'Strong Reactions', when the temperature rise was instantaneous after the introduction of a spark with a total temperature rise in excess of 50 °F; and 'Weak Reactions', when the rate of temperature rise was relatively slow after the introduction of a spark with a total temperature rise of more than 41 °F but less than 50°F.

Where a limited amount of reaction was observed with very low rate of temperature rise after the introduction of a spark with a total temperature rise of less than 41 °F, it was designated as 'Limited Reactions' and classified as no ignition. The hydrocarbon mixture flammability was significantly affected (widened) by the presence of hydrogen sulfide. In addition, operating pressure and temperature had a strong influence on mixture ignition characteristics.

Other studies were performed to determine safe conditions for underbalanced drilling using compressed air and liquid nitrogen. The main objectives were:

- to establish flammability of mixtures of air, live heavy oil and drilling mud as a function of pressure, and

- to determine optimum composition of vitiated air (nitrogen-air mixture), based on flammability data, in order to minimize ignition or explosion potential during underbalanced drilling operations.

Currently, there are no general "rules-of-thumb" which can be used to predict if an underbalanced drilling operation will be conducted in a safe, effective manner. (Metha, 1996) Using exhaust gas for underbalanced drilling has killed the market for nitrogen membrane units. (jonralph)

Hydrogen Sulfide Effects

Studies have also been conducted to determine flammability of complex mixtures of fuel gases containing H_2S, hydrocarbon condensate and drilling mud in de-oxygenated air (consisting of 5 % O_2 with the balance being N_2). Flammability tests at realistic reservoir pressures and temperatures and at the types of operating conditions which might be encountered during sour underbalanced drilling operations should be conducted for each project. The goal is to establish hydrogen sulfide concentration effects on flammability. Establishing safe design and operation of underbalanced drilling projects in sour hydrocarbon fields using de-oxygenated air containing 5% oxygen with the balance being nitrogen is important.

It was determined that de-oxygenated air containing 5 % oxygen was the benchmark for a safe underbalanced drilling operation in reservoirs containing very small amounts of hydrogen sulfide (up to 3000 ppm). This particular composition of deoxygenated air is economically achievable. Work was conducted at near-atmospheric conditions and is not valid at elevated pressures and temperatures. The pressure range chosen was from 0.0 to 3000 psig.

It is well known that increases in pressure and temperature have a widening effect on flammability range. Therefore, it was concluded that optimizing compositions at atmospheric conditions using correlations and extending the values to higher pressures and temperatures would lead to the "worst-case" flammability scenario.

Again, it must be stressed that results are highly case-specific. They are valid only for specific fuel gas, hydrocarbon and drilling mud mixtures and the run conditions investigated. The test parameters were designed for a specific set of reservoir conditions; thus, the ignition characteristics described herein should **NOT** be applied to other reservoirs.

It should **NOT** be assumed that de-oxygenated air containing five percent oxygen by volume with the balance being nitrogen can be safely used during an underbalanced drilling operation for a hydrocarbon system containing other gases. The flammability limits for each system must be tested. (Metha, 1996)

Also note that the underbalanced drilling discussed here does not relate specifically to mixing the gas at the surface to create underbalanced fluids. Rather the gas is added subsurface to create an underbalanced fluid. This is in contrast to **Impact Technologies** methods but still gives one insight into how the fluids could behave downhole. The exhaust gas system could be used for FLASH ASJ drilling.

Field Applications

Over the past two decades, the underbalanced drilling technology has evolved significantly. It can yield benefits such as

- increasing ROP (reduced well cost)
- reducing formation damage (increased productivity)
- limiting lost circulation problems
- reducing differential sticking
- providing formation testing/evaluating while drilling and
- determining TD from production rate or water influx.

Underbalanced drilling has several advantages over conventional drilling, but it also has several disadvantages as well. ***The principle advantage is that the penetration rates are usually 3-6***

times greater that mud drilling. The disadvantage is that the penetration rates are higher. Although penetration rates are higher, you're basically limited by the rig crew's capability to be able to "keep-up" and also recognize when the well "tells" them that something is happening downhole that isn't "right". There problems can lead one to a "fishing" job.

In well pre-planning, determine what a "safe" penetration rate would be, even though the capability exists to drill faster and, adhere to it during implementation. Plan to schedule enough time for "circulating" before making connections to make sure you have a reasonable clean annulus prior to shutting down the injection gas. If one is using coiled tubing, the requirements are different.

The people responsible have to be educated, that once the air is cut-off "mother nature" takes over (gravity), and the cuttings in the annulus will fall, as "air" has very little carrying capacity. "Velocity", is the primary carrying agent for straight "air" drilling (commonly called "Dusting"). (Redman69)

That said, by 2003, out of over 15,000 wells drilled under "so called" UBD conditions in North America, approximately 9,000 wells were drilled with truly underbalanced conditions over the entire planned depth/length and completion. Worldwide, the percentage drilled through the pay zone and completed underbalanced is considerably less. A variety of techniques have been employed relevant to different applications, such as:

- air drilling and use of air hammers
- flow drilling
- gas injection (via drill string; parasite string; inner string)
- mist and foam drilling.

Depending on the application and availability, gases such as air, deoxygenated air created through membrane separation or exhaust gas recompression, vitrified air, cryogenic nitrogen and natural gas have been injected in order to achieve these conditions. (Pratt) Another method is being tried in Australia using natural gas and nitrogen. Weatherford is championing this system. (Santarelli)

Using Exhaust Gas For Drilling

Diesel Powered Generator

A schematic of an exhaust gas system is shown in Figure 1 below. The engine supplies the input to the catalytic converter which eliminates oxygen from the stream. Through a series of heat exchangers and scrubbers the gas is made ready for using in the underbalanced drilling operation. Note that the final injection stream has no oxygen.

A modified version of this technique utilizing two engines has been used successfully on remote Canadian locations for many years. (Pratt) It should be noted that drilling with exhaust gas units can cause very serious problems. (CamT) This occurs when the gas generated was not treated properly or when surface equipment fails.

Exhaust gas systems are not as simple as one would believe. One can't just hook up a compressor to some diesel engine exhaust and go with it. If this is done, you'll also have no drillpipe, no casing, and no surface injection piping. The compressors can also be damaged. If one is under the impression that membranes give bad corrosion with oxygen, saltier water and temperature, then one should see what a poorly controlled exhaust gas corrosion management system can do. Fortunately this is extremely rare, however it does occur 2 or 3 times every 4 to 6 months. (Kevin S) A well controlled exhaust gas system produces approximately 87% N_2 and 13% CO_2 as the injection gas as shown in Figure 1.

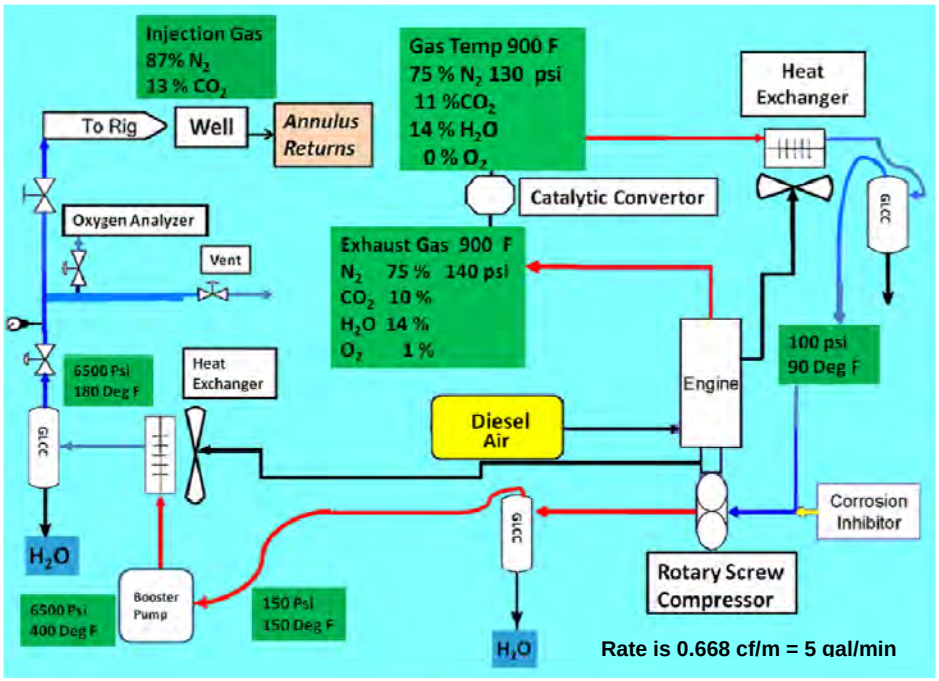

Figure 1: Diesel Exhaust Gas Schematic

Diesel Powered Exhaust Gas HP Requirements

The generator can create 486 HP. The horsepower requirements for the other equipment shown in Figure 1 are for the heat exchanger—25 HP, for the rotary screw compressor—3 HP, for the booster pump—0 HP (pressure driven), and for the second heat exchanger—25 HP. The total horsepower requirement is 53 HP. The oxygen analyzer is battery powered. These horsepower requirements are well within the range of that provided by the generator.

An example of a diesel powered exhaust gas system is shown in Figure 2. This is an example of how a field application layout using exhaust gas from 2 generators for underbalanced drilling looks. (Pratt)

Figure 2: Exhaust Gas Field Equipment Layout

Propane Powered Generator

Another exhaust gas system is that driven by propane and air. The schematic is displayed below. Note that there are few differences from the diesel exhaust system. The most compelling one is that propane burns at a higher temperature than diesel—1031 compared to 900 respectively.

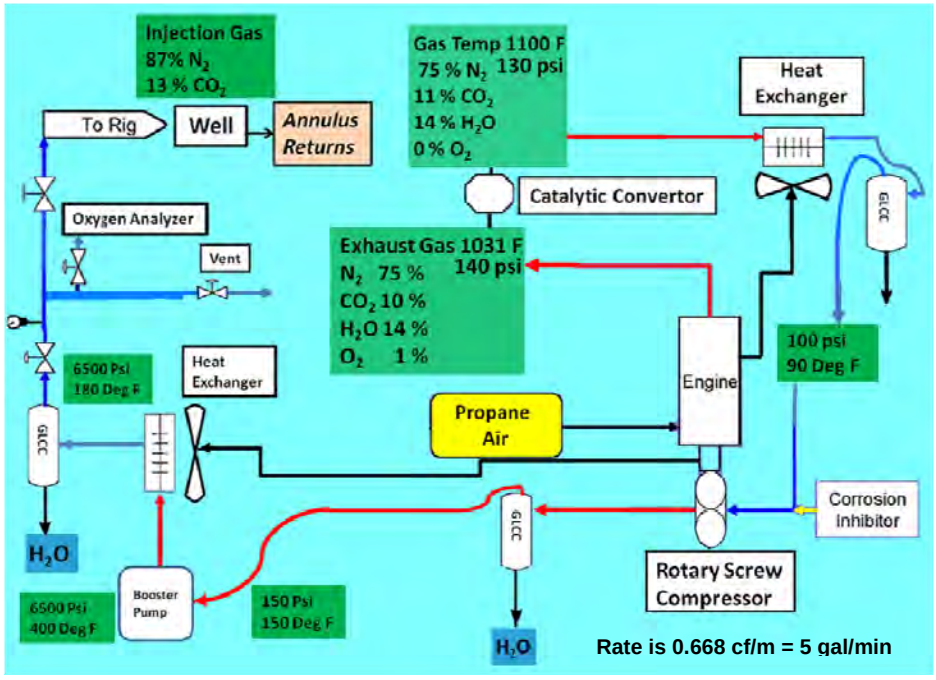

Figure 3: Propane Exhaust System

Propane Powered Exhaust Gas HP Requirements

The propane powered generator creates 97.7 HP. The requirements for the other equipment are for the first heat exchanger it is 25 HP. For the rotary screw compressor the requirements are 3 HP. The requirement for the booster pump is that the entrance pressure be at least 90 psi. No other power requirements are necessary. For the second heat exchanger to power requirements are 25 HP. The total horsepower requirement is 53. These requirements are well within that provided by the generator.

Now that the two exhaust systems have been explored the two most common nitrogen systems will be discussed.

Nitrogen Drilling

Cryogenic Systems

In contrast to the exhaust gas system, one of the fluids used in underbalanced drilling operations is cryogenic nitrogen, the liquid form of nitrogen, which is at a temperature of -321°F. Some of the characteristics of it are it is transported in tractor/trailer bulkers and stored at the drilling location in "Queen storage tanks" (typically 503 barrels).

The cryogenic N_2 is pressure transferred to a Cryogenic N_2 pumping unit which is capable of pumping 1 to 80 scfm at 1 to 50,000 psi or greater. The pumps are generally from the fracing industry. The N_2 pumper has a liquid N_2 storage tank, (about 63 barrels) and that is held at a fixed pressure, pressure feeding a downstream pump. This pump then pre-charges the liquid nitrogen to a couple hundred psi and forces it to the cryogenic pumps, which is usually a triplex. The triplex pressurizes the cryogenic nitrogen to its operating pressure and forces it to the heat convertor, which converts the cryogenic nitrogen to gaseous nitrogen at 77°F.

For the average two-phase system drilling a 6 1/4" hole with saltwater and nitrogen, it takes about 200 gpm water and about 1500 scfm nitrogen (11,221 gpm) at a drilling pressure of 1100 psi. (KevinS) These numbers are important to remember since the FLASH ASJ system requires a higher pressure and 5 gpm availability for the drilling fluid.

Cryogenic nitrogen is not inexpensive when compared to other gas methods. The cryogenic pumping equipment and cryogenic storage equipment can run about $15-$20K per day; then there is the cost of the nitrogen—30 scm * $0.75/scm * 24 (pumping about 75—85 % of the time on underbalanced drilling jobs, but there are also cryogenic losses so one can almost say pumping is 100%).

Cryogenic nitrogen costs vary on location and weather conditions. For example, if one is in Alberta, Canada, where there is one of the world's largest N_2 factories, costs are significantly lower than if one is in South Dakota where one may only get 1 bulker of nitrogen every 24 hours delivered. The cost delivered to site in Canada, including trucking and standard losses run about $0.75/scm.

Deoxygenated Air Systems

A schematic for this system is shown in Figure 4 below. Note that the engine drives the compressors.

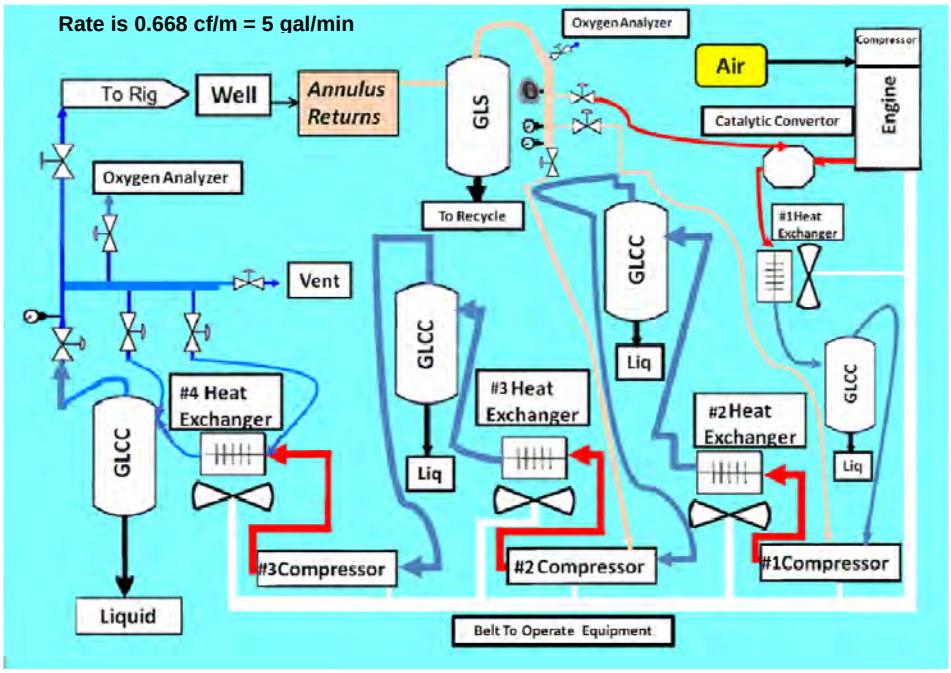

Figure 4: Nitrogen System Schematic

An example deoxygenated air system for 1500 scfm at 2200 psi costs around CAN $2.8 Mil and takes 6 months to build. The system is extremely portable. However, one of the disadvantages is the remaining 5% oxygen which given the right downhole chemistry causes massive corrosion. Some mud companies are close to conquering this 10 year old problem, however only close. On a high rate, remote location, this is the only economical way to go, unless you have exhaust gas or a gas line you can tie into. There is also air, but this is not very common in places outside of the U. S.; most likely due to lack of experience elsewhere. (KevinS) This system would not be a replica of Figure 4 above. This information is included for reference.

Deoxygenated Air System HP Requirements

The power is supplied by either a diesel or propane driven generator/compressor. The Kaeser combination provides between 48 and 111 HP available to run the equipment. The first heat exchanger requires an estimated 35 HP. The available data does not included information to determine the horsepower requirements. This estimate is taken from other equipment reviewed for this project. The first compressor requires 3 HP. The remaining heat exchangers require 25 HP each. The remaining compressors require 3 HP each. The total HP requirement is 122. This is slightly higher than the combination generator/compressors reviewed for this study. It may be necessary to modify the schematic in order to get within the HP limits.

This study shows that using nitrogen or exhaust gas for underbalanced drilling is not unheard of. The EPA requirements have complicated this use by limiting nitrogen in the exhaust from off road equipment. Some of the limits are listed in the next section.

EPA Off Road Standards

There is a requirement that off road diesel equipment must meet exhaust emission standards. Some of the requirements are summarized below. This information is included as reference to

the steps EPA may take for future requirements on exhaust emissions which could affect the skid built for enhanced geothermal drilling applications.

Tier 1-3 Standards

The first Federal standards (Tier 1) for new nonroad (or off-road) diesel engines were adopted in 1994 for engines over 50 hp. The requirements were to be phased-in from 1996 to 2000. In 1996, a Statement of Principles (SOP) pertaining to nonroad diesel engines was signed between EPA, California Air Resources Board and engine makers (including Caterpillar, Cummins, Deere, Detroit Diesel, Deutz, Isuzu, Komatsu, Kubota, Mitsubishi, Navistar, New Holland, Wis-Con, and Yanmar). On August 27, 1998, EPA signed the final rule reflecting the SOP provisions. The 1998 regulation introduced Tier 1 standards for equipment under 50 hp and increasingly more stringent Tier 2 and Tier 3 standards for all equipment with phase-in schedules from 2000 to 2008. Tier 1-3 standards were met through advanced engine design, with no or only limited use of exhaust gas after treatment such as oxidation catalysts. Tier 3 standards for NO_x+ HC are similar in stringency to the 2004 standards for highway engines; however Tier 3 standards for PM (Particle Matter) were never adopted.

Tier 4 Standards

On May 11, 2004, the EPA signed the "final" rule introducing Tier 4 emission standards, which are to be phased-in over the period of 2008-2015. Tier 4 standards require PM and NO_x emissions be further reduced by about 90%. Such emission reductions can be achieved through the use of control technologies—including advanced exhaust gas after treatment—similar to those required by the 2007-2010 standards for highway engines.

Nonroad Diesel Fuel

The other element for nonroad equipment is diesel. At the Tier 1-3 stage, sulfur content in nonroad diesel fuels was not limited. The oil industry specification was 0.5% (wt., max), with the average in-use sulfur level of about 0.3% = 3,000 ppm. To enable sulfur-sensitive control technologies in Tier 4 engines—such as catalytic particulate filters and NO_x absorbers—EPA mandated reductions in sulfur content in nonroad diesel fuels, as follows:

- 500 ppm effective June 2007 for nonroad, locomotive and marine (NRLM) diesel fuels
- 15 ppm (ultra-low sulfur diesel) effective June 2010 for nonroad fuel, and June 2012 for locomotive and marine fuels

The Figure below shows the EPA timeline for reduced particle matter and NO_x implementation. Included are the years when new emissions are active as well as the NO_x, hydrocarbon, carbon monoxide, and particle matter limits. (Caterpillar)

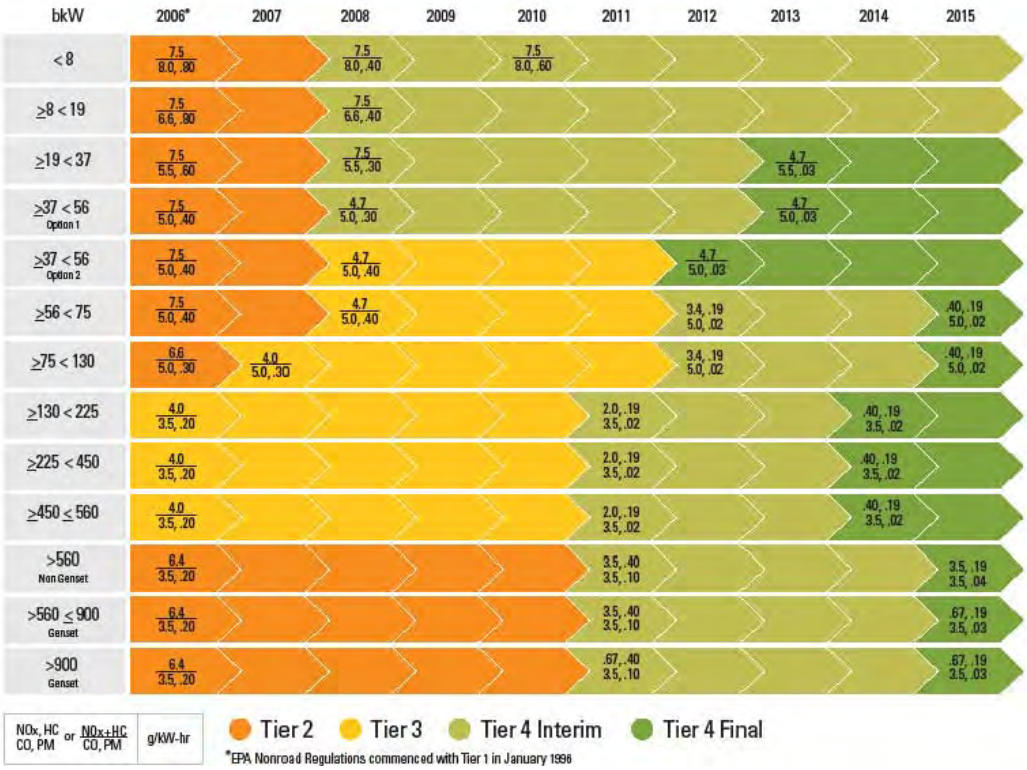

Figure 5: EPA Emission Requirements--Nonroad

Industries Where Applicable

The nonroad standards cover mobile *nonroad diesel engines* of all sizes used in a wide range of construction, agricultural and industrial equipment. Examples of regulated applications include farm tractors, excavators, bulldozers, wheel loaders, backhoe loaders, road graders, diesel lawn tractors, logging equipment, portable generators, skid steer loaders, or forklifts.

EPA defined *nonroad engines* as based on the principle of mobility/portability, and includes engines installed

(1) on self-propelled equipment,

(2) on equipment that is propelled while performing its function, or

(3) on equipment that is portable or transportable, as indicated by the presence of wheels.

In other words, nonroad engines are all internal combustion engines except motor vehicle (highway) engines, stationary engines (or engines that remain at one location more than 12 months), engines used solely for competition, or aircraft engines.

Effective May 14, 2003, the definition of nonroad engines was changed to also include all diesel powered engines—including stationary ones—used in California agricultural operations. This

change applies only to engines sold in California. Stationary engines sold in other states are not classified as nonroad engines.

The nonroad diesel emission regulations are not applicable to all nonroad diesel engines. Exempted are the following nonroad engine categories:

- Engines used in railway locomotives; those are subject to separate EPA regulations.
- Engines used in marine vessels, also covered by separate EPA regulations. Marine engines below 37 kW (50 hp) are subject to Tier 1-2—but not Tier 4—nonroad standards. Certain marine engines that are exempted from marine standards may be subject to nonroad regulations.
- Engines used in underground mining equipment. Diesel emissions and air quality in mines are regulated by the Mine Safety and Health Administration (MSHA).
- Hobby engines (below 50 cm^3 per cylinder)

A new definition of a compression-ignition (diesel) engine is used in the regulatory language since the 1998 rule. The definition focuses on engine cycle, rather than ignition mechanism, with the presence of a throttle as an indicator to distinguish between diesel-cycle and otto-cycle operation. Regulating power by controlling the fuel supply in lieu of a throttle corresponds with lean combustion and diesel-cycle operation. This language allows the possibility that a natural gas-fueled engine equipped with a sparkplug is considered a compression-ignition engine. (DieselNet)

So what do these requirements mean for oil field equipment? The next section details some examples.

Compressor Review

EPA has entered into an agreement with several companies who have agreed to limit exhaust of NO_x and particular matter. These companies were listed previously.

Two compressor manufacturers were reviewed—Cummins and Caterpillar. In both cases the company was proud that they were in compliance with EPA nonroad diesel requirements. Even with the engines meeting EPA standards, there is enough nitrogen + carbon dioxide exhaust volume being emitted that the exhaust can be the gas source for the **Impact Technology** FLASH ASJ system.

One would still need to choose a generator that could support the rates needed for this application. In order for a generator to meet the rate requirements for the FLASH ASJ system, it must be capable of producing exhaust gas at a rate of 8,898 ft^3/min. Examples of the Cummins engines are the Genset PC880 series (Appendix A, page A-1). Caterpillar diesel examples are in the PRIME 1360 ekW, 1700 kVA engine series Appendix A, page A-9.

One could also use 2 much smaller generators—4000 ft^3/min each. This arrangement may allow for more rate variations. It could also lower the acquisition costs. Appendix A, page A-5 is an example of the ± 4000 rated generator from Cummins. A Cat PRIME 580 eKW example is included on page A-15.
More information from each company is included in Appendix A. Each generator highlighted will produced enough exhaust gas to meet FLASH ASJ requirements for a 2" 5000' wellbore.

Ancillary Equipment Sources For Exhaust Gas And Nitrogen Systems

In order to successfully apply the exhaust gas system several pieces of ancillary equipment must be used. This section is targeted toward locating this equipment. See Appendix B for more information on the ancillary equipment types and sources.

Using Figures 1 and 3 as an example, the ancillary equipment is listed as it appears on this figure. The first item is the catalytic converter. PTX purifiers are used to control commercial equipment exhaust powered with engines using unleaded gasoline, diesel fuel, or LPG, allowing the safe use of such equipment in enclosed spaces. PTX purifiers are used on forklifts, trucks, floor sweepers, underground locomotives, stationary or portable engines. (Cohn) These catalytic converters may be purchased from Optimized Process Design. They do not have literature available on the Internet. The contact information is OPD, 25610 Clay Road, Katy, TX 77493. The phone number is (281) 371-7500.

There are also several other prominent catalytic converter sources. One of them is BASF. The contact information is BASF Catalysts LLC, 101 Wood Avenue, Iselin, NJ 08830-0770. The phone number is (732) 205-5000. The web site is www.basf-catalysts.com. A description of one of their products begins on page B-1of Appendix B.

These catalytic convertors have temperature ranges from 200 to 3500°F. If the temperature exceeds the maximum, the matrix holding the catalyst will melt. The minimum temperature is necessary to make the catalyst activate. There are some catalysts that can be used at lower temperatures but they are not completely commercial yet. (Holroyd)

According to the heat exchanger computer program (Heat Exchange Calculator) it might be necessary to put two heat exchangers in series in order to prevent metal fatigue with the large heat changes expected for propane or diesel exhaust systems. They would also have to be larger than the miniature heat exchangers discussed in the previous paragraphs. However, specialized high temperature heat exchangers can be purchased from Munters. Their high temperature heat exchangers can be used in applications where the input temperature is 1400 to 2000°F. These exchangers are not overly big. Information on them is in Appendix B beginning on page Appendix B-3. Their contact information is 225 South Magnolia Avenue, Buena Vista, VA 24416. The phone number is (540) 291-1111. The fax number is (540) 291-3333. Their web page is www.nunstershightemperature.com.

For the scrubbers it is suggested that **Impact** use the **Tulsa University** designed separators. It should be fairly inexpensive to design and fabricate them for the throughput necessary for rate, temperature and pressure ranges expected. **Impact** or MSI should be able to manufacture the

two phase separator equipment required. Appendix B, page B-8 contains some of MSI's information.

The rotary screw compressor is marketed by Kaeser. More information can be obtained at http://us.kaeser.com/Products. The closest distributor is MIS Group, Inc. The phone number is (713) 671-9565. The address is 9402 North Loop E, Houston, TX 77029-1228. Or the Kaeser number is (800) 777-7873. Some more compressor information is contained in Appendix B on page B-9.

The booster pump is manufactured by Haskel. It has the capability to pressure gases at 60 psi to 9000 psi. It is pressure driven. The contact information is Haskel International, Inc., 100 East Graham Place, Burbank, California 91502. The phone number is (818) 843-4000. The fax number is (818)556-2549. Their web page is www.haskel.com. Information on this pump begins on page Appendix B-13.

The oxygen analyzer can be purchased from Alpha Omega Instruments Corporation. It is located at 30 Martin Street, Cumberland, RI 02864. The phone number is (800) 262-5977. The web site is http://www.aoi-corp.com. The analyzers which could be used are Series 2520 & 3520 Portable Oxygen Analyzers. The product information sheet is in Appendix B on page B-12.

Figure 4 shows the ancillary equipment that might be required for extracting nitrogen from air. Some of the equipment is described above. The remainder is included below.

The combination engine with compressor can be purchased from Kaeser. Their contact information is P. O. Box 2143, 96410 Coburg, Germany. The phone number is 49-9561 640-0. The fax number is 49-9561 640130. The web page is www.kaeser.com. Information on this combination is in Appendix B beginning on page Appendix B-22.

For the miniature air cooled heat exchangers, www.wholesalehydraulics.com is a good source. They market several brands—American Heat Transfer, American Standard Thermal Transfer, and Young Radiator for example. These are all manufacturers of miniature air cooled heat exchangers. Depending on the model, cooling rates range from 1 to 1000 gpm. They do not have brochures that one can download but they do have brief descriptions of several of their heat exchangers.

The toll free number is 1-800-329-6888**.** E-mail is info@wholesalehydraulics.com. The parent company is Advanced Fluid Power, Inc. It is located in Mobile, Alabama. Advanced Fluid Power, Inc. has over 75 years of combined experience. The address is I-10 Industrial Parkway, Theodore, Alabama 36582. Examples of their product lines are in Appendix B on page B-6.

If one chooses a reciprocating compressor, it can be provided by Dresser Rand or GE. The Dresser contact information is Dresser-Rand, West8 Tower Suite 1000, 10205 Westheimer Road, Houston, TX 77042. The phone number is (713) 354-6100. An example of their reciprocating compressor is shown in Appendix B on page B-11.

Now that the compressors and ancillary equipment have been reviewed, what are the exhaust gas fluid properties which might be utilized in the underbalanced drilling operations?

Fluid Properties

Exhaust Gas

A physical properties study of the typical cleaned up exhaust gas is made up of 87 % Nitrogen and 13 % Carbon Dioxide was conducted. See Figure 1 above. Some of the exhaust gas mixture physical properties were determined and are included in Table 1 below.

Table 1: 87 % Nitrogen + 13 % Carbon Dioxide Mixture Physical Properties

English Units		Normal Freezing Point (1 atm)		Gas Phase Properties @ 68°F & @1 atm		Liquid Phase Properties @ B P& @ 1 atm		Triple Point		Critical Point		
		Temp.	Latent Heat of Vaporization	Specific Gravity	Specific Heat (Cp)	Specific Gravity	Specific Heat (Cp)	Temp.	Pressure	Temp.	Pressure	Density
Substance	Mol. Weight	° F	BTU/lb	Air = 1	BTU/lb °F	Water = 1	BTU/lb °F	°F	psia	°F	psig	lb/cu ft
N_2 + CO_2 Mixture	29.40	-273.3	---	---	7.21	---	12.95	-373.0	1.00	-178.9	1073.4	25.99

The phase diagram for exhaust gas is shown in Figure 6. The nitrogen—carbon dioxide mixture is shown in black. The important features are that it goes supercritical at -180 . Low temperatures are required to drive it to the supercritical region. The carrying capacity of this fluid might be lower compared to carbon dioxide since the molecular weight is 29 while it is 44 for CO_2.

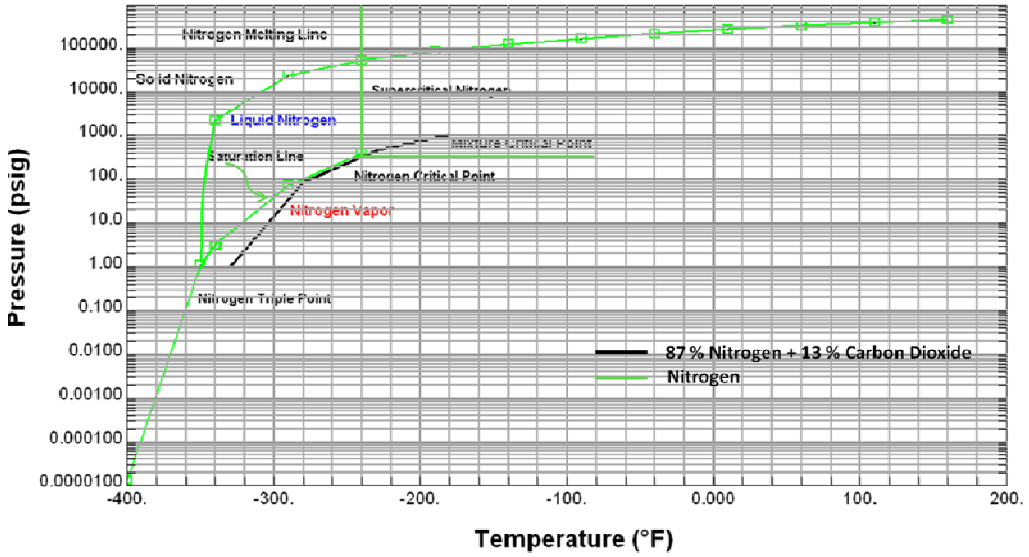

Figure 6: 87 % Nitrogen + 13 % Carbon Dioxide Mixture Phase Diagram

On Figure 6 the nitrogen phase diagram is included for reference. It is depicted in green. The conversion of 1 ft^3 of this mixture would be between that of carbon dioxde—533 ft^3 and that of nitrogen which is 694 ft^3 at 60°F and 14.696 psi. If one assumes each element contributes its respective amount of volume to the expansion, then the number would be 673 ft^3 (0.87 *694 ft^3 + 0.13 * 533 ft^3), however it is unclear if one can really assume that the mixture would vaporize in this manner.

Sample Of Expanded Physical Properties—Nitrogen + Carbon Dioxide Mixture

The table shows some more physical properties of the 87 % nitrogen + 13 % carbon dioxide mixture. The differences at these two temperatures—60 and 70°F—are slight. These two temperatures were chosen because they are the ambient temperature range which might be most frequently encountered.

Table 2: Expanded 87 % Nitrogen + 13 % Carbon Dioxide Mixture Physical Properties List

Temp., °F	Press., psig	Density, lbm/ft^3	Enthalpy, (Btu/lbm)	Entropy, (Btu/lbm-°R)	Heat Capacity, C_v (Btu/lbm-°R)	Heat Capacity, C_p (Btu/lbm-°R)
60	0	0.08	139.93	1.5185	0.17457	0.24257
	100	0.61	139.07	1.3782	0.17516	0.24601
	1000	5.50	131.67	1.2187	0.17997	0.27792
	2000	10.88	124.81	1.1604	0.18419	0.30948
	3000	15.73	119.84	1.1239	0.18724	0.32979
	4000	19.83	116.71	1.0978	0.18950	0.33932
	5000	23.21	115.01	1.0780	0.19132	0.34239
	6000	26.00	114.36	1.0623	0.19293	0.34232
	8000	30.35	115.06	1.0384	0.19589	0.33924
	10000	33.62	117.34	1.0205	0.19865	0.33582
70	0	0.08	142.36	1.5231	0.17477	0.24275
	100	0.60	141.53	1.3829	0.17532	0.24602
	1000	5.37	134.45	1.2239	0.17987	0.27614
	2000	10.61	127.88	1.1663	0.18388	0.30585
	3000	15.34	123.11	1.1301	0.18685	0.32545
	4000	19.37	120.08	1.1042	0.18908	0.33521
	5000	22.71	118.42	1.0845	0.19090	0.33883
	6000	25.49	117.77	1.0687	0.19251	0.33930
	8000	29.85	118.44	1.0448	0.19545	0.33697
	10000	33.14	120.69	1.0269	0.19819	0.33398
100	0	0.07	149.65	1.5374	0.17535	0.24328
	100	0.56	148.91	1.3966	0.17582	0.24612
	2000	5.03	142.66	1.2390	0.17970	0.27176
	3000	9.87	136.92	1.1829	0.18319	0.29684
120	0	0.07	154.52	1.5460	0.17575	0.24365
	100	0.54	153.83	1.4052	0.17618	0.24625
	1000	4.83	148.07	1.2485	0.17969	0.26945
	2000	9.45	142.80	1.1932	0.18290	0.29206
	3000	13.67	138.93	1.1587	0.18546	0.30828

The 60 and 70°F enthalpy curves are depicted in the Figure below. Note the similarity at the two temperatures reported. There is, however, some separation.

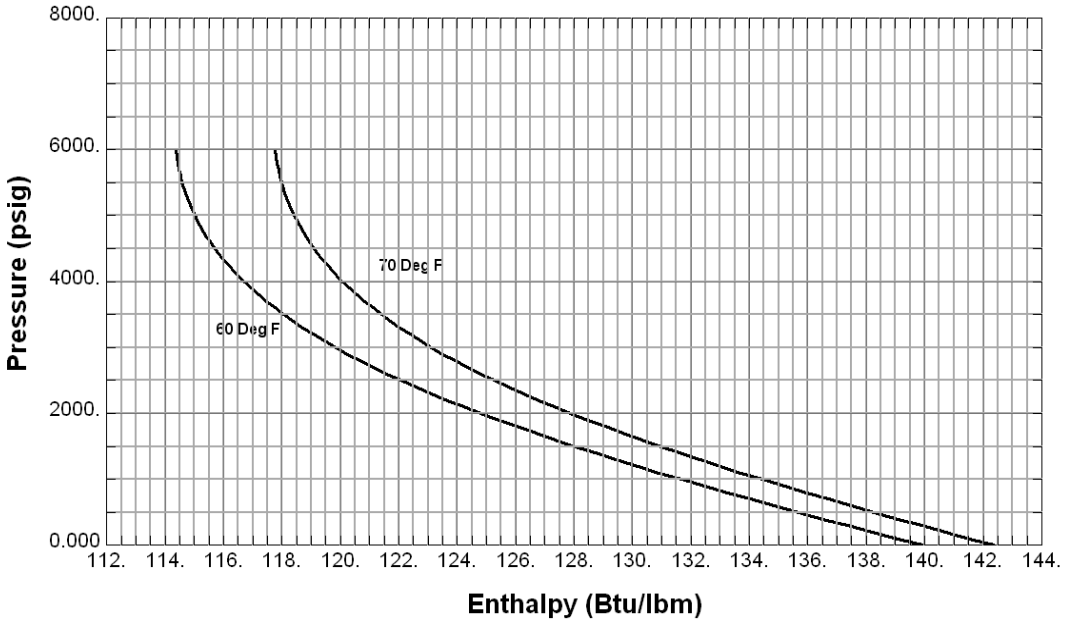

Figure 7: 87 % Nitrogen + 13 % Carbon Dioxide Enthalpy Curves

The 60 and 70°F entropy curves for the nitrogen—carbon dioxide mixture are shown in the Figure below. Unlike the enthalpy curves the entropy curves are essentially on top of each other. See Figure 8.

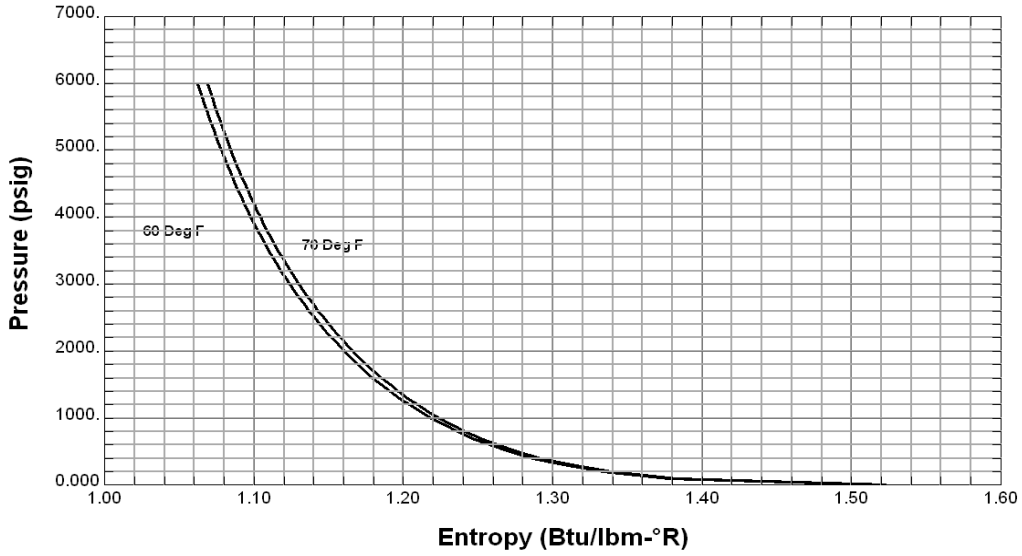

Figure 8: 87 % Nitrogen + 13 % Carbon Dioxide Mixture Entropy Curves

The 60 and 70 density-pressure plots are included for the nitrogen—carbon dioxide mixture.

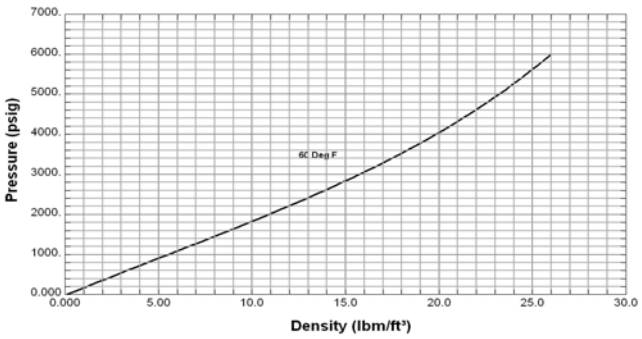

Figure 9: 87 % Nitrogen + 13 % Carbon Dioxide 60 Degree F Density Curve

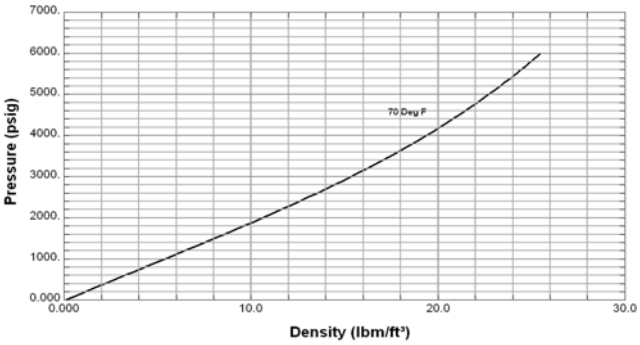

Figure 10: 87 % Nitrogen + 13 % Carbon Dioxide 70 Degree F Density Curve

Because they are so close, the plots are shown separately. The density values for 100 and 120 are depicted in Figure 11 below. The 120 values are shown in magenta. Note that there is some divergence between these curves.

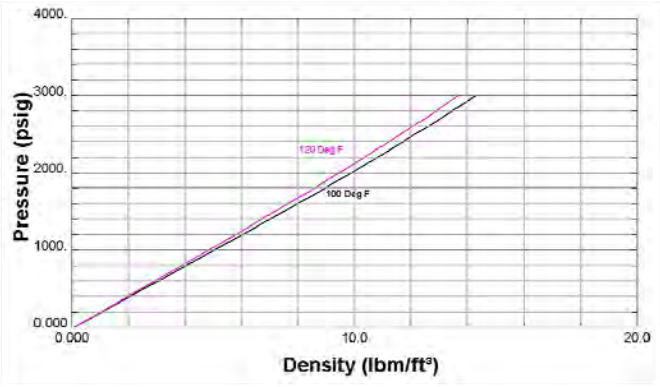

Figure 11: 87 % Nitrogen + 13 % Carbon Dioxide 100 & 120 Degree F Density Curves

The constant volume heat capacities at 60 and 70 are also shown separately because they too are also very close. The variances are slight throughout the pressure range investigated.

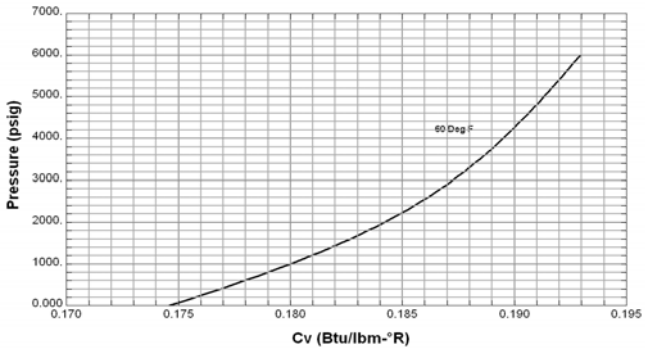

Figure 12: 87 % Nitrogen + 13 % Carbon Dioxide Constant Volume @ 60 Degrees F

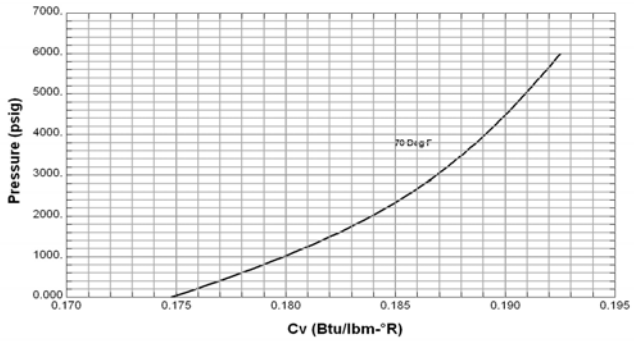

Figure 13: 87 % Nitrogen + 13 % Carbon Dioxide Constant Volume @ 70 Degrees F

The heat capacities for 60 and 70°F at constant pressure are shown in the Figure below. Note that in the pressure range (Highlighted by red line) important for this work the differences are almost indistinguishable.

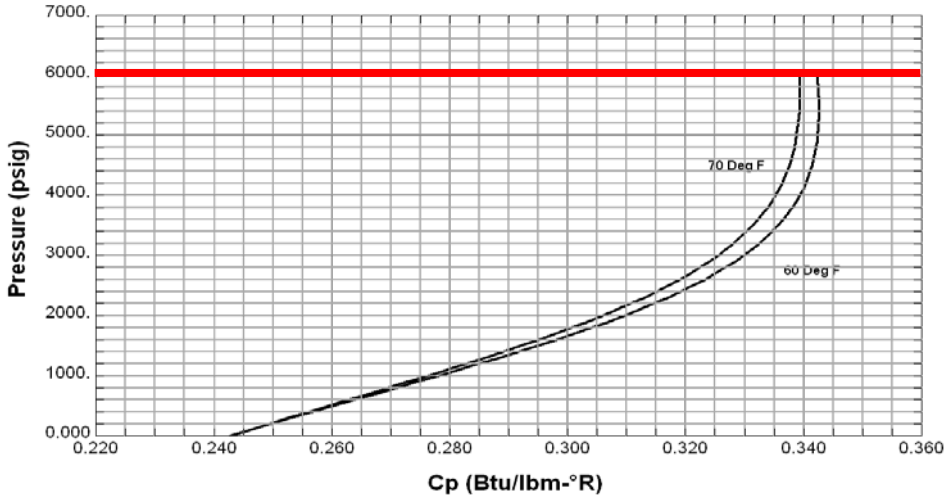

Figure 14: 87 % Nitrogen + 13 % Carbon Dioxide Constant Pressure Heat Capacities

Flue Gas

Flue gas was also reviewed. It is defined as the gas that exits to the atmosphere via a flue, which is a pipe for conveying exhaust gases from a fireplace, oven, furnace, boiler or steam generator. Quite often, it refers to the combustion exhaust gas produced at power plants. The emissions are different for each source.

Flue gas emissions from fossil fuel combustion refer to the combustion product gas resulting from 10 to 25 volume percent or more of flue gas. Its composition depends on what is being burned, but it will usually consist of mostly nitrogen (typically more than two-thirds) derived from the combustion air, carbon dioxide (CO_2) and water vapor as well as excess oxygen (also derived from the combustion air). This is closely followed in volume by water vapor created by combustion of the hydrogen in the fuel with atmospheric oxygen. Much of the 'smoke' seen

pouring from flue gas stacks may in fact be water vapor forming a cloud as it contacts cool air. It further contains a small percentage of pollutants such as particulate matter, carbon monoxide, nitrogen oxides and sulfur oxides.

A typical flue gas from the combustion of fossil fuels will also contain nitrogen oxides (NO_x), sulfur dioxide (SO_2) and particulate matter. The nitrogen oxides are derived from the nitrogen in the air as well as from any nitrogen containing compounds in the fossil fuel. Sulfur dioxide is derived from any sulfur-containing compounds in the fuels. The particulate matter is composed of very small particles of solid materials and very small liquid droplets which give flue gases their smoky appearance.

At power plants, flue gas is often treated with a series of chemical processes and scrubbers, which remove pollutants. Electrostatic precipitators remove particulate matter and flue gas desulfurization captures the sulfur dioxide produced by burning fossil fuels, particularly coal. Nitrogen oxides are treated either by modifications to the combustion process to prevent their formation, or by high temperature or catalytic reaction with ammonia or urea. In either case, the aim is to produce nitrogen gas, rather than nitrogen oxides.

The steam generators in large power plants and the process furnaces in large refineries, petrochemical and chemical plants, and incinerators burn large amounts of fossil fuels and therefore emit large amounts of flue gas. The table below presents the total amounts of flue gas typically generated by the burning of fossil fuels such as natural gas, fuel oil and coal. Data in the table were obtained by stoichiometric calculations. (Gas Emissions)

Table 3: Flue Gas Generated By Fossil Fuel Combustions

Combustion Data	Fuel Gas	Fuel Oil	Coal
Fuel Properties:			
Gross heating value, Btu/scf	1,093		
Gross heating value, Btu/gal		150,000	
Gross heating value, Btu/lb			11,150
Molecular weight	18		
Specific gravity		0.9626	
Gravity, °API		15.5	
Carbon/hydrogen ratio by weight		8.1	
weight % carbon			61.2
weight % hydrogen			4.3
weight % oxygen			7.4
weight % sulfur			3.9
weight % nitrogen			1.2
weight % ash			12.0
weight % moisture			10.0
Combustion Air:			
Excess combustion air, %	12	15	20
Wet Exhaust Flue Gas:			
Amount of wet exhaust gas, scf/10^6 Btu of fuel	11,600	11,930	12,714

CO_2 in wet exhaust gas, volume %	8.8	12.4	13.7
O_2 in wet exhaust gas, volume %	2.0	2.6	3.4
Molecular weight of wet exhaust gas	27.7	29.0	29.5
Dry Exhaust Flue Gas:			
Amount of dry exhaust gas, scf/10^6 Btu of fuel	9,510	10,600	11,554
CO_2 in dry exhaust gas, volume %	10.8	14.0	15.0
O_2 in dry exhaust gas, volume %	2.5	2.9	3.7
Molecular weight of dry exhaust gas	29.9	30.4	30.7

Note: scf is standard cubic feet at 60 °F and 14.696 psia.

It is of interest to note that the total amount of flue gas generated by coal is only 10 percent higher than the flue gas generated by natural gas. ***This means that changing to gas fired electrical plants will have virtually no impact on air emissions released.***

Also in the US there are a range of emerging technologies for removing pollutants emitted from power plants. One of these is the deployment of technologies to remove mercury from flue gas—typically by adsorption on sorbents or by capture in inert solids as part of the flue gas desulfurization product. There is very little performance data from large-scale industrial applications of such technologies. None has achieved significant worldwide market penetration so valid conclusions based on this implementation are premature.

Conclusions and Recommendations

History has shown that successful underbalanced drilling applications using exhaust gas have been applied for over two decades. A brief review of available diesel and propane powered generators indicates that the exhaust gas rate is sufficient to be applied with **Impact Technologies'** FLASH ASJ system. The ancillary equipment required for safe operation of an exhaust gas drilling system is also available. If one wanted to pursue the flue gas system for underbalanced drilling, it is expected that similar equipment would be required to use flue gas as that for exhaust gas drilling. The equipment required for nitrogen-carbon dioxide systems which haven't been combusted also are available.

It is recommended that serious consideration of the exhaust gas and nitrogen systems be undertaken.

References

CamT, Posted on Underbalanced Drilling Thread, December 31, 2003.
http://drillingclub.proboards.com/index.cgi?board=ubd&action=display&thread

Caterpillar, "Guide to EPA Tier 4 Emissions for Diesel Generator Sets", 2011.

Cohn, J. G., "Catalytic Converters for Exhaust Emission Control of Commercial Equipment Powered by Internal Combustion Engines", Environmental Health Perspectives, Vol. 10, pp. 159-164, April 1975.

DieselNet, "Emission Standards, Nonroad Diesel Engines", Dieselnet.org, Downloaded March, 2011.

EPA Program Update, "Reducing Air Pollution From Nonroad Engines," United States Environmental Protection Agency, EPA420-F-03-011, April 2003.

Felber, B., "Phase I: Underbalanced, Abrasive Drilling With Supercritical Carbon Dioxide, Water, and Nitrogen", Internal **Impact Technologies, LLC** report issued September 2, 2008.

Felber, B., "An Evaluation of Aqueous Viscosifiers", Internal **Impact Technologies, LLC** report issued May 21, 2009.

Felber, B., "An Evaluation of Possible Carbon Dioxide Replacement Systems", Internal **Impact Technologies, LLC** report issued October 15, 2010.

Felber, B., "A Summary of Possible Air Separation Systems", Internal **Impact Technologies, LLC** report issued November 30, 2010.

Felber, B., "Xanvis L Viscosity Relationships Vs Temperature For Use In FLASH ASJ™ Drilling Systems", Internal **Impact Technologies, LLC** report issued December 1, 2011.

Gas Emissions From Fossil Fuel Combustion, Wikipedia, http://en.wikipedia.org/wiki/flue_gas_emissions_from_fossil_fuel_combustion, Downloaded April 2011.

Heat Exchange Calculator, http://www.exergyllc.com/calculator.php, Exergy Miniature Heat Exchangers, Calculations conducted March 2012.

Holroyd, J. A., "Low Temperature Oxidation Catalyst Development And Applications", Presented at the American Filtration & Separation Society Annual Conference, Valley Forge, PA, May 2008.

Jonralph, Posted on Chemical Engineering Other Topics, June 13, 2001. http://www.eng-tips.com/viewthread.cfm?qid=7819&page=48

KevinS, Posted on Underbalanced Drilling Thread, March 11, 2004 . *http://drillingclub.proboards.com/index.cgi?board=ubd&action=display&thread*

Mehta, S.A., Moore, R.G., Samuel, P., Laureshen, C.J., Bennion, D.B., and Teichrob, R., "High Pressure Flammability Limits Of Drilling Mud/Live Heavy Oil Mixtures In Pure Air And Nitrogen/Air Mixtures", Proceedings of Sixth UNITAR International Conference on Heavy Oil and Tar Sands, Houston, TX, February 1995.

Mehta, S. A., Moore, R.G., Laureshen, C. J., Samuel, P., Teichrob, A. R., Bennion, O. B., "Safety Considerations For Underbalanced Drilling Of Horizontal Wells Using Air Or Oxygen-Containing Gas", CIM Paper 95-135, Presented At The Sixth Petroleum Conference Of The South Saskatchewan Section, The Petroleum Society Of CIM, Regina, Saskatchewan, CA, October 1995.

Mehta, S. A., Moore, R. G., Pratt, C. A., (Kip), Gair, S. D., Hoyer, C.W.J. "High-Pressure Flammability of Drilling Mud/Condensate/Sour Gas Mixtures in De-Oxygenated Air for Use in Underbalanced Drilling Operations", SPE 37067, Presented at 1996 Conference on Horizontal Well Technology, Calgary, Alberta, CA, November 1996.

Pratt, C. A. (Kip), "Underbalanced Drilling: The Past, The Present and The Future" SPE Distinguished Lecturer Presentation, 2003.

Redman69, Posted on Underbalanced Drilling Thread, April 8, 2003
http://drillingclub.proboards.com/index.cgi?board=ubd&action=display&thread

Santelli, N., Posted on Underbalanced Drilling Thread, Mar 31, 2003.
http://drillingclub.proboards.com/index.cgi?board=ubd&action=display&thread

Appendix A—Example Generator Brochures

Cummins

and Caterpillar

ISO 9001:2000

PowerWorld®
Diesel Generator

GensetModel:PC880

POWERBYCUMMINS

110V-440V 3P4W

Standard Features and Characteristics

● QUALITY STANDARDS

- ○ The POWERWORLD generator set compliance with all main standards, such as ISO8528 GB/T2820-97), GB755 BS5000, VDE0530, ISO3046, IEC34-1, CSA22-2, AS1359, ISO14001.
- ○ Diesel engine and alternator from the exclusive manufacturer in china and their quality assurance.
- ○ Other standards and certifications can be considered on request.

● ASSEMBLY

- ○ The engine and alternator are close coupled by means of an SAE flange . A full torsional analysis has been carried out to guarantee no harmful vibration will occur b
- ○ Anti-vibration pads are affixed between engine alternator feet and the base frame. Thus ensuring complete vibration isolation of the rotating assemblies and enabling the machine to be placed on an uneven surface without any detrimental effects.
- ○ For durability and corrosion resistance, all iron and steel surfaces of canopy fabrications have been treated for coating by grit blast cleaning. Then covered by special three layers painting which provides an excellent corrosion resistant surface.

● CONTROL SYSTEM AND PROTECTION

- ○ Controllers are available for all applications. The controller system is used to start and stop the engine , indicate electric date and protect the generator set. See controller features inside.
- ○ The revolving parts are covered by safety net , and the place which easy to scald and got an electric shock all to have been put on obvious warning slogan

● WARRANTY

- ○ Each POWERWORLD generating set has been got through 2 hours load test for running 0%, 25%, 50%, 75%, 100% and 110% load, all protective devices and control function are simulated and checked before despatch.
- ○ POWERWORLD Company provides one-source responsibility for the generator set and accessories.
- ○ Engine and Alternator are guaranteed for a period of 12 months from the date of commissioning or 18 months from shipping, whichever occurs first.
- ○ Convenience for operation and maintenance, backed by CUMMINS and STAMFORD global service

RATINGS: All three-phase units are rated at 0.8 power factor. Standby ratings : Standby ratings apply to installations served by a reliable utility source. The standby rating is for this rating. Ratings are in according with ISO-3046/1, BS 5514 ,AS 2789 , and DIN 6271. Prime Power Ratings: Prime power ratings apply to installations where utility power is unavailable or unreliable. At varying load, the number of generator set operating hours is unlimited. A 10% overload capacity is available for one hour in twelve. Ratings are in accordance with ISO-8528/1, overload capacity in accordance with ISO-3046/1, BS 5514, AS 2789, and DIN 6271. For limited running time and base load ratings, consult the factory. The generator set manufacturer reserves the right to change the design or specifications without notice and without any obligation or liability whatsoever. GENERAL GUIDELINES FOR DERATION: Altitude: Derate 2.0% per 300m (984 ft) elevation above 1000m (3279 ft) up to a maximum elevation of 2450m (8000 ft). More than 2450m (8000ft), please contacts with us or our dealer seek the help. Temperature: Derate 6.0% per 11 (20) temperature above 40 (104).

Rating Range

		RPM1500 50Hz
Standby:	kW	880
	kVA	1100
Prime:	kW	800
	kVA	1000

GENERATOR SET RATINGS

Alternator Model	STAMFORD				MARATHON		
Frequency and Speed	50Hz 1500rpm				50Hz 1500rpm		

Prime Power Data

Class-TEMP Rise( )	Cont.H-125K/40				Cont.H-125K/40		
Voltage series star	380	400	415	440	380	400	415
Voltage parallel star	190	200	208	220	190	200	208
Voltage series delta	220	230	240	254	220	230	240
Rating capacity(kVA)	1000	1030	1000	1000	1025	1025	1025
Rating power(kW)	800	824	800	800	820	820	820
Power efficiency(%)	95.0	95.1	95.3	95.4	95.1	95.1	95.1
Input power(kW)	842	866	839	839	863	863	863

Standby Power Data

Class-TEMP Rise( )	Standby.H-125K/40				Standby.H-150K/40		
Voltage series star	380	400	415	440	380	400	415
Voltage parallel star	190	200	208	220	190	200	208
Voltage series delta	220	230	240	254	220	230	240
Rating capacity(kVA)	1060	1070	1060	1060	1075	1075	1075
Rating power(kW)	848	856	848	848	860	860	860
Power efficiency(%)	94.7	94.9	95.1	95.3	94.9	94.9	94.9
Input power(kW)	895	902	892	890	906	906	906

ALTERNATOR

Specification	1500RPM 50HZ
Type	4-Pole, Rotating Field
Exciter type	Brushless, Self excited
Voltage regulator	Solid State, Volts/Hz
Voltage regulation	1.0%
Insulation	Class H
Protection	IP23
Rated power factor	0.8
Stator winding	Double layer concentric
Winding pitch	Two thirds
Winding leads	12
Maximum overspeed	2250 Rev/min
Sustained short circuit	Self excited machines do not sustain a short circuit current
Waveform distortion	No load < 1.5% Non-distorting balanced linear load < 5.0%
Altitude	1000 m

- Alternators meet the requirement of BS EN 60034 and the relevant section of other international standards such as BS5000, VDE 0530, NEMA MG1-32, IEC34, CSAC22.2-100, As1359, and other standards and certifications can be considered on request.
- The 2/3 pitch design avoids excessive neutral currents. With the 2/3 pitch and carefully selected pole and tooth designs, ensures very low waveform distortion.
- Brushless alternator with brushless pilot exciter for excellent load response.
- The insulation system is class H, easy parallelling with mains or other generators, standard 2/3 pitch stator windings avoid excessive neutral currents.
- Backed by worldwide service network

DIESEL ENGINE

- KTA38-G5 diesel engines are manufactured by CHONGQING CUMMINS Engines Company Limited.

Application Data

EngineSpecifications	1500RPM 50HZ
Manufacturer	CUMMINS
Number of cylinders	12
Cylinder arrangement	60° V
Cycle	Four stroke
Aspiration	Turbocharged Aftercooler
Compression ratio	13.9:1
Bore Stroke	159 mm 159mm
Displacement	37.8litres
Direction of rotation	Clockwise viewed from front
Max.Power at rated rpm	970kW
Estimated total weight(dry)	4231kg
Frequency regulation steady state	0.25%
Mean piston speed	7.9m/s

Exhaust

Exhaust System	1500RPM 50HZ
Maximum back pressure	10.05 kPa (3 in Hg)
Exhaust gas flow (max)	3306 litre/s
Exhaust gas temperature (max)	513 (955℉)

Lubrication

Lubrication system	1500RPM 50HZ
Oil Pressure At idle speed At governed speed	 138kPa 310-448kPa
Maximum Oil Temperature	121 ℃(250℉)
Total System Capacity (with Combo Filter)	135 litre(35.7 US gal)

Engine Electrical

Engine Electrical System	1500RPM 50HZ
Battery charging alternator:	
Ground(negative/positive)	Negative
Volts(DC)	24V
Starter motor rated voltage(DC)	24V
Battery voltage	12V
Battery charging ampere	35A
Maximum allowable resistance of cranking circuit	0.002 ohm
Minimum Recommended Battery Capacity:	
Cold Soak @ 10 ℉ and Above	1200 CCA
Cold Soak @ 0 to 10 ℉ ℉	1280 CCA
Cold Soak @ -18 to 0℉ ℉	1800 CCA

Fuel

Fuel System	1500RPM 50HZ
Type of injection	Direct Injection Cummins PT
Maximum restriction at PT fuel injection pump with clean fuel filter with dirty fuel filter	 13.4kPa 26.8kPa
Maximum allowable head on injector return line	6.5 in Hg
Maximum fuel flow to injection pump	TBA litre/hour

Fuel consumption	1500RPM 50HZ
Standby power	228 litre/hr
100% prime power	209 litre/hr
75% prime power	161 litre/hr
50% prime power	113 litre/hr
25% prime power	65 litre/hr
Continuous power	N.A litre/hr

Specifications may change without notice

Http://www.dieselgeneratorcn.com

Application Data

Cooling System

Cooling System	1500RPM 50HZ
Total system capacity	
Engine Only	30 litres
Radiator	71 litres
Fan gas flow	29950m³/hr
Thermostat operation range	82 - 95 ¥
Maximum water temperature	100 (212¥) &»
Minimum Pressure of radiator cap	69kPa
Max. coolant temp. permitted	
for Standby Power	104 (220¥) &»
for Prime Power	100 (212¥) &»

NOTE:

All data is based on:

1. Engine operating with fuel system, water pump, lubricating oil pump, air cleaner and exhaust silencer; not included are battery charging alternator, fan, and optional driven components.
2. Engine operating with fuel corresponding to grade No. 2-D per ASTM D975.
3. ISO 3046, Part 1, Standard Reference Conditions of:
   Barometric Pressure : 100 kPa (29.53 in Hg)
   Air Temperature : 25 (77¥) &»
   Altitude : 110 m (361 ft)
   Relative Humidity : 30%
   Air Intake Restriction : 254 mm H2O (10 in H2O)
   Exhaust Restriction : 51 mm Hg (2 in Hg)

TBA: To Be Determined

CONTROLLERS

GTR-168 MANUAL CONTROLLER

The Model GTR-168is a Manual Engine Control Module designed to control the engine via a key switch and pushbuttons on the front panel. The module is used to start and stop the engine and indicate fault conditions, automatically shutting down the engine and indicating the engine failure by LED, giving true, first up fault annunciation.

Panel introduction:

- Indicator type frequency, voltmeter and ampere meter demonstration unit's electrical parameter.
- The voltage change-over switch and the rheotrope uses for to choose the different phase voltage and current to display.
- The big red button uses for the operator to stop the genset peremptorily
- The oil pressure gauge, coolant temperature gauge and the battery voltage gauge.
- The controller. And an integral anti-tamper LCD hours run counter is also provided.
- If the customer needs to use the preheating function, we will be able to increase the preheating button.

Protection:

Low Oil Pressure
High Engine Temperature
Auxiliary Shutdown
Over speed

DC Supply: 8 to 35 V Continuous.

PLC5110 CONTROLLER

Panel introduction:

- Indicator type frequency, voltmeter and ampere meter demonstration unit's electrical parameter.
- The voltage change-over switch and the rheotrope uses for to choose the different phase voltage and current to display.
- The oil pressure gauge, coolant temperature gauge and the battery voltage gauge.
- The controller.
- Preheating button.

Protection:

Over Speed Shutdown.
Low Oil Pressure Shutdown.
High Engine Temp Shutdown.
Charger failure alarm.
Mains failure alarm.
Optional Under speed Protection.

DC Supply: 8 to 35 V Continuous.

PLC5220 INTELIGENT CONTROL SYSTEM

The AMF25 is an Automatic Mains Failure module with generator monitoring, protection and start facilities. The controller has a large LCD screen, display the generator's each parameter, running and alarm information. The off/replacement button, mode switch button, start/stop button and the LED indicator light, makes the user easy to operate and maintain the generator.

Panel introduction:

- Indicator or digital type frequency, voltmeter and ampere meter demonstration unit's electrical parameter.
- The big red button uses for the operator to stop the genset peremptorily
- The controller.

Function:

- Communication: RS232 connection, uses the industry rank MODBUS protocol can easily communicate with others intelligence control system.
- Display function: LCD screen can display the generator's parameter and the control system's running information.
- Set up parameter: Engineer can set up the controller parameter from the control panel or through the PC, 6 programmable fan-out may satisfy the user each kind of demand.
- Protection: The control system can protect the generator set, manage each kind of electrical failure.
- Control Function of ATS.

DC Supply: 8 to 35 V Continuous.

Standard Features and Accessories

Paralleling System

- ❑ Reactive Droop Compensator
- ❑ Voltage Adjust Control
- ❑ Voltage Regulator Relocation Kit

Controller System

- ❑ Common Failure Relay Kit
- ❑ Customer Connection Kit(Except Open Style)
- ❑ Communications Products and PC Software
- ❑ Engine Pre-alarm Sender Kit
- ❑ Remote Annunciator Panel
- ❑ Remote Audiovisual Alarm Panel
- ❑ Remote Emergency Stop Kit
- ❑ PCRC series control system, with RS232 or RS485 communication connection and communication agreement.

Miscellaneous Accessories

- ❑ _____
- ❑ _____
- ❑ _____
- ❑ _____
- ❑ _____

Dimensions and Weights

Open Style

Overall Size, L*W*H(mm)	4850*1830*2400
Weight(radiator model),net,Kg	8900Kg

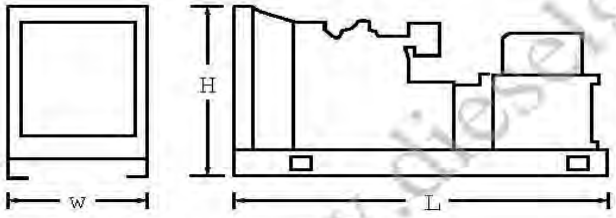

Soundproof Style

Overall Size, L*W*H(mm)	N/A
Weight(radiator model),net,Kg	N/A

NOTE: This drawing is provided for reference only and should not be used for planning installation. Contact your local distributor for more detailed information.

DISTRIBUTED BY:

Standard Features

- Battery, Battery Rack and Battery Cables
- Integral Vibration Isolation
- Oil Drain Extension
- Air cleaner ,Heavy Duty
- 3 Pole Circuit Breaker
- Heavy duty industrial type exhaust silencer with flexible pipe(supplied loose).

Maintenance and Literature

- General Maintenance Literature Kit
- Test Certificate and design paper
- Quality certificate and Maintenance card

Accessories

Enclosed Unit

- ❑ Sound Enclosure
- ❑ Weather Enclosure (with enclosed critical silencer)
- ❑ Weather Housing (with roof-mounted critical silencer)
- ❑ Trailer(Causes the genset easily to move)

Open Unit

- ❑ Exhaust Silencer, Critical kit
- ❑ Flexible Exhaust Connector, Stainless Steel

Cooling System

- ❑ Block Heater (recommended for ambient temperatures below 0 ¥)
- ❑ Radiator Duct Flange
- ❑ Remote Radiator Cooling

Fuel System

- ❑ Auxiliary Fuel Pump
- ❑ Flexible Fuel Lines
- ❑ Mechanical dipstick or fuel level sensor
- ❑ Subbase Fuel Tank with Day Tank
- ❑ Fuel fill cap with breather
- ❑ 10 hours running tank
- ❑ Automatic fuel--providing device
- ❑ Hand primer pump

Electrical System

- ❑ Battery Charger, Equalize/Float Type

Engine and Alternator

- ❑ 3 or 4 Pole Circuit Breaker with Shunt Trip
- ❑ Fuel/Water Separator
- ❑ Oil Preheater
- ❑ Air Preheater
- ❑ Alternator Strip Heater

Maintenance and Literature

- ❑ Maintenance Kit (includes air, oil, and fuel filters)
- ❑ Overhaul Literature Kit

Specifications may change without notice

Http://www.dieselgeneratorcn.com

Model: DFHA
KW rating: 620 standby
560 prime
Frequency: 50
Fuel type: Diesel

Generator set data sheet

Our energy working for you.™

Cummins Power Generation

Exhaust emission data sheet:	**EDS-251**
Exhaust emission compliance sheet:	
Sound performance data sheet:	**MSP-249**
Cooling performance data sheet:	
Prototype test summary data sheet:	**PTS-226**
Standard set-mounted radiator cooling outline:	**0500-3134**
Optional set-mounted radiator cooling outline:	
Optional heat exchanger cooling outline:	
Optional remote radiator cooling outline:	

Fuel consumption

	Standby				Prime				Continuous
	kW (kVA)				kW (kVA)				kW (kVA)
Ratings	620 (775)				560 (700)				
Load	1/4	1/2	3/4	Full	1/4	1/2	3/4	Full	Full
US gph	12.6	23.2	33.0	44.7	11.7	20.7	30.7	40.3	
L/hr	48	88	125	169	44	78	116	153	

Engine

	Standby rating	Prime rating	Continuous rating
Engine manufacturer	Cummins Inc.		
Engine model	QST30-G1		
Configuration	Cast iron, 50°V 12 cylinder		
Aspiration	Turbocharged and aftercooled		
Gross engine power output, kWm (bhp)	701.2 (940.0)	634.1 (850.0)	
BMEP at rated load, kPa (psi)	1840.9 (267.0)	1661.6 (241.0)	
Bore, mm (in)	140.0 (5.51)		
Stroke, mm (in)	165.1 (6.50)		
Rated speed, rpm	1500		
Piston speed, m/s (ft/min)	8.3 (1634.0)		
Compression ratio	14.0:1		
Lube oil capacity, L (qt)	132.5 (140.0)		
Overspeed limit, rpm	2100 ± 50		
Regenerative power, kW	78.00		

Fuel flow

Fuel flow at rated load, L/hr (US gph)	355.8 (94.0)	
Maximum inlet restriction, mm Hg (in Hg)	101.6 (4.0)	
Maximum return restriction, mm Hg (in Hg)	254.0 (10.0)	

Air	Standby rating	Prime rating	Continuous rating
Combustion air, m^3/min (scfm)	45.6 (1610.0)	42.4 (1500.0)	
Maximum air cleaner restriction, kPa (in H_2O)	6.2 (25.0)		
Alternator cooling air, m^3/min (scfm)	96.8 (3420.0)		

Exhaust			
Exhaust flow at rated load, m^3/min (cfm)	130.1 (4596.0)	119.6 (4225.0)	
Exhaust temperature, °C (°F)	537.8 (1000.0)	526.7 (980.0)	
Maximum back pressure, kPa (in H_2O)	10.2 (41.0)		

Standard set-mounted radiator cooling			
Ambient design, °C (°F)	40 (104)		
Fan load, kW (HP)	18.4 (24.7)		
Coolant capacity (with radiator), L (US gal)	200.6 (53.0)		
Coolant system air flow, m^3/min (scfm)	707.5 (25000		
Total heat rejection, MJ/min (Btu/min)	30.9 (29140)	27.1 (25560)	
Maximum cooling air flow static restriction, kPa (in H_2O)	0.12 (0.5)		

Optional set-mounted radiator cooling			
Ambient design, °C (°F)			
Fan load, kW_m (HP)			
Coolant capacity (with radiator), L (US gal)			
Cooling system air flow, m^3/min (scfm)			
Total heat rejection, MJ/min (Btu/min)			
Maximum cooling air flow static restriction, kPa (in H_2O)			

Optional heat exchanger cooling			
Set coolant capacity, L (US gal)			
Heat rejected, jacket water circuit, MJ/min (Btu/min)			
Heat rejected, after-cooler circuit, MJ/min (Btu/min)			
Heat rejected, fuel circuit, MJ/min (Btu/min)			
Total heat radiated to room, MJ/min (Btu/min)			
Maximum raw water pressure, jacket water circuit, kPa (psi)			
Maximum raw water pressure, aftercooler circuit, kPa (psi)			
Maximum raw water pressure, fuel circuit, kPa (psi)			
Maximum raw water flow, jacket water circuit, L/min (US gal/min)			
Maximum raw water flow, aftercooler circuit, L/min (US gal/min)			
Maximum raw water flow, fuel circuit, L/min (US gal/min)			
Minimum raw water flow @ 27 °C (80 °F) Inlet temp, jacket water circuit, L/min (US gal/min)			
Minimum raw water flow @ 27 °C (80 °F) Inlet remp, after-cooler circuit, L/min (US gal/min)			
Minimum raw water flow @ 27 °C (80 °F) Inlet temp, fuel circuit, L/min (US gal/min)			
Raw water delta P @ min flow, jacket water circuit, kPa (psi)			
Raw water delta P @ min flow, after-cooler circuit, kPa (psi)			
Raw water delta P @ min flow, fuel circuit, kPa (psi)			
Maximum jacket water outlet temp, °C (°F)			
Maximum after-cooler inlet temp, °C (°F)			
Maximum after-cooler inlet temp @ 25 °C (77 °F) ambient, °C (°F)			

Optional remote radiator cooling[1]	
Set coolant capacity, L (US gal)	

Our energy working for you.™

www.cumminspower.com

D-3412 (7/08)

Cummins Power Generation

Max flow rate @ max friction head, jacket water circuit, L/min (US gal/min)			
Heat rejected, jacket water circuit, MJ/min (Btu/min)			
Total heat radiated to room, MJ/min (Btu/min)			
Maximum friction head, jacket water circuit, kPa (psi)			
Maximum static head, jacket water circuit, m (ft)			
Maximum jacket water outlet temp, °C (°F)			

Weights[2]

Unit dry weight kgs (lbs)	7676 (16922)
Unit wet weight kgs (lbs)	7973 (17578)

Notes:

[1] For non-standard remote installations contact your local Cummins Power Generation representative.

[2] Weights represent a set with standard features. See outline drawing for weights of other configurations.

Derating factors

Standby	Rated power available up to 1524 m (5000 ft) at ambient temperatures up to 35 °C (95 °F). Above 1524 m (5000 ft), derate at 4% per 305 m (1000 ft), and 2% per 11 °C (1% per 10 °F) above 35 °C (95 °F).
Prime	
Continuous	

Ratings definitions

Emergency standby power (ESP):	**Limited-time running power (LTP)**:	**Prime power (PRP)**:	**Base load (continuous) power (COP)**:
Applicable for supplying power to varying electrical load for the duration of power interruption of a reliable utility source. Emergency Standby Power (ESP) is in accordance with ISO 8528. Fuel Stop power in accordance with ISO 3046, AS 2789, DIN 6271 and BS 5514.	Applicable for supplying power to a constant electrical load for limited hours. Limited Time Running Power (LTP) is in accordance with ISO 8528.	Applicable for supplying power to varying electrical load for unlimited hours. Prime Power (PRP) is in accordance with ISO 8528. Ten percent overload capability is available in accordance with ISO 3046, AS 2789, DIN 6271 and BS 5514.	Applicable for supplying power continuously to a constant electrical load for unlimited hours. Continuous Power (COP) is in accordance with ISO 8528, ISO 3046, AS 2789, DIN 6271 and BS 5514.

Our energy working for you.™

www.cumminspower.com

D-3412 (7/08)

Power Generation

Alternator data

Three phase table[1]		105 °C	125 °C	125 °C								
Feature code		B325	B324	B360								
Alternator data sheet number		310	309	309								
Voltage ranges		110/190 thru 127/220 220/380 thru 254/440	110/190 thru 127/220 220/380 thru 254/440	220/380 thru 254/440								
Surge kW		650	644	644								
Motor starting kVA (at 90% sustained voltage)	Shunt											
	PMG	2250	2000	2000								

Full load current amps at standby rating	120/208	220/380	230/240	240/416
	2151	1177	1118	1076

[1] Single phase power can be taken from a three phase generator set at up to 40% of the generator set nameplate kW rating at unity power factor.

Formulas for calculating full load currents:

Three phase output

$$\frac{\text{kW} \times 1000}{\text{Voltage} \times 1.73 \times 0.8}$$

Single phase output

$$\frac{\text{kW} \times \text{SinglePhaseFactor} \times 1000}{\text{Voltage}}$$

Cummins Power Generation
1400 73rd Avenue N.E.
Minneapolis, MN 55432 USA
Phone: 763 574 5000
Fax: 763 574 5298

Warning: Back feed to a utility system can cause electrocution and/or property damage. Do not connect to any building's electrical system except through an approved device or after building main switch is open.

Our energy working for you.™

www.cumminspower.com

D-3412 (7/08)

Power Generation

DIESEL GENERATOR SET

CATERPILLAR®

Image shown may not reflect actual package.

PRIME
1360 ekW 1700 kVA 60 Hz 1800 rpm 12 470 Volts

Caterpillar is leading the power generation marketplace with Power Solutions engineered to deliver unmatched flexibility, expandability, reliability, and cost-effectiveness.

FEATURES

FUEL/EMISSIONS STRATEGY
- EPA Certified for Stationary Emergency Application (EPA Tier 2 emissions levels)

DESIGN CRITERIA
- The generator set accepts 100% rated load in one step per NFPA 110 and meets ISO 8528-5 transient response.

FULL RANGE OF ATTACHMENTS
- Wide range of bolt-on system expansion attachments, factory designed and tested
- Flexible packaging options for easy and cost effective installation

SINGLE-SOURCE SUPPLIER
- Fully prototype tested with certified torsional vibration analysis available

WORLDWIDE PRODUCT SUPPORT
- Cat dealers provide extensive post sale support including maintenance and repair agreements
- Cat dealers have over 1,800 dealer branch stores operating in 200 countries
- The Cat® S•O•S℠ program cost effectively detects internal engine component condition, even the presence of unwanted fluids and combustion by-products

CAT 3512C DIESEL ENGINE
- Reliable, rugged, durable design
- Four-stroke-cycle diesel engine combines consistent performance and excellent fuel economy with minimum weight

CAT EMCP 3 SERIES CONTROL PANELS
- Simple user friendly interface and navigation
- Scalable system to meet a wide range of customer needs
- Integrated Control System and Communications Gateway

SEISMIC CERTIFICATION
- Seismic Certification available
- Anchoring details are site specific, and are dependent on many factors such as generator set size, weight, and concrete strength. IBC Certification requires that the anchoring system used is reviewed and approved by a Professional Engineer
- Seismic Certification per Applicable Building Codes: IBC 2000, IBC 2003, IBC 2006, IBC 2009, CBC 2007
- Pre-approved by OSHP and carries an OPA#(OSP-0084-01) for use in healthcare projects in California

PRIME 1360 ekW 1700 kVA

60 Hz 1800 rpm 12 470 Volts

CATERPILLAR®

FACTORY INSTALLED STANDARD & OPTIONAL EQUIPMENT

System	Standard	Optional
Air Inlet	• Single element canister type air cleaner with service indicator	[ ] Dual element & heavy duty air cleaners (with pre-cleaners) [ ] Air inlet adapters & shutoff
Cooling	• Radiator fan and fan drive • Fan and belt guards • Coolant level sensors* • Cat Extended Life Coolant*	[ ] Coolant level switch gauge [ ] Heat exchanger and expansion tank
Exhaust	• Exhaust manifold - dry - dual - 8 in • 203 mm (8 in) ID round flanged outlet	[ ] Mufflers [ ] Stainless steel exhaust flex fittings [ ] Elbows, flanges, expanders & Y adapters
Fuel	• Secondary fuel filters • Fuel cooler* • Fuel priming pump • Flexible fuel lines-shipped loose	[ ] Duplex secondary fuel filter [ ] Primary fuel filter with fuel water separator
Generator	• Class F insulation • Cat digital voltage regulator (CDVR) with kVAR/PF control, 3-phase sensing • Winding temperature detectors • Anti-condensation space heaters	[ ] Oversized generators [ ] Bearing temperature detector [ ] Cross current compensation transformer
Power Termination	• Bus bar (NEMA mechanical lug holes) • Right hand cable entry • Top or bottom cable entry	[ ] Left hand cable entry
Governor	• ADEM™ 3	[ ] Load share module
Control Panel	• EMCP 3.1 • User Interface panel (UIP) - rear mount • AC & DC customer wiring area (right side) • Emergency stop pushbutton	[ ] EMCP 3.2 ... [ ] EMCP 3.3 [ ] Option for right or left mount UIP [ ] Local & remote annunciator modules [ ] Digital I/O Module [ ] Generator temperature monitoring & protection [ ] Remote monitoring software
Lube	• Lubricating oil and filter • Oil drain line with valves • Fumes disposal • Gear type lube oil pump	[ ] Oil level regulator [ ] Deep sump oil pan [ ] Electric & air prelube pumps [ ] Manual prelube with sump pump [ ] Duplex oil filter
Mounting	• Rails - engine / generator / radiator mounting • Anti-vibration mounts (shipped loose)	[ ] Spring-type vibration isolator [ ] IBC Isolators
Starting/Charging	• 24 volt starting motor(s) • Batteries with rack and cables • Battery disconnect switch	[ ] Battery chargers (10 & 20 Amp) [ ] 45 amp charging alternator [ ] Oversize batteries [ ] Ether starting aids [ ] Heavy duty starting motors [ ] Barring device (manual) [ ] Air starting motor with control & silencer
General	• Right hand service • Paint - Caterpillar Yellow (with high gloss black rails & radiator) • SAE standard rotation • Flywheel and flywheel housing - SAE No. 00	[ ] CSA certification [ ] CE Certificate of Conformance [ ] Seismic Certification per Applicable Building Codes: IBC 2000, IBC 2003, IBC 2006, IBC 2009, CBC 2007 * Not included with packages without radiators

PRIME 1360 ekW 1700 kVA

60 Hz 1800 rpm 12 470 Volts

CATERPILLAR®

SPECIFICATIONS

CAT GENERATOR

SR4B Generator

Frame Size	2730
Excitation	Permanent Magnet
Pitch	0.6670
Number of poles	4
Number of bearings	2
Number of Leads	006
Insulation	Class F
IP Rating	Drip Proof IP22
Alignment	Closed Coupled
Overspeed capability- % of rated	125
Wave form	002.00
Paralleling kit/Droop transformer	Standard
Voltage Regulator	3 Phase sensing with volts/Hz
Telephone influence factor	Less than 50

CAT DIESEL ENGINE

3512C ATAAC, V-12, 4 stroke, water-cooled diesel

Bore	170.00 mm (6.69 in)
Stroke	190.00 mm (7.48 in)
Displacement	51.80 L (3161.03 in^3)
Compression Ratio	14.7:1
Aspiration	TA
Fuel System	Electronic unit injection
Governor Type	ADEM3

CAT EMCP SERIES CONTROLS

- EMCP 3.1 (Standard)
- EMCP 3.2 / EMCP 3.3 (Option)
- Single location customer connector point
- True RMS AC metering, 3-phase
- Controls
  - Run / Auto / Stop control
  - Speed Adjust
  - Voltage Adjust
  - Emergency Stop Pushbutton
  - Engine cycle crank
- Digital Indication for:
  - RPM
  - Operating hours
  - Oil pressure
  - Coolant temperature
  - System DC volts
  - L-L volts, L-N volts, phase amps, Hz
  - ekW, kVA, kVAR, kW-hr, %kW, PF (EMCP 3.2 / 3.3)
- Shutdowns with common indicating light for:
  - Low oil pressure
  - High coolant temperature
  - Low coolant level
  - Overspeed
  - Emergency stop
  - Failure to start (overcrank)
- Programmable protective relaying functions: (EMCP 3.2 & 3.3)
  - Under and over voltage
  - Under and over frequency
  - Overcurrent (time and inverse time)
  - Reverse power (EMCP 3.3)
- MODBUS isolated data link, RS-485 half-duplex (EMCP 3.2 & 3.3)
- Options
  - Vandal door
  - Local annunciator module
  - Remote annunciator module
  - Input / Output module
  - RTD / Thermocouple modules
  - Monitoring software

PRIME 1360 ekW 1700 kVA

60 Hz 1800 rpm 12 470 Volts

CATERPILLAR®

TECHNICAL DATA

Open Generator Set - - 1800 rpm/60 Hz/12 470 Volts	DM8261	
EPA Certified for Stationary Emergency Application (EPA Tier 2 emissions levels)		
Generator Set Package Performance		
Genset Power rating @ 0.8 pf	1700 kVA	
Genset Power rating with fan	1360 ekW	
Coolant to aftercooler		
Coolant to aftercooler temp max	47 ° C	117 ° F
Fuel Consumption		
100% load with fan	364.5 L/hr	96.3 Gal/hr
75% load with fan	286.2 L/hr	75.6 Gal/hr
50% load with fan	201.8 L/hr	53.3 Gal/hr
Cooling System[1]		
Air flow restriction (system)	0.12 kPa	0.48 in. water
Air flow (max @ rated speed for radiator arrangement)	2075 m³/min	73278 cfm
Engine Coolant capacity with radiator/exp. tank	390.8 L	103.2 gal
Engine coolant capacity	156.8 L	41.4 gal
Radiator coolant capacity	234.0 L	61.8 gal
Inlet Air		
Combustion air inlet flow rate	124.7 m³/min	4403.7 cfm
Exhaust System		
Exhaust stack gas temperature	388.4 ° C	731.1 ° F
Exhaust gas flow rate	293.5 m³/min	10364.9 cfm
Exhaust flange size (internal diameter)	203.2 mm	8.0 in
Exhaust system backpressure (maximum allowable)	6.7 kPa	26.9 in. water
Heat Rejection		
Heat rejection to coolant (total)	580 kW	32985 Btu/min
Heat rejection to exhaust (total)	1213 kW	68983 Btu/min
Heat rejection to aftercooler	443 kW	25193 Btu/min
Heat rejection to atmosphere from engine	118 kW	6711 Btu/min
Heat rejection to atmosphere from generator	71.6 kW	4071.9 Btu/min
Alternator[2]		
Motor starting capability @ 30% voltage dip	2788 skVA	
Frame	2730	
Temperature Rise	105 ° C	189 ° F
Lube System		
Sump refill with filter	310.4 L	82.0 gal
Emissions (Nominal)[3]		
NOx g/hp-hr	4.33 g/hp-hr	
CO g/hp-hr	.41 g/hp-hr	
HC g/hp-hr	.13 g/hp-hr	
PM g/hp-hr	.032 g/hp-hr	

[1] For ambient and altitude capabilities consult your Cat dealer. Air flow restriction (system) is added to existing restriction from factory.
[2] UL 2200 Listed packages may have oversized generators with a different temperature rise and motor starting characteristics. Generator temperature rise is based on a 40 degree C ambient per NEMA MG1-32.
[3] Emissions data measurement procedures are consistent with those described in EPA CFR 40 Part 89, Subpart D & E and ISO8178-1 for measuring HC, CO, PM, NOx. Data shown is based on steady state operating conditions of 77°F, 28.42 in HG and number 2 diesel fuel with 35° API and LHV of 18,390 btu/lb. The nominal emissions data shown is subject to instrumentation, measurement, facility and engine to engine variations. Emissions data is based on 100% load and thus cannot be used to compare to EPA regulations which use values based on a weighted cycle.

PRIME 1360 ekW 1700 kVA

60 Hz 1800 rpm 12 470 Volts

CATERPILLAR®

RATING DEFINITIONS AND CONDITIONS

Meets or Exceeds International Specifications: AS1359, CSA, IEC60034-1, ISO3046, ISO8528, NEMA MG 1-22, NEMA MG 1-33, UL508A, 72/23/EEC, 98/37/EC, 2004/108/EC

Prime - Output available with varying load for an unlimited time. Average power output is 70% of the prime power rating. Typical peak demand is 100% of prime rated ekW with 10% overload capability for emergency use for a maximum of 1 hour in 12. Overload operation cannot exceed 25 hours per year. Prime power in accordance with ISO3046. Prime ambients shown indicate ambient temperature at 100% load which results in a coolant top tank temperature just below the alarm temperature.

Ratings are based on SAE J1349 standard conditions. These ratings also apply at ISO3046 standard conditions.

Fuel rates are based on fuel oil of 35° API [16° C (60° F)] gravity having an LHV of 42 780 kJ/kg (18,390 Btu/lb) when used at 29° C (85° F) and weighing 838.9 g/liter (7.001 lbs/U.S. gal.). Additional ratings may be available for specific customer requirements, contact your Cat representative for details. For information regarding Low Sulfur fuel and Biodiesel capability, please consult your Cat dealer.

PRIME 1360 ekW 1700 kVA

60 Hz 1800 rpm 12 470 Volts

CATERPILLAR®

DIMENSIONS

Package Dimensions		
Length	6452.6 mm	254.04 in
Width	2324.5 mm	91.52 in
Height	2711.4 mm	106.75 in
Weight	15 926 kg	35,111 lb

NOTE: For reference only - do not use for installation design. Please contact your local dealer for exact weight and dimensions. (General Dimension Drawing #2846050).

Performance No.: DM8261

Feature Code: 512DE6D

Gen. Arr. Number: 2524216

Source: U.S. Sourced

October 27 2010

16297658

www.CAT-ElectricPower.com

DIESEL GENERATOR SET

CATERPILLAR®

Image shown may not reflect actual package.

PRIME
580 ekW 725 kVA
50 Hz 1500 rpm 400 Volts

Caterpillar is leading the power generation marketplace with Power Solutions engineered to deliver unmatched flexibility, expandability, reliability, and cost-effectiveness.

FEATURES

FUEL/EMISSIONS STRATEGY
- Low Fuel consumption

FULL RANGE OF ATTACHMENTS
- Wide range of bolt-on system expansion attachments, factory designed and tested
- Flexible packaging options for easy and cost effective installation

SINGLE-SOURCE SUPPLIER
- Fully prototype tested with certified torsional vibration analysis available

WORLDWIDE PRODUCT SUPPORT
- Cat dealers provide extensive post sale support including maintenance and repair agreements
- Cat dealers have over 1,800 dealer branch stores operating in 200 countries
- The Cat® S•O•S℠ program cost effectively detects internal engine component condition, even the presence of unwanted fluids and combustion by-products

CAT® 3412C TA DIESEL ENGINE
- Reliable, rugged, durable design
- Field-proven in thousands of applications worldwide
- Four-stroke-cycle diesel engine combines consistent performance and excellent fuel economy with minimum weight

CAT GENERATOR
- Designed to match the performance and output characteristics of Cat diesel engines
- Single point access to accessory connections
- UL 1446 recognized Class H insulation

CAT EMCP 3 SERIES CONTROL PANELS
- Simple user friendly interface and navigation
- Scalable system to meet a wide range of customer needs
- Integrated Control System and Communications Gateway

PRIME 580 ekW 725 kVA

50 Hz 1500 rpm 400 Volts

CATERPILLAR®

FACTORY INSTALLED STANDARD & OPTIONAL EQUIPMENT

System	Standard	Optional
Air Inlet	• Single element canister type air cleaner • Service indicator	[ ] Dual element air cleaner [ ] Heavy-duty air cleaner
Cooling	• Radiator with guard • Coolant drain line with valve • Fan and belt guards • Cat® Extended Life Coolant • Low coolant level alarm or shutdown	[ ] Radiator duct flange [ ] Jacket water heater with shutoff valve [ ] Heat exchanger and expansion tank
Exhaust	• Stainless steel exhaust flex and ANSI style outlet flange, gasket, bolts and mating weld flange, shipped loose	[ ] Mufflers (10 or 35 dBA) [ ] Elbow kit and through-wall installation kit [ ] Manifold and turbocharger guards
Fuel	• Primary and secondary fuel filters • Water separator • Fuel priming pump • Flexible fuel lines	[ ] Manual transfer pump [ ] Choice of three Automatic Transfer Systems
Generator	• Class H insulation • Class F temperature rise • VR6 Voltage Regulator, 3-phase sensing, 2:1 Volts/Hz • Reactive droop • Extension box • Bus bar connection • Segregated low voltage (AC/DC) wiring panel	[ ] Digital Voltage Regulator with kVAR/PF control [ ] Anti-condensation space heater [ ] Oversize and premium generators [ ] Circuit breakers, IEC Compliant, 3-pole or 4-pole with shunt trip
Governor	• PEEC - Cat Electronic	[ ] Electronic load sharing
Control Panels	• EMCP 3.1 (mounted inside power center) • Rear facing • Speed adjust • Emergency stop pushbutton • Voltage adjustment	[ ] EMCP 3.2 ... [ ] EMCP 3.3 [ ] Right-hand mounting of control panel [ ] Local annuniciator modules (NFPA 99/110) [ ] Remote annunicator modules (NFPA 99/110) [ ] Discrete I/O module
Lube	• Lubricating oil and filter • Oil drain line with valves • Fumes disposal	[ ] Manual sump pump
Mounting	• Formed steel base • Linear vibration isolators between base and engine-generator	[ ] Integral fuel tank base [ ] Sub base fuel tank [ ] Wide base [ ] Skid base
Starting/Charging	• 45 amp charging alternator • Fuel shutoff solenoid • 24 volt starting motor • Battery with rack and cables	[ ] Heavy-duty starting system [ ] 5 or 10 amp battery charger [ ] Oversize batteries [ ] Ether starting aid [ ] Battery disconnect switch
General		[ ] Enclosures - sound attenuated, weather protective [ ] Automatic transfer switches (ATS) [ ] Floor standing circuit breakers [ ] EU Certificate of Conformance (CE)

PRIME 580 ekW 725 kVA

50 Hz 1500 rpm 400 Volts

CATERPILLAR®

SPECIFICATIONS

CAT SR4B GENERATOR

Frame Size.....597
Excitation.....Self Excited
Pitch..... 0.8000
Number of poles.....4
Number of bearings..... Single Bearing
Insulation..... UL 1446 Recognized Class H with tropicalization and antiabrasion
IP Rating.....Drip Proof IP22
Alignment..... Pilot Shaft
Overspeed capability - % of rated..... 180
Wave form..... Less than 5% deviation
Paralleling kit/Droop transformer..... Standard
Voltage regulator.3 Phase sensing with selectible volts/Hz
Voltage regulation.....Less than +/- 1/2% (steady state) Less than +/- 1% (no load to full load)
Telephone Influence Factor..... Less than 50
Harmonic distortion..... Less than 5%

CAT DIESEL ENGINE

3412C TA V-12, 4-stroke-cycle watercooled diesel
Bore - mm..... 137.20 mm (5.4 in)
Stroke - mm..... 152.40 mm (6.0 in)
Displacement - L..... 27.02 L (1648.86 in^3)
Compression Ratio..... 13.0:1
Aspiration..... TA
Fuel system.....Pump and Lines
Governor type..... PEEC - Cat Electronic

CAT CONTROL PANELS

- EMCP 3.1 (Standard)
- EMCP 3.2 / EMCP 3.3 (Option)
- Single location customer connector point
- True RMS metering, 3-phase
- Controls
  - Run / Auto / Stop control
  - Speed Adjust
  - Voltage Adjust
  - Emergency Stop Pushbutton
  - Engine cycle crank
- Digital Indication for:
  - RPM
  - Operating hours
  - Oil pressure
  - Coolant temperature
  - System DC volts
  - L-L volts, L-N volts, phase amps, Hz
  - ekW, kVa, kVAR, kW-hr, % kW, PF (EMCP 3.2 / 3.3)
- Shutdowns with indicating lights for:
  - Low oil pressure
  - High coolant temperature
  - Low coolant level
  - Overspeed
  - Emergency Stop
  - Failure to start (overcrank)
- Programmable protective relay functions: (EMCP 3.2 & 3.3)
  - Under and over voltage
  - Under and over frequency
  - Overcurrent (time and inverse time)
  - Reverse power (EMCP 3.2 & 3.3)
- MODBUS isolated data link RS–485 half-duplex (EMCP 3.2 & 3.3)
- Options
  - Vandal door
  - Local annunciator module
  - Remote annunciator module
  - Input / Output module
  - RTD / Thermocouple Modules
  - Monitoring software

PRIME 580 ekW 725 kVA

50 Hz 1500 rpm 400 Volts

CATERPILLAR®

TECHNICAL DATA

Open Generator Set - - 1500 rpm/50 Hz/400 Volts	DM0627	
Package Performance		
Genset Power rating @ 0.8 pf	725 kVA	
Genset Power rating with fan	580 ekW	
Fuel Consumption		
100% load with fan	153.7 L/hr	40.6 Gal/hr
75% load with fan	117.5 L/hr	31.0 Gal/hr
50% load with fan	82.5 L/hr	21.8 Gal/hr
Cooling System[1]		
Air flow restriction (system)	0.12 kPa	0.48 in. water
Air flow (max @ rated speed for radiator arrangement)	1236 m³/min	43649 cfm
Engine coolant capacity	59.0 L	15.6 gal
Radiator coolant capacity	84.0 L	22.2 gal
Engine Coolant capacity with radiator/exp. tank	143.0 L	37.8 gal
Exhaust System		
Combustion air inlet flow rate	44.2 m³/min	1560.9 cfm
Exhaust stack gas temperature	534.0 °C	993.2 °F
Exhaust gas flow rate	125.4 m³/min	4428.5 cfm
Exhaust flange size (internal diameter)	203.2 mm	8.0 in
Exhaust system backpressure (maximum allowable)	6.7 kPa	26.9 in. water
Heat rejection		
Heat rejection to coolant (total)	347 kW	19734 Btu/min
Heat rejection to exhaust (total)	571 kW	32473 Btu/min
Heat rejection to atmosphere from engine	95 kW	5403 Btu/min
Heat rejection to atmosphere from generator	27.3 kW	1552.5 Btu/min
Alternator[2]		
Motor starting capability @ 30% voltage dip	1815 skVA	
Frame	597	
Temperature Rise	105 °C	189 °F
Lube System		
Sump refill with filter	139.0 L	36.7 gal
Emissions[3]		
NOx mg/nm3	2932.1 mg/nm³	
CO mg/nm3	171.7 mg/nm³	
HC mg/nm3	102.6 mg/nm³	
PM mg/nm3	45 mg/nm³	

[1] For ambient and altitude capabilities consult your Cat dealer. Air flow restriction (system) is added to existing restriction from factory.
[2] UL 2200 Listed packages may have oversized generators with a different temperature rise and motor starting characteristics. Generator temperature rise is based on a 40°C ambient per NEMA MG1-32.
[3] Emissions data measurement procedures are consistent with those described in EPA CFR 40 Part 89, Subpart D & E and ISO8178-1 for measuring HC, CO, PM, NOx. Data shown is based on steady state operating conditions of 77°F, 28.42 in HG and number 2 diesel fuel with 35° API and LHV of 18,390 btu/lb. The nominal emissions data shown is subject to instrumentation, measurement, facility and engine to engine variations. Emissions data is based on 100% load and thus cannot be used to compare to EPA regulations which use values based on a weighted cycle.

PRIME 580 ekW 725 kVA

50 Hz 1500 rpm 400 Volts

CATERPILLAR®

RATING DEFINITIONS AND CONDITIONS

Meets or Exceeds International Specifications: AS1359, CSA, IEC60034-1, ISO3046, ISO8528, NEMA MG 1-22, NEMA MG 1-33, UL508A, 72/23/EEC, 98/37/EC, 2004/108/EC

Prime - Output available with varying load for an unlimited time. Average power output is 70% of the prime power rating. Typical peak demand is 100% of prime rated ekW with 10% overload capability for emergency use for a maximum of 1 hour in 12. Overload operation cannot exceed 25 hours per year. Prime power in accordance with ISO3046. Prime ambients shown indicate ambient temperature at 100% load which results in a coolant top tank temperature just below the alarm temperature.

Ratings are based on SAE J1349 standard conditions. These ratings also apply at ISO3046 standard conditions.

Fuel rates are based on fuel oil of 35° API [16° C (60° F)] gravity having an LHV of 42 780 kJ/kg (18,390 Btu/lb) when used at 29° C (85° F) and weighing 838.9 g/liter (7.001 lbs/U.S. gal.). Additional ratings may be available for specific customer requirements, contact your Cat representative for details. For information regarding Low Sulfur fuel and Biodiesel capability, please consult your Cat dealer.

PRIME 580 ekW 725 kVA

50 Hz 1500 rpm 400 Volts

CATERPILLAR®

DIMENSIONS

Package Dimensions		
Length	**4485.0 mm**	**176.57 in**
Width	**1798.1 mm**	**70.79 in**
Height	**1986.7 mm**	**78.22 in**
Weight	**5693 kg**	**12,551 lb**

NOTE: For reference only - do not use for installation design. Please contact your local dealer for exact weight and dimensions. (General Dimension Drawing #2923106).

Performance No.: DM0627

Feature Code: 412DEQ9

Gen. Arr. Number: 1492443

Source: European Sourced

October 27 2010

16282242

www.CAT-ElectricPower.com

Appendix B—Example Ancillary Equipment Brochures

BASF
The Chemical Company

PTX™ and DPX™

For mining applications

Product data

Watery eyes. Itchy throats. Headaches and nausea. They are the "occupational hazards" of almost everyone who works with diesel equipment. Worse yet, the fumes and noxious chemicals emitted from this machinery can lead to long-term health problems, causing increased sick time and employee turnover.

Yet with BASF ingenuity, your company can do more than improve the work environment of its employees. You can actually enhance productivity; protect workers and materials on the job site, while complying with today's increasingly stringent anti-pollution legislation.

As a world leader in emissions control technologies, BASF has extensive experience in reducing carbon monoxide (CO), hydrocarbons (HC) and particulate matter (PM) produced in diesel engine environments, including mining.

PTX Diesel Oxidation Catalyst
BASF innovative PTX catalyst was specifically designed to control carbon monoxide and hydrocarbon emissions from diesel engines.

- Reduces CO up to 95%
- Reduces HC up to 95%
- Extremely durable
- Withstands up to 590°C (1100°F)
- Simple to install
- Easy to clean and maintain

DPX™ Diesel Particulate Filter
BASF DPX soot filter is remarkably effective for eliminating soot and other pollutants.

- Proven on tens of thousands vehicles retrofitted worldwide
- Verified by the US EPA
- Can reduce PM,CO, HC by 90+%
- Can regenerate at normal diesel operating temperatures

About BASF
As the world's leading chemical company, BASF's portfolio ranges from chemicals, plastics, performance products, agricultural products and fine chemicals to crude oil and natural gas. BASF's intelligent system solutions and high-value products help its customers to be more successful. BASF develops new technologies and uses them to open up additional market opportunities. It combines economic success with environmental protection and social responsibility, thus contributing to a better future.

BASF Emission Control Technologies for Retrofit Mining Applications			
Technology	**Carbon Monoxide**	**Hydrocarbons**	**Particulate Matter**
PTX	✓	✓	
DPX	✓	✓	✓

BASF

The Chemical Company

BASF DPX™ Diesel Particulate Filter

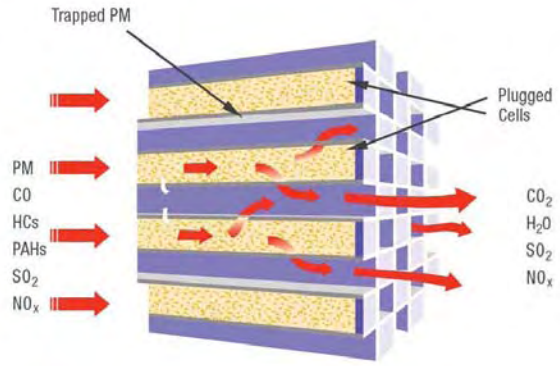

BASF PTX™ Diesel Oxidation Catalyst

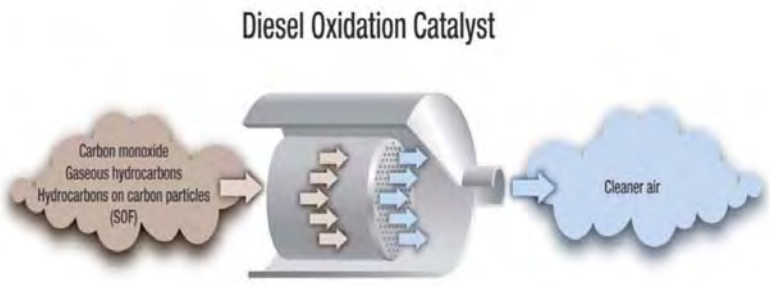

BASF Catalysts LLC
101 Wood Avenue
Iselin, NJ 08830-0770
Telephone: 732 205-5000
Fax: 732 205-5915
Web site: www.basf-catalysts.com

BF-8503 Rev. 11/2006

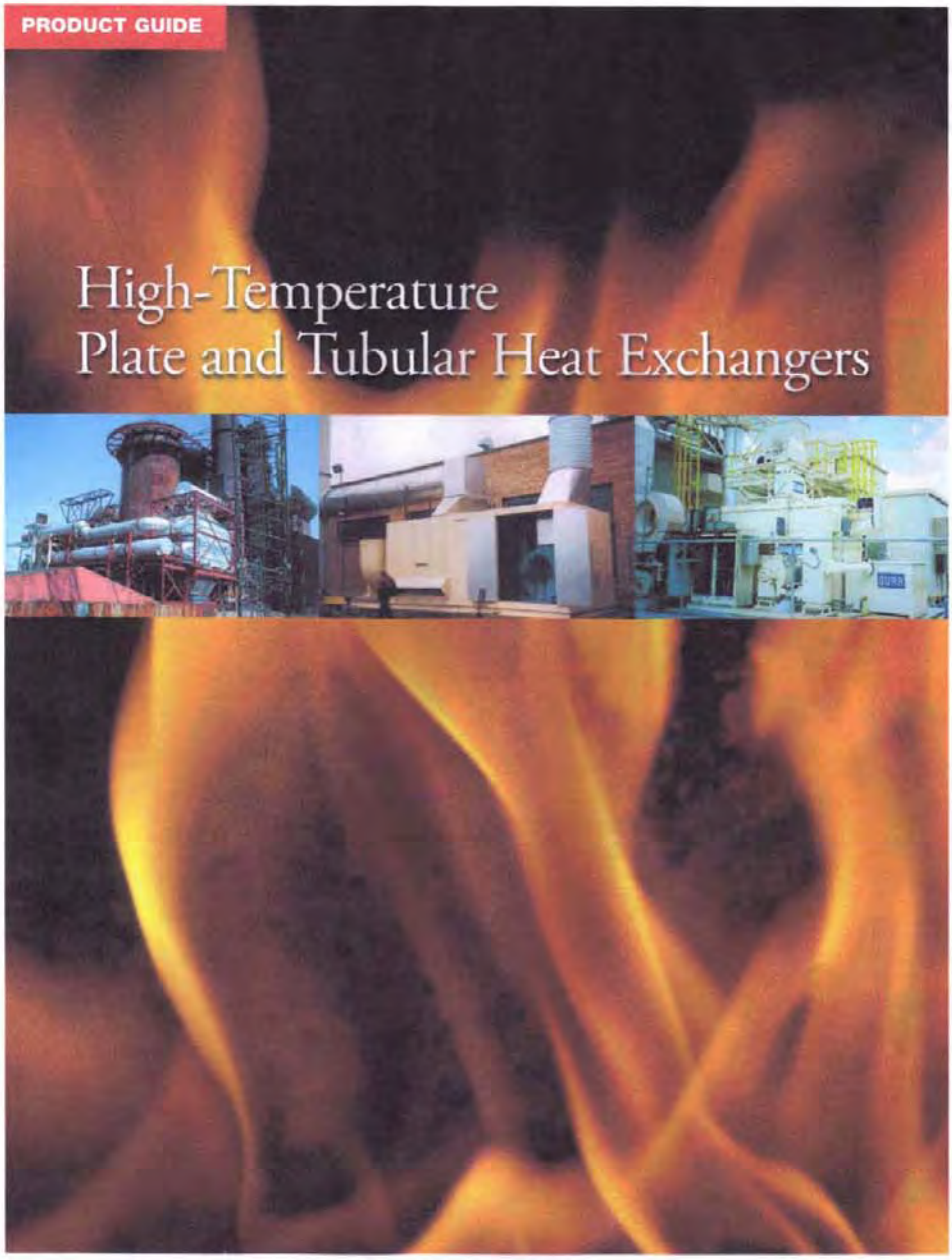

Munters

Des Champs Products

Introduction

Pioneering Advanced Technology for Industrial Energy Conservation

Founded in 1974 with the invention of the Z-Duct plate air-to-air heat exchanger, Munters - Des Champs Products has led the industry in the design, engineering, and manufacture of air-to-air energy saving systems, industrial heat exchangers, packaged make-up air, and dehumidification systems. The company quickly earned a reputation for innovation by manufacturing a unique, efficient heat exchanger for the F-14 fighter plane. This aluminum plate heat exchanger proved to be cost effective and found a ready market in the private sector. Eighteen patents and a host of new products later, Munters offers virtually all types of air-to-air heat exchangers and energy recovery systems including equipment durable enough to withstand the effects of high temperatures and rugged operating environments. These industrial heat exchangers are able to perform under harsh conditions in temperatures as high as 2000°F with special construction.

Munters understands the customer's needs and offers engineered solutions to meet specific requirements. Our line of industrial heat exchangers includes the Thermo-Z plate heat exchanger and the Thermo-T tubular heat exchanger. Custom designs may include multiple airflow configurations and variable spacings to achieve the desired heat exchanger effectiveness and pressure differentials while maintaining specific size.

Thermo-Z™

The Munters Thermo-Z plate heat exchanger recovers heat from energy-consuming processes up to 1400°F. Thermo-Z is typically constructed of heavy gauge alloy stainless steel, providing a smooth, continuous path for minimum air resistance. Heat transfer plates are completely seam-welded to prevent cross-contamination, and optional expansion joints enable flange-to-flange ductwork installation without the need to compensate for thermal expansion. Custom designs are offered, with effectiveness values up to 85%.

Thermo-T™

The Munters Thermo-T tubular heat exchanger recovers heat from energy-consuming processes at temperatures up to 1800°F. Heat transfer tubes are fully welded to the tube sheets, ensuring minimum cross-contamination. Integral expansion joints make the Thermo-T ideal for high-temperature applications. Single and multi-pass models are available with effectiveness values up to 80%.

Product Testing

Munters - Des Champs Products utilizes modern testing instruments and procedures to ensure a high quality product. All heat exchangers are fully pressure-tested for leaks and inspected for structural integrity.

Research and Development

Research and Development is the core of Munters - Des Champs Products and the source of all our products. Listening to and working closely with our customers has made us the first to bring to market new products to address new applications. Munters is committed to providing custom engineered solutions to challenging problems.

Thermo-Z™

High-Temperature Plate Heat Exchangers

Thermo-Z

The Thermo-Z plate heat exchanger is designed to recover heat from energy consuming processes up to 1400°F. Energy can be recovered and returned as process make-up air, used to preheat combustion air, or used for plant or office heating.

Thermo-Z offers fully adjustable plate thickness and plate spacing. Combine this with the unmatched flexibility in materials of construction and flow patterns, and Thermo-Z is the obvious choice for your high temperature heat recovery application.

To meet unique performance or configuration requirements, multiple flow patterns are available. For harsh environments, the Thermo-Z can be integrated with a tubular heat exchanger (Thermo-T) to provide the ultimate in effectiveness, reliability and value.

Construction

The Thermo-Z heat exchanger is designed and constructed for an industrial environment. Proper material selection is crucial to the life of a heat exchanger. Typically, Thermo-Z is constructed with heavy gauge 304L, 316L, or 309S stainless steel plates that provide a smooth, continuous path for minimum air resistance. These materials provide superior performance in high temperature or corrosive environments. Optional materials are available to meet specific needs.

The heat transfer plates are completely seam welded to ensure against cross-contamination. Spacing is achieved with raised and depressed truncated conical dimples, providing uniform plate pitch. The height of these dimples can be varied at the time of manufacture to establish the desired plate spacing necessary to meet exact performance requirements.

The inner casing is constructed of the same material as the heat transfer matrix. It is welded to the matrix at certain peripheral locations to assure an air-tight seal.

Optional Expansion Joints With Welded Outer Casing

Thermal stress is another major factor in high-temperature heat exchanger design. At high temperatures, Munters' integral expansion joints allow the heat exchanger matrix to expand without causing excessive stress.

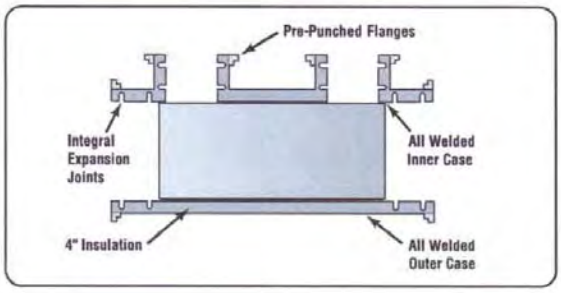

The outer casing remains cool because of the layer of high-temperature insulation. Therefore, it will not expand as a result of process temperature changes. The internal casing is secured to the cold outer casing by means of integral thermal expansion joints. These joints allow the inner matrix/casing assembly to move freely without undue forces being imposed on it by the rigid, cool external casing. The heat exchanger (with its cold flanges) can be installed flange-to-flange to the ductwork without the need to compensate for the thermal expansion of the heat exchanger.

Features and Benefits

- Standard operation to 1400°F
- Effectiveness to 85%
- Pressure differentials to 28" W.C. standard
- Fully-welded construction
- Near zero cross-contamination
- Custom designs
- Variable plate spacing
- Integration with Thermo-T
- More cost effective than shell and tube heat exchangers

Applications

- Oxidizers
- Ovens
- Dryers
- Furnaces
- Solid Waste Recovery
- Annealing Operations
- Solvent Recovery
- Anywhere hot air is wasted

Standard and Custom Engineered Construction

Standard Construction

- All-welded heat transfer matrix (standard 0.030 inches thick)
- Standard 0.5-inch plate spacing
- All-welded casing (minimum 0.105 inches thick)
- 2" x 2" x 1/4" pre-punched flange connections
- Highly effective counterflow pattern
- Ready to be field installed and insulated

Custom Construction

- Broad selection of materials
- Insulated double-wall construction with integral thermal expansion joints
- Seven airflow patterns
- Designed to meet user requirements
- Complete systems
- Matrix cleaning options

Computer Analysis

Munters will supply a complete Thermodynamic Output as well as a Financial Analysis showing simple payback.

Munters **ZDUCT PAYBACK**

Des Champs Products

225 South Magnolia Ave. Buena Vista, VA 24416
Phone: (540) 291-1111 Fax: (540) 291-3333

10/6/2008 5:27:43 PM Ver. 4.2.26
dctindustrial@munters.com

Order Name	Energy Recovery	Location	Virginia
Order Number	0	Prepared By	JLC
(Qty) Model	(1)SRICF	Unit Tag	HX-1
Representative	Munters	Engineering Firm	OEM
Altitude	1000		

INPUT DATA:

[illegible]	[illegible]

OUTPUT DATA:

[illegible]	[illegible]	[illegible]	[illegible]	[illegible]	[illegible]
[illegible]	[illegible]	[illegible]	[illegible]	[illegible]	[illegible]

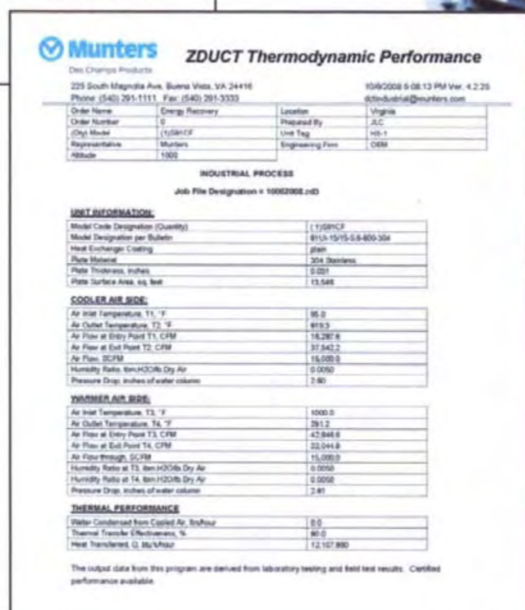

Munters **ZDUCT Thermodynamic Performance**

Des Champs Products

225 South Magnolia Ave. Buena Vista, VA 24416
Phone: (540) 291-1111 Fax: (540) 291-3333

10/6/2008 5:08:13 PM Ver. 4.2.25
dctindustrial@munters.com

Order Name	Energy Recovery	Location	Virginia
Order Number	0	Prepared By	JLC
(Qty) Model	(1)SRICF	Unit Tag	HX-1
Representative	Munters	Engineering Firm	OEM
Altitude	1000		

INDUSTRIAL PROCESS

Job File Designation = 10062008.rd3

UNIT INFORMATION:

Model Code Designation (Quantity)	(1)SRICF
Model Designation per Bulletin	811J-15/15-5.8-800-304
Heat Exchanger Coating	plain
Plate Material	304 Stainless
Plate Thickness, inches	0.031
Plate Surface Area, sq. feet	13,546

COOLER AIR SIDE:

Air Inlet Temperature, T1, °F	95.0
Air Outlet Temperature, T2, °F	819.3
Air Flow at Entry Point T1, CFM	16,287.8
Air Flow at Exit Point T2, CFM	37,542.2
Air Flow, SCFM	15,000.0
Humidity Ratio, lbm.H2O/lb Dry Air	0.0050
Pressure Drop, inches of water column	2.60

WARMER AIR SIDE:

Air Inlet Temperature, T3, °F	1000.0
Air Outlet Temperature, T4, °F	281.2
Air Flow at Entry Point T3, CFM	42,848.6
Air Flow at Exit Point T4, CFM	22,044.8
Air Flow through, SCFM	15,000.0
Humidity Ratio at T3, lbm.H2O/lb Dry Air	0.0058
Humidity Ratio at T4, lbm.H2O/lb Dry Air	0.0058
Pressure Drop, inches of water column	2.81

THERMAL PERFORMANCE

Water Condensed from Cooled Air, lbs/hour	0.0
Thermal Transfer Effectiveness, %	80.0
Heat Transferred, Q, btu's/hour	12,107,880

The output data from this program are derived from laboratory testing and field test results. Certified performance available.

Munters

Des Champs Products

225 South Magnolia Avenue • Buena Vista, VA • 24416
540.291.1111 • Fax 540-291-3333 • dctindustrial@munters.com • www.muntershightemp.com

Air Cooled - HEAT EXCHANGER

MOBILE AIR COOLED HEAT EXCHANGERS		
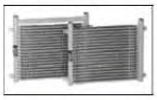 MODEL SEARCH	mount on Mobile Equipment mounts in front of Engine Radiator pressure to 300 PSI flow rate 1GPM to 100 GPM CALL 800-329-6888	AMERICAN HEAT TRANSFER AMERICAN STANDARD THERMAL TRANSFER YOUNG RADIATOR

SMALL AIR COOLED HEAT EXCHANGERS		
 MODEL SEARCH	different flow rates up to 25 GPM AC, or DC Motor Drive with or without Motor can mount behind Electric Motor CALL 800-329-6888	AMERICAN HEAT TRANSFER AMERICAN STANDARD THERMAL TRANSFER YOUNG RADIATOR

AC or DC Fan Drive		
 MODEL SEARCH	explosion proof option flow rates of 1 to 30 GPM 1, 2, 4 Fan Drives CALL 800-329-6888	AMERICAN HEAT TRANSFER AMERICAN STANDARD THERMAL TRANSFER YOUNG RADIATOR

HEAVY DUTY AIR COOLED HEAT EXCHANGER		
 MODEL SEARCH	different flow rates of 1 to 600 GPM pressure to 300 PSI AC, DC or Hydraulic Motor Drive NPT, SAE, or Flanged connections CALL 800-329-6888	AMERICAN HEAT TRANSFER AMERICAN STANDARD THERMAL TRANSFER YOUNG RADIATOR

HEAY DUTY INDUSTRIAL HEAT EXCHANGERS		
 MODEL SEARCH	different flow rates 20 to 1000 GPM Steel or Stainless Steel AC, DC, or Hydraulic Motor Driven Severe Duty Construction CALL 800-329-6888	AMERICAN HEAT TRANSFER AMERICAN STANDARD THERMAL TRANSFER YOUNG RADIATOR

MOBILE AIR COOLED HEAT EXCHAGERS		
	with or without Fans Single, Double, or Quad fans AC, or DC voltages for fans flow rates up to 150 GPM CALL 800-329-6888	AMERICAN HEAT TRANSFER AMERICAN STANDARD THERMAL TRANSFER YOUNG RADIATOR

TEMPERATURE SWITCH		
 MODEL SEARCH	with in-tank Thermal Wet Bulb sensor adjustable temperture settings Start and Stop Fan CALL 800-329-6888	AMERICAN HEAT TRANSFER AMERICAN STANDARD THERMAL TRANSFER YOUNG RADIATOR

COMPACT AIR COOLED HEAT EXCHANGER		
 MODEL SEARCH	MOUNT IN REAR OF ELECTRIC MOTOR uses Electric Motor Fan to Cool CALL 800-329-6888	AMERICAN HEAT TRANSFER AMERICAN STANDARD THERMAL TRANSFER YOUNG RADIATOR

COMPACT AIR COOLED HEAT EXCHANGER		
 MODEL SEARCH	For Industrial or Mobile applications AC, DC, or Hydraulic Motor driven fan flow rates of 1 GPM to 150 GPM Single or Double Fans CALL 800-329-6888	AMERICAN HEAT TRANSFER AMERICAN STANDARD THERMAL TRANSFER YOUNG RADIATOR

LARGE AIR COOLED HEAT EXCHANGERS		
 MODEL SEARCH	flow rates up to 1000 GPM EXPLOSION PROOF OPTION CALL 800-329-6888	AMERICAN HEAT TRANSFER AMERICAN STANDARD THERMAL TRANSFER YOUNG RADIATOR

COMPACT AIR COOLED HEAT EXCHANGER		
 MODEL SEARCH	1, 2, 4 FAN COOLED Heat Exchanger AC or DC drives flow rates 1 to 30 GPM CALL 800-329-6888	AMERICAN HEAT TRANSFER AMERICAN STANDARD THERMAL TRANSFER YOUNG RADIATOR

LARGE AIR COOLED HEAT EXCHANGERS		
	different flow rates of 10 to 1000 GPM THERMAL CAPACITY TO 750 hp (560 Kw) AC, DC or Hydraulic Motor Driven in Steel or Stainless Steel CALL 800-329-6888	AMERICAN HEAT TRANSFER AMERICAN STANDARD THERMAL TRANSFER YOUNG RADIATOR

Products & Services

msi multiphase systems integration

Multiphase Technology Design & Manufacturing

MSI has earned an excellent worldwide reputation through Research, Development & Modeling of Multiphase Separation Technologies, achieving world leading expertise in the design of compact gas, oil, water, and solids separation systems and technologies. We offer design, fabrication, installation, and troubleshooting of the following technologies:

GLCC – Gas-Liquid Cylindrical Cyclone compact separators
LLCC – Liquid-Liquid Cylindrical Cyclone compact separators
LLHC – Liquid-Liquid Hydrocyclone (Deoling and FWKO)
SLHC – Solid-Liquid Hydrocylone for solids removal
SD – Slug Damper

Consulting & Engineering Solutions
Multiphase Technology Design & Manufacturing
Oilfield Services
Research & Development
Technical Training

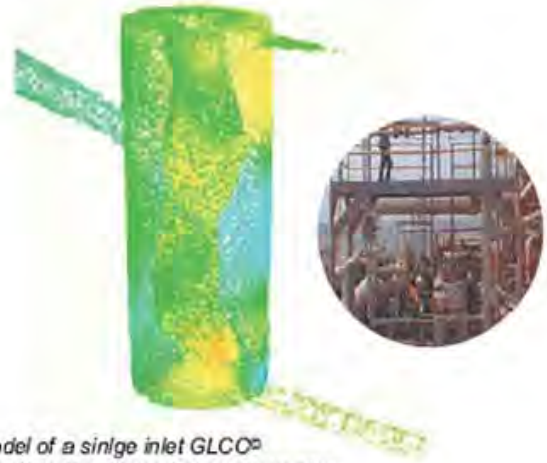

CFD model of a sinlge inlet GLCC®
(Gas-Liquid Cylindrical Cyclone) compact separator

Sitemap | Privacy Policy | Terms of Use

KAESER COMPRESSORS

More Compressed Air for Less Energy

Lower Long Term Costs

Energy costs are a significant portion of any compressed air system's total lifetime cost. In fact, the amount of energy required to run a compressor for just one year can exceed the compressor purchase price. Over a period of 10 years, energy normally totals 70% of the overall costs.

Since Kaeser's energy-saving screw compressors deliver up to 20% more air per kilowatt, the cost-efficient choice is clear.

The Revolutionary Sigma Control

Sigma Control automatically regulates and monitors the compressor. It is an industrial-based PC with a real-time operating system. Easy-to-understand, color-coded LEDs indicate operating status. The four-line, plain-text display with touch keys and menu-guided screens offer clear function choices.

The Energy-saving Sigma Profile Airend

Larger, slower-running airends are more efficient and deliver more compressed air for the same input power. Kaeser's Sigma Profile airends are optimized and designed to operate at the lowest possible speeds. Every Kaeser rotary screw compressor is equipped with a highly efficient airend and will quickly pay for itself through power cost savings.

The Proprietary Sigma Profile

Kaeser's proprietary Sigma Profile airend was introduced in 1975. It is up to 20% more efficient than conventional rotary screw designs, offering more compressed air per kilowatt.

Efficiency and reliability are designed into the Sigma Profile airend with excellent airend inlet flow characteristics and a five-to-six lobe, assymmetrical design. Kaeser also uses precision-aligned, high-quality roller bearings designed to withstand the most demanding conditions and extend service life.

Kaeser continues to refine and improve the airend design, and as a result, the optimized Sigma Profile airends offer unparalleled performance.

DRESSER-RAND.

Bringing energy and the environment into harmony.®

ESH Horizontal, Single-Throw Process Compressors

Application versatility and unmatched dependability.

The ESH horizontal single-throw reciprocating compressor is one of the simplest and most basic of all compressor designs. ESH compressors have unmatched versatility and dependability. Basic components are pre-engineered, pre-assembled and pre-tested. The final selection is verified by special computer programs that will calculate the performance, select cylinders, frames and distance pieces, compute the gas and inertia loads and torsional stresses which will be encountered in your service.

Features

- All running gear components are pressure-lubricated with filtered oil, distributed through internal rifle-drilled passages (see Figure 1 below). The complete system is protected by an oil pressure shutdown switch. Units have a pressure gauge and a crankcase window-type oil level indicator. Oil filter is automotive cartridge-type for easy replacement.
- Cylinders for any gas or pressure are available for either lubricated or non-lubricated service. Cylinder materials include cast iron, nodular iron and steel.
- Main, crankpin and crosshead pin bearings are full-floating - free to rotate on the bearing journal and within the bearing housing. Due to the unique design having pressurized oil on both sides of the floating bearings, friction is reduced and wear is distributed evenly on both sides of the bearing.
- ESH compressors can be packaged for ease of installation and reduced installation costs (see Figure 2 below).
- Piston rods are induction hardened for reduced wear and longer life in continuous heavy-duty operation. Standard material is AISI 4142 carbon steel; other materials available as required including our tungsten-carbide coating.
- Full-floating rod packing with latest technology, non-metallic packing ring materials are vented and water-cooled which contribute to long, trouble-free operation with minimum leakage.
- Pistons are provided with latest technology, non-metallic piston ring and rider band materials to ensure maximum reliability.

ESH Model Data

Stroke, in. (mm)	7 (178)	11 (279)
Max BHP (kW)	70 (52)	180 (134)
Max RPM	600	450
(A) Length, in. (mm)	125 (3175)	125 (3175)
(B) Piston Removal, in. (mm)	43 (1092)	66 (1676)

(C) Width, in. (mm)	40 (216)	40 (216)
(D) Height, in. (mm)	30 (762)	30 (762)
Weight, lbs. (kg)	2550 (1157)	6030 (2735)

Weight does not include driver or sheave.

- Length = average distance along axis running perpendicular to crankshaft from outer head to outer head with standard cylinders and API Type B distance piece.
- Piston Removal = average distance required to remove piston and rod with standard cylinders and API Type B distance piece.
- Width = average distance along axis running from drive-end of crankshaft to oil pump.
- Height = average distance from top of foundation/skid to top of frame.

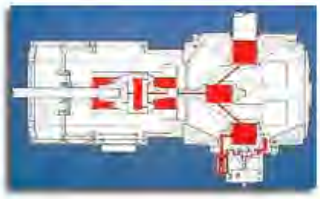

Figure 1. Pressurized Oil to All Bearing Surfaces

Figure 2. Two-Stage Tandem ESH Package with Overhead Motor Mount

Dresser-Rand
Reciprocating Operations
100 Chemung Street
Painted Post, NY 14870 USA
Tel: (Int'l +1) 607-937-2011
Fax: (Int'l +1) 607-937-2905

Haskel
INTERNATIONAL, INC.

GAS BOOSTER CATALOG

OUR PRODUCTS ARE BACKED BY OUTSTANDING TECHNICAL SUPPORT, AN EXCELLENT REPUTATION FOR RELIABILITY AND WORLDWIDE DISTRIBUTION

TABLE OF CONTENTS

Haskel International, Inc.
Burbank, California, USA

Haskel Energy Systems, Ltd.
Sunderland, England, U.K.

Haskel International, Inc. has almost 50 years of hydraulic and pneumatic engineering experience in the design and manufacture of their wide range of air driven gas boosters.

Located in Burbank, California, U.S.A., with an additional manufacturing plant in Sunderland, United Kingdom, the company is supported by a worldwide network of offices and distributors.

Haskel air driven gas boosters now offer the most complete range of models in this industry, whether measured by ultimate pressure, flow or output horsepower capability; or by variety of gases with which they are compatible.

Continuous investment in the most modern machinery and technology ensures that Haskel will remain the leader in this field.

GENERAL DESCRIPTION

Haskel Gas Boosters consist of a large area reciprocating air drive piston directly coupled by a connecting rod to a small area gas piston. The gas piston operates in a high-pressure gas barrel section. Each gas barrel end cap contains high-pressure inlet and outlet check valves. The air drive section includes a cycling spool and pilot valves that provide continuous reciprocating action when air is supplied to the air drive inlet.

Isolation of the gas compression chambers from the air drive section is provided by three sets of dynamic seals. The intervening two chambers are vented to atmosphere. This design prevents air drive contamination from entering the gas stream.

Cooling is provided by routing the cold exhausted drive air through an individual jacket surrounding the gas barrel and also through an intercooler on the interstage line (two-stage models only).

- **Air Driven – No Electrical Requirement**
- **No Airline Lubricator Required**
- **Hydrocarbon Free – Separation Between Air and Gas Sections**
- **Pressures to 39,000 psi (2690 bar)**
- **Wide Range of Models**
- **Built in Cooling (most models)**
- **Standard & Custom Systems Available**
- **Suitable for Most Gases**

Acceptable operating temperatures for Haskel Gas Booster Compressors

There are two distinct sections: the air drive section and the gas barrel section.

Air Drive Section

The ambient air condition is normally all that need be considered since this will usually determine the temperature of the air or gas drive seals and other static components. Standard air drive sections should cycle reliably within an ambient range of -4°C to +65°C (25° to 150°F). Lower temperatures will cause excessive air/gas leakage; higher temperatures reduce seal life.

Drive air directly from a compressor should ideally be warm before entering the air gas drive.

Gas Barrel Section

Low temperatures normally have little effect on the operation of standard parts and seals. The heat from the compressing gas helps to balance out an acceptable temperature. Maximum average acceptable temperature 115°C (240°F).

HASKEL AIR OR GAS DRIVEN GAS BOOSTER COMPRESSORS ARE SUITABLE FOR TRANSFER AND PRESSURIZATION OF:

1. Nitrogen (N_2)
2. Helium (He)
3. Breathing Air (N_2O_2)
4. Nitrous Oxide (N_2O)
5. Carbon Dioxide (CO_2)
6. Neon (Ne)
7. Argon (Ar)
8. Sulphur Hexafluoride (SF_6)
9. Oxygen (O_2) – maximum safe working pressure 345 bar (5000 psi)
10. Carbon Monoxide (CO) *
11. Hydrogen (H_2) *
12. Methane (CH_4) *
13. Ethylene (C_2H_4) *
14. Deuterium (D_2) *
15. Natural Gas (CH_4) – often contains a high proportion of CO_2 & N_2 *

* For these gases (10 – 15), the gas booster must be operated in a safe and well-ventilated area and vent(s) piped to controlled environment.

Liquefied type gases (propane, CO_2, nitrous oxide, halons, etc.) can be boosted as a liquid or gas in controlled applications. Consult your Haskel distributor or the factory for precise recommendations.

Haskel boosters are noted for their cleanliness and can handle pure gases such as oxygen without risk of any contamination. (Special cleaning required – advise factory.)

BASIC TYPES OF GAS BOOSTERS

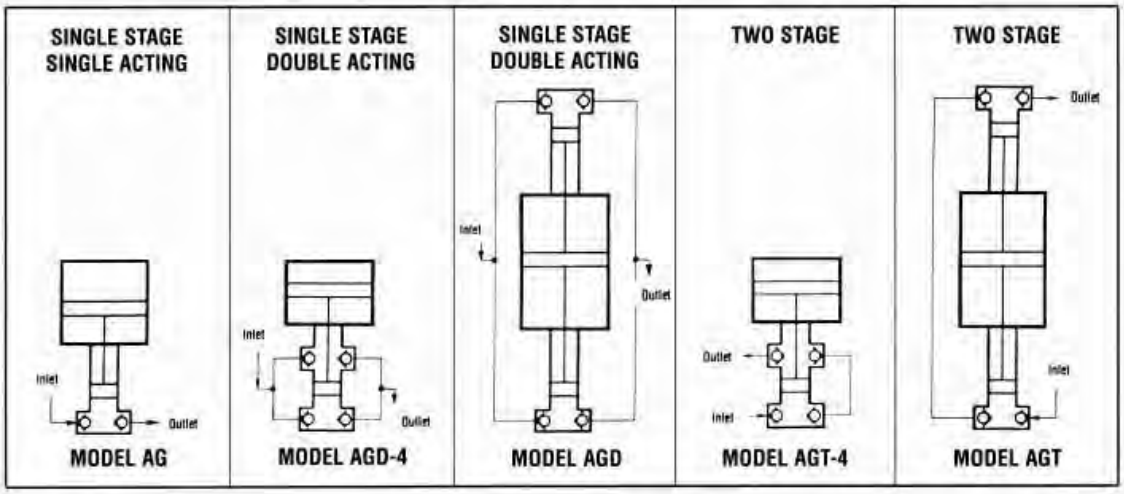

Haskel AG-152
High-ratio gas booster compressor, single acting, single stage, double air head.

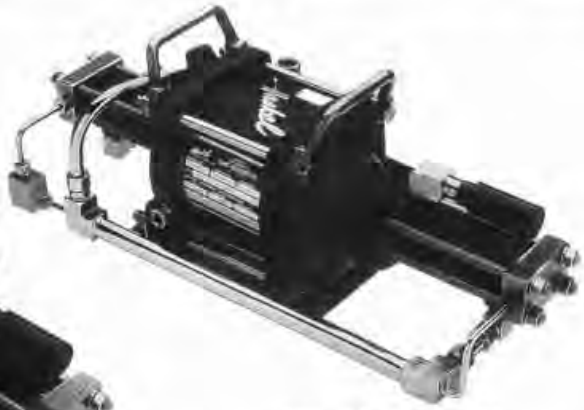

Haskel AGT-30/75
Two stage gas booster compressor, single air head.

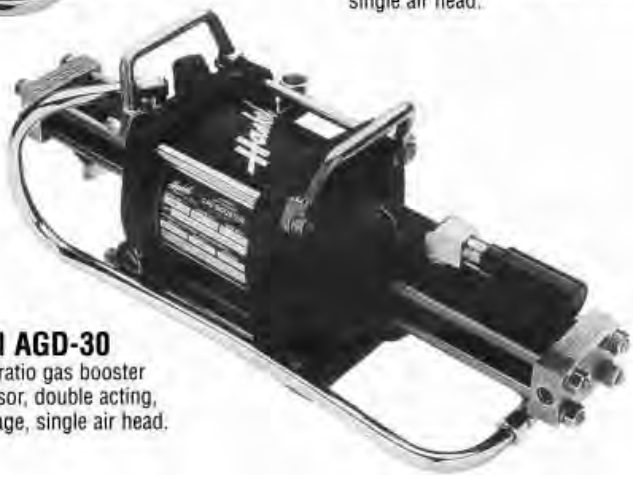

Haskel AGD-30
Medium ratio gas booster compressor, double acting, single stage, single air head.

MODEL SELECTION CHART

Model No.	Curve On Page	Maximum Rated Gas Supply (Psig)	Maximum Rated Gas Outlet (Psig)	Static Outlet (Stall) Pressure Formula	Piston Displ. Cu. In. Per Cycle	Min. Inlet Gas Pressure: Max. Outlet Gas Pressure: Max Compression Ratio:
AG-15	9	2250	2250	15 Pa	6.2	3.5 bar (50 psi) 155 bar(2250 psi) 20:1
AG-30	9	4500	4500	30 Pa	3.1	7 bar (100 psi) 310 bar(4000 psi) 25:1
AG-62	9	9000	9000	60 Pa	3.1	14 bar (200 psi) 620 bar(9000 psi) 25:1
AG-75	9	11250	11250	75 Pa	1.2	17 bar (250 psi) 775 bar(11,250 psi) 25:1
AG-152	9	20000	20000	150 Pa	1.2	17 bar (250 psi) 1380 bar(20,000 psi) 25:1
AG-233	9	22500	22500	225 Pa	1.2	17 bar (250 psi) 1380 bar(22,500 psi) 25:1
AG-303	10	39000	39000	300 Pa	0.89	34 bar (500 psi) 2690 bar(39,000 psi) 20:1
AGD-1.5	10	300	300	1.5 Pa + Ps	60	ATM 20.7 bar(300 psi) 10:1
AGD-4	10	1250	1250	4 Pa + Ps	19.3	ATM (1/4 ATM AGT-4) 86.2 bar(1250 psi) 10:1 (100:1 AGT-4)
AGD-7	10	2500	2500	7 Pa + Ps	26.4	1.7 bar (25 psi) 172 bar(2500 psi) 20:1
AGD-15	10	5000	5000	15 Pa + Ps	12.4	3.5 bar (50 psi) 345 bar(5000 psi) 20:1
AGD-30	10	9000	9000	30 Pa + Ps	6.2	7 bar (100 psi) 620 bar(9000 psi) 25:1
AGD-32	11	5000	5000	30 Pa + Ps	12.4	3.5 bar (50 psi) 310 bar(4500 psi) 20:1
AGD-62	11	9000	9000	60 Pa + Ps	6.2	14 bar (200 psi) 620 bar(9000 psi) 25:1
AGD-75	11	20000	20000	75 Pa + Ps	2.4	17 bar (250 psi) 1380 bar(20,000 psi) 25:1
AGD-152H	11	25000	25000	150 Pa + Ps	2.4	17 bar (250 psi) 1724 bar(25,000 psi) 25:1
AGT-4	11	1250	1250	4 Pa + Ps	10	1/4 ATM 86.2 bar(1250 psi) 100:1
AGT-7/15	11	(1) 6 Pa to 2500 (3) 5000	5000	15 Pa + 2 Ps	13.2	1.7 bar (25 psi) 276 bar(4000 psi) 50:1
AGT-7/30	12	(1) 2 Pa to 2500 (3) 5000	9000	30 Pa + 4 Ps	13.2	1.7 bar (25 psi) 379 bar(5500 psi) 100:1
AGT-15/30	12	(1) 15 Pa to 2500	9000	30 Pa + 2 Ps	6.2	3.5 bar (50 psi) 586 bar(8500 psi) 50:1
AGT-32/62	12	(1) 30 Pa to 2500	9000	60 Pa + 2 Ps	6.2	7 bar (100 psi) 621 bar(9,000 psi) 50:1
AGT-15/75	12	(1) 3.5 Pa to 5000	20000	75 Pa + 5 Ps	6.2	3.5 bar (50 psi) 897 bar(13,000 psi) 100:1

LEGEND: **Ps** = Gas Supply Pressure **Pa** = Drive Pressure **Po** + Gas Outlet Pressure

PERFORMANCE CURVES — AG SERIES

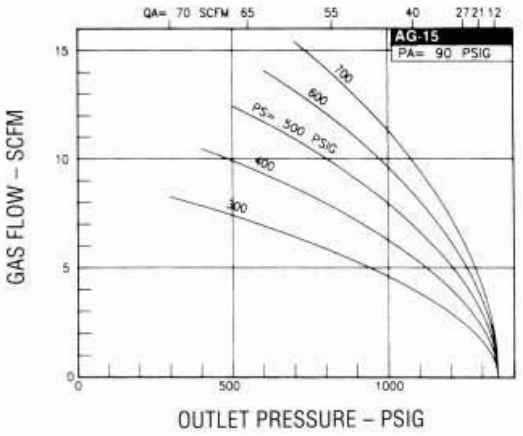

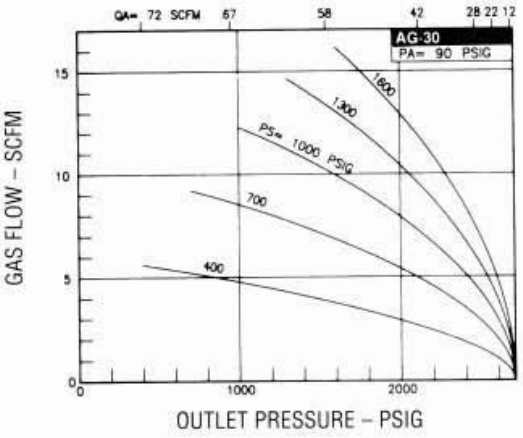

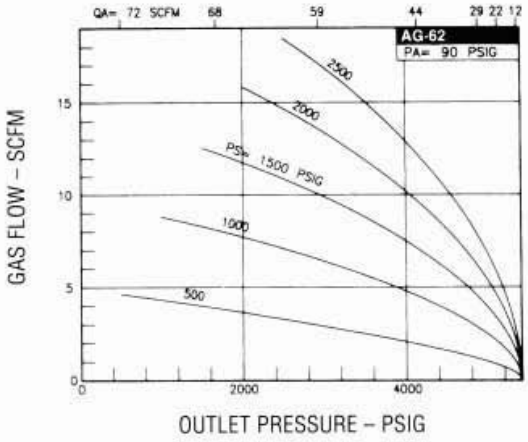

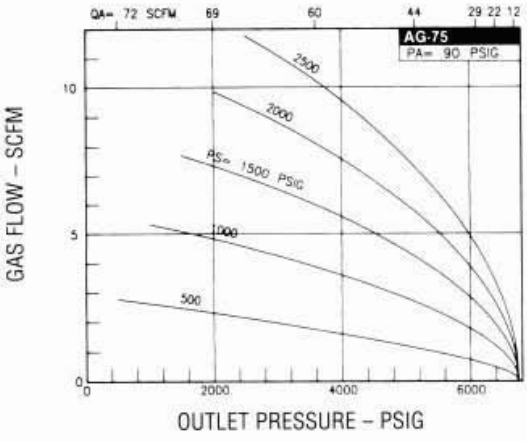

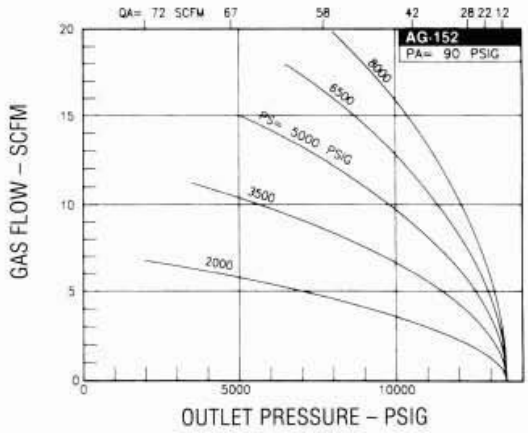

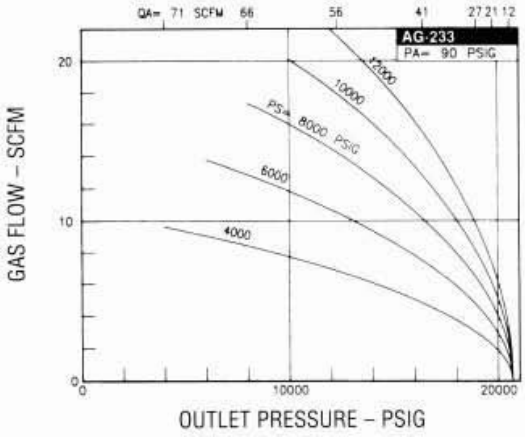

PERFORMANCE CURVES / WEIGHT and DIMENSIONAL INFORMATION

14" — AGT SERIES

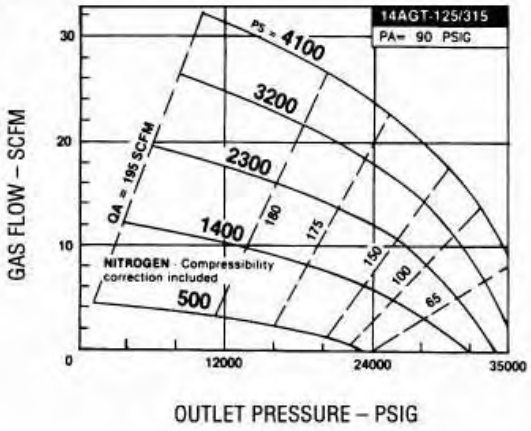

Single acting, single stage, single air head AG–15

Net weight 11 Kg
Boxed weight 13 Kg
Box dimensions 51 x 39 x 39 cm

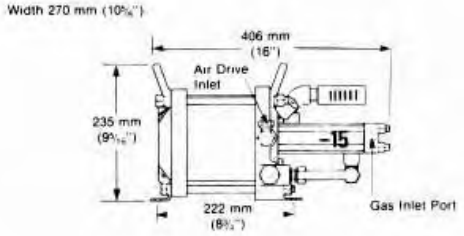

Inlet/Outlet Gas Ports: Interchangeable 3/8" SAE or 1/4" Superpressure

---

Single acting, single stage, single air head AG–30

Net weight 12 Kg
Boxed weight 13 Kg
Box dimensions 44 x 37 x 33 cm

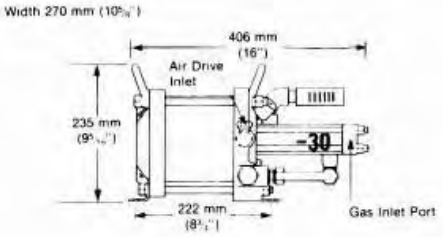

Inlet/Outlet Gas Ports: Interchangeable 3/8" SAE or 1/4" Superpressure

Single acting, single stage, double air head AG–62

Net weight 15 Kg
Boxed weight 18 Kg
Box dimensions 67 x 42 x 49 cm

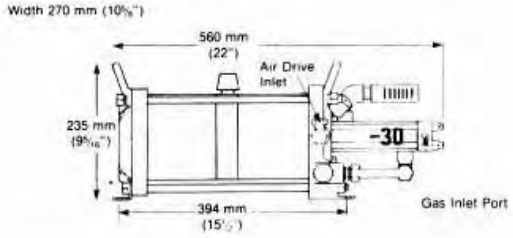

Inlet/Outlet Gas Ports: Interchangeable 3/8" SAE or 1/4" Superpressure

---

Single acting, single stage, single air head AG–75

Net weight 12 Kg
Boxed weight 14 Kg
Box dimensions 51 x 39 x 40 cm

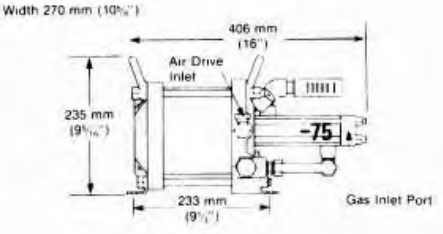

Inlet/Outlet Gas Ports: Interchangeable 3/8" SAE or 1/4" Superpressure

Single acting, single stage, double air head AG–152

Net weight 15 Kg
Boxed weight 18 Kg
Box dimensions 66 x 41 x 50 cm

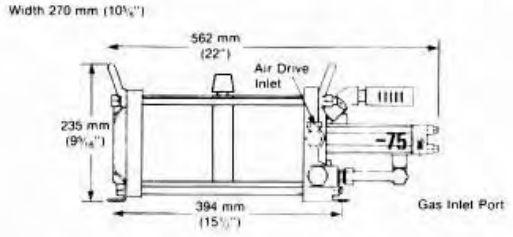

Inlet Gas Port: Interchangeable 3/8" SAE or 1/4" Superpressure
Outlet Gas Port: 1/4" Superpressure

Consult factory for information on additional Haskel products

AIR DRIVEN LIQUID PUMPS

AIR DRIVEN AIR PRESSURE AMPLIFIERS

HIGH PRESSURE VALVES, FITTINGS, TUBING & SYSTEMS COMPONENTS

SPECIAL SYSTEMS

CHEMICAL INJECTION PUMPS

HIGH PRESSURE GAS REGULATORS

Haskel International, Inc.
North America • South America
100 East Graham Place
Burbank, California 91502 • USA
Telephone: (818) 843-4000
Fax: (818) 556-2549 or (818) 841-4291

Haskel Energy Systems Ltd.
Europe • Middle East • India
North Hylton Road
Sunderland SR5 3JD • England • U.K.
Tel: 44-191-549-1212
Fax: 44-191-549-0911

Haskel (Asia) Pte. Ltd.
23 Tagore Lane #03-07
Tagore 23 Warehouse Complex
Singapore 787601
Tel: 65-455-7599 • Fax: 65-455-2341

Haskel Australasia Pty. Ltd.
P.O. Box 267
Salisbury, Qld. 4107, Australia
Tel: 61-7-3277-5118
Fax: 61-7-3277-6129

Haskel Hochdrucksysteme GmbH
D-46485 Wesel
Fritz-Haber Strasse • Germany
Tel: 49-281-96-48-000
Fax: 49-281-96-48-020

Haskel General Rheumatic
4 rue du haut de la Cruppe
F-59650 Villeneuve d'Ascq • France
Tel: 33-320-04-66-00 • Fax: 33-320-33-31-95

Haskel Benelux B.V.
Cobaltstraat 29
2718 RW Zoetermeer • Netherlands
Tel: 31-79-361-84-72 • Fax: 31-79-360-05-60

Haskel España S.R.L.
Paseo Urbaburu 31 • Edif.5 • 1° Planta
Locales 1 y 2 • Pol.27 Markulene
20115 Astigarraga • Guipuzkoa • Spain
Tel: 34-943-47-45-66 • Fax: 34-943-45-11-36

Haskel Energy Systems Limited
Unit 14, Airways Industrial Estate,
Pitmedden Road
Dyce, Aberdeen AB21 0DT • Scotland
Tel: 01224-771784 • Fax: 01224-723642

Haskel Italiana S.R.L.
via Varese 17/B
21013 Gallarate • Varese • Italy
Tel: 0039-0331-701133 • Fax: 0039-0331-701130

For further information on Haskel products, visit our website at: www.haskel.com

GB-GL
Printed in USA.

KAESER COMPRESSORS

www.kaeser.com

Portable Compressors
MOBILAIR M13-M270

With the world-renowned SIGMA PROFILE

Free air delivery: 1.2 to 26.9 m³/min

KAESER COMPRESSORS

Save energy with the KAESER SIGMA PROFILE

Made in Germany

KAESER's renowned MOBILAIR range of portable compressors is manufactured in a state-of-the-art production facility located directly next to the KAESER main plant in Coburg, Northern Bavaria. Equipped with the very latest technology, the recently modernised portable compressor plant boasts TÜV (German Technical Inspection Agency) certified sound testing facilities for free-field sound level measurement, an advanced powder coating installation and highly efficient production logistics. With minimal turn-around time, KAESER's highly qualified personnel are able to assemble portable compressors of all sizes and equipment levels to suit our customers' specific needs.

Compressed air as a versatile energy source

With 90 years experience in machine construction and engineering, KAESER KOMPRESSOREN is one of the world's leading compressor manufacturers and compressed air system providers. KAESER's comprehensive range of products and services ensures that every compressed air systems user will find a solution that meets his or her exact needs.

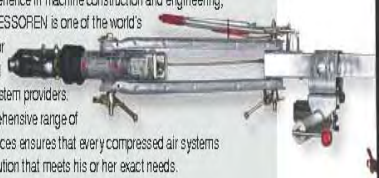

MOBILAIR M model shown

SIGMA PROFILE

Every KAESER rotary screw airend is equipped with energy-saving SIGMA PROFILE rotors. Components manufactured to the highest standards and precision aligned roller-bearings ensure long service life with maximum reliability.

User-friendly design

MOBILAIR portable compressors are simple to operate, provide excellent component accessibility and are easy to maintain. Features also include automatic monitoring and shutdown.

Patented Anti-Frost Control

Specially developed by KAESER for portable compressors, the patented Anti-Frost Control automatically regulates operating temperature in relation to ambient. This innovative system therefore prevents breakers from freezing up and significantly extends air-tool service life.

Fluid circulation and compressed air production

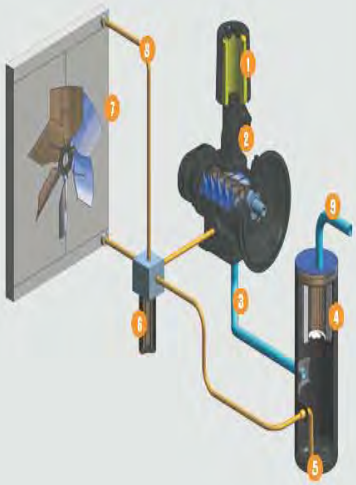

1. Intake air
2. Rotary screw airend
3. Fluid/air mixture
4. Fluid separator
5. Fluid with compression heat
6. Thermostatic valve, or Anti-Frost Control with micro-fluid filter
7. Fluid cooler
8. Cool oil
9. Compressed air

KAESER's comprehensive range of products and services

Compressed air system solutions for every application

Exceptional power and versatility

Compressed air and more...

The MOBILAIR portable compressors in this product group provide exceptional versatility. Optionally available with synchronous generators and / or compressed air treatment components, these compressors are also offered in various maximum pressure versions. This large selection of possible configurations therefore ensures that an appropriate model is available to meet the needs of virtually any application.

MOBILAIR M64G

Technical Specifications

Model	FAD m³/min	Working pressure bar	Engine	Rated engine power kW	Operational weight kg	Fuel tank capacity l	Air connection	Compressed air treatment	Generator option kVA
M36	3.9	7	Kubota V 2403	36.0	1145	80	2 x G¾, 1 x G1	Option	13 (Standard)
M45	4.2/4.15	7/10	Kubota V 2203	35.4	995	80	2 x G¾, 1 x G1	Option	8.5
M52	5.2	7	Kubota V 2203	35.4	1225	105	2 x G¾, 1 x G1	Option	8.5
M64	6.4/5.0	7/10	Kubota V 2403T	43.3	1230	105	2 x G¾, 1 x G1	Option	8.5/13
M70	7.0*/5.4*	7*/10*	Kubota V 2003-T	43.3	1230	105	2 x G¾, 1 x G1	Option	–
M80	8.1/6.8/6.1/5.5	7/10/12/14	Kubota V 3307 DI-T	54.6	1480	150	3 x G ¾, 1 x G1½	Option	8.5/13
M100	10.2/8.5/7.2/6.4	7/10/12/14	Kubota V 3800 DI-T	71.7	1495	150	3 x G ¾, 1 x G1½	Option	8.5/13
M122	11.1/10.1/9.5/8.2/7.3	7/8.6/10/12/14	Deutz TCD 2012 L04	83.0	1865	170	3 x G ¾, 1 x G1½	Option	–

*Only for export outside of the EU

KAESER COMPRESSORS

www.kaeser.com

KAESER – The world is our home

As one of the world's largest compressor manufacturers, KAESER KOMPRESSOREN is represented throughout the world by a comprehensive network of branches, subsidiary companies and authorised partners in over 60 countries.

With innovative products and services, Kaeser Kompressoren's experienced consultants and engineers help customers to enhance their competitive edge by working in close partnership to develop progressive system concepts that continuously push the boundaries of performance and compressed air efficiency. Moreover, the decades of knowledge and expertise from this industry-leading system provider are made available to each and every customer via the Kaeser group's global computer network.

These advantages, coupled with KAESER's worldwide service organisation, ensure that all products operate at the peak of their performance at all times and provide maximum availability.

KAESER KOMPRESSOREN GMBH
P.O. Box 2143 – 96410 Coburg – GERMANY – Tel +49 9561 640-0 – Fax +49 9561 640130
www.kaeser.com – e-mail: productinfo@kaeser.com

SERIES 2520 & 3520
Portable Oxygen Analyzers

ALPHA OMEGA
INSTRUMENTS

FEATURES	***BENEFITS***
√ State-of-the-Art Sensor Technology	High Precision Measurements.
√ Light Weight/Compact Design	Easy to Carry and Transport.
√ Rapid Speed of Response	Senses Changes in Gas Composition in Seconds.
√ Built-in NICAD Batteries	Provides >12 Hours of Continuous Operation with the Optional DC Sample Pump in Use.
√ Uses Standard NICAD's	Replacement Batteries Can be Purchased Worldwide.
√ Built-in Battery Charger	Can be Powered From AC Adapter.
√ Minimum Maintenance	Low Cost of Ownership.

System Description

Series 2520 Portable *Percent* Oxygen Analyzer

The Series 2520 Portable Percent Oxygen Analyzer is a light-weight, easy-to-use analyzer that provides accurate and repeatable percent oxygen measurements in a variety of gases. The rugged and compact design of the Series 2520 makes it ideal for industrial applications where spot oxygen measurements need to be made. The Series 2520 can be configured with one of several measuring ranges from 0-1% to 0-100% oxygen. The standard Series 2520 Portable Percent Oxygen Analyzer is equipped with a 3-1/2 digit liquid crystal display, in-line filter, built-in NICAD batteries, and an AC adapter that provides the ability to recharge the NICAD batteries even while powering the analyzer from the adapter.

The Series 2520 Portable Percent Oxygen Analyzer features a patented, extended life oxygen sensor with EES (Enhanced Electrolyte System) that provides exceptional measurement accuracy and stability. For applications where carbon dioxide is present in the sample gas, the EES retards passivation of the sensor anode by allowing the products of oxidation to dissolve in the electrolyte. In effect, the sensor is renewed continuously, resulting in an increase in sensor life. The output from the sensor is temperature compensated.

Series 3520 Portable *Trace* Oxygen Analyzer

The Series 3520 Portable Trace Oxygen Analyzer is a high precision instrument designed to provide accurate trace oxygen measurements in a variety of laboratory and process gases. The Series 3520 can be configured with one of several measuring ranges from 0-50 parts per million (ppm) to 0-10,000 ppm. The Series 3520 is equipped with either a 3-1/2 or 4-1/2 digit liquid crystal display (depending on the range selected), built-in NICAD batteries, and an AC adapter that provides the ability to recharge the NICAD batteries even while powering the analyzer from the adapter.

The 3520 features an advanced electrochemical oxygen sensor. The improved mechanical design of the sensor ensures longer life and virtually eliminates leakage of caustic electrolyte, a nagging problem associated with sensors that require periodic electrolyte maintenance. The output from the sensor is temperature compensated. In addition, the sensor is equipped with manual isolation valves so that during times of inactivity, the sensor can be kept inerted and ready for use. A major advantage of the Series 3520 is that it does not require users to apply a correction factor to the readings when exposed to different gas compositions. With other analyzer types, if correction factors are not applied, readings can be off by a factor of three!

Specifications	Series 2520	Series 3520
Measurement Ranges:	0-1, 0-5, 0-10, 0-25, 0-50, and 0-100%.	0-50, 0-100, 0-500, 0-1,000, 0-5,000, and 0-10,000 ppm.
Accuracy:	± 1% of full scale.	± 1% of full scale.
Linearity:	± 1% of full scale.	± 1% of full scale.
Response Time:	90% of full scale in <15 seconds.	90% of full scale in <20 seconds typical.
Sensor Type:	Electrochemical.	Electrochemical.
Temperature Compensation:	Standard.	Standard.
Operation Temperature Range:	40° to 100°F (5° to 38° C).	40° to 100°F (5° to 38° C).
Sample Gas Pressure Limits:	0.1 to 1.0 psig.	0.1 to 1.0 psig.
Sample Flow Rate:	1.0 to 2.0 SCFH (0.5 to 1.0 liters/minute).	1.0 to 2.0 SCFH (0.5 to 1.0 liters/minute).
Power Source:	Rechargeable NICAD batteries or 115 VAC/60 Hz using the AC adapter.	Rechargeable NICAD batteries or 115 VAC/60 Hz using the AC adapter.
Analog Output:	Not available.	Not available.
Warranty:	Two years electronics/1 year sensor.	Two years electronics/1 year sensor.
Enclosure:	Polycarbonate-rated NEMA 1.	Polycarbonate-rated NEMA 1.
Display:	3-1/2 digit liquid crystal display.	3-1/2 or 4-1/2 digit liquid crystal display.
Gas Connections:	Quick connect.	1/4"compression fittings.
Dimensions:	5.8" H x 6.7" W x 3.4" D.	5.8" H x 8.8" W x 3.4" D.
Weight:	<2 pounds.	<4 pounds.

Optional Equipment

DC Sample Pump
High Capacity Filter
Pressure Regulator
Flow Meter

Call Us Toll Free
800-262-5977

ALPHA OMEGA INSTRUMENTS

Alpha Omega Instruments Corp., 30 Martin Street, Cumberland, RI 02864
Telephone: 800.262.5977 or 401.333.8580, Fax: 401.333.5550
Email: aomega@aoi-corp.com, Web Site: http://www.aoi-corp.com

PRISM® ALPHA MEMBRANE

NITROGEN GENERATION
DESIGN & REFERENCE MANUAL

AIR PRODUCTS AND CHEMICALS, INC.
PRISM MEMBRANES
11444 LACKLAND ROAD
ST. LOUIS, MISSOURI 63146

PHONE: 314-995-3300 OR 800-635-8842
FAX: 314-995-3500

QOP-43-06 Rev. B

TABLE OF CONTENTS

1.0 SAFETY

The PRISM® Alpha membrane is utilized for the production of high purity nitrogen gas (0.1-5% oxygen impurity). The nitrogen product and oxygen-enriched waste streams produced by the membrane can be hazardous if proper precautions are not taken.

Gaseous nitrogen is colorless, odorless, inert, tasteless, non-corrosive, and non-flammable. Nitrogen is non-toxic but can act as an asphyxiant by displacing the necessary amount of oxygen in the air to sustain life (a minimum of 19% oxygen is required for life support). Safety procedures must be established and followed before entering any enclosed or poorly ventilated area containing nitrogen generating equipment or piping. **WARNING: The nitrogen gas generated by the membrane cannot support life.**

The waste gas stream of the membrane can be enriched with oxygen concentrations as high as 50%. While oxygen itself will not burn, it will readily support the combustion of materials, which under normal circumstances would not burn, and it will accelerate the burning of materials, which will burn, such as many building materials and clothing. All oxygen-enriched streams from the membrane must be vented outdoors, at least 12 feet (3.7 meters) above grade, into an area that will minimize contact with personnel and equipment. The oxygen-enriched gas should be vented away from any enclosures, any areas with inadequate air circulation, or areas near combustion sources.

After installing the membrane separators, the piping containing nitrogen must immediately (upon start-up) be thoroughly leak-checked to prevent the possibility of nitrogen leakage into the area surrounding the equipment. **WARNING: Nitrogen leaks into confined areas may result in a *decrease of the oxygen content below safe breathing levels.***

WARNING: Operation of the PRISM Alpha membrane separator above the rated design pressure or temperature may be hazardous. Do not connect it to compressed air sources that can exceed its maximum rated pressure without installing appropriate pressure controls and safety relief devices in the compressed air supply line.

Specific procedures must be developed for maintenance of the equipment on which the membrane separator is located. Appropriate labels must be continuously displayed in all areas where personnel might be exposed to a nitrogen atmosphere under normal or upset conditions.

Note: Disassembly of the PRISM Alpha membrane separator should not be attempted without express permission of an Air Products PRISM membrane service representative. Failure to obtain permission may void the warranty or cause damage to the separator. Specific procedures must be followed during the disassembly/reassembly operation.

Self-locking clamp nuts on the v-band clamps retaining the removable end caps on the DE8100 and DE8060 must not be re-used for safety reasons.

For additional information see

- Safety Grams at this link:
    - Safetygram - Gaseous Nitrogen
    - Safetygram - Dangers of Oxygen-Deficient Atmospheres
    - Safetygram - Oxygen and Oxygen-Enriched Mixture Hazards
- Material Safety Data Sheets (MSDS) at this link
    - Nitrogen Material Safety Data Sheet (MSDS)
    - Oxygen Material Safety Data Sheet (MSDS)

2.0 PRISM® ALPHA MEMBRANES

2.1 How PRISM Alpha Membranes Work

The PRISM Alpha membrane uses asymmetric hollow fiber membrane technology to separate and recover nitrogen from compressed air. Atmospheric air contains 78% nitrogen, 21% oxygen, and 1% other gases. The PRISM Alpha membrane uses the principle of selective permeation to produce high purity nitrogen. Each gas has a characteristic permeation rate, which is a function of its ability to dissolve and diffuse through a membrane. Oxygen is a "fast" gas and is selectively diffused through the membrane wall while nitrogen is allowed to travel along the inside of the fiber, thus creating a nitrogen rich product stream. The oxygen enriched gas, or permeate, is vented from the membrane separator at atmospheric pressure. The driving force for the separation is the difference between the partial pressure of the gas on the inside of the hollow fiber and that on the outside.

A typical membrane separator contains thousands of fibers, which are bundled and encased at both ends in epoxy resin. The ends of the bundles are cut which leaves the fiber bores open on both ends, allowing the gas to travel from one end to the other. The bundles of fibers are enclosed in a suitable casing (see Typical PRISM Alpha Membrane Separator Construction Drawing, Section 8.0). The casing protects the fibers and routes the gas properly from feed to product end.

In the PRISM Alpha membrane separator, compressed air flows down the inside of hollow fibers. "Fast" gases - oxygen, carbon dioxide, and water vapor, and a small amount of "slow" gases, pass through the membrane wall to the outside of the fibers. They are collected at atmospheric pressure as the permeate, or waste stream, and should be vented to a safe location (see Safety, Section 1.0). Most of the "slow" gases and a very small amount of the "fast" gases continue to travel through the fiber until they reach the end of the membrane separator, where the product nitrogen gas is piped to the application.

3.0 FEED AIR SUPPLY

3.1 Feed Air Quality

The feed gas for a membrane separator system is typically compressed air at a pressure of 60 psig (4.1 barg) to as high as 350 psig (24.1 barg), which may be supplied from a plant air system or a dedicated compressor. Depending on the source, the air may contain various contaminants, the most common of which are water and compressor lubricants. Atmospheric pollutants, particularly in heavily industrialized areas, may also be present.

Air entering the compressor carries with it dust, atmospheric contaminants, and water vapor. Inside the compressor, oil aerosols, vapors, and other solid particles resulting from compressor wear may be added to the compressed air stream. The compressed air should be treated to remove any condensed liquids, entrained mists, and solid particulates before entering the membrane separator. Occasionally vapor phase contaminants will also have to be removed from the feed stream. The degree of clean-up required depends upon the particular contaminants present, the effects those contaminants will have on the performance and lifetime of the membrane separator, and the final nitrogen purity requirements. Pre-treatment steps typically include cooling, filtration, and final temperature and/or pressure control.

Air Inlet Specifications

Component	Continuous Maximum ppm by Volume
Hydrogen	10
Carbon Monoxide	35
Carbon Dioxide	350
Methane	10
Acetylene	1.0
Ethane	1.0
Ethylene	1.0
Propylene	1.0
Propane	1.0
Butane and heavier hydrocarbons	0.1
Particulate Matter	2.5 mg/m^3

The above contaminants will not harm the membrane material, even in much greater concentrations. They will all permeate across the membrane to varying degrees. For cases where concentrations are higher than listed there may be residual contaminants in the nitrogen gas stream. Consult Air Products PRISM® Membranes for technical advice.

If any of the contaminants listed below exist, consult Air Products PRISM Membranes.

Sulfur Dioxide
Hydrogen Sulfide
Mercaptans
Ammonia
Chlorides or Chlorine
Oxides of Nitrogen (NO or NO_2)
Acid Fumes
Solvent Vapors
Coal Dust
Smoke / Soot
Ozone

In some cases, it may be desirable to treat the compressed air before it enters the membrane separator(s) with one of the following:

- Air dryers (refrigeration, desiccant, or membrane) to reduce water vapor / prevent condensation
- Activated carbon adsorption filters to remove oil vapors
- Molecular sieve beds to remove undesirable chemical vapors

3.2 Compressor Selection

The typical air compressor used on membrane separator systems is an air-cooled, oil flooded rotary screw machine operating at normal pressures between 60 psig (4.1 barg) and 350 psig (24.1 barg). In some cases, specifically when trace amounts of compressor oil are not permitted in the final nitrogen product gas, "oil-free" compressors (including dry screw, non-lubed reciprocating, or centrifugal compressors) may be required. It is important to determine the effect, if any, on user's product quality or on process safety when ppm (parts per million) levels of compressor lubricant are present in the final nitrogen gas. Activated carbon adsorbers may also be used to remove hydrocarbon and lubricant vapors, as well as other potential vapor phase contaminants, from the air supply or product stream.

3.3 Air Receiver Tank

An air receiver tank or water separator equipped with an automatic drain is normally installed downstream of the compressor. These devices serve as knockouts for bulk liquids that condense after compression and aftercooling, thereby reducing the load on the filtration system and minimizing the chance for liquids to reach the membrane separator. Liquid oil on the membrane will cause fouling and significantly decrease the system performance, resulting in reduced nitrogen flow or off-specification purity. In addition, the air tank provides buffer volume for the compressor controls in order to reduce the air pressure fluctuations. Since the membrane separation process is steady state and continuous, the air tank need not store a large volume of compressed air. Follow compressor manufacturer recommendations for minimum tank volume.

3.4 Compressor Installation

Air compressors must be installed according to manufacturer's recommended instructions. For indoor installations, locate the machine the proper distance from walls and corners. This installation practice will assist in preventing compressor overheating due to poor ventilation and will provide adequate maintenance clearance. Ducting compressor cooling air into and out of the building is recommended to prevent heat buildup and negative room pressures, especially in confined areas. Water-cooled aftercoolers may be necessary in installations where ventilation is restricted or where high ambient temperatures are common.

WARNING: Operation of the PRISM Alpha membrane separator above the rated design pressure may be hazardous. Do not connect it to compressed air sources that can exceed its maximum rated pressure without installing appropriate pressure controls and safety relief devices in the compressed air supply line.

Care should be taken so that the air compressor does not ingest hydrocarbon vapors or fumes or excessive dust. If necessary, special intake filters for removal of the foreign matter should be installed, or if possible, the air source should be piped from a remote location where uncontaminated air is available.

3.5 Condensate Disposal

Provisions must be made for proper disposal of the oily water condensate that will be present if a lubricated compressor is used. Dumping oily condensate into municipal sewers generally is not permitted.

4.0 DESIGN

4.1 Design Considerations

Requested separator model performance tables are attached. In sizing for the required nitrogen flow, the operating pressure drop across all upstream filters and regulators must be accounted for when determining the feed pressure to the membrane separator. The typical time-to-change filter element pressure drop of 10 psid (0.7 bard) will rarely be encountered with the recommended six-month element change schedule. If the pressure fluctuates and no pressure regulator will be used, size the membrane separator based on the lowest feed air pressure that will be encountered. If the range of the pressure fluctuation is more than 10% of the minimum pressure, it is advisable to install a pressure regulator before the filter to eliminate the fluctuation.

The "operating temperature" is the average membrane separator temperature. The design temperature loss is 10°F (6°C) across a membrane separator, even in a heated enclosure. Therefore, to achieve an average membrane separator temperature of 115°F (46°C), it should be fed with air that has been heated to 120°F (49°C), and the temperature drop across the separator must be no more than 10°F (6°C)

4.2 Nitrogen Production

The requested separator model performance tables are attached. These tables show the volume flow of nitrogen that can be produced by a given membrane separator at a variety of temperatures and pressures, with purities ranging from 95-99.5% oxygen-free gas. Consult Air Products PRISM Membranes for those applications requiring purities greater than 99.5%. The tables also indicate the volume flow of feed air required at each condition. IMPORTANT: The design pressure shown on the performance tables is the pressure at the inlet to the membrane separator (i.e., the pressure **after** any filters and/or regulators and/or feed air heaters). These tables represent the estimated OEM performance.

In order to determine what size membrane separator is required for an application, the following must be determined:

- Nitrogen Purity and Flow Requirements
- Available Feed Pressure and Flow
- Desired Nitrogen Usage Pressure
- Ambient Extremes
- Nitrogen Usage Pattern (Continuous or Intermittent)

4.3 Enriched Oxygen Production

PRISM Alpha membrane separators can be used to produce oxygen-enriched air, with oxygen levels ranging from 25-50% oxygen. The oxygen-enriched air exits the permeate port, and is at ambient pressure. Please contact Air Products PRISM Membranes to determine the appropriate size membrane separator for your application. The following information is required:

- Oxygen-Enriched Air Purity and Flow Requirements
- Available Feed Pressure and Flow
- Ambient Extremes
- Oxygen-Enriched Air Usage Pattern (Continuous or Intermittent)

4.4 Pressure Effects

Any size PRISM Alpha membrane separator will produce more nitrogen and consume more compressed air when fed with higher pressure. The recovery of the membrane separator (nitrogen/air ratio) will increase as it is fed with higher-pressure air. See the pressure sensitivity graph in Section 10.1.

4.5 Temperature Effects

Any size PRISM Alpha membrane separator will produce more nitrogen when operated at a higher temperature, but will also consume a relatively greater quantity of compressed air (reduced recovery). Please refer to the temperature sensitivity graph in Section 10.2. ***The membrane separator must be operated at a temperature that is, at a minimum, 10°F (6°C) greater than the dew point of the feed air. This is necessary to ensure that water vapor and oil vapor in the feed air will not condense on the membrane. LIQUID OIL WILL PERMANENTLY DAMAGE THE MEMBRANE.*** The membrane can tolerate liquid water, but the performance will decline when wet and will not return to specification until clean, dry air has been run through it for a sufficient amount of time to dry the fiber. Any water or oil that is introduced to the membrane separator must remain in vapor form while in contact with the membrane.

The maximum discharge temperature expected from the compressor should dictate the membrane separator operating temperature. Air Products PRISM Membranes recommends a normally closed inlet valve wired to close if there is less than a 10°F (6°C) differential between the inlet air and the membrane separator operating temperature. This valve should be placed upstream of the membrane separator in order to protect it from damage due to hot feed air. Refer to Section 5.3 for additional information on the inlet valve.

4.6 Purity Effects

The PRISM Alpha membrane is more efficient when producing product containing greater concentrations of oxygen. Typical membrane N2 recovery at 120 psig (8.3 barg) and 115°F (46°C) is:

Nitrogen Purity	Recovery % (N2 flow x 100/Air flow)	
	N1 separator	P3 separator
95%	44%	53%
99%	24%	34%

For this reason, the membrane separator should be designed using the appropriate purity for the application. Over-designing for higher nitrogen purity (less oxygen) than required may result in more and/or larger membrane separators being required, a larger compressor, and greater power consumption.

4.7 Pressure Drop

The feed-to-N2 product pressure drop across the membrane separator varies with operating pressure, operating temperature, product purity, and membrane separator length. The first three parameters all affect the flow through the membrane separator, and the greater the flow through the membrane separator, the greater the pressure drop. For example, operating a given membrane separator under given operating conditions at 95% nitrogen will cause a greater pressure drop than operating at 99% nitrogen, due to the greater quantity of throughput at 95%. Typical pressure drops are listed in the table below.

Typical Pressure Drop for 95% O2-Free Product at Maximum Separator Temperature

Model	Separator Temperature °F (°C)	Separator Inlet Pressure psig (barg)	Pressure Drop psid (bard)
PA6050-N1	180 (82)	220 (15.2)	7 (0.5)
PA4050-N1	130 (54)	220 (15.2)	4 (0.3)
PA4030-N1	130 (54)	220 (15.2)	2 (0.14)
DE8100-P1	130 (54)	220 (15.2)	10 (0.7)
DE8060-P1	130 (54)	220 (15.2)	6 (0.4)
PA4050-N1	130 (54)	220 (15.2)	4 (0.3)
PA4030-N1	130 (54)	220 (15.2)	2 (0.14)
PA3030-N1	130 (54)	220 (15.2)	2 (0.14)
PA3020-N1	130 (54)	220 (15.2)	<1 (<0.07)
PA3010-N1	130 (54)	220 (15.2)	<1 (<0.07)
PA1020-P1	130 (54)	220 (15.2)	<1 (<0.07)
PA1010-P1	130 (54)	220 (15.2)	<1 (<0.07)
PA6050-P3	180 (82)	220 (15.2)	5 (0.35)
PA4050-P3	130 (54)	220 (15.2)	3 (0.2)
PA4030-P3	130 (54)	220 (15.2)	<1 (<0.07)

4.8 Dew point

Since water is a "fast" gas, most of the water vapor that is fed to the membrane separator will exit with the oxygen enriched air, or permeate (waste gas). Refer to the graph in Section 10.3 that indicates the dew point in the nitrogen gas (dependent upon inlet conditions and nitrogen purity).

4.9 Product Purity Greater Than 99.5%

Consult Air Products PRISM Membranes for those applications requiring product purity greater than 99.5%.

5.0 MEMBRANE SEPARATOR SYSTEM CONTROLS AND INSTRUMENTATION

(See Typical PRISM Alpha® Membrane Separator System Flow Diagram - Section 9.0)

5.1 Filtration

Air entering the compressor carries with it dust, hydrocarbon vapors, and water vapor. Inside the compressor, oil aerosols, vapors, and other solid particles resulting from compressor wear may be added to the compressed air stream. As the air exits the compressor, it is cooled in the aftercooler and undergoes further cooling in the piping that causes oil and water vapors to condense. These liquid contaminants must be removed prior to entering the membrane separator system in order to ensure stable performance and long service life.

Coalescing filters must be installed upstream of the membrane separator in order to remove both bulk and aerosol liquid water and liquid compressor oil:

Filtration must remove solids and liquids 0.01 micron and larger.
Filtration must remove 99.999% of oil aerosols; remaining oil content 0.001 ppm w/w

Filter Construction: Must be fitted with an automatic drain and differential pressure (time-to-change) indicator.

Typically, 2-3 coalescing filters in series are required to remove the contaminants to the required levels. It is usually a staged removal process in which each filter is specifically designed to either precede or follow another specific filter in order to provide the required contaminant removal.

With proper filtration, the only remaining contaminants in the compressed feed air will be in the vapor phase, with water and oil possibly at the saturation point.

Coalescing filters can handle limited liquid (oil plus water) and particulate loads. It may be necessary to install a moisture separator to protect the coalescing filters from flooding and to ensure a coalescing element life of greater than six months. The moisture separator must meet the construction specifications for the coalescing filters, and the efficiency rating must be selected to insure removal to a level that is less than the liquid loading limit of the coalescing filter that follows. Generally, a moisture separator will not be required with a well-maintained compressor that includes some mechanism (e.g., routinely drained receiver, water separator or filter) to remove liquid water. However, compressed air quality should always be checked prior to installing a PRISM Alpha membrane separator. If, after blowing down the lines, the compressed air supply is visibly contaminated with liquid water, oil, or particulates, a moisture separator must be installed. A moisture separator must also be installed if experience indicates the coalescing filter life to be less than six months.

Automatic condensate drains are required for removal of the condensate generated by the filtration train. Typically, an automatic drain is installed on each filter housing. Float-type drains are commonly used. Timed drains are sometimes used, but the time intervals must be set carefully. Opening the drain too frequently and for too long an interval can reduce the operating pressure and affect membrane separator performance. High liquid level switches may be installed to detect a drain failure, in which case the system should be shut down immediately.

To reduce hydrocarbon vapor content, an activated carbon adsorber may be installed after the liquid removal stages. Food and drug applications or special electronic uses may require oil vapor removal.

All filters must be sized for the maximum possible inlet flow and rated for the maximum pressure and temperature that could be encountered. Careful consideration must be given to all operating conditions (e.g., startup, shutdown, etc) in addition to normal operating conditions.

5.2 Pressure Regulation

A pressure regulator should be installed before the filtration if the compressed air supply fluctuates. A fluctuating air supply will cause variations in the product flow rate and purity. Ideally, the air supply pressure should be controlled to ± 1 psi (0.07 bar).

5.3 Inlet Solenoid Valve

A solenoid valve placed at the membrane separator inlet can act as a safety device if its position is normally closed. The valve should be wired to open **only** if the feed air is at least 10°F (6°C) cooler than the membrane separator operating temperature. This automatic shut-off will prevent damage and loss of performance due to condensation of water and oil vapor on the membrane.

5.4 Membrane Separator

The membrane separator will produce nitrogen whether oriented vertically or horizontally. However, it is important to recognize that the orientation should be made to prevent the collection of condensate in the feed and permeate ports. Liquid water in the membrane separator will decrease its performance. It will not permanently damage the membrane separator, however, unless oil is also present (see Section 4.5). Liquid water accumulation in the carbon steel end caps of the Model DE8100 and DE8060 membrane separators may eventually cause particulate formation and severely decrease the performance and life.

5.5 Feed Air Piping: The orientation of the feed inlet nozzle is important for the model DE8060 and DE8100 membrane separators. On these models, the inlet nozzle should always point downward in order to prevent collection of any liquids or particulates on the membrane.

5.6 Vent Piping: The performance shown in the performance tables assumes that the permeate gas exits the permeate port at essentially atmospheric pressure. Therefore, any vent (permeate) piping should be sized appropriately to prevent backpressure at the permeate port. The vent lines must be piped outdoors at least 12 ft (3.7 m) above grade to prevent flammability hazards to nearby personnel and/or machinery. If it is not possible to pipe the permeate this way, insure adequate ventilation is provided to dilute the oxygen-enriched gas to safe levels (see Safety, Section 1.0). Vent piping should be shielded to prevent accumulation of rain or foreign matter. Piping should be configured such that there is no way for condensate to run backwards into the membrane separator if condensate forms outside the boundary of the nitrogen system. The opportunity for condensate to form will be minimized if the membrane separators and vent (permeate) piping are kept warm during shutdown.

Anaerobic TFE-type pipe thread sealants (SWAK is one common brand name) should not be used for installation of fittings into the permeate port of the 4-inch and smaller membrane separators which have ABS shells. These sealants are not compatible with ABS and will rapidly weaken the mechanical strength of the plastic, generally resulting in cracking. If fittings are to be installed in the permeate port, it is recommended that the threads be sealed using standard PTFE tape or seal nuts. Typically, the pressure at the permeate port will be near atmospheric, so the potential for leakage is minimal.

5.7 Nitrogen Gas Piping: The nitrogen gas outlet nozzle may be oriented in any direction since the gas is very dry.

Appropriate safety labels should be continuously displayed in all areas where personnel might be exposed to a nitrogen atmosphere under normal or upset conditions.

5.8 Feed Air Heater

A feed air heater is usually installed after the filters and upstream of the membrane separator. This enables the membrane separator to be operated at a controlled temperature that is necessary for steady performance. It also enables the user to operate at the temperature necessary to obtain the desired performance. Heating is typically accomplished using an electric resistance heater immersed in the air stream. Other heating methods include steam, hot water, or other re-circulated fluids that might be available. The heater should be sized based on the ambient temperature extremes. A feed air heater is critical when the membrane separator is fed with compressed air that is saturated with oil and/or water vapor as would typically be the case when fed directly from a feed air compressor. ***The membrane separator must operate at a higher temperature, at least 10°F (6°C), than the compressed feed air in order to prevent liquid oil and water from condensing on the membrane.*** If the membrane separator is operating in a controlled, indoor environment with compressed air that has been treated with a compressed air dryer to a dew point below the operating temperature of the membrane separator, it can be safely operated without a heater. However, a greater volume of nitrogen will be produced using a feed air heater (see attached Performance Tables).

Proper safety interlocks should be included which prevent runaway overheating of the heater. Runaway heaters may result in membrane separator damage, personnel hazards, or potential fire. The control circuits should be separate and independent from the protective interlock circuits to provide positive protection in case of heater upset.

5.9 Oxygen Analyzer

An oxygen analyzer will display the level of oxygen in the nitrogen product gas produced by the membrane separator. The analyzer should be able to send signals to the delivery and vent solenoid valves in order to prevent off-specification nitrogen from being delivered to the storage tank or the application.

Dual analyzers or a single fail-safe analyzer should be utilized in safety-sensitive applications. A calibration bypass valve should be included when dual analyzers are used in order to allow calibration of one analyzer "off-line" so that neither production of nor assurance of nitrogen purity is interrupted.

5.10 Flow Meter

A flow meter can be installed downstream of the membrane separator in order to measure the volume of nitrogen generated. There are a wide variety of flow meters that may be used. The need for pressure and temperature compensation depends on the type flow meter used, the location of the flow meter, and the user requirements. If the flow meter is not temperature and pressure compensated, the flow must be corrected if the nitrogen is not at the design pressure and temperature of the meter.

5.11 Needle Valve

A needle valve may be installed downstream of the membrane separator in order to provide a convenient manual flow/purity adjustment.

5.12 Flow Limiting Devices

A backpressure regulator may be used to limit the flow through the membrane separator so the system cannot be overdrawn. Frequently the backpressure regulator is used for a coarse flow adjustment, and the needle valve is used for fine-tuning to the desired purity. This type of device works best where variations in downstream conditions are minimal.

A constant differential pressure flow valve is another device which can be used to limit the flow through a membrane separator, thereby keeping the oxygen level from exceeding specification. This device keeps a constant flow through the system regardless of downstream pressure fluctuations (e.g., changing levels of a nitrogen storage tank).

5.13 Delivery Solenoid Valve

A solenoid valve may be installed downstream of the back pressure regulator, and can be wired to "deliver" the nitrogen if it has the correct oxygen content, and to "vent" the gas if the oxygen concentration is too high. This valve assures the user that if, for some reason, the membrane separator produces off-specification nitrogen, the nitrogen will be diverted and not delivered to the application.

5.14 Check Valve

A check valve should be installed if a nitrogen storage tank is used to store nitrogen gas produced by the PRISM Alpha membrane separator. The check valve will prevent back-flow and loss of the stored gas through the membrane separator when it is not in operation. A check valve should also be installed if there is potential for any other contaminating gases or vapors that may be present downstream to flow back into the membrane separator.

5.15 Enclosure Heater

If the membrane separator is in an enclosure, an enclosure heater is recommended to keep it warm. An enclosure heater will allow for a faster start-up (the membrane separator will reach its maximum flow for a given pressure more quickly) by reducing the warm-up time required.

The use of an enclosure heater can also minimize or eliminate the need to insulate the membrane separator in order to minimize temperature loss and thereby attain the expected performance.

5.16 Nitrogen Storage Tank

A nitrogen product receiver tank may be desirable in order to provide storage of nitrogen gas. The tank should be sized appropriately for peak usage periods that exceed the membrane separator capacity or as backup during brief equipment downtimes. Use the following formula to size the tank:

Define:

Storage Pressure = P_2 (Generally storage pressure equals N2 discharge pressure)

Usage Pressure = P_1

Desired Storage Volume in SCF (standard cubic feet)

Calculate tank size required :

$$\frac{Volume(SCF)\,x\,14.7}{(P2-P1)}$$

Note: To convert tank size from cubic feet to gallons, multiply the above result by 7.5.

5.17 Piping - General

All pipe and pipe threads should be clean and free of rust, welding slag, particulates, grease, water, or cutting oils before connection to the membrane separator system. Dirt, grease, and scale that enter the membrane separator may cause premature fouling or failure of the filtration system, resulting in temporary or permanent loss of nitrogen flow or off-specification purity.

As noted in section 5.6, anaerobic TFE-type pipe thread sealants should not be used on the permeate ports of the 4" and smaller membrane separators as they are incompatible with the ABS shell material.

A typical PRISM Alpha membrane separator system flow diagram is shown in Section 9.0.

6.0 PRE-INSTALLATION, START-UP AND OPERATION

6.1 Pre-Installation

PRISM Alpha® membrane separators can be used with oil lubricated, water lubricated, and non-lubricated compressors.

Before installing the membrane separator, verify the following:

a) The maximum pressure that could be encountered is less than the pressure rating of all the system components, including the membrane separator.
b) The maximum temperature that could be encountered is less than the temperature rating of all the system components, including the membrane separator.
c) The line sizes are adequate for the expected flows and allowable pressure drop.
d) The inlet air meets the specifications as described in Section 3.1.

Open the compressed air line at the connection point and allow any accumulated water, oil, or particulates to blow out. Use extreme caution to prevent accidents or injuries during this operation.

If, after blowing out the line, the compressed air is visibly contaminated with water, oil, or particulates, a moisture separator (sized for the supply air flow and pressure) must be installed before the coalescing filters to protect the membrane and prolong the filter life.

A shut off valve (ball or gate valve) of the same size as the supply line should be installed before the filter and membrane separator so they can be isolated.

Connect the nitrogen rich gas to a storage tank or directly to the application. Route the filter drain line to a suitable location.

6.2 Start-up and Operation

Open the air supply to the membrane separator and check for any leaks. ***Nitrogen leaks in enclosed or confined areas can be fatal.*** Some automatic drains may leak air until the pressure builds up to about 10 psig (0.7 barg). It will then seal, except when discharging accumulated water and oil.

The filter differential pressure indicators and drains should be inspected on a regular frequent schedule. If the filter differential pressure indicator shows high differential pressure on either the moisture separator (if applicable) or the coalescing filters, all of the filter elements must be changed. It is recommended that replacement filter elements be kept in inventory as spares. If the coalescing filter elements' life is consistently less than six months and the sizing confirmed to be correct, a moisture separator should be installed. If the filters' life remains less than six months with a moisture separator installed, compressor maintenance or excessive line corrosion and/or contamination is indicated. If any decrease is observed in the drain rate of the filter, it should be depressurized and the bowl removed. If the liquid level in the bowl is above the automatic drain float, the drain is not operating properly and should be replaced.

Filter elements should be replaced on a regular schedule, preferably every six months, and at least once per year. When replacing the filter element, wash the filter bowl and automatic drain with warm soapy water to remove any accumulated oil. Fill the bowl during washing to verify the automatic drain is operating.

For extended shut down of the membrane separator, turn off the air supply and allow the pressure to decrease. Shut off the power to the system (de-energizing the heaters, solenoids, analyzers, etc.)

6.3 Intermittent or Cyclic Operation

When a PRISM Alpha membrane separator is de-pressurized, air from the atmosphere may enter through the permeate vent piping. On restarting, the air in the membrane separator will result in a short period of higher-than-design oxygen in the product gas stream. There may also be a short delay before the membrane separator "warms-up" to its design temperature. This delay can be minimized through the use of insulation and heated enclosures.

7.0 MAINTENANCE

The membrane separator system is a relatively simple, passive device with few moving parts that require maintenance. However, it is important to remember that the system operates under pressure, and proper precautions (including system depressurization and positive isolation from external pressure sources) must be taken any time piping connections or filter housings must be disconnected or any maintenance performed. Failure to do so could result in injury to operating and maintenance personnel.

The recommended routine maintenance is as follows:

a) Replacement of the filter elements every six months if the air supply is not clean, with a minimum frequency of annual replacement (regardless of air quality).
b) Replacement of the oxygen analyzer sensor, if an analyzer is used and the sensor is the type that requires regular replacement.

There are no repairable components within the PRISM® Alpha membrane separator, and any attempt to disassemble it could lead to damage and void the warranty.

To ensure the performance of the PRISM Alpha membrane separator and to obtain maximum compressor life, **all compressor maintenance schedules recommended by the compressor manufacturer should be followed.**

7.1 Filter Elements

If the filter differential pressure indicator gives a "time-to change" indication on any filter, all of the filter elements must be changed. Continuing to operate for an extended period after any of the differential indicators have indicated "time-to-change" could result in low air pressure, and consequently high oxygen content, as well as permanent loss of performance due to reduced removal efficiency of the filters. Continued operation in this mode will eventually cause failure of the filter elements and more rapid and severe contamination of the membrane separator.

Visual inspection of the filter elements should be performed periodically to verify the elements' integrity. If there is no change in the differential pressure indicators after a long period of operation, the elements may be damaged, and the air may be bypassing the elements.

7.2 Filter Automatic Drains

If a high water level is observed in a filter, the automatic drain is not functioning correctly and the membrane separator system should be shut down. Extended operation with malfunctioning automatic drains could result in liquid water and oil entering the membrane separator. These contaminants will lead to high oxygen content in the nitrogen stream as well as damage to the membrane separator, so inspections should be frequent. See Section 5.1 concerning the use of high liquid level switches.

7.3 High Oxygen Content in the Nitrogen Gas

Before attempting to troubleshoot the PRISM Alpha membrane separator, verify that the nitrogen usage is at or below the design level. **High flow will result in high oxygen content.**

Another possible cause of off-specification nitrogen is low feed air pressure, due either to low pressure at the filters or a high-pressure drop across the filters. The latter will be indicated on the differential pressure indicator.

High oxygen content may also be caused by failure of the automatic drains as discussed in section 7.2.

7.4 Oxygen Analyzer

There are several types of oxygen analyzers that may be selected for use with the PRISM Alpha membrane separator. Some analyzers use a fuel cell that will expire and must be replaced. A ***regular replacement schedule is recommended*** for the fuel cell if this is the case. An expired fuel cell cannot be calibrated, may fail instantaneously (will not slowly decline), and many fuel cells in the failure mode indicate the product purity is better (less oxygen) than the actual purity. For this reason, regular calibration and replacement schedules are critical. Safety sensitive applications should use dual analyzers (see Section 5.9).

Contact Air Products PRISM Membranes (314-995-3300 or 1-800-635-8842) for additional technical assistance with membrane applications.

8.0 TYPICAL PRISM® ALPHA MEMBRANE SEPARATOR CONSTRUCTION DRAWING

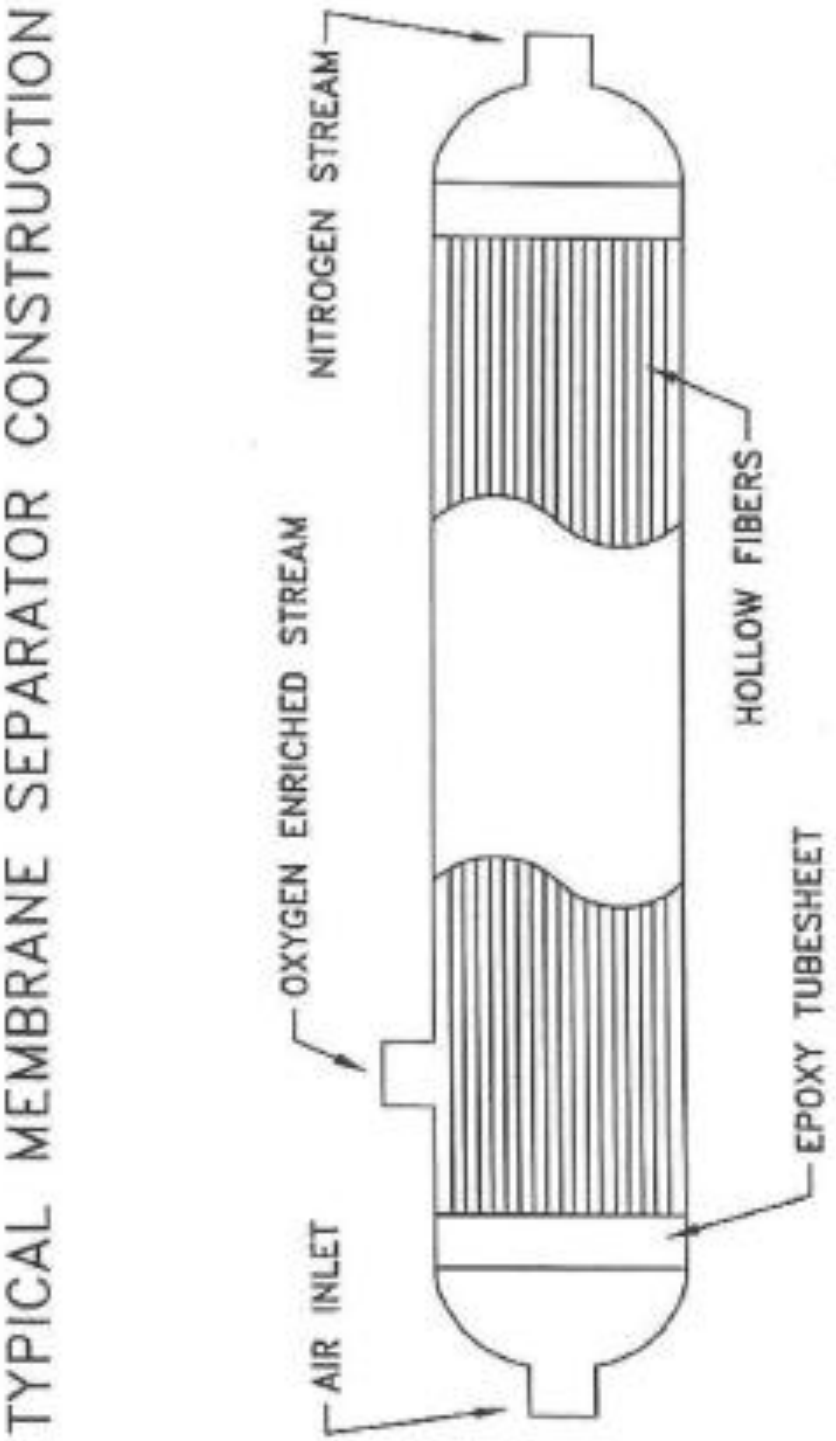

9.0 TYPICAL PRISM® ALPHA MEMBRANE SEPARATOR SYSTEM FLOW DIAGRAM

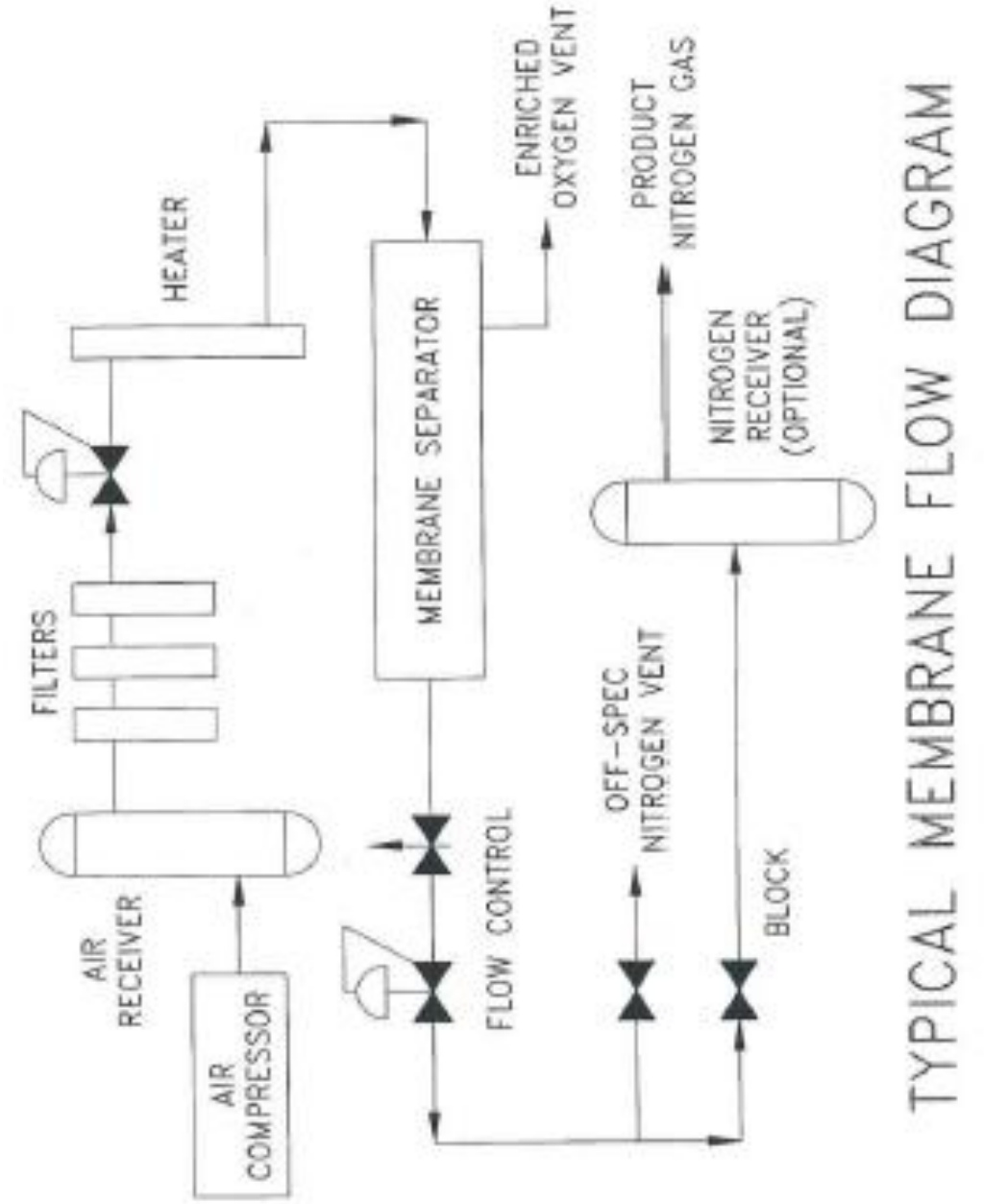

10.0 OPERATING VARIABLES

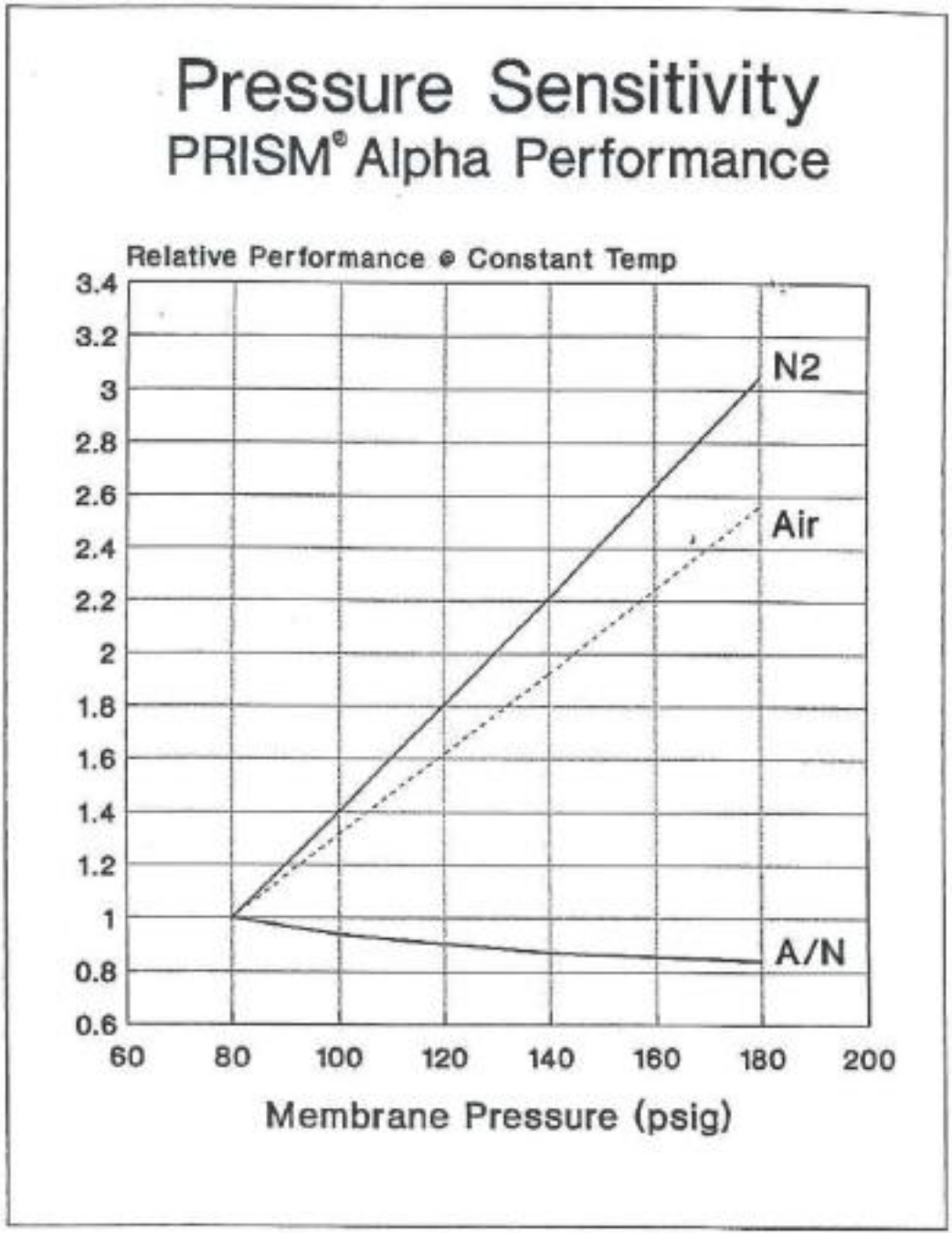

Temperature Sensitivity
PRISM® Alpha Performance

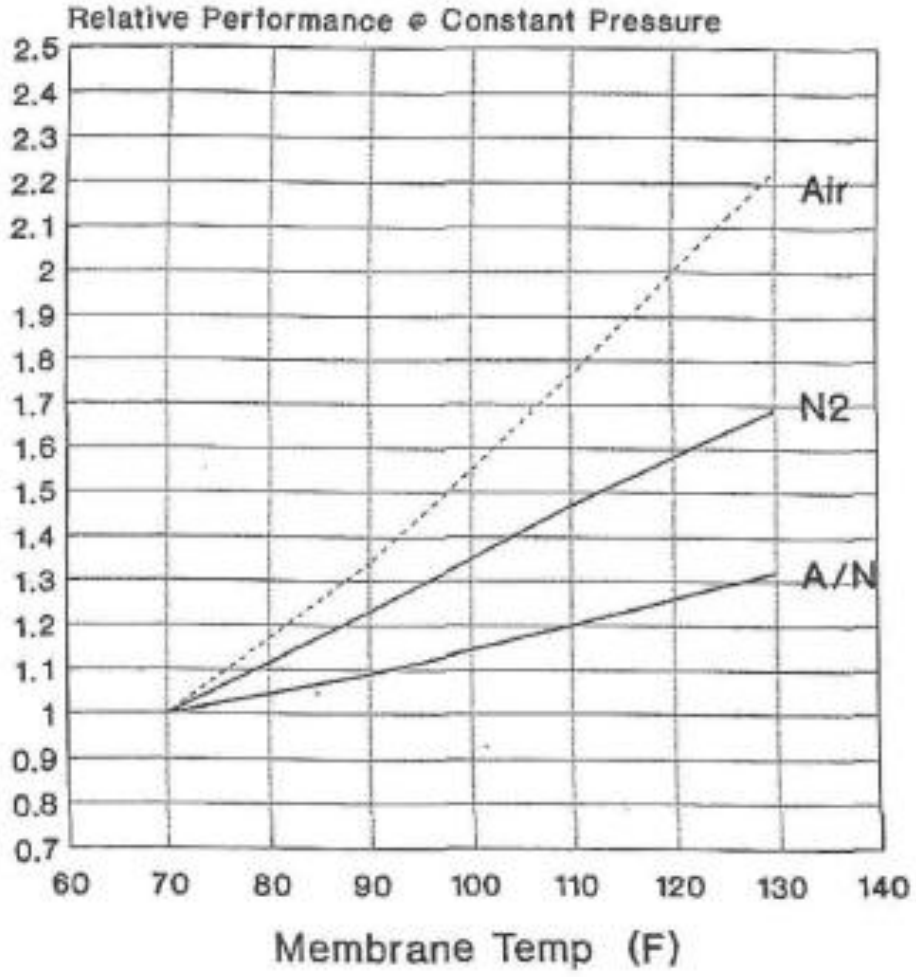

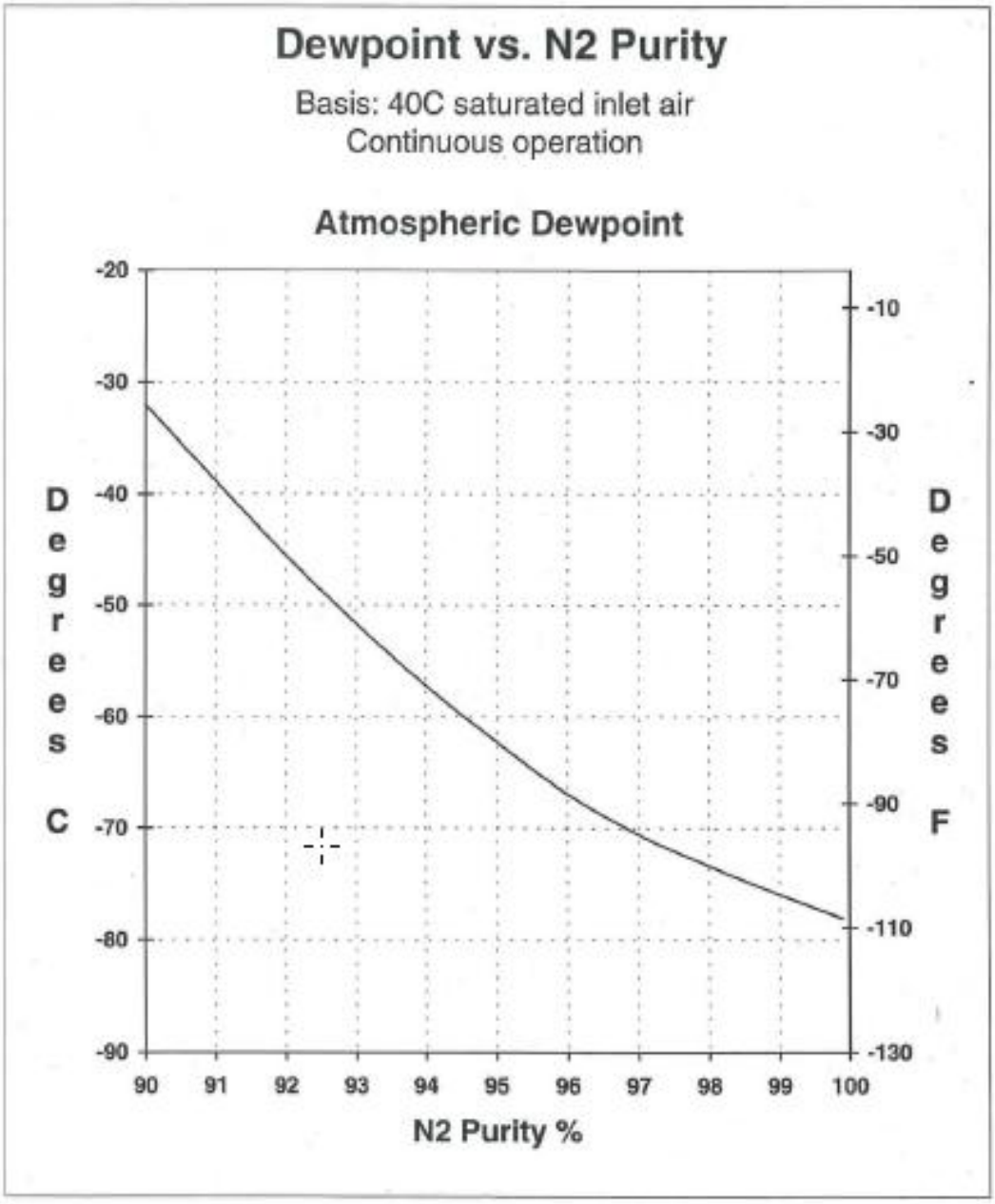
Dewpoint vs. N2 Purity
Basis: 40C saturated inlet air
Continuous operation
Atmospheric Dewpoint
Degrees C
-20
-30
-40
-50
-60
-70
-80
-90
Degrees F
-10
-30
-50
-70
-90
-110
-130
90
91
92
93
94
95
96
97
98
99
100
N2 Purity %

11.1 1 to 4 Inch Diameter PRISM Membrane Installation Guide

AIR PRODUCTS

1 to 4 Inch Diameter PRISM® Membrane Installation Guide

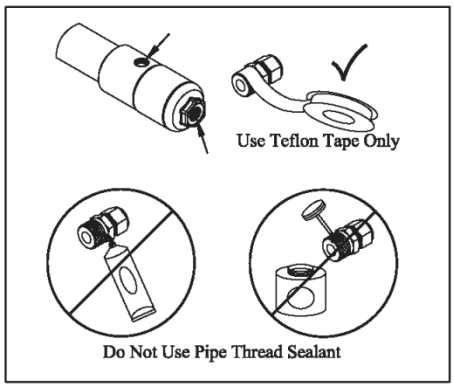

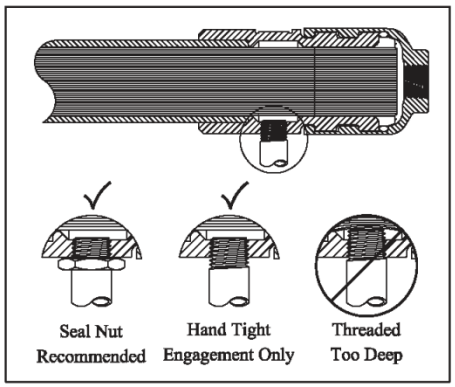

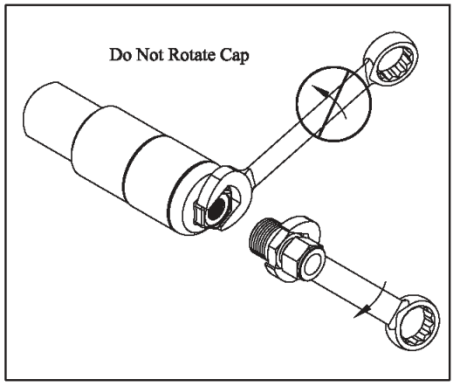

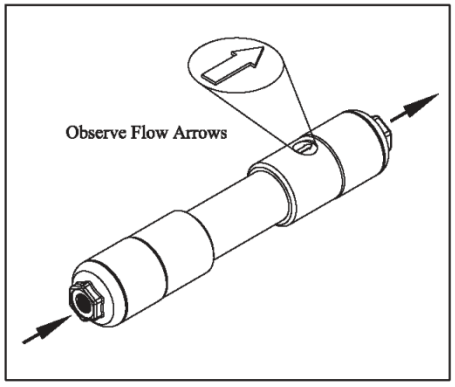

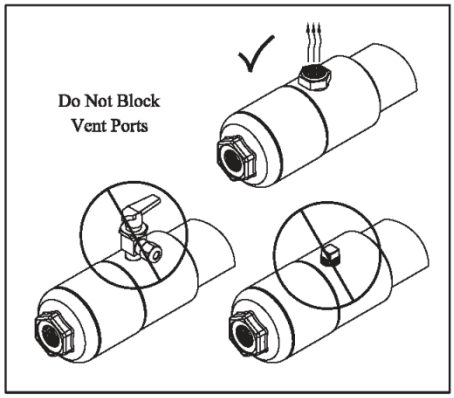

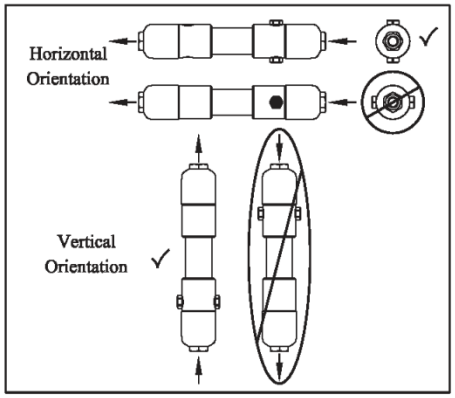

QOP-43-07 (PRISM Membrane Installation Guide)
Rev C

Page 1 of 2

11.2 PA6 PRISM Membrane Installation Guide

PA6 PRISM® Membrane Installation Guide

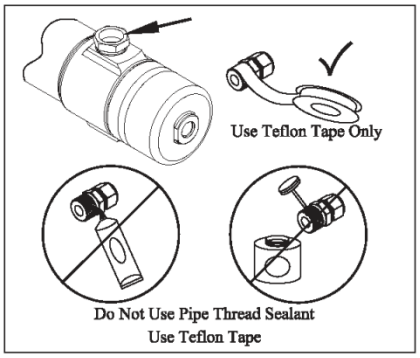

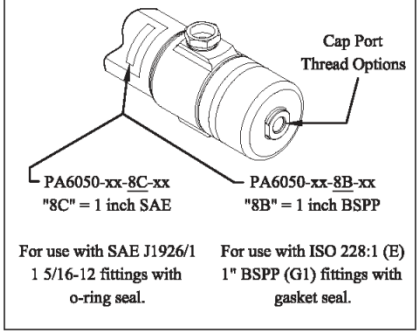

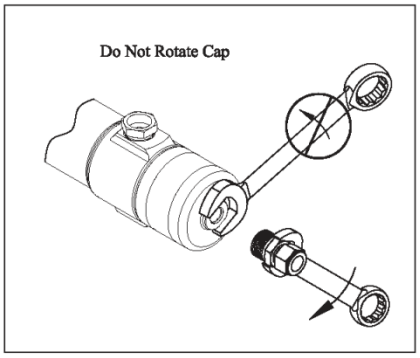

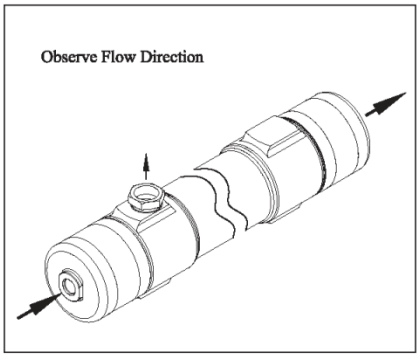

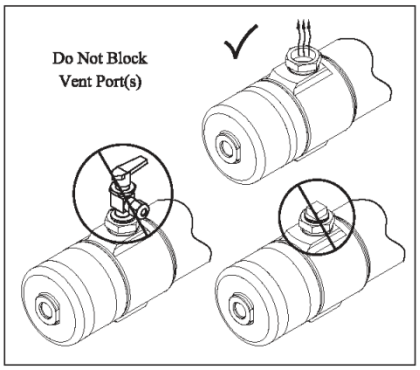

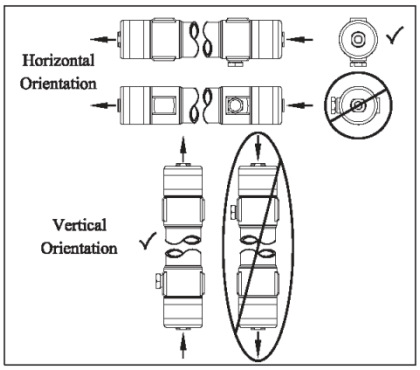

For More Information

To learn more about our global gas generation capabilities or to tell us more about your needs, contact us at:

Air Products and Chemicals, Inc.
PRISM Membranes
11444 Lackland Road
St. Louis, MO 63146-3544
Tel 800-635-8842
Fax 314-995-3500

tell me more
www.airproducts.com/membranes

Page 2 of 2

Table of Contents

Xanvis L Viscosity Relationships Vs Temperature For Use In FLASH ASJ™ Drilling Systems

Study Conducted For

Impact Technologies LLC

In Support Of

DE-EE0002783

December 1, 2011

Work Performed by

Betty Felber, Ph D.

Consultant

Table of Contents

List of Figures

List of Tables

Introduction

The purpose of this work is to report existing and determine new viscosities of Xanvis L for use in the **Impact Technologies, LLC** FLASH ASJ™ drilling system. Also to derive viscosity equations for fresh water and brines for use when Xanvis L laboratory viscosities have not been measured.

Literature reviews of technical papers and laboratory experiments were used. The object of this report is to put into one place the Xanvis L viscosity information.

Executive Summary

The polymer is to be used as a carrier in the underbalanced drilling fluid required to drill a 2", 5000 ft well. To fill this wellbore it requires a minimum volume of 109 ft^3 (815.38 gallons). This volume is that required to have gases present in the entire drilling column. The Xanvis L is an effective carrier as long as the downhole temperatures are less than 180°F.

Other polysaccharide polymers can be used at higher temperatures. Geovis XT is included for consideration at these higher temperatures.

It should be noted that density of biopolymer solutions does not apply since the solutions are thixotropic.

Synthetic ASTM Seawater Analysis

Because ASTM Seawater is used in many viscosity measurements, it is helpful to know exactly what the formulation is. ASTM Seawater Composition is designated as ASTM.D1141. It is assumed that this is the "seawater" used in all applications when Seawater is referred to.

Formulation for artificial seawater is listed in the following table or one could simply purchase the ASTM Seawater formulation to be dissolved in 1 liter of water. Generally the pH is brought up to 8.0. This seawater has a TDS of about 35,000 ppm.

Table 1: ASTM Seawater Composition

Salt	Grams/liter
NaCl	24.6
KCl	0.67
$CaCl_2 * 2\ H_2O$	1.36
$MgSO_4 * 7\ H_2O$	6.29
$MgCl_2 * 6\ H_2O$	4.66
$NaHCO_3$	0.18

The viscosity data gathered from SPE papers, technical bulletins and laboratory measurements taken for **Impact Technologies, LLC** follow.

Viscosity Relationships

Xanthan solution viscosities can be measured over a wide range of shear rates. One of the important industry problems is determining from laboratory measurements which fluid will have the most desirable properties under field conditions. Higher viscosities translate into lower

particle settling velocities. Xanthan is an excellent polymer to use under these conditions. Data from **Impact Technologies** Fluids and results from reviewed published data are included in this section. The reviewed solutions are listed in the following Table. Data are arranged in increasing Wt % polymer concentration. The 0.875 Wt % Xanvis data is listed in the **Impact Technologies Fluids Data** section.

Table 2: Xanthan Viscosity Source Materials

Polymer, #/bbl	Polymer, Wt %	Temp., °F	Brine	Source
0.50	0.14	74	Seawater	SPE 64982
0.75	0.21	120	2 % KCl	Drilling Fluids Rheology
0.84	0.24	Room	Fresh	SPE 13907
1.00	0.29	80	2 % KCl	Drilling Fluids Rheology
1.00	0.29	120	2 % KCl	Drilling Fluids Rheology
1.00	0.29	74	Seawater	SPE 64982
1.00	0.29	120	2 % KCl	Drilling Fluids Rheology
1.00	0.29	75&78	Seawater	Drilling Fluids Rheology
1.25	0.36	80	2 % KCl	Drilling Fluids Rheology
1.25	0.36	75&78	Seawater	Drilling Fluids Rheology
1.50	0.43	80	2 % KCl	Drilling Fluids Rheology
1.50	0.43	120	3 % KCl	SPE 62790
1.50	0.43	250	3 % KCl + 0.25 #/bbl Na_2SO_3	SPE 62790
1.50	0.43	75	3 %KCl	SPE 62790
1.50	0.43	75	Seawater	SPE 64982
1.50	0.43	200	Seawater +0.25 #/bbl Na_2SO_3	SPE 64982
1.50	0.43	250	Seawater +0.25 #/bbl Na_2SO_3	SPE 64982
1.50	0.43	75	Seawater	SPE 64982

1.50	0.43	100	2 % KCl	Xanvis Sales Bulletin
1.50	0.43	180	2 % KCl	Xanvis Sales Bulletin
1.50	0.43	280	10 #/gal NaCl	Xanvis Sales Bulletin
1.50	0.43	280	Seawater	Xanvis Sales Bulletin
1.50	0.43	120	2 % KCl	Drilling Fluids Rheology
1.50	0.43	75&78	Seawater	Drilling Fluids Rheology
1.50	0.43	75	2 % KCl	Xanvis Sales Bulletin
1.50	0.43	75	3 % KCl	Xanvis Sales Bulletin
1.50	0.43	78	11 ppg $CaCl_2$	Xanthan Formulated Systems
1.50	0.43	78	Saturated NaCl	Xanthan Formulated Systems
1.50	0.43	78	Seawater	Xanthan Formulated Systems
1.50	0.43	Room	Fresh Water	SPE 19736
1.50	0.43	Room	2 % KCl	SPE 19736
2.00	0.57	80	2 % KCl	Drilling Fluids Rheology
2.00	0.57	75&78	Seawater	Drilling Fluids Rheology
2.00	0.57	85	11 #/bbl $CaCl_2$ + 0.3 #/bbl $NaSO_3$	Xanthan Formulated Systems
2.00	0.57	280	11 #/bbl $CaCl_2$ + 1 #/bbl MgO + 0.3 #/bbl $NaSO_3$	Xanthan Formulated Systems
2.00	0.57	280	11 #/bbl $CaCl_2$ + 0.3 #/bbl $NaSO_3$	Xanthan Formulated Systems
2.00	0.57	78	Seawater	Xanthan Formulated Systems
2.00	0.57	78	Saturated NaCl	Xanthan Formulated Systems
2.00	0.57	78	11 ppg $CaCl_2$	Xanthan Formulated Systems

2.00	0.57	75	3 % KCl	Xanvis Sales Bulletin
2.00	0.57	75	2 % KCl	Xanvis Sales Bulletin
2.00	0.57	75	11.4 ppg $CaCl_2$ + 0.25 #/bbl Na_2SO_3 +1.00 #/bbl MgO	SPE 64982
2.00	0.57	120	3 % KCl	SPE 62790
2.20	0.63	80	Saturated NaCl + 1 #/bbl MgO	Xanthan Formulated Systems
2.20	0.63	300	Saturated NaCl + 1 #/bbl MgO	Xanthan Formulated Systems
2.25	0.64	80 & 300	10 #/bbl $CaCl_2$ + 1 #/bbl MgO**	Xanthan Formulated Systems
2.25	0.64	80 & 300	11 #/bbl $CaCl_2$ + 1 #/bbl MgO**	Xanthan Formulated Systems
2.25	0.64	80 & 300	11.3 #/bbl $CaCl_2$ + 1 #/bbl MgO**	Xanthan Formulated Systems
2.50	0.71	75	Seawater	SPE 64982

**Only @ 1 shear rate

Impact Technologies Fluids Data

The purpose of this work is to determine the viscosity relationships over the expected temperature range. The concentration chosen was 0.875 Wt % which is the concentration used in the underbalanced drilling fluids for ASJ.

A total of 10 tests were conducted using 0.875 Wt % Xanvis L in combinations of fresh and 150,000 ppm NaCl. The temperatures ranges studied were from 30 to 140°F. The results are listed in the following Table and shown in the following Figures.

Table 3: 0.875 Wt % Data Various Temperatures

Polymer, Wt %	Brine	Shear Rate, sec^{-1}	Viscosity, cP	Temperature, °F
0.875	Fresh	7.34	4,550	30
		14.68	2,505	
		36.69	1,124	
		73.38	636	
0.875	Fresh	0.37	62,000	40
		0.73	33,500	
		1.83	14,480	
		3.67	8,400	
		7.34	5,000	

		14.68	2,543	
		36.69	1,133	
		73.38	611	
0.875	150,000 ppm NaCl	0.37	28,000	40
		0.73	14,400	
		1.83	6,720	
		3.67	3,440	
		7.34	1,940	
		14.68	1,080	
		36.69	504	
		73.38	290	
0.875	Fresh	7.34	4,600	69.4
		14.68	2,440	
		36.69	1,072	
		73.38	592	
0.875	Fresh	0.37	60,400	72
		0.73	33,500	
		1.83	15,200	
		3.67	8,400	
		7.34	4,500	
		14.68	2,450	
		36.69	1,040	
		73.38	600	
0.875	Fresh	7.34	3,240	140
		14.68	1,990	
		36.69	960	
		73.38	598	

This Figure shows the temperature dependence for 0.875 Wt % Xanvis L solutions. Unless otherwise noted the solutions are in fresh water. The data at 30, 40, and 72°F are nearly equivalent. The 40°F data were replicated 3 times. The values on this plot are the numeric averages of these runs. The 30 degree Fahrenheit data is the numeric average of 2 runs. The 72 and 140 degree data are individual tests. Even the 140°F data—green—is very close especially at the higher shear rates which are the most likely rates that will be encountered in underbalanced drilling applications.

The 40°F solution in 150,000 ppm NaCl was replicated 2 times. The plot shows the numeric average of these runs.

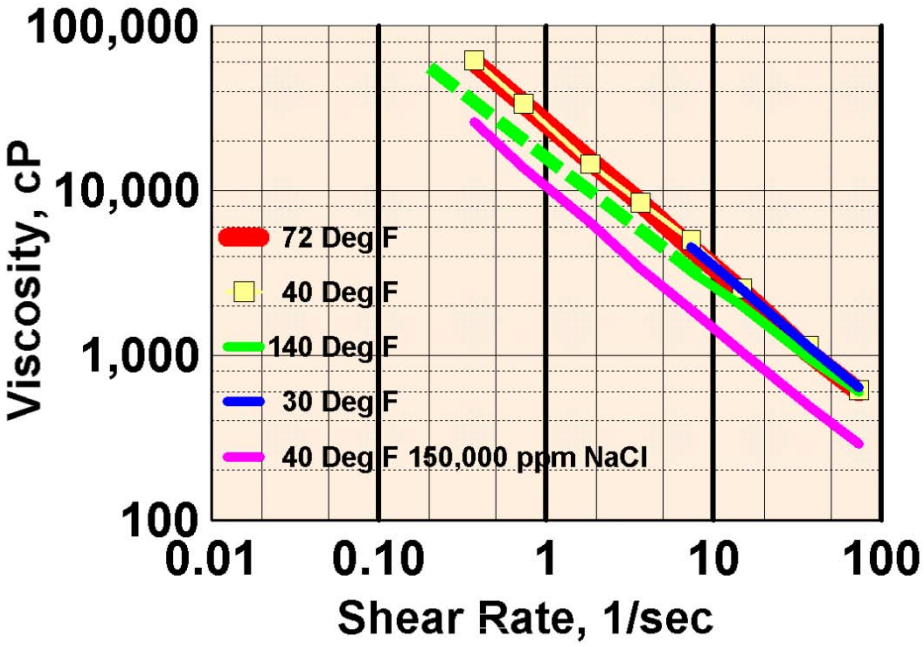

Figure 1: 0.875 Wt % Xanvis L Viscosities Various Temperatures Fresh & 150,000 ppm NaCl

Figure 2 shows the viscosity–shear rate results for the coolest temperature studied and one near room temperature. This data shows that at these temperatures the viscosities are nearly equal for the 0.875 Wt % Xanvis L solutions in fresh water. The 30 data were replicated twice while

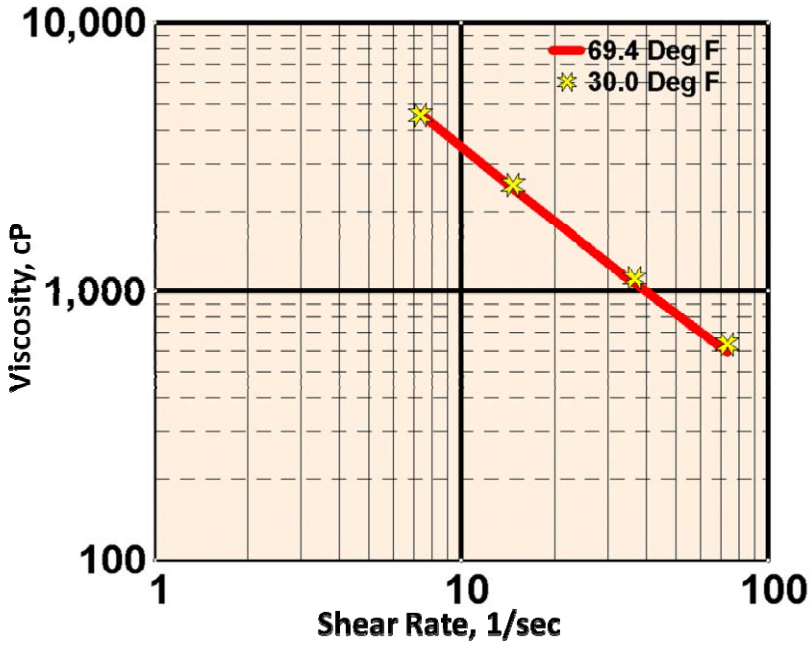

Figure 2: 0.875 Wt % Xanvis L Viscosities, 69.4 & 30 Deg F, Fresh Water

the 69.4°F was not. This 30°F is the same included in Figure 1 above.

A comparison with other Xanvis work is shown below. The outside work was conducted by Kelco personnel.

Comparison With Other Xanvis Work

This data reflects some of the viscosities recently measured for 0.875 wt % Xanvis L solutions. Comparison data from Kelco at lower polymer concentrations and lower temperatures are also included.

This Figure shows some of the viscosity data that is available for Xanvis L. The 0.88 Wt % data was measured at the Bartlesville laboratory of Clean Tech Innovations, LLC during June 2011. This data was taken using a Brookfield LV Series Viscometer with the LV-3 spindle. The concentrated polymer solutions were diluted using fresh water—Sapulpa drinking water. The Figure depicts some of the 72 and 140 °F data generated with the 0.875 Wt % polymer solutions.

The data are consistent with normal viscosity measurements. The lower the temperature is the higher the measured viscosities. This inverse relationship is directly opposite of the Xanvis L concentration which also influences the viscosities. There is a direct correlation with concentration. The lower the concentration the lower the viscosities are.

Two temperatures for the 0.875 wt % Xanvis L are shown. The red solid line represents some of the data taken at 72°F. The highest viscosity recorded was 60,400 cP. The direct comparison of the 72°F at a shear rate of 7.34 sec^{-1} shows that it is 4,500 cP while the data at 140°F is 3,240 cP. The light green, dashed line is an estimation of what the viscosities might be at lower shear rates for the 140°F solutions.

For comparison data created by Kelco scientists is included. This work was reported in SPE papers. The data chosen was the highest weight percent that was reported—0.71 Wt %. The comparison data was generated at 75 °F using ASTM Seawater. (SPE 64982) This work is depicted by the dashed brown line.

The other comparison data chosen was because the temperature (120°F) is close to the highest temperature in this work—140°F. Their work utilized 0.57 Wt % Xanvis L in 3% KCl. This is the highest polymer concentration that they reported at this temperature. (SPE 62790) It is shown by the dashed blue line. The effect of lower polymer concentration contributes to the lower viscosities as well as the 120°F.

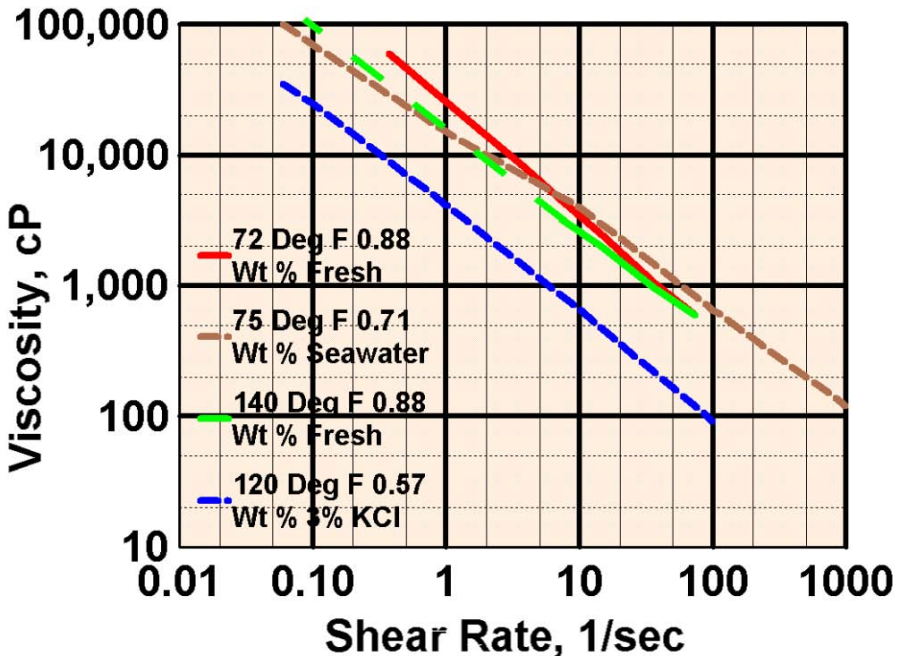

Figure 3: Comparison Xanvis Concentrations And Temperatures

Other Kelco data are discussed below. Most of the Kelco data was generated with low polymer concentrations.

Kelco Technical Bulletin Data

The viscosities reported here were determined by Kelco personnel. They were disclosed in the various Technical Bulletins prepared by Kelco. Each Table represents only the data given in the Figure(s) immediately following the Table.

Table 4 lists the viscosity numbers at various concentrations based on specific shear rates and brine concentrations.

Table 4: 0.63 Wt % Xanvis Data 80 and 300 Deg F

Polymer, Wt %	Brine	Shear Rate, sec^{-1}	Viscosity, cP	Temperature, °F
0.63	Saturated NaCl + 1 lb/bbl MgO	5	1,000	80
		10	600	
		100	100	
		1000	22	
0.63	Saturated NaCl + 1 lb/bbl MgO	5	305	300
		10	190	
		100	50	
		1000	14	

The Figure below depicts the effects on temperature of 0.63 Wt % Xanvis L at various shear rates. The polymer is dissolved in saturated NaCl plus 1 lb/bbl MgO. The data is consistent in that the 300°F viscosities are lower than those reported at 80°F. The data source is the Kelco Formulated Systems Technical Bulletin.

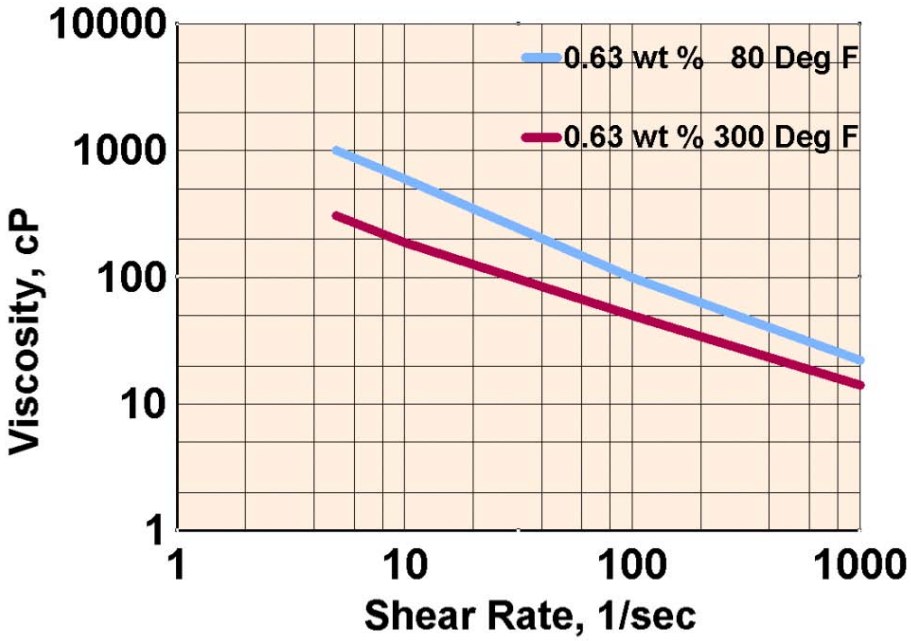

Figure 4: 0.63 Wt % Xanthan Viscosities At 80 & 300 Deg F

This Table shows the data collected at 85 and 280°F for 0.57 Wt % Xanvis.

Table 5: 0.57 Wt % Xanvis 85 and 280 Deg F

Polymer, Wt %	Brine	Shear Rate, sec^{-1}	Viscosity, cP	Temperature, °F
0.57	11 ppg $CaCl_2$	5	1,020	85
	+ 0.3	10	700	
	lb/bbl Na_2SO_3	100	180	
		300	80	
0.57	11 ppg $CaCl_2$	5	180	280
	+ 0.3	10	180	
	lb/bbl Na_2SO_3	100	46	
	+ 1 lb/bbl MgO	300	30	
0.57	11 ppg $CaCl_2$	18	38	280
	+ 0.3	20	38	
	lb/bbl Na_2SO_3	100	30	
		300	20	

Using 0.57 Wt % Xanvis the 85 and 280°F viscosity effects were studied in 11 ppg of $CaCl_2$ plus 0.3 lb/bbl of Na_2SO_3. In one instance—depicted by the yellow line—1 lb/bbl of MgO was added to the brine. What this shows is that not only is it necessary to add sodium sulfite to the brine and for increased stability at higher temperatures (275°F) magnesium oxide also helps to stabilize Xanvis L.

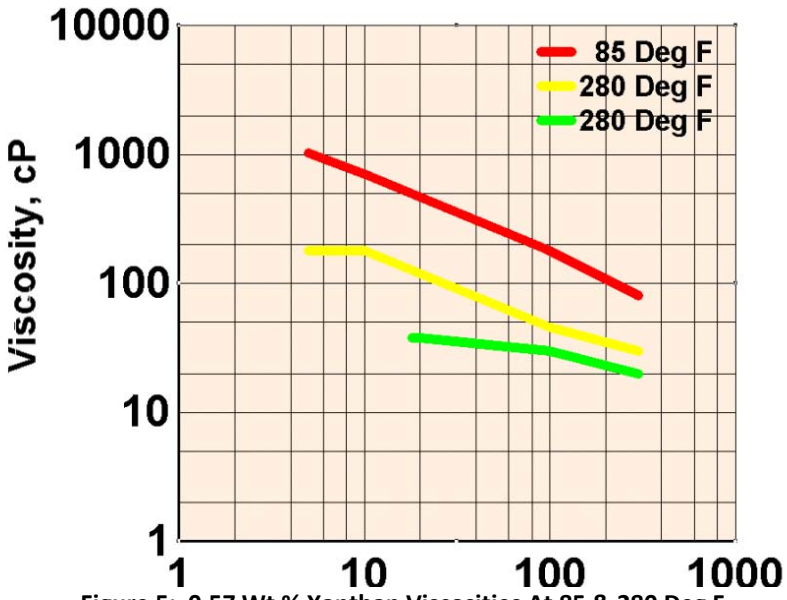

Figure 5: 0.57 Wt % Xanthan Viscosities At 85 & 280 Deg F

The data list for 0.64 Wt % Xanvis L at various temperatures occurs in the following Table. There are three different brines reported.

Table 6: 0.64 Wt % Xanvis L--Various Temperatures And Brines

10 ppg $CaCl_2$ + 1 lb/bbl MgO	
Temperature, °F	Viscosity, cP
80	107
100	100
150	87
200	75
300	12.5
11 ppg $CaCl_2$ + 1 lb/bbl MgO	
Temperature, °F	Viscosity, cP
80	130
100	124
150	111
200	92
300	37.5
11.3 ppg $CaCl_2$ + 1 lb/bbl MgO	
Temperature, °F	Viscosity, cP
80	149
100	135
150	121

200	109
300	70

The comparison of 0.64 Wt % Xanvis L viscosities at various temperatures and brines is shown in the following Figure. The $CaCl_2$ brines are stabilized with 1 lb/bbl MgO. As expected the heavier brine 11.3 ppg $CaCl_2$ has the highest viscosity throughout the temperature range studied. All of these viscosities were taken at 100 sec^{-1}.

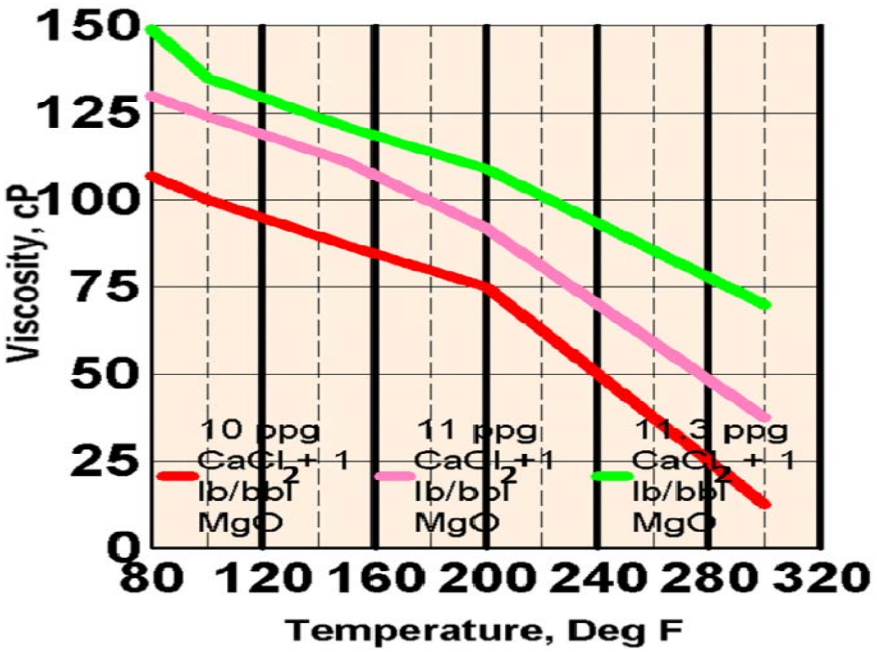

Figure 6: 0.64 Wt % Xanvis L At Various Temperatures in Various Calcium Chloride Brines

All of the following measurements were taken at 78 . The brines are seawater, saturated NaCl and 11.0 ppg of $CaCl_2$. This table lists the input data for Figure 7.

Table 7: Various Xanvis L Polymer Concentrations--Low Shear Rates--78 Deg F

Polymer, Wt %	Brine	Shear Rate, sec^{-1}	Viscosity, cP	Temperature,
0.43	Seawater	0.0636	28,000	78
		5.1	890	
0.57	Seawater	0.0636	59,000	78
		5.1	1300	
0.43	Saturated NaCl	0.0636	33,000	78
		5.1	840	
0.57	Saturated NaCl	0.0636	62,000	78
		5.1	1280	

0.43	11 ppg $CaCl_2$	0.0636	9,000	78
		5.1	500	
0.57	11 ppg $CaCl_2$	0.0636	19,000	78
		5.1	700	

Note that the shear rate range is narrow compared to some of the other data reported. Also that the $CaCl_2$ brines have lower viscosities than those diluted with NaCl brines.

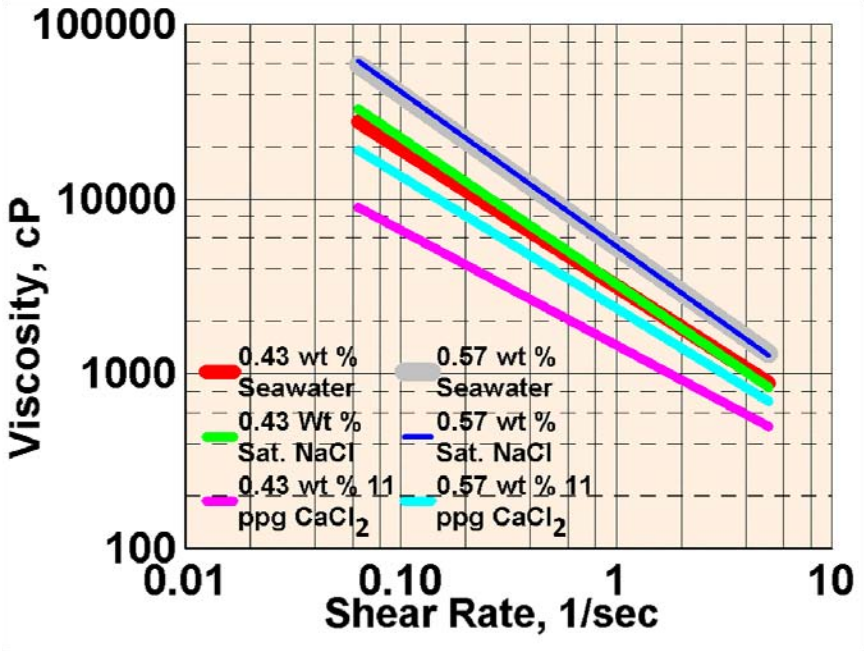

Figure 7: 0.43 & 0.57 Wt % Xanvis L In Three Different Brines At 78 Deg F

Other data shows the relationship of concentration in 3% KCl. The Figure below depicts this relationship at 75 . Once again the shear rate range is restricted.

Table 8: 0.43 And 0.57 Wt % Xanvis In 3 % KCl Low Shear At 75 Deg F

Polymer, Wt %	Brine	Shear Rate, sec^{-1}	Viscosity, cP	Temperature,
0.43	3 % KCl	0.0636	33,000	75
		5.1	820	
0.57	3 % KCl	0.0636	62,000	75
		5.1	1200	

Laboratory bench tests have shown that 0.57 Wt % fluids could be used in the **Impact Technologies, LLC** ASJ drilling applications. The 0.43 Wt % data is included for reference.

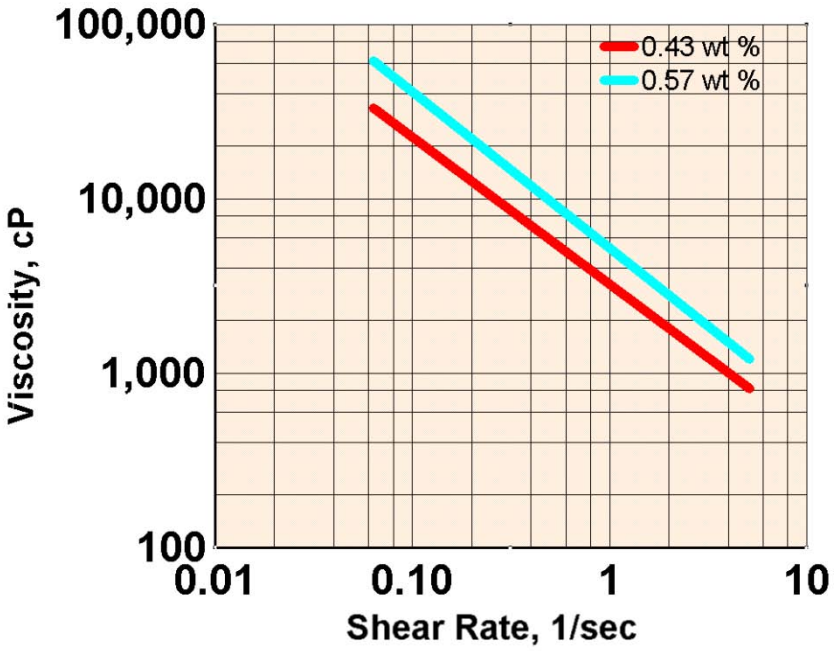

Figure 8: 0.43 & 0.57 Wt % Xanvis L in 3 % KCl At 75 Deg F

An example of the same polymer concentrations but in 2 % KCl at 75°F is listed in the Table below and shown in the Figure.

Table 9: 0.43 And 0.57 Wt % Xanvis in 2 % KCl At 75 Deg F

Polymer, Wt %	Brine	Shear Rate, sec^{-1}	Viscosity, cP	Temperature, °F
0.43	2 % KCl	0.1	20,000	75
		1	3,100	
		10	400	
		100	70	
		1000	13	
0.57	2 % KCl	0.1	40,000	75
		1	4,500	
		10	700	
		100	100	
		1000	19	

Note that the shear rate range is larger compared to the 2 % KCl brines above. Once again the 0.57 Wt % polymer fluid would be applicable to the ASJ work.

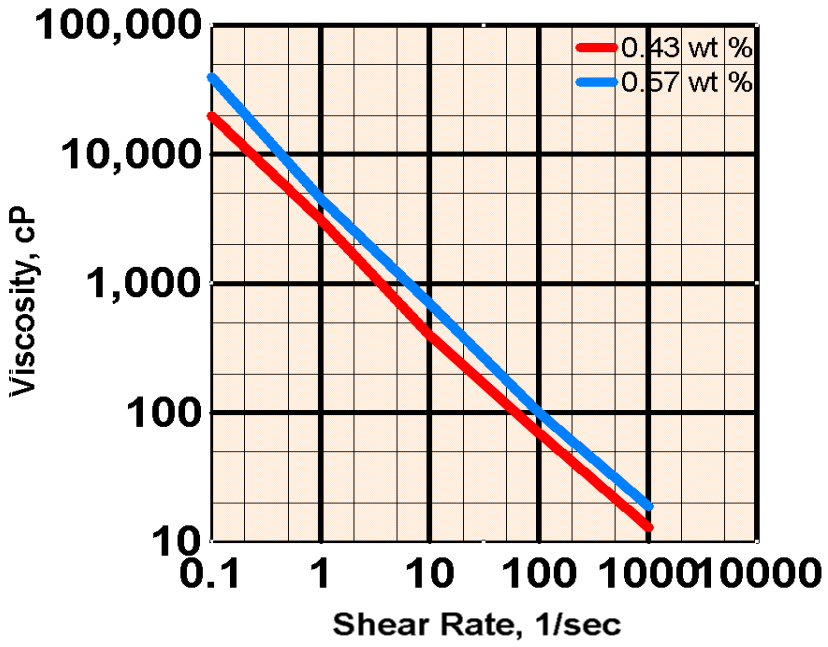

Figure 9: 0.43 & 0.57 Wt % Xanthan In 2 % KCl At 75 Deg F

This Table lists 0.43 Wt % Xanvis diluted in 2 % KCl. The data was taken at 100 and 180°F.

Table 10: 0.43 Wt % Xanvis in 2 % KCl at 100 and 180 Deg F

Polymer, Wt %	Brine	Shear Rate, sec^{-1}	Viscosity, cP	Temperature, °F
0.43	2 % KCl	0.1	16,000	100
		1	2,800	
		10	380	
		100	68	
		1000	13	
0.43	2 % KCl	0.1	4,800	180
		1	1,500	
		10	290	
		100	58	
		1000	11	

The effect of 100 and 180 °F temperatures on 0.43 Wt % polymer solutions in 2 % KCl is shown below. Over this range of shear rates the differnces are nominal until the very low shear rates. The low rates are less than those expected to be encountered in ASJ field applications.

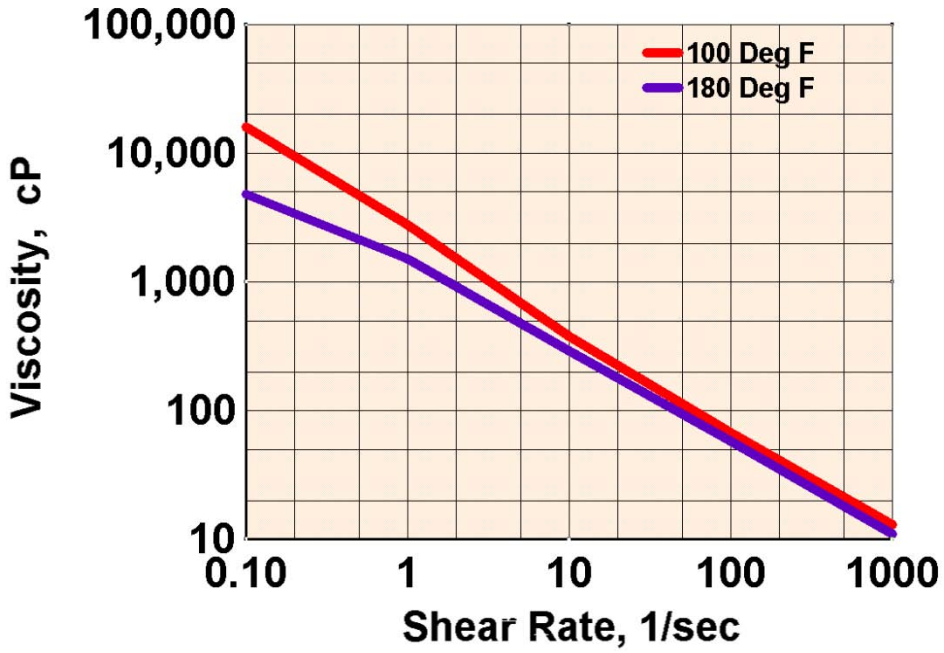

Figure 10: 0.43 Wt % Xanvis In 2 % KCl At 100 & 180 Deg F

The Table below and the following Figure show the temperature effects for a shear rate of 100 sec^{-1}. The 0.43 Wt % solutions were tested in seawater and 10 lb/bbl NaCl.

Table 11: 0.43 Wt % Various Temperatures In Seawater And 10 ppg NaCl

Seawater	
Temperature, °F	Viscosity, cP
75	82
124	71
210	60
255	51
280	16
10 lb/bbl NaCl	
Temperature, °F	Viscosity, cP
75	100
124	88
210	76.6
255	66
280	68

Xanvis L solutions are generally stable up to 250°F. In order to make more stable Xanvis L in saturated NaCl solutions at higher temperatures—up to 300°F—one must add low molecular weight alcohols, oxygen scavengers, or anti-oxidants. To increase the stability to 350°F the

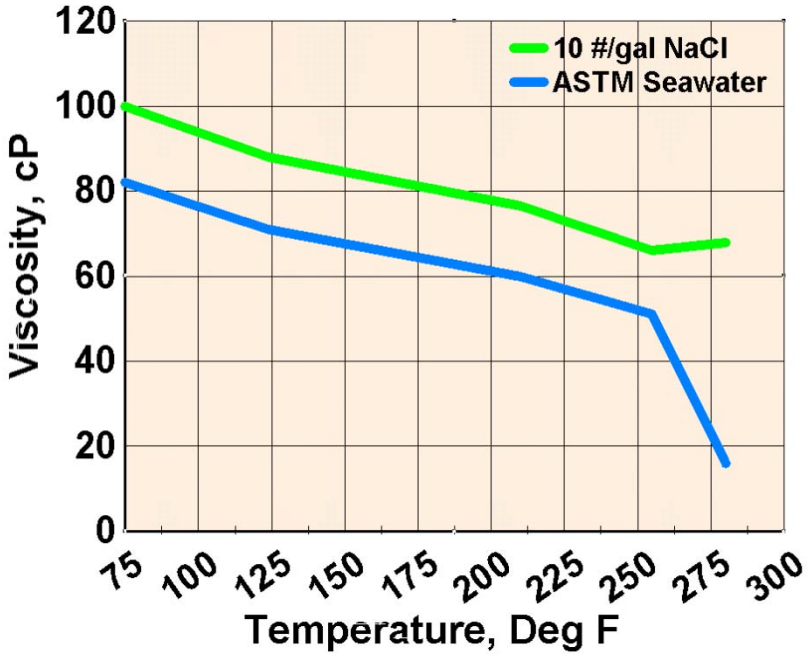

Figure 11: 0.43 Wt % Xanvis in Seawater & 10 ppg NaCl At Various Temperatures

Xanvis must be dissolved in formate brines. Even though one can add these chemicals to the Xanvis, it is recommended that one use Xanthan formulated for higher temperature use.

More drilling fluids formulations are given in the Kelco Drilling Fluid Rheology Bulletin. Examples for 120°F at various Xanvis L concentrations are listed below and shown in Figure 12.

Table 12: Various Xanvis L Low Concentrations In 2 % KCl At 120 Deg F

Polymer, Wt %	Brine	Shear Rate, sec^{-1}	Viscosity, cP	Temperature, °F
0.21	2 % KCl	0.06	680	120
		0.1	610	
		1	380	
		10	120	
		100	26	
		1,000	5	
0.29	2 % KCl	0.06	1,600	120
		0.1	1,450	
		1	700	
		10	180	
		100	35	
		1,000	7	
0.49	2 % KCl	0.06	10,500	120

		0.1	8,000	
		1	1,900	
		10	360	
		100	65	
		1,000	11	

Even though the concentrations reported here are too low for the ASJ applications, it does show the polymer concentration relationships and gives some insight to what might happen when the polymer solutions are exposed to elevated temperatures—120°F. The viscosities are similar over the shear rate range studied. The polymers were diluted with 2 % KCl.

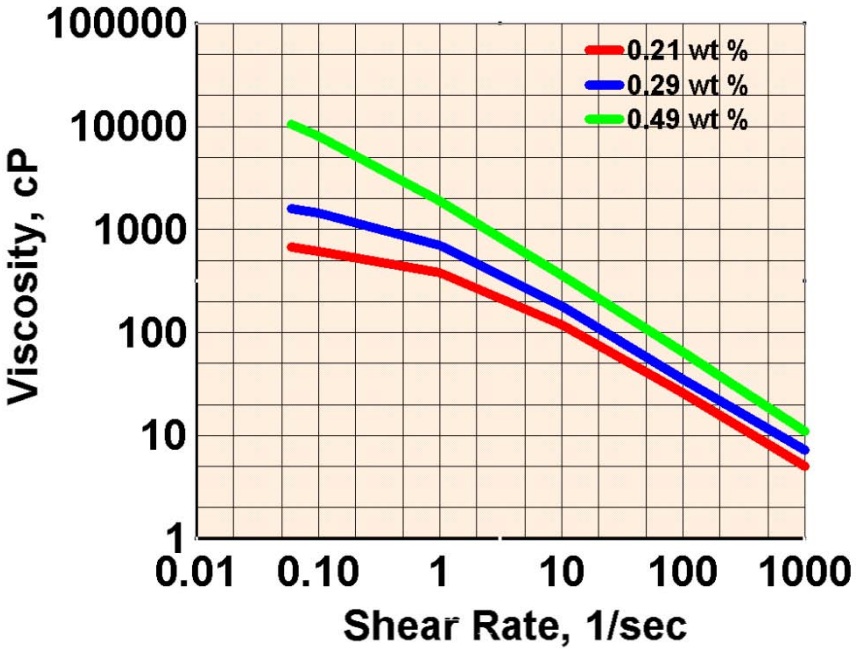

Figure 12: Various Low Concentration Xanvis Solutions in 2 % KCl At 120 Deg F

Other low shear rate data are reported below. The concentrations show that at these low shear rates the higher concentration Xanvis has the highest viscosity. This data was measured at 80°F using polymers diluted by 2 % KCl.

Table 13: Various Xanvis L Concentrations In 2 % KCl At Low Shear Rates And 80 Deg F

Polymer, Wt %	Brine	Shear Rate, sec^{-1}	Viscosity, cP	Temperature, °F
0.29	2 % KCl	0.06	9,500	80
		5.1	440	
0.36	2 % KCl	0.06	18,500	80
		5.1	640	
0.43	2 % KCl	0.06	31,000	80
		5.1	860	
0.57	2 % KCl	0.06	56,000	80
		5.1	1,350	

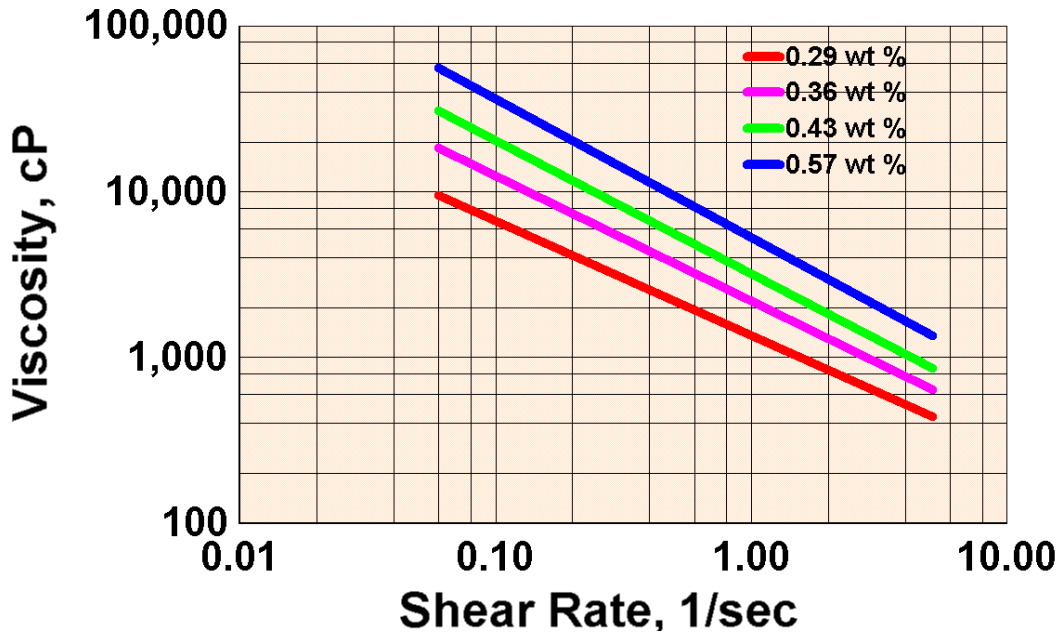

Figure 13: Various Xanvis Concentrations In 2 % KCl At Room Temperature

The following data were extracted from SPE papers which reported Xanthan viscosities.

Other Viscosity Measurement Sources

SPE papers

Some of the earliest Xanthan data was published in 1985. The chart and figure shows some of the viscosities reported. (Clark, 1989)

Table 14 lists the data collected from the Clark work.

Table 14: Fresh Water 0.24 And 0.48 Wt % Xanthan At Room Temperature

Polymer, Wt %	Brine	Shear Rate, sec^{-1}	Viscosity, cP	Temperature, °F
0.24	Fresh	0.001	58,061	Room
		0.1	1,700	
		1	580	
		5.2	237	
		10	116	
		100	30	
		170	25	
		479	13	
		1000	10	
0.48	Fresh	0.01	48,000	Room
		0.1	18,000	
		1	4,000	
		10	800	
		100	160	
		1000	18	

The purpose for including this Figure is to depict the viscosities over a very large shear rate range. The experiments were conducted in fresh water at room temperature. The curves are consistent since the lower polymer concentration has the lower viscosity.

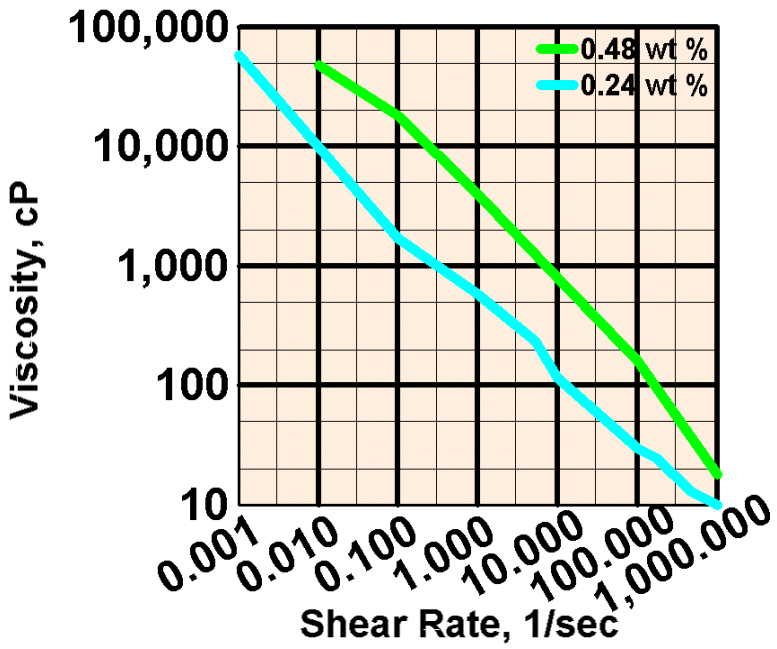

Figure 14: 0.24 & 0.48 Wt % Xanthan In Fresh Water At Room Temperature

Table 15 lists the data collected from this work. The differences are within experimental error.

Table 15: 0.48 Wt % Xanthan In Fresh Water & 2 % KCl At Room Temperature

Polymer, Wt %	Brine	Shear Rate, sec^{-1}	Viscosity, cP	Temperature, °F
0.48	Fresh	0.01	100,000	Room
		0.1	21,100	
		1	4,000	
		10	540	
		100	80	
		1000	7.8	
0.48	2 % KCl	0.1	20,000	Room
		1	4,000	
		10	580	
		100	85	

Data in Figure 15 are from a 0.48 Wt % xanthan solution made with and without potassium chloride. This Figure shows the viscosity similarities in fresh water and 2 % KCl at this polymer

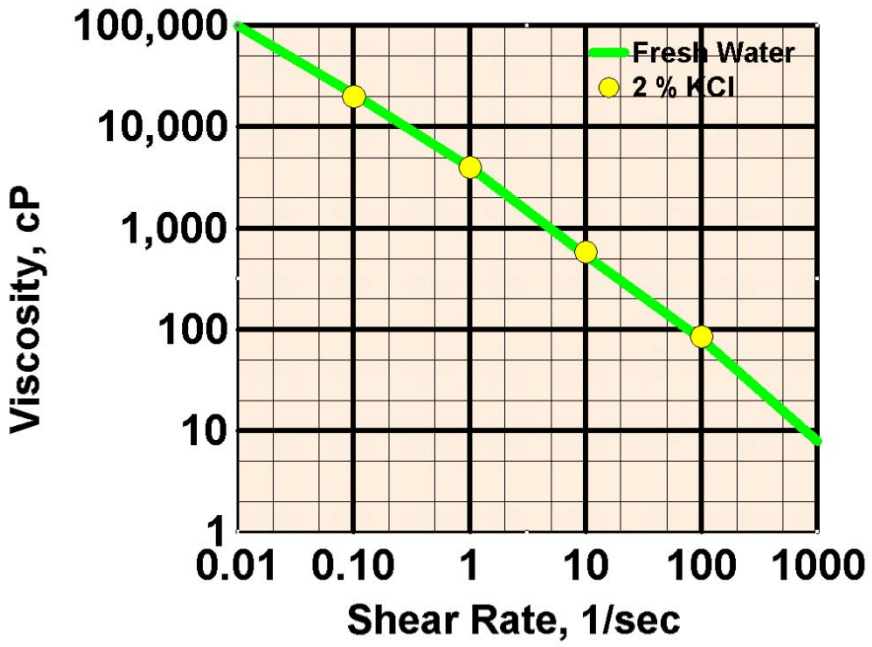

Figure 15: 0.48 Wt % Xanthan In Fresh & 2 % KCl At Room Temperature

concentration. These experiments were also conducted at room temperature. This data indicates that Xanthan polymer viscosities are unaffected by low alkali salt concentrations. (Clark, 1989)

Another example of the viscosity versus concentration effects is given below. The work was conducted at room temperature. The solutions were mixed in ASTM seawater. A constant shear rate of 0.06 sec^{-1} was used to measure these viscosities. (Navarrete, 2001) Table lists the data.

Table 16: Various Xanvis Concentrations In Seawater At Room Temperature

Polymer, Wt %	Brine	Viscosity, cP	Temperature, °F
0.17	Seawater	3,000	Room
0.23		6,500	
0.29		11,500	
0.34		20,000	
0.4		30,000	
0.46		40,000	
0.51		51,250	
0.57		64,250	

To compare these polymer concentrations the data are shown in the Figure below. As the table states the polymer was dissolved in ASTM seawater and this work was conducted at room temperature.

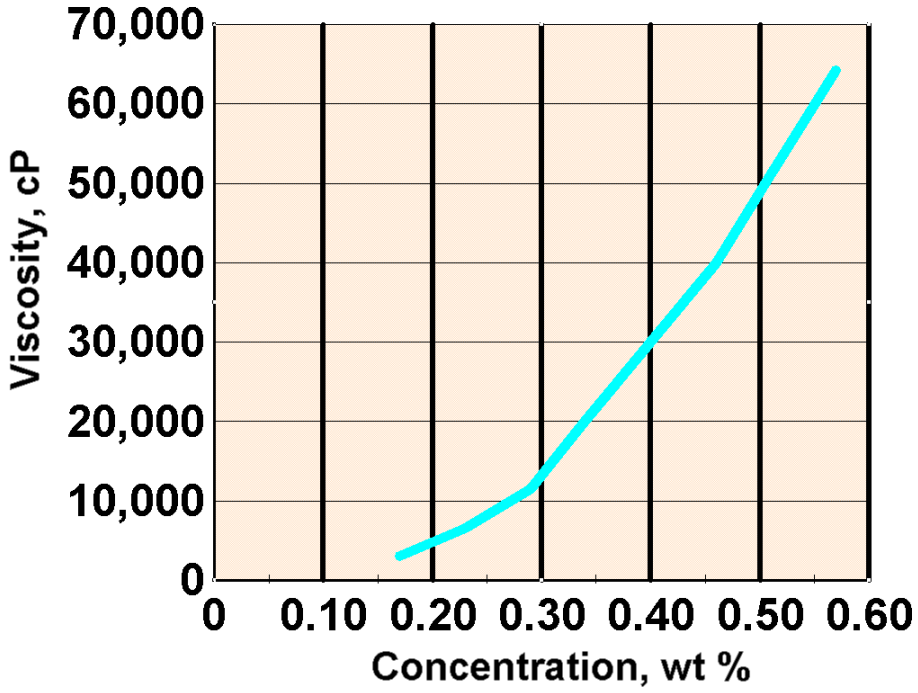

Figure 16: Various Xanthan Concentrations In Seawater At Room Temperature

The Table below lists the data shown in Figure 17. Using seawater at room temperature, results are consistent. The lowest polymer concentration produces the lowest viscosities.

Table 17: 0.14, 0.29, & 0.71 Wt % Xanthan In Seawater At Room Temperature

Polymer, Wt %	Brine	Shear Rate, sec^{-1}	Viscosity, cP	Temperature, °F
0.14	Seawater	0.06	650	Room
		0.1	600	

		1	360	
		10	80	
		100	18	
		1,000	5	
0.29	Seawater	0.06	10,100	Room
		0.1	9,000	
		1	1,800	
		10	380	
		100	45	
		1,000	9	
		1,000	5	
0.71	Seawater	0.06	100,000	Room
		0.1	70,000	
		1	15,000	
		10	4,000	
		100	650	
		1000	120	

No explanation was offered as to why the 0.14 Wt % polymer solution viscosities curved at shear rates of 1 and lower. This would not be significant for the ASJ applications since the shear rates would be much higher than 1.

From our laboratory work we have shown that only the 0.71 Wt % polymer solution would be suitable for our applications with respect to lifting the impact solids in the base drilling fluid and the rock solids produced during drilling.

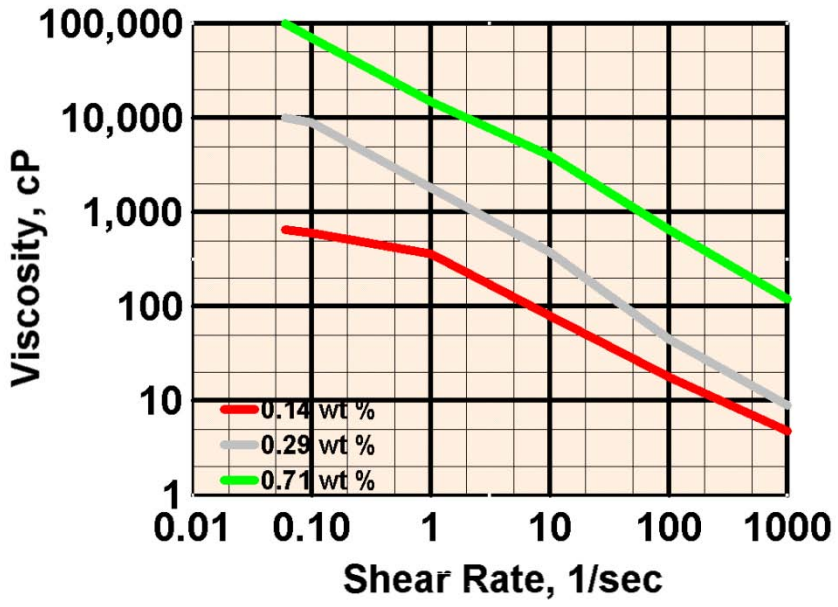

Figure 17: Three Xanthan Concentrations in Seawater At Room Temperature

To test the effects of 11.4 ppg $CaCl_2$ brine containing 0.25 lb/bbl Na_2SO_3 and 1 lb/bbl of MgO at room temperature on 0.57 Wt % Xanthan, a few viscosities were reported. The results are listed in the Table below and shown in Figure 18.

Table 18: 0.57 Wt % Xanvis In 11.4 ppg Calcium Chloride At Room Temperature

Polymer, Wt %	Brine	Shear Rate, sec^{-1}	Viscosity, cP	Temperature, °F
0.57	11.4 ppg $CaCl_2$ + 0.25 lb/bbl Na_2SO_3 and 1 lb/bbl MgO	100	20	Room
		350	9.8	
		1000	9.0	

The Xanthan was directly hydrated in this brine. One can see that it wasn't too effective. This work shows that if it is necessary to use brines with higher concentrations of divalent ions, it is advisable to hydrate the Xanvis in fresh water in high polymer concentrations then dilute the polymer solution with the divalent brines. This allows the Xanvis to be more successful in producing higher viscosities.

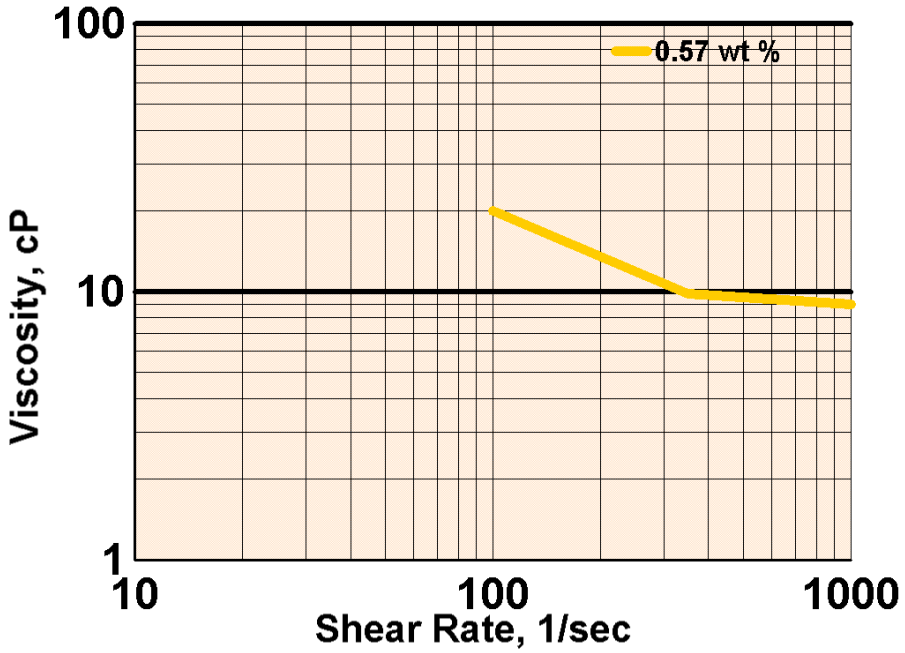

Figure 18: 0.57 Wt % Xanthan In Calcium Chloride At Room Temperature

Other Xanthan viscosities show that at higher temperatures the viscosities are affected. (Navarrete, 2000) Table 19 contains these results.

Table 19: 0.43 Wt % Xanthan In 3 % KCl At 75 And 120 Deg F

Polymer, Wt %	Brine	Shear Rate, sec^{-1}	Viscosity, cP	Temperature, °F
0.43	3 % KCl	0.06	33,000	75
		0.1	26,000	
		1	3,200	
		10	450	

		100	65	
0.43	3 % KCl	0.06	10,000	120
		0.1	8,500	
		1	2,000	
		10	380	
		100	50	
0.57	3 % KCl	0.06	35,000	120
		0.1	25,000	
		1	4,200	
		10	650	
		100	91	
0.43	3 % KCl + 0.25 lb/bbl Na_2SO_3	0.06	100,000	250
		0.1	70,000	
		1	15,000	
		10	4,000	
		100	650	
		1000	120	

The Figure below shows the comparison between polymer concentrations of 0.43 and 0.57 Wt %. It looks as though the Xanthan is beginning to disintegrate at 250°F since there is a sharp viscosity reversal at 10 sec^{-1}.

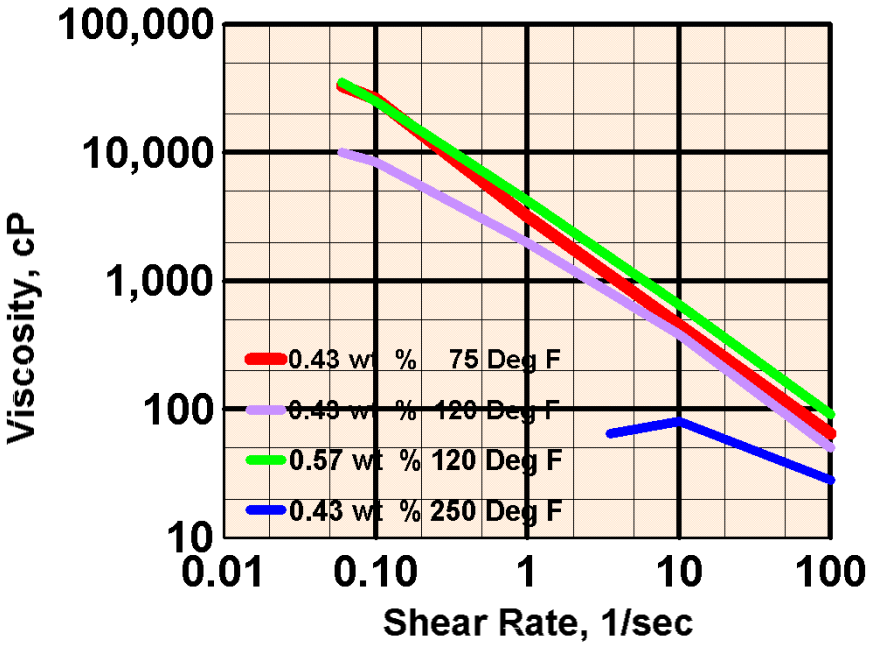

Figure 19: 0.43 & 0.57 Wt % Xanthan In 3 % KCl At Three Temperatures

Other work has demonstrated high temperature effects. (Navarrete, 2001) ASTM seawater was used as the base brine for these experiments. The polymer concentration was 0.43 Wt %. The Table below lists this data.

Table 20: 0.43 Wt % Xanvis At 200 And 250 Deg F

Polymer, Wt %	Brine	Shear Rate, sec^{-1}	Viscosity, cP	Temperature, °F
0.43	Seawater + 0.25 lb/bbl Na_2SO_3	0.15	1,100	200
		1	700	
		10	220	
		100	48	
0.43	Seawater + 0.25 lb/bbl Na_2SO_3	5.5	36	250
		10	32	
		100	18	

It should be noted that when temperatures of 200°F or higher are expected to be encountered when using Xanvis L, it is necessary to add 0.25 lb/bbl sodium sulfite to stabilize the fluid. Even then the fluids might not be too stable.

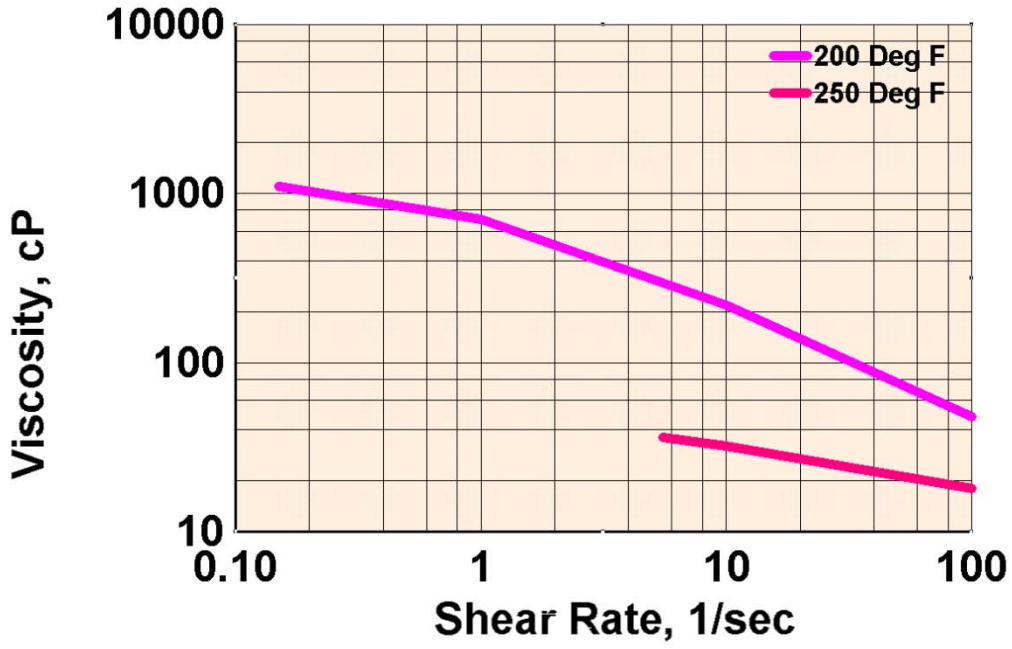

Figure 20: 0.43 Wt % Xanvis L In Seawater At 200 & 250 Deg F

To overcome some of the high temperature characteristics of Xanvis, high temperature biopolymers have been developed. These polymers might be better suited for use when drilling geothermal wells especially as total depth is approached.

Derivation Of Xanvis Viscosity Equations

This work was conducted because of the temperature limitations of the Brookfield viscometer available at Clean Technology Solutions, LLC. The highest temperature one can reach is 160°F. This temperature doesn't represent the highest temperature that Xanvis is a viable component of the underbalanced drilling fluids so it is necessary to be able to calculate representative viscosities at temperature greater than 160°F. Conversely, it is necessary to be able to calculate Xanvis viscosities at temperatures lower than those at the Brookfield lower limit. These temperatures might not be the lowest temperatures achieved as the underbalanced drilling fluids expand as they exit the nozzles downhole.

Techniques Employed

Using 213 viscosity samples, two equations have been derived. One is for polymer solutions in fresh water. The other is for polymer solutions dissolved in brines.

The first step was to determine the components necessary to determine the viscosities. The variables to choose from were polymer concentration, temperature, shear rate, salt concentration and ionic strength. The units were weight percent, degrees °F, sec^{-1}, ppm and ionic strength which is unit less. A review of some of the concepts behind ionic strength follow.

What is Ionic Strength?

Whenever ones deal with ionic solutions, one should be aware of their ionic strength since it affects the ion activity. For comparing experimental results, we work with solutions that have comparable ionic strength, which is a quantity representing interactions of ions with water molecules and other ions in solution. This quantity is usually represented by I.

$$I = \frac{1}{2}\sum_{i=1}^{n} z_i^2 \; m_i$$

where m_i is the concentration of the *i*th ion concentration. The summation, Σ, is taken over all the possible ions in the solution. For example what is the ionic strength for a 1.0 M NaCl solution?

Using the simple formula for ionic strength *I* given above, the result is

1 molar*charge^2 + 1 molar*charge^2

1 Molar Na*1^2 + 1 Molar Cl*1^2 or

I = ½ (1*1^2 + 1*1^2)

= 1.00 (a unit less quantity)

But one might notice that the concentrations given here are Molar. Therefore one has to first calculate the total molar concentration for the solution.

The molar concentrations were calculated for each species in the solutions studied. In order to do this the molecular weight for each salt present in the solutions were calculated. These molecular weights were then transformed into molarity. The molarities were then added to determine the total solution molality.

Once the ionic strengths for each solution were determined then the statistical analysis was begun.

Statistical Analysis

Correlation coefficients between the proposed components were determined. The purpose of this section of the work was to define which variables are independent. Independent variables are those where the correlations coefficients are less than 0.5.

The first task is to determine which variables to use to derive the viscosity equations. The variables considered were polymer concentration, temperature, shear rate, ionic strength and the combinations of each of these variables. The plot below shows the correlation coefficients of the various combinations taken two at a time. For example temperature and polymer taken together produce the highest correlation coefficient. The lowest combination is that of shear rate and ionic strength. The analysis is reported with the first grouping using temperature and the combinations. The second grouping is based on polymer with the other variable. The third grouping uses shear as the base.

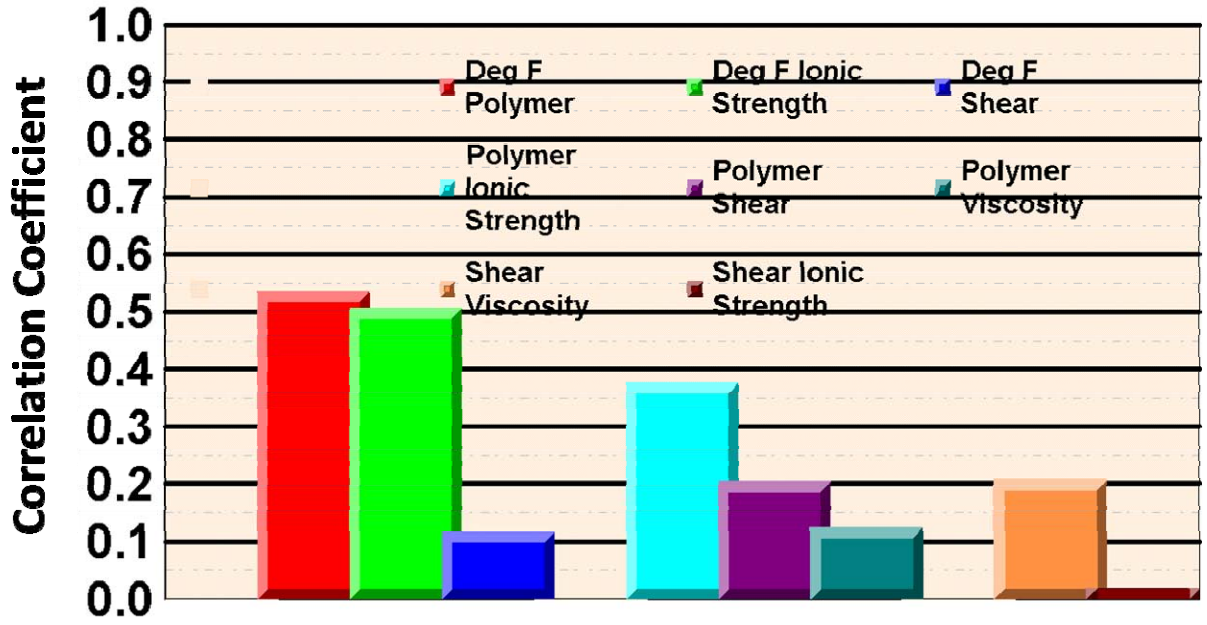

Figure 21: Correlation Coefficient Results

The correlation work results were then used to develop two viscosity equations. They are shown in the next paragraphs.

For Fresh Water

This equation is based on polymer concentration (Wt %), temperature (°F) and shear rate (sec^{-1}). The viscosity determined is thus reported in natural logarithms. The units for viscosity are centipoise. R squared is 0.977.

$$\ln Viscosity\ (centipoise) = 2.487 * \ln\left(Polymer\ Concentration\ (wt\%)\right) + (-0.134 * \ln\left(Temperature\ (°F)\right) + (-0.735 * \ln\left(Shear\ Rate\ (sec^{-1})\right) + 10.635$$

For Brines

The equation for brines is based on polymer concentration (Wt %), temperature (°F), shear rate (sec^{-1}) and ionic strength. The viscosity determined is thus reported in natural logarithms. The units for viscosity are centipoise. R squared is 0.989.

$$\ln Viscosity\ (centipoise) = 1.044 * \ln\left(Polymer\ Concentration\ (wt\%)\right) + (-0.706 * \ln\left(Temperature\ (°F)\right) + (-0.788 * \ln\left(Shear\ Rate\ (sec^{-1})\right) + 0.225 * \ln(Ionic\ Strength) + 11.708$$

There are 213 data points used for this derivation.

High Temperature Biopolymer

Geovis ®XT

Under specific operating conditions the use of Geovis XT may be preferred over standard xanthan products. These unique biopolymers offer improved performance under high temperature conditions, especially in fresh to brackish, low salinity systems (≤ 15% monovalent salts).

Example viscosities are given in the Table below. The three solutions viscosities were measured at 75°F.

Table 21: Geovis XT In Fresh, Seawater And 9.2 ppg NaCl At 75 Deg F

	Viscosity, cp	
Fresh Water	5.1 sec^{-1}	0.06 sec^{-1}
1.00 lb/bbl (0.29 wt %)	750	40,000
1.25 lb/bbl (0.36 wt %)	1,000	57,000
Seawater		
1.00 lb/bbl (0.29 wt %)	660	31,000
1.25 lb/bbl (0.36 wt %)	800	44,000
9.2 lb/gal NaCl		
1.00 lb/bbl (0.29 wt %)	575	28,500
1.25 lb/bbl (0.36 wt %)	800	39,000

More data are given for 0.29 wt % Geovis XT at 75 and after 1 hour off exposure to 300°F.

Table 22: Geovis XT In Seawater At 75 And 300 Deg F

Seawater + Na_2SO_3	Viscosity, cP	
Shear Rate, sec^{-1}	@ 75°F	@300°F
0.06	35,000	
0.51		2,900
5.10	700	
1.00		1,800
10	410	330
100	56	48
1000	11	7.8

The Figure below shows the viscosities of Geovis XT in ASTM Seawater + 0.25 lb/bbl Na_2SO_3 at 75°F and after 1 hour of exposure at 300°F.

One can see that the viscosities don't vary significantly until the lower shear rates. These low rates do not prevail under underbalanced drilling field conditions. Also under most field conditions, Geovis XT is preferred at higher temperatures. The thermal stability of Geovis XT is illustrated in Figure 22. Note that the concentration of Geovis XT is 50% less than the xanthan used. This alone would lower the solution costs.

Of significant importance is that Geovis XT retains a high degree of viscosity over a relatively wide shear rate range when exposed to elevated temperatures. This allows for using this polymer in bentonite free, low salinity formulations for high temperature applications. The temperature limitation for Geovis XT is approximately 320°F.

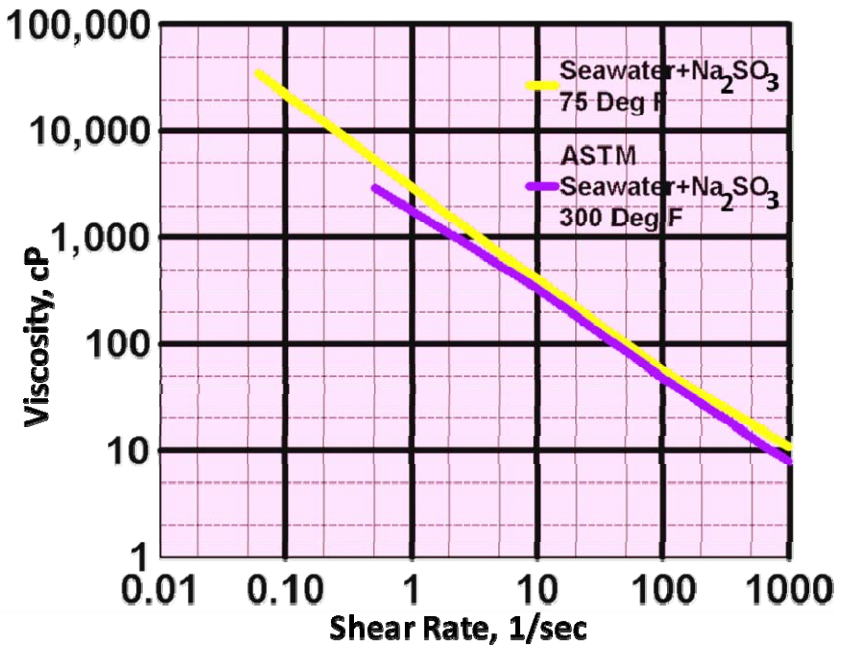

Figure 22: 0.29 Wt % Geovis XT in Seawater At 75 & 300 Deg F

The Table below of lists the viscosity comparison of Geovis and Xanthan.

Table 23: Viscosity Comparison Of 0.29 Wt % Geovis And 0.57 Wt % Xanthan In Seawater At Various Temperatures

0.29 Wt % Geovis XT in Seawater	
Temperature,	Viscosity, cP
77	46
133	44
240	40.5
258	42.5
283	42.5
285	42.5
297	39
302	39
0.57 Wt % Xanthan in Seawater	
Temperature,	Viscosity, cP
77	78
133	70
240	55
258	37.5
283	12
285	9

297	8
302	4

As with any polymer-based system, oxygen scavengers are recommended to assure maximum polymer stability when fluids are exposed to elevated temperatures for extended periods of time.

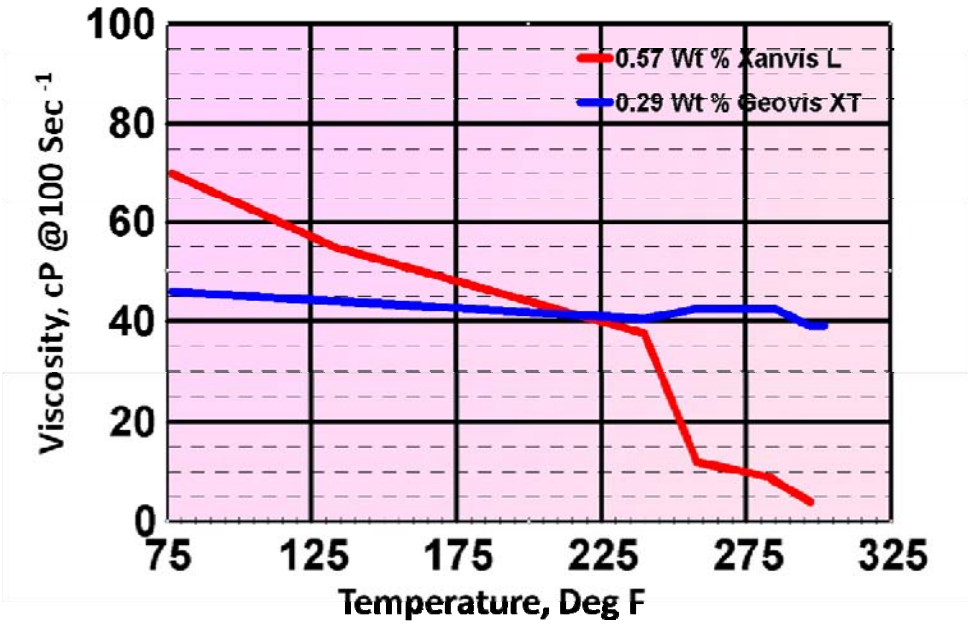

Figure 23: Comparison Xanvis L & Geovis XT Viscosities At Various Temperatures

The fact that the Geovis viscosities are essentially constant throughout the temperature range is significant. This means that the polymer solution carrying capacity is relatively constant as well.

Conclusions and Recommendations

It is recommended that Geovis or another high temperature resistant polymer be tested at temperatures approaching those expected to be encountered when drilling geothermal wells. It will be necessary to design the reaction vessels since the temperatures will be greater than 212 . The vessels must also be designed to withstand pressures necessary to keep water liquid.

References

Clark, P. E., "Oilfield Fluid Rheology: The Use of a Controlled Stress-Measuring System To Determine Oilfield Fluid Properties", SPE 19736, presented at 64th Annual Technical Conference and Exhibition, San Antonio, TX, October 1989.

Clark, P. E., Halvaci, M., Ghaeli, H., and Parks, H. F., SPE/DOE 13907, "Proppant Transport by Xanthan and Xanthan-Hydroxypropyl Guar Solutions: Alternatives to Crosslinked Fluids", presented at SPE/DOE Low Permeability Gas Reservoirs, Denver, CO, May 1985.

Kelco Oilfield Group, High Temperature Biopolymers, Technical Bulletin, September 2005.

Kelco Oilfield Group, Rheology Technical Bulletin, September 2006.

Kelco Oilfield Group, Xanthan Formulated Systems, Technical Bulletin, September 2005.

Kelco Oilfield Group, Xanvis L Sales Bulletin, September 2005.

Navarrete, R. C., Seheult, J. M., and Coffey, M. D., "New Bio-Polymers for Drilling, Drill-In, Completions, Spacer Fluids and Coiled Tubing Applications", IADC/SPE 62790, presented at 2000 IADC/SPE Asia Pacific Drilling Technology, Kuala Lumpur, Malaysia, September 2000.

Navarrete, R. C., Seheult, J. M., and Coffey, M. D., "New Biopolymers for Drilling, Drill-In, Completions, Spacer, and Coil-Tubing Fluids, Part II", SPE 64982, presented at 2001 SPE International Symposium on Oilfield Chemistry, Houston, Texas, February 2001.

Appendix—High Temperature Polymer—Geovis XT

Kelco Oil Field Group

A HUBER COMPANY

Product Bulletin

GEOVIS™ XT

A High Viscosity, Thermally Stable Biopolymer for Rheology Control

Description

GEOVIS XT polymer is a high molecular weight polysaccharide used to enhance the low shear rate viscosity of water based circulating systems.

Function

The primary function of ***GEOVIS XT*** is to optimize the rheological profile of drilling fluids by increasing viscosity at low shear rates (less than 5.1 sec^{-1}), while maintaining plastic viscosity at a minimum value. In so doing, it improves suspension and solids carrying capacity, especially under low flow rate conditions. ***GEOVIS XT*** is functional in makeup waters ranging from fresh to low salinity brines including seawater and <10% monovalent salt systems.

Features

GEOVIS XT exhibits extended power law behavior in water base systems to optimize hydraulic efficiency. Unlike other biopolymers, these properties are evident even at low concentrations of 0.75 to 1.0 lb/bbl. This allows fluids to be formulated with a relatively low concentration of biopolymer and reduces daily maintenance treatments needed to maintain a specific LSRV. Due to its unique molecular structure, ***GEOVIS XT*** retains a higher degree of low shear rate viscosity at elevated temperatures (300° - 310°F) when compared to other commercial polysaccharides. ***GEOVIS XT*** is more cement compatible than other biopolymers, making it an ideal candidate in the formulation of cement spacer fluids.

Mixing

For optimum hydration, ***GEOVIS XT*** should be added through a conventional rig hopper at the rate of 10 minutes per 25 lb bag. Care should be exercised when mixing under low shear conditions to avoid unhydrated polymer and eliminate waste. Polymer can be slurried into a mineral oil, glycol or alcohol to improve dispersion and mixing efficiency.

Concentration

For most applications, 0.75 to 1.25 lb/bbl should be adequate to maintain an LSRV >25,000 cP. As with other polysaccharides, pH should be maintained in the range of 8.0 to 9.0 for maximum stability. In applications where BHT is above 200°F, use of an oxygen scavenger will prolong polymer life.

Limitations

Optimum performance is achieved in fresh water to low salinity monovalent brines where total salt content is <15%. Under higher salt concentrations, LSRV is suppressed, and may not fully develop even under prolonged mixing. Upper temperature application range is approximately 310° - 325°F. In excess of these temperatures, viscosity recovery is limited, although the addition of commercial clays can improve overall fluid stability.

Toxicology and Safety

GEOVIS XT is non-hazardous and can be used in environmentally sensitive areas.

General Information

Chemical Name: Polysaccharide
Bulk Density: 40 – 50 lb/ft3
Appearance: Cream colored dry powder, <40 mesh
DOT Classification: Non-hazardous, Non-toxic
Packaging: 25 lb or 25 Kg multi-ply, lined bags

Rev. 09/05

Kelco Oil Field Group ▪ 10920 W. Sam Houston Pkwy North, Ste 800 ▪ Houston, TX 77064 ▪ (713) 895-7575

www.kofg.com

Appendix D
Operational Control Program
by Dr. Ozbayoglu

Computer Program on Heat Transfer – Temperature Distribution – Hydraulic Calculations for Abrasive Jet Drilling

Report

Evren Ozbayoglu

This report describes the basic execution principles and the theoretical background about the computer program developed for Impact Technologies in order to estimate the temperature and pressure distribution inside the wellbore during abrasive drilling using CO_2 and N_2. The report consists of an introduction part, theory part, the algorithm, and "manual" sections.

Introduction

One of the major challenges in drilling operations is to estimate the pressure and temperature distribution inside the wellbore accurately. This is required for assuring correct equipment usage, efficient hole cleaning, maximizing drilling efficiency and minimizing the cost per foot. In conventional drilling operations, the fluid inside the drillstring and annular section can be considered as "same", except the fact that the fluid inside the annulus also contains solid particles due to cuttings and formation contamination, and a negligible amount of formation fluid since usually the conditions are overbalanced, i.e., bottomhole pressure is greater than the formation pressure. However, in abrasive jet drilling, the phase inside the string is single phase (either liquid of supercritical), and after the jet, the fluid shifts to gas phase inside the annulus. Therefore, inside the annulus, there will be gas flowing with a very high velocity, drilled cuttings and some formation fluid since the conditions will be usually underbalanced, i..e., bottomhole pressure is less than the formation pressure.

The temperature and pressure distribution inside a wellbore is a challenging problem, but many work have been conducted and there is a good understanding of the problem when conventional drilling is concerned. For this case, since the fluid is incompressible, the calculation methods are relatively straightforward. However, many approaches available in the literature considers the formation having a constant temperature gradient and related temperature distribution (infinite potential assumption), therefore they ignore the cooling effect of the circulating fluid on the formation around the vicinity of the wellbore. This can be included only by a proper and realistic heat transfer model.

The determination of distribution of temperature and pressure inside the wellbore is much more challenging for abrasive drilling due to the presence of a compressible fluid inside the annulus. Also,

when the fluid passes through the jet and changes phase, a significant temperature drop is observed, which is known as Joule Thompson effect. This phenomenon is not observed for conventional drilling operations.

During the scope of this project, a computer program is developed which is capable of estimating temperature and pressure distribution inside the wellbore for both compressible and incompressible fluids considering both Joule Thompson effect and formation cooling.

Theory

This section consists of three parts; i) heat transfer model, ii) hydraulic model, and iii) properties of CO_2.

Heat Transfer Model

In order to determine the temperature distribution inside the wellbore, the following heat transfer model is developed.

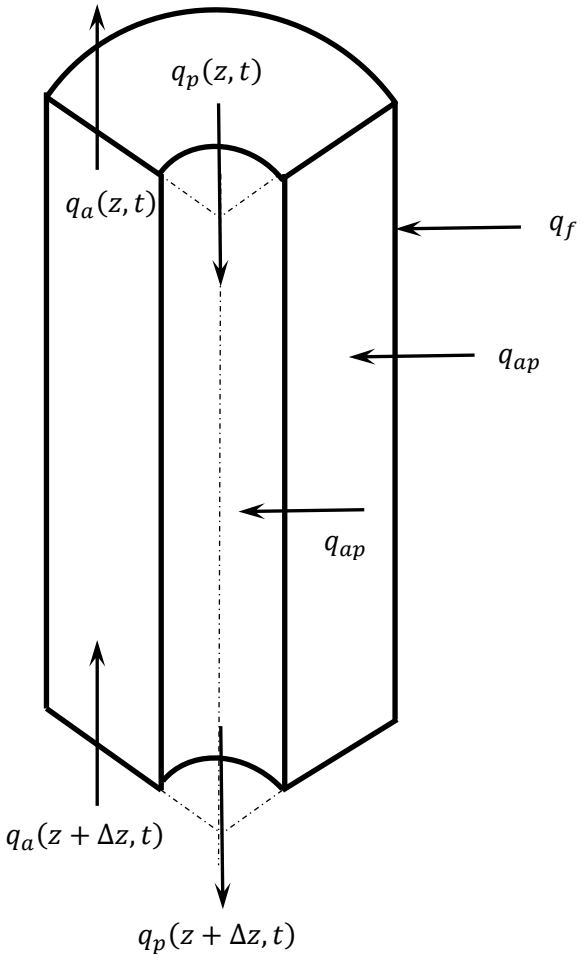

According to this model;

The heat rate in drillpipe at z

$q_p(z) = \dot{m}\, c_p\, T_p(z)$

The heat rate in annulus at z

$q_a(z) = \dot{m}\, c_p\, T_a(z)$

The heat rate from annulus to drillpipe

$$q_{ap} = \frac{\dot{m}\, c_p}{B}\left(T_a - T_p\right)\Delta z$$

where

$$B = \frac{\dot{m}\, c_p}{2\,\pi\, r_p\, U_p}$$

The heat transfer from formation to annulus

$$q_{af} = 2\,\pi\, r_w\, U_a (T_w - T_a)\Delta z = \frac{\dot{m}\, c_p}{A}\left(T_f - T_a\right)\Delta z$$

where

$$A = \frac{\dot{m}\, c_p}{2\,\pi\, r_w\, U_a}\left[\frac{k_f + r_w\, U_a\, f(t_D)}{k_f}\right]$$

In order to solve this model numerically, the values of overall heat transfer coefficients must be determined. Overall heat transfer coefficients are

$$\frac{1}{U_p} = \frac{1}{h_p} + \frac{r_{pi}}{k_{st}}\ln\left(\frac{r_{po}}{r_{pi}}\right) + \frac{r_w}{r_{po}}\frac{1}{h_a}$$

between pipe and annulus, and

$$\frac{1}{U_a} = \frac{1}{h_a} + \frac{r_{ci}}{k_{st}}\ln\left(\frac{r_{co}}{r_{ci}}\right) + \frac{r_{ci}}{k_e}\ln\left(\frac{r_{w\prime}}{r_{co}}\right)$$

between annulus and formation. Here, h_p and h_a can be determined by

$$h_p = \left(\frac{k_f}{2\, r_{pi}}\right)\left(\frac{3.65 + \left(0.00668\, N_{Re}\, N_{Pr}\, 2\, r_{pi}\right)}{1 + 0.04\left(N_{Re}\, N_{Pr}\, 2\, r_{pi}\right)^{0.666}}\right) \text{ for } N_{Re} \geq 10{,}000$$

$$h_p = 0.023\, {N_{Re}}^{0.8}\, {N_{Pr}}^{0.4}\, \frac{k_f}{2\, r_{pi}} \text{ for } N_{Re} < 10{,}000$$

$$h_a = \left(\frac{k_f}{2\, r_w}\right)\left(\frac{3.65+(0.00668\, N_{Re}\, N_{Pr}\, 2\, r_w)}{1+0.04\, (N_{Re}\, N_{Pr}\, 2\, r_w)^{0.666}}\right) \text{ for } N_{Re} \geq 10{,}000$$

$$h_a = 0.023\, {N_{Re}}^{0.8}\, {N_{Pr}}^{0.4}\, \frac{k_f}{2\, r_w} \text{ for } N_{Re} < 10{,}000$$

respectively. In these equations, the term N_{Re} is expressed for fluid inside the pipe as

$$N_{Re} = \frac{2\, r_{pi}\, \dot{m}}{A_p\, \mu_p}$$

and for fluid inside the annulus as

$$N_{Re} = \frac{2\, (r_w - r_{po})\, \dot{m}}{A_a\, \mu_p}$$

considering that A_p and A_a are cross-sectional areas of flow for pipe and annulus, respectively. N_{Pr} for both pipe and annulus is defined as

$$N_{Pr} = \frac{c_p\, \mu_p}{k_f}$$

It should be noted that μ_p and k_f values should be defined for both fluid inside the pipe and annulus separately.

The transient heat flow from the formation to the wellbore wall

$$q_f = \frac{2\, \pi\, k_f}{f(t_D)}(T_f - T_a)\Delta z$$

where

$$T_f = T_{sf} + g_T\, z$$

Here, $f(t_D)$ is defined as

$$f(t_D) = 1.1281\,\sqrt{t_D}\,(1 - 0.3\,t_D) \quad \text{for} \quad 10^{-10} \le t_D \le 1.5$$

and

$$f(t_D) = (0.4063 + 0.5 \ln t_D)\left(1 + \frac{0.6}{t_D}\right) \quad \text{for} \quad t_D > 1.5$$

where

$$t_D = \frac{\alpha_f\, t}{{r_w}^2}$$

and

$$\alpha_f = \frac{k_e}{c_f\, \rho_f}$$

Energy balance applied to the control volume yields;

In drillpipe

$$q_p(z) + q_{ap} = q_p(z + dz)$$

In annulus

$$q_a(z + dz) + q_{af} = q_a(z) + q_{ap}$$

Therefore, using the heat flux definitions and the proper calculus based on the model described, and combining, the governing differential equation can be obtained as

$$A\,B\,\frac{\partial^2 T_p}{\partial z^2} - B\,\frac{\partial T_p}{\partial z} - T_p + T_{sf} + g_T\, z$$

General solution of this differential equation which will be used for estimating fluid temperature inside the drillpipe

$$T_p = \gamma\, e^{\varepsilon_1 z} + \delta\, e^{\varepsilon_2 z} + g_T\, z - B\, g_T + T_{sf}$$

and fluid temperature inside the annulus

$$T_a = (1 + \varepsilon_1\, B)\gamma\, e^{\varepsilon_1 z} + (1 + \varepsilon_2\, B)\delta\, e^{\varepsilon_2 z} + g_T\, z + T_{sf}$$

where

$$\varepsilon_1 = \frac{1}{2\,A}\left(1 - \sqrt{1 + \frac{4\,A}{B}}\right)$$

$$\varepsilon_2 = \frac{1}{2\,A}\left(1 + \sqrt{1 + \frac{4\,A}{B}}\right)$$

Applying boundary conditions

$$T_p(z = 0) = T_{inlet}$$

$$\left.\frac{\partial T_p}{\partial z}\right|_{z=D} = c$$

and considering the fact that there will be a temperature reduction due to Joule Thompson effect (sudden expansion) when the fluid changes the phase after the jet;

$$T_p - T_a = \Delta T|_{z=D}$$

the following equation constants are determined;

$$\gamma = -\frac{\left(T_{inlet} + B\ g_T - T_{sf}\right)\varepsilon_2\ e^{\varepsilon_2 D} + g_T + \xi}{\varepsilon_1\ e^{\varepsilon_1 D} - \varepsilon_2\ e^{\varepsilon_2 D}}$$

$$\delta = \frac{\left(T_{inlet} + B\ g_T - T_{sf}\right)\varepsilon_1\ e^{\varepsilon_1 D} + g_T + \xi}{\varepsilon_1\ e^{\varepsilon_1 D} - \varepsilon_2\ e^{\varepsilon_2 D}}$$

where

$\xi = f(\Delta T, D)$

Finally, the wellbore wall temperature can be obtained as

$$T_w = B\frac{\partial T_p}{\partial z} + T_p = T_a + \left(T_{sf} + g_T\ z - T_a\right)\frac{\dot{m}\ c_p}{2\ \pi\ r_w\ U_a\ A}$$

Hydraulic Modeling

The following schematic drawing is used to describe the pressure distribution inside the wellbore.

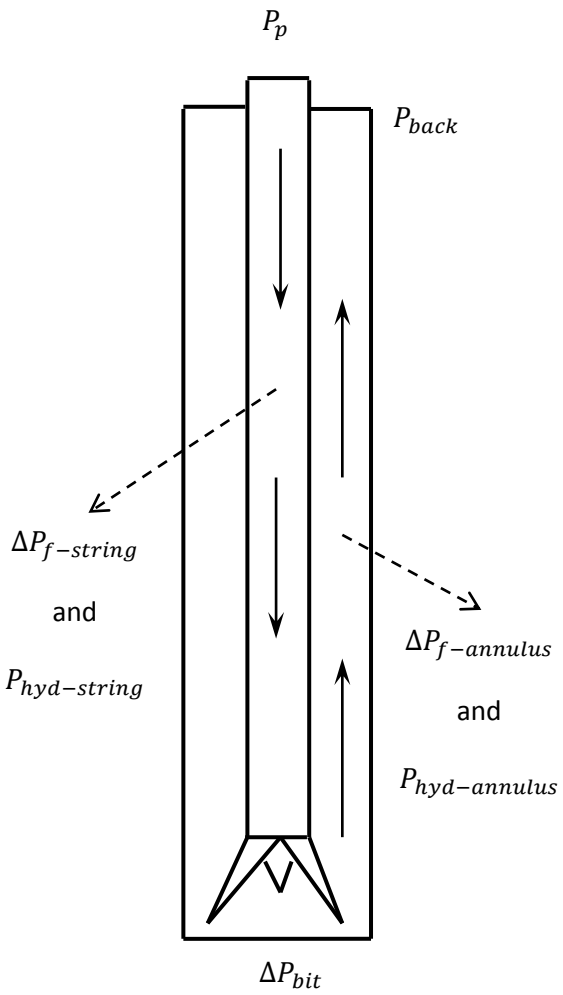

Pump pressure is defined as

$$P_p = \Delta P_{f-string} - P_{hyd-string} + \Delta P_{bit} + \Delta P_{f-annulus} + P_{hyd-annulus} + P_{back}$$

Here,

$$\Delta P_{f-string} = \frac{f_f \, \rho \, v^2}{r_{pi}}$$

$$\Delta P_{f-annulus} = \frac{f_f \, \rho \, v^2}{r_h}$$

where

$$r_h = r_w - r_{po}$$

$$\Delta P_{bit} = \frac{\rho \, Q^2}{2 \, C_d \, {A_n}^2}$$

(C_d is the discharge coefficient, and usually considered as 0.95 for jet nozzles)

$$P_{hyd} = \rho \, g \, D$$

f_f is expressed as a function of N_{Re} using Colebrooks' equation for turbulent flow,

$$\frac{1}{\sqrt{f_f}} = 4 \log\left(N_{Re}\sqrt{f_f}\right) - 0.395$$

and

$$f_f = \frac{16}{N_{Re}}$$

for laminar flow. N_{Re} inside the string is defined as

$$N_{Re} = \frac{2 \, \rho \, v \, r_{pi}}{\bar{\mu}}$$

where

$$\bar{\mu} = \mu_p + \frac{\tau_y \, r_{pi}}{3 \, v}$$

N_{Re} inside the annulus is defined as

$$N_{Re} = \frac{\rho\, v\, 2\, r_h}{\bar{\mu}}$$

where

$$\bar{\mu} = \mu_p + \frac{\tau_y\, r_h}{4\, v}$$

The criteria for laminar to turbulent transition is assumed to be $N_{Re} = 2100$, which is not necessarily to be correct if the fluid has a significant yield stress. However, for this study, the fluid is considered to have no yield stress.

<u>Temperature Drop at the Bit</u>

Due to Joule-Thompson effect, there will be a temperature drop while a compressible fluid flows through a nozzle due to the large pressure drop at the bit. The sudden pressure drop causes an instantaneous volumetric expansion, causing a sudden drop in temperature. Since CO_2 or N_2 will be injected in liquid or supercritical phase through the pipe, while they are passing through the nozzle, the state of phase will change due to pressure drop, which will lead to a temperature decrease. This phenomenon is explained by the general definition of

$$T_2 = \frac{T_1}{\left(\frac{P_1}{P_2}\right)^{\frac{k-1}{k}}}$$

where k is the Joule-Thompson coefficient, defined by the change of pressure with respect to change in temperature at constant enthalpy;

$$k = \left.\frac{\partial P}{\partial T}\right|_H$$

k value shows variations according to the atomic structure of the gas phase, i.e., monoatomic, diatomic and triatomic molecular structures have different *k* values ranging from 1.0 to 1.4.

Influx from Formation

The program can also take the influx from a formation into consideration. Influx causes an increase in the liquid volume inside the annulus, causing an increase in the hydrostatic pressure as well as frictional losses. Also, the temperature distribution inside the wellbore is affected by the influx.

- During this influx consideration, some assumptions are used;
- Productivity index of the formation causing influx is assumed to be constant
- Temperature of the influx is assumed to be equal to the temperature due to geothermal gradient of the field
- Formation pressure is assumed to be equal to the pressure due to normal pressure gradient of the field
- Influx is assumed to be water

The productivity index is defined as

$$PI = \frac{Q}{P_f - P_{ann}}$$

Since annulus may be containing gas, flow rate is converted into mass rate using the in-situ density, which can be determined using real gas law. Total flow inside the annulus becomes the summation of influx rate and volumetric flow rate of the circulation fluid.

Solids in the Wellbore

During the abrasive drilling process, solids are injected through the drillpipe. The contribution of the solids inside the drillpipe is included into consideration as the hydrostatic pressure. The influence of solids inside the pipe on frictional losses is considered only due to density change. The change in the viscosity of the fluid due to presence of solids is ignored.

The mixture density inside the annulus is determined as

$$\rho_{mix} = \rho_f(1 - C_{s1}) + \rho_{s1}C_{s1}$$

Inside the annulus, there are two different solids; i) abrasive solids injected through the drillpipe, and ii) cuttings generated due to drilling process. Therefore, the mixture density inside the annulus considers

both solids types as well as the fluid inside the annulus. As inside the pipe, frictional losses are modified regarding with the change in density due to presence of solids and cuttings inside the annulus.

$$\rho_{mix} = \rho_f\left(1 - (C_{s1+}C_{s2})\right) + \rho_{s1}C_{s1} + \rho_{s2}C_{s2}$$

Additional Water Injection at the Surface

One more option that the program provides is; besides CO_2 or N_2, water can also be injected with these fluids, if needed. The program takes the influence of the additional injected water into consideration for density, viscosity, and fluid specific heat as a mixture. The mixture concentration distribution is determined by using mass rates, i.e., injected liquid has a concentration equal to

$$C_l = \frac{\dot{m}_l}{\dot{m}_l + \dot{m}_f}$$

CO_2 Properties

In order to conduct the calculations for temperature and pressure distribution inside the wellbore, the physical properties of CO_2 must be well defined. The properties include the phase, density, viscosity and thermal conductivity.

The following figures are presenting the physical properties of CO_2 as a function of pressure and temperature.

The phase behavior of CO_2 is described as

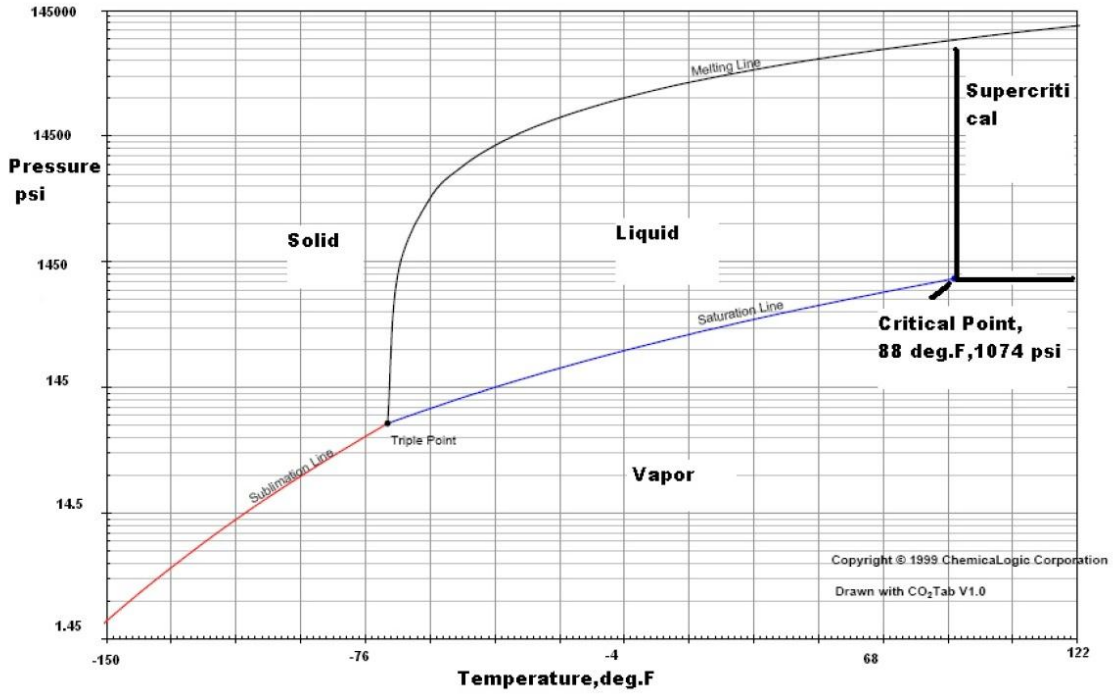

Density of CO_2 is described as shown in the following figure;

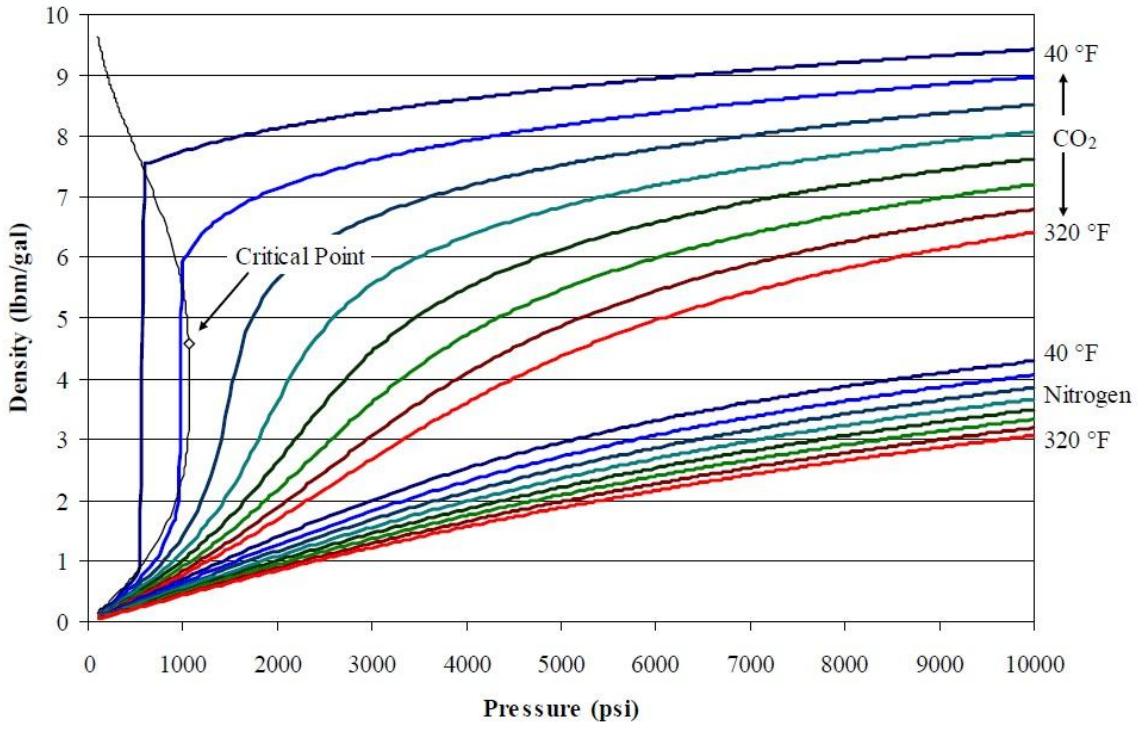

Viscosity of CO_2 is given as

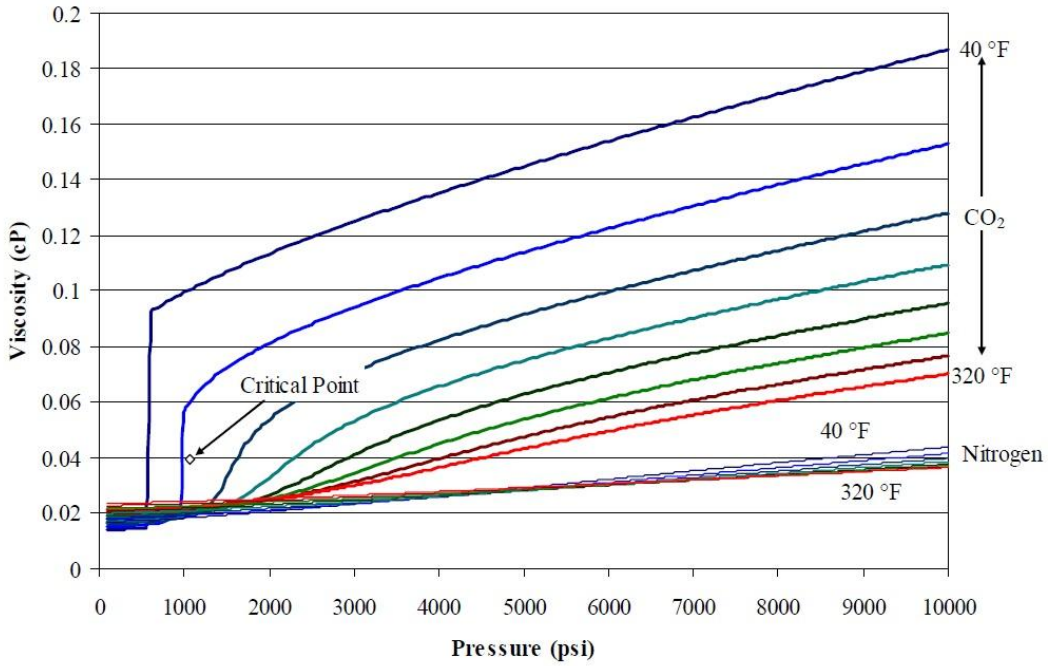

Heat capacity of CO_2 is presented in the following figure;

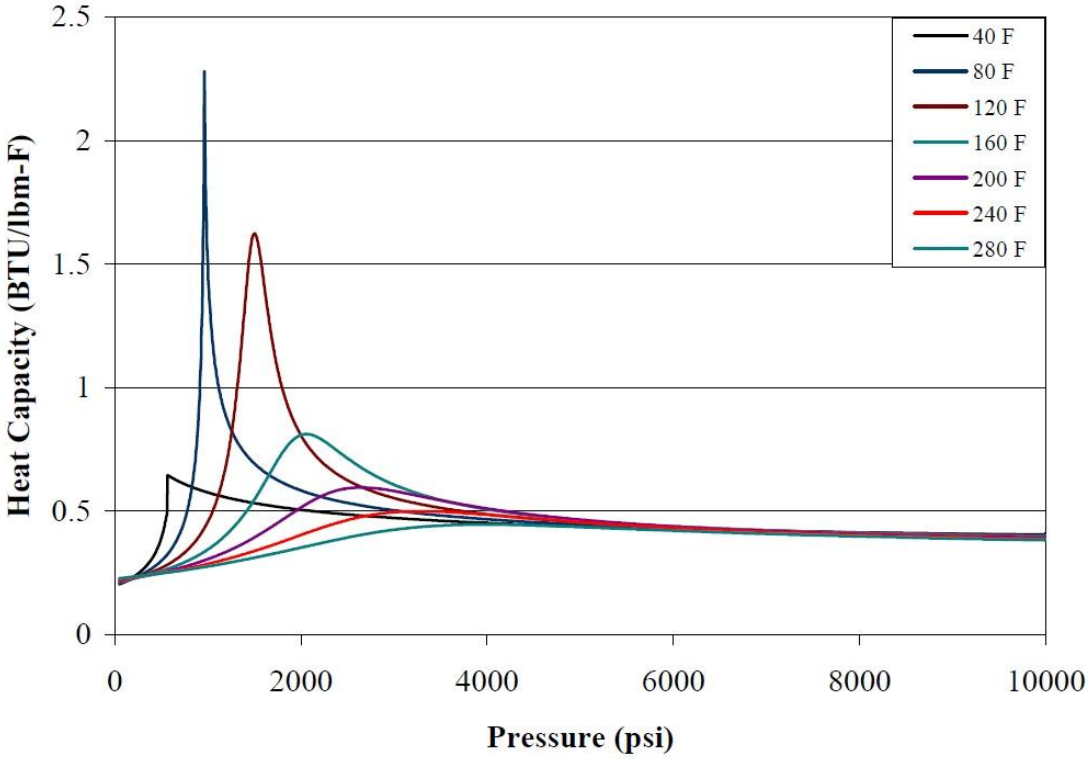

Using the figures presented above, multiple regression techniques are applied after digitizing process for the data given. Then, the following empirical correlations are obtained to define the CO_2 properties;

Density:

$\rho = 4.020134 + 0.000338\,P + 0.000002\,P^2 - 0.04184\,T + 0.000088\,T^2$ for gas phase

$\rho = 6.93583 + 0.00079\,P - 0.036157\,T + 0.000063\,T^2$ for liquid phase and supercritical phase

Viscosity

$\mu = 0.013968\,P^{0.51833}\,T^{-0.548697}$ for gas phase. Since the values are usually around 0.02 cp, this value can also be used as a constant.

$\mu = 0.00000171\,\rho^{4.1878176}$ for liquid phase

$\mu = 1.1\,(0.013968\,P^{0.518333}T^{-0.548697})$ for supercritical phase

Thermal conductivity

$k_f = 0.009$ for gas phase

$k_f = 0.0073\frac{\rho}{7.48} + 0.0036$ for liquid phase

$k_f = 0.015523 + 0.000068\,T^{-0.599136}\,P^{1.0725}$ for supercritical phase

Phase behavior boundaries are approximated using the following equations;

$P_{cr} = 305.0675 + 5.5718\,T + 0.0339\,T^2$

If $> P_{cr}$, then it is liquid phase. Otherwise, the phase is considered as gas.

N_2 Properties

Nitrogen properties are determined using N_2 phase diagrams, and density, viscosity and heat capacity information as a function of temperature and pressure.

Density:

$\rho = 0.318951 + \ 0.000536\, P - 0.003891\, T + 0.000002\, T^2$ for gas phase

$\rho = 0.818951 + 0.000536\, P - 0.003891\, T + 0.000002\, T^2$ for liquid phase and supercritical phase

Viscosity

$\mu = 0.021821627 - 0.00000124\, P + 4.07E - 10\, P^2 - 0.00001512\, T + 1.0307E - 8\, T^2$ for all phases

Thermal conductivity

$k_f = 0.01117$ for all phases

Phase behavior boundaries are approximated using the following equations;

$P_{cr} = 8071.4 + 53{,}142\, T + 0.0882\, T^2$

If $> P_{cr}$, then it is liquid phase. Otherwise, the phase is considered as gas.

Basic Algorithm of the Computer Program

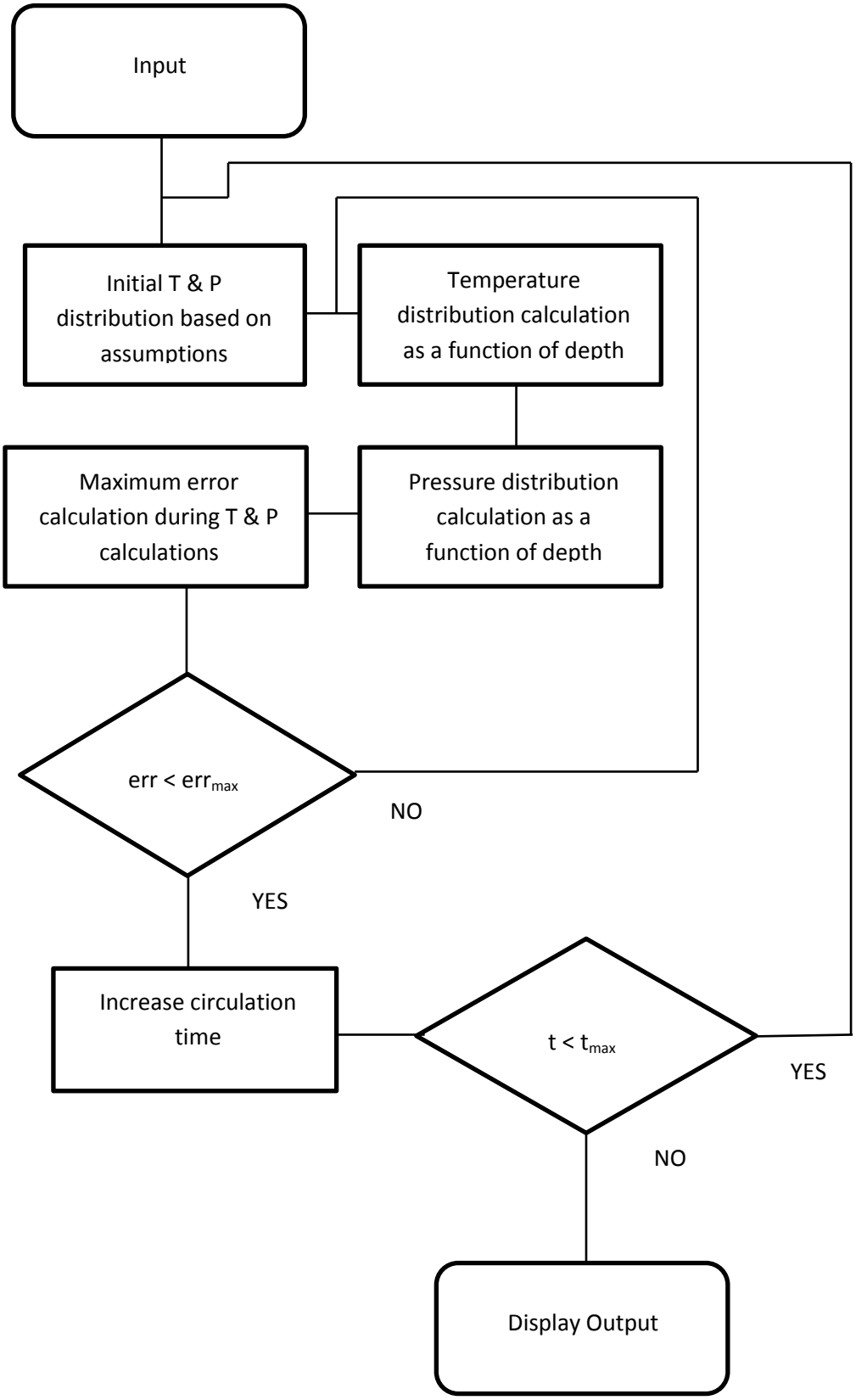

Manual for the Program

The program has prepared in two different versions; 1) inputs manually entered through the screen by the user, and 2) inputs read from an input file.

First version is prepared to be user friendly while entering the data. Each data required is entered by following the instructions given on the screen, since which data and the required unit is mentioned. A typical input screen is as shown in the figure.

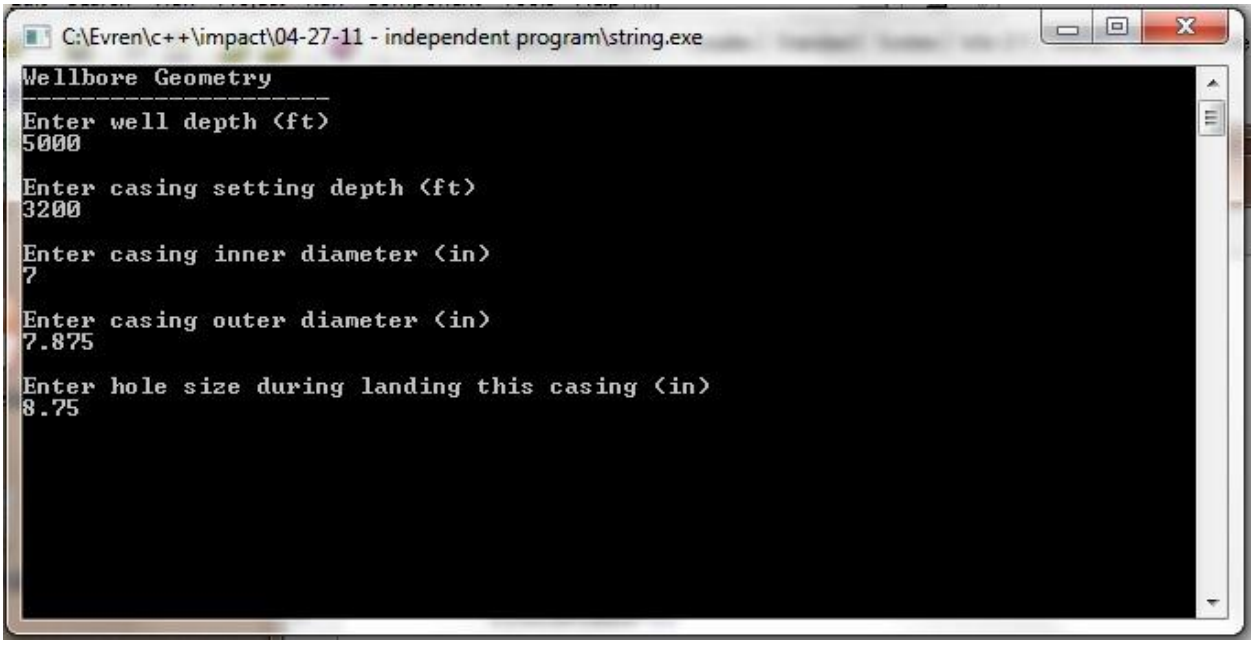

Second version is a direct file input. The input file is shown below:

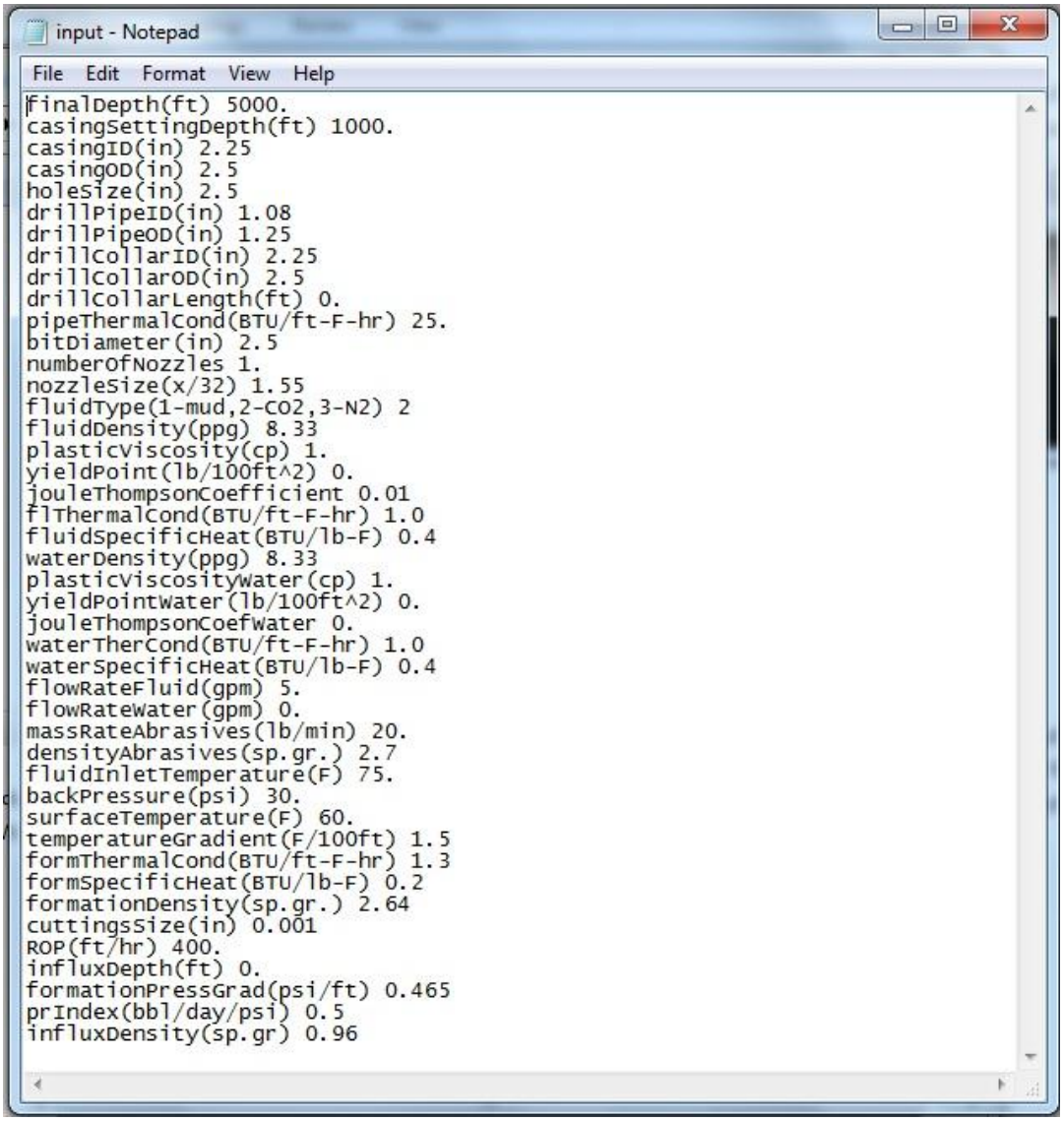

When inputs are completed, the program executes, and prints the results as a table to “out.dat” text file. This file can be directly used in excel by “data import” and “text from file” options. Since the data in the text file is separated by a space from each other, excel will directly recognize, and will put each and every data point in a different cell. Then, any plot can be determined using this data.

A typical out file is shown in the following figure.

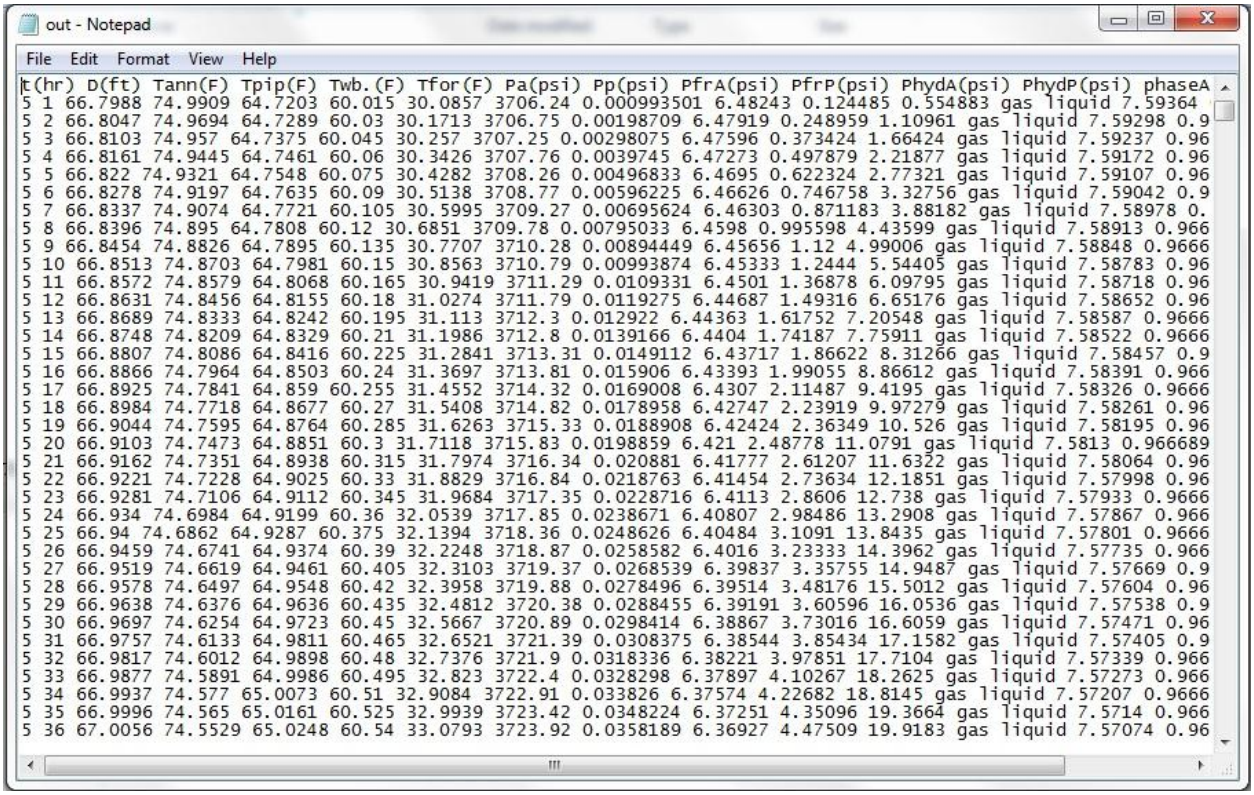

This file is transferred to excel using the “data import” utility.

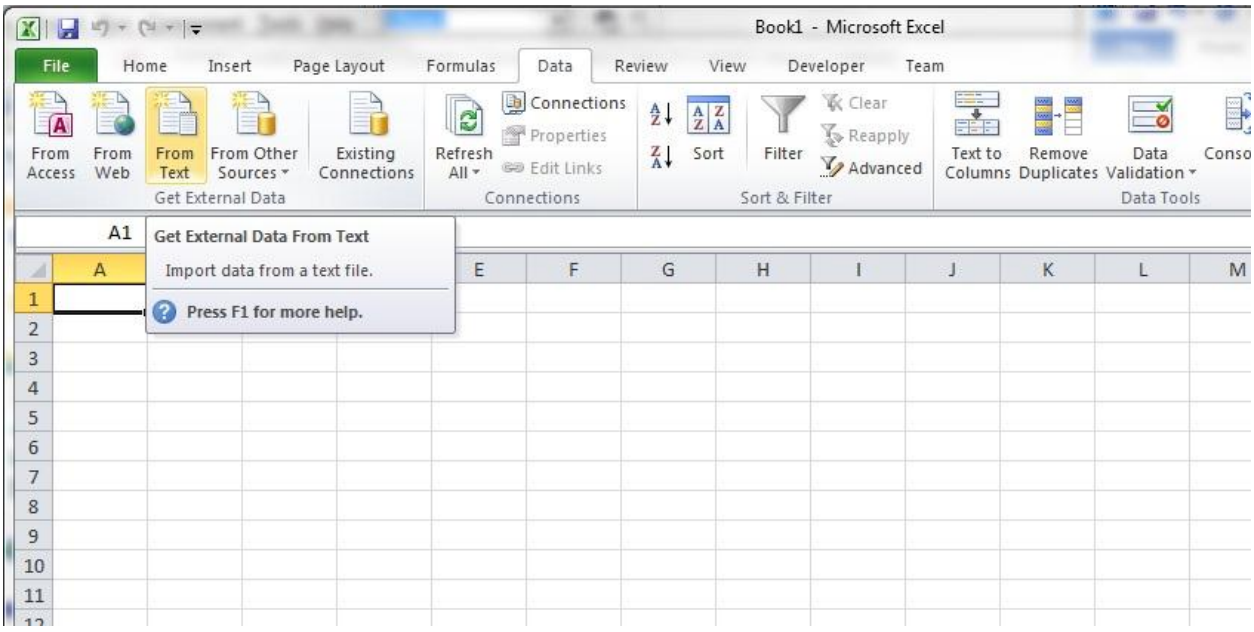

After selecting the file “out.dat” from the folder that it is generated, steps should be followed.

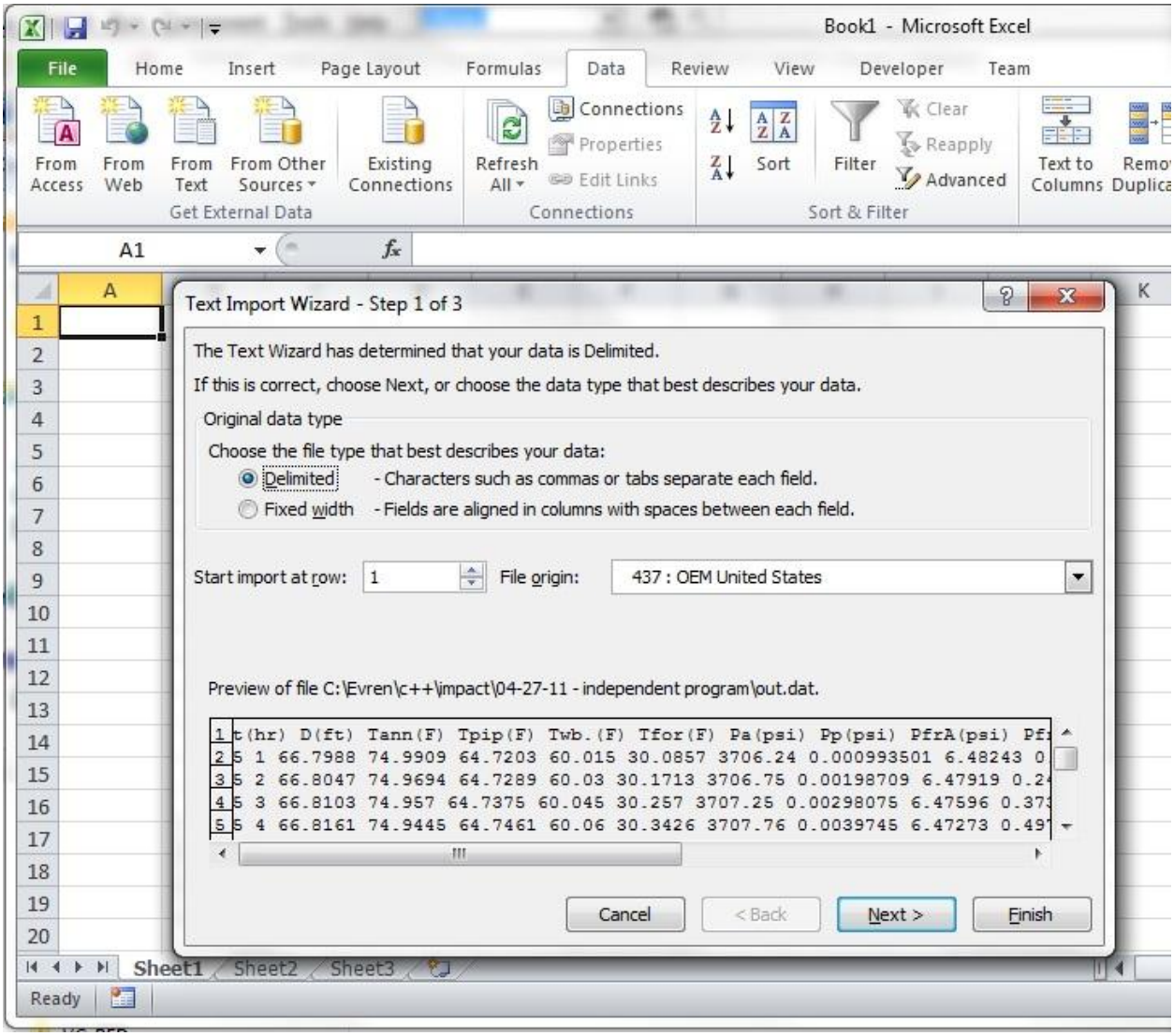

In the “delimiters” box, “space” should be marked.

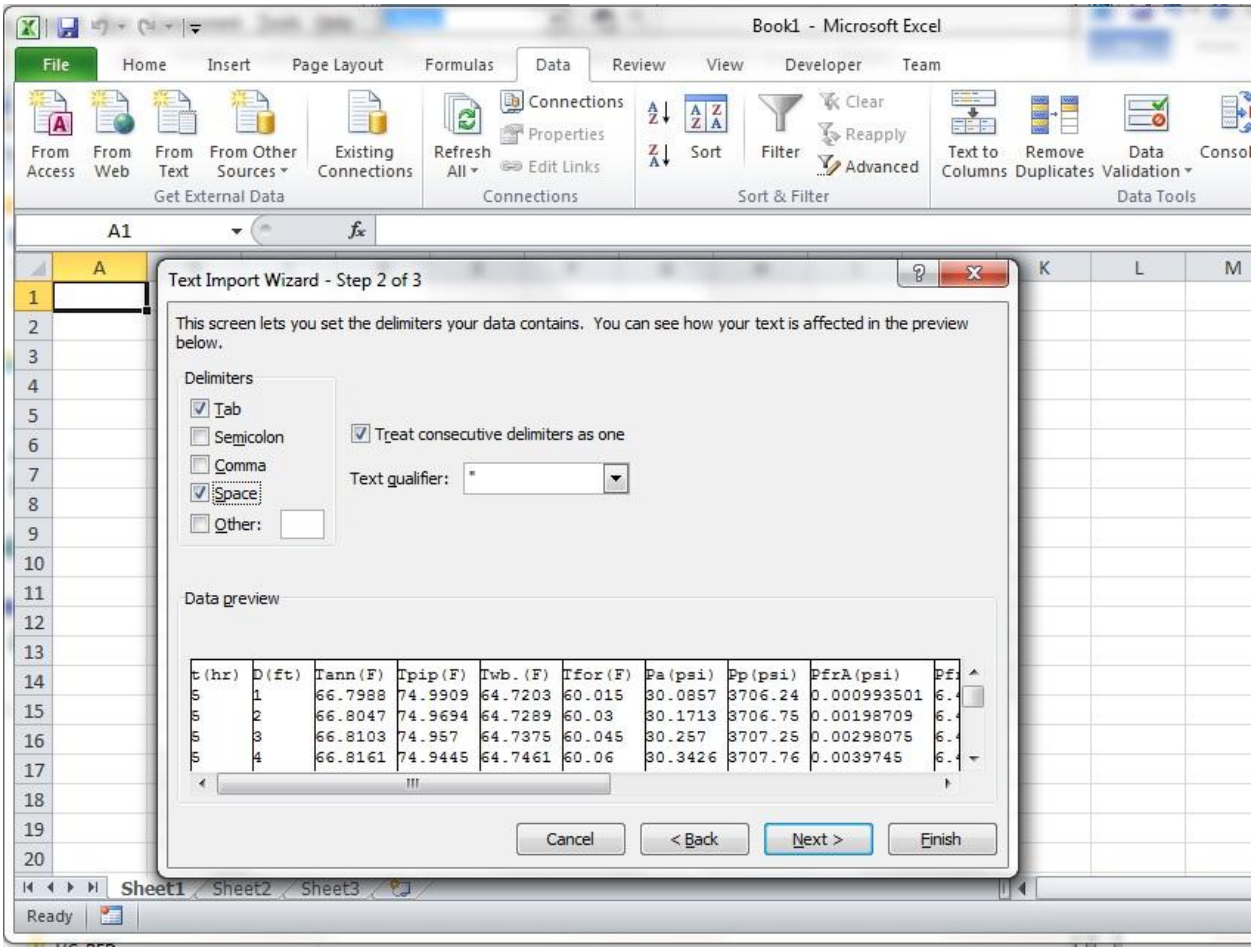

After pressing “Finish” all the data will be transferred onto excel such that, each data point will be recorded on a separate cell.

In case of a failure in calculation during the program is running, an error message will pop up, mentioning that the inputs should be modified.

Nomenclature

α	heat diffusivity of formation
A_p	cross-sectional area of inside of the drillpipe

A_a	cross-sectional area of inside of the annulus
C_d	jet discharge coefficent
c_f	specific heat of formation
ΔP_f	frictional pressure losses
ΔP_{bit}	pressure loss at the bit
D	total depth
c_p	specific heat of drilling fluid
f_f	friction factor
g	gravitational constant
g_T	geothermal gradient
h_a	coefficient of heat transfer of fluid in annulus
h_p	coefficient of heat transfer of fluid in drillpipe
D	well depth
k_{st}	thermal conductivity of pipe or casing
k_e	thermal conductivity of formation and/or cement
k_f	thermal conductivity of drilling fluid
$\dot{m}$	mass flow rate
μ_p	plastic viscosity
$\bar{\mu}$	effective viscosity
N_{Pr}	Prandtl number
N_{Rep}	Reynolds number for drillpipe
N_{Rea}	Reynolds number for annulus
P_{hyd}	hydrostatic pressure
Q	volumetric flow rate
q_{ap}	conductive heat flow across drillpipe
q_{af}	conductive heat flux from formation
q_a	convective heat flow in the annulus

q_p	convective heat flow in the drillpipe, BTU/hr
ρ_f	density of formation, lb/gal
ρ	density of drilling fluid, lb/gal
r_{pi}	drillpipe inner radius
r_{po}	drillpipe outer radius
r_{ci}	casing inner radius
r_{co}	casing outer radius
r_w	wellbore radius
t	circulation time
τ_y	yield stress
T_{inlet}	drillpipe inlet fluid temperature
T_{sf}	surface earth temperature
T_w	temperature at wellbore-formation interface
T_a	fluid temperature in the annulus
T_p	fluid temperature in the drillpipe
T_f	temperature of the formation
t_D	dimensionless time
U_p	overall heat transfer coefficient from annulus to drillpipe
U_a	overall heat transfer coefficient from formation to annulus
v	velocity

Subscripts

g	gas phase
l	liquid phase
mix	mixture
$1,2$	upstream, downstream conditions
s	Solid

APPENDIX

C++ source code for the software developed

```
//---------------------------------------------------------------------------

#include <vcl.h>
#include <conio.h>
#include <stdio.h>
#include <iostream.h>
#include <fstream.h>
#include <stdlib.h>
#include <math.h>
#pragma hdrstop

//---------------------------------------------------------------------------


// variable declarations

int choice, fluidType, fail;
const double e=2.718281828, pi=3.141592654;

// depth - wellbore configuration
double finalDepth;
double casingSettingDepth, casingID, casingOD, holeSize;

// drillstring properties
double drillPipeOD, drillPipeID;
double drillCollarOD, drillCollarID, drillCollarLength;
double pipeThermalConductivity;
// double pipeSpecificHeat;

// bit information
double bitDiameter, numberOfNozzles, nozzleSize;

// fluid properties
double fluidDensity, plasticViscosity, yieldPoint;
double waterDensity, plasticViscosityWater, yieldPointWater;
double fluidThermalConductivity, fluidSpecificHeat, fluidSpecificHeatPipe;
double waterThermalConductivity, waterSpecificHeat;
double overallHeatTransferCoefficientPipeAnnulus;
double overallHeatTransferCoefficientAnnulusFormation;
double flowRate, massFlowRate;
double massFlowRateFluid, massFlowRateWater;
double flowRateFluid, flowRateWater;
double fluidInletTemperature;
double jouleThompsonCoefficient, jouleThompsonCoefficientWater, cPovercV;
double ha, hp;

// abrasive solids
double massRateAbrasives, densityAbrasives;

// pressure - temperature info
double backPressure;
```

```
double surfaceTemperature, temperatureGradient;

// formation properties
double formationThermalConductivity, formationSpecificHeat, formationDensity,
cuttingsSize;

// influx properties
double influxRate, influxDepth, formationPressureGradient, prIndex, influxMassRate,
influxDensity;

// other variables
double circulationTime, circulationTime2, dcirculationTime, finalCirculationTime, depth,
dDepth;
double temperatureInsidePipe[2][20000], temperatureInsideAnnulus[2][20000],
temperatureWellbore[2][20000], temperatureFormation[20000], tBottomhole;
double tfModified, tD;
double pressureInsidePipe[2][20000], pressureInsideAnnulus[2][20000];
double frictionAnnulus[20000], frictionPipe[20000], hydrostaticPipe[20000],
hydrostaticAnnulus[20000];
double hydrostaticPressure, frictionalPressureLoss, bitPressureLoss;
double stringID[20000], stringOD[20000], casID[20000], casOD[20000], boreSize[20000],
boreSizeOld[20000];
double cementThermalConductivity;
double bitUpstreamPressure, bitDownstreamPressure, bitPressureDrop,
bitUpstreamTemperature, bitDownstreamTemperature;
double maxErr, err, printMaxErr;
double deltaT, delT[20000];
double cuttingsConcentration[20000], ROP, transportRatio;
int fluidPhase, phaseInsidePipe[20000], phaseInsideAnnulus[20000];
int errDepth;
bool printErr, screenInput;

// temporary parameters, can be removed later
double parUa[20000], parUp[20000], parK1[20000], parK2[20000];


void clearScreen()
{
 // cleans the screen
     getch();
     clrscr();

}



void inputPage()
{

  bool check;
  int morePipe,i,pipeNo;
  char defDum1[15],defDum2[23],defDum3[13],defDum4[13],defDum5[13];
  char defDum6[16],defDum7[16],defDum8[18],defDum9[18],defDum10[22];
  char defDum11[29],defDum12[16],defDum13[16],defDum14[17],defDum15[28];
  char defDum16[18],defDum17[21],defDum18[23],defDum19[25],defDum20[27];
  char defDum21[28],defDum22[18],defDum23[26],defDum24[28],defDum25[23];
  char defDum26[27],defDum27[28],defDum28[19],defDum29[19],defDum30[26];
  char defDum31[25],defDum32[25],defDum33[18],defDum34[22],defDum35[29];
```

```
 char defDum36[29],defDum37[27],defDum38[25],defDum39[17],defDum40[11];
 char defDum41[16],defDum42[27],defDum43[21],defDum44[21];
//   clrscr();

//   printf("Please enter the input type\n");
//   printf("\n");
//   printf("For manual input, press '0', then press ENTER\n");
//   printf("For file input, press '1', then press ENTER\n");
//   printf("\n");

//   cin >> screenInput;

   screenInput=1;
   switch (screenInput)
   {
     case 0: // Manual Input
     {

       printf("Input Data:\n");
       printf("\n");
       printf("(Press any key to continue ...)\n");
       getch();
       clrscr();

       printf("Wellbore Geometry\n");
       printf("---------------------\n");
       printf("Enter well depth (ft)\n");
       cin >> finalDepth;
       printf("\n");

       printf("Enter casing setting depth (ft)\n");
       cin >> casingSettingDepth;
       printf("\n");

       if (casingSettingDepth>0)
       {
         printf("Enter casing inner diameter (in)\n");
         cin >> casingID;
         printf("\n");

         printf("Enter casing outer diameter (in)\n");
         cin >> casingOD;
         printf("\n");

         printf("Enter hole size during landing this casing (in)\n");
         cin >> holeSize;
         printf("\n");
       }
       clrscr();

       printf("Drillstring Properties\n");
       printf("---------------------\n");
       printf("Enter drillpipe inner diameter (in)\n");
       cin >> drillPipeID;
       printf("\n");

       printf("Enter drillpipe outer diameter (in)\n");
       cin >> drillPipeOD;
```

```
        printf("\n");

        printf("Enter drill collar length (ft)\n");
        cin >> drillCollarLength;
        printf("\n");

        if (drillCollarLength>0)
        {
          printf("Enter drill collar inner diameter (in)\n");
          cin >> drillCollarID;
          printf("\n");

          printf("Enter drill collar outer diameter (in)\n");
          cin >> drillCollarOD;
          printf("\n");
        }

        printf("Enter thermal conductivity of the pipe (BTU/ft-F-hr)\n");
        cin >> pipeThermalConductivity;
        printf("\n");

//        printf("Enter specific heat of the pipe (BTU/ft-F-hr)\n");
//        cin >> pipeSpecificHeat;
//        printf("\n");

        clrscr();

        printf("Bit Properties\n");
        printf("----------------------\n");
        printf("Enter bit diameter (in)\n");
        cin >> bitDiameter;
        printf("\n");

        printf("Enter number of nozzles \n");
        cin >> numberOfNozzles;
        printf("\n");

        printf("Enter nozzle size \n");
        cin >> nozzleSize;
        printf("\n");

        clrscr();

        printf("Fluid Properties\n");
        printf("----------------------\n");
        printf("Select fluid type\n");
        printf(" \n");
        printf("1 - Mud\n");
        printf("2 - CO2\n");
        printf("3 - N2\n");
        printf(" \n");
        printf("(please select the fluid type, then press ENTER\n");
        cin >> fluidType;
        clrscr();

        switch (fluidType)
        {
          case 1:
```

```
      {
        printf("Enter mud density (ppg)\n");
        cin >> fluidDensity;
        printf("\n");

        printf("Enter plastic viscosity (cp)\n");
        cin >> plasticViscosity;
        printf("\n");

        printf("Enter yield point (lb/100ft^2)\n");
        cin >> yieldPoint;
        printf("\n");

        printf("Enter thermal conductivity of the fluid (BTU/ft-F-hr)\n");
        cin >> fluidThermalConductivity;
        printf("\n");

        printf("Enter specific heat of the fluid (BTU/lb-F)\n");
        cin >> fluidSpecificHeat;
        printf("\n");

        clrscr();
        break;
      }

      case 2:
      {
// CO2 properties are calculated in the program (these are dummy values)
        fluidDensity=1.;
        plasticViscosity=1.;
        yieldPoint=1.;
        fluidThermalConductivity=1.;
        fluidSpecificHeat=1.;

        break;
      }

      case 3:
      {
// N2 properties are calculated in the program (these are dummy values)
        fluidDensity=1.;
        plasticViscosity=1.;
        yieldPoint=1.;
        fluidThermalConductivity=1.;
        fluidSpecificHeat=1.;

        break;
      }
    }

    printf("Enter flow rate (gpm)\n");
    cin >> flowRateFluid;
    printf("\n");

    printf("Enter flow rate of water injected (gpm) (if no, enter 0)\n");
    cin >> flowRateWater;
    printf("\n");
```

```
        printf("Enter fluid inlet temperature (F)\n");
        cin >> fluidInletTemperature;
        printf("\n");

        printf("Enter backpressure (psi)\n");
        cin >> backPressure;
        printf("\n");

        clrscr();

        printf("Abrasive Solids Information\n");
        printf("----------------------\n");
        printf("Enter mass rate of abrasive solids (lb/min)\n");
        cin >> massRateAbrasives;
        printf("\n");

        printf("Enter density of abrasive solids (sp.gr)\n");
        cin >> densityAbrasives;
        printf("\n");

        clrscr();

        printf("Temperature Information\n");
        printf("----------------------\n");
        printf("Enter surface temperature (F)\n");
        cin >> surfaceTemperature;
        printf("\n");

        printf("Enter temperature gradient (F/100ft)\n");
        cin >> temperatureGradient;
        printf("\n");

        clrscr();

        printf("Formation Properties\n");
        printf("----------------------\n");
        printf("Enter thermal conductivity of the formation (BTU/ft-F-hr)\n");
        cin >> formationThermalConductivity;
        printf("\n");

        printf("Enter specific heat of the formation (BTU/lb-F)\n");
        cin >> formationSpecificHeat;
        printf("\n");

        printf("Enter formation density (sp.gr.)\n");
        cin >> formationDensity;
        printf("\n");

        printf("Enter influx depth (ft) (if no flux, set depth to 0)\n");
        cin >> influxDepth;
        printf("\n");

        if (influxDepth>0)
        {
          printf("Enter productivity index for influx (bbl/day/psi) (suggested value =
0.5)\n");
          cin >> prIndex;
          printf("\n");
```

```
          printf("Enter formation pressure gradient (psi/ft) (if not known, enter
0.465)\n");
          cin >> formationPressureGradient;
          printf("\n");

          printf("Enter influx density (sp.gr) (if no flux, set depth to 0)\n");
          cin >> influxDensity;
          printf("\n");
        }


        printf("Enter average cuttings size (in)\n");
        cin >> cuttingsSize;
        printf("\n");

        printf("Enter rate of penetration (ft/hr)\n");
        cin >> ROP;
        printf("\n");


        clrscr();

       break;
      }

      case 1:  // File input
      {
        ifstream inFile;
        inFile.open ("input.dat");
        inFile >> defDum1 >> finalDepth;
        inFile >> defDum2 >> casingSettingDepth;
        inFile >> defDum3 >> casingID;
        inFile >> defDum4 >> casingOD;
        inFile >> defDum5 >> holeSize;
        inFile >> defDum6 >> drillPipeID;
        inFile >> defDum7 >> drillPipeOD;
        inFile >> defDum8 >> drillCollarID;
        inFile >> defDum9 >> drillCollarOD;
        inFile >> defDum10 >> drillCollarLength;
        inFile >> defDum11 >> pipeThermalConductivity;

        inFile >> defDum12 >> bitDiameter;
        inFile >> defDum13 >> numberOfNozzles;
        inFile >> defDum14 >> nozzleSize;

        inFile >> defDum15 >> fluidType;
        inFile >> defDum16 >> fluidDensity;
        inFile >> defDum17 >> plasticViscosity;
        inFile >> defDum18 >> yieldPoint;
        inFile >> defDum19 >> jouleThompsonCoefficient;
        inFile >> defDum20 >> fluidThermalConductivity;
        inFile >> defDum21 >> fluidSpecificHeat;

        inFile >> defDum22 >> waterDensity;
        inFile >> defDum23 >> plasticViscosityWater;
        inFile >> defDum24 >> yieldPointWater;
        inFile >> defDum25 >> jouleThompsonCoefficientWater;
```

```
        inFile >> defDum26 >> waterThermalConductivity;
        inFile >> defDum27 >> waterSpecificHeat;
        inFile >> defDum28 >> flowRateFluid;
        inFile >> defDum29 >> flowRateWater;

        inFile >> defDum30 >> massRateAbrasives;
        inFile >> defDum31 >> densityAbrasives;

        inFile >> defDum32 >> fluidInletTemperature;
        inFile >> defDum33 >> backPressure;
        inFile >> defDum34 >> surfaceTemperature;
        inFile >> defDum35 >> temperatureGradient;
        inFile >> defDum36 >> formationThermalConductivity;
        inFile >> defDum37 >> formationSpecificHeat;
        inFile >> defDum38 >> formationDensity;
        inFile >> defDum39 >> cuttingsSize;
        inFile >> defDum40 >> ROP;

        inFile >> defDum41 >> influxDepth;
        inFile >> defDum42 >> formationPressureGradient;
        inFile >> defDum43 >> prIndex;
        inFile >> defDum44 >> influxDensity;


        inFile.close();

//      clrscr();
      break;
      }
    }
/*
  finalDepth=5.;        // 15000
  casingSettingDepth=0.;  // 10000
  casingID=2.25;
  casingOD=2.5;
  holeSize=2.5;
  drillPipeID=1.08;
  drillPipeOD=1.25;
  drillCollarID=2.25;
  drillCollarOD=2.5;
  drillCollarLength=0.;
  pipeThermalConductivity=25;
//  pipeSpecificHeat=600;
  bitDiameter=2.5;
  numberOfNozzles=1;
  nozzleSize=1.55;
  fluidType=2.;
  fluidDensity=8.33;
  plasticViscosity=1.;
  yieldPoint=0;
  jouleThompsonCoefficient=0.01;
  fluidThermalConductivity=1.0;    // 0.33
  fluidSpecificHeat=0.4;          // 1.1

  waterDensity=8.33;
  plasticViscosityWater=1.;
  yieldPointWater=0;
  jouleThompsonCoefficientWater=0.;
```

```
  waterThermalConductivity=1.0;    // 0.33
  waterSpecificHeat=0.4;          // 1.1

  flowRateFluid=5.;
  flowRateWater=0.;

  massRateAbrasives=20.;
  densityAbrasives=2.7;

  fluidInletTemperature=75.;
  backPressure=30.;
  surfaceTemperature=60.;
  temperatureGradient=1.5;
  formationThermalConductivity=1.3;
  formationSpecificHeat=0.2;
  formationDensity=2.64;
  cuttingsSize=0.001;
  ROP=400.;

  influxDepth=0.;
  formationPressureGradient=0.465;
  prIndex=0.5;
  influxDensity=0.96;
*/

  if (influxDepth == 0)
  {
    influxDensity=8.;
    prIndex=0.1;
    formationPressureGradient=0.465;
    waterDensity=8.33;
    plasticViscosityWater=1.;
    yieldPointWater=0;
    jouleThompsonCoefficientWater=0.;
  }

  if (casingSettingDepth == 0)
  {
    casingID=bitDiameter-1.;
    casingOD=bitDiameter;
    holeSize=bitDiameter;
  }

  if (drillCollarLength == 0)
  {
    drillCollarID=drillPipeID;
    drillCollarOD=drillPipeOD;
  }

}


void unitConversion()
{
 // converting units to proper field units for calculations (if needed)

//  finalDepth    // ft
//  casingSettingDepth  // ft
```

```
  casingID=casingID/12.;   // in to ft
  casingOD=casingOD/12.;   // in to ft
  holeSize=holeSize/12.;   // in to ft
  drillPipeID=drillPipeID/12.;  // in to ft
  drillPipeOD=drillPipeOD/12.;  // in to ft
  drillCollarID=drillCollarID/12.;   // in to ft
  drillCollarOD=drillCollarOD/12.;   // in to ft
//  drillCollarLength    // ft
//  pipeThermalConductivity  // BTU-ft/(ft^2-hr-F)
//  pipeSpecificHeat     //  BTU/(lb-F)
  bitDiameter=bitDiameter/12.;  // in to ft
  nozzleSize=nozzleSize/32.;  // in*32 to in
  fluidDensity=fluidDensity*7.48;  // lb/gal to lb/ft^3
  plasticViscosity=plasticViscosity*2.4191;   // cp to lb/(ft-hr)
  yieldPoint=yieldPoint*100.;   // lb/100-ft^2 to lb/ft^2
  waterDensity=waterDensity*7.48;  // lb/gal to lb/ft^3
  influxDensity=influxDensity*62.4;  // sp.gr to lb/ft^3
  plasticViscosityWater=plasticViscosityWater*2.4191;   // cp to lb/(ft-hr)
  yieldPointWater=yieldPointWater*100.;   // lb/100-ft^2 to lb/ft^2
//  fluidThermalConductivity    // BTU-ft/(ft^2-hr-F)
//  fluidSpecificHeat    //  BTU/(lb-F)
  flowRateFluid=flowRateFluid*8.020833;  // gpm to ft^3/hr
  flowRateWater=flowRateWater*8.020833;  // gpm to ft^3/hr
  backPressure=backPressure*144.;   // psi to lb/ft^2
  massRateAbrasives=massRateAbrasives*60.;  // lb/min to lb/hr
  densityAbrasives=densityAbrasives*62.4;  // sp.gr to lb/ft^3
  formationPressureGradient=formationPressureGradient*144.;
//  surfaceTemperature   // F
//  surfaceTemperature   // F
  temperatureGradient=temperatureGradient/100.;  // F/100-ft to F/ft
//  formationThermalConductivity   // BTU-ft/(ft^2-hr-F)
//  formationSpecificHeat    //   BTU/(lb-F)
  formationDensity=formationDensity*62.4;   // sp.gr. to lb/ft^3
  cuttingsSize=cuttingsSize/12.;          // in to ft
  prIndex=prIndex*0.0016247;       // bbl/day/psi to ft^3/hr/lb/ft^2
// ROP     // ft/hr

}


void outputPage()
{
 //   printf("Results written on 'out.dat' file \n");
 //   printf(" \n");

    if (printErr==1)
    {
 //     printf("\n");
 //     printf("Forced convergence : ");
 //     cout << printMaxErr;
 //     printf(" at ");
 //     cout << errDepth;
 //     printf (" ft");
 //     printf("\n");
 //     printf("\n");
    }

 //   printf("Press any key to continue ...");
```

```
}


void intro()
{

 //   printf("Welcome to Impact Design Program\n");
 //   printf("\n");
 //   printf("Press any key to continue ..\n");
 //   clearScreen();

}


void intro1()
{

 //   printf("Please press '1' to continue, '0' for EXIT, then press ENTER\n");
 //   printf("\n");

}


void fluidPropertyDetermination(double t, double p, double s)
{
  double phaseP;

 // this section requires modification according to the fluid in use

    if (p<=0.)
     p=0.001;

    switch (fluidType)
    {
      case 1:
      {
        fluidPhase=0;

        fluidDensity=fluidDensity;

        plasticViscosity=plasticViscosity;
        yieldPoint=yieldPoint;

        fluidThermalConductivity=fluidThermalConductivity;
        fluidSpecificHeat=fluidSpecificHeat;

        jouleThompsonCoefficient=jouleThompsonCoefficient;
        cPovercV=1.;

        break;
      }

      case 2:     // CO2
      {
       // phase calculation
        phaseP=305.0675+5.5718*t+0.0339*pow(t,2.);
        if (p<phaseP) // gas phase
        {
```

```
          fluidPhase=1;
 //         if (t<=0)
           fluidDensity=4.020134+p*0.000338+0.000002*pow(p,2.)-
0.041840*t+0.000088*pow(t,2.);
 //         else
 //          fluidDensity=0.00238*pow(p,1.82064)*pow(t,-1.18085);
          if (fluidDensity<0.05)
           fluidDensity=0.05;
          else if (fluidDensity>10.)
           fluidDensity=10.;
          fluidDensity=fluidDensity*7.48;

 //         plasticViscosity=0.013968*pow(p,0.518333)*pow(t,-0.548697);
 //         if (plasticViscosity<0.0001)
 //          plasticViscosity=0.0001;
          plasticViscosity=0.02;
          plasticViscosity=plasticViscosity*2.4191;
          yieldPoint=0.0012;

       //   fluidThermalConductivity=0.015523+0.000068*pow(t,-0.599136)*pow(p,1.0725);
          fluidThermalConductivity=0.009;
          fluidSpecificHeat=0.201961+0.00008037237057561171*t-1.4522474376118E-
08*pow(t,2.)+8.06809443440048E-13*pow(t,3.);

       //  jouleThompsonCoefficient=0.0012; // F/psi
          jouleThompsonCoefficient=0.012;
          cPovercV=1.37;
        }

        if (p>=phaseP) // liquid phase
        {
          fluidPhase=0;

      //    fluidDensity=1.389954*pow(p,0.356736)*pow(t,-0.311397);      //
fluidDensity=-0.0007*pow(t,2.)+0.0323*t+7.3848;
          fluidDensity=6.935830+p*0.000790+0.000000*pow(p,2.)-
0.036157*t+0.000063*pow(t,2.);
          if (fluidDensity>12.)
           fluidDensity=12.;

          plasticViscosity=0.0000171*pow(fluidDensity,4.18781759);     //
plasticViscosity=-0.00007*pow(t,2.)-0.0012*t+1.1116;     //
plasticViscosity=0.013968*pow(p,0.518333)*pow(t,-0.548697);
          if (plasticViscosity<0.0001)
           plasticViscosity=0.0001;
          plasticViscosity=plasticViscosity*2.4191;
          fluidDensity=fluidDensity*7.48;
          yieldPoint=0.;

      //    fluidThermalConductivity=-0.000004*pow(t,2.)+0.0001*t+0.0613;        //
fluidThermalConductivity=0.015523+0.000068*pow(t,-0.599136)*pow(p,1.0725);
          fluidThermalConductivity=0.0073*fluidDensity/7.48+0.0036;
      //    fluidSpecificHeat=0.497;
          fluidSpecificHeat=195645.*pow((fluidDensity/7.48),-6.306);

       //   jouleThompsonCoefficient=0.0012; // F/psi
          jouleThompsonCoefficient=0.0012;
          cPovercV=1.05;
```

```
        }

        if ((p>1054.)&&(t>87.65)) // supercritical phase
        {
          fluidPhase=2;

          // fluidDensity=1.389954*pow(p,0.356736)*pow(t,-0.311397);
          fluidDensity=6.935830+p*0.000790+0.000000*pow(p,2.)-
0.036157*t+0.000063*pow(t,2.);
          if (fluidDensity>10.)
           fluidDensity=10.;

          fluidDensity=fluidDensity*7.48;
          plasticViscosity=1.1*(0.013968*pow(p,0.518333)*pow(t,-0.548697));
          if (plasticViscosity<0.0001)
           plasticViscosity=0.0001;
          plasticViscosity=plasticViscosity*2.4191;
          yieldPoint=0.;

          fluidThermalConductivity=0.015523+0.000068*pow(t,-0.599136)*pow(p,1.0725);
       //   fluidSpecificHeat=0.201961+0.00008032370575611 71*t-1.4522474376118E-
08*pow(t,2.)+8.06809443440048E-13*pow(t,3.);
          fluidSpecificHeat=0.497;

       //   jouleThompsonCoefficient=0.0012; // F/psi
          jouleThompsonCoefficient=0.0015;
          cPovercV=1.05;
        }


        break;
      }

      case 3:     // N2
      {
       // phase calculation
        phaseP=0.0882*pow(t,2.)+53.142*t+8071.4;
        if (p<phaseP) // gas phase
        {
          fluidPhase=1;
          if (t<0)
           fluidDensity=0.318951+p*0.000536-0.000000*pow(p,2.)-
0.003891*t+0.000002*pow(t,2.);
          else
           fluidDensity=0.023887*pow(p,0.662326)*pow(t,-0.212517);
          if (fluidDensity<0.01)
           fluidDensity=0.01;
          else if (fluidDensity>10.)
           fluidDensity=10.;
          fluidDensity=fluidDensity*7.48;

          plasticViscosity=0.021821627261426+p*-1.24207108829138E-06+4.07329587745606E-
10*pow(p,2.)+t*-0.00001512006347938 47+1.30689389694566E-08*pow(t,2.);
          if (plasticViscosity<0.0001)
           plasticViscosity=0.0001;
          plasticViscosity=plasticViscosity*2.4191;
          yieldPoint=0.;
```

```
       //   fluidThermalConductivity=0.015523+0.000068*pow(t,-0.599136)*pow(p,1.0725);
          fluidThermalConductivity=0.01117;
          fluidSpecificHeat=0.231961+0.00008033237057561171*t-1.4522474376118E-
08*pow(t,2.)+8.06809443440048E-13*pow(t,3.);

       //  jouleThompsonCoefficient=0.0012; // F/psi
          jouleThompsonCoefficient=0.012;
          cPovercV=1.39;
        }

        if (p>=phaseP) // liquid phase
        {
       //   fluidDensity=0.023887*pow(p,0.662326)*pow(t,-0.212517);
          fluidDensity=0.818951+p*0.000536-0.000000*pow(p,2.)-
0.003891*t+0.000002*pow(t,2.);
          if (fluidDensity<0.05)
           fluidDensity=0.05;
          else if (fluidDensity>12.)
           fluidDensity=12.;
          fluidDensity=fluidDensity*7.48;

          plasticViscosity=0.021821627261426+p*-1.24207108829138E-06+4.07329587745606E-
10*pow(p,2.)+t*-0.00001512006347938 47+1.30689389694566E-08*pow(t,2.);
          if (plasticViscosity<0.0001)
           plasticViscosity=0.0001;
          plasticViscosity=plasticViscosity*2.4191;
          yieldPoint=0.;

       //   fluidThermalConductivity=0.015523+0.000068*pow(t,-0.599136)*pow(p,1.0725);
          fluidThermalConductivity=0.01117;
          fluidSpecificHeat=0.231961+0.00008033237057561171*t-1.4522474376118E-
08*pow(t,2.)+8.06809443440048E-13*pow(t,3.);

       //   jouleThompsonCoefficient=0.0012; // F/psi
          jouleThompsonCoefficient=0.0012;
          cPovercV=1.39;
        }

        if ((p>1054.)&&(t>87.65)) // supercritical phase
        {
          fluidPhase=2;
          fluidDensity=0.818951+p*0.000536-0.000000*pow(p,2.)-
0.003891*t+0.000002*pow(t,2.);
      //    fluidDensity=0.023887*pow(p,0.662326)*pow(t,-0.212517);
          if (fluidDensity<0.05)
           fluidDensity=0.05;
          else if (fluidDensity>10.)
           fluidDensity=10.;
          fluidDensity=fluidDensity*7.48;

          plasticViscosity=0.021821627261426+p*-1.24207108829138E-06+4.07329587745606E-
10*pow(p,2.)+t*-0.00001512006347938 47+1.30689389694566E-08*pow(t,2.);
          if (plasticViscosity<0.0001)
           plasticViscosity=0.0001;
          plasticViscosity=plasticViscosity*2.4191;
          yieldPoint=0.;

       //   fluidThermalConductivity=0.015523+0.000068*pow(t,-0.599136)*pow(p,1.0725);
```

```
          fluidThermalConductivity=0.01117;
          fluidSpecificHeat=0.231961+0.00080323705756117l*t-1.4522474376118E-
08*pow(t,2.)+8.06809443440048E-13*pow(t,3.);

       //   jouleThompsonCoefficient=0.0012; // F/psi
          jouleThompsonCoefficient=0.0015;
          cPovercV=1.39;
        }

        break;
      }
    }

}


void fluidPropertyMixture()
{
  double flowRateF, flowRateW, flowRateT;

    flowRateF=massFlowRateFluid/fluidDensity;
    flowRateW=massFlowRateWater/waterDensity;
    flowRateT=flowRateF+flowRateW;

    fluidDensity=fluidDensity*(flowRateF/flowRateT)+waterDensity*(flowRateW/flowRateT);

plasticViscosity=plasticViscosity*(flowRateF/flowRateT)+plasticViscosityWater*(flowRateW/
flowRateT);
    yieldPoint=yieldPoint*(flowRateF/flowRateT)+yieldPointWater*(flowRateW/flowRateT);

fluidThermalConductivity=fluidThermalConductivity*(flowRateF/flowRateT)+waterThermalCondu
ctivity*(flowRateW/flowRateT);

fluidSpecificHeat=fluidSpecificHeat*(flowRateF/flowRateT)+waterSpecificHeat*(flowRateW/fl
owRateT);

jouleThompsonCoefficient=jouleThompsonCoefficient*(flowRateF/flowRateT)+jouleThompsonCoef
ficientWater*(flowRateW/flowRateT);

    flowRate=flowRateT;
}


void overallHeatTransferEstimation(int k)
{
  double rpi, rpo, kp, rci, rco, rb, rbo, ka, ke, kt;
  double nRep, nRea, nPrp, nPra, aP, aA, mP, mA, cpP, cpA;
  double temp, pres;
  double mixF, mixI, mFR;
  int infD;

  // definitions
    infD=influxDepth;
    mFR=massFlowRate;
    kt=pipeThermalConductivity;
    ke=formationThermalConductivity;

    rpi=stringID[k]/2.;
```

```
    rpo=stringOD[k]/2.;

    rci=casID[k]/2.;
    rco=casOD[k]/2.;
    rb=boreSize[k]/2.;
    rbo=boreSizeOld[k]/2.;

    aP=pi*pow(rpi,2.);
    aA=pi*(pow(rb,2.)-pow(rpo,2.));

   // modified pipe temperature
    if (k==1)
     temp=temperatureInsidePipe[0][k];
    else
     temp=(temperatureInsidePipe[0][k]+temperatureInsidePipe[0][k-1])/2.;

    pres=pressureInsidePipe[0][k];
    fluidPropertyDetermination(temp, pres/144., k);
    fluidPropertyMixture();

   // pipe
    mP=plasticViscosity;
    kp=fluidThermalConductivity;
    cpP=fluidSpecificHeat;
    fluidSpecificHeatPipe=cpP;


   // modified annulus temperature
    if (k==1)
     temp=temperatureInsideAnnulus[0][k];
    else
     temp=(temperatureInsideAnnulus[0][k]+temperatureInsideAnnulus[0][k-1])/2.;

    pres=pressureInsideAnnulus[0][k];
    fluidPropertyDetermination(temp, pres/144., k);
    fluidPropertyMixture();

   // annulus
    ka=fluidThermalConductivity;
    cpA=fluidSpecificHeat;
    mA=plasticViscosity;


   // influx contribution
    influxMassRate=prIndex*(formationPressureGradient*influxDepth-
pressureInsideAnnulus[0][infD])*influxDensity;

mixF=(massFlowRate/fluidDensity)/((massFlowRate/fluidDensity)+(influxMassRate/influxDensi
ty));

mixI=(influxMassRate/influxDensity)/((massFlowRate/fluidDensity)+(influxMassRate/influxDe
nsity));

    if (k<=infD)
    {
      if ((formationPressureGradient*influxDepth)>pressureInsideAnnulus[0][infD])
      {
        temp=temp*mixF+temperatureFormation[infD]*mixI;
```

```
        pres=pressureInsideAnnulus[0][k];
        fluidPropertyDetermination(temp, pres/144., k);
        fluidPropertyMixture();
        mA=mixF*plasticViscosity+mixI*plasticViscosityWater;
        mFR=mFR+influxMassRate;
      }
    }


   // NReP, NReA, NPrP and NPrA calculations
    nRep=(2.*rpi*massFlowRate)/(aP*mP);
    nRea=(0.816*2.*(rb-rpo)*mFR)/(aA*mA);

    nPrp=cpP*mP/kp;
    nPra=cpA*mA/ka;

   // Heat Transfer Coefficients, ha and hp
    if (nRep<=10000.)

hp=(kp/(2.*rpi))*(3.65+(0.00668*nRep*nPrp*(2.*rpi))/(1+0.04*(pow((nRep*nPrp*2.*rpi),0.666
));
    else
     hp=0.023*pow(nRep,0.8)*pow(nPrp,0.4)*kp/(2.*rpi);   // N/s-m-K

    if (nRea<=10000.)

ha=(ka/(2.*rb))*(3.65+(0.00668*nRea*nPra*(2.*rb))/(1+0.04*(pow((nRea*nPra*2.*rb),0.666)))
);
    else
     ha=0.023*pow(nRea,0.8)*pow(nPra,0.4)*ka/(2.*rb);    // N/s-m-K

   // Overall heat transfer coefficients, Ua and Up

overallHeatTransferCoefficientPipeAnnulus=1/((1/hp)+(rpi/kt)*log(rpo/rpi)+(rb/rpo)*(1/ha)
);   // N/s-m-K
//    overallHeatTransferCoefficientPipeAnnulus=30.;

overallHeatTransferCoefficientAnnulusFormation=1/((1/ha)+(rci/kt)*log(rco/rci)+(rci/ke)*l
og(rbo/rco));   // N/s-m-K
//    overallHeatTransferCoefficientAnnulusFormation=1.0;
}


void tfCalculation(double d)
{
  int i;

  // no modification is conducted at this moment
    i=d;

tfModified=(2.*(surfaceTemperature+temperatureGradient*d)+0.*temperatureWellbore[0][i])/2
.;
}



void formationTemperatureDetermination(int d, double ta, double tf)
{
```

```
  double kf, cf, rb, ua, alfa, ttd, df;

     overallHeatTransferEstimation(d);

     ua=overallHeatTransferCoefficientAnnulusFormation;

     kf=formationThermalConductivity;
     cf=formationSpecificHeat;
     df=formationDensity;
     rb=boreSize[d]/2.;

     tfCalculation(d);

     tf=(tf+tfModified)/2.;    // tfModified=tf

     alfa=kf/(cf*df);
     ttd=alfa*circulationTime/pow(rb,2.);   // dimensionless

     if (ttd<=1.5)
      tD=1.1281*pow(ttd,0.5)*(1.-0.3*pow(ttd,0.3));
     else
      tD=(0.4063+0.5*log(ttd))*(1.+0.6/ttd);

     if (d==1)
      temperatureWellbore[1][d]=(kf*tf+rb*ua*tD*ta)/(kf+rb*ua*tD);
     else
      temperatureWellbore[1][d]=(kf*tf+rb*ua*tD*ta)/(kf+rb*ua*tD);

 //    temperatureWellbore[1][d]=ta+(surfaceTemperature+(temperatureGradient-
deltaT/finalDepth)*d-ta)*(kf/(kf+rb*ua*tD));
     temperatureWellbore[1][d]=ta+(surfaceTemperature+(temperatureGradient)*d-
ta)*(kf/(kf+rb*ua*tD));

}


void temperatureUpdate()
{
  double ta, tp, tf;
  int i;


    i=finalDepth;
    ta=temperatureInsideAnnulus[1][i];
    tf=surfaceTemperature+temperatureGradient*i;
    formationTemperatureDetermination(i, ta, tf);

    for (i=finalDepth-1; i>=1; i--)
    {
      ta=(temperatureInsideAnnulus[1][i]+temperatureInsideAnnulus[1][i+1])/2.;
      tf=surfaceTemperature+temperatureGradient*i;
      formationTemperatureDetermination(i, ta, tf);
    }

}
```

```
void temperatureCalculation(int j, double tf)
{
  double a, b;
  double ta, ta1, ta2, tp, tp1, tp2;
  double c1, c2, c3, c4, k1, k2;
  double tpC1, tpC2, taC1, taC2;
  double rpi, uP;
  double rb, uA;
  double tpInlet, ts, tg, h;
  double ke, eps1, eps2, gama, delta;
  double dt, epsilon;
  double mFRT, mixI, mixF;
  double gamaDum,gama1,delta1;
  double failDum1, failDum2;
  int fd, inD;


    tpInlet=fluidInletTemperature;
    ts=surfaceTemperature;
    tg=temperatureGradient;
    h=finalDepth;
    fd=h;
    ke=formationThermalConductivity;
    inD=influxDepth;

    overallHeatTransferEstimation(j);
    uP=overallHeatTransferCoefficientPipeAnnulus;
    uA=overallHeatTransferCoefficientAnnulusFormation;

    rb=boreSize[j]/2.;
    rpi=stringID[j]/2.;

  // influx influence
    influxMassRate=prIndex*(formationPressureGradient*influxDepth-
pressureInsideAnnulus[0][inD])*influxDensity;
 //
mixF=(massFlowRate/fluidDensity)/((massFlowRate/fluidDensity)+(influxMassRate/influxDensi
ty));
 //
mixI=(influxMassRate/influxDensity)/((massFlowRate/fluidDensity)+(influxMassRate/influxDe
nsity));

   // influx contribution
    mFRT=0.;

    if (j<=inD)
    {
     if ((formationPressureGradient*influxDepth)>pressureInsideAnnulus[0][inD])
      {
        mFRT=influxMassRate;
      }
    }


  // temperature calculation methodology - I

    a=((massFlowRate+mFRT)*fluidSpecificHeatPipe/(2.*pi))*((ke+tD)/(rb*uA*ke));       //
lb/hr
```

```
    b=(massFlowRate*fluidSpecificHeatPipe/(2.*pi*rpi*uP));                          //
ft

    eps1=1./(2.*a)+1./(2.*a)*pow((1.+4.*a/b),0.5);
    eps2=1./(2.*a)-1./(2.*a)*pow((1.+4.*a/b),0.5);

    failDum1=eps1;
    if (failDum1<0)
     failDum1=-failDum1;
    failDum2=eps2;
    if (failDum2<0)
     failDum2=-failDum2;

    if ((failDum1>0.1)||(failDum2>0.1))
    {
      clrscr();
      printf("Unstable conditions !! .. \n");
      printf("\n");
      printf("Please change inputs (increase nozzle size, reduce flow rate, etc)\n");
      printf("\n");
      fail=1;
      eps1=0.00000001;
      eps2=-0.00000001;
      gama1=1.;
      delta1=1.;
    }

    if (fail==0)
     gama1=(eps1*pow(e,(eps1*fd))-eps2*pow(e,(eps2*fd)));
    gama=-((tpInlet+b*(tg)-ts)*eps2*pow(e,(eps2*fd))+tg+deltaT/fd*3.)/gama1;
//    delta=((tpInlet+b*(tg)-
ts)*eps1*pow(e,(eps1*fd))+tg+deltaT/fd)/(eps1*pow(e,(eps1*fd))-eps2*pow(e,(eps2*fd)));
//    gamaDum=deltaT/fd;
//    gama=gamaDum-((tpInlet+b*(tg)-ts)*eps2*pow(e,(eps2*fd))+tg)/(eps1*pow(e,(eps1*fd))-
eps2*pow(e,(eps2*fd)));
//    gamaDum=deltaT/fd*(eps1*pow(e,(eps1*fd))-
eps2*pow(e,(eps2*fd))+eps1*pow(e,(eps1*fd))*eps2*pow(e,(eps2*fd)))/(eps1*pow(e,(eps1*fd))
*(eps1*pow(e,(eps1*fd))-eps2*pow(e,(eps2*fd))));
//    gama=gamaDum-((tpInlet+b*(tg)-ts)*eps2*pow(e,(eps2*fd))+tg)/(eps1*pow(e,(eps1*fd))-
eps2*pow(e,(eps2*fd)));
//    gama=deltaT/fd-((tpInlet+b*(tg)-
ts)*eps2*pow(e,(eps2*fd))+tg)/(eps1*pow(e,(eps1*fd))-eps2*pow(e,(eps2*fd)));
//    gama=gamaDum+((-tpInlet-b*(tg)+ts)*eps1*pow(e,(eps1*fd))-
tg)/(eps1*pow(e,(eps1*fd))-
eps2*pow(e,(eps2*fd)))*eps2*pow(e,(eps2*fd))/eps1*pow(e,(eps1*fd))-
tg/eps1*pow(e,(eps1*fd));
    if (fail==0)
     delta1=(eps1*pow(e,(eps1*fd))-eps2*pow(e,(eps2*fd)));
    delta=((tpInlet+b*(tg)-ts)*eps1*pow(e,(eps1*fd))+tg-deltaT/fd/3.)/delta1;

 // original
 //   tp=k1*pow(e,(c1*j))+k2*pow(e,(c2*j))+tf-tg*a;           // K
 //   ta=k1*c3*pow(e,(c1*j))+k2*c4*pow(e,(c2*j))+tf;          // K

  // modified
    tfCalculation(j);
    tf=tfModified;
```

```
   // modified annulus temperature
    if (j==1)
    {
//      ta1=(1.+eps1*b)*gama*pow(e,(eps1*j))+(1.+eps2*b)*delta*pow(e,(eps2*j))+tg*j+ts-
deltaT/fd*j;
//      ta2=(1.+eps1*b)*gama*pow(e,(eps1*j))+(1.+eps2*b)*delta*pow(e,(eps2*j))+tg*j+ts-
deltaT;
      ta1=(1.+eps1*b)*gama*pow(e,(eps1*j))+(1.+eps2*b)*delta*pow(e,(eps2*j))+tg*j+ts;
      ta2=(1.+eps1*b)*gama*pow(e,(eps1*j))+(1.+eps2*b)*delta*pow(e,(eps2*j))+tg*j+ts;
      ta=(ta1+ta2)/2.;
    }
    else
    {
//      ta1=(1.+eps1*b)*gama*pow(e,(eps1*j))+(1.+eps2*b)*delta*pow(e,(eps2*j))+tg*j+ts-
deltaT/fd*j;
//      ta2=(1.+eps1*b)*gama*pow(e,(eps1*j))+(1.+eps2*b)*delta*pow(e,(eps2*j))+tg*j+ts-
deltaT;
      ta1=(1.+eps1*b)*gama*pow(e,(eps1*j))+(1.+eps2*b)*delta*pow(e,(eps2*j))+tg*j+ts;
      ta2=(1.+eps1*b)*gama*pow(e,(eps1*j))+(1.+eps2*b)*delta*pow(e,(eps2*j))+tg*j+ts;
      ta=(ta1+ta2)/2.;
    }

    if (ta<1.)
    {
      ta=10.;
      fail=1;
    }

   // modified pipe temperature

    if (j==1)
    {
      tp1=tpInlet;
//      tp2=gama*pow(e,(eps1*j))+delta*pow(e,(eps2*j))+tg*j-b*(deltaT/fd+tg)+ts;     //
modified due to Joule Thompson
      tp2=gama*pow(e,(eps1*j))+delta*pow(e,(eps2*j))+tg*j-b*tg+ts;
    }
    else
    {
//      tp1=gama*pow(e,(eps1*j))+delta*pow(e,(eps2*j))+tg*j-b*(deltaT/fd+tg)+ts;     //
modified due to Joule Thompson
//      tp2=gama*pow(e,(eps1*j))+delta*pow(e,(eps2*j))+tg*j-b*(deltaT/fd+tg)+ts;     //
modified due to Joule Thompson
      tp1=gama*pow(e,(eps1*j))+delta*pow(e,(eps2*j))+tg*j-b*tg+ts;
      tp2=gama*pow(e,(eps1*j))+delta*pow(e,(eps2*j))+tg*j-b*tg+ts;

    }
    tp=(tp1+tp2)/2.;

    if (tp<1.)
    {
      tp=10.;
      fail=1;
    }

    tpC1=tp;
    taC1=ta;
```

```
  // temperature calculation methodology - II
 /*
    a=(massFlowRate*fluidSpecificHeatPipe)/(2.*pi*rpi*uP);    // has a unit of meter
    b=(rb*uA)/(rpi*uP);    // dimensionless

    c1=(b/(2.*a))*(1.+pow((1.+4./b),0.5));       // has a unit of 1/meter
    c2=(b/(2.*a))*(1.-pow((1.+4./b),0.5));       // has a unit of 1/meter

    c3=1.+(b/2.)*(1.+pow((1.+4./b),0.5));        // dimensionless
    c4=1.+(b/2.)*(1.-pow((1.+4./b),0.5));        // dimensionless

   // unit has changed to F due to modifications conducted
    k2=(tg*a-(tpInlet-ts+tg*a)*pow(e,(c1*h))*(1.-c3))/(pow(e,(c2*h))*(1.-c4)-
pow(e,(c1*h))*(1.-c3));    // K
    k1=tpInlet-k2-ts+tg*a;    // K

  // original
 //   tp=k1*pow(e,(c1*j))+k2*pow(e,(c2*j))+tf-tg*a;           // K
 //   ta=k1*c3*pow(e,(c1*j))+k2*c4*pow(e,(c2*j))+tf;          // K

  // modified

    tfCalculation(j);
    tf=tfModified;

   // modified pipe temperature
    if (j==1)
    {
      tp1=k1*pow(e,(c1*j))+k2*pow(e,(c2*j))+tf-tg*a;           // K
      tp2=k1*pow(e,(c1*j))+k2*pow(e,(c2*j))+(temperatureWellbore[0][j]+tf)/2.-tg*a;
    }
    else
    {
      tp1=k1*pow(e,(c1*j))+k2*pow(e,(c2*j))+tf-tg*a;
      tp2=k1*pow(e,(c1*j))+k2*pow(e,(c2*j))+(temperatureWellbore[0][j]+tf)/2.-tg*a;
    }
    tp=(tp1+tp2)/2.;

   // modified annulus temperature
    if (j==1)
    {
      ta1=k1*c3*pow(e,(c1*j))+k2*c4*pow(e,(c2*j))+tf-delT[j];
      ta2=(k1*c3*pow(e,(c1*j))+k2*c4*pow(e,(c2*j))+(tf+temperatureWellbore[0][j])/2.)-
delT[j];
      ta=(ta1+ta2)/2.;
    }
    else
    {
      ta1=k1*c3*pow(e,(c1*j))+k2*c4*pow(e,(c2*j))+tf-delT[j];
      ta2=(k1*c3*pow(e,(c1*j))+k2*c4*pow(e,(c2*j))+(tf+temperatureWellbore[0][j])/2.)-
delT[j];
      ta=(ta1+ta2)/2.;
    }

    tpC2=tp;
    taC2=ta;
```

```
   // combining method - I and method - II
    temperatureInsidePipe[1][j]=(tpC1+tpC2)/2.;

    temperatureInsideAnnulus[1][j]=(taC1+taC2)/2.;
 */
  // should be removed if method-II is also used
    temperatureInsidePipe[1][j]=tpC1;
    temperatureInsideAnnulus[1][j]=taC1;

    parUa[j]=uA;
    parUp[j]=uP;
}


void bitPressure(double pipeT, double annT)
{
  double a,pA,k,tA;
//  double q;
  double flowRateF, flowRateW, flowRateT;
  int fd;

    flowRateF=massFlowRateFluid/fluidDensity;
    flowRateW=massFlowRateWater/waterDensity;
    flowRateT=flowRateF+flowRateW;

    k=cPovercV;
    fd=finalDepth;
    fluidPropertyDetermination(pipeT, pressureInsidePipe[0][fd]/144., fd);

    flowRateF=massFlowRateFluid/fluidDensity;
    flowRateW=massFlowRateWater/waterDensity;
    flowRateT=flowRateF+flowRateW;

    fluidPropertyMixture();
   // pipeT is the temperature at the bottom inside the pipe
   // annT is the termperature at the bottom inside the wellbore
   //   q=massFlowRate/fluidDensity;
    a=pi/4.*numberOfNozzles*pow(nozzleSize,2.);


bitPressureDrop=0.00008311*144.*fluidDensity/7.48*pow((flowRate/8.020833),2.)/(pow(0.95,2
.)*pow(a,2.));
    pA=pressureInsidePipe[0][fd]-bitPressureDrop;

    if (pA<0)
     pA=pressureInsideAnnulus[0][fd];

    fluidPropertyDetermination(annT, pA/144., fd);
    fluidPropertyMixture();

    tA=pipeT/pow((pressureInsidePipe[0][fd]/pressureInsideAnnulus[0][fd]),(k-1.)/k);

  //  deltaT=bitPressureDrop/144.*jouleThompsonCoefficient;
    deltaT=(pipeT-tA)*(1-flowRateW/flowRateT);

}
```

```
void pressureCalculation()
{
  int w, infD, fd;
  double t, p, tp;
  double pa, pp, dpf, dpfT, phyd, phydT;
  double nre, v, q, dhyd, a, ff;
  double mixF, mixI, mFR, mA;
  double solidCc;

    pa=backPressure;
    infD=influxDepth;
    fd=finalDepth;

    dpfT=0.;
    phydT=0.;

   // start from exit towards the bottom through the annulus
    for (w=1; w<=finalDepth; w++)
    {
      t=temperatureInsideAnnulus[1][w];
      p=pressureInsideAnnulus[0][w];
      fluidPropertyDetermination(t, p/144., w);
      fluidPropertyMixture();
      mA=plasticViscosity;

      mFR=massFlowRate;
     // influx contribution
      influxMassRate=prIndex*(formationPressureGradient*influxDepth-
pressureInsideAnnulus[0][infD])*influxDensity;

mixF=(massFlowRate/fluidDensity)/((massFlowRate/fluidDensity)+(influxMassRate/influxDensi
ty));

mixI=(influxMassRate/influxDensity)/((massFlowRate/fluidDensity)+(influxMassRate/influxDe
nsity));

     // solids contribution

solidCc=cuttingsConcentration[w]/100.+(massRateAbrasives/densityAbrasives)/((massFlowRate
/fluidDensity)+(influxMassRate/influxDensity)+(massRateAbrasives/densityAbrasives));
      if (solidCc >= 1.0)
       solidCc=0.99;

      if (w<=infD)
      {
        if ((formationPressureGradient*influxDepth)>pressureInsideAnnulus[0][infD])
        {
          t=t*mixF+temperatureFormation[infD]*mixI;
          fluidPropertyDetermination(t, p/144., w);
          fluidPropertyMixture();
          mA=mixF*plasticViscosity+mixI*plasticViscosityWater;
          mFR=mFR+influxMassRate;
        }
      }
```

```
     // hydrostatic pressure
      phyd=(fluidDensity*mixF+influxDensity*mixI)*(1-
solidCc)+(densityAbrasives+formationDensity)/2.*solidCc;
      hydrostaticAnnulus[w]=phyd+phydT;
      phydT=hydrostaticAnnulus[w];

     // frictional pressure
      phyd=fluidDensity*mixF+influxDensity*mixI;
      q=mFR/(phyd*60.);
      a=pi/4.*(pow(boreSize[w],2.)-pow(stringOD[w],2.));
      dhyd=boreSize[w]-stringOD[w];
      v=q/a;
      nre=phyd*v*0.816*dhyd*60./mA;

      if (nre<=2100)
       ff=16./nre;
      else
       ff=0.0791/pow(nre,0.25);

//      if (fluidPhase==1)
//       ff=0.56/(pow(dhyd,0.333));

      dpf=2*ff*phyd*pow(v,2.)/(dhyd*0.816)/(32.2*3600.);
      frictionAnnulus[w]=dpf+dpfT;
      dpfT=frictionAnnulus[w];

     // total pressure
      pa=pa+dpf+phyd;
      pressureInsideAnnulus[1][w]=pa;

      phaseInsideAnnulus[w]=fluidPhase;

    }


   // call bit pressure loss
    tp=temperatureInsidePipe[1][w-1];
    bitPressure(tp, t);

   // bit upstream pressure = pressure inside the pipe at the bottom
    bitUpstreamPressure=pressureInsideAnnulus[1][w-1]+bitPressureDrop;

    pp=bitUpstreamPressure;
    pressureInsidePipe[0][w-1]=pp;

    dpfT=0.;
    phydT=0.;

   // from bottom to surface through the pipe
    for (w=finalDepth; w>=1; w--)
    {
      t=temperatureInsidePipe[1][w];
      p=pressureInsidePipe[0][w];
      fluidPropertyDetermination(t, p/144., w);
      fluidPropertyMixture();

     // hydrostatic pressure
```

```
solidCc=(massRateAbrasives/densityAbrasives)/((massFlowRate/fluidDensity)+(massRateAbrasi
ves/densityAbrasives));
      if (solidCc >= 1.0)
       solidCc=0.99;

      phyd=fluidDensity*(1-solidCc)+densityAbrasives*solidCc;
      hydrostaticPipe[fd+1-w]=phyd+phydT;
      phydT=hydrostaticPipe[fd+1-w];

     // frictional pressure
      q=massFlowRate/(fluidDensity*60.);
      a=pi/4.*pow(stringID[w],2.);
      dhyd=stringID[w];
      v=q/a;
      nre=fluidDensity*v*dhyd*60./plasticViscosity;

      if (nre<=2100)
       ff=16./nre;
      else
       ff=0.0791/pow(nre,0.25);

//      if (fluidPhase==1)
//       ff=0.56/(pow(dhyd,0.333));

      dpf=2*ff*fluidDensity*pow(v,2.)/dhyd/(32.2*3600.);

      frictionPipe[w]=dpf+dpfT;
      dpfT=frictionPipe[w];
     // total pressure
      pp=pp+dpf-phyd;
      pressureInsidePipe[1][w]=pp;

      phaseInsidePipe[w]=fluidPhase;
    }

    for (w=1; w<=finalDepth; w++)
    {
      pressureInsidePipe[0][w]=pressureInsidePipe[1][w];
      pressureInsideAnnulus[0][w]=pressureInsideAnnulus[1][w];
    }


}


void initialize()
{

  int i, fd;

    fd=finalDepth;

    for (i=1; i<=fd; i++)
    {
     // initial temperature set (formation temperature)
      temperatureWellbore[0][i]=surfaceTemperature;
      temperatureInsidePipe[0][i]=surfaceTemperature+(temperatureGradient)*i;
```

```
      temperatureInsideAnnulus[0][i]=surfaceTemperature;
      temperatureFormation[i]=surfaceTemperature+(temperatureGradient)*i;

      fluidPropertyDetermination(temperatureInsideAnnulus[0][i],
pressureInsideAnnulus[0][i]/144., i);

      pressureInsideAnnulus[0][i]=backPressure+fluidDensity*i;

      phaseInsideAnnulus[i]=0;
      phaseInsidePipe[i]=0;

      cuttingsConcentration[i]=0;
    }

    temperatureInsidePipe[0][1]=fluidInletTemperature;
    tBottomhole=temperatureInsideAnnulus[0][fd];

    for (i=1; i<=fd; i++)
    {
     // initial guess (if you find a better dPf estimation (empirical), use it and modify
the equation
      pressureInsidePipe[0][i]=pressureInsideAnnulus[0][fd];
    }

    fluidPropertyDetermination(temperatureInsidePipe[0][1],
pressureInsidePipe[0][1]/144., 1);
    bitPressureDrop=0.;
    massFlowRateFluid=fluidDensity*flowRateFluid;
    massFlowRateWater=waterDensity*flowRateWater;
    massFlowRate=massFlowRateFluid+massFlowRateWater;

}


void geometryDescription()
{
  int i;

  for (i=1; i<=finalDepth; i++)
  {
     if (i<=casingSettingDepth)
     {
       boreSize[i]=casingID;
       boreSizeOld[i]=holeSize;
       casOD[i]=casingOD;
       casID[i]=casingID;
     }
     else
     {
       boreSize[i]=bitDiameter;
       boreSizeOld[i]=bitDiameter;
       casOD[i]=bitDiameter;
       casID[i]=bitDiameter;
     }

     if (i>(finalDepth-drillCollarLength))
     {
       stringOD[i]=drillCollarOD;
```

```
      stringID[i]=drillCollarID;
     }
     else
     {
      stringOD[i]=drillPipeOD;
      stringID[i]=drillPipeID;
     }

  }


}



void convergenceCheck()
{
  int errC;

    maxErr=0;
    err=0;
    errDepth=0;

    for (errC=1; errC<=finalDepth; errC++)
    {
      err=temperatureInsidePipe[1][errC]-temperatureInsidePipe[0][errC];
      if (err<0)
       err=-err;
      if (err>maxErr)
      {
        maxErr=err;
        errDepth=errC;
      }
      temperatureInsidePipe[0][errC]=temperatureInsidePipe[1][errC];

      err=temperatureInsideAnnulus[1][errC]-temperatureInsideAnnulus[0][errC];
      if (err<0)
       err=-err;
      if (err>maxErr)
      {
        maxErr=err;
        errDepth=errC;
      }
      temperatureInsideAnnulus[0][errC]=temperatureInsideAnnulus[1][errC];

      err=temperatureWellbore[1][errC]-temperatureWellbore[0][errC];
      if (err<0)
       err=-err;
      if (err>maxErr)
      {
        maxErr=err;
        errDepth=errC;
      }
      temperatureWellbore[0][errC]=temperatureWellbore[1][errC];
    }
}
```

```
// cuttings transport verification
void cuttingsTransportCheck()
{
  double dc, a, b, denC, denF, vsOld, vs, me, cc;
  double nRep, vf, errSlip;
  double aw, ab;
  int i;
  const g=32.198;


    dc=cuttingsSize;
    denC=formationDensity;

    for (i=1; i<=finalDepth; i++)
    {

      vs=1000.;
      errSlip=1000.;

      fluidPropertyDetermination(temperatureInsideAnnulus[1][i],
pressureInsideAnnulus[1][i]/144., i);
      fluidPropertyMixture();

      denF=fluidDensity;

      aw=(pi/4)*(pow(casID[i],2.)-pow(stringOD[i],2.));
      ab=(pi/4)*pow(casID[i],2.);
      vf=massFlowRate/(denF*aw);

      do
      {
        vsOld=vs;
        me=plasticViscosity+yieldPoint*dc/vf;
        nRep=dc*denF*vsOld/me;

        if (nRep<=1.)
        {
          a=40.;
          b=-1.;
        }
        if ((nRep>1.) && (nRep<1000.))
        {
          a=22.;
          b=-0.5;
        }
        if (nRep>=1000.)
        {
          a=1.5;
          b=0.;
        }

        vs=pow(((dc*g*pow(3600.,2.)/a)*(denC-denF)/denF*pow(nRep,-b)),0.5);
        errSlip=vs-vsOld;
        if (errSlip<0)
         errSlip=-errSlip;
      }
      while (errSlip>0.0001);
```

```
    cc=(ROP*ab)/(aw*(vf-vs));

    cuttingsConcentration[i]=cc*100.;
    transportRatio=1.-vs/vf;
    }
}



// main program
#pragma argsused
int main(int argc, char* argv[])
{

 double massOld, massErr;
 int tt, dd, counter, errCounter, cntr;
 char phasePipe[10], phaseAnnulus[10];

  fail=0;
  intro();

  do
  {

    choice=0;

    intro1();

 //   cin >> choice;

    choice=1;
    switch (choice)
    {
      case 0: // Exit
      {
        exit('0');
        break;
      }

      case 1:  // Continue
      {
  //      clrscr();

        inputPage();

        unitConversion();
     //  main

        finalCirculationTime=5.;  // define this properly later
        circulationTime=0;
        dcirculationTime=5.;

        geometryDescription();
  //      printf("Calculation in progress ");

        ofstream outfileDum ("out.lvm");
        outfileDum.close();
```

```
        ofstream outfile ("out.lvm", ios::app);

       // initiate the file
        outfile << "t(hr) " << "D(ft) " << "Tann(F) " << "Tpip(F) " << "Twb.(F) " <<
"Tfor(F) " << "Pa(psi) " << "Pp(psi) " << "PfrA(psi) " << "PfrP(psi) " << "PhydA(psi) "
<< "PhydP(psi) " << "phaseA " << "phaseP" << "Cc " << "Rt " << endl;
 //       outfile << "-----------------------------------------------------"<< endl;

       // loop for time
        while (circulationTime<finalCirculationTime)
        {
 //         printf(".");
          initialize();

          printErr=0;
          errCounter=0;
          circulationTime=circulationTime+dcirculationTime;

          cntr=0;
       // loop for convergence
          do
          {
            if (fail==1)
             goto unstableCase;
            cntr=cntr+1;
            massOld=massFlowRate;
            errCounter=errCounter+1;

           // depth loop
            for (dd=1; dd<=finalDepth; dd++)
            {
              temperatureCalculation(dd, temperatureWellbore[0][dd]);
            }
            pressureCalculation();

            temperatureUpdate();

            convergenceCheck();

            if (errCounter>50)
            {
              printErr=1;
              printMaxErr=maxErr;
              maxErr=0.01;
            }

            fluidPropertyDetermination(temperatureInsidePipe[0][1],
pressureInsidePipe[0][1]/144., 1);
            massFlowRateFluid=fluidDensity*flowRateFluid;
            massFlowRateWater=waterDensity*flowRateWater;
            massFlowRate=massFlowRateFluid+massFlowRateWater;


         // to make sure mass rate is stable between two iterations
            massErr=massFlowRate-massOld;
            if (massErr<0)
             massErr=-massErr;
```

```
            if (cntr>200)
             massErr=0.9;
          }
          while ((maxErr>=0.05) || (massErr>=1.));

          cuttingsTransportCheck();

         // writing information into a file
  //        circulationTime2=0;
  //        while (circulationTime2<finalCirculationTime)
  //        {
  //          circulationTime2=circulationTime2+dcirculationTime;

            for (counter=1; counter<=finalDepth; counter++)
            {
              if (phaseInsideAnnulus[counter]==0)
               strcpy(phaseAnnulus, "liquid");
              if (phaseInsideAnnulus[counter]==1)
               strcpy(phaseAnnulus, "gas");
              if (phaseInsideAnnulus[counter]==2)
               strcpy(phaseAnnulus, "supercrt");
              if (phaseInsidePipe[counter]==0)
               strcpy(phasePipe, "liquid");
              if (phaseInsidePipe[counter]==1)
               strcpy(phasePipe, "gas");
              if (phaseInsidePipe[counter]==2)
               strcpy(phasePipe, "supercrt");
  /*
         char op1[10];
         char op2[10];
         char op3[10];
         char op4[10];
         char op5[10];
         char op6[10];
         char op7[10];
         char op8[10];
         char op9[12];
         char op10[12];

         sprintf(op1, "%4d ", circulationTime);
         sprintf(op2, "%5d ", counter);
         sprintf(op3, "%5d ", temperatureInsideAnnulus[1][counter]);
         sprintf(op4, "%5d ", temperatureInsidePipe[1][counter]);
         sprintf(op5, "%5d ", temperatureWellbore[1][counter]);
         sprintf(op6, "%5d " ,temperatureFormation[counter]);
         sprintf(op7, "%7d ", pressureInsideAnnulus[1][counter]/144.);
         sprintf(op8, "%7d ", pressureInsidePipe[1][counter]/144.);
         sprintf(op9, "%9c ", phaseAnnulus);
         sprintf(op10, "%9c ", phasePipe);

              outfile << op1 << op2 << op3 << op4 << op5 << op6 << op7 << op8 << op9 <<
op10 << endl;
   */
              outfile << circulationTime << " " << counter << " " <<
temperatureInsideAnnulus[1][counter] << " " << temperatureInsidePipe[1][counter] << " "
<< temperatureWellbore[1][counter]
```

```
              << " " << temperatureFormation[counter] << " " <<
pressureInsideAnnulus[0][counter]/144. << " " << pressureInsidePipe[0][counter]/144. << "
" << frictionAnnulus[counter]/144. << " " << frictionPipe[counter]/144. << " " <<
              hydrostaticAnnulus[counter]/144. << " " << hydrostaticPipe[counter]/144.
<< " " << phaseAnnulus << " " << phasePipe << " " << cuttingsConcentration[counter] << "
" << transportRatio << " " << endl;

            }
   //       }
         }

   //     clrscr();

         outfile.close();
         outputPage();


   //     clearScreen();
         break;
      }


      default:  // continue
      {
        choice=1;

 //       clrscr();

        inputPage();
     // main

        outputPage();

 //       clearScreen();
        break;
      }
    }

  unstableCase:
   if (fail == 1)
   {
      clrscr();
 //    printf("Stable solution is not possible with the current input data.\n");
 //    printf("\n");
 //    printf("Either 'freezing' or 'physically impossible' situation.\n");
 //    printf("\n");
 //    printf("Suggestions:.\n");
 //    printf("   - Change nozzle size\n");
 //    printf("   - Change backpressure\n");
 //    printf("   - Change flow rate\n");
 //    printf("   - Add water into the system\n");
 //    printf("\n");
 //    printf("Please modify the input information.\n");
 //    printf("\n");
 //    printf("(Press any key to continue ...)\n");
 //    getch();
 //    clrscr();
      ofstream outfileDum ("out.lvm");
```

```
      outfileDum.close();
   }

  choice=0;
  }
  while (choice != 0);

    return 0;
}
//---------------------------------------------------------------------------
```